A GEOMORPHOLOGICAL INTERPRETATION OF SALTMARSH CHANNEL NETWORK MORPHOLOGY AND FUNCTION

BEVERLEY JOANNE ADAMS

UNIVERSITY COLLEGE LONDON

THESIS SUBMITTED FOR THE DEGREE OF DOCTOR OF PHILOSOPHY

MARCH 2001

SOME DIAGRAMS

EXCLUDED ON

INSTRUCTION FROM

THE UNIVERSITY

ABSTRACT

Although tidal channel networks are a near-ubiquitous feature of saltmarsh environments developed on the marine sedimentary shores of Britain, only limited progress has been made towards achieving a scientific understanding of their morphological characteristics and the physical functions that they perform.

Based on data acquired from a combination of high resolution aerial photography and field survey, a range of descriptive indices and morphometric measures are used to characterise planimetric, longitudinal and cross-sectional adjustment in saltmarsh channel networks from 29 localities around England and Wales. In accordance with the extensive methodological approach employed during this exploratory phase of the study, regularities and distinguishing features of the selected formations are interpreted in terms of broad-scale environmental controls, which represent the relative intensity of erosional versus resistive forces. While statistical analyses suggest that creek morphology reflects a multiplicity of influences, the strongest bivariate associations, between tidal prism and cross-sectional geometry, are consistent with the finding of earlier process studies that creek morphology is principally adapted to perform a conveyance function.

Theoretically-based mathematical models are employed to more fully elucidate relations of causality between creek morphology and function. This intensive investigation utilises Brancaster Marsh, Norfolk as an illustrative case study. The availability of airborne laser altimetry (lidar) for this site facilitates the evaluation of alternative models of channel function. Optimality models of angular geometry are implemented at a network-scale, and cross-sectional adjustments are modelled with reference to the concept of stability shear stress.

While of interest from a geomorphological perspective, the insights offered into creek morphology and function are also relevant to the field of coastal engineering. Here, they provide an empirical basis for post-project appraisal, and may lead to theoretical guidelines for the design of tidal channel networks, as an integral component of saltmarsh restoration and flood defence realignment schemes.

TABLE OF CONTENTS

	page
ABSTRACT	**1**
TABLE OF CONTENTS	**2**
LIST OF FIGURES	**7**
LIST OF TABLES	**15**
LIST OF PLATES	**17**
LIST OF SYMBOLS	**19**
ACKNOWLEDGEMENTS	**22**
1. INTRODUCTION	**23**
1.1 THE NATURE OF SALTMARSH ENVIRONMENTS	**23**
1.1.1 Controls on distribution	**23**
1.1.2 Classes of coastal saltmarsh	**27**
1.2 SALTMARSH FUNCTION AND VALUE	**29**
1.3 THE IMPORTANCE OF SALTMARSH CHANNEL NETWORKS	**31**
1.3.1 Evolutionary status	**32**
1.3.2 Physical functions	**32**
1.3.3 The challenge of saltmarsh restoration and channel network design	**35**
1.4 PREVIOUS RESEARCH ON CHANNEL NETWORK GEOMORPHOLOGY	**37**
1.4.1 Channel network morphology	**37**
1.4.2 Conceptualising controls on channel network geomorphology	**39**
1.4.3 Environmental influences	**40**
1.4.4 Developmental sequence	**41**
1.4.5 Formative processes	**47**
1.4.6 Modelling relations between channel network morphology and function	**49**
1.5 UNRESOLVED ASPECTS OF SALTMARSH CHANNEL NETWORK MORPHOLOGY AND FUNCTION	**50**
1.6 AIMS AND OBJECTIVES	**53**
1.7 THESIS STRUCTURE	**53**

2. RESEARCH DESIGN 54

2.1 METHODOLOGICAL APPROACH 54

2.2 MORPHOLOGICAL CHARACTERISATION 57

2.2.1 Study site selection 57
2.2.2 Acquisition strategy for planimetric, cross-sectional and longitudinal data 63
2.2.3 Methods of characterisation 67

2.3 INTERPRETATION OF NETWORK MORPHOLOGY 71

2.3.1 Controlling elements and independent variables 72
2.3.2 Analytical procedure 74

2.4 EVALUATION OF PHYSICAL FUNCTION 75

2.4.1 Theoretically-based mathematical models 75
2.4.2 Case study location: Brancaster Marsh, Norfolk 76
2.4.3 Data acquisition strategy 81

3. PLANIMETRIC CHARACTERISATION 84

3.1 INTRODUCTION 84

3.2 DATA ACQUISITION 84

3.2.1 Network delineation 85
3.2.2 Morphometric indices 89
3.2.3 Frequency data 92
3.2.4 Length data 92
3.2.5 Area data 94
3.2.6 Image registration 97

3.3 DESCRIPTIVE CHARACTERISATION 98

3.4 MORPHOMETRIC CHARACTERISATION 106

3.4.1 Uncertainty in area measurement 107
3.4.2 Intra-site variability 111
3.4.3 Creek density 112
3.4.4 Percentage channel cover 116
3.4.5 Link-based texture 118
3.4.6 Mean link length 122
3.4.7 Sinuosity of the principal channel 129

3.5 SCALE DEPENDENCE 136

3.6 SUMMARY OF KEY FINDINGS 144

4. LONGITUDINAL CHARACTERISATION 146

4.1 INTRODUCTION 146

4.2 DATA ACQUISITION 146

4.3 EXPLORATORY DATA ANALYSIS 150

4.3.1 Standardised profiles 159

4.3.2 Discontinuities in longitudinal adjustment 165

4.4 MORPHOMETRIC EXPRESSIONS OF LONGITUDINAL ADJUSTMENT 182

4.4.1 Network gradient 183

4.4.2 Profile concavity 187

4.5 SCALE DEPENDENCE 189

4.6 SUMMARY OF KEY FINDINGS 190

5. CROSS-SECTIONAL CHARACTERISTISATION 192

5.1 INTRODUCTION 192

5.2 DATA ACQUISITION 192

5.3 DESCRIPTIVE CHARACTERISATION 195

5.3.1 Cross-sectional facets 196

5.3.2 Conceptualising spatial scales of morphologic variability 204

5.4 QUANTITATIVE EXPRESSION OF CROSS-SECTIONAL FORM 216

5.4.1 Constituent variables 216

5.4.2 Width:depth ratio 223

5.4.3 Cross-sectional area 231

5.5 SCALE DEPENDENCE 237

5.6 SUMMARY OF KEY FINDINGS 239

6. INTERPRETATION OF CHANNEL NETWORK MORPHOLOGY 241

6.1 INTRODUCTION 241

6.2 EXTERNAL CONTROL DATA 241

6.2.1 Tidal range 242
6.2.2 Hydraulic duty 248
6.2.3 Tidal prism 255
6.2.4 Relative sea level change 257
6.2.5 Percentage silt-clay 262
6.2.6 Vegetative composition 268
6.2.7 Intertidal gradient 270
6.2.8 Coastal setting 273

6.3 MULTICOLLINEARITY 274

6.4 INTERDEPENDENCE BETWEEN MORPHOMETRIC DESCRIPTORS 280

6.5 BIVARIATE ASSOCIATIONS 287

6.5.1 Mutual dependence on an intermediary variable 289
6.5.2 Causal effects 299

6.6 MULTIVARIATE RELATIONS 308

6.7 SUMMARY OF KEY FINDINGS 311

7. THEORETICAL BASES FOR THE EVALUATION OF PHYSICAL FUNCTION 313

7.1 INTRODUCTION 313

7.2 OPTIMAL ANGULAR GEOMETRY 314

7.2.1 Model definition 314
7.2.2 Cost criteria 316
7.2.3 Theoretical responses 317
7.2.4 Data acquisition 322
7.2.5 Model performance 332

7.3 EQUILIBRIUM CROSS-SECTIONAL ADJUSTMENT 345

7.3.1 Stability shear stress criteria 346
7.3.2 Model definition 348
7.3.3 Data acquisition 349
7.3.4 Model performance 359

7.4 SUMMARY OF KEY FINDINGS 362

8. DISCUSSION 365

8.1 EVALUATION OF SALTMARSH CHANNEL NETWORK MORPHOLOGY AND FUNCTION 365

8.2 IMPLICATIONS FOR SALTMARSH RESTORATION 372

8.2.1 Design guidelines 373

8.2.2 Post-project appraisal 386

9. CONCLUSIONS 392

9.1 SUMMARY OF KEY FINDINGS 392

9.2 RECOMMENDATIONS FOR FURTHER RESEARCH 393

REFERENCES 396

APPENDIX 1 DETAILS OF AERIAL PHOTOGRAPHIC COVERAGE 419

APPENDIX 2 DESCRIPTION OF EXTENSIVE STUDY LOCALITIES 420

LIST OF FIGURES

Figure 1.1 Vertical range of coastal saltmarsh and intertidal flats (adapted from Klein, 1985; and Burd, 1989)

Figure 1.2 (a) Relation between tidal range and the lateral extent of saltmarsh development in an unconstrained system; and (b) landward and seaward limits imposed on marsh extent

Figure 1.3 Classification of British saltmarshes

Figure 1.4 Artificial creek systems from the Dutch Waddens (after Beeftink, 1977a)

Figure 1.5 Tiered model conceptualising geomorphological controls on channel network morphology

Figure 1.6 Schematic representation of saltmarsh channel network development

Figure 1.7 Transitional stages involved in saltmarsh channel network formation

Figure 1.8 Truncation of creek networks by the construction of an embankment during land reclamation in The Wash (after Kestner, 1979)

Figure 2.1 Logistical framework diagram

Figure 2.2 Factors taken into account in the selection of study sites for the extensive analysis

Figure 2.3 Regional variability in creek development for increasing network complexity. Linear; linear-dendritic; dendritic and complex relate to broad classes of planimetric form

Figure 2.4 Percentage frequency of saltmarsh creek formations of varying planimetric complexity, by region of the UK (based on data obtained from Pye and French (1993))

Figure 2.5 Geographic distribution of study localities

Figure 2.6 Structuring and evaluation of analytical approaches employed in the study of channel network planimetry

Figure 2.7 Alternative definitions of network sinuosity based on: (a) channel links; (b) Hortonian ordering; and (c) Hortonian ordering of an adjusted network; and (d) the principal channel

Figure 2.8 Schematic representation of associations cited in the literature between controlling elements and dependent network properties

Figure 2.9 Evaluation of modelling approaches employed in studying form-function relations in tidal channel networks

Figure 2.10 Site map for Brancaster Marsh, Norfolk

Figure 2.11 Lidar coverage of Brancaster Marsh overlaid with high resolution aerial photography (courtesy of Environment Agency)

Figure 3.1 Schematic representation of the methodological procedures employed to produce data for the descriptive and morphometric characterisation of network planimetry.

Figure 3.2 Definition diagrams for length and area measures required to compute morphometric expressions of: (a) creek density (*D*); (b) percentage channel cover (*%C*); (c) link-based texture (*F*); (d) mean link length (*L*); and (e) principal channel sinuosity (*S*)

Figure 3.3 Decision rules used in identifying the principal channel for sinuosity measures

Figure 3.4 Delimiting marsh area (*A*) in: (a) 'Closed' saltmarsh; and (b) 'Open' saltmarsh systems (adapted from Chapman, 1974)

Figure 3.5 Delineation of *A* based on: (a) Minimum area; (b) Equidistant area; and (c) Maximum area decision rules

Figure 3.6 Dendritic planimetric formations

Figure 3.7 Rectangular planimetric formations

Figure 3.8 Parallel planimetric formations

Figure 3.9 Linear planimetric formations

Figure 3.10 Schematic representation of: (a) elongate; and (b) expansive network structures.

Figure 3.11 Irregular decisions made in the definition of minimum, equidistant and maximum contributing areas.

Figure 3.12 (a) Percentage and (b) absolute magnitude of increase in A_{eq} and A_{max} relative to A_{min}

Figure 3.13 Intra-site variability in *D* at selected UK study sites and from US examples documented in the literature. Error bars reflect differences in *A* computed according to minimum, equidistant and maximum decision rules

Figure 3.14 Frequency distribution of *D* computed using: (a) A_{min}; (b) A_{eq}; and (c) A_{max} decision rules

Figure 3.15 Geographic variability in *D*. Margins of uncertainty about A_{eq} are reflected by the upper (A_{min}) and lower (A_{max}) error bars

Figure 3.16 Frequency distribution of *%C* computed using: (a) A_{min}; (b) A_{eq}; and (c) A_{max} decision rules

Figure 3.17 Geographic variability in *%C*. Margins of uncertainty about A_{eq} are reflected by the upper (A_{min}) and lower (A_{max}) error bars.

Figure 3.18 Relations between: (a) L_T, N_L; and (b) A_C and N_L, as alternative measures of channel network extent

Figure 3.19 Frequency distribution of *F* computed using: (a) A_{min}; (b) A_{eq}; and (c) A_{max} decision rules

Figure 3.20 Geographic variability in *F*. Margins of uncertainty about A_{eq} are reflected by the upper (A_{min}) and lower (A_{max}) error bars

Figure 3.21 Frequency distribution of mean lengths for: (a) the sample population; (b) exterior; and (c) interior links

Figure 3.22 Geographic variability in L

Figure 3.23 Schematic representation of variations in mean link length (L) with creek density (D_{eq}). Error bars reflect uncertainty in D relating to A_{min} and A_{max} decision rules

Figure 3.24 Scatter plot showing the degree of association between average exterior and interior link lengths

Figure 3.25 Geographic variability in L_{EXT}/L_{INT}

Figure 3.26 Frequency distribution of values obtained for: (a) principal channel sinuosity (S), and partial measures of: (b) network-scale sinuosity (S_N); (c) tortuosity (S_T); and (d) meander asymmetry (S_A)

Figure 3.27 Proportional representation of network- and reach-scale sinuosity terms (primary axis), with ensemble sinuosity organised in decreasing order of magnitude (secondary axis). Threshold values suggested by Leopold *et al.* (1964) are marked, together with supplementary divisions identified during the present analysis

Figure 3.28 Separation of the ensemble signal for each study locality into absolute measures of: (a) tortuous (S_T); (b) asymmetric meandering (S_A); and (c) network-scale sinuosity (S_N). Data are organised in decreasing magnitude of S

Figure 3.29 Schematic representation of sinuous adjustment along the principal channel through network- and reach-scale signals

Figure 3.30 Scatter plots showing statistically significant associations recorded for the sample networks between: (a) D and A (computed using minimum, equidistant and maximum decision rules); (b) F and A; (c) L and A; (d) L_{EXT} and A; (e) L_{INT} and A

Figure 3.31 Scatter plot showing relations between: (a) L_T and A (computed using minimum, equidistant and maximum decision rules); and (b) A_C and A

Figure 3.32 Schematic diagram showing: (a) progressive reduction in D with increasing marsh area due to the influence of master channels; and (b) scale-free behaviour of $\%C$

Figure 4.1 Schematic representation of the methodological procedure employed in the acquisition of longitudinal profile data

Figure 4.2 Mean sampling interval for channel bed elevation data at study localities

Figure 4.3 Longitudinal profiles grouped according to those displaying: *linear* (a1-a5) u*pwardly concave* (b1-b14); and *composite* (c1-c10) patterns of descent.

Figure 4.4 Schematic representation of the method employed for converting survey results to standardised longitudinal profiles for: (a) continuous; and (b) discontinuous patterns of vertical fall. Channel bed elevation is expressed as a function of total vertical fall and distance from the channel head as a % of total distance to the lower measurement boundary

Figure 4.5 Ensemble of standardised longitudinal profiles for: (a) the full sample population; (b) linear responses; (c) upwardly concave reaches; (d) linear reaches coupled with headwater drop-off; and (e) composite responses

Figure 4.6 Schematic characterisation of longitudinal profiles, as a hierarchy of superimposed discontinuities of varying spatial frequency and amplitude

Figure 4.7 Relation of local bed slope to distance from the channel head for the subset of profiles exhibiting: minor irregularities (a1-a17); and high amplitude fluctuations (b1-b12). The location of major tributaries along the principal channel is recorded by substantial changes in link frequency

Figure 4.8 Definition sketch for computing the Index of Concavity for: (a) continuous and (b) discontinuous sample profiles

Figure 4.9 Frequency distribution of values obtained for G_N

Figure 4.10 Geographic variability in G_N.

Figure 4.11 Variability in G_N and $\sum d$ computed from diagrammatic representations of: (a) tidal; and (b) fluvial longitudinal profiles documented in the literature (names of individual networks are recorded in an abbreviated form)

Figure 4.12 Values obtained for the Index of Concavity, ranked in ascending order to reflect the relation between I and profile shape

Figure 4.13 Frequency distribution of the Index of Concavity (I)

Figure 4.14 Scatter plot showing the statistically significant association between G_N and A (computed using the minimum, equidistant and maximum decision rules described in Section 3.2.5)

Figure 5.1 Schematic representation of the methodological procedure used to acquire data for the descriptive and morphometric characterisation of cross-sectional adjustment

Figure 5.2 Frequency histogram showing the mean sampling interval between cross-sections at each study locality

Figure 5.3 Definition diagram showing the cross-sectional facets that may be present in tidal creeks. (-------) represents the envelope of variability observed for each component

Figure 5.4 Classificatory model summarising at-a-station and downstream variations in cross-sectional shape

Figure 5.5 Application of the classificatory model for cross-sectional adjustment to the suite of sample networks. Responses observed in the upper, central and lower sectors are expressed on a three tier scale of increasing constraint in depth relative to width, ranging from 'laterally constrained', to 'balanced' and 'over-widened'

Figure 5.6 (a) Dimensional and (b) standardised plots showing w_b as a function of distance along the course of the principal channel for the population of study localities

Figure 5.7 Study localities displaying: (a) concave; and (b) linear or convex patterns of downstream width adjustment

Figure 5.8 (a) Dimensional and (b) standardised plots showing d_b as a function of distance along the course of the principal channel for the population of study localities

Figure 5.9 Bank elevation expressed as: (a) a function of distance for the population of study sites; and (b) standardised distance for selected localities exhibiting a fall towards the seaward margin

Figure 5.10 (a) Dimensional and (b) standardised plots, showing w/d as a function of distance along the course of the principal channel for the population of study localities

Figure 5.11 Study localities displaying: (a) irregular adjustment in *w/d* along the course of the network; and (b) regular convex, concave and linear patterns of increase in *w/d*

Figure 5.12 Schematic representation of the continuum in *w/d* adjustment for the sample networks. Endmember responses correspond with extreme 'estuarine' and 'laterally constrained' behaviour

Figure 5.13 Average *w/d* for: (a) upper; (b) central; and (c) lower sectors of the principal channel at each study locality

Figure 5.14 Extended classificatory model, summarising at-a-station and downstream variations in cross-sectional shape and *w/d*

Figure 5.15 (a) Dimensional and (b) standardised plots showing A_S as a function of distance along the course of the principal channel, for the population of study localities

Figure 5.16 Envelope of variability in A_S and 'best-fit' second order polynomial function for localities exhibiting a 'regular' response along the course of the principal channel

Figure 5.17 Box and whisker plot showing the sample median and interquartile range of A_S. Localities are ranked in order of decreasing median values

Figure 5.18 Median cross-sectional area computed for: (a) upper; (b) central; and lower sectors of the principal channel at each study locality

Figure 5.19 Departure between the terminal value of cross-sectional area and the median of response (A_{SL}) recorded for stations within the lower 75-100% of the sample networks

Figure 5.20 Scatter plots showing statistically significant levels of scale dependence for: (a) width:depth ratio (w/d_L); and (b) cross-sectional area (A_{SL})

Figure 6.1 Definition diagram for the calculation of hydraulic duty

Figure 6.2 Statistical characteristics of input series for the calculation of hydraulic duty: (a) mean marsh surface elevation ($\overline{E}$); (b) Mean High Water Spring (*MHWS*); and (c) Highest Astronomical Tide (*HAT*)

Figure 6.3 Summary of methodological procedures used to compute *HAT* and *MHWS* for standard and secondary ports (with Tables (T) and Parts (P) from the Hydrographic Office (1997))

Figure 6.4 (a) Maximum hydraulic duty (H_{max}); and (b) spring hydraulic duty (H_{sp})

Figure 6.5 Definition diagram showing input measures involved in the computation of maximum total tidal prism (P_{TM}) from channelised (P_C) and platform (P_P) components, for an idealised tidal network

Figure 6.6 (a) Channelised (P_C) and (b) platform (P_P) components of (c) maximum tidal prism (P_{TM}), with margins of uncertainty about the best estimate expressed by error bars

Figure 6.7 (a) Geographical distribution of channelised prism (P_C) expressed as a percentage of the total maximum tidal prism (P_{TM}); and (b) the frequency distribution of values obtained

Figure 6.8 Schematic representation of conditions influencing the percentage of total maximum tidal prism (P_{TM}) accounted for by the channelised component (P_C)

Figure 6.9 (a) Geographical distribution of sea level change (*SLC*); and (b) the frequency distribution of values obtained

Figure 6.10 Geographical variability in: (a) average; (b) downstream; and (c) at-a-station readings of sediment cohesiveness (*%silt-clay*)

Figure 6.11 Geographical variability in: (a) the difference between channel bed readings of sediment cohesiveness (*%silt-clay*) for sample stations in the headwaters (He) and at the limit of vegetative cover (Mo); and (b) the difference between channel bank (Ba) and bed (Be) readings at the limit of vegetative cover

Figure 6.12 (a) Geographical distribution of spring tidal range (*STR*); and (b) the frequency distribution of responses, organised into classes specified by Davies (1964)

Figure 6.13 (a) Geographical distribution of values recorded for intertidal gradient (G_I) which are grouped into classes of tidal range (Davies, 1964); and (b) the frequency distribution of responses

Figure 6.14 'Box-whisker' plots showing associations between: (a) class of vegetative cover and spring tidal range (*STR*); and (b) type of coastal setting and intertidal gradient (G_I)

Figure 6.15 'Box-whisker' plots showing associations between network planimetry and planimetric measures of: (a) creek density; (b) % channel cover; (c) link-based texture; (d) principal channel sinuosity; (e) network-scale sinuosity; (f) tortuosity; and (e) meander asymmetry

Figure 6.16 Scatter plots showing statistically significant ($\alpha = .05$) associations which are in part attributable to mutual dependence on marsh area cover, between: (a) creek density (D_{eq}) and total prism (P_{TM}); (b) D_{eq} and intertidal gradient (G_I); (c) mean link length ($\overline{L}$) and P_{TM}; (d) network gradient (G_N) and P_{TM}; (e) width:depth ratio (w/d_L) and P_{TM}; (f) cross-sectional area (A_{SL}) and P_{TM}; (g) A_{SL} and channelised prism (P_C); (h) w/d_L and P_C; (i) G_N and P_C; and (j) G_N and G_I

Figure 6.17 Schematic representation of coherence between the maximum theoretical extent of creek development as defined by base level, and the varied position of the seaward limit of vegetative cover recorded at the sample networks

Figure 6.18 (a) Percentage offset between the limit of vegetative cover and maximum horizontal extent of saltmarsh development defined by *MLW*; (b) percentage offset between total elevation change ($\sum H$) along the principal channel and the maximum vertical range defined by *MTR*; and (c) scatter plot showing the relation between horizontal and vertical percentages

Figure 6.19 Scatter plots showing statistically significant ($\alpha = .05$) associations between: (a) creek density (D_{eq}) and percentage silt-clay (*%silt-clay*); (b) D_{eq} and spring tidal range (*STR*); (c) percentage channel cover (*%C*) and *STR*; (d) mean link length ($\overline{L}$) and *STR* (e) profile concavity (*I*) and intertidal gradient (G_I); (f) *I* and He-Mo *%silt-clay*; (g) network gradient (G_N) and He-Mo *%silt-clay*; (h) G_N and *%silt-clay*; (i) G_N and maximum hydraulic duty (H_{max}); (j) width:depth ratio (w/d_L) and *STR*.

Figure 6.20 'Box-whisker' plots showing associations between: (a) network planimetry and *STR*; (b) coastal setting and *I*; (c) vegetative cover and D_{eq}; (d) vegetative cover and *L*; (e) vegetative cover and *%C*; and (f) vegetative cover and w/d_L.

Figure 7.1 Definition diagram showing major (θ_1) and minor (θ_2) branching angles, the junction angle (ψ) and costs (c) for the tributaries and receiving channel (c_0)

Figure 7.2 Schematic representation of stages involved in the simplification of cost criteria using hydraulic geometry relations

Figure 7.3 Graphical representation of theoretical responses predicted by optimum models of branching geometry for: (a) major branching angle (θ_1); (b) minor branching angle (θ_2) and (c) junction angle (ψ), with varying values of exponent **k** and symmetry ratio α

Figure 7.4 Schematic representation of changes in branching angle accompanying downstream increases in slope and/or velocity (exponent **k**) and discharge asymmetry (α)

Figure 7.5 Schematic representation of the methodological procedure employed in: (a) measuring 'local' branching angles θ_1 and θ_2; and (b) computing symmetry ratios α_N, α_A and α_P, for evaluation of the optimal model of angular geometry

Figure 7.6 Definition diagram showing node (N) and local (L) junction angle measures

Figure 7.7 Linearised representation of the Brancaster network, highlighting the subset of 60 junctions used to evaluate the performance of the model of optimal angular geometry

Figure 7.8 Schematic representation of the procedure involved in computing maximum tidal prism (P_M) for a selected cross-section

Figure 7.9 Frequency distribution of: (a) α_P; and (b) α_N, for the sample of 60 junctions employed in evaluating the model of optimal angular geometry

Figure 7.10 Graphical representation of the minimum network-wide offset between observed and expected angles at Brancaster Marsh, for: (a) θ_1; (b) θ_2 and (c) ψ

Figure 7.11 Predicted angles for: (a) θ_1; (b) θ_2 and (c) ψ, corresponding with 'best' values of **k** obtained using the model of optimal angular geometry. Results recorded for fluvial networks by Roy (1985)* are included for comparison

Figure 7.12 Combined hydraulic geometry exponent (b+f) for downstream changes in channel cross-sectional area (A_{SP}) with peak discharge (Q_P), showing: (a) discontinuity in adjustment along the course of the Brancaster network; and (b) separate power functions fitted to the headward reaches and central/lower sectors

Figure 7.13 Schematic representation of the methodological procedure employed in obtaining predicted and observed measures of peak ebb tidal discharge, for the evaluation of stability shear stress as a principle governing equilibrium cross-sectional geometry

Figure 7.14 Sequence of diagrams showing the progressive inundation of the Brancaster system as tidal stage rises from 2.3 m OD to a maximum of 2.6 m OD

Figure 7.15 Schematic representation of the instrument array employed in the acquisition of stage and velocity data for a section in the lower reaches of the Brancaster network

Figure 7.16 Stage-time curves for a sequence of tides at the Brancaster network. Over-marsh tides on 25-26th October 2000 clearly exceed bankfull elevation

Figure 7.17 Area-stage plot showing an abrupt transition in the area contributing flow to a cross-section towards the mouth of the Brancaster network

Figure 7.18 Velocity-stage curves for the sequence of tides at the instrumental set-up station towards the mouth of the Brancaster network

Figure 7.19 Stage-discharge plots computed using the hypsometric model and through field validation, for the instrument set-up station towards the mouth of the Brancaster network

Figure 7.20 Comparison of cross-sectional profiles for the instrument set-up station acquired by field surveying and from the lidar coverage

Figure 7.21 (a) Observations of the cross-sectional parameter $A_{SP}R_P^{1/6}$ as a function of Q_P and τ_C for 60 sample stations throughout the Brancaster network; and (b) observations of the cross-sectional parameter $A_{SP}R_P^{1/6}$ as a function of Q_P, and τ_C, taking into account a potential error margin of up to 37% in Q_P. The theoretical line (__) is given by Equation 7.26, with the error margins (_ _) reflecting cumulative uncertainty for the input series

Figure 8.1 Conceptual model showing design guidelines for saltmarsh channel networks involving the minimum power loss model of angular geometry and stability shear stress as the physical principle governing cross-sectional capacity

Figure 8.2 Performance of the stability shear stress model for the extensive sample of channel networks, with Q_P driven by: (a) *MHWS* and (b) *HAT*

Figure 8.3 Schematic representation of: (a) the frequency-stage plot enabling marsh surface elevation to be established for an inundation frequency of 450-500 annual events; and (b) the arrangement of contributing areas, principal (S_P) and subsidiary (S_S) creeks, and sample stations in a hypothetical restoration project of similar size to Tollesbury and Abbotts Hall schemes

Figure 8.4 Graphical representation of: (a) creek width (w); and (b) width:depth ratio (w/d), expressed as a function of tidal prism for various scenarios of channel depth (d)

Figure 8.5 Schematic representation of: (a) planimetric characteristics; and (b) downstream changes in channel width and depth, resulting from the application of design guidelines to a hypothetical restoration project. Shaded areas in (b) represent the envelope of natural variability

Figure 8.6 Comparison between the morphological characteristics of channel networks observed in saltmarsh restoration schemes at Abbots Hall and Tollesbury in the Blackwater Estuary and results obtained for 29 networks from throughout England and Wales

LIST OF TABLES

Table 2.1 Extensive and intensive research methodologies adapted to the study of saltmarsh channel networks morphology and function (adapted from Sayer, 1992)

Table 3.1 Categories and visually distinguishing characteristics of saltmarsh channel network planimetry

Table 3.2 Occurrence of space filling saltmarsh channel formations and unconfined networks that may be sub-extended and/or underdeveloped

Table 3.3 Statistical characteristics for area-based measures of: creek density *D* (for the population as a whole and divided according to scale dependence into small, intermediate and large formations); percentage channel cover *%C*; link-based texture *F*; link lengths *L*; and principal channel sinuosity *S*

Table 3.4 Categories of balanced and imbalanced link lengths, with study localities arranged according to mean channel spacing

Table 3.5 Correlation matrix showing statistically significant (α = .05) levels of association between appropriately transformed measures of marsh area and planimetric descriptors

Table 3.6 Breakdown of creek density (*D*) into constituent elements of marsh area (*A*) and total channel length (L_T), showing the theoretical length of channel required for 'intermediate' and 'large' networks to achieve the same density as the 'small' system

Table 4.1 Offset recorded between the maximum magnitude of vertical fall and channel bed elevation at the limit of vegetative cover. Adjusted fall was computed by regression analysis

Table 4.2 Height of stepped channel head and vertical drop-off between zero datum and channel bed elevation at the loci of re-curvature, for channel reaches encountering various forms of topographic obstruction at the rear of the marsh

Table 4.3 Statistical characteristics for morphometric measures of: network gradient G_N; and the Index of concavity *I*

Table 4.4 Correlation matrix showing **statistically significant** (α = .05) levels of association between appropriately transformed measures of marsh area coverage and morphometric descriptors.

Table 5.1 Statistical characteristics for cross-sectional measures of: average width:depth ratio ($w{:}d_L$); and median cross-sectional area (A_{CL}) recorded in the lower sector of the principal channel at each study locality

Table 5.2 Correlation matrix showing **statistically significant** (α = .05) levels of association between appropriately transformed measures of marsh area coverage and morphometric descriptors

Table 6.1 Statistical characteristics for variables describing potential environmental controls on channel network morphology

Table 6.2 Details of revised local reference (RLR) records used to compute sea level change for each study site

Table 6.3 Classification scheme used to establish the dominant vegetative community at each site, based on previous studies by *Adam (1981) and **Burd (1989)

Table 6.4 Classification expressing the degree of random versus structural control exerted over network morphology by coastal setting

Table 6.5 Correlation matrix showing **statistically significant** (α = .05) levels of multicollinearity between appropriately transformed variables describing potential controlling elements

Table 6.6 Correlation matrix showing **statistically significant** (α = .05) levels of association between appropriately transformed morphometric descriptors

Table 6.7 Correlation matrix showing **statistically significant** (α = .05) levels of association between appropriately transformed environmental control and morphometric response variables (Spearman's rank correlation coefficients are distinguished by *). Partial correlation coefficients are also recorded for significant zero order associations

Table 6.8 Summary of regression analysis for the morphometric descriptors, using the full set of transformed 'independent' controls (r_t) and the subset comprising measures that were pre-selected on the basis of statistically significant (α = .05) bivariate correlations (r_m). The multiple coefficient of determination (R^2) is recorded for each equation, together with partial regression coefficients (b) and beta weights (B) for every variable

Table 7.1 Statistics for the mean and (standard deviation) of angular characteristics at the subset of 60 junctions satisfying selection criteria for θ_1, θ_2, ψ and α. Values recorded in a range of fluvial networks by Roy (1985)* are included for comparison

Table 7.2 Spearman's rank correlation coefficients for symmetry ratios (α) based on link frequency (N), contributing area (A) and maximum tidal prism (P)

Table 7.3 Responses obtained using the model of optimal angular geometry for the 'best' value of **k**, mean angular residual and percentage of angular variance explained. Results recorded by Roy (1985)* for a selection of fluvial networks are included for comparison

Table 7.4 Hydraulic exponents computed using a range of independent variables for the selected network at Brancaster Marsh. Results recorded elsewhere in the literature for tidal networks are included for comparison

Table 7.5 Summary of the input parameters and values used to evaluate the performance of stability shear stress (τ_S) as a principle governing the cross-sectional geometry of Brancaster network

Table 8.1 Correlation matrix showing statistically significant (α = .05) levels of association for the offset between observed and predicted values of $A_S R^{1/6}$ (that were computed for *MHWS* and *HAT* conditions), and external environmental controls

LIST OF PLATES

Plate 2.1 (a) 1:5000 scale panchromatic aerial photograph (courtesy of the Environment Agency) showing Hut marsh on Scolt Head Island, Norfolk; and (b) the same area depicted on a 1:10 000 scale map (courtesy of Ordnance Survey)

Plate 2.2 Photo mosaic for Brancaster Marsh depicting: (a) mid-marsh communities dominating vegetative cover on the marsh platform; (b) concentration of *Attriplex portulacoides* along creek margins; (c) bank retreat through mass failure reflecting the binding action of halophytic species; (d) prominence of pioneer species as marsh surface elevation diminishes towards Mow Creek

Plate 3.1 Aerial photographic coverage depicting the network selected at each study locality (courtesy of Environment Agency, NERC and Cambridge University)

Plate 3.2 Localised variability in the reflectance characteristics of creek bed and banks, at Stiffkey marshes, Norfolk

Plate 4.1 Contrasting morphological characteristics displayed by: (a) a 'dead-end' channel reach, Isle of Walney; and (b) 'through-flowing' headwaters, Hamford Water

Plate 4.2 Headwater adjustment occurring as: (a) *stepped* descent, Scolt Head Island; and (b) *gradual* descent, River Loughor

Plate 4.3 Headwaters devolving through: (a) 'bridging over', Holbeach, The Wash; and (b) 'grassing in', River Leven

Plate 4.4 Discontinuities in longitudinal adjustment: (a) small-scale bedforms, Brancaster marshes; (b) livestock crossing point, Duddon Estuary; (c) thalweg obstruction, Lymington; (d) local obstruction by bank fall debris, River Ribble; (e) through-flowing reaches arising from channel capture, River Orwell; (f) collecting pool caused by migration of a sand bank across the channel mouth, Maplin Sands; (g) shell ridge blocking channel outflow, River Crouch; and (h) channel bed depression around a major junction, River Dovey

Plate 5.1 Bank/wall facet of cross-sectional profiles displaying: (a) die back, Keyhaven, The Solent; (b) overhanging vegetation, Holbeach, The Wash; (c) vertical wall, Stiffkey; (d) minor undercut, River Dovey; and (e) substantial undercut, River Crouch

Plate 5.2 Toe facet of cross-sectional profiles displaying: (a) smoothly concave descent, The Middleway, River Roach; (b) prominent active bench, The Swale; (c) algal colonisation, River Beaulieu; (d) pioneer colonisation, Butterwick, The Wash; (e) densely vegetated inactive bench, River Leven

Plate 5.3 Floor facet of cross-sectional profiles displaying: (a) abrupt transition between a sandy floor segment and silty toe facet, Scolt Head Island; (b) algal colonisation, River Carew; (c) confined lateral development, Maplin Sands; (d) extensive lateral development, River Ribble; (e) freely meandering thalweg feature, Isle of Walney; (f) minor thalweg development, Brancaster marshes; and (g) deeply incised thalweg, Lymington marshes

Plate 5.4 Relic step facet of cross-sectional profiles displaying: (a) lateral offset and contrasting halophytic colonisation between upper and lower margins, Holbeach, The Wash; and (b) abandoned channel wall transcending a vertical offset of ~0.4 m between upper and lower banks, Duddon Estuary

Plate 5.5 Headwater cross-sectional profiles characterised by: (a) an over-widened floor facet, River Loughor; and (b) constrained lateral adjustment, River Carew

Plate 5.6 Cross-sectional profiles in the upper reaches, displaying: (a) symmetrical triangular adjustment, The Ribble; (b) an extended floor facet, Pagham Harbour; (c) asymmetrical toe protrusion with offset floor, Maplin Sands; and (d) persistence of relic steps, River Leven

Plate 5.7 Cross-sectional adjustment in the central reaches, displaying: (a) sustained toe concavity, Devil's Reach, River Roach; (b) confined floor and thalweg feature, Severn Estuary; and (c) shortened toe facet and offset floor on the outside apex of a bend, Lymington marshes

Plate 5.8 Cross-sectional adjustment in the lower reaches, displaying: (a) dominant thalweg with adjacent incised flow lines, River Colne; (b) amplified bank convexity arising from the diminished influence of root binding, Butterwick, The Wash; and (c) toe facet degraded by erosive action, River Blackwater

Plate 6.1 Horizontal zonation observed between: (a) mid-marsh species at the landward boundary; and (b) pioneer species at the seaward limit of vegetative colonisation, Butterwick, The Wash

Plate 6.2 Classes of vegetative composition dominated by: (a) *Atriplex portulacoides*, Saltfleet marshes; and (b) *Limonium vulgare* and *Puccinellia maritima*, River Colne; (c) *Spartina spp.*, River Carew; (d) *Elytrigia spp.*, Holbeach, The Wash; and (e) *Festuca rubra* and *Armeria maritima*, Duddon Estuary

Plate 6.3 Channel development extending from the limit of vegetative cover to *MLW*, showing: (a) non-vegetated yet channelised reaches, Isle of Walney; (b) mudmounds, Severn Estuary; and (c) incised thalweg, River Orwell

Plate 6.4 Convex descent to base-level across: (a) a narrow non-vegetated margin at the River Roach; and (b) mudflats bordering the main channel of the Severn Estuary

Plate 7.1 Junctions in the Brancaster network showing: (a) an asymmetrical example from the central reaches where a minor branch adjoins a considerably larger major channel; and (b) a rare example of near-symmetrical branching in the lower reaches

Plate 8.1 High resolution aerial photography showing saltmarsh restoration projects at: (a) Tollesbury; and (b) Abbotts Hall, in the Blackwater Estuary, Essex

Plate 8.2 Development of secondary flow lines in relation to artificial 'creeks' comprising drainage lines on former reclaimed land, which has subsequently been restored to saltmarsh at: (a) Hamford Water, Essex; and (b) Pagham Harbour, Sussex

LIST OF SYMBOLS

A	Marsh area
A_C	Area occupied by tidal creeks
A_E	Area contributing flow to a particular cross-section at a given tidal stage
A_{eq}	Marsh area corresponding with an equidistant area decision rule
A_{min}	Marsh area corresponding with a minimum area decision rule
A_{max}	Marsh area corresponding with a maximum area decision rule
A_S	Cross-sectional area
A_{SL}	Mean cross-sectional area for the lower sector of the principal channel
A_{SP}	Cross-sectional area corresponding with peak discharge
b	Width exponent for hydraulic geometry equation
Ba-Be %silt clay	Difference between the *% silt clay* content of sediments on the bank and bed of the principal channel
c	Cost-function employed in the calculation of optimal branching angles
%C	Percentage channel cover
d	Distance from the channel head measured by field survey
$\sum d$	Cumulative downstream length measured by field survey
d_b	Bankfull depth
$\bar{d}_b$	Mean channel depth
D	Creek density
D_{eq}	Creek density corresponding with an equidistant area decision rule
E	Predicted optimal angular characteristics in a tidal channel network
$\bar{E}$	Mean marsh surface elevation
E_o	Elevation corresponding with base level
f	Depth exponent for hydraulic geometry equation
F	Link-based texture or frequency
g	Gravitational constant
G_I	Intertidal gradient
G_N	Network gradient
H	Bed elevation with respect to zero datum at channel head
$\sum H$	Total vertical fall with respect to zero datum at channel head
ΔH_{50}	Height difference between bed elevation at mid-distance and a straight line joining the start and end nodes of a longitudinal profile

H_{max}	Maximum hydraulic duty corresponding with the highest astronomical tidal level
H_{sp}	Spring hydraulic duty corresponding with the mean high water spring tidal level
HAT	Level of highest astronomical tide predicted from Admiralty tide tables
He-Mo %silt clay	Difference between the *% silt clay* content of sediments at the head and mouth of the principal channel
I	Langbein's Index of Concavity
k	Hydraulic geometry exponent in cost model of optimal angular geometry
L	Local junction angle measure
L	Mean link length
L_{EXT}	Exterior mean link length
L_{INT}	Interior mean link length
L_I	Width of intertidal zone
L_H	Total pathlength of half meanders along the principal channel
L_L	Linear length of the principal channel
L_S	Sinuous length of the principal channel
L_T	Total sinuous channel length
L_W	Total pathlength of whole meanders along the principal channel
m	Velocity exponent for hydraulic geometry equation
MHWS	Level of mean high water spring predicted from Admiralty tide tables
MLWS	Level of mean low water spring predicted from Admiralty tide tables
MTR	Mean tidal range predicted from Admiralty tide tables
n	Manning's friction coefficient
N	Node junction angle measure
N_L	Frequency of constituent links
N_{EXT}	Frequency of exterior links
N_{INT}	Frequency of interior links
O	Observed angular characteristics in a tidal channel network
P_C	Channelised component of tidal prism
P_M	Maximum tidal prism computed from lidar terrain data
P_P	Platform component of tidal prism
P_S	Spring tidal prism computed from lidar terrain data
P_{TM}	Maximum total tidal prism
Q	Dominant discharge
Q_E	Discharge at a given tidal stage

Q_P	Peak discharge
R	Hydraulic radius
R_P	Hydraulic radius corresponding with the stage of peak tidal discharge
s	Energy gradient
S	Principal channel sinuosity
S_A	Reach-scale channel asymmetry
S_N	Network-scale sinuosity
S_P	Sample station along the principal creek within a tidal network
S_S	Sample station along a subsidiary creek within a tidal network
S_T	Reach-scale tortuosity
SLC	Relative sea level change
STR	Spring tidal range
U_{cr}	Critical entrainment velocity
v	Velocity of tidal flow
v_C	Critical velocity at which material is entrained from the creek margin
v_P	Peak velocity of channelised tidal flow
w_b	Bankfull width
$w{:}d$	Ratio of bankfull width to depth
$w{:}d_L$	Mean ratio of bankfull width to depth for the lower sector of the principal channel
W	Wetted perimeter
$\mathbf{z}$	Slope exponent for hydraulic geometry equation
α	Symmetry ratio in optimality model
β	Branching angle measured directly from photographic coverage
θ_1	Major branching angle at a tidal confluence
θ_2	Minor branching angle at a tidal confluence
ρ	Fluid density
ψ	Junction angle at a tidal confluence
τ_{bk}	Critical shear stress at the channel bank
τ_C	Critical shear stress at which material is entrained from the creek margin
τ_P	Peak shear stress along the creek margin
τ_S	Stability shear stress of the creek margin
% silt clay	*% silt clay* content of sediments sampled within the principal channel

ACKNOWLEDGEMENTS

I would like to acknowledge the invaluable assistance of a number of people during the course of my research training in the Department of Geography at University College London. First, the intellectual guidance and words of wisdom offered by Dr. Jon French have left a lasting imprint on myself, and my approach towards academic research. Encouragement and advice from Dr. Nick Clifford and Dr. Tom Spencer are also much appreciated. Second, the financial assistance provided by the NERC (studentship number GT/4/96/185/MAS) is acknowledged, together with support from the Environment Agency (Anglian Region), who were the partners in this Case Award. From the EA, I would particularly like to thank Mark Dixon and Jane Rawson for their input, and Peter Fitzpatrick and Becky Allen for supplying such fantastic aerial photography and lidar data. Third, I would like to thank Lewis and Mat Disney for assistance in the RSU, and Ian Usher, Chris Knell and Lan Wang for computer support. A final word of thanks is due to Anne 'The Maps', Chris Chromarty, Janet Hope and the lab team, Cath Pyke and the members of the Drawing Office, and Dr. Jacquie Burgess, for helping in moments of need.

The epic fieldwork campaign of 1999 simply could not have taken place without the tireless efforts of Al, Chris, Alison, Emma, Sophie and Ben. Immense thanks are also due to Helen Gavin and Katie Prebble, who on numerous occasions were prepared to go beyond the call of duty. I would like to thank the organisations and individuals who kindly allowed access to the study sites, and in particular acknowledge Eddie Wiseman at the Hampshire Wildlife Trust and Michael Roony from English Nature for logistical assistance.

Immeasurable thanks are due to my parents - Rita and Gordon Adams, my grandmother – Blanche Trump, and the rest of my family, for their unfailing interest and support throughout my education. The encouragement and advice of Andree and Dr. Derek Lee has also been a guiding light. I am tremendously grateful to Sharon, Rick and Elliot West for their acceptance, enthusiasm, and help with my work.

For me, the most important message of thanks goes to my partner Adam West, who truly is a kindred spirit. You have helped me to find the way, overcome seemingly insurmountable obstacles, and made the impossible my reality. How can I possibly begin to thank you?

1. INTRODUCTION

1.1 THE NATURE OF SALTMARSH ENVIRONMENTS

Coastal saltmarshes may be defined as depositional environments, which develop through the successional colonisation by halophytic vegetation, of fine-grained sediments accumulated within the inter-tidal zone of low-energy, temperate shorelines. On the basis of these characteristics, *coastal saltmarshes* are distinguished from mangals, which are widely regarded as their tropical counterpart (Steers, 1959, 1977; Thom, 1967; Chapman, 1977) and other halophytic communities that colonise above the limit of tidal influence (Dijkema, 1987; Burd, 1989) and in land bound salt deserts (Chapman, 1974). Although these latter communities share some of the biological and sedimentary characteristics of saltmarshes, they are fundamentally different in many respects and as such fall beyond the scope of this thesis. Inter-tidal mud and sand flats are often found in close proximity to saltmarshes. Distinguished by the absence or the limited development of vegetative cover, tidal flats have generally been studied as discrete depositional environments (Klein, 1985; Amos, 1995).

1.1.1 Controls on distribution

The global distribution and geomorphic characteristics of saltmarshes can be explained as the manifestation of an envelope of physical environmental controls (Redfield, 1965; Frey and Bassan, 1985; Allen and Pye, 1992) comprising: (1) sediment supply; (2) wind/wave climate; (3) tidal hydrodynamics; (4) indigenous halophytic vegetation; and (5) environmental change.

As a depositional environment, the development of stable saltmarshes very much depends on an adequate *supply of sediment*. This may be in the form of imported allochthonous deposits (Pestrong, 1970, 1972; French and Spencer, 1993), or produced in situ as autochthonous peats (Reimold, 1977). Early work by Richards (1934) identified a direct relationship between availability of appropriate coastal sedimentary material and the upward growth of the marsh surface, whereby an inadequate 'reservoir' (Dalby, 1970, p.300) precludes saltmarsh development. Allen and Duffy (1998b) also observed that the abundance and composition of sediment available around the coastline affects rates of deposition and marsh growth, whereby marsh evolution rapidly proceeds if sediments are

readily available and easily deposited. Further advances have been made in understanding the location and rate of marsh development by Gleason *et al.* (1979), Pethick *et al.* (1990) and Leonard *et al.* (1995), through studies concerning the manner in which species of marsh surface vegetation enhance rates of sediment entrainment. The presence of benthic microbes and marsh dwelling animals has also been shown to be important in stabilising entrained marsh substrates (see Van Straaten and Kuenen, 1957; Ranwell, 1972; Daiber, 1977; Frey and Bassan, 1985; also Underwood and Peterson, 1993).

Intensity of the *wind-wave climate* limits the grain-size of sediments transported within the inter-tidal zone. Pethick (1992) thus inferred that saltmarshes are the low-energy equivalent of beaches, being predominantly composed of sand, mud and clay rather than shingle or cobbles. Chapman (1974) and Steers (1977) noted that spits, bars and barrier islands afford protection from direct wave attack, which together with estuaries (Yapp *et al.*, 1917), embayments and coasts fronted by offshore sand banks (Reed *et al.,* 1985; Pye, 1992) are calm settings, favourable for saltmarsh development. Erosion of fronting tidal flats (Allen and Duffy, 1998a), the marsh surface and its seaward edge (Pethick, 1992) are reported as natural responses to intensified wave activity during stormy conditions. However, Pethick (1992) also notes their ability to recover given a sufficient return interval between high intensity events.

Tidal hydrodynamics are the driving force behind sediment entrainment and transportation within the inter-tidal zone (Steers, 1977). As such, they strongly influence temporal and spatial patterns of deposition, and thereby saltmarsh development (Evans and Collins, 1987; Allen and Duffy, 1998b). A number of feedback mechanisms have been identified which serve to mediate the interaction between patterns of tidal inundation and the growth of coastal saltmarshes (Ranwell, 1972; Burd, 1989). As illustrated by the surface profile in Figure 1.1, pioneer saltmarsh vegetation begins to colonise once an inter-tidal surface accretes to a level at which it emerges for a period of time during low water. The emergence threshold supporting halophytic colonisation is thought to occur just below Mean High Water Neap (*MHWN*) (Chapman, 1977). The maximum elevation to which the marsh surface can rise before becoming fully terrestrialised, corresponds with the upper limit of tidal inundation defined by Highest Astronomical Tide (*HAT*) (see Allen, 1997). The difference between *MHWN* and *HAT* therefore determines the vertical range available for saltmarsh development, which is in turn a function of tidal range. In the words of Davies (1964, p.137) the degree of variation in water level '*determines the altitudinal limits within which saltmarsh can be built*'. Since tidal range varies

considerably between different parts of the world, and especially around the coast of Britain, there is considerable spatial variability in the vertical range supporting saltmarsh formation.

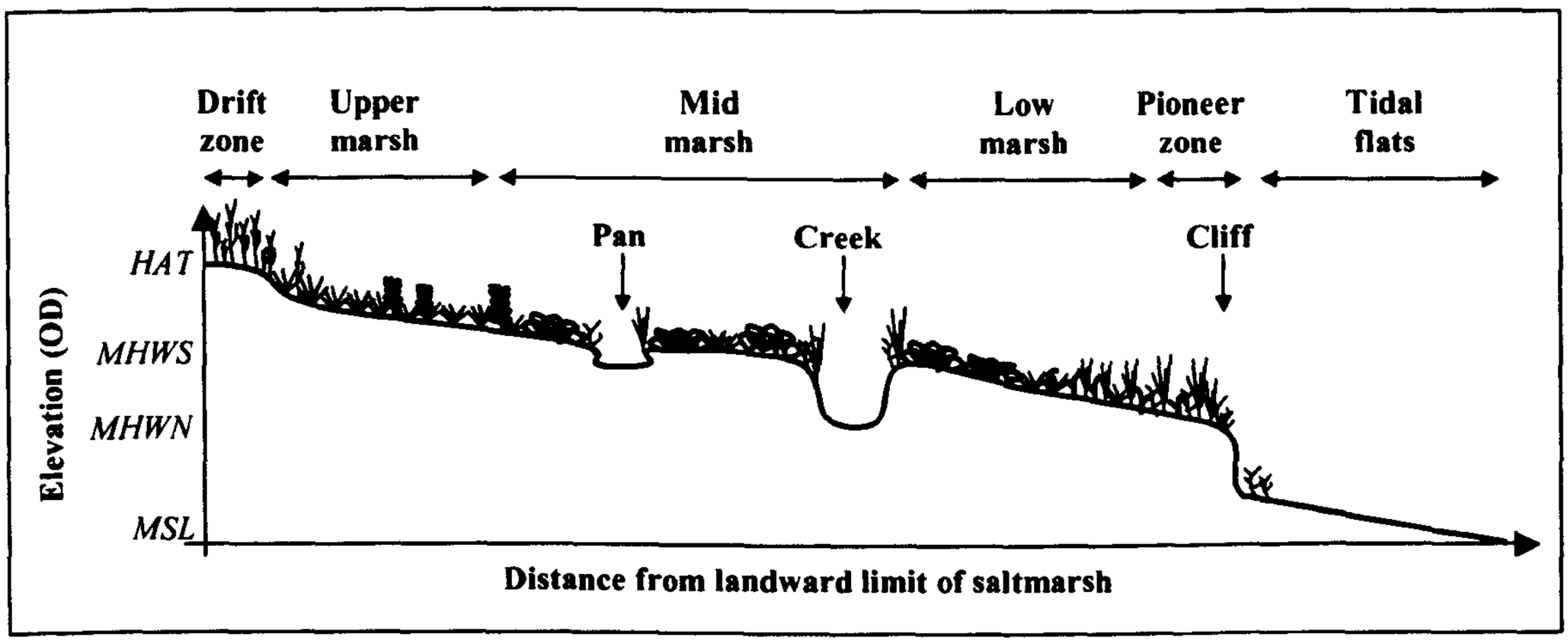

Figure 1.1 Vertical range of coastal saltmarsh and inter-tidal flats (adapted from Klein, 1985; and Burd, 1989).

Tidal range also affects the horizontal extent of marsh development. On the basis that over time the surface of a coastal marsh evolves towards a fairly constant gradient (Beeftink, 1965, 1977a; French, 1989, 1993; French and Reed, 2001), it follows that sites with a large range can *potentially* support a wide swath of saltmarsh, while a smaller range limits the lateral extent of marsh growth (Figure 1.2a). However, the *actual* width of marsh that develops is often limited by a combination of natural and artificial controls. As shown in Figure 1.2b, human intervention in the guise of sea wall construction (see for example Kestner, 1979; Pye, 1995) may constrain the landward extent of marsh growth, while periodic migration of the main tidal channel (Chapman, 1974; Gray, 1972; Pringle, 1995) imposes a natural limit on seaward development. Coastal saltmarshes may therefore be divided into categories of *constrained* or *unconstrained* system.

Climatic limits exert a fundamental level of influence over the composition of inter-tidal vegetation (Ranwell, 1972; Chapman, 1977; Steers, 1977; Adam, 1978, 1981). Salt tolerant or halophytic species support different levels of sediment entrainment, which has important implications for the rate of marsh growth. Superimposed on these geographically extensive trends, Ranwell (1972) expressed the biological and morphological zonation of saltmarsh vegetation in terms of localised physical environmental controls. Segregation of the salt marsh ecosystem into sub-habitats (Figure 1.1) reflects the ability of species to accommodate variability in factors including:

sediment type; duration and depth of tidal inundation; and soil drainage (Zedler *et al.*, 1999; Sanderson *et al.*, 2000). The classification of saltmarsh ecosystems in this way has been widely implemented to monitor the rate of growth and patterns of change in saltmarsh habitats (see for example Reimold, 1977; Clarke *et al.*, 1993).

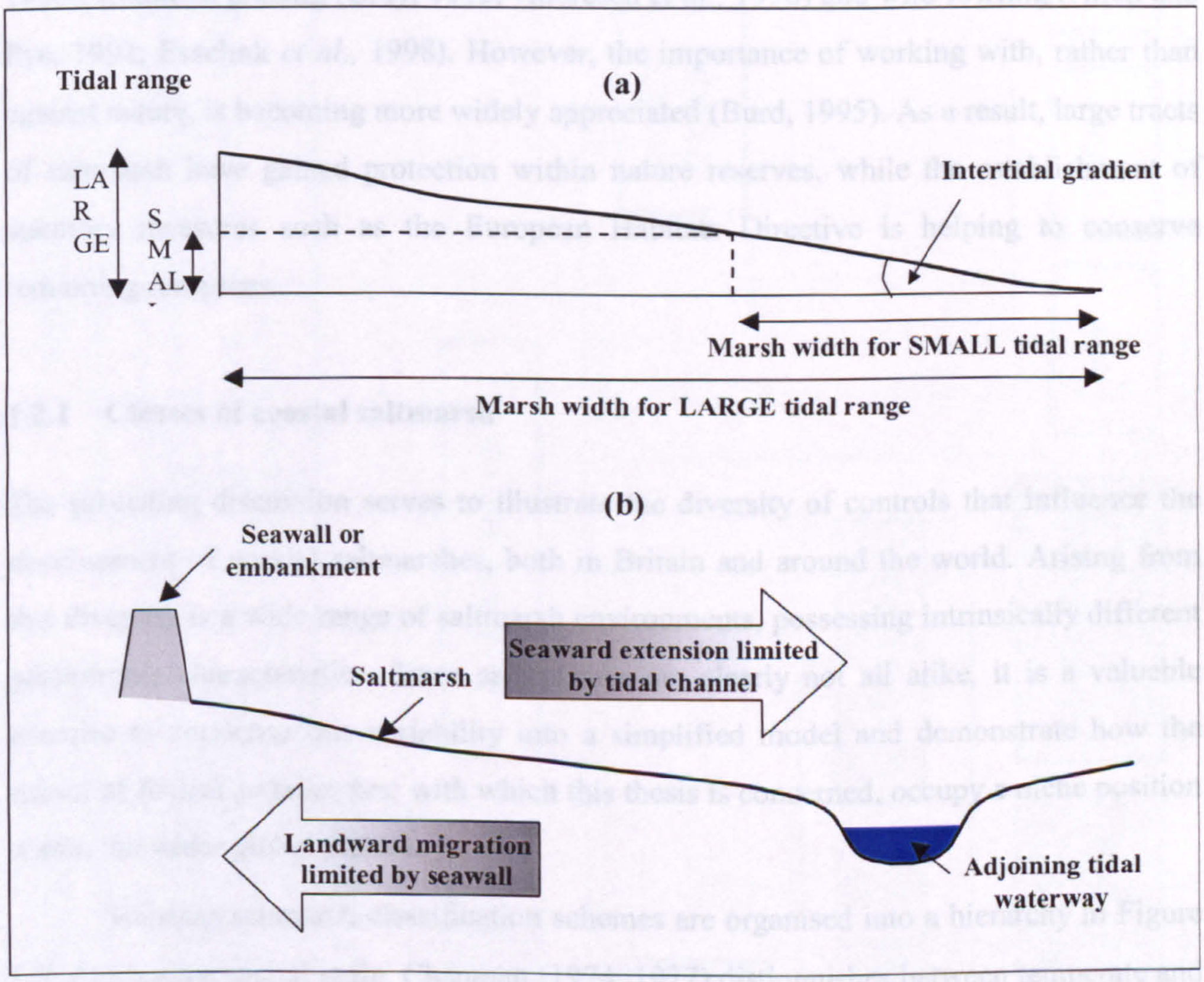

Figure 1.2 (a) Relation between tidal range and the lateral extent of saltmarsh development in an unconstrained system; and (b) landward and seaward limits imposed on marsh extent.

In the words of Frey and Bassan (1985, p.225) saltmarshes are *'to some extent a measure of coastal stability and equilibrium'*. This observation points to the ability of depositional saltmarsh environments to accommodate environmental change. Indeed, the development of saltmarshes was originally interpreted by (Redfield, 1972, p.37) as *'the interaction of the accumulation of sediment and a rising sea level'*. Comments have been made concerning the dynamic adjustment of saltmarshes to sea-level perturbation (Redfield, 1965; Steers, 1977; Wolaver *et al.*, 1988; Patrick and DeLaune, 1990; Allen, 1992; Pye, 1992; Reed, 1995; French, *et al.*, 1995; French and Spencer, 2001). In most

instances, sea-level rise is perceived to be a driving force behind marsh accretion (Pethick, 1980; Reed, 1990), inasmuch that stable marshes develop at a pace commensurate with long-term changes in relative sea level (Pye, 1992; Cahoon *et al.,* 1996).

Environmental change, in the guise of human intervention, has also shaped the distribution of saltmarshes through activities such as reclamation (Kestner, 1979; Pye, 1995), livestock grazing (Gray, 1972; Andresen *et al.,* 1990) and wild fowling (Allen and Pye, 1992; Esselink *et al.,* 1998). However, the importance of working with, rather than against nature, is becoming more widely appreciated (Burd, 1995). As a result, large tracts of saltmarsh have gained protection within nature reserves, while the establishment of statutory measures such as the European Habitats Directive is helping to conserve remaining resources.

1.2.1 Classes of coastal saltmarsh

The preceding discussion serves to illustrate the diversity of controls that influence the development of coastal saltmarshes, both in Britain and around the world. Arising from this diversity is a wide range of saltmarsh environments, possessing intrinsically different geomorphic characteristics. Since saltmarshes are clearly not all alike, it is a valuable exercise to condense this variability into a simplified model and demonstrate how the subset of *British saltmarshes,* with which this thesis is concerned, occupy a niche position within the wider global picture.

Existing saltmarsh classification schemes are organised into a hierarchy in Figure 1.3. At a macro spatial scale, Chapman (1974, 1977) distinguishes between temperate and tropical climatic zones, which support the development of saltmarshes and mangals respectively. For the subset experiencing temperate climatic conditions, Chapman goes on to identify major regional saltmarsh floras. British marshes fall within the North European set. Dijkema (1987) recognises further sub-European classes, based on the biosedimentary origin of substrates. In this instance, British marshes generally occur on allochthonous substrates. A useful distinction is also made between geological settings, with marshes throughout England and Wales occurring on marine, sedimentary shores and Scottish marshes forming on predominantly rocky shores. The difference between these environments is significant, since sediment supplies are comparatively scarce on rocky coasts, a factor limiting the rate of marsh growth compared with sedimentary shores. According to Ranwell (1972), sedimentary shores are also more *maritime* (i.e. dominated

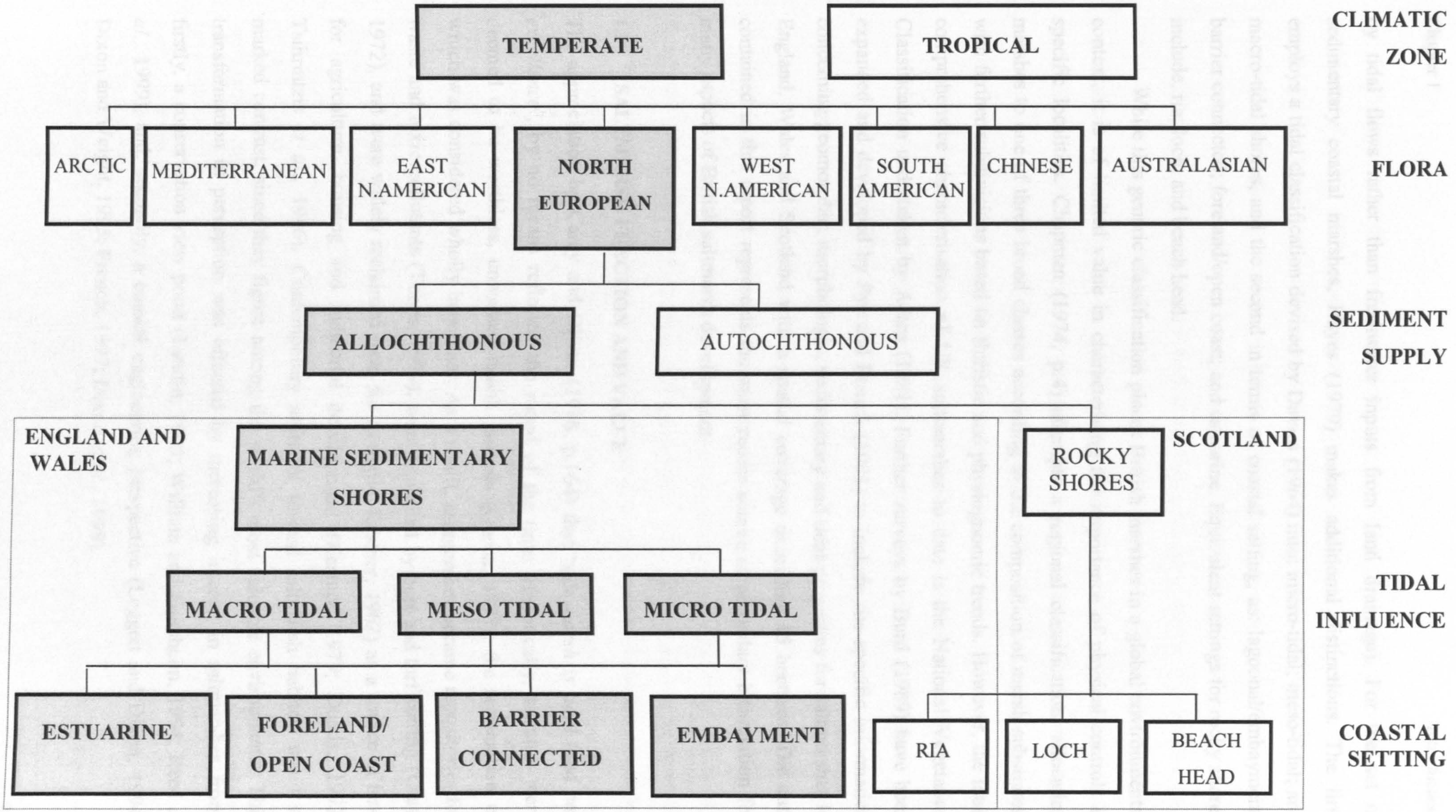

Figure 1.3 Classification of British saltmarshes.

by tidal flows rather than freshwater inputs from land drainage). For the set of sedimentary coastal marshes, Hayes (1979) makes additional distinctions. The first employs a tidal classification devised by Davies (1964) into: micro-tidal; meso-tidal; and macro-tidal shores, and the second in terms of coastal setting, as: lagoonal/embayment; barrier connected; foreland/open coast; and estuarine. Equivalent settings for rocky shores include: ria; loch; and beach head.

While this generic classification places British marshes in a global environmental context, it is of limited value in characterising the importance of physical controls at specific localities. Chapman (1974, p.4) attempts a regional classification, allocating marshes to one of three broad classes according to the composition of marsh substrates, with further subdivisions based on floristic and physiognomic trends. However, the most comprehensive characterisation of UK saltmarshes to date is the National Vegetation Classification undertaken by Adam (1981). Further surveys by Burd (1989) have been expanded and developed by Pye and French (1993) to include site-specific information concerning geomorphic, morphologic, sedimentary and tidal properties for saltmarshes in England, Wales and Scotland with a spatial coverage exceeding 15 hectares. The data contained in this report represents the most recent source of secondary information for many aspects of British saltmarsh development.

1.2 SALTMARSH FUNCTION AND VALUE

The appreciation by Carey and Oliver (1918, p.164) that '*salt marsh is tidal land par excellence*', by no means reflected the mood of the time. Historically, marshes were deemed to be worthless, unwanted health hazards (Queen, 1977), the reclamation of which was considered wholly beneficial. As a result, saltmarshes became repositories for waste and toxic pollutants (Tubbs, 1999), were exploited by peat and turf cutting (Gray, 1972), and were widely reclaimed (see, for example, Kestner, 1962) as a source of land for agriculture, housing and industrial development (Kestner, 1979; Doody, 1992; Tsihrintzis *et al.*, 1996). Contemporary attitudes toward saltmarsh habitats stand in marked contrast, since they figure among the world's most valuable environments. This transformation in perception was effected by increasing interest in saltmarshes from, firstly, a conservation view point (Landin, 1993; William and Florsheim, 1994; Reed *et al.*, 1999), and, secondly, a coastal engineering perspective (Leggett and Dixon, 1994; Dixon and Weight, 1995; French, 1997; Dixon *et al.*, 1998).

Ecological studies initially established the value of marshes for biological production (Nixon, 1980), aquaculture, waste-water assimilation and as an important habitat for wild fowl and animal species (Beeftink, 1977b; Queen, 1977). With tangible benefits such as these, environmentalists have turned negative perceptions into united support for the conservation and preservation of coastal saltmarshes (Marcus, 1994). In Great Britain alone, some 82% of tidal marshland is under statutory protection (Burd, 1989), since it is regarded as a rare and threatened national habitat. The ecological significance of saltmarshes in the U.S. has gained recognition to such an extent that the legacy of investment in diking and draining has in a number of locations been abandoned, and reclaimed agricultural land restored to its native saltmarsh habitat (Brooke, 1992; Haltiner *et al.,* 1997; Roman *et al.*, 1995; Tsihrintzis *et al.*, 1996).

In Britain, the ecological value of saltmarshes has to some extent been overshadowed by the emerging role of marshes as a natural line of coastal defence against flooding and erosion. The engineering significance of saltmarshes as a type of flood insurance policy (Pethick, 1992) is twofold. First, the marsh surface performs critical dissipative and sediment supply functions during the onset of storm conditions (Brampton, 1992). By mitigating excess wave and tidal energy (Moeller *et al.,* 1996; Shi *et al.*, 2000), the presence of saltmarsh in front of an embankment or seawall reduces the likelihood of overtopping (Dixon and Weight, 1995). The marsh surface also acts as a reservoir of sediment, which can be released during storm events to replenish an eroding foreshore (Pethick, 1992), yet will recover as 'normal' sedimentary processes are restored. The second function relates to the re-establishment of saltmarsh on reclaimed marginal land. While the value of engineered saltmarshes for coastal protection was originally recognised in the Netherlands (Esselink *et al.,* 1998), the development of artificial marshes as a *sustainable* form of flood defence has more recently received attention in a U.K. context through managed retreat or flood defence realignment schemes (French, 1997, 1999).

Flood defence realignment involves returning tidal circulation to reclaimed marginal land, and if undertaken on tide-dominated coasts where the magnitude of wind/wave energy is comparatively low, may result in the restoration of a stable saltmarsh environment (Toft *et al.,* 1994; French, 1999). Marshland created in this way provides a low cost method of maintaining the level of flood defence, where the saltmarsh fronting existing sea walls is deteriorating through erosion. This problem is particularly acute in south-east England, where relative sea level rise is perceived to be responsible for a

phenomenon known as coastal squeeze (Titus, 1991; Burd, 1995). Under natural circumstances, unconstrained saltmarshes respond to an increase in tidal activity or erosion by migrating landward. However, in many locations this 'roll over' is obstructed by an embankment or sea wall, such that the saltmarsh is instead squeezed into a zone of progressively decreasing width, until it is completely destroyed. By retreating the line of flood defence roll over can recommence. Realignment is also an option where hard defences have fallen into disrepair. In certain instances, it may be more cost effective in the long term to realign defences, rather than perform repairs. Realignment is a particularly attractive management strategy where historical land reclamation has distorted the natural shape and extent of the inter-tidal zone. This condition is prevalent in estuarine environments, where prior reclamation is responsible for disequilibrium between morphology and hydrodynamic processes (Burd, 1995). Flood defence realignment is a means of returning estuaries to their natural shape, and in so doing restoring the balance between process and form which is pivotal to stability in the coastal zone (Pethick, 1994, 1996).

The ecological and economic benefits of using saltmarshes to support and replace high cost, hard defences with a lower cost, ecologically and environmentally sound option (Agriculture Select Committee, 1998), are increasingly apparent. The promise of sustainable protection is most alluring. Whereas hard defences offer little assurance against accelerating rates of sea level rise (see Environment Agency, 1998), it is generally accepted that saltmarshes offer at least a medium-term solution, so long as they continue to accrete at a commensurate rate (French, 1993; Reed, 1990, 1995).

1.3 THE IMPORTANCE OF SALTMARSH CHANNEL NETWORKS

Channel networks are a *near-ubiquitous* feature of coastal saltmarsh environments (Chapman, 1977). In the first recorded definition of saltmarsh to explicitly include tidal channels, Steers and Thomas (1929, p.342) describe the marshes of Norfolk as '*a level plain cut up by an intricate series of minor creeks draining into major ones*'. Subsequent definitions by Letzsch and Frey (1980a) and Allen (1997, 2000) allude to the prominence of channels, which may otherwise be referred to as creeks, gullies, gutters, or sloughs (a U.S. term). Taking Great Britain as an example, creek development is evident in more than 90% of saltmarsh systems (Pye and French, 1993). The outstanding 10% of sites comprise marshes from the rocky shores of Scottish lochs, which as noted in Section 1.2.1, form under markedly different environmental conditions. In addition to their

widespread occurrence, other compelling evidence that channel networks are an essential feature of coastal marshes lies in: (1) their evolutionary status as an integral component from the initial stages of saltmarsh development; and (2) a number of key physical functions through which they maintain a stable and healthy saltmarsh environment. These factors are important considerations in the emerging realm of channel network design, where creek systems are seen to be an integral component of saltmarsh restoration and flood defence realignment schemes (French, 1996; French and Reed, 2001).

1.3.1 Evolutionary status

Channel development is an intrinsic morphological component of coastal saltmarshes from the earliest stages of formation (Ragotzkie, 1959; Pestrong, 1970; 1972). Conceptual models of their development (see for example Beeftink, 1977a; Kestner, 1979; also Steel and Pye, 1997) suggest that marshes tend to 'grow up' around their creek system, rather than the channel network incising into a saltmarsh surface that has already formed. The progressive growth of tidal creeks across bare inter-tidal flats has been observed during the earliest stages of marsh evolution in naturally evolving, engineered and artificial systems. The development of creek networks within 'natural' tidal environments has been studied at locations ranging from Solway Firth (Marshall, 1962; Bridges and Leeder, 1976), to the north coast of France (Fenies and Faugeres, 1998), San Francisco Bay (Pestrong, 1970) and Korea (Adams *et al.*, 1990). Experimental evidence from the U.S. demonstrates that proto-creeks also form in 'engineered' inter-tidal zones, once tidal circulation is re-established within marsh restoration schemes (Haltiner and Williams, 1987; Williams and Florsheim, 1994; Coates *et al.*, 1995). In the U.K., this response has been mirrored at the flood defence realignment site on Northey Island in the Blackwater Estuary (NRA, 1994). Channel initiation has also been observed on the pristine surface of dredgings deposited along the banks of the River Orwell (JR French, personal communication), and in abandoned reclamations (see French *et al.*, 2000) bordering the River Blyth, Suffolk.

1.3.2 Physical functions

The widespread occurrence and evolutionary status of channel networks raises obvious questions as to physical functions that they may perform. Evidence from the literature suggests that channel networks support the successful development and maintenance of saltmarsh environments by: (1) the dispersal of water and sediment through the marsh

system (Pestrong, 1970, 1972; Letzsch and Frey, 1980a; Hartnall, 1984; Collins *et al.*, 1987; Stoddart *et al.*, 1989; Esselink *et al.*, 1998; French and Spencer, 1993; Reed *et al.*, 1999; Wang *et al.*, 1999; Christiansen *et al.*, 2000); (2) drainage of the marsh surface (Knighton *et al.*, 1992; French *et al.*, 1995; Allen, 1997); and (3) the dissipation of flood tidal energy (Pethick, 1992).

Creek networks have been likened to the arteries and veins of the saltmarsh. In an elegant address, Sidney Lanier (1878, cited in Chapman, 1974, p.45) recognised how,

> *'...the grace of the sea doth go*
> *About and about through the intricate channels that flow here and there, everywhere*
> *Till his waters have flooded the uttermost creeks...*
> *And the marsh is meshed with a million veins'.*

Lanier employs this analogy with the circulatory system to great effect (see also Carey and Oliver, 1918, p.167), evoking a persuasive image of the essential, yet abstruse nature of channel formations. Bridges and Leeder (1976) also liken the flood and ebb flows passing through inter-tidal channels to the pattern of circulation in arteries and veins. Comparing the modes of operation, arteries convey blood and nutrients away from the heart in a manner that is broadly comparable to the main channel of a creek network distributing tidal flow and sediment through the marsh. Veins complete the circuit returning blood to the heart, just as the channel network collects tidal flow from the marsh surface. This distributive function is clearly central to the health of the system, inasmuch that the delivery of sediment to any depositional environment can be seen as a 'life giving process' (Bridges and Leeder, 1979, p.534). According to this model, tidal creeks are a sustaining feature of progressive saltmarsh development (Redfield, 1972), providing that the rate of deposition keeps pace with rates of sea level change (Reed, 1995).

Employing terminology from the fluvial literature, a number of authors refer to tidal creeks as *drainage* networks (see for example Steers, 1959; Pestrong, 1965; Ranwell, 1972). Yapp *et al.* (1917, p.81) describes saltmarsh channel networks as '*drainage systems... comparable to those of a river basin on land*', on the basis of a marked visual similarity between the form of saltmarsh and river channel networks. Over and above their common branching nature, saltmarsh channels are often orientated in a similar manner to gravity driven river networks (Steers, 1977; Bayliss-Smith *et al.*, 1979) and exhibit similar morphometric characteristics (Woldenberg, 1972). Fluvial systems perform a drainage function, which given the physical resemblance could also apply to saltmarsh networks.

Observation of tidal flow through a mature saltmarsh system suggests that this is indeed the case. Semi-diurnal neap tidal exchange (subsequently referred to as an 'under-marsh' tide) is usually concentrated within the channel network (Reed, 1987), with the creeks providing a pathway along which flood tidal flow and sediment gain access to the system (see also Carey and Oliver, 1918). As the tide turns and begins to retreat, the water level falls at the mouth of the system. This sets up a hydraulic gradient that drives the drainage of flow held within the creeks. The marsh surface is frequently inundated on higher spring tides (an 'over-marsh' event). As the tide begins to ebb, sheet flow may initially predominate across the marsh edge (French and Stoddart, 1992; Allen, 1997). However, as water levels fall, the flow is progressively diverted through the creek network, which from then on resembles a fluvial drainage network, as the creeks comprise the main conduit for surface and subsoil flows (Chapman, 1974).

Despite the similarity in form and function, there are obvious differences between the flow regimes of fluvial networks and saltmarsh creeks. Whereas the former convey uni-directional flows and formative bankfull events occur intermittently, the latter are subject to bi-directional tidal flows and comparatively frequent inundation. This form-process paradox (Knighton *et al.,* 1992) has been explained by Pestrong (1970, 1972) in terms of increased correspondence between the flow regimes with distance from the source of tidal flow. In essence, Pestrong suggests that ebb flows dominate in the headwater reaches, (see also Williams and Harvey, 1983), which consequently bear a strong physical resemblance to a river system. As the relative importance of flood tidal fluxes increases toward the mouth, it is theorised that network morphology diverges from the classic fluvial form.

Their channelised form and bi-directional flow regime has also lead to the perception of saltmarsh creeks as a scale version of tidal estuaries (Pethick, 1992; Coates *et al.,* 1995; Toft *et al.,* 1994). Wright *et al.* (1973) observe a landward exponential decrease in the width of estuarine channels, which has been linked with increased frictional effects and the dissipation of excess flood tidal energy. By analogy, Langbein (1963) claims that saltmarsh channels also perform a dissipative function. Pethick (1992, p.54) observes that progressive channel bifurcation exacerbates this effect, going so far as to describe the development of marsh creeks as *'a morphological devise to dissipate tidal wave energy'*. The discordant orientation of reaches within an otherwise ebb aligned system is further proposed by French (1996) to be indicative of localised dissipation. Limited empirical evidence is provided by Ward (1978), Stoddart *et al.* (1987, 1989) and

French and Stoddart (1992) to suggest that velocities diminish as tidal flow is directed into smaller creeks through the increasingly dissected network. Although results such as these are desirable given the potential value of coastal saltmarshes as a means of dissipating storm tidal energy, the notion that channels evolve to perform a dissipative function is inconsistent with the results of process-studies and models of network development (French and Reed, 2001). As such, it cannot be overlooked that the dissipation of tidal velocity may be simply a by-product of efficient branching network structures (Haggett and Chorley, 1969; Leopold, 1971; also Rodriguez-Iturbe *et al.,* 1992).

1.3.3 The challenge of saltmarsh restoration and channel network design

In light of the widespread occurrence of channel networks in British marshes, their enduring presence from the earliest stages of saltmarsh formation, and life giving functions that they appear to perform, it is reasonable to surmise that creek development is an essential component of stable saltmarsh environments. Since the success of saltmarsh restoration and flood defence realignment schemes rests on the re-establishment of stable marshes (Haltiner *et al.,* 1997), the importance of including a channel network as an integral component of the project is apparent (Reed *et al.,* 1999). As shown in Section 1.3.1, studies of saltmarsh development suggest that given time, a natural channel network and saltmarsh will evolve on newly created tidal land. However, time is at a premium in coastal defence programmes. Rather than waiting for nature to take its course, experience from the U.S. (Williams and Florsheim, 1994; Coates *et al.,* 1995) demonstrates that incorporating an element of channel network design can reduce the time required for saltmarsh restoration (see also Johnson, 1996).

In the earliest example of design implementation, Dutch farmers achieved their objective of creating new inter-tidal land (see Beeftink, 1977a; Esselink *et al.,* 1998), by digging parallel lines of drainage known locally as *Gruppen* (Kestner, 1979). Although unnatural in appearance (Figure 1.4), the provision of a basic creek formation promoted sediment dispersal and accumulation within the inter-tidal zone (Steers, 1959). However, the marshes were reclaimed in their youth, so it is impossible to ascertain if these channel networks, of artificial origin, supported other physical functions such as the dissipation of tidal energy.

Judging from the scarcity of literature on the subject, the formulation of specific design guidelines promoting the establishment of correctly functioning saltmarsh channel networks is very much in its infancy. Recent approaches to network design in the U.S. pay

Figure 1.4 Artificial creek systems from the Dutch Waddens (after Beeftink, 1977a).

close attention to natural forms as well as processes and functions (Coates *et al.*, 1995). Recommendations made by Williams and Florsheim (1994) include replicating the natural functions of tidal channels through the provision of a template or outline creek network based on the form of nearby systems. The use of relic channel networks preserved on reclaimed tidal land has accordingly been proposed as a basis for contemporary design in British restoration schemes. Burd (1995) notes that the optimum method of re-establishing a creek network is to excavate the original system. However, this approach is fundamentally flawed because of the implicit assumption that environmental conditions have remained constant since the time at which the relic creek system was originally established. The evolutionary nature of marsh systems means that this is rarely the case. To be effective, channel network design should reflect relations between the set of *contemporary* environmental controls, network morphology and function. To support the successful implementation of flood defence realignment schemes there is clearly a pressing need to establish a formal geomorphology of saltmarsh channel networks.

1.4 PREVIOUS RESEARCH ON CHANNEL NETWORK GEOMORPHOLOGY

1.4.1 Channel network morphology

Variability in the form of saltmarsh channel networks around Britain, and indeed the world, has attracted the interest of a number of authors (Chapman, 1974; Steers, 1977). Within the body of previous research on channel network morphology, a fundamental distinction can be made between studies focusing on *planimetric* (Knighton *et al.,* 1992; Shi *et al.,* 1995), *longitudinal* (Collins *et al.,* 1987) and *cross sectional* (Pestrong, 1965, 1970; Coates *et al.,* 1995) planes of adjustment.

Observations concerning the planimetric structure of saltmarsh channel networks were initially *descriptive* in nature. At a network scale, terminology ascribed to fluvial systems by Zernitz (1932) and Howard (1967) is used to record obvious visual patterns in and contrasts between planimetric structures (see for example Ragotzkie, 1959). Dendritic is the term most frequently employed (Pestrong, 1965; Steers, 1977; Frey and Bassan, 1985; Knighton *et al.,* 1992; Fenies and Faugeres, 1998), although alternative expressions include: trellis and rectangular (Pestrong, 1965; Steers, 1977); reticulate (Tubbs, 1999); parallel (Pestrong, 1965); anastomosing (Zernitz, 1932); candelabra (Ragotzkie, 1959); herringbone (Adam, 1990); simple and tortuous (Chapman, 1974); linear and complex (Pye and French, 1993).

The emergence of morphometry, defined as *'the quantitative expression of form'* (Gardiner and Park, 1978, p.2), introduced an empirical basis for studying the planimetric characteristics of tidal networks. In a bid to better understand relations between morphological (related to form) and dynamic factors (formative processes), Ragotzkie (1959) applies *geometric* measurements to quantify patterns in channel development. Employing methods of analysis introduced by Horton (1932, 1945) for fluvial systems, this work represents an important advance from observation-based studies to the quantification of morphologic properties. Pestrong (1965) subsequently established the first quantitative geomorphology of tidal channel systems. Topologic information and key geometric measurements were obtained from aerial photographs, in order to characterise the principal features of network planimetry in several U.S. marshes. Selected measures of network structure and composition and channel form and included: Hortonian 'laws' of network composition (Horton, 1945; Schumm, 1956); channel frequency; length; sinuosity; angle of convergence; and drainage density. Subsequent studies employ morphometric indices to characterise and compare creek formations (Myrick and Leopold,

1963; Woldenberg, 1972; Coates *et al.,* 1995) and to identify temporal changes in planimetry associated with network development (Knighton *et al.,* 1992; Shi *et al.,* 1995).

Comparatively few studies have addressed the cross-sectional characteristics of saltmarsh channel networks in any detail. Pestrong (1965) provides an early visualisation of spatial changes in channel shape along the course of U.S. tidal networks (see also Myrick and Leopold, 1963). Although specific reference to British formations is made by a limited number of authors (Steers, 1977; Bayliss-Smith *et al.,* 1979; French and Stoddart, 1992), tidal creeks appear to exhibit a broadly similar morphology. Collins *et al.* (1987) introduce qualitative expressions such as triangular and semicircular to describe cross sectional form, terminology which is expanded by Everts (1980, cited in Coates *et al.,* 1995) and Wells *et al.* (1990) to include trapezoidal, parabolic U-shaped and V-shaped. Coates *et al.* (1995) simplify these composite expressions of cross-sectional adjustment into three distinct facets comprising: (1) upper slope; (2) channel wall; and (3) toe segment. An additional thalweg facet is referred to by Bridges and Leeder (1976).

Quantitative expressions of cross-sectional adjustment include: bank slope (Well *et al.,* 1990); width:depth ratio (Collins *et al.,* 1987; Zeff, 1988); and depth:tidal range ratio (Allen, 1985a). Measurements of width and depth as individual parameters are recorded in studies of hydraulic geometry (Myrick and Leopold, 1963; Pestrong, 1965; Woldenberg, 1972), the basic premise being that over time cross sectional form adjusts to accommodate formative flows experienced by the system. The mechanisms of bank failure responsible for temporal change in cross sectional form (Pestrong, 1970) are widely discussed in the literature (Marshall, 1962; Letzsch and Frey, 1980a, 1980b; Allen, 1985a, 1985b). Hydrodynamic processes are regarded as the governing force (Friedrichs, 1995), although invertebrates are seen to play a subordinate role in bed and bank destabilisation (Van Straaten and Kuenen, 1957; Frey and Bassan, 1985; Hughes, 1999).

The longitudinal profile of tidal channels has received considerably less attention than the other planes of morphologic adjustment. From the limited examples of longitudinal form that are documented in the literature, profile shape remains a matter of some dispute. Pestrong (1965) observes considerable irregularity in the longitudinal profiles of 'trunk' channels, together with a fundamental lack of conformity to the concave upward shape of terrestrial streams. In marked contrast, Ayles and Lapointe (1996) record pronounced upward concavity, interpreted by Collins *et al.* (1987) as a sign that the network is still actively eroding. Anomalous features of profile morphology include a rapid 'drop of' close to the mouth of the system (Ayles and Lapointe, 1996), and

deeps and shallows (Bridges and Leeder, 1976; Collins *et al.*, 1987) along the channel floor. Morphometric expressions of longitudinal adjustment are also scarce, with an isolated reference to the measure of network gradient made by Collins *et al.* (1987).

1.4.2 Conceptualising controls on channel network geomorphology

Diversity in the morphological characteristics of saltmarsh channel networks only becomes meaningful when sufficient information is available to *interpret* and *explain* its meaning. Examination of the literature suggests that the complexity observed in planimetric, cross-sectional and longitudinal form can be traced to a number of key geomorphic controls. The schematic model in Figure 1.5 has been devised to conceptualise the manner in which these controls exert influence over, and are manifested in channel network morphology.

Controls on the form of tidal creeks can be conceptualised in terms of two separate scales of influence. The *boundary conditions* under which British saltmarshes develop are important at the broadest geographical scale, and as such are represented at base of the model (Figure 1.5). In accordance with observations by a number of authors, it is reasonable to suggest that regional diversity is present in environmental controls such as: sediment composition (Allen, 1989; Pye and French, 1993); halophytic vegetation (Adam, 1979, 1981; Burd, 1989); tidal influences (Allen, 1992); and relative sea level change (Environment Agency, 1998), which may from the outset affect the processes involved in the development of channel networks. Superimposed on this geographically *extensive* suite of influences are locally important, or *site specific* factors. Previous research indicates that the spatio-temporal development of individual networks is the second important determinant of form. Comprising the upper tier of the model, the *developmental sequence* represents the stages and characteristic morphologies through which networks may pass.

Application of this two-tiered approach to interpreting the form of saltmarsh creek networks means that seemingly complex morphological characteristics can, in theory, be separated into those arising from broad environmental controls, and others related to the developmental status of the system. The tiers are linked by core formative processes, whose operation is affected by the environmental setting, but which in turn influence specific characteristics of network development. The following part of this introduction summarises the current state of understanding concerning the geomorphologic controls and process regimes that determine the form of tidal channel networks.

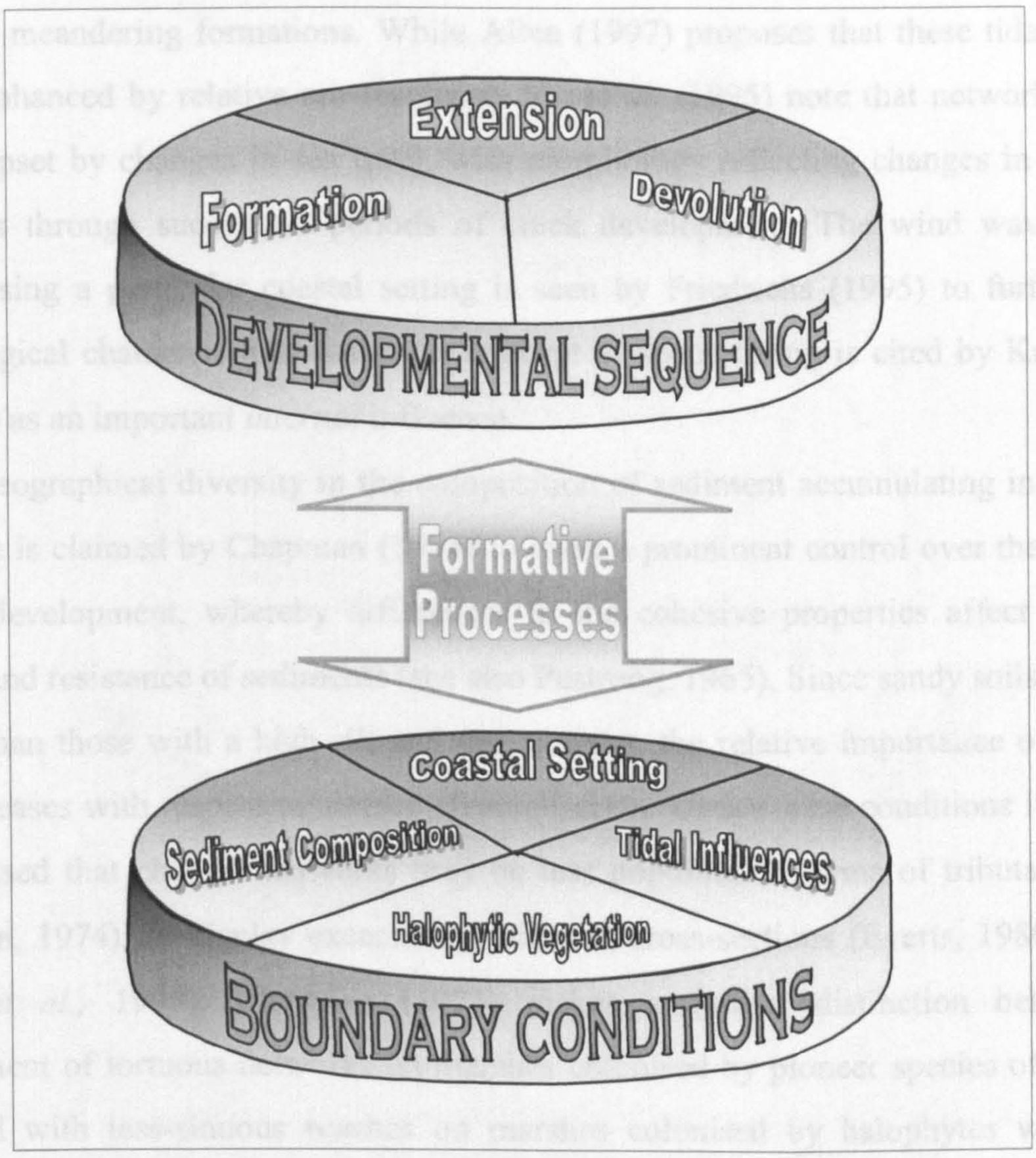

Figure 1.5 Tiered model conceptualising geomorphological controls on channel network morphology.

1.4.3 Environmental influences

Controls exerted on the form of channel networks by the physical environment in which saltmarshes develop, have received considerably less attention than either their temporal development or the formative process regime. In recognition, Chapman (1974, p.32) acknowledges that the existence of different creek systems *'demands investigation by physiographers of the conditions underlying their formation'*.

Unlike fluvial systems, where considerable time is required for the adjustment process (Richards, 1988), tidal systems are seen to respond rapidly (Knighton *et al.,* 1992; Friedrichs, 1995; Allen, 1997; Haltiner *et al.,* 1997; Mulrennan and Woodroffe, 1998), and as such bare the imprint of contemporary influences. Of the limited references made to *external* controls (Haltiner *et al.,* 1997; Allen, 2000), Ranwell (1972) suggests that spatial variability in tidal range is responsible for the development of 'sharp' versus 'sluggish' channel networks, the former occurring in large ranges where steeply sloping inter-tidal shelves enhance gravity driven drainage. Smaller ranges are linked with

elaborate, meandering formations. While Allen (1997) proposes that these tidal controls may be enhanced by relative sea level rise, Shi *et al.* (1995) note that network stability may be upset by changes in sea level, with morphology reflecting changes in boundary conditions through successive periods of creek development. The wind wave climate characterising a particular coastal setting is seen by Friedrichs (1995) to further affect morphological characteristics, while the concept of space-filling is cited by Knighton *et al.* (1992) as an important *internal* influence.

Geographical diversity in the composition of sediment accumulating in the inter-tidal zone is claimed by Chapman (1974) to exert a prominent control over the extent of channel development, whereby differences in the cohesive properties affect the shear strength and resistance of sediments (see also Pestrong, 1965). Since sandy soils are better drained than those with a high silt and clay content, the relative importance of through-flow increases with respect to surface channelisation. Under these conditions it has been hypothesised that channel networks may be less populous in terms of tributary growth (Chapman, 1974), or display excessively widened cross-sections (Everts, 1980, cited in Coates *et al.,* 1995). Chapman (1974) makes a further distinction between the development of tortuous networks on marshes colonised by pioneer species of *Spartina*, compared with less-sinuous reaches on marshes colonised by halophytes with a less aggressive root ball. Ranwell (1972) suggests that the density of channel development is correlated with the relative potential of species to trap sediment, while the absolute amount of vegetative cover is noted by Frey and Bassan (1985) to be proportional with the degree of creek meandering.

1.4.4 Developmental sequence

Saltmarsh channel network development has received considerable attention in the literature. By piecing together information drawn from an array of studies, the schematic representation in Figure 1.6 summarises the key stages of development and mechanisms involved in the growth of saltmarsh channel networks.

Conceptual advances were made in understanding the geomorphic significance of channel networks through studying the processes involved in creek *formation*. A clue to the origin of tidal networks is provided by Steers (1959, p.75), who notes that creeks are essentially '*unenclosed parts of the surface on which marsh has grown*'. The sequence of stages involved in the transition between pristine tidal flats and a saltmarsh surface dissected by creek systems is depicted in Figure 1.7.

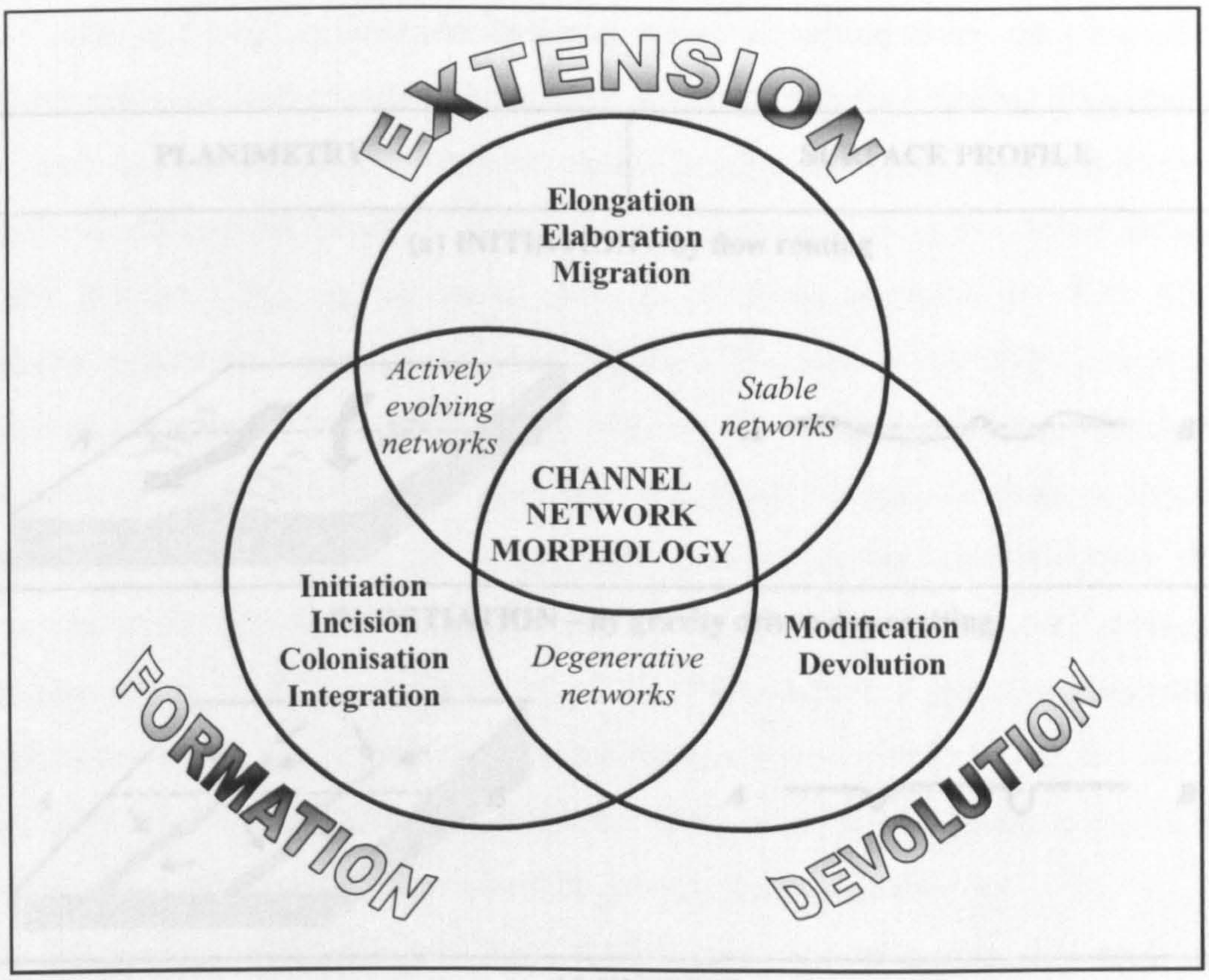

Figure 1.6 Schematic representation of saltmarsh channel network development.

Several hypotheses have been put forward to explain the initiation of proto-channel networks. The first explanations by Yapp *et al.* (1917) and Carey and Oliver (1918) begin the story of tidal channel initiation with observations concerning the widespread development of topographic irregularities on sediment rich inter-tidal surfaces. As shown in Figure 1.7a, embryo creek development is explained in terms of flow routing around these raised mounds, whereby the tide *'drains away from between the hummocks of the developing marsh, and soon cuts shallow, winding channels'* (Yapp *et al.*, 1917, p.81).

Inspired by models of fluvial channel formation (Horton, 1932, 1945), Pestrong (1965) presents an alternative explanation (see also Steers, 1977), proposing that flow routing arises in a similar manner to rill development (Figure 1.7b), in response to the incising effect of gravity driven flow across a sloping inter-tidal surface. Chapman (1974) distinguishes between these modes of creek initiation in terms of physical setting, with hummock growth prevalent on low gradient flats in the lee of a spit or bar, and incising rills prominent on the sloping banks of an estuary (see, for example, Allen, 1985a). Whichever initiating mechanism is seen to dominate, Chapman (1974, p.29) goes on to note that, *'in the early stages of marsh development it is often difficult to determine the course of future creeks, even the main creek'*.

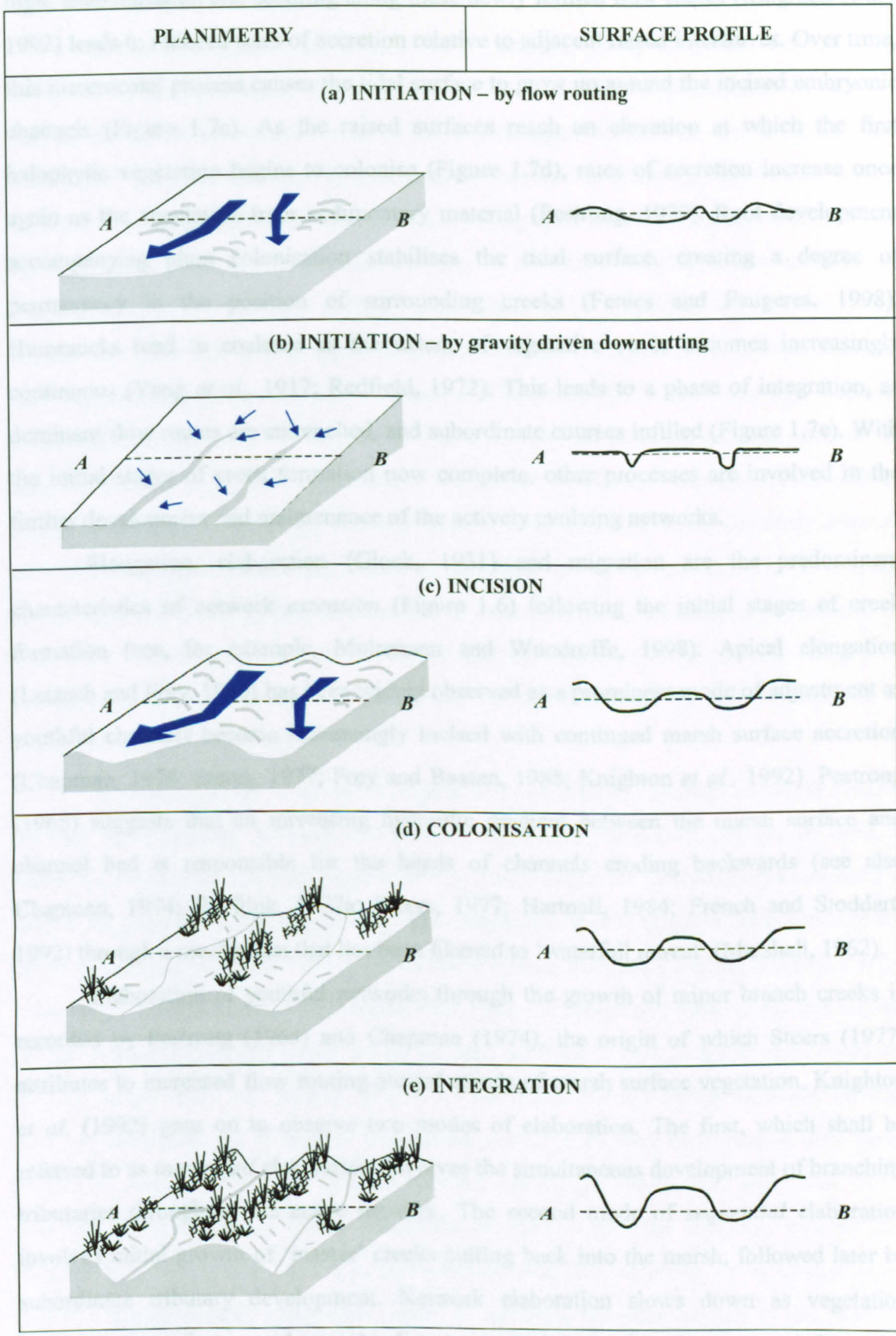

Figure 1.7 Transitional stages involved in saltmarsh channel network formation.

Although frequent tidal inundation ensures that sedimentation rates are generally high, channelisation and scouring along these newly formed flow routes (Knighton *et al.*, 1992) leads to reduced rates of accretion relative to adjacent raised interfluves. Over time, this incremental process causes the tidal surface to grow up around the incised embryonic channels (Figure 1.7c). As the raised surfaces reach an elevation at which the first halophytic vegetation begins to colonise (Figure 1.7d), rates of accretion increase once again as the vegetation traps sedimentary material (Pestrong, 1970). Root development accompanying plant colonisation stabilises the tidal surface, creating a degree of permanency in the position of surrounding creeks (Fenies and Faugeres, 1998). Hummocks tend to coalesce as the extent of vegetative cover becomes increasingly continuous (Yapp *et al.*, 1917; Redfield, 1972). This leads to a phase of integration, as dominant flow routes are entrenched, and subordinate courses infilled (Figure 1.7e). With the initial stages of creek formation now complete, other processes are involved in the further development and maintenance of the actively evolving networks.

Elongation, elaboration (Glock, 1931) and migration are the predominant characteristics of network *extension* (Figure 1.6) following the initial stages of creek formation (see, for example, Mulrennan and Woodroffe, 1998). Apical elongation (Letzsch and Frey, 1980) has been widely observed as a prominent mode of adjustment as youthful channels become increasingly incised with continued marsh surface accretion (Chapman, 1974; Steers, 1977; Frey and Bassan, 1985; Knighton *et al.*, 1992). Pestrong (1965) suggests that an increasing hydraulic gradient between the marsh surface and channel bed is responsible for the heads of channels eroding backwards (see also Chapman, 1974; Beeftink, 1977a; Steers, 1977; Hartnall, 1984; French and Stoddart, 1992) through a mechanism that has been likened to 'waterfall retreat' (Marshall, 1962).

Elaboration of youthful networks through the growth of minor branch creeks is recorded by Pestrong (1965) and Chapman (1974), the origin of which Steers (1977) attributes to increased flow routing around stands of marsh surface vegetation. Knighton *et al.* (1992) goes on to observe two modes of elaboration. The first, which shall be referred to as *integrated* elaboration, involves the simultaneous development of branching tributaries throughout the entire network. The second mode of *sequential* elaboration involves initial growth of 'master' creeks cutting back into the marsh, followed later by subordinate tributary development. Network elaboration slows down as vegetation becomes more dense, and root binding presents increased resistance to deformation (Pestrong, 1965). Elaboration ceases all together when the area of marsh is fully drained

(Knighton *et al.*, 1992), with tributaries hydraulically serving a particular marsh surface 'catchment' (Allen, 1997; Rigon *et al.*, 1999).

Lateral migration (Yapp *et al.*, 1917; Pestrong, 1965; Chapman, 1974; Steers, 1977; and Frey and Bassan, 1985; Gabet, 1998) is the final characteristic of network development to be considered. From an initially straightforward route across barren inter-tidal flats, the course followed by tidal channels becomes increasingly tortuous as flow is diverted around vegetated patches of raised topography. In response, the creeks which develop after the initial stages of marsh formation are likely to follow a more sinuous and discordant course (Pestrong, 1965). Furthermore, once vegetation has become fully established across the marsh, network growth through surface erosion is superseded by bank undercutting (Chapman, 1974; French and Stoddart, 1992) and slumping (Marshall, 1962; Letzsch and Frey, 1980b; Allen, 1985a, 1985b) which cause existing channels to migrate. Collins *et al.* (1987) document the impact of channel capture, resulting from lateral meandering, on network development. The interconnection of previously separate networks significantly alters the pattern of tidal flow through the system. This may result in renewed elaboration, where reaches which were previously isolated receive additional flow from the integrated sources. Chapman (1974) identified lateral erosion, along with elongation and elaboration, as characteristic processes leading to the development of *stable* saltmarsh channel networks.

In addition to the progressive degeneration of channel networks as marsh systems become terrestrialised, network *devolution* incorporates discordant changes in form or structure, which occur as a response to abrupt modifications to the boundary conditions in which the channel system was initiated and subsequently developed. In the absence of sea level rise, Allen envisages (1997) that a stable coastal saltmarsh evolves towards a stage when surface inundation ceases and the tidal lands are essentially won (Carey and Oliver, 1918). Paradoxically, devolution of the channel network is seen to accompany evolution of this nature (Frey and Bassan, 1985). As the marsh surface builds vertically through ongoing accretion, the frequency of inundation decreases, and the effective tidal flows which previously maintained an open channel (Marshall, 1962) occur less often. In the absence of high velocity flows, vegetation encroaches into the channels, in a manner referred to by Yapp *et al.* (1917) as retrogression (see also Chapman, 1974; Collins *et al.*, 1987). Infilling is rapid (Ragotzkie, 1959) as sediment becomes trapped by the sward of vegetation. Channel bridging and infilling are characteristic features of networks that have reached the final degenerative stage of development (Chapman, 1974).

The network devolution thus described is limited to systems that are approaching the upper vertical limit of marsh growth, as determined by maximum high tidal levels. However, changes in the local boundary conditions have been shown to *modify* network morphology as it evolves towards this stage. Pringle (1995) suggests that a shift in base level may alter the morphology of coastal saltmarshes and their channel network. Base level represents the lowest elevation to which the channel bed can fall before gravity driven flow ceases (due to a zero energy gradient), and is usually determined by the minimum water level in the tidal inlet from which the marsh receives flow (French and Stoddart, 1992). According to Inglis and Kestner (1958, 1959) and Marshall (1962), fluctuations in the proximity of this inlet to the marsh edge initiates changes in creek morphology, with creeks becoming more incised and experiencing renewed apical erosion.

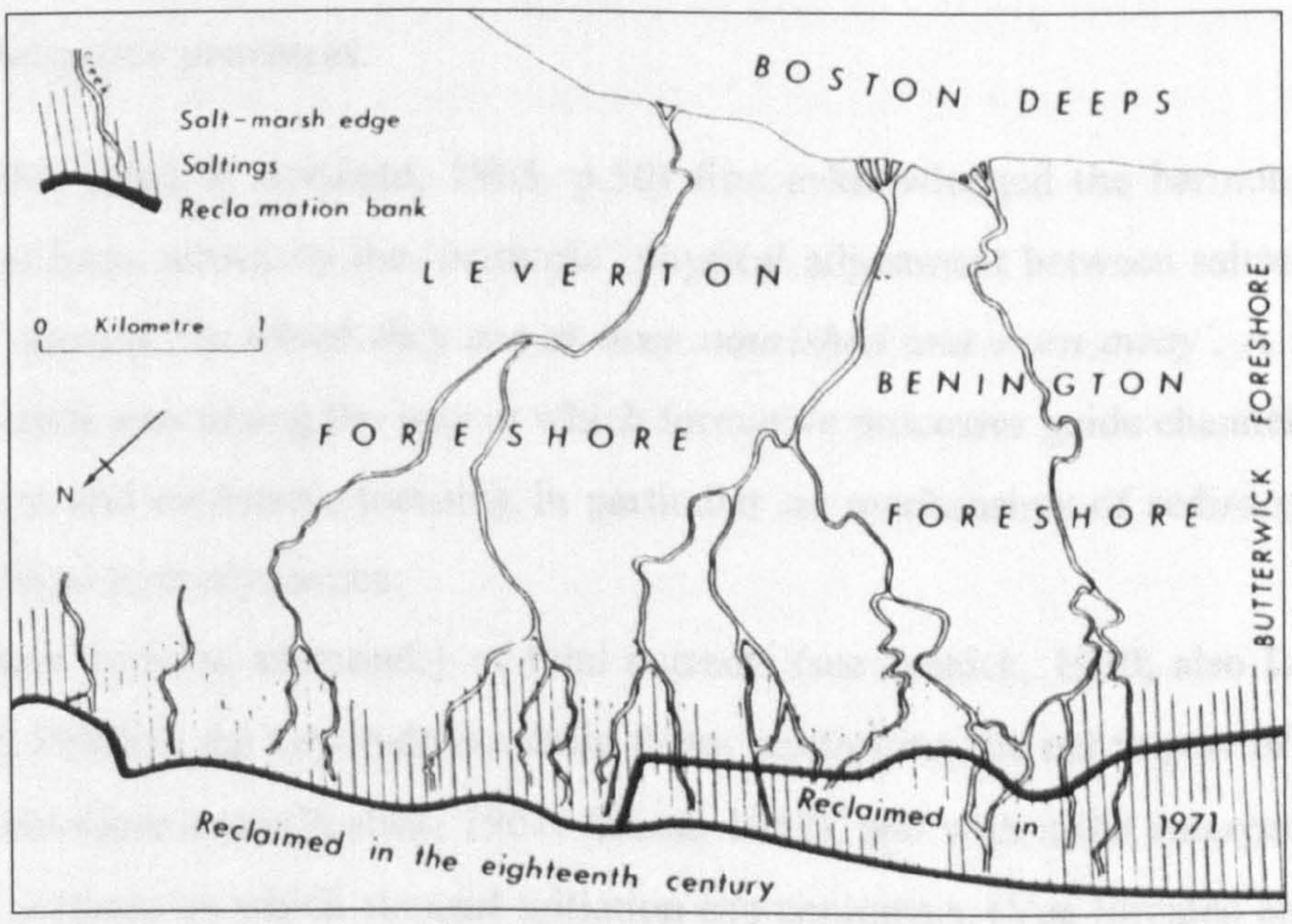

Figure 1.8 Truncation of creek networks by the construction of an embankment during land reclamation in The Wash (after Kestner, 1979)

The evolution of a channel network can also be distorted by obstructing the route of tidal flow through the system. As a result of large shell ridges blocking the mouth of channel systems which had otherwise formed and developed naturally, Greensmith and Tucker (1965, 1966) report pronounced changes in the course and size of master creeks, while Hartnall (1984) notes renewed creek development in a discordant pattern. Artificial intervention in a system through the reclamation of tidal land also alters flow patterns, as the width of the marsh is reduced and creek networks are truncated (Kestner, 1979) by the

construction of a seawall or embankment (see Figure 1.8). Over and above the modification to network morphology resulting from truncation, Pye (1995) notes that creeks whose heads become connected to the borrow pit, which results from the extraction of material to form an embankment, adjust to the new flow conditions by deepening and widening.

Natural and artificial adjustments to the boundary conditions are therefore linked with extraneous modifications to the morphology of existing creek networks. However, Pringle (1995) suggests that saltmarsh systems also respond to adjustments such as these with *cyclic* phases of marsh formation (see also Chapman, 1974; Kestner, 1979), whereby loss of marsh in one location is accompanied by renewed initiation elsewhere. On occasion, the devolutionary phase is thereby seen to complete the developmental sequence and feed-back to the initial stage of channel building and marsh formation.

1.4.5 Formative processes

Shaler (1886, cited in Redfield, 1965, p.50) first acknowledged the harmony between process and form, struck by the '*beautiful*' physical adjustment between saltmarshes and their tidal streams *'by which they are at once nourished and worn away'*. A substantial literature exists concerning the way in which formative processes guide channel initiation, development and evolution, focusing in particular on mechansims of sedimentation and the role of tidal hydrodynamics.

Phase duration asymmetry of tidal currents (see Pethick, 1980; also Lincoln and Fitzgerald, 1988) is the key hydrodynamic factor controlling the net import of sediments into the near-shore zone (Postma, 1961; Groen, 1967), and with it the emergence of new inter-tidal surfaces on which channel initiation can commence (Van Straaten and Kuenen, 1957). The departure from symmetrical tides arises as the duration of the flood phase of the tidal cycle is shortened by shallow water distortion (Pugh, 1987; French and Stoddart, 1992), an effect that is commensurate with an increase in flood velocity.

With sufficient accumulation of sedimentary material, channel initiation may proceed via hummock growth or rill incision. The former occurs through random accretion patterns coupled with ebb flow channelisation (Chapman, 1974), and the latter by gravity driven flows (Pestrong, 1965). According to Pestrong (1970), the raised mounds and rill banks attract sedimentation, while a comparatively high shear strength resists deformation by ebb tidal scouring. The hydraulic gradient that this creates leads to

the scouring and progressive reinforcement of ebb aligned proto-channel networks. As vegetation begins to colonise the accreting inter-tidal surface, further channel network development is controlled by a complex temporal and spatially varied hydrodynamic regime (see French and Stoddart, 1992). On a *temporal* scale, the amount of tidal power available to perform work within the saltmarsh system continues to be influenced by the degree of phase duration asymmetry (Pestrong, 1965; Boon, 1975; Ward, 1978, 1981; Lincoln and Fitzgerald, 1988). Through an increase in flood tide velocity, asymmetry is responsible for the import of sediments into and mobilisation of material within channel reaches (Settlemeyer and Gardner, 1977; Wolaver *et al.,* 1988; Stoddart *et al.*, 1989).

However, superimposed on basic tidal asymmetry are an additional set of hydrodynamic influences arising from the interaction between tidal flows and marsh morphology. Of particular significance is the distinction made by French and Stoddart (1992) between morphologically active and inactive flows. The difference between these regimes lies in the relative potential of the tidal flows to transport sediment and perform erosive work. Empirical studies (Bayliss-Smith *et al.,* 1979; Green *et al.,* 1986; French and Stoddart, 1992; Pringle, 1995) record high magnitude velocity pulses on the flood and ebb phases of overmarsh tides, which are absent on undermarsh cycles (see Reed, 1987). The velocity transients are attributed to a discontinuous relationship between the tidal stage and prism of flow (Ward, 1978; Pethick, 1980; Healey *et al.,* 1981), whereby tidal flow is constrained by a topographic threshold, namely the marsh surface (see also Woolnough *et al.,* 1995), and then rapidly released.

Flood transients occur at bankfull stage as the tide spills over the creek banks, and are associated with vertical advection (French and Stoddart, 1992) and lateral dispersal (Hartnall, 1984; Stoddart *et al.,* 1987, 1989; French and Spencer, 1993; French *et al.,* 1995; Esselink *et al.*, 1998; Reed *et al.*, 1999; Christiansen *et al.*, 2000) of sediments away from the channel network. Leonard *et al.* (1995) and Leonard and Luther (1995) document the enhancing effect of halophytic vegetation on sediment drop-out and deposition. According to Steers (1959), differential rates of sedimentation across the vegetated marsh surface are responsible for the development of levees and topographic discontinuities (Hartnall, 1984; Frey and Bassan, 1985; Collins *et al.,* 1987). Network elaboration is the net result, as secondary flow routing around these irregularities forms subsidiary creeks (see Amos, 1995). Ebb transients occur when overmarsh flows become channelised within the creek network (Pestrong, 1965) as the stage falls below bankfull (Green *et al.,* 1986; French and Stoddart, 1992). The high velocity achieved by flows

pouring from the marsh surface (Chapman, 1974) into the channel, have sufficient power to perform the erosive work associated with headward retreat and bank undercutting. As such, ebb transients are considered to be directly responsible for network elongation and channel migration (Pestrong, 1970).

French and Stoddart (1992) summarise the *spatial* relationships between formative flows, sediment deposition and creek morphological development using two models. In 'Model 1', flood velocities are progressively attenuated towards the headwaters of the system, where flows *'simply back up against channel slopes as water in a reservoir gradually being filled'* (Pestrong, 1965, p.20). In contrast, the headwaters are seen to experience high ebb velocities of prolonged duration. The result is a bi-directional regime in the lower reaches of the network, with ebb dominated flows in the upper reaches. The morphological implications are noted as rapid headward erosion and the development of ebb-aligned channel formations (French and Stoddart, 1992). In 'Model 2', researchers claim that ebb flows are dominant throughout the creek system, with accelerated flood flows responsible for sedimentation during low frequency storm conditions (Bayliss-Smith *et al.,* 1979). The distinction is between 'normal' tides, during which hydrodynamic processes maintain and extend the network, and storm-driven sedimentation that guides network elaboration. French and Stoddart (1992) suggest that these models operate in parallel, and go on to note that morphologically active flows become increasingly intermittent during latter stages of network evolution as the marsh surface approaches the upper limit of growth. Channel infilling is prevalent as undermarsh tides continue to introduce sediment, but there is insufficient energy to distribute this material out across the marsh surface. Modification of tidal flows by the growth of an obstructing bar or spit (Greensmith and Tucker, 1965, 1966; Hartnall, 1984) is seen to result in the redirection or even reversal of flood and ebb flows. The re-distribution of tidal energy in this way may be reflected by changes in reach-scale geometry and the development of discordant channel alignments.

1.4.6 Modelling relations between channel network morphology and function

The formal expression of relations between the morphology of tidal channel networks and the physical functions that they perform is of interest from both a scientific standpoint, and as a source of guidance for the design and management of restored saltmarshes (French, 1996). Of the limited examples documented in the literature, Randerson (1979) and Allen (1997) offer *conceptual* models of the links between network morphology,

sediment dispersal and drainage functions. The majority of *mathematical* models are essentially empirical and serve to establish basic associations between independent controls and dependent measures of creek geometry (for a review see Hume, 1991; also Gao and Collins, 1994; Van Dongeren and De Vried, 1994). Initial progress has been made towards identifying peak tidal discharge as the dominant independent factor influencing tidal channel development, through the approach referred to as hydraulic geometry (Myrick and Leopold, 1963; Woldenberg, 1972). While preliminary findings from the U.S. indicate that morphological adjustment is highly correlated with peak discharge or tidal prism (Haltiner and Williams, 1987; Coates *et al.,* 1995), similar associations for British creek systems have yet to be obtained.

The mechanics that may underpin these empirical associations have already been addressed in the context of process studies (see for example French and Stoddart, 1992). Building on this understanding, several authors (Mehta *et al.,* 1976; Friedrichs, 1995) attempt to explore relations between function and form using a more *deterministic* approach. In both instances, progress is made through the transition from a black-box to a grey-box model (Kirkby *et al.,* 1987), which incorporates certain aspects of the physical processes involved in morphological adjustment. Various hydrodynamic models (Schuepfer *et al.,* 1988; Boon and Byrne, 1981; Falconer and Chen, 1991; French and Clifford, 2000) yield promising results for predicting the driving forces that may determine the morphology of inter-tidal reaches (including the channels), but have yet to be specifically applied to saltmarsh environments. The aspect of sediment dispersal, that serves to counteract erosional effects, has been addressed in models by Allen (1992), French (1993), and Woolnough *et al.* (1995). Although simulating the general pattern of surface accretion, these models fail to consider the influence exerted by tidal creeks over patterns of deposition. Lastly, a novel contribution is made by French (1996), who employs a *probablistic* approach (see also Langbein, 1963) to evaluate network function in terms of optimality principles that have proved to be useful in the evaluation of fluvial networks (Roy, 1983, 1985).

1.5 UNRESOLVED ASPECTS OF SALTMARSH CHANNEL NETWORK MORPHOLOGY AND FUNCTION

The preceding review has established the important role played by tidal channel networks in the development and functioning of coastal saltmarshes. Their presence in more than 90% of British marshes is testimony to this. Although *initial* progress has been made

towards interpreting the morphology and understanding the function of saltmarsh channel networks, the following unresolved areas require further research:

1. The morphological characteristics of saltmarsh channel networks can be conveniently divided into three planes of analysis: network planimetry; channel longitudinal profile; and cross sectional form. Previous studies have focused on planimetry as the most visually distinct feature of network form, with descriptive expressions and simple morphometric measures employed in a small number of studies to characterise patterns of adjustment. However, channel long profile and cross sectional characteristics are arguably of equal importance in characterising how the growth and adjustment of creek formations is manifested morphologically. The idea of an *equilibrium* network that is in alignment with its boundary conditions, requires adjustment through all planes. Limited progress has been made towards characterising the cross sectional features of British saltmarsh channel networks, while longitudinal characteristics remain open to debate. Preliminary advances clearly need to be made in establishing a *'characteristic geomorphology'* of British saltmarsh channel networks, before it is possible to begin interpreting trends in and developing explanations for natural morphological variations.

   Although descriptive expressions are valuable as crude indicators of variability, the implementation of morphometric measures represents an important methodological development, with the potential to advance studies of form towards a standardised, and more objective inventory of channel network morphology. The simplification of complex phenomena, such as saltmarsh creek planimetry, can only work if characteristic and distinguishing morphometric information is obtained. A number of morphometric approaches have been tested on tidal channel networks. However, it remains to be established which provide the most useful representation of form.

2. The general occurrence of inter-tidal marshes has been tied into an envelope of geographically diverse environmental controls. It is claimed that the same factors affect the nature of channel network development. Previous research indicates that the growth of saltmarsh creek systems occurs through stages of formation, extension and devolution, driven by a process regime that is variable on both spatial and temporal

scales. Although Knighton *et al.* (1992) make the valid point that historic inevitability should not be assumed from this model of developmental controls, it is likely that each channel network bears some imprint of the dominant influences imposed during its evolution.

Comparatively little progress has been made towards relating environmental and developmental controls, both individually and collectively, to channel network morphology. Descriptive characterisation and limited morphometric analysis of network planimetry provide evidence of spatial variability in the appearance and underlying geometric structure of saltmarsh channel networks. However, the manner in which specific 'external' and 'internal' controls are related to these differences is largely unknown. In the words of Chapman (1974, p.32), *'the existence of different creek systems demands investigation by physiographers of the conditions underlying their formation'*. It may be that heterogeneity is the expression of different permutations of environmental control, while morphological trends are an expression of consistency within the developmental sequence (Figure 1.6). A coherent *interpretation* is clearly required of the complex structure and form of channel networks, in terms of key geomorphological controls.

3. In light of the valuable physical functions that saltmarsh channel networks appear to perform, progress needs to be made in determining which of these are most important in controlling morphological development. Previous empirical studies have tended to focus on the adjustment process in larger estuarine systems and U.S. saltmarsh environments. Since this approach serves as a useful exploratory tool, there is a pressing need for similar models for British marshes. However, it is important to recognise that the results obtained ultimately offer only a limited insight into the physical processes at work. A more theoretical approach is called for, which addresses morphological adjustment in terms of causal mechanisms. Deterministic and probablistic models are available, which complement and build upon empirical findings, and most importantly are suitable for application to tidal channel networks. It remains for these mathematical models to be evaluated as bases for establishing the manner in which physical function is manifest in network morphology. This may lead to more theoretically-informed guidelines for channel network design as part of flood defence realignment and saltmarsh restoration schemes.

1.6 AIMS AND OBJECTIVES

On the basis of the foregoing discussion of the unresolved questions concerning the geomorphological interpretation of saltmarsh channel network morphology and function, the main aim of this study is to:

Improve the scientific understanding of the morphology and function of natural saltmarsh channel networks.

With particular reference to British marshes, a number of specific objectives are identified:

1. **To characterise the morphology of saltmarsh channel networks**
2. **To demonstrate how physical environmental controls relate to natural variability in saltmarsh channel network morphology**
3. **To investigate relations between saltmarsh channel network morphology and function**
4. **To consider the implications of results obtained for the engineering of functional channel systems within restored marshes.**

1.7 THESIS STRUCTURE

The methodological framework employed to address the aim and objectives identified above is outlined in Chapter 2. Thereafter, characterisation of channel network planimetry in British saltmarshes is undertaken in Chapter 3, with longitudinal and cross-sectional adjustment addressed in Chapter 4 and Chapter 5 respectively. In Chapter 6, patterns of morphological behaviour emerging from the analysis are interpreted in terms of physical environmental controls. Theoretically-based mathematical models are employed in Chapter 7, in order to explore relations of causality between creek morphology and function. The main findings are discussed in Chapter 8, together with their practical implications for saltmarsh restoration schemes. In Chapter 9, the key conclusions that can be drawn from this study are presented, together with a series of recommendations for future research.

2. RESEARCH DESIGN

2.1 METHODOLOGICAL APPROACH

The interpretation of saltmarsh channel network morphology is a comparatively new research interest with a limited history of scientific work. With relatively little background research to build on, the study of network structure and function is very much in its preliminary stages, in terms of both the methodological constructs that are in place to characterise channel formations, and also the explanatory capability to interpret regularities in form.

In the search for appropriate research designs in geomorphology, Richards (1996) distinguishes between *extensive* and *intensive* methodologies. The extensive approach employs a large number (*Large-N*) of samples to formulate generalisations about complex geomorphological phenomena by empirical methods of statistical inference. It is most effectively utilised where research is exploratory by nature. In contrast, *intensive* methods focus on a small number (*Small-N*) of case studies to investigate causal mechanisms in greater detail. In this instance, generalisations are made by theoretical reasoning.

Extensive and intensive research approaches are often perceived to be at opposite ends of a methodological continuum (Richards, 1996), where the most suitable strategy is adopted depending on the research needs and nature of the paradigm under consideration. Extensive methods have become synonymous with a *positivist* approach, whereby the presence of physical relations between elements of a natural system is inferred from evidence of a statistical correlation between independent (causal) and dependent (response) variables. As noted by Sayer (1992) and summarised in Table 2.1, the extensive approach seeks to answer questions about regularities and patterns between study sites, and distinguishing features of a sample population. Although empirical observation alone cannot reveal causal behaviour, it points towards dependency and suggests lines of further enquiry. The objective of intensive analysis is *'to provide an explanation for the mechanisms generating the observed patterns in an extensive investigation'* (Richards, 1996, p.174). Viewed in this light, these seemingly dichotomous approaches to geomorphic research are in fact complementary. As Wolpert (1993) observes, much of scientific reasoning is counter-intuitive. Without empirical results as a starting point, the development of theoretical models on the basis of common sense alone becomes a hit and miss affair. Intensive research necessarily asks a different and more

probing set of questions compared with its extensive counterpart (see Table 2.1). In geomorphology, the transition is typically marked by a reduction in spatial scale to investigate the finer aspects of system operation and functionality. This involves concentrating on a smaller number of study locations and, in some circumstances, extends to laboratory based analysis (see, for example, Mosley, 1976; Lane, 1995). Boundary conditions imposed by the choice of study site for intensive analysis are addressed in Section 2.3, suffice to say that *'meticulous description of local boundary conditions is now as critical to successful experimentation and interpretation as the development of fundamental theory'* (Richards, 1996, p.184).

	EXTENSIVE	INTENSIVE
Research questions	• What are the regularities, common patterns and distinguishing features of the channel network population? • How widely are these characteristics distributed or represented?	• How does a function or process operate in a particular saltmarsh environment? • What produces distinguishing network characteristics?
Relations	Substantial relations of connection	Formal relations of causality
Nature of account	Empirical generalisations about patterns in form, lacking in explanatory penetration	Causal explanations for network characteristics at specific sites which may or may not be 'representative'
Typical methods	• Large-scale survey of a wide geographical range of study localities • Statistical analysis	• Small-scale study of individual networks in their causal context • Quantitative measurements

Table 2.1. Extensive and intensive research methodologies adapted to the study of saltmarsh channel network morphology and function (adapted from Sayer, 1992).

Experimental methodology has typically involved the separate implementation of extensive and intensive approaches, depending on the nature of the investigation and required level of explanatory power (see, for example, French and Clifford, 2000). In line with the objectives of this thesis, as stated in Section 1.6 and outlined by the logistical framework diagram in Figure 2.1, the present study involves the initial application of a geographically *extensive* approach to the characterisation and interpretation of morphological development in saltmarsh channel networks throughout Britain. The results obtained subsequently guide the theoretically and spatially *intensive* evaluation of physical functions performed at an illustrative case study site. Details of the extensive-intensive methodological procedures are described in the following sections.

GENERAL AIM	**To improve the scientific understanding of the morphology and function of natural saltmarsh channel networks**			
SPECIFIC OBJECTIVE	1. To characterise the morphology of saltmarsh channel networks.	2. To establish how physical environmental controls relate to natural variability in channel network morphology.	3. To assess the performance of theoretical mathematical models for evaluating causal relations between morphology and function.	4. To develop practical recommendations for the engineering of functional channel systems within restored marshes.
SCALE OF ANALYSIS	Extensive	Extensive	Intensive	N/A
APPROACH	Descriptive and morphometric characterisation of network morphology in marshes from around Britain.	Investigate relations of connection between physical control variables and diagnostic indicators of channel form.	Test the ability of theoretically-based models to predict morphological characteristics at a selected case study site.	Demonstrate how findings from the extensive and intensive analyses may be implemented in restoration design and post-project appraisal.
DATA REQUIRED	• Network planimetry • Longitudinal profiles • Cross-sectional geometry	a) Physical environment: tidal influence; sediment composition; coastal configuration; sea level change. b) Morphometric data: planimetric descriptors; longitudinal descriptors; cross-sectional indices.	a) Angular geometry: branching angles; surrogate measures for dominant discharge. b) Cross-sectional geometry: branching angles; surrogate measures for discharge; cross-sectional area; hydraulic radius; dominant discharge; tidal stage data.	a) Design guidelines: area coverage; surface elevation; tidal stage data; lidar terrain model; sediment composition. b) Post project appraisal: planimetric, longitudinal and cross-sectional descriptors.
SOURCES OF DATA	• Aerial photography • Field surveying • Photography, surveying and observation	a) Physical environment: tide tables; marsh surface elevation; field sampling; maps and aerial photos; Permanent Service for Mean Sea Level b) Morphometric data	• Aerial photography • Lidar coverage • Field-based measurements of velocity, stage and cross-sectional geometry	• Aerial photography • Lidar coverage • Field-based measurements of stage and sediment composition
HOW TO ADDRESS OBJECTIVE	Quantify network-wide behaviour using optimal morphometric descriptors and summarise natural morphological variability in terms of classificatory models.	Use statistical analyses to investigate empirical relations between 'optimal' morphometric indicators and potentially important environmental controls.	Compare predicted results from models of: (a) optimal angular geometry and (b) equilibrium cross-sectional geometry, with observed morphological characteristics.	a) Employ model of optimal angular geometry to define creek alignment, and mechanism of stability shear stress to define cross-sectional characteristics. b) Compare morphological characteristics of example restoration projects with results from extensive analysis

Figure 2.1 Logistical framework diagram.

2.2 MORPHOLOGICAL CHARACTERISATION

As summarised by the logistical framework diagram (Figure 2.1), the *characterisation* of saltmarsh channel network morphology is consistent with the level of understanding provided by an *extensive* scale of analysis. In the present context, characterisation denotes the process of describing a tidal channel network in terms of a specified set of attributes, and where possible adheres to the key requirements as outlined by Mosley (1987, p.304) that, *'the set of attributes, procedures and scales of measurement are defined so that objective reproducible results can be obtained as far as possible'*. The distinction between planimetric, longitudinal and cross-sectional planes of adjustment was introduced in Section 1.4.1, and provides an appropriate analytical framework for establishing the manner in which morphological adjustment proceeds. With reference to the methodological procedure outlined in Table 2.1, the following sections describe the study approach implemented in the 'large-scale survey' of regularities, distinguishing characteristics and variability within the national population of saltmarsh channel networks occurring on marine sedimentary shores (Figure 1.3).

2.2.1 Study site selection

Success of the extensive research strategy in addressing the first objective outlined in Figure 2.1, depends upon the selection of study sites that encompass a *Large-N* (Richards, 1996) sample of channel network formations. The selection of an appropriate number and geographic distribution of study sites requires careful attention, to ensure that morphologic diversity is captured in conjunction with regional variability in key environmental controls. In the Database of British Saltmarshes, Pye and French (1993) provide details of 175 saltmarsh localities, each covering an area >15 hectares. The choice of sites for the present study from this set of potential locations was informed by the set of factors summarised in Figure 2.2.

The presence of a creek system is an obvious initial consideration. Pye and French (1993) report that channel network development is evident in >90% of British saltmarsh localities. In the remaining 10% of sites, creeks are either absent or artificial by nature. These are predominantly confined to Scottish lochs and the rias of south-west England, which as shown in Figure 1.3, fall into a separate class of 'rocky shore' marshes. Since the present study is restricted to active saltmarsh environments, proto systems transcending fronting tidal flats (see, for example, Van Straaten and Kuenen, 1957; Allen, 1985a) are

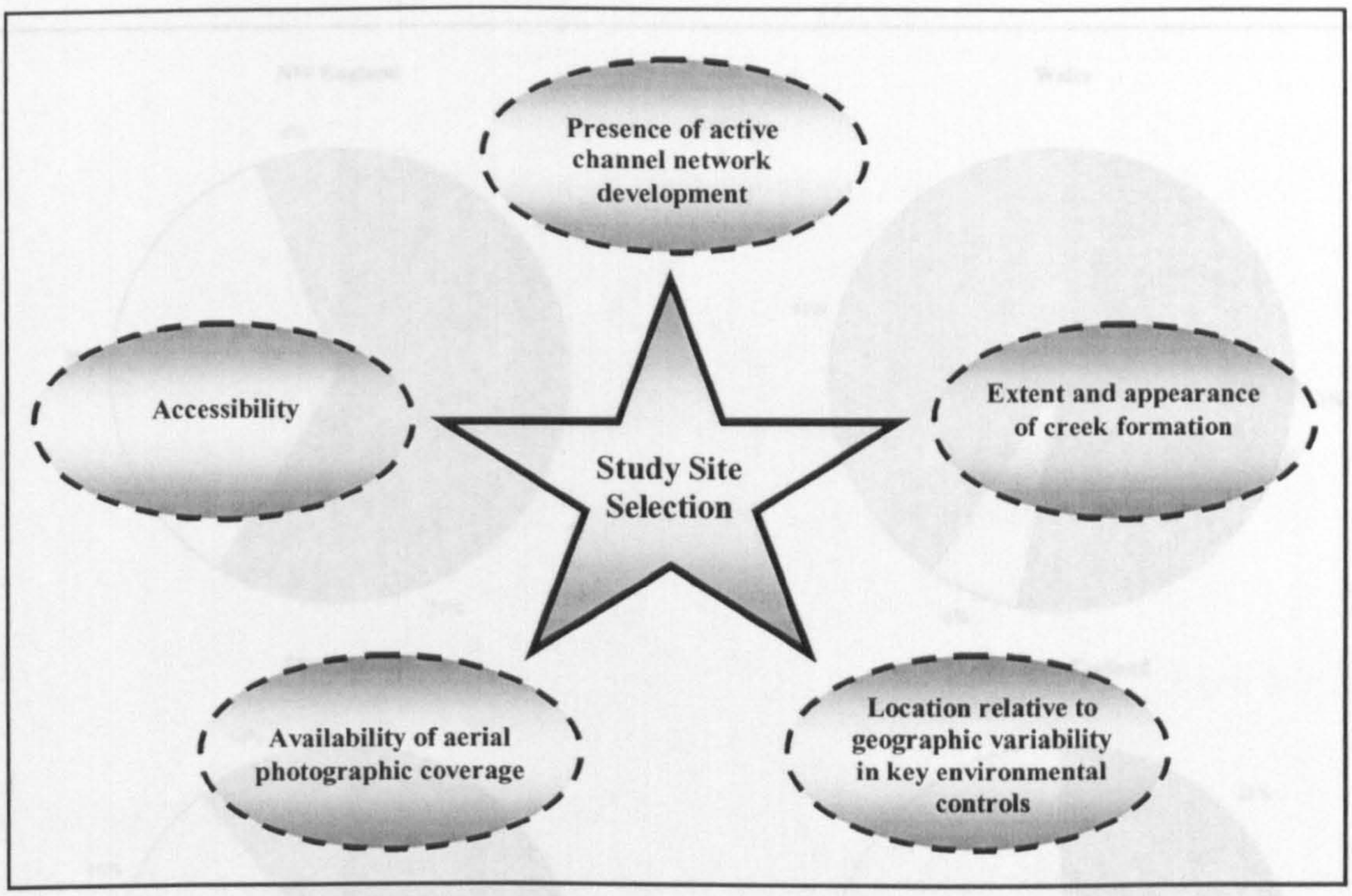

Figure 2.2 Factors taken into account in the selection of study sites for the extensive analysis.

precluded, together with relic networks on reclaimed land that no longer reflect local boundary conditions.

The *extent* of channel development is another important consideration. Significant morphologic diversity has been observed in the planimetry of British tidal networks (see Section 1.4), including patterns ranging from simple and dendritic to trellis, rectangular, parallel, anastomosing, herringbone and candelabra. For an extensive study, it is desirable to include the full range of morphological diversity. This can best be achieved by implementing a purposive sampling strategy (Norcliffe, 1977). As a starting point, Pye and French (1993) employ a basic categorisation of channel networks to summarise the complexity of planimetric form. Although descriptive by nature, the classes of linear, linear-dendritic, dendritic and complex/absent provide a basic indication of national variability. Classified according to these groupings, the pie charts in Figure 2.3 confirm that spatial variability is present in planimetric form. Network morphology throughout England and Wales is dominated by linear, linear-dendritic and dendritic systems, with complex formations figuring less prominently. Wales exhibits the full range of morphologies, while network development in Scottish marshes is predominantly complex or absent. On the basis of these results, it is reasonable to propose a broad-scale distinction between the marine sedimentary shores of England and Wales, which clearly

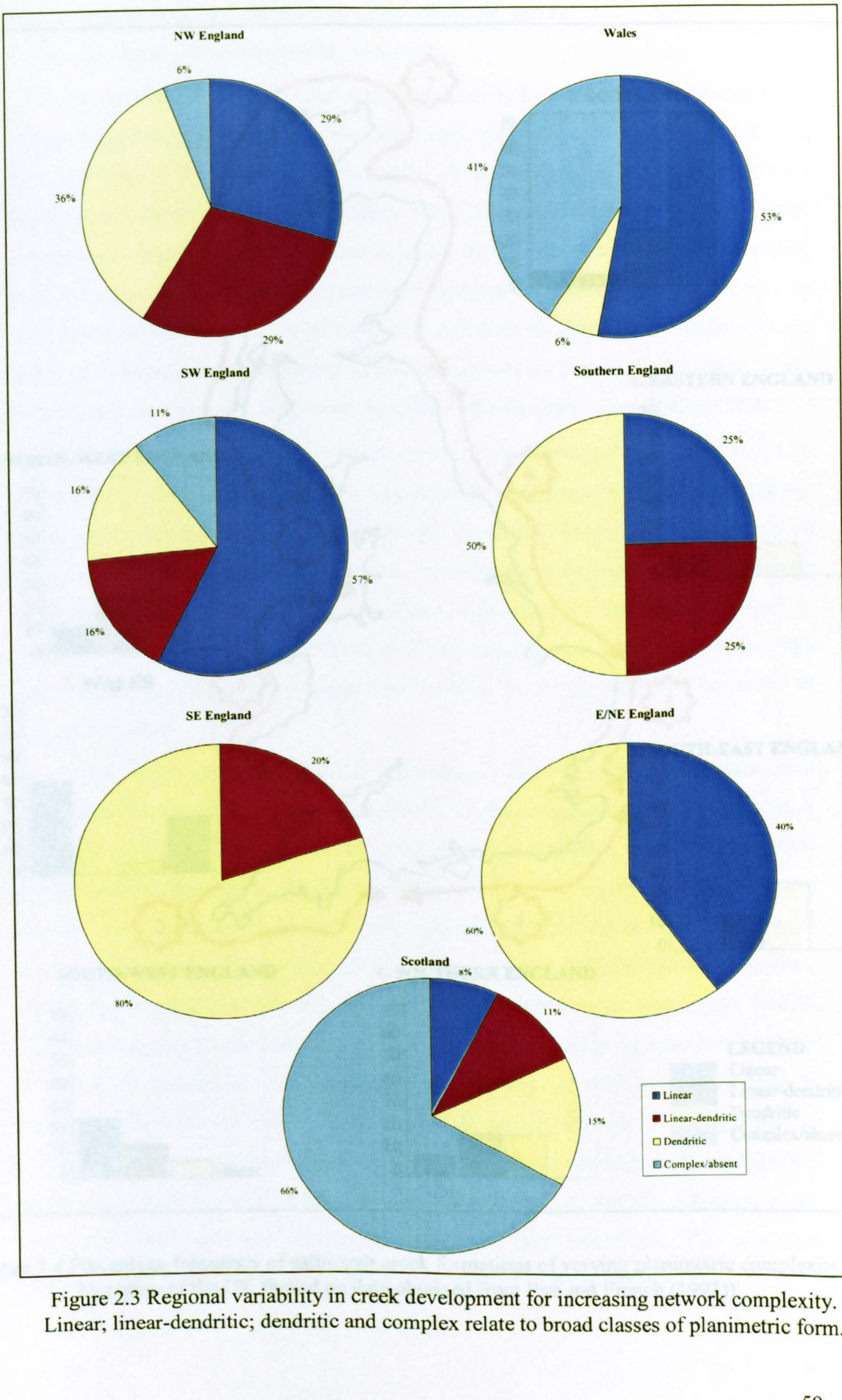

Figure 2.3 Regional variability in creek development for increasing network complexity. Linear; linear-dendritic; dendritic and complex relate to broad classes of planimetric form.

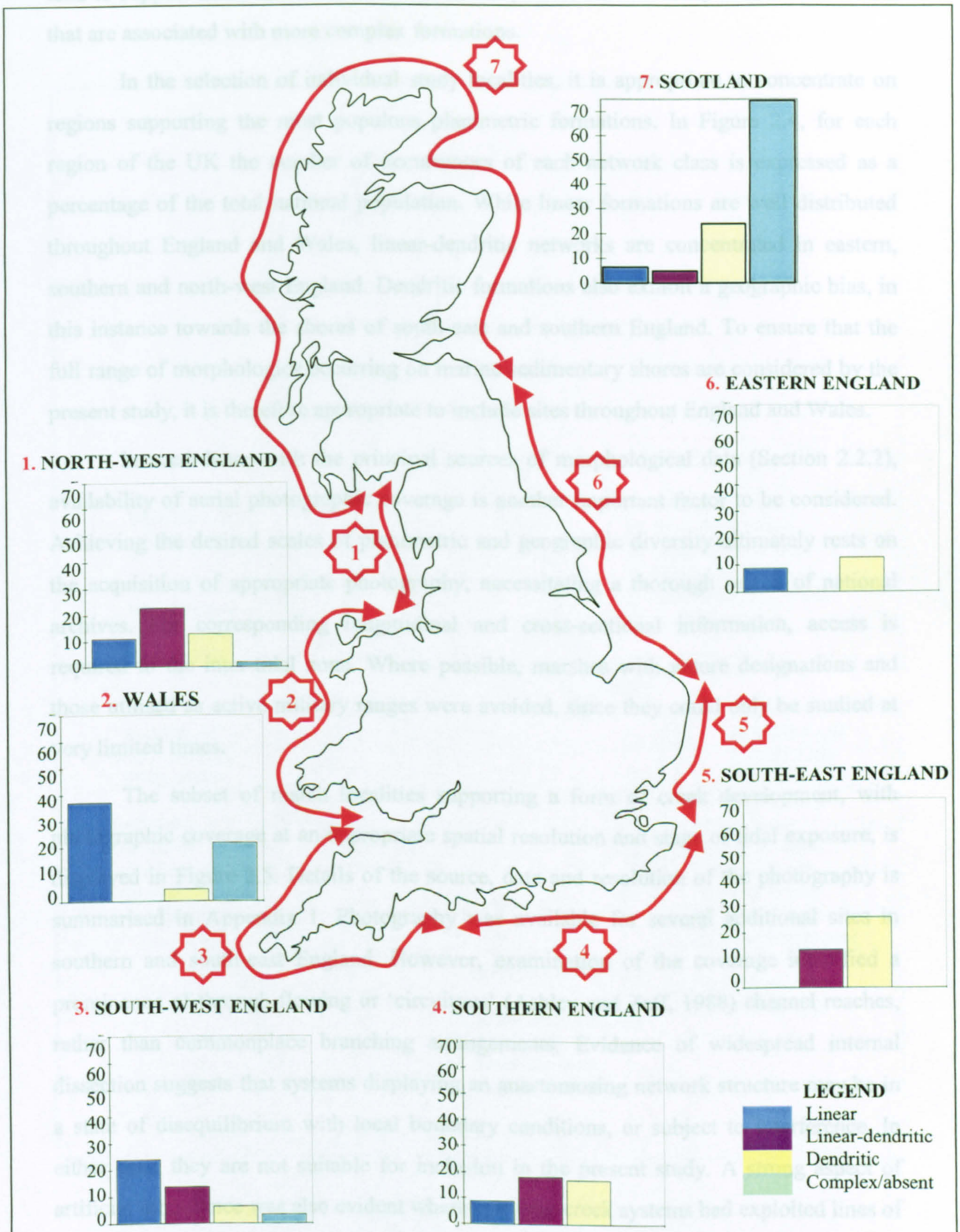

Figure 2.4 Percentage frequency of saltmarsh creek formations of varying planimetric complexity, by region of the UK (based on data obtained from Pye and French (1993)).

tend to support linear and dendritic creek development, and the rocky shores of Scotland that are associated with more complex formations.

In the selection of individual study localities, it is appropriate to concentrate on regions supporting the most populous planimetric formations. In Figure 2.4, for each region of the UK the number of occurrences of each network class is expressed as a percentage of the total national population. While linear formations are well distributed throughout England and Wales, linear-dendritic networks are concentrated in eastern, southern and north-west England. Dendritic formations also exhibit a geographic bias, in this instance towards the shores of south-east and southern England. To ensure that the full range of morphologies occurring on marine sedimentary shores are considered by the present study, it is therefore appropriate to include sites throughout England and Wales.

In accordance with the principal sources of morphological data (Section 2.2.2), availability of aerial photographic coverage is another important factor to be considered. Achieving the desired scales of planimetric and geographic diversity ultimately rests on the acquisition of appropriate photography, necessitating a thorough search of national archives. For corresponding longitudinal and cross-sectional information, access is required to the inter-tidal zone. Where possible, marshes with nature designations and those utilised as active military ranges were avoided, since they could only be studied at very limited times.

The subset of marsh localities supporting a form of creek development, with photographic coverage at an appropriate spatial resolution and stage of tidal exposure, is displayed in Figure 2.5. Details of the source, date and resolution of the photography is summarised in Appendix 1. Photography was available for several additional sites in southern and south-east England. However, examination of the coverage identified a prominence of through-flowing or 'circuitous' (Ashley and Zeff, 1988) channel reaches, rather than commonplace branching arrangements. Evidence of widespread internal dissection suggests that systems displaying an anastomosing network structure may be in a state of disequilibrium with local boundary conditions, or subject to interference. In either case, they are not suitable for inclusion in the present study. A strong aspect of artificial inheritance was also evident where evolving creek systems had exploited lines of weakened resistance along former drainage ditches (see, for example, Knighton *et al.*, 1992; also Mulrennan and Woodroffe, 1998) and field boundaries. This precluded marshes bordering the River Stour, and in some areas of Pagham Harbour.

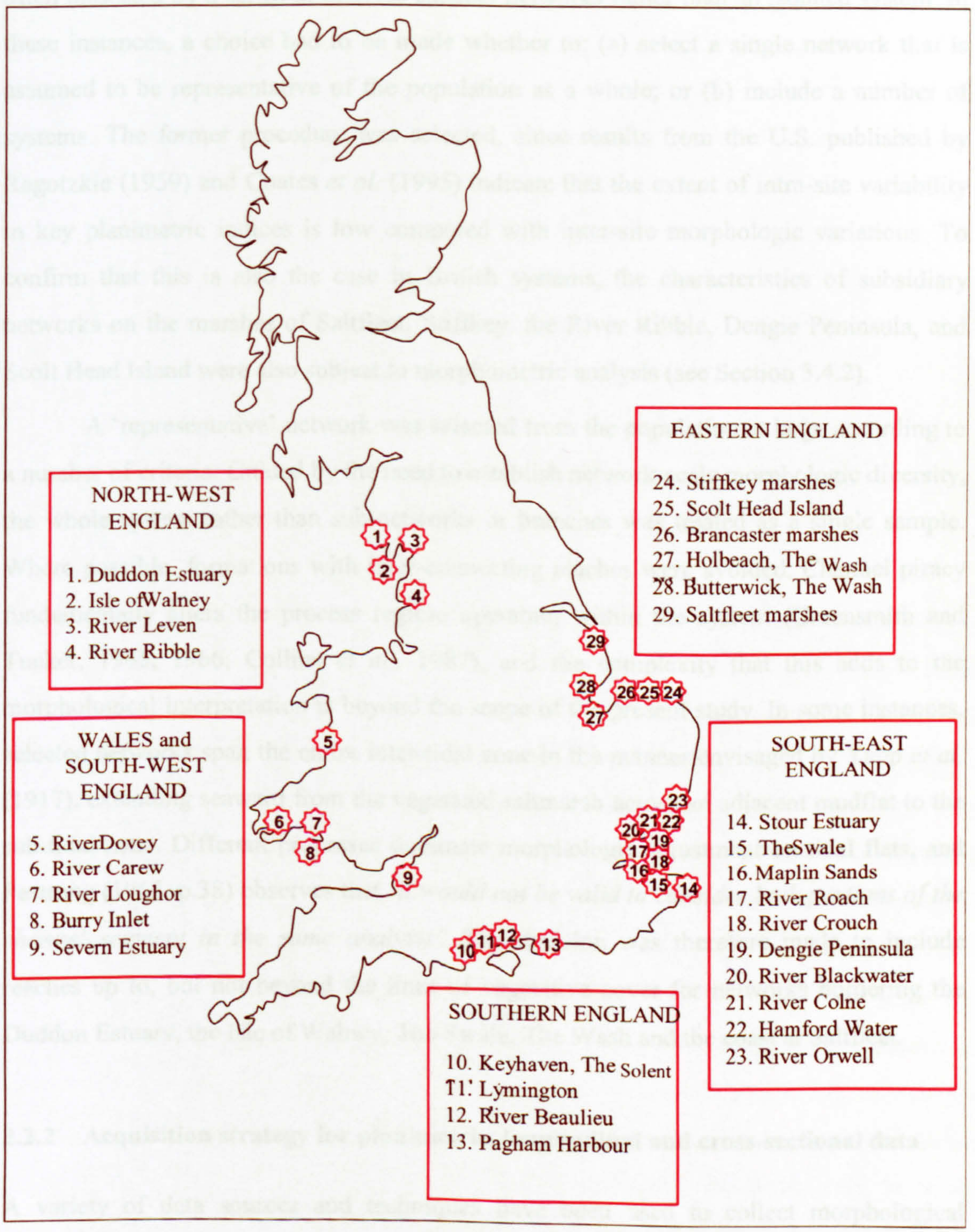

Figure 2.5 Geographic distribution of study localities

Having established a set of study sites for the extensive analysis, it became apparent from the photography that marshes occupying a substantial spatial coverage are often dissected by a series of discrete channel networks rather than an isolated system. In these instances, a choice had to be made whether to: (a) select a single network that is assumed to be representative of the population as a whole; or (b) include a number of systems. The former procedure was selected, since results from the U.S. published by Ragotzkie (1959) and Coates *et al.* (1995) indicate that the extent of intra-site variability in key planimetric indices is low compared with inter-site morphologic variations. To confirm that this is also the case in British systems, the characteristics of subsidiary networks on the marshes of Saltfleet, Stiffkey, the River Ribble, Dengie Peninsula, and Scolt Head Island were also subject to morphometric analysis (see Section 3.4.2).

A 'representative' network was selected from the population at large according to a number of criteria. Guided by the need to establish network-scale morphologic diversity, the whole system rather than sub-networks or branches was treated as a single sample. Where possible, formations with inter-connecting reaches were avoided. Channel piracy fundamentally alters the process regime operating within the system (Greensmith and Tucker, 1965, 1966; Collins *et al.,* 1987), and the complexity that this adds to the morphological interpretation is beyond the scope of the present study. In some instances, selected networks span the entire inter-tidal zone in the manner envisaged by Yapp *et al.* (1917), extending seaward from the vegetated saltmarsh across an adjacent mudflat to the sub-tidal zone. Different processes dominate morphologic adjustment on tidal flats, and Pestrong (1965, p.38) observes that *'it would not be valid to consider both portions of the channel segment in the same analysis'.* The decision was therefore made to include reaches up to, but not beyond the limit of vegetative cover for networks bordering the Duddon Estuary, the Isle of Walney, The Swale, The Wash and the coast at Saltfleet.

2.2.2 Acquisition strategy for planimetric, longitudinal and cross-sectional data

A variety of data sources and techniques have been used to collect morphological information about coastal environments (see Anders and Byrnes, 1991; Donoghue *et al.*, 1994; Thieler and Danforth, 1994; Collier *et al.,* 1995; also Donoghue and Shennan, 1995). However, the optimum methodological procedure is very much determined by the scale of the study and nature of information required.

Plate 2.1 (a) 1:5000 scale panchromatic aerial photograph (courtesy of the Environment Agency) showing Hut marsh on Scolt Head Island, Norfolk; and (b) the same area depicted on a 1:10 000 scale map (courtesy of Ordnance Survey).

For the detailed *planimetric* mapping of saltmarsh channel networks, field-based studies are constrained by the large volume of measurements that are involved. Conventional sources of network data, such as topographic map sheets, have also been criticised for their unfaithful and abstracted depiction of network composition (Haggett and Chorley, 1965; Chorley and Dale, 1972; Anders and Byrnes, 1991). The problem is particularly acute in the case of Ordnance Survey (O.S.) representations of saltmarsh creeks around the British coastline. Plate 2.1a illustrates a 1:5000 scale aerial photograph supplied by the Environment Agency, covering Hut Marsh on Scolt Head Island. The same area is depicted in Plate 2.1b on the corresponding 1:10 000 O.S. map. The reduction in information content between the two scenes is substantial. Firstly, the central and upper reaches of the channel networks are mapped at a constant width, whereas the actual width is clearly varied. Secondly, many smaller creeks have been omitted on the map, which are readily detected on the photography. In other instances, entire networks that are depicted on the photographic coverage are absent from corresponding map sheets. The omission of these features may to some extent be justified, since the remit of the Ordnance Survey is to map areas *above* the Mean High Water (*MHW*) mark. Recording features of shoreline below *MHW* is the responsibility of the Hydrographic Office. Unfortunately the national coverage of bathymetric charts is poor, and the maps are infrequently updated. Although a new series of Coastal Zone Maps are under development

as a joint venture between the Ordnance Survey and Hydrographic Office (Collier *et al.*, 1995), these were not available in time for the present study.

The value of remote sensing data as a source of information for coastal morphology has long been recognised (Wolf, 1983; Mitsch and Gosselink, 1986; see also Donoghue *et al.*, 1994; Reid-Thomas *et al.*, 1995; Cracknell, 1999; Moore, 2000). Satellite sensors such as Landsat MSS (Buttera, 1983), Landsat TM (Reid Thomas *et al.*, 1995) and SPOT (Hardisky *et al.*, 1986) have been successfully used for general mapping purposes in saltmarsh and wetland environments. However, they are of limited value for recording the planimetric characteristics of saltmarsh channel networks. The spatial resolution of these systems (75m, 30m and 10m respectively) is insufficient to record creeks that are less than 10m wide (Bayliss-Smith *et al.*, 1979; French and Stoddart, 1992). Airborne multi-spectral data provided by sensors such as the Compact Airborne Spectrographic Imager (CASI) and Airborne Thematic Mapper (ATM) have become more widely used in coastal mapping (Reid Thomas *et al.*, 1995; Green *et al.*, 1998; Smith *et al.*, 1998). However, detailed spectral information still comes at a cost in terms of spatial resolution. In contrast, high-resolution vertical aerial photography has been effectively employed in a number of studies (Chapman, 1974; Frey and Bassan, 1985), to illustrate the planimetric characteristics of channel network formations. Photographic coverage offers a detailed, yet synoptic record of the coastal zone, which is ideal for studying channel networks. Given an appropriate flying height, aerial photography has potential to record the smallest reaches of the system. A resolution of 1:3000 is observed by Coates *et al.* (1995) to provide an optimal record, although imagery of up to 1:25 000 has been used to study tidal channels (Knighton *et al.*, 1992; Shi *et al.*, 1995). Timing of the overflight is an additional consideration. Network planimetry may be captured in its entirety, providing that the coverage coincides with a low tidal stage. Otherwise, regions of the creek system are likely to be submerged.

A number of techniques (see Ichoku *et al.*, 1996), including feature extraction and on-screen digitising, have been used to delineate channel networks on digital imagery. Most automated algorithms utilise terrain models as base data (Chorowicz *et al.*, 1992), which is inappropriate for the present study because elevation data for the inter-tidal zone are scarce. Others have exploited the detailed spectral information offered by multispectral satellite imagery (Wang *et al.*, 1983; Ichoku *et al.*, 1996) to trace the channel, as distinct from its vegetated banks. However, this approach is also unsuitable, since it relies on a consistent pattern of digital numbers (DN) to demarcate the course of

the channel. In some instances, heterogeneity arises in DN values at the boundary between the channel and surrounding vegetated interfluves. In other cases, the low reflectance of standing water together with directional shading results in abrupt changes in contrast, which distort and fragment the digital representation of the channel (see Plate 3.2). On-screen digitising is a simple yet effective alternative for obtaining quantitative network information (Astaras, 1985; Astaras *et al.,* 1990). Advances in scanning equipment, image processing software and data handling capabilities mean that a channel network can be converted to a digital format, and conveniently analysed using a manual desk-based approach.

At present, a direct rather than remote approach to data acquisition is most appropriate for the acquisition of *longitudinal* and *cross-sectional* information. The extraction of elevation data from digital imagery is problematic. Traditional photogrammetric methods (see Wolf, 1983) are time consuming to implement. Furthermore, the transient nature of coastal areas, and paucity of benchmarks, means that establishing elevation readings relative to Ordnance Datum is difficult. The problem is compounded by an absence of contour lines and spot heights below mean high water (Collier *et al.*, 1995), and a lack of up-to-date hydrographic charts for the inter-tidal zone. New mapping techniques employing airborne laser altimetry (lidar) data (Gomes Pereira and Wicherson, 1999; Irish and Lillycrop, 1999 Hill *et al.*, 2000) have the potential to yield detailed coverage of Britain's marshes. However, datasets are currently available for only a limited number of coastal localities.

Of the possible direct approaches, the method of sounding adopted by Myrick and Leopold (1963) to obtain channel bed elevation data is inappropriate for the present study, due to the shallowness of creeks in the upper reaches of many tidal networks. Traditional techniques of field-based surveying described by Collins *et al.* (1987) and Ayles and Lapointe (1996), instead provide a straightforward source of longitudinal and cross-sectional data. For the longitudinal profile, bed elevation readings can be obtained at designated positions along the course of the network, while for measures of cross-sectional form (Zeff, 1988, 1999; Coates *et al.,* 1995), the distance between creek margins and bank and bed elevations are also readily surveyed. Although the more detailed facets of channel cross-sections are also of interest in the characterisation process, given the sample size required for an extensive study of this kind, are more appropriately recorded by observation (Rhoads and Thorne, 1996) than through an in-depth survey of each cross-section (see Knight, 1981).

2.2.3 Methods of characterisation

With the objective being an effective characterisation of saltmarsh channel networks, and having identified appropriate sources of primary data, the challenge is to establish a set of descriptors which most effectively record regularity and variability in the principal planes of morphological adjustment. Without *a priori* knowledge concerning the history of saltmarsh development at many of the study localities, it is assumed that in the short term at least, tidal channel networks tend towards a state of adjustment with contemporary boundary conditions (Leopold *et al.,* 1964). As such, the planimetric, longitudinal and cross-sectional characteristics of interest are those governed by, or closely related to physical environmental controls. In anticipation of the second objective of this thesis, which seeks to establish relations between physical controls and morphological characteristics, employing a methodological approach which facilitates the geomorphic interpretation of selected measures in terms of deterministic rather than random influences, is of pivotal importance.

Although developed in the realm of fluvial geomorphology, a substantial number of approaches to network characterisation are documented in the literature, which can be readily translated to a tidal context. *Descriptive* methods of analysis figure prominently in studies concerning all three morphological planes. They represent a useful starting point from which generic trends in: the branching structure and orientation of creek formations (Zernitz, 1932; Howard, 1967); cross-sectional shape (Rosgen, 1994); and manner of longitudinal descent (Hack, 1957), can be established. Although yielding a nominal scale of measurement, this rudimentary method of comparative analysis provides a basis for establishing distinguishing features, which may otherwise go unnoticed if statistical procedures alone are utilised in the search for pattern and regularity. *Quantitative* morphologic expressions, in the form of morphometric indices (Gardiner and Park, 1978), have also been widely implemented in the characterisation of fluvial networks (Horton, 1945; Schumm, 1956; Melton, 1958a; Strahler, 1958, 1964; Abrahams, 1984). Although their application in tidal systems has so far been limited (see, for example, Woldenberg, 1972; Zeff, 1988; Knighton *et al.,* 1992; Coates *et al.,* 1995), a numerical approach employing higher order measurements is particularly well suited to the development of an empirical basis for morphological characterisation.

The characterisation of *longitudinal* adjustment, has typically been undertaken using graphical representations of downstream changes in bed elevation (Morisawa, 1962;

Myrick and Leopold, 1963; Yang, 1971; Collins *et al.*, 1987; French and Stoddart, 1992), while sequences of profiles are widely employed as indicators of variability in *cross-sectional* shape (Pestrong, 1965; Collins *et al.*, 1987; French and Stoddart, 1992). Although each of these approaches promises a useful initial insight into the natural variability of channel morphology, a limited selection of morphometric indices have also been used to quantify network-wide patterns of adjustment (Collins *et al.*, 1987; Zeff, 1988, 1999).

The selection of appropriate measures for *planimetric* characterisation is somewhat more involved. Previous studies at a network scale (Figure 2.6) have typically focused on: (1) pattern; (2) textural; and (3) organisational characteristics. Their history of implementation suggests pronounced variability in the performance of associated descriptors. While the geomorphological significance of pattern and textural measures are widely accepted, the discriminatory power of measures of channel organisation is more questionable. Approaches based on hierarchical topological ordering and fractal geometry have proved useful as a means of channel network simulation (Abrahams, 1984; Agnese *et al.*, 1996). However, there is little evidence to suggest that the measures obtained are distinguishable from other biological branching structures, such as a tree or the human respiratory system (see Kirchner, 1993). The ability of organisational descriptors to characterise tidal formations, as distinct from other types of network, is therefore called into question. Furthermore, the geomorphological interpretation of results obtained remains unclear, since meaningful associations with physical environmental controls have proved elusive (Werritty, 1972). In view of these limitations, and in the absence of alternative organisational measures, their omission from the present study is reasonably justified.

From the subsets of pattern and textural indicators (Figure 2.6), a comprehensive characterisation of network density, channel spacing and sinuosity is not feasible by descriptive methods alone. A set of 'optimal descriptors' of network form, defined by Gardiner (1978) as *'those morphometric variables which economically express the most important* [morphological] *attributes'*, are instead required. Since a substantial number of inter-correlated expressions are documented in the literature (see Strahler, 1964; Abrahams, 1984), preferred measures are identified with regard to the sub-set of conceptually irreducible elements distinguished by Gardiner (1978) in a study of redundancy in channel network indices.

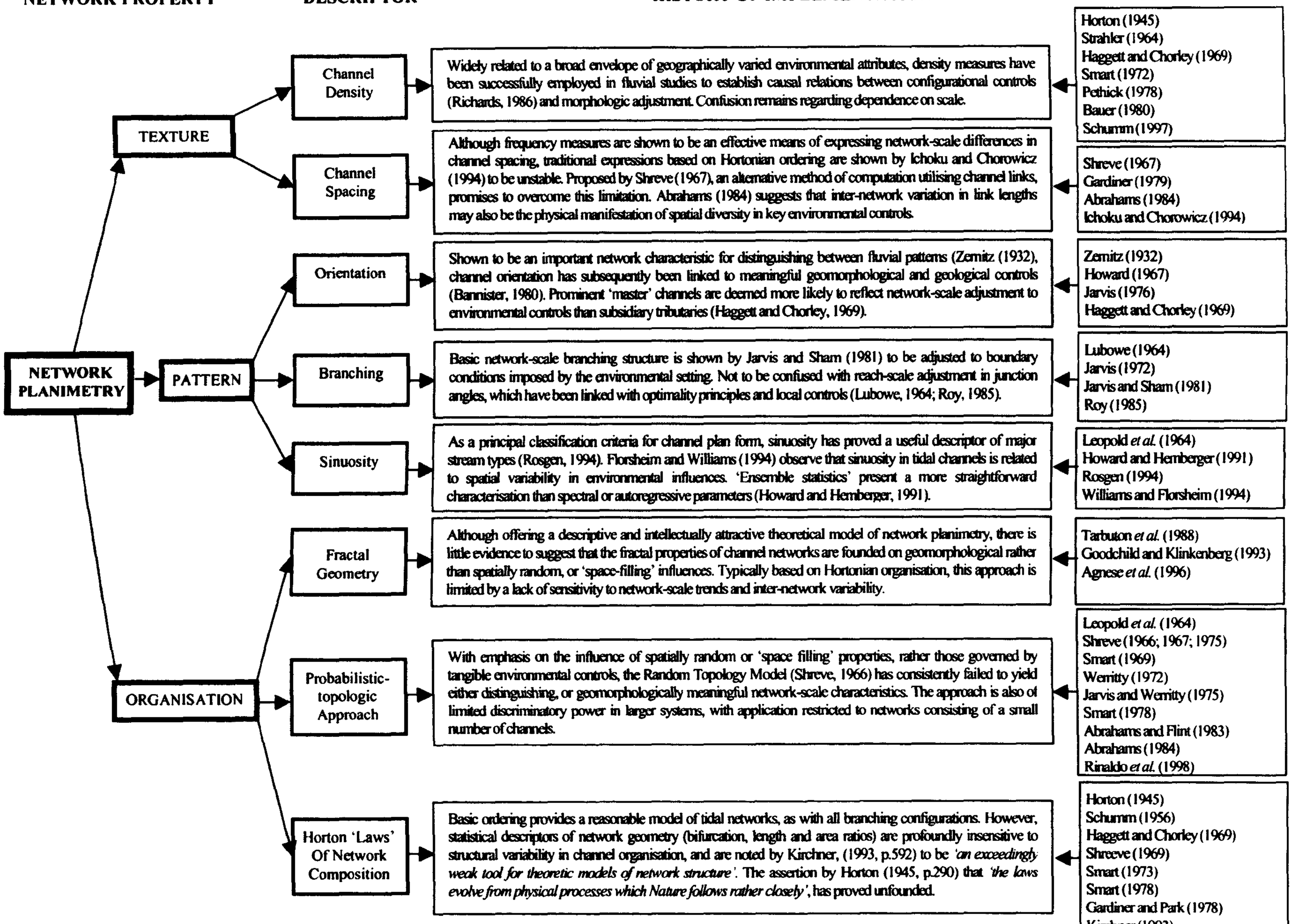

Figure 2.6 Structuring and evaluation of analytical approaches in the study of channel network planimetry.

Claimed by Coates *et al.* (1995) to be the single most important parameter of network planimetry, *creek density* is expressed in the conventional form as a ratio between the total channel length and area (Horton, 1945). Portraying the 'completeness', rather than degree of surface dissection, channel spacing or frequency (Schumm, 1956) is conceptually distinct from density, and equally difficult to ascertain from visual examination alone. A range of morphometric indices have been proposed for its quantification, the optimal of which is defined by Shreeve (1967) and later referred to by Ichoku and Chorowicz (1994) as '*link-based texture*'. The potential of *mean link length* to distinguish between the spacing of channels is recognised by Abrahams (1984). A composite measure of mean link length involves both total channel length and link frequency, and stands apart from density and frequency indices because it is not dependent on area. A further distinction between exterior and interior link lengths (see also Mock, 1971) is made by a number of authors (see Schumm, 1956; Krumbein and Shreve, 1970), the systematic behaviour of which promises insight into the operation of spatially varied environmental controls (Abrahams, 1984). *'Percentage channel cover'* is proposed here as an alternative textural measure, which reflects the mutual adjustment of channel width and length to imposed boundary conditions. The complexity of computing a three-dimensional expression of channel volume, which Gregory (1977) suggests provides the most realistic basis for density measures, is preclusive. Other excluded expressions that exhibit pronounced inter-correlation with the above indices (Gardiner, 1978) include: the constant of channel maintenance (Schumm, 1956); and length of overland flow (Horton, 1945).

The traditional definition of *sinuosity*, as applied in fluvial classifications of planimetric form (see Knighton, 1998), expresses the ratio between the straight and sinuous lengths of a channel reach. However, as shown in Figure 2.7a, calculating a network wide sinuosity as the sum of sinuous or straight measures relating to individual reaches or *links*, masks wandering in the principal channel axis. This represents a significant limitation of the technique, since the route followed by the central channel is most likely to reflect morphological adjustment to imposed boundary conditions (Haggett and Chorley, 1969). The implementation of an alternative sinuosity measure based on Hortonian ordering (Figure 2.7b) effectively distinguishes the meandering central channel, but is notoriously unstable with regard to subtle changes in topological organisation. In Figure 2.7c, the addition of a single channel towards the headwaters significantly alters the sinuosity measure for the principal channel, and indeed the network as a whole.

Depicted in Figure 2.7d, an alternative measure of principal channel sinuosity provides an *ensemble* measure, capturing both reach-scale detail *and* network-scale adjustment. Although this measure requires subjective delineation of the principal channel from the headwaters through to the mouth of the system, appropriate guidelines are documented to ensure that this is carried out according to prescribed decision rules (see Horton, 1945; Strahler, 1964). Following the technique proposed by Howard and Hemberger (1991), sinuosity can then be unpacked into the constituent signals that characterise superimposed scales of meandering.

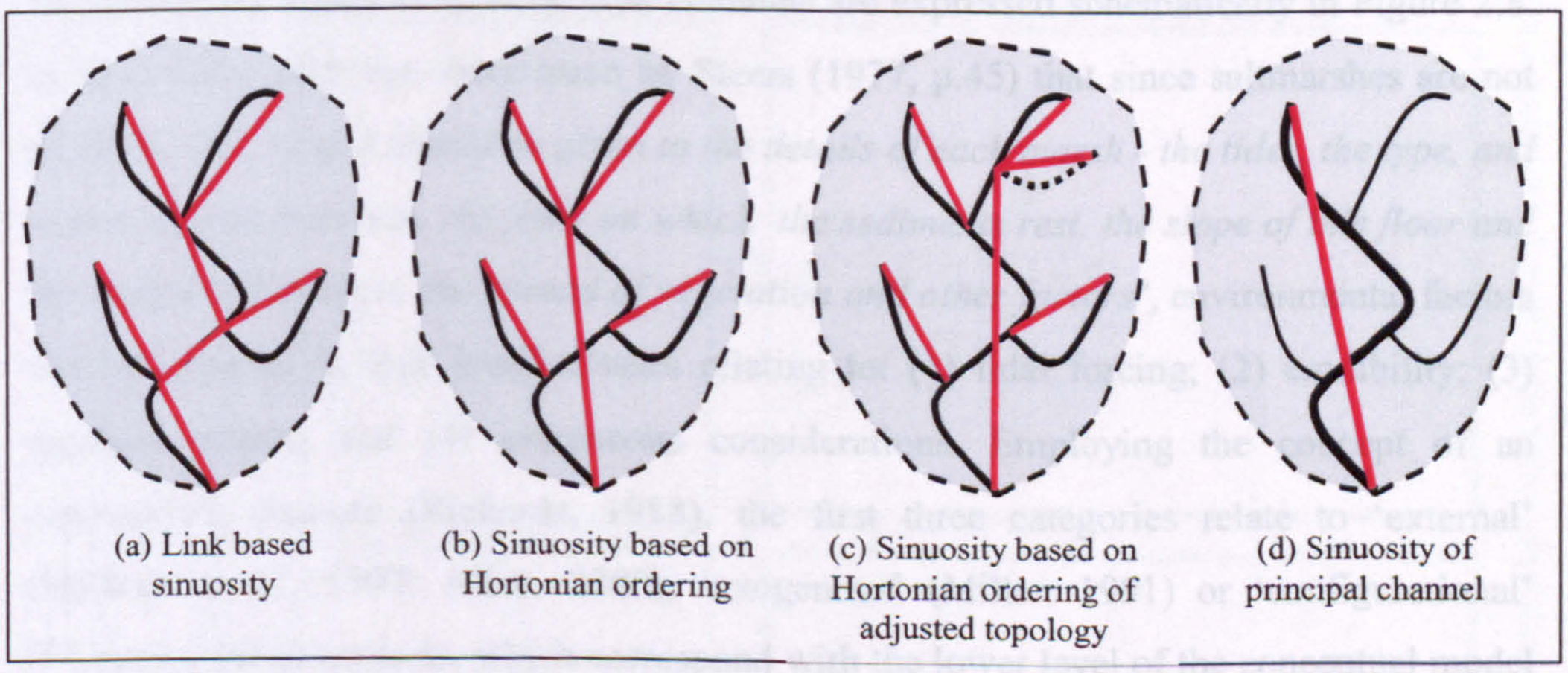

Figure 2.7 Alternative definitions of network sinuosity based on: (a) channel links; (b) Hortonian ordering; and (c) Hortonian ordering of an adjusted network; and (d) the principal channel.

While an exploratory, descriptive analysis provides a means of teasing out elementary trends in morphological behaviour, morphometric indices introduce an important element of standardisation to the characterisation procedure. As such, this combined methodological approach provides a sound basis for establishing regularities and patterns of variability in the geographically extensive sample of tidal channel networks.

2.3 INTERPRETATION OF NETWORK MORPHOLOGY

In line with the second objective of this thesis (see Figure 2.1), the interpretative phase of the study seeks to establish associations between optimal morphometric descriptors and physical environmental influences. Although Pestrong (1970) rightly acknowledges the academic value of an improved level of understanding, in practical terms this would also be of immense benefit in the design of channel systems. The construction of tidal

networks has until present been modelled on 'similar' (Collins *et al.,* 1987; Zeff, 1999) or 'nearby' (Williams and Harvey, 1983) formations, which closely resemble the project site. However, formal relations of connection clearly provide the basis for developing a better appreciation of the physical manifestation of regional diversity in boundary conditions.

2.3.1 Controlling elements and independent variables

Controlling elements (Melton, 1958a) that may exert a degree of influence over the morphological characteristics of tidal channels are expressed schematically in Figure 2.8. In accordance with the observation by Steers (1977, p.45) that since saltmarshes are not all alike, *'full weight should be given to the details of each marsh - the tides, the type, and means of sedimentation, the floor on which the sediments rest, the slope of this floor and the irregularities on it, the spread of vegetation and other factors'*, environmental factors can be grouped in four broad classes relating to: (1) tidal forcing; (2) erodibility; (3) gradient effects; and (4) extraneous considerations. Employing the concept of an *explanatory cascade* (Richards, 1988), the first three categories relate to 'external' (Haltiner *et al.,* 1997; Allen, 2000), 'exogenous' (Miller, 1991) or 'configurational' (Richards, 1986) controls, which correspond with the lower level of the conceptual model in Figure 1.5. In addition to these motive and resistive effects, the fourth category incorporates 'internal', 'endogenous', or 'direct' controls, which instead reflect differences in the developmental sequence depicted on the upper level of the model. In the literature, numerous references are made to adjustment between controlling elements and both planimetric and cross-sectional geometry. However, citations concerning longitudinal modification are comparatively rare.

Descriptive variables, defined in the singular by Melton (1958a, p.442) as *'a mathematical object that assumes values obtained by a particular method of measuring a corresponding element'*, are recorded in the literature for embodying the key environmental characteristics of the study localities. From the potential parameters (Figure 2.8), only a subset can realistically be quantified. A combination of data sources is required for their measurement. Variables such as %silt-clay content and vegetative cover are best obtained through field observation, while tidal range, inter-tidal gradient and sea level change are readily derived from secondary records. Direct and remote sources are combined in the calculation of indices such as tidal prism and hydraulic duty (Allen, 1997). Given the *Large-N* sample of study localities, there is no obvious means of

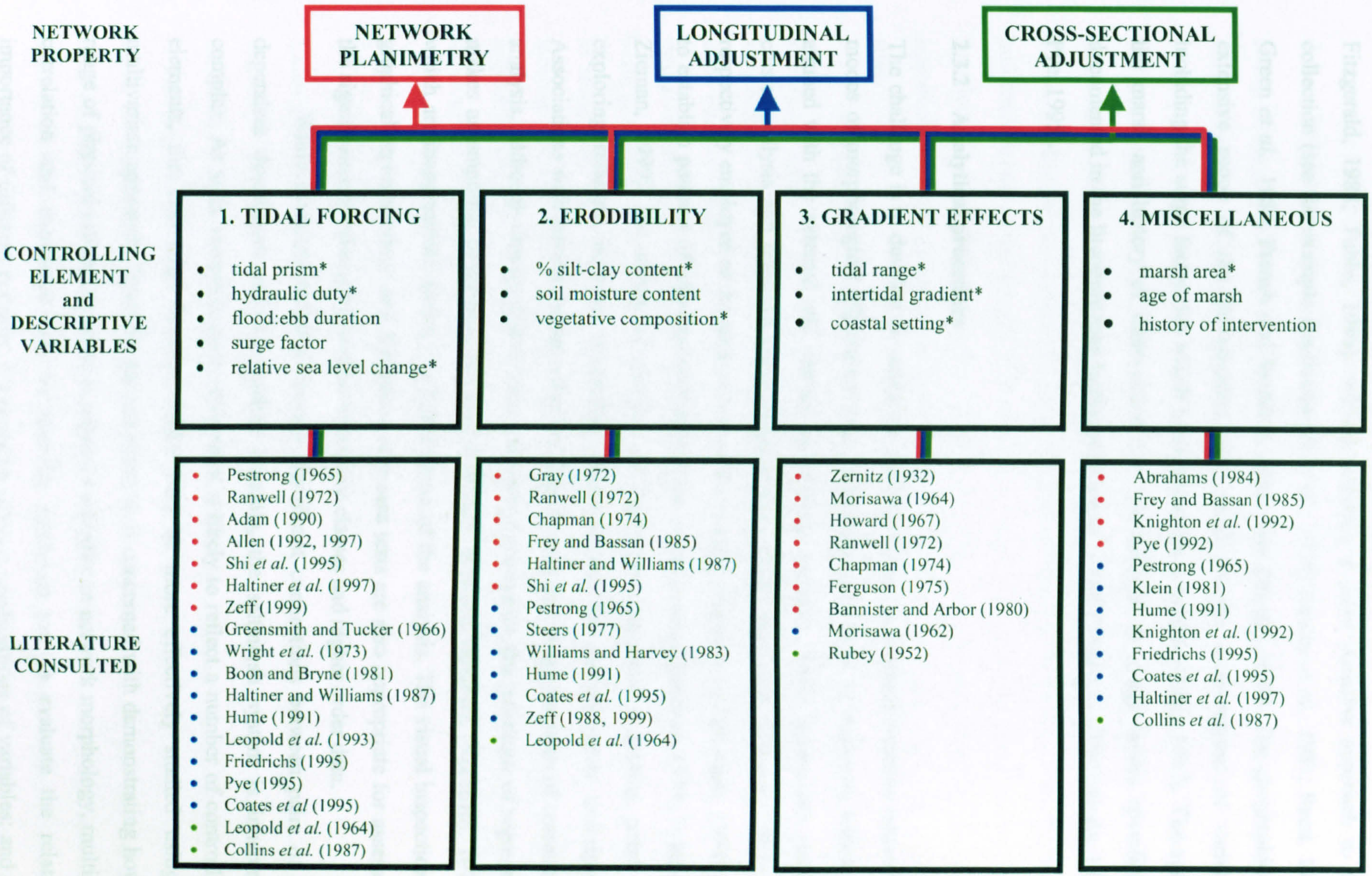

Figure 2.8 Schematic representation of associations cited in the literature between controlling elements and dependent network properties (* represents the subset of variables which can realistically be quantified).

quantifying temporally varying properties like soil moisture content (Pestong, 1965) and flood:ebb duration (Pestrong, 1965; Ranwell, 1972; Wright *et al.,* 1973; Lincoln and Fitzgerald, 1988; Tubbs, 1999), without adopting a more intensive approach to data collection (see for example Bayliss-Smith *et al.,* 1979; Healey *et al.,* 1981; Reed, 1985; Green *et al.,* 1986; French and Stoddart, 1992; also Pringle, 1995). The geographically extensive scope of the investigation also precludes the measurement of variables including the surge factor, for which limited data are available (Pugh, 1987). The age of the marsh and history of intervention are also difficult to gauge unless specifically documented in the literature (see Inglis and Kestner, 1958; Chapman, 1974; Doody, 1992; Pye, 1995).

2.3.2 Analytical procedure

The challenge is to develop an analytical procedure that successfully unpacks systematic modes of morphological adjustment into characteristic patterns of response, which are attuned with the external and internal controlling elements. While approaches such as cluster analysis and principal components (Davis, 1985; Shaw and Wheeler, 1997) are respectively employed in the study of networks as a classificatory tool (Rosgen, 1994) and to establish patterns of interdependence between variable sets (Gardiner, 1978; Tyler and Zieman, 1999), the *statistical analysis of dependence* provides a starting point for exploring relations between controlling elements and the morphometric descriptors. Associations with environmental variables may be explored using methods of correlation analysis. Although closely related from a statistical viewpoint, the technique of regression makes assumptions concerning the causal relation between variables (Norcliffe, 1977), which are inappropriate during this initial phase of the analysis. The visual inspection of graphical representations and difference of means tests are also appropriate for assessing the significance of relations between descriptive classes and higher order data.

While bivariate analyses identify significant connections between pairs of the dependent descriptors and independent controls, the saltmarsh system is inherently complex. As such, morphological adjustment is likely to reflect a number of controlling elements, the interaction between which may be more effectively studied using a multivariate approach. Since the present research is concerned with demonstrating how a range of physical influences relate to natural variability in network morphology, multiple correlation and regression may be usefully employed to: (1) evaluate the relative importance of different controls; (2) establish optimal combinations of variables; and (3)

infer causal relations which can be explored in more detail through the implementation of an intensive mode of analysis.

2.4 EVALUATION OF PHYSICAL FUNCTION

A logical progression from the exploratory characterisation and interpretation of saltmarsh channel network morphology, involves the further investigation of 'substantial relations of connection', in the search for 'formal relations of causality' (see Table 2.1). In line with the third objective outlined in Figure 2.1, the evaluation of physical function seeks to establish which of the key physical functions (Section 1.3.2) are important in controlling the morphological adjustment of saltmarsh channel networks. As noted in Section 1.4.6 and summarised schematically in Figure 2.9, a range of models have been used to link function and form. Following a brief evaluation of the various approaches, Section 2.4.1 introduces the two theoretical mathematical models that have been selected for the present study.

Following the observation by Richards (1996, p.172) that *'as the scientific knowledge about a phenomena increases, so the methods required to extend that knowledge further are likely to be adapted'*, the transition from an extensive towards a more intensive methodological procedure is necessary to improve explanatory power. The intensive strategy is synonymous with increases in both the conceptual level and spatial scale of analysis. As such, it typically involves the detailed analysis of a *Small-N* number of study sites. Considerations leading to the identification of an appropriate case study location are described in Section 2.4.2. Strategies employed in data acquisition for the respective models are introduced in Section 2.4.3, although details of the methods involved are reserved for the relevant sections of Chapter 7.

2.4.1 Theoretically-based mathematical models

Success of the intensive study depends, to a large extent, on selecting appropriate theoretical bases from the range of approaches documented in the literature. The summary diagram in Figure 2.9 indicates that models of differing complexity have been employed in studying tidal channel networks. Black-box empirical models (Kirkby *et al.* 1987), based on regression equations and hydraulic geometry relations, are the most widely reported. Although particularly useful during exploratory phases of analysis, these offer limited explanatory power. The small number of theoretical mathematical models (Lawrence, 1996) reflects the complex parameterisations involved in modelling

interactions between creek morphology, process and function. While the absence of white-box, or process models, confirms that there is some way to go before physically-based modelling can be implemented in the study of saltmarsh channel networks, intermediate grey-box models (Kirkby *et al.,* 1987) incorporate some knowledge of process and the conditions under which adjustment proceeds. Furthermore, they are consistent with the 'top-down' approach called for by Pethick (1996), whereby their application proceeds with a fairly high level of abstraction, rather than the detail of a 'bottom-up' strategy. Although successfully employed in the investigation of specific process mechanisms (Knight, 1981; French and Stoddart, 1992), this latter approach has been criticised for its failure to accommodate broad-scale interactions within the system as a whole.

Grey-box theoretical approaches can usefully be divided into two distinct classes (see Knighton, 1998):

1. Deterministic model - based on physical laws which are known to control the behaviour of natural systems; and
2. Probablistic model - based on the tendency of natural systems to adjust in response to guiding theoretical principles.

Research efforts have tended to concentrate on the former approach, with limited application of the latter in tidal systems. Of the deterministic models, the application by Friedrichs (1995) of the physically-based concept of stability shear stress to explain the adjustment of cross-sectional geometry, satisfies the criteria outlined by Kirkby (1996) for a 'good model'. While the physical basis appears sound, the model is simplistic and of general applicability to saltmarsh channel networks under a range of environmental conditions. Although the model by Mehta *et al.* (1976) employs a similar approach, it is less readily implemented. Of the probablistic models, initial findings by French (1996) suggest that the branching geometry of saltmarsh creeks may be adjusted to minimise various operation and maintenance 'costs', which in turn provide an indication of which physical functions the network is most likely to perform.

2.4.2 Case study location: Brancaster Marsh, Norfolk

A number of 'rules' govern the choice of study locality in intensive research. Of foremost importance is *'the identification of the properties of the site that have led to its selection in order that the mechanisms under investigation might be expected to produce*

DETERMINISTIC MODELLING APPROACH

Physical mechanisms have recently been employed by a number of authors as a basis for predicting various modes of morphological adjustment. Friedrichs (1995) uses a stability shear stress threshold to predict cross-sectional geometry, building on the less readily implemented deterministic approach of Mehta *et al.* (1976). Although numerical models are successfully employed by French and Clifford (2000), Falconer and Chen (1991) Schuepfer *et al.* (1988) and Boon and Byrne (1981) in morphodynamic studies, saltmarsh channel networks are treated as a general part rather than specific feature of the wider intertidal system.

KEY REFERENCES

Mehta *et al.* (1976)
Boon and Byrne (1981)
Schuepfer *et al.* (1988)
Falconer and Chen (1991)
Friedrichs (1995)
French and Clifford (2000)

PROBABLISTIC MODELLING APPROACH

Modelling approach with the least number of documented applications* in the study of tidal channel networks. Optimality criteria applied to branching geometry by French (1996) to ascertain which physical functions saltmarsh creeks are most likely to perform. Based on the hypothesis that tidal channels are adjusted to minimise energy expenditure, Langbein (1963a, 1963b) derived hydraulic geometry equations.

KEY REFERENCES

Langbein (1963a, 1963b)
French (1996)

PROBABLISTIC

DETERMINISTIC

EMPIRICAL

EMPIRICAL MODELLING APPROACHES

Most widely documented* of the modelling approaches, numerous empirical associations in a range of estuarine channels (for example Myrick and Leopold, 1963; Wright *et al.*, 1973; Chantler, 1974; Pethick, 1994, 1996), tidal inlets (see O'Brien, 1969; Johnson, 1973; Hume, 1991; Gao and Collins 1994) and U.S. creeks (Haltiner and Williams, 1987; Coates *et al.*, 1995) suggest causal links between the drainage function performed by tidal channels and cross-sectional geometry.

KEY REFERENCES

Simons and Albertson (1960)
Myrick and Leopold (1963)
Leopold *et al.* (1964)
O'Brien (1969)
Woldenberg (1972)
Johnson (1973)
Wright *et al.* (1973)
Chantler (1974)
Haltiner and Williams (1987)
Zeff (1988), (1999)
Hume (1991)
Pethick (1994), (1996)
Gao and Collins (1994)
van Dongeren and de Vried (1994)
Coates *et al* (1995)

Figure 2.9 Evaluation of modelling approaches employed in studying form-function relations in tidal channel networks.
(*width of box is proportional to number of studies documented in the literature)

observable events consistent with the hypothesis being evaluated' (Richards, 1996, p.184). For the present study, these considerations include the selection of a site, which is perceived to be in a stable state of adjustment with contemporary environmental controls, and lacking in obvious artificial intervention due to reclamation, the construction of seawalls, or training of the adjoining tidal waterway. In terms of network morphology, the choice of site was also guided by: (1) an absence of through flowing reaches which complicate flow patterns; (2) the lack of obvious internal degradation; and (3) avoiding systems where headward reaches have obviously exploited lines of least resistance such as borrow pits. Richards (1996) goes on to recognise that practical considerations are also important. The availability of high-resolution, remotely sensed terrain data was a primary concern, together with ease of access for the acquisition of complementary field measurements.

For the present study, Brancaster Marsh situated on the north Norfolk coast is selected as an illustrative case study. From an historical perspective, the expanse of saltmarsh of which this is an example, has developed during the latter stages of the Holocene marine transgression, through the deposition of inorganic mud in the lee of a complex band of fronting sand and shingle structures (Steers, 1959, 1977; Pye, 1992). The site experiences meso-tidal conditions, with mean high water spring (*MHWS*) tides attaining a stage of 3.25m OD and the highest astronomical tide estimated at 3.95m OD (Hydrographic Office, 1997). Marsh surface elevation is at a level of approximately 2.5m OD, and as such is inundated during high neap and spring tides. Freshwater runoff from the land is negligible. The sample network is situated in a back-barrier setting (Figure 2.10), which affords protection from wave action. The channel floor is incised into a resistant sandy substratum that was laid down during former conditions of high energy wave activity (Steers, 1959). Field samples (see Section 6.2.4) indicate that the substrate comprises on average 6% silt-clay, whereas the channel wall exhibits a markedly higher value of 46%. The discordant nature of bed and bank materials may affect the relative ease of entrainment, and ultimately the susceptibility of the channel margins to deformation by tidal action. The principal channel drains freely into the adjacent Mow Creek, which constitutes the main connection to the harbour at Brancaster Staithe. There is no indication of intervention in the regime of this waterway, through dredging or training wall construction. The rear of the system adjoins a golf course, which is also protected by the fronting dune ridge. Areas of higher terrain partially enclose the marsh platform, creating in the terminology of Chapman (1974), a semi-closed marsh. The

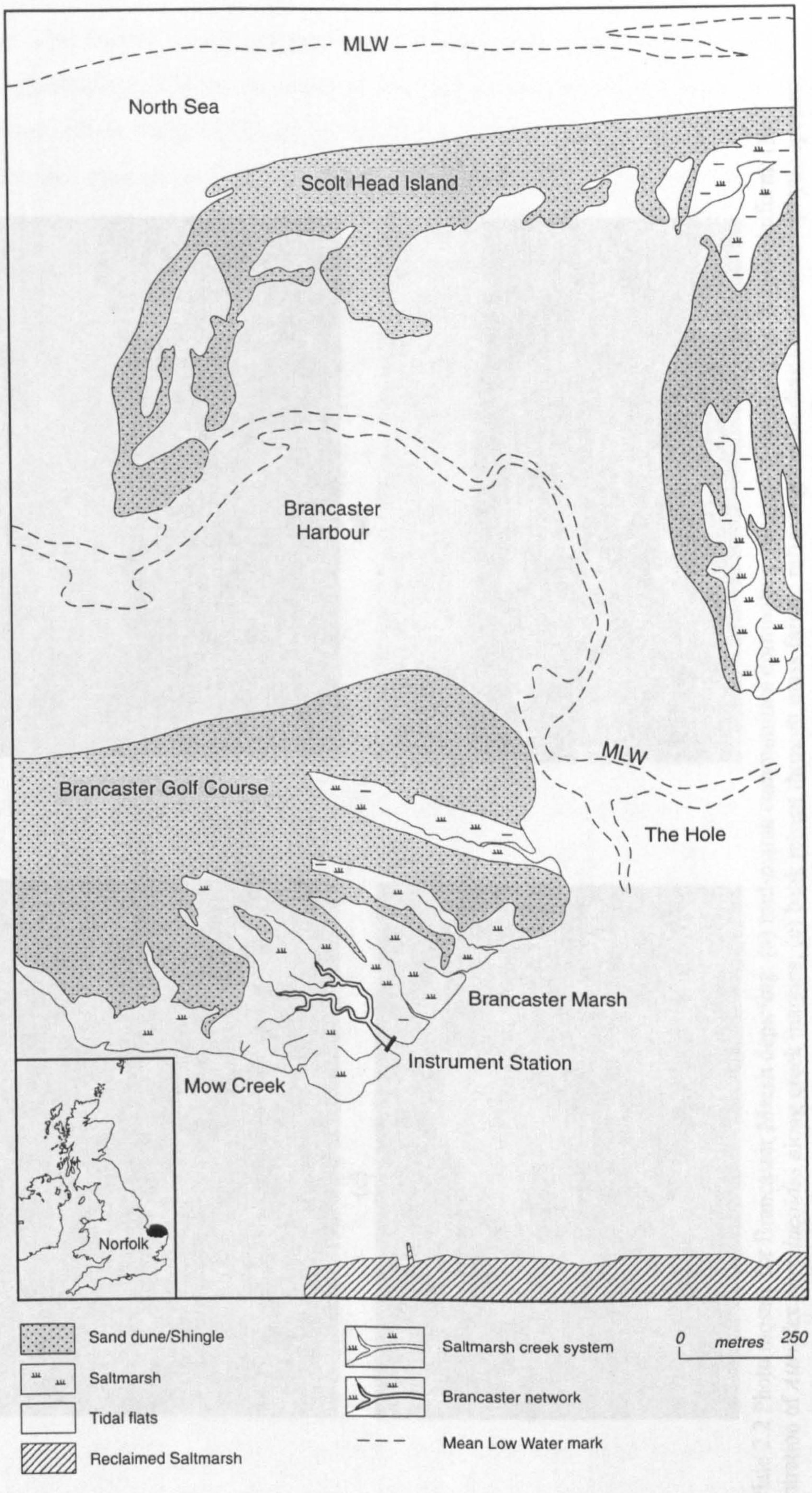

Figure 2.10 Site map for Brancaster Marsh, Norfolk.

(a)

(b)

(c)

(d)

Plate 2.2 Photo mosaic for Brancaster Marsh depicting: (a) mid-marsh communities dominating vegetative cover on the marsh platform; (b) concentration of *Attriplex portulacoides* along creek margins; (c) bank retreat through mass failure reflecting the binding action of halophytic species; (d) prominence of pioneer species as marsh surface elevation diminishes towards Mow Creek.

conditions. The floristic cover comprises mid-marsh communities (Adam, 1981; Burd, 1989), in which diagnostic species such *as Puccinellia maritima* and *Limonium vulgare* are prominent (Plate 2.2a). *Attriplex portulacoides* is also widespread, although swards are concentrated throughout the headwaters and along creek margins (Plate 2.2b) where root binding action supports bank retreat by mass failure (Plate 2.2c). Pioneer species including *Spartina spp.* and *Salicornia spp.* are prevalent towards the front edge of the marsh, where surface elevation diminishes (Plate 2.2d). The site is managed by the National Trust, and in recognition of floristic and accompanying ecological diversity, lies within the North Norfolk Coast Site of Special Scientific Interest. It is also designated as a Ramsar Site, SPA, area of Heritage Coast and Area of Outstanding Natural Beauty (NRA, 1995).

2.4.3 Data acquisition strategy

A combination of remotely sensed imagery and field-based measures comprise the principal sources of data for this intensive phase of the study. For the model of optimal angular geometry, the measurement of branching angles from high-resolution aerial photography (see, for example, Pieri, 1985) is preferable to reliance on the abstracted representation of blue-line topographic maps (see Lubowe, 1964; Roy, 1985), or imprecise nature of field-based compass measurements (Howard, 1971).

Following translation from a fluvial (Roy, 1983) to a tidal context (French, 1996), an expression for the 'dominant' (Myrick and Leopold, 1963) or geomorphologically significant discharge associated with ebb drainage, is the other parameter driving this model. Discharge is used to compute a ratio between the tributaries at any particular junction. As such, the *relative* rather than absolute magnitude of responses is important. Since the acquisition of actual discharge readings at multiple stations throughout a network is problematic (Roy, 1985), a range of surrogate measures have been employed in its place, including link magnitude (Pieri, 1985) and upstream area (Roy, 1985; French, 1996). As outlined previously in Section 2.2.2, both of these series are readily obtained from scanned photographic coverage by the procedure of on-screen digitising. In studies by Haltiner and Williams (1987) and Coates *et al.* (1995), tidal prism is also implemented as a proxy for discharge. Various procedures have been employed to compute prism, including time integrated discharge readings (Wright *et al.,* 1973; De Jonge, 1992; French and Stoddart, 1992) and planimetering topographic maps (Boon and Byrne, 1981). However, the advent of high-resolution terrain data supports a far more straightforward

method of calculation. Discussed below in the context of hypsometric models, the total tidal prism for a given area of marsh can be measured as the volume held between the marsh surface and a given tidal datum.

An alternative approach to data acquisition is needed for the model of cross-sectional geometry, because a*bsolute* discharge readings are required at sample stations throughout the creek system. The use of current meters for the direct calculation of discharge from velocity measures is widely documented (Postma, 1961; Ward, 1978, 1981; Carling, 1981; Reed *et al.,* 1985; Lincoln and Fitzgerald, 1988; Stoddart *et al.,* 1989; Wells *et al.,* 1990; French and Clifford, 1992; Pringle, 1995). Although this approach has proved useful for 'at-a-station' readings (see for example Roman, 1984; De Jonge, 1996), 'downstream' measurements (Myrick and Leopold, 1963; Bayliss-Smith *et al.,* 1979; Knight, 1981; French and Stoddart, 1992) are fundamentally constrained by logistical factors, such as the required number of sensors.

Discharge readings may otherwise be generated using a hypsometric model (see, for example, Wright *et al.,* 1973; Boon, 1975; Settlemeyer and Gardner, 1977; Pethick, 1980, 1996; Boon and Byrne, 1981; Fitzgerald and Nummedale, 1983; Hume, 1991). Although originally implemented in the study of landscape evolution (Langbein, 1947; Strahler, 1962, 1964; Schumm, 1956; Moglen and Bras, 1995), Ragotzkie and Bryson (1955) modified the basic area-altitude model to yield conveyance-storage relations, which Boon (1975) subsequently employed as a basis for generating discharge measures in tidal creeks. Successful implementation of the hypsometric model depends upon the availability of remotely sensed imagery for the site, and an accurate terrain model. While it has already been established that high resolution aerial photography is the optimum media for mapping saltmarsh channel networks, a range of sources have previously been employed for terrain data. High density surveying (Collins *et al.,* 1987; Haltiner and Williams, 1987; French and Stoddart, 1992), topographic maps and charts (Gao and Collins, 1994) and sequential photography (Boon, 1975; Pethick, 1980) are the most widely documented. However for the present study, newly available airborne lasar altimetry (Hill *et al.*, 2000) is the most appropriate source. The Environment Agency flew the lidar coverage (see Figure 2.11) during 1997 under low tidal conditions. With a spatial resolution resampled to 2m and sub-millimetre vertical precision (P. Butcher, personal communication), it provides a high-density grid of elevation readings. Rather than resorting to time consuming field-based surveys, channel cross-sections were recorded using the standard profiling facility of Erdas Image software (Erdas, 1997).

The model is also driven by temporal changes in tidal stage, the prediction of which is presently limited by the complex parameterisation of shallow water distortions (see for example Boon, 1975; Boon and Byrne, 1981; Falconer and Chen, 1991; Friedrichs and Madsen, 1992). Stage measurements were acquired using an automated pressure sensor system (see Reed *et al.*, 1999).

Despite the fairly widespread application of the hypsometric model in tidal environments, it is important to verify the accuracy of discharge measurements computed by this 'remote' method, by comparison with data recorded directly in the field. The final phase of data acquisition therefore involves: (1) the installation of a flow meter at a sample cross section in the Brancaster network during tidal conditions which are likely to produce a dominant discharge capable of performing geomorphic work; and (2) surveying the cross-sectional profile to establish the degree of modification since the lidar coverage was originally acquired.

Figure 2.11 Lidar coverage of Brancaster Marsh, overlaid with high-resolution aerial photography (courtesy of Environment Agency).

3. PLANIMETRIC CHARACTERISATION

3.1 INTRODUCTION

Initial observations concerning the planimetric structure of tidal channels were descriptive in nature (Ragotzkie, 1959; Chapman, 1974; Marshall, 1962). Based on the visual interpretation of aerial photography, these studies contributed little more than an overview of the most general network characteristics. With the advent of morphometric methods of analysis (Doornkamp and King, 1971; Gardiner and Park, 1978), a range of topological and geometrical measures of network form have been developed in a bid to translate qualitative diversity into formal quantitative expressions (see Schumm, 1956; also Strahler, 1964). However, their application to the interpretation of saltmarsh creek morphology is limited. It remains for a systematic investigation to be undertaken, as a means of establishing the commonplace, distinguishing and unusual characteristics of tidal channel network planimetry.

The extensive methodological approach introduced in Chapter 2 is implemented in the following characterisation, for the sample of study localities depicted in Figure 2.5. Techniques used to obtain qualitative expressions of form are described in Section 3.2, together with procedures employed in the generation of optimal morphometric descriptors. Working with this database, a combination of descriptive (Section 3.3) and statistical (Section 3.4) approaches are used to explore the characteristics of planimetric adjustment, and to lay foundations for the establishment of formal relations of connection and causality with physical environmental controls. Internal control exerted by scale dependence over the results obtained is considered in Section 3.5, while key findings are presented in Section 3.6.

3.2 DATA ACQUISITION

The characterisation of network planimetry employs the optimal descriptors of texture and pattern, which were introduced in Section 2.2.3 (see also Figure 2.6) as: (1) density and spacing; and (2) orientation, branching and sinuosity. A combination of qualitative and quantitative methods is appropriate for establishing characteristics of, and differences between the sample networks. Descriptive techniques yielding generic classes are most appropriate for the analysis of network scale patterns in orientation and branching, while

morphometric indices are readily computed for creek density, channel frequency, mean link lengths, percentage channel cover and network sinuosity. The following section describes the procedures involved in the acquisition of data to undertake a characterisation based on these descriptive and statistical measures.

3.2.1 Network Delineation

Aerial photography constitutes the primary source of data for characterising channel network planimetry. The vertical photographic coverage obtained for the selected network at each study locality is displayed in Plate 3.1. Insights into network planimetry, obtained directly from these photographic prints, are fundamentally constrained by the resolution of the coverage. For example, high-resolution 1:3000 coverage facilitates a fairly accurate interpretation of network planimetry by visual analysis alone, whereas flow lines are more difficult to identify on 1:13 000 imagery. In several instances, the interpretation of basic network patterns is also compromised by exaggerated adjustment in the width dimension. Due to pronounced channel widening along the River Carew (Plate 3.1.6) and River Orwell (Plate 3.1.24), orientation and branching characteristics are difficult to distinguish. In answer to these limitations, an enhanced representation of each sample network was produced from the hard-copy photographs. Following the methodological procedure outlined in Figure 3.1, imagery was converted into a digital format using a flatbed scanner, at a resolution commensurate with the nominal scale of the coverage (see Appendix 1). Panchromatic and colour photographs were converted to a common 8-bit greyscale format, which enhances the contrast between tidal channels and the background of marsh surface vegetation.

As a precursor to the extraction of morphometric data, it is important to recognise that the reliability of geometric measurements extracted from the photography depends on the magnitude of, and ability to compensate for errors introduced during the photographic process. A preliminary accuracy assessment was therefore completed (Adams *et al.*, 1998), to ascertain the influence of distortions from camera effects, shrinkage and relief displacement (Wolf, 1983) on measurements obtained from the photographic coverage of each study site. Results suggest that the total magnitude of error present in the photography is of the same order of magnitude as the sampling resolution, and that using the central 60% of the frame essentially removes the effects of distortions inherent in the scanned imagery.

DIAGRAM ON THIS PAGE EXCLUDED UNDER INSTRUCTION FROM THE UNIVERSITY

Plate 3.1 (cont.) Aerial photographic coverage depicting the network selected at each study locality. Scale bar represents 100m.

The technique of on-screen digitising (Astaras *et al.*, 1990), using Erdas Imagine image processing software (Erdas, 1997), was subsequently employed as a means of producing abstracted representations for the descriptive characterisation, and generating input data for the morphometric analysis. Channel reaches were delineated by tracing the channel mid-point, as the best approximation to the mean flow route through the system. To improve visual interpretation for the descriptive phase of analysis, omitting source channels from the digitisation procedure reduced the degree of network elaboration. Although the network is no longer depicted in its entirely, the loss of reaches that according to Haggett and Chorley (1969) are least likely to reflect underlying environmental controls, is a reasonable trade off against the simplified visual representation and increased potential to identify regularities and discontinuities between the skeletonised planimetric structures. Details of the routine involved in the extraction of geometric data are provided in Sections 3.3.3-3.3.6.

3.2.2 Morphometric Indices

From a practical viewpoint, advances in computer technology mean that producing an *inventory* of planimetric morphometry has become a feasible undertaking. The input parameters required to compute the morphometric expressions of: creek density (D);

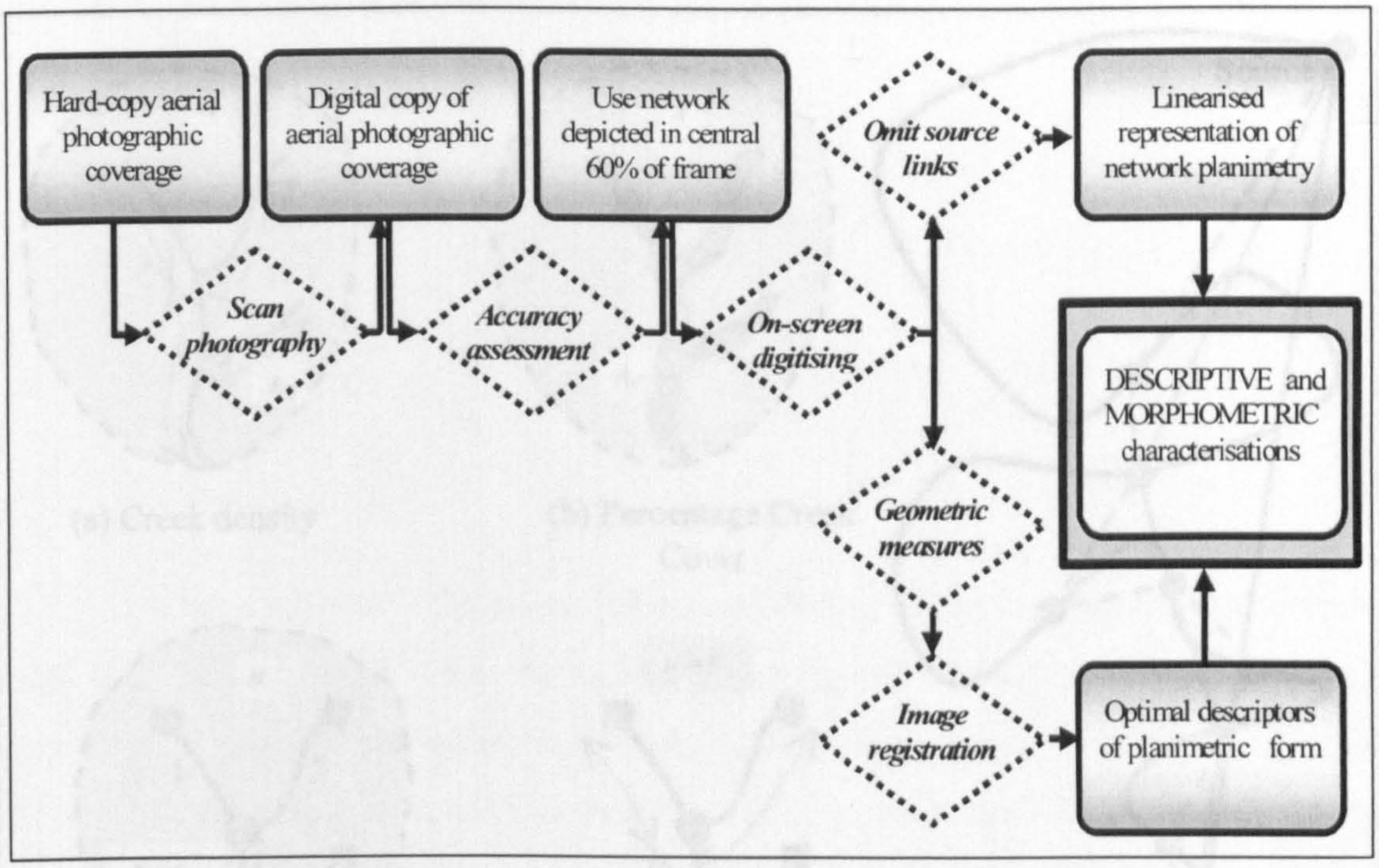

Figure 3.1 Schematic representation of the methodological procedures employed to produce data for the descriptive and morphometric characterisation of network planimetry

percentage channel cover (*%C*); link-based texture or frequency (*F*); and mean link length (*L*), are summarised by the definition diagrams in Figure 3.2a-d. An equivalent definition diagram for principal channel sinuosity (*S*) is depicted in Figure 3.2e, and includes the disassociation of this ensemble statistic into constituent network- (S_N) and reach-scale components of asymmetry (S_A) and tortuosity (S_T).

Computed according to Equation 3.1, input parameters for the calculation of creek density are the total sinuous length of channel (L_T) and the marsh area (A) (Figure 3.2a). As indicated by Equation 3.2, the computation of percentage channel cover requires the total surface area occupied by tidal creeks (A_C), in addition to marsh area (Figure 3.2b). Link-based texture (Equation 3.3) is defined in terms of marsh area and the total number of links (Shreve, 1966) within the network (N_L), where a link is defined and depicted in Figure 3.2c as, a '*channel segment between a source and the first junction downstream* [◆——●], *between successive junctions* [●——●], *or between the outlet and the first junction upstream* [●——◆]' (Werner and Smart, 1973, p.272). Mean link length (Equation 3.4) is an amalgam of the total sinuous channel length and number of constituent links. A further distinction made by Shreve (1967) between exterior (L_{EXT}) and interior (L_{INT}) mean link lengths (see also Smart, 1978), was achieved by subdividing length and frequency measures into their respective class, according to position within the network.

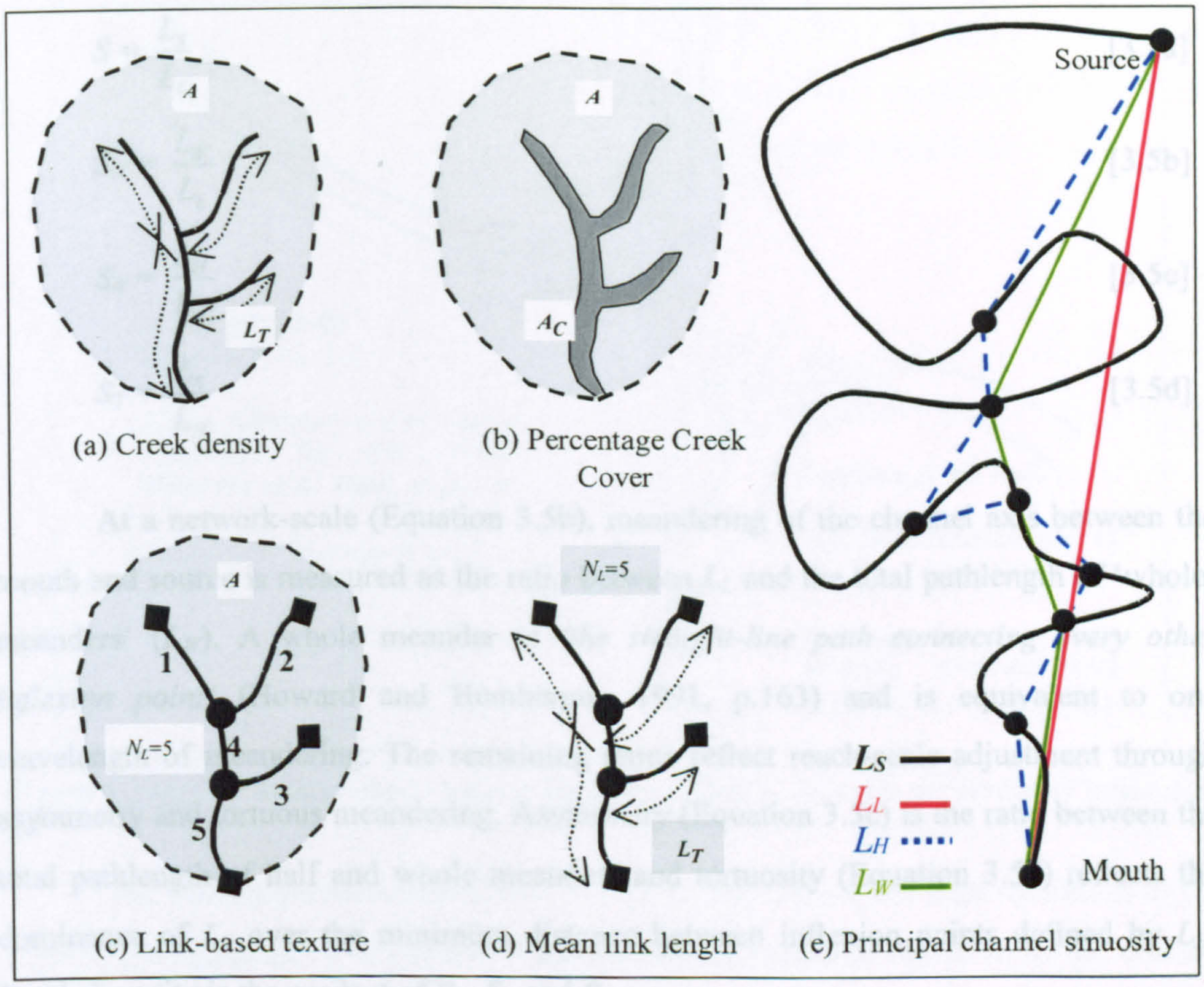

Figure 3.2 Definition diagrams for length and area measures required to compute morphometric expressions of: (a) creek density (D); (b) percentage channel cover ($\%C$); (c) link-based texture (F); (d) mean link length (L); and (e) principal channel sinuosity (S).

$$D = \frac{L_T}{A} \quad [3.1]$$

$$\%C = \frac{A_C}{A} \quad [3.2]$$

$$F = \frac{N_L}{A} \quad [3.3]$$

$$L = \frac{L_T}{N_L} \quad [3.4]$$

Total sinuosity of the principal channel (Equation 3.5a) is computed as the ratio between the sinuous (L_S) and linear (L_L) length of the principal channel (Figure 3.2e). Equations 3.5b-d unpack this composite term into three constituent spatial scales. These are based on subdividing the formation into 'half-meanders' (L_H), which are defined as *'segments of stream lying between successive inflexion points* [●] *(locations where the channel curvature changes sign downstream)*' (Howard and Hemberger, 1991, p.163).

$$S = \frac{L_S}{L_L} \quad [3.5a]$$

$$S_N = \frac{L_W}{L_L} \quad [3.5b]$$

$$S_A = \frac{L_H}{L_W} \quad [3.5c]$$

$$S_T = \frac{L_S}{L_H} \quad [3.5d]$$

At a network-scale (Equation 3.5b), meandering of the channel axis between the mouth and source is measured as the ratio between L_L and the total pathlength of 'whole-meanders' (L_W). A whole meander is *'the straight-line path connecting every other inflexion point'* (Howard and Hemberger, 1991, p.163) and is equivalent to one wavelength of meandering. The remaining terms reflect reach-scale adjustment through asymmetry and tortuous meandering. Asymmetry (Equation 3.5c) is the ratio between the total pathlength of half and whole meanders and tortuosity (Equation 3.5d) reflects the dominance of L_S over the minimum distance between inflexion points defined by L_H. Total sinuosity is the product of S_N, S_A and S_T.

3.2.3 Frequency Data

Straightforward counting of the total number of links within each network (N_L) was carried out by visual examination of scanned and enlarged hard copies of the photographic coverage. For the benefit of subsequent analysis involving mean link lengths, a distinction was made between the frequency of exterior (N_{EXT}) and interior (N_{INT}) links.

3.2.4 Length Data

Manual on-screen digitising was employed as the most reliable technique for obtaining accurate length data. The total sinuous channel length (L_T) was computed for each network, by translating the digital representation from a raster into a vector format. As depicted in Figure 3.2, the central course followed by each channel within the network was traced using Imagine software, to create a vector layer consisting of 'sinuous' channel lengths, which are at this stage measured in pixel units. To ensure that the length data were collected in a format appropriate for the computation of mean link lengths, a distinction was made between exterior and interior reaches.

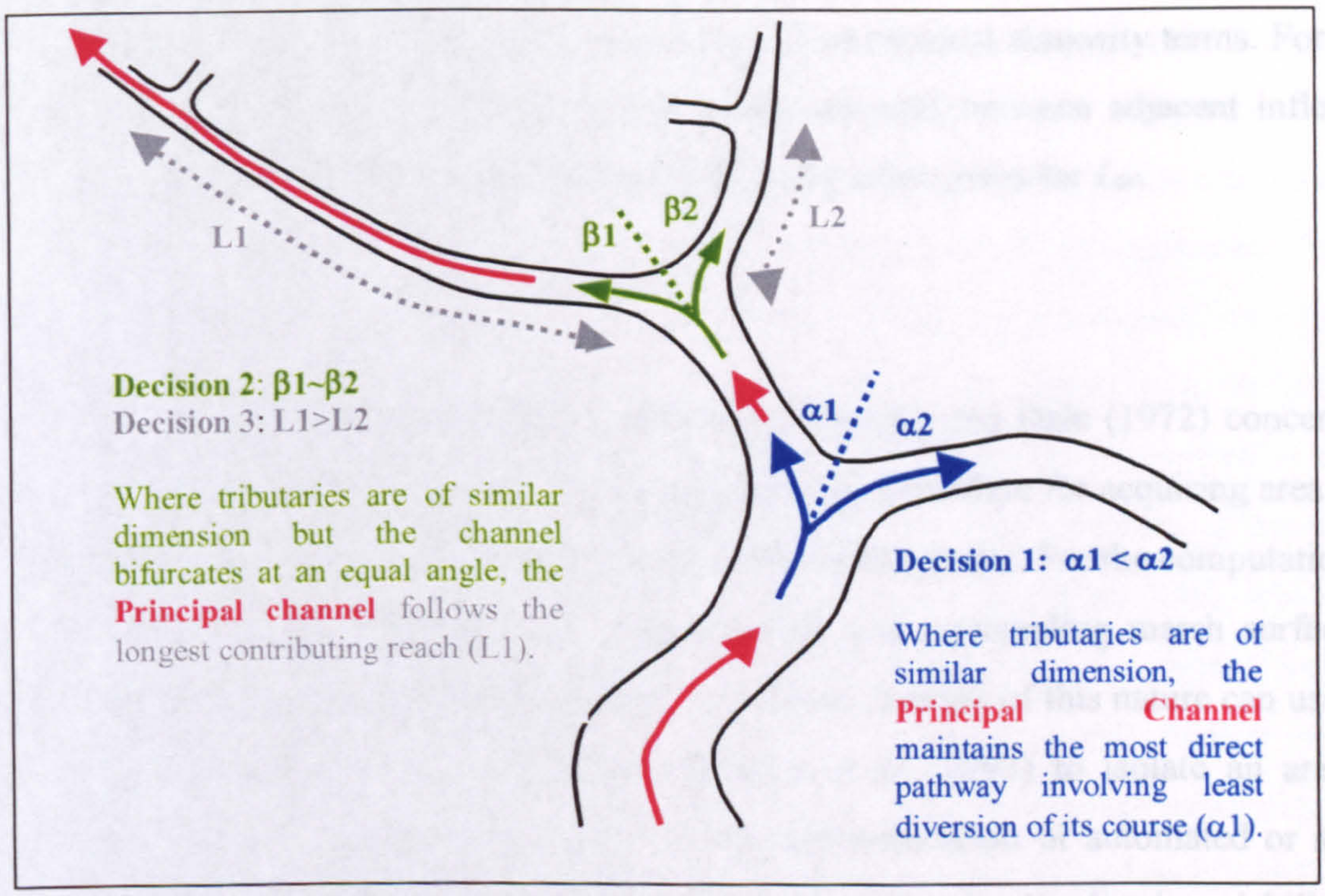

Figure 3.3 Decision rules used in identifying the principal channel for sinuosity measures.

The potential measurement error for L_T is small, since the high resolution of the original photographic coverage and scanning procedure ensure depiction of the channel networks in their entirety. Field validation confirms that even creeks which are partially bridged by dense vegetation may be discerned on the photography, due to visual contrasts between the reflectance characteristics of vegetation occurring on the better drained channel banks compared with the marsh interior. Although the 'roofed-in' channels described by Yapp *et al.* (1917) are not so readily distinguished from the imagery, these are likely to account for a comparatively small percentage of the total network length at a limited number of sites.

For the sinuosity measurements, a series of decision rules proposed by Gravelius (1914, cited in Horton, 1945, p.281) and Horton (1945) and outlined in Figure 3.3, were employed to determine the course of the principal channel. Commencing at the outlet, the dominant channel of each sample network was identified as the widest, or most branched, and traced towards the headwaters. Where reaches of a similar dimension met at a junction (Decision 1), the dominant tributary was selected as the channel maintaining the greatest continuity with respect to the orientation of the downstream reach. If tributaries branched at a similar angle (Decision 2), the channel supporting the longer upstream reach was identified as dominant (Decision 3).

Sinuosity of the principal channel was computed by digitising the sinuous (L_S) and linear (L_L) courses between the outlet and headwaters of each network. Inflexion points

were then identified, facilitating the measurement of constituent sinuosity terms. For half (L_H) meander pathlengths, the linear distance was recorded between adjacent inflexion points. A reading was similarly digitised between every other point for L_W.

3.2.5 Area Data

Contrary to the cartographic problems outlined by Chorley and Dale (1972) concerning the delineation of channel lengths in fluvial systems, the procedure for acquiring area data poses considerably more of a challenge in saltmarsh environments. For the computation of A_C, radiometric contrast between the creek network and surrounding marsh surface is clearly apparent on the scanned prints (Plate 3.1). Basic contrast of this nature can usually be manipulated through feature extraction (Sonka *et al.*, 1993) to isolate an area of interest. However as illustrated in Plate 3.2, the implementation of automated or semi-automated image segmentation algorithms was precluded by localised variability in channel reflectance characteristics, coupled with indistinct creek margins. Manual on-screen digitising was instead employed to delineate a boundary around the channel margin, and the enclosed channel area calculated (in pixel units) as a standard function of Imagine software.

Plate 3.2 Localised variability in the reflectance characteristics of creek bed and banks, at Stiffkey marshes, Norfolk.

Developed for the characterisation of fluvial networks, the measure of drainage density reflects the extent of channel formation within a given 'basin' area, the boundary of which is defined by topographic maxima (see for example Strahler, 1964; also Chorley and Dale, 1972). Based on this definition, the computation of an equivalent 'creek density' for tidal networks is complicated, since the basin analogy is not readily applied to many saltmarsh systems (see Pestrong, 1965). As illustrated in Figure 3.4a, in 'closed' saltmarshes (Chapman, 1974) the area served by a particular channel network is fairly well defined by pronounced topographic barriers such as embankments or seawalls. However, flow boundaries are far less distinct in 'open' marshes (Figure 3.4b), which are considerably more common in the sample population. Although several authors (Hartnall, 1984; Collins *et al.*, 1987; Knighton *et al.*, 1992) allude to marsh surface micro-topography, there is no record of pronounced topographic boundaries separating the morphologically active flows received by inter-digitating networks (Charbreck, 1988).

Although creek density measures are recorded for study localities in the U.S. (Ragotzkie, 1959; Pestrong, 1965; Coates *et al.*, 1995), Australia (Knighton *et al.*, 1992) and the River Dovey in Wales (Shi *et al.*, 1995), in all cases there is no record of the decision rule employed in measuring area. Following Woolnough *et al.* (1995), it is logical that tidal flows on established marshes must, on average, follow a consistent pathway, since sustained randomness in flow patterns is unlikely to support the initiation, development and maintenance of a stable channel network configuration. Delineation of a realistic measure for A therefore depends on identifying the most *probable* area of marsh served by each network. In the absence of topographic boundaries, a number of standardised decision rules (see also Rinaldo *et al.*, 1999) could be implemented, including: (1) minimum area; (2) equidistant area; and (3) maximum area.

As depicted in Figure 3.5a, a 'minimum' area (A_{min}) may be demarcated by connecting the headward or source channels, forming a polygon within which flow is more likely to move in towards the network than be directed outwards into an adjacent system. The equidistant rule (A_{eq}) arises from the recommendation by Charbreck (1988) that the midpoint between adjacent creeks be used as an arbitrary boundary (Figure 3.5b). In accordance with the observation by French and Stoddart (1992) that a proportion of overmarsh tidal flow leaves the system directly across the marsh edge, rather than being routed through the channel network, a modified version of the equidistant rule is applicable along the seaward margin. A similar equidistant boundary can be established between the marsh edge and nearest landward channel, forming the equivalent of a fluvial

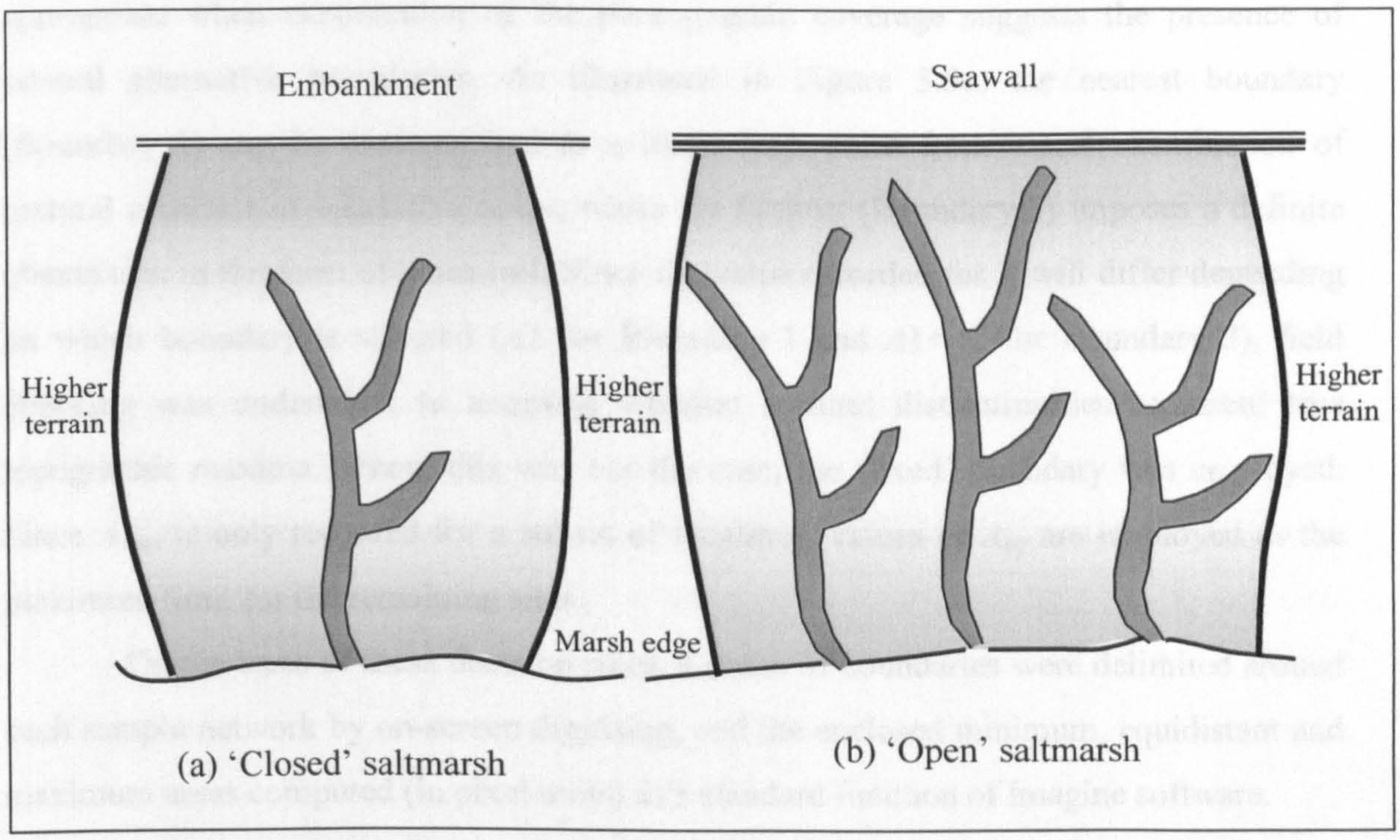

Figure 3.4 Delimiting marsh area (*A*) in: (a) 'Closed' saltmarsh; and (b) 'Open' saltmarsh systems (adapted from Chapman, 1974).

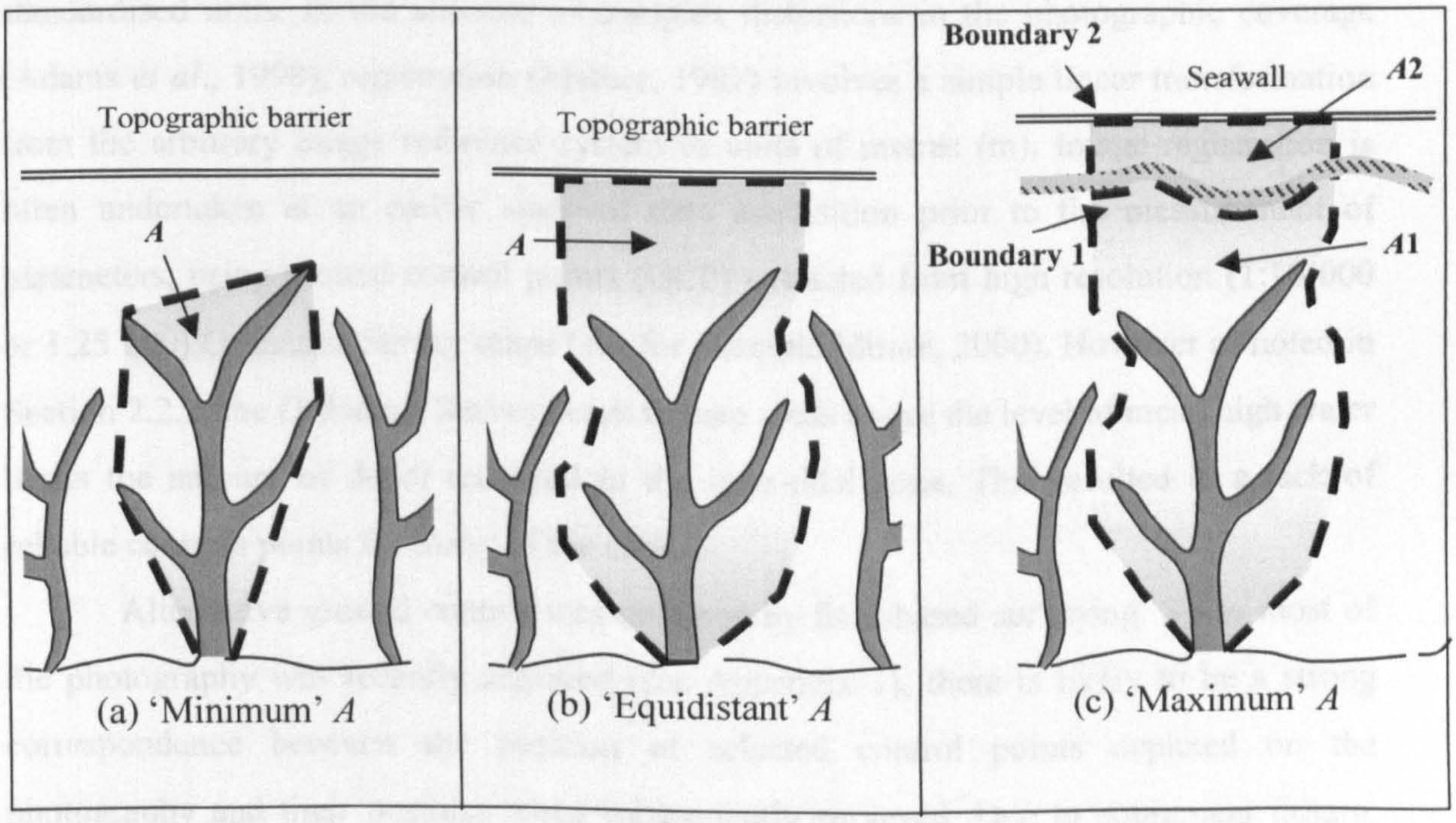

Figure 3.5 Delineation of *A* based on: (a) Minimum area; (b) Equidistant area; and (c) Maximum area decision rules.

'inter-basin' area (Schumm, 1956). The computation of a 'maximum' area (A_{max}) is appropriate when examination of the photographic coverage suggests the presence of several alternative boundaries. As illustrated in Figure 3.5c, the nearest boundary (Boundary 1) can be distinguished as a likely high point from visual examination of textural contrasts in vegetative cover, while the farthest (Boundary 2) imposes a definite obstruction in the form of a seawall. Since the value recorded for A will differ depending on which boundary is selected ($A1$ for Boundary 1 and $A1+A2$ for Boundary 2), field checking was undertaken to ascertain whether textural discontinuities represent true topographic maxima. Where this was not the case, the 'fixed' boundary was employed. Since A_{max} is only recorded for a subset of localities, values of A_{eq} are employed as the maximum limit for the remaining sites.

On the basis of these decision rules, a series of boundaries were delimited around each sample network by on-screen digitising, and the enclosed minimum, equidistant and maximum areas computed (in pixel units) as a standard function of Imagine software.

3.2.6 Image Registration

To facilitate inter-network comparison between dimensional morphometric measures such as creek density, the basic length and area parameters need to be converted into standardised units. In the absence of complex distortions in the photographic coverage (Adams *et al.*, 1998), registration (Mather, 1987) involves a simple linear transformation from the arbitrary image reference system to units of metres (m). Image registration is often undertaken at an earlier stage of data acquisition prior to the measurement of parameters, using ground control points (GCP) extracted from high resolution (1:10 000 or 1:25 000) Ordnance Survey maps (see for example Moore, 2000). However as noted in Section 2.2.2, the Ordnance Survey remit to map areas above the level of mean high water limits the amount of detail recorded in the inter-tidal zone. This resulted in a lack of reliable controls points for many of the sites.

Alternative ground control was obtained by field-based surveying. Since most of the photography was recently acquired (see Appendix 1), there is likely to be a strong correspondence between the position of selected control points depicted on the photography and their position when subsequently surveyed. Due to equipment failure, field survey data were not available for networks at Burry Inlet, Lymington, Maplin Sands and the River Crouch. For these sites, control points were instead obtained from 1:10 000 scale maps. Where recent lidar coverage was available for the Brancaster marshes, a basic

linear transformation was performed using Imagine software. Elsewhere, registration was performed using a least squares fit to generate a scaling factor. The distance (in metres) between points of known position was surveyed in an arbitrary co-ordinate system, and related to the distance between corresponding pixel positions on the scanned imagery.

The resulting coefficients of determination range between $R^2 = 0.98$-0.99. High values such as these indicate that the linear model provides an appropriate transformation. Further analysis of the confidence limits about the regression coefficient translates to an error margin in *D* (computed according to the equidistant decision rule) of <5% for transformations involving field survey, and ≤10% for map-derived control points. Having obtained the necessary scaling information, length and area measurements were converted from pixel units to metres, and input into Equations 3.1-3.5 to compute expressions for *D*, *F*, *%C*, *L* and *S*.

3.3 DESCRIPTIVE CHARACTERISATION

The descriptive account of *British Salt Marshes* by Chapman (1974), represents the first comprehensive record of the diverse morphological characteristics exhibited by marsh systems throughout England, Wales and Scotland. A similar qualitative approach represents a useful starting point for the present characterisation of tidal channel network planimetry at the 29 study localities. It also corresponds closely with the technique employed by Zernitz (1932) to gain insight into the planimetric patterns characterising fluvial networks. With reference to the classes of network pattern introduced by Zernitz (1932) and expanded by Howard (1967), visual analysis of the linearised networks (Figure 3.6-3.9) suggests that the sample formations can be divided into four broad planimetric categories, the characteristics of which are summarised in Table 3.1.

In accordance with observations by a number of authors (Pestrong, 1965; Steers, 1977; Frey and Bassan, 1985; Knighton *et al.*, 1992; Fenies and Faugeres, 1998), *dendritic* networks are most common, dominating 70% of the sample population. The abstracted representations in Figure 3.6 are characterised by a large degree of variability in channel orientation. Although systematic parallelism is evident in the upper reaches of networks on Scolt Head Island and the River Colne (Figure 3.6d-e), the *overall* orientation is nevertheless dendritic. Differing degrees of elaboration can be identified within the networks. From the most elaborate (Figure 3.6a-i), which display a large

CLASS	FREQUENCY and *(%)*	DISTINGUISHING CHARACTERISTICS	VISUAL REPRESENTATION
Dendritic	21 *(70%)*	• Branching occurs in a wide range of directions, with channels adjoining the master creeks at all angles. Subsidiary channels tend to meander randomly across the marsh surface. • Sub-sets of 'constrained' networks exhibit re-curved channel forms, and locally restricted tributary development.	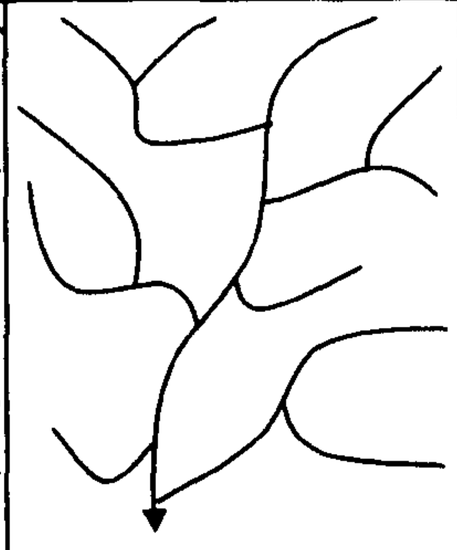
Rectangular	3 *(10%)*	• Right-angled bends dominate the form of master channels, giving a highly sinuous appearance. Adjoining creeks enter at an obtuse orientation. • Re-curved channels are prevalent in upper reaches of the network.	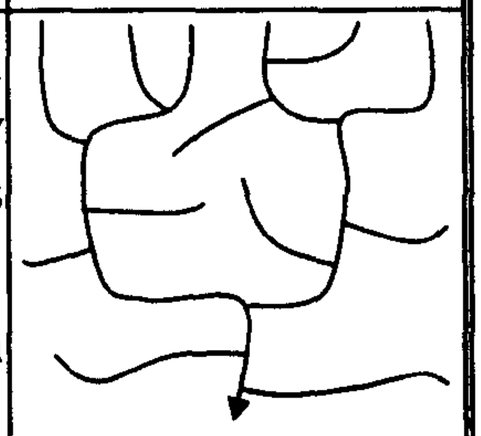
Parallel	4 *(13%)*	• Straight master creeks follow a parallel orientation throughout the network, producing a characteristic 'candelabra' appearance. Minor channels usually adjoin at an acute angle, although discordant arrangements are evident in the lower reaches of some networks.	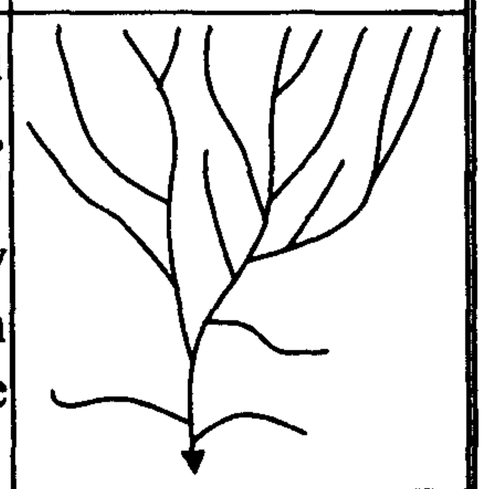
Linear	2 *(7%)*	• Branching planimetry is dominated by a single master creek. Subsidiary creeks are sparse, and where present adjoin the central channel at an obtuse angle. • Headwater reaches are often re-curved.	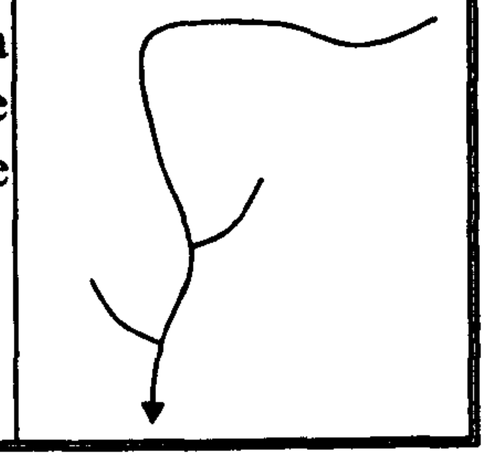

Table 3.1 Categories and visually distinguishing characteristics of saltmarsh channel network planimetry.

number of branching creeks, channel frequency decreases through formations with an intermediate level of development (Figure 3.6j-o) to the most basic systems (Figure 3.6p-r). Particularly close spacing between the numerous tributaries at Lymington (Figure 3.6o) produces a network structure that may be likened to the pinnate formation identified by Zernitz (1932).

A sub-set of spatially '*constrained*' dendritic networks can be identified, where channel development is limited in certain areas of the network. In Figures 3.6s-u, creeks are virtually absent along part of the principal channel. In each case, a sparsity of channel formation coincides with the presence of adjacent networks situated in close proximity.

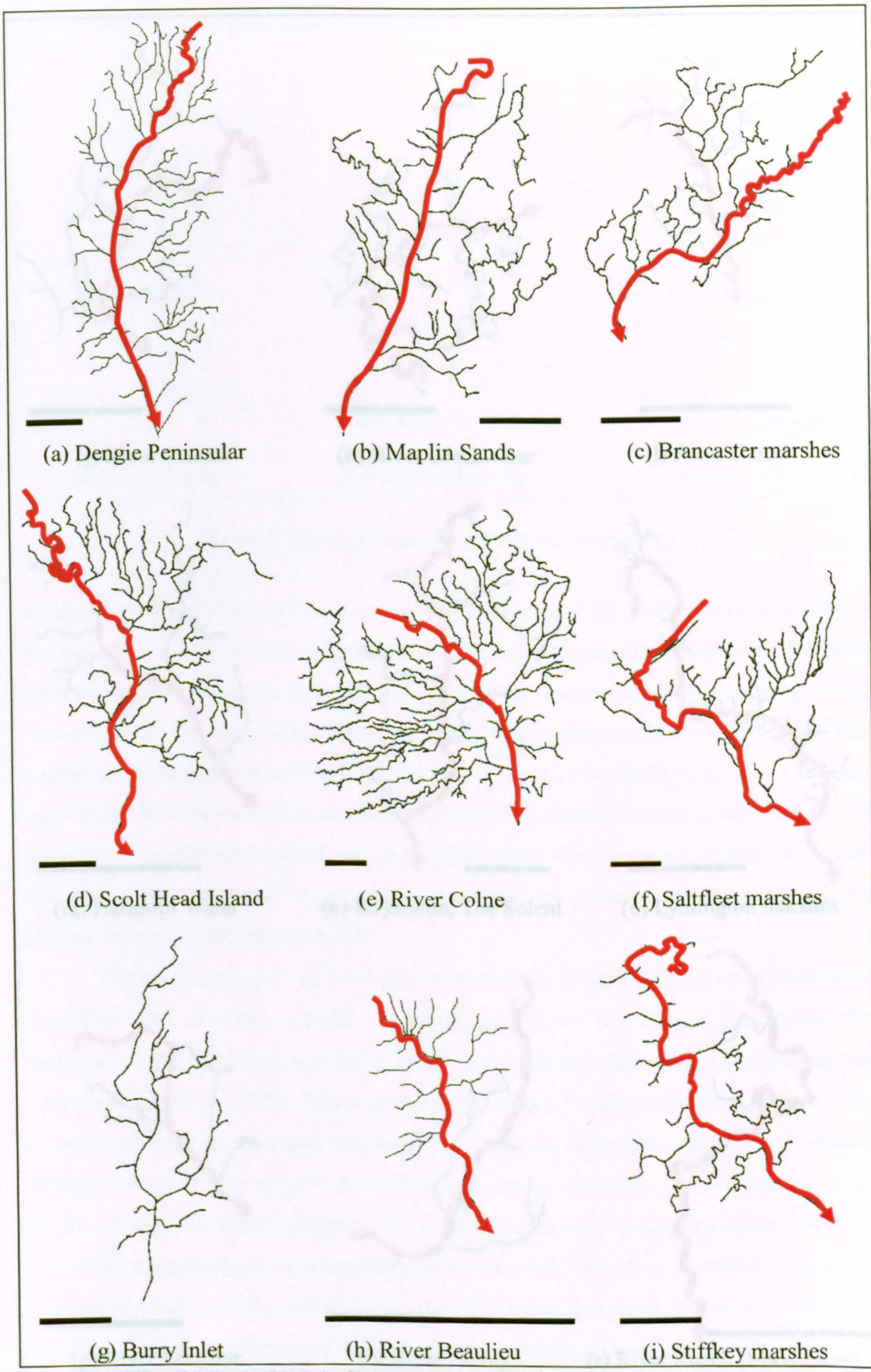

(a) Dengie Peninsular (b) Maplin Sands (c) Brancaster marshes

(d) Scolt Head Island (e) River Colne (f) Saltfleet marshes

(g) Burry Inlet (h) River Beaulieu (i) Stiffkey marshes

Figure 3.6 Dendritic planimetric formations. The red line corresponds with the surveyed principal channel (see also Figure 3.3) and scale bar represents 100m.

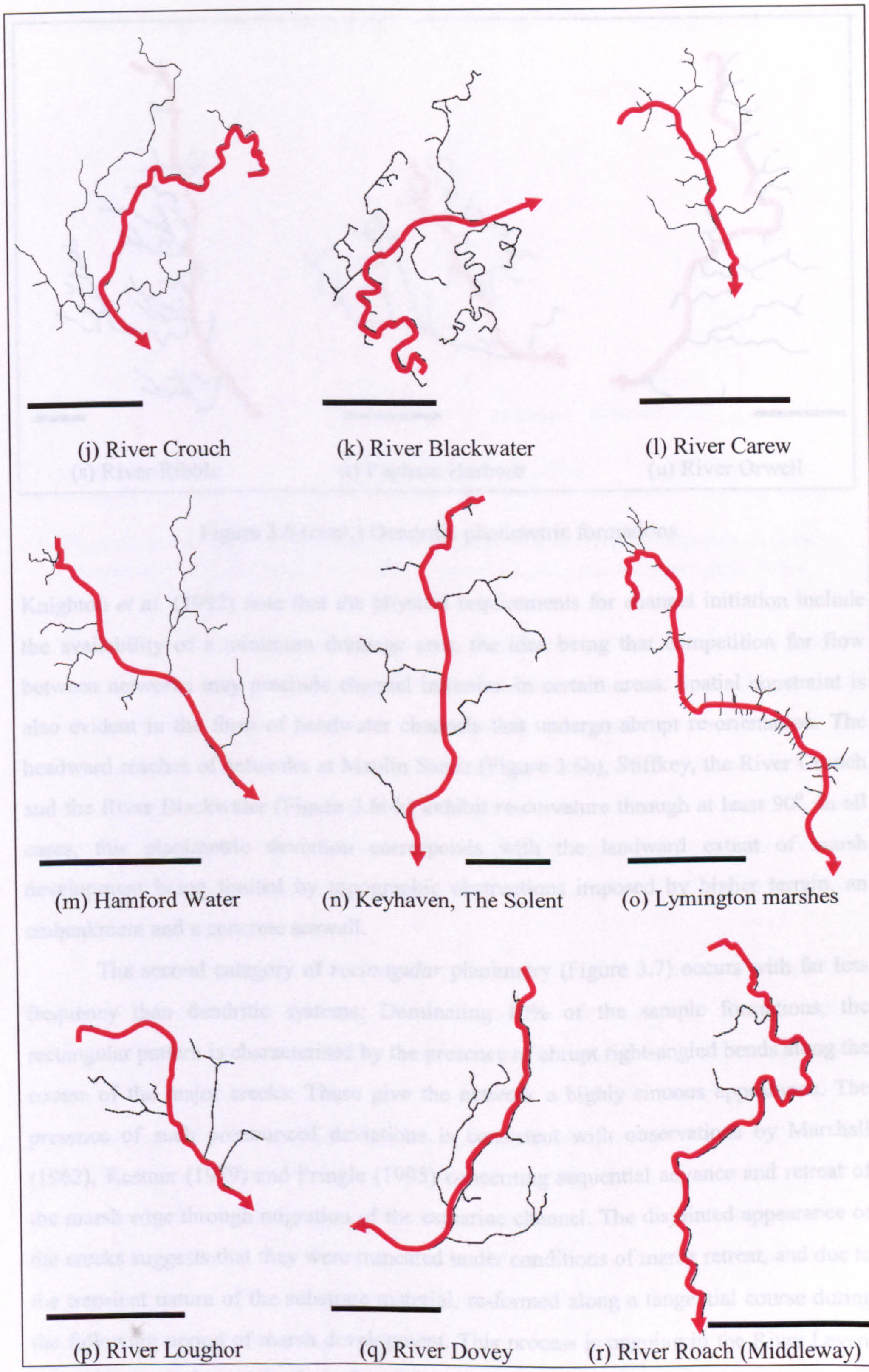

(j) River Crouch (k) River Blackwater (l) River Carew

(m) Hamford Water (n) Keyhaven, The Solent (o) Lymington marshes

(p) River Loughor (q) River Dovey (r) River Roach (Middleway)

Figure 3.6 (cont.) Dendritic planimetric formations.

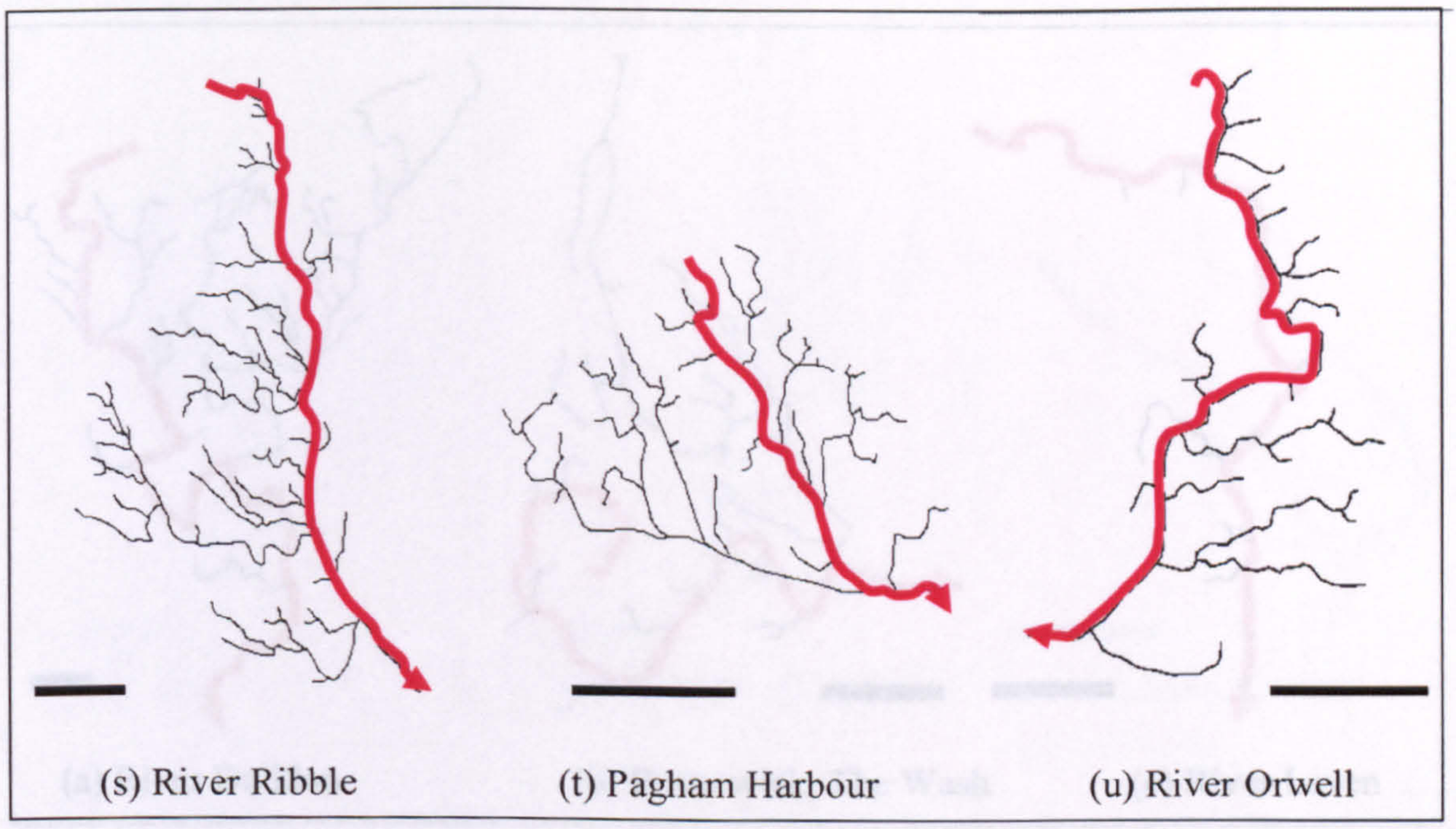

(s) River Ribble (t) Pagham Harbour (u) River Orwell

Figure 3.6 (cont.) Dendritic planimetric formations.

Knighton *et al.* (1992) note that the physical requirements for channel initiation include the availability of a minimum drainage area, the idea being that competition for flow between networks may preclude channel initiation in certain areas. Spatial constraint is also evident in the form of headwater channels that undergo abrupt re-orientation. The headward reaches of networks at Maplin Sands (Figure 3.6b), Stiffkey, the River Crouch and the River Blackwater (Figure 3.6i-k) exhibit re-curvature through at least 90°. In all cases, this planimetric deviation corresponds with the landward extent of marsh development being limited by topographic obstructions imposed by higher terrain, an embankment and a concrete seawall.

The second category of *rectangular* planimetry (Figure 3.7) occurs with far less frequency than dendritic systems. Dominating 10% of the sample formations, the rectangular pattern is characterised by the presence of abrupt right-angled bends along the course of the major creeks. These give the network a highly sinuous appearance. The presence of such pronounced deviations is consistent with observations by Marshall (1962), Kestner (1979) and Pringle (1995) concerning sequential advance and retreat of the marsh edge through migration of the estuarine channel. The disjointed appearance of the creeks suggests that they were truncated under conditions of marsh retreat, and due to the transient nature of the substrate material, re-formed along a tangential course during the following period of marsh development. This process is ongoing in the River Leven, where lower reaches of the formation (Plate 3.1.3) have been replaced by a proto-channel

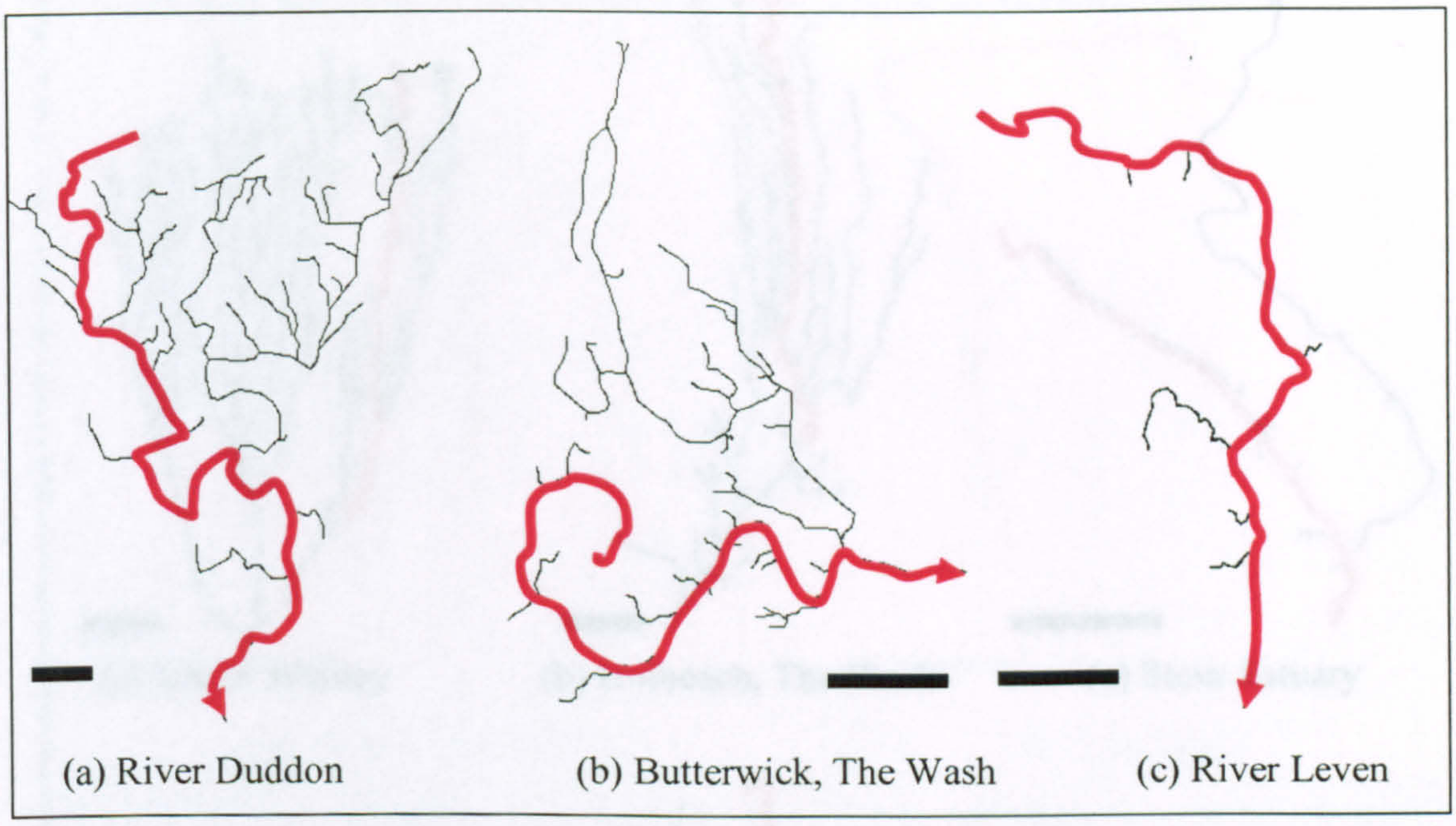

Figure 3.6 Rectangular planimetric formations. The red line corresponds with the surveyed principal channel (see also Figure 3.3) and scale bar represents 100m.

that is carving a deviant route across the inter-tidal flats towards the main tidal channel. Re-curved creeks are also apparent in the upper reaches of the network, although they have in this instance formed in response to topographic obstructions imposed by earth and concrete embankments. Minor channels in the lower reaches adjoin the master creeks at an obtuse angle, further enhancing the rectangular appearance of the system. Network elaboration is polarised between systems on the Duddon Estuary and at Butterwick, The Wash (Figure 3.7a-b) where creek development is abundant, and the River Leven where channel development is sparse.

A third category of *parallel* formation characterises 13% of the sample population (Table 3.1). In these cases (Figure 3.8), planimetry is dominated by straight, closely spaced creeks that follow a parallel orientation from the headwaters through to the mouth of the system. In appearance, they correspond with the fluvial class of parallel, slope-driven networks identified by Zernitz (1932), yet in a tidal context form a structure similar to the 'candelabra' networks observed by Ragotzkie (1959). The major channels converge at an acute angle. However, discordant alignments are evident in the lower reaches of networks at Holbeach, The Wash and in the Stour Estuary (Figure 3.8b-c). Network elaboration is polarised between populous formations at the Isle of Walney and Holbeach study sites (Figure 3.8a-b), compared with sparse network development fringing the River Roach and Stour Estuary (Figure 3.8c-d).

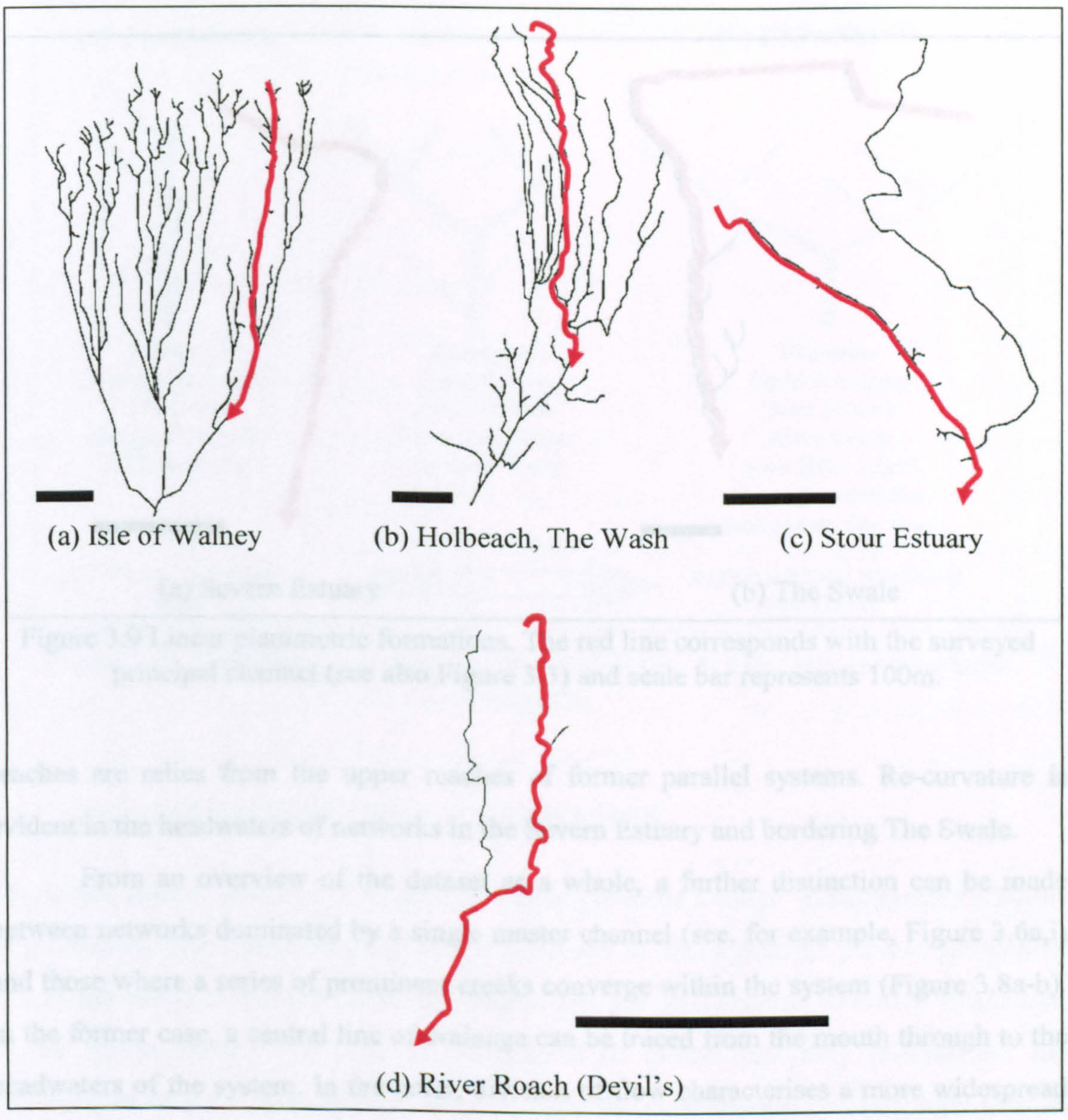

(a) Isle of Walney (b) Holbeach, The Wash (c) Stour Estuary

(d) River Roach (Devil's)

Figure 3.8 Parallel planimetric formations. The red line corresponds with the surveyed principal channel (see also Figure 3.3) and scale bar represents 100m.

The final group of *linear* networks (Figure 3.9), which occupy 7% of the sample population, represent an addition to the original classification scheme devised by Zernitz (1932). Dominated by a central master creek extending from the headwaters through to the mouth of the system, these networks are characterised by a general lack of branching. In the case of the Severn Estuary (Figure 3.9a), subsidiary channels are all but absent, while limited development is evident at The Swale (Figure 3.9b). For both of these sites, adjacent networks (see Plate 3.1) display equally sparse tributary development. There is a striking resemblance between these formations and the upper reaches of parallel networks at the Isle of Walney and Holbeach, The Wash (Figure 3.8a-b). It may be that linear

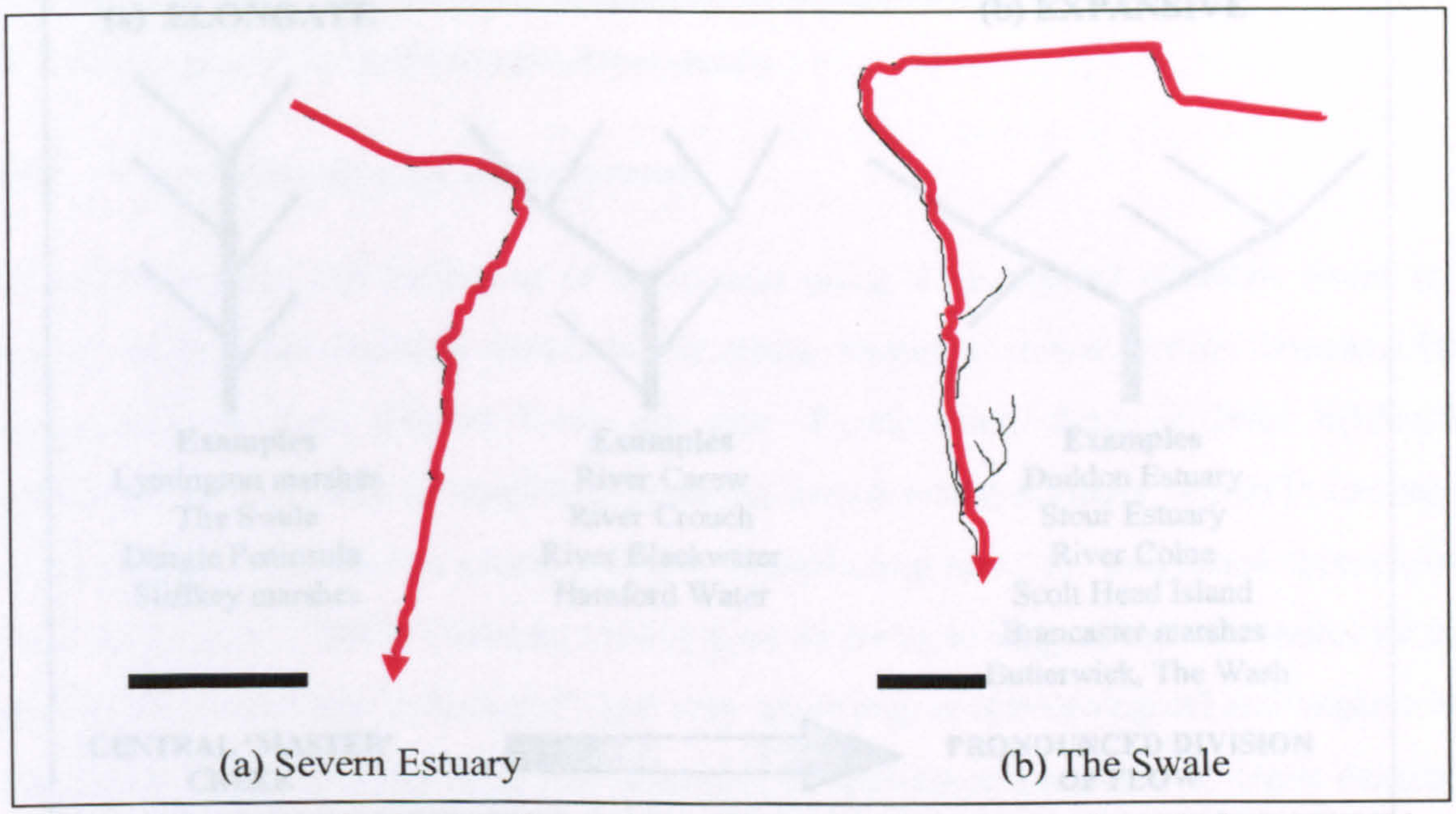

(a) Severn Estuary (b) The Swale

Figure 3.9 Linear planimetric formations. The red line corresponds with the surveyed principal channel (see also Figure 3.3) and scale bar represents 100m.

reaches are relics from the upper reaches of former parallel systems. Re-curvature is evident in the headwaters of networks in the Severn Estuary and bordering The Swale.

From an overview of the dataset as a whole, a further distinction can be made between networks dominated by a single master channel (see, for example, Figure 3.6a,i) and those where a series of prominent creeks converge within the system (Figure 3.8a-b). In the former case, a central line of drainage can be traced from the mouth through to the headwaters of the system. In the latter, division of flow characterises a more widespread network of 'distributaries' extending through the marsh. The distinction between these '*elongate*' (see Ferguson, 1979) and '*expansive*' structures is expressed schematically in Figure 3.10. Physical influences underpinning these structures are complex (Abrahams, 1984), and can be traced back through the developmental sequence to the manner in which flows were originally routed across the tidal flats. The tendency towards flow convergence may reflect factors such as the shape of the area served by the evolving creek system, together with random factors like the microtopography of the inter-tidal surface. For the present localities, smaller networks tend to be dominated by a central channel, while intermediate and large formations often display a major confluence in their lower reaches. In cases such as the Isle of Walney and Holbeach, The Wash, this junction is situated beyond the limit of halophytic colonisation. Although these creeks appear to be part of a bigger formation, adjacent reaches are treated separately according to network boundaries employed in the present study.

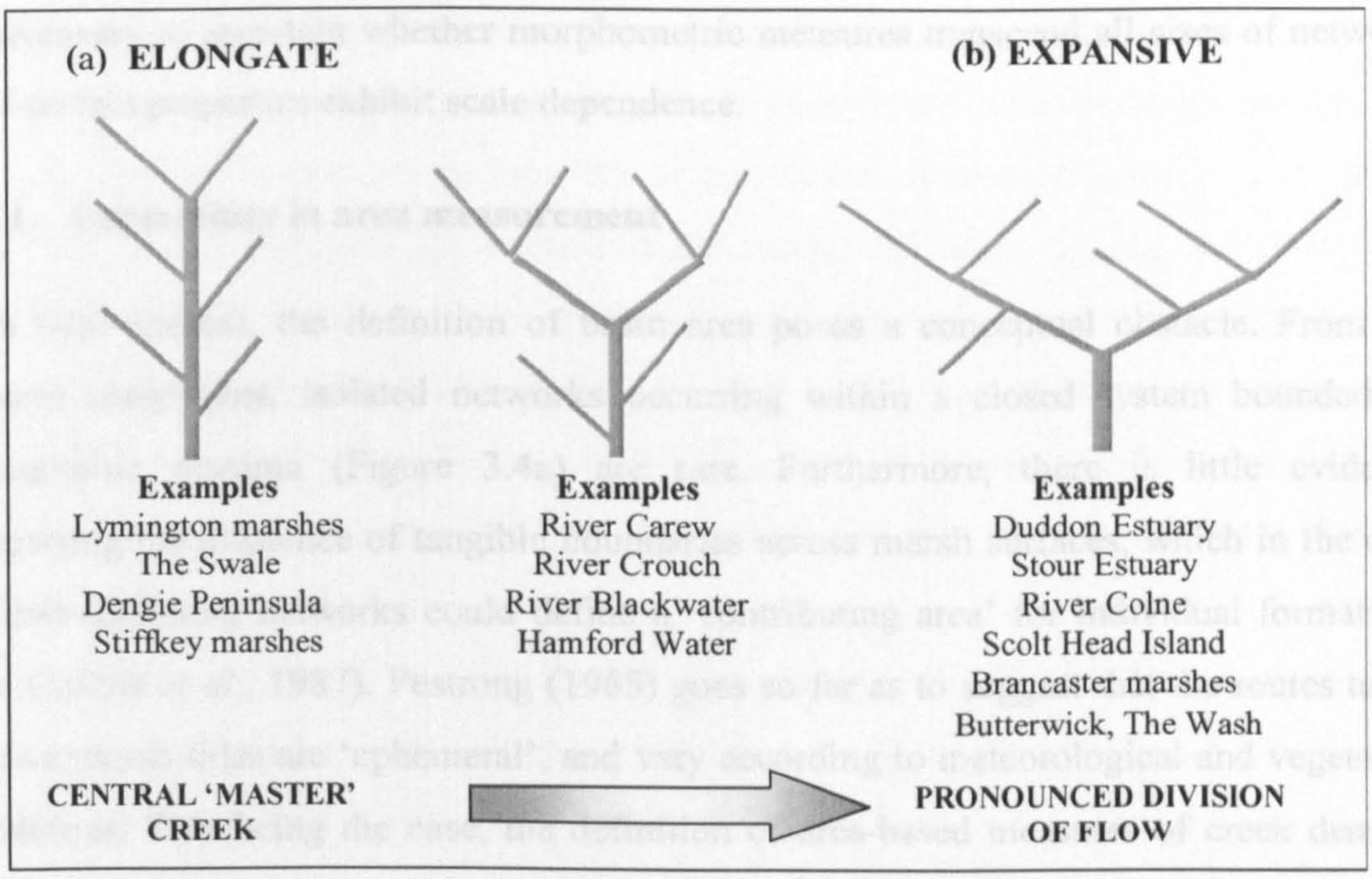

Figure 3.10 Schematic representation of: (a) elongate; and (b) expansive network structures.

3.4 MORPHOMETRIC CHARACTERISATION

The morphometric phase of this characterisation proceeds through an exploratory analysis of planimetric adjustment recorded by the measures of: creek density; percentage channel cover; link-based frequency; mean link length; and principal channel sinuosity. Evaluation of the results commences with an assessment of factors that may compromise the performance of these indices. First, uncertainty in the measurement of contributing marsh area is addressed as a key consideration in the generation of textural indices. Second, a comparative analysis of supplementary formations is undertaken to confirm that the selected networks are indeed representative.

Having thereby identified potential sources of error in the morphometric data, statistical characteristics of the indices are addressed in detail. Returning to the research objectives outlined in Figure 2.1, characterisation of planimetric morphology can take place at both generic and site-specific levels. The exploratory phase commences with an analysis of the general statistical properties for each measure as applied to the population of sample networks. The accompanying examination of inter-site variability establishes the extent to which 'optimal' descriptors (Gardiner, 1978) yield distinguishing characteristics that can be carried forward to the interpretative phase of the analysis. A key assumption here, is that systematic trends and patterns of variability are primarily correlated with external environmental controls. To confirm that this is indeed the case, it

is necessary to ascertain whether morphometric measures transcend all sizes of network, or if certain properties exhibit scale dependence.

3.4.1 Uncertainty in area measurement

In a tidal context, the definition of basin area poses a conceptual obstacle. From the present study sites, isolated networks occurring within a closed system bounded by topographic maxima (Figure 3.4a) are rare. Furthermore, there is little evidence supporting the existence of tangible boundaries across marsh surfaces, which in the case of inter-digitating networks could define a 'contributing area' for individual formations (see Collins *et al.*, 1987). Pestrong (1965) goes so far as to suggest that the routes taken by overmarsh tides are 'ephemeral', and vary according to meteorological and vegetative conditions. This being the case, the definition of area-based measures of creek density, percentage channel cover and link-based texture is subject to some uncertainty. The challenge is therefore to define the most likely contributing area surrounding each of the sample networks, based on the decision rules in Figure 3.5.

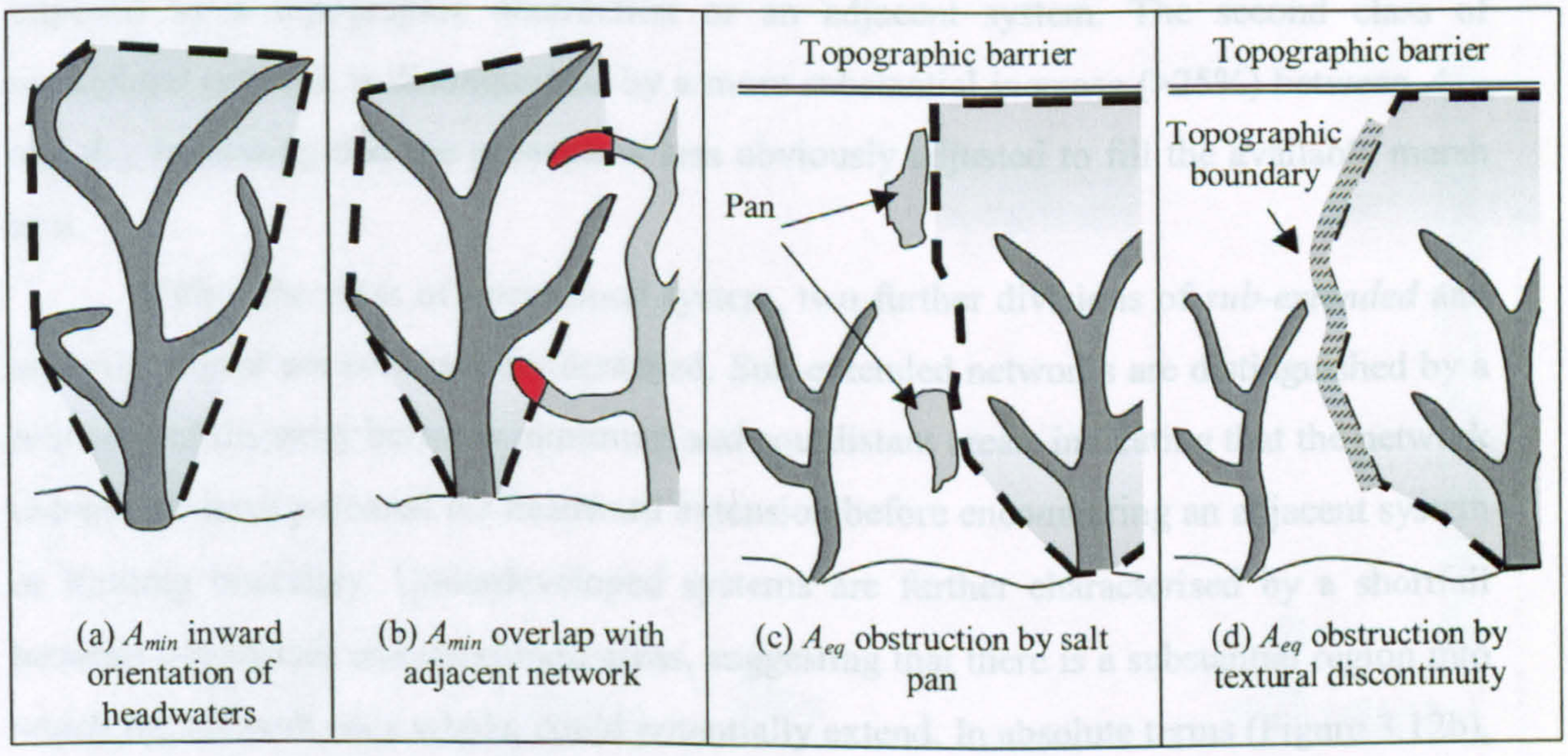

Figure 3.11 Irregular decisions made in the definition of minimum, equidistant and maximum contributing areas.

Practical application of the theoretical decision rules demonstrates that certain procedures are more appropriate in some study localities than others. Minimum and equidistant contributing areas could be defined for all networks, whereas a maximum area was appropriate at only 43% of the sites. Irregular decisions that had to be made in the definition of minimum area involved: (1) channel curvature leading to the re-orientation

of channel heads (Figure 3.11a), in which instance the outermost edge of the channel bend was selected as the alternative pinnacle; and (2) inter-digitating channel reaches from an adjacent network encroaching into the area between sources (Figure 3.11b), which although rare is accepted as a unavoidable margin of error in A_{min} measures. The definition of equidistant area was relatively straightforward, except where: (1) isolated pans that could collect a portion of the tidal flow had developed in the intervening area (Figure 3.11c); and (2) the presence of obvious textural discontinuities between networks imposed a topographic boundary that did not necessarily coincide with the loci of bisection (Figure 3.11d).

The percentage increase in contributing area associated with the transition from minimum to equidistant and maximum decision rules is shown in Figure 3.12a. Results suggest that the study localities can be divided into two broad categories. The first class of *space filling* network (see Table 3.2) is distinguished by a minimal increase (<25%) between areas defined according to minimum and equidistant decision rules, with a minor additional increment associated with the maximum measure. These networks are characterised by headwater reaches that are approaching the limit of development imposed by a topographic obstruction or an adjacent system. The second class of *unconfined* network is distinguished by a more substantial increase (>25%) between A_{min} and A_{eq}, indicating that the network is less obviously adjusted to fill the available marsh area.

Within the class of unconfined system, two further divisions of *sub-extended* and *underdeveloped* network can be identified. Sub-extended networks are distinguished by a pronounced disparity between minimum and equidistant areas, indicating that the network extremities have potential for headward extension before encountering an adjacent system or limiting boundary. Underdeveloped systems are further characterised by a shortfall between equidistant and maximum areas, suggesting that there is a substantial region into which the network, as a whole, could potentially extend. In absolute terms (Figure 3.12b), the margin of uncertainty associated with this effect is substantial at the River Ribble, The Swale and Saltfleet marshes. It is interesting to note that these sub-divisions are not mutually exclusive, and that unconfined networks may display both sub-extended and underdeveloped characteristics.

In the absence of an indepth investigation, it is unclear which of the decision rules is most appropriate for defining the area of contributing flow in tidal systems. Since they may all be equally valid, it is necessary to carry forward all three measures to the

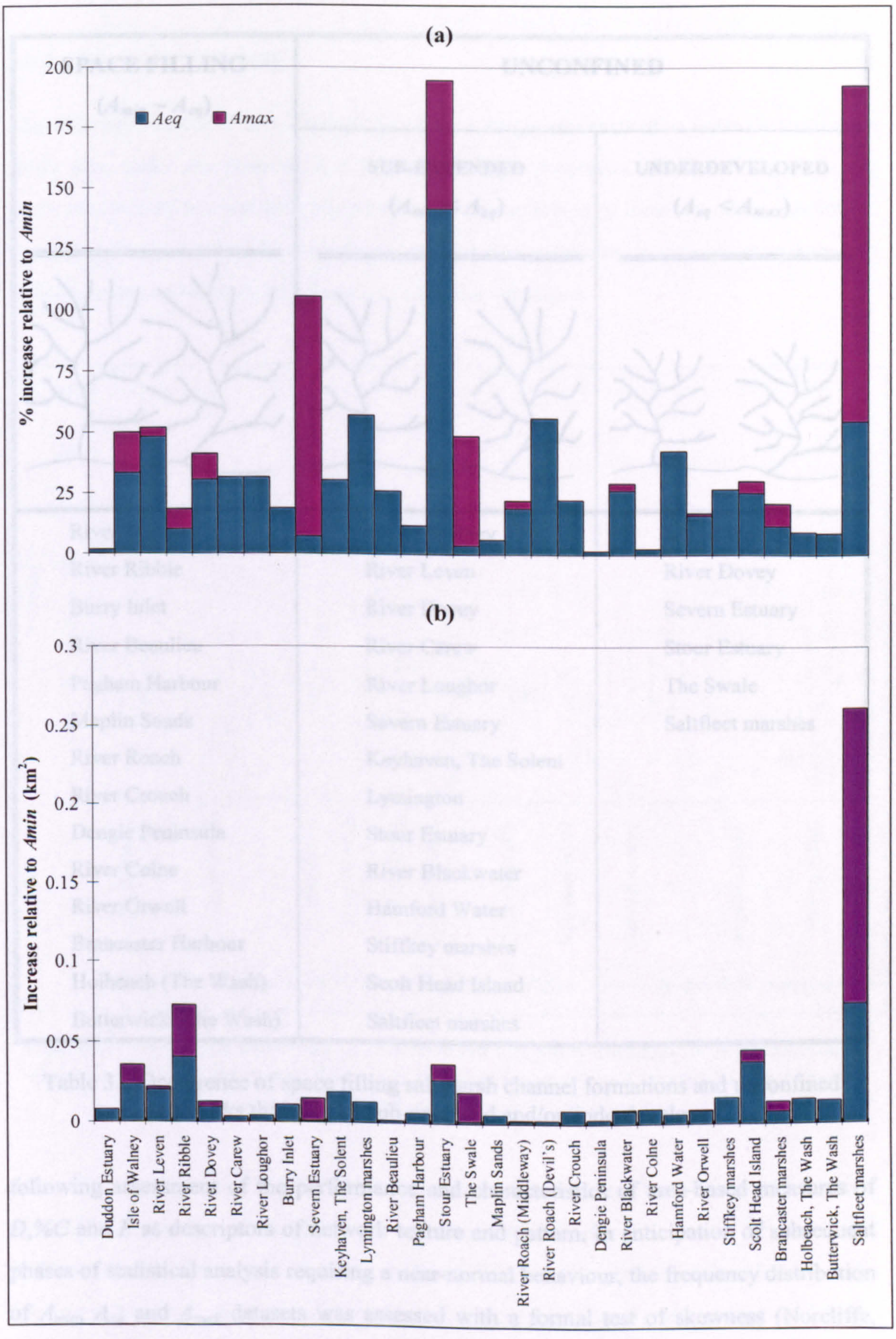

Figure 3.12 (a) Percentage and (b) absolute magnitude of increase in A_{eq} and A_{max} relative to A_{min}.

SPACE FILLING ($A_{min} \sim A_{eq}$)	UNCONFINED	
	SUB-EXTENDED ($A_{min} < A_{eq}$)	UNDERDEVELOPED ($A_{eq} < A_{max}$)
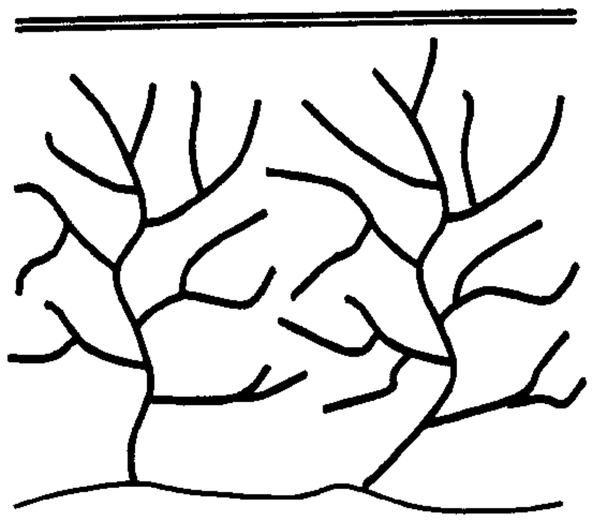	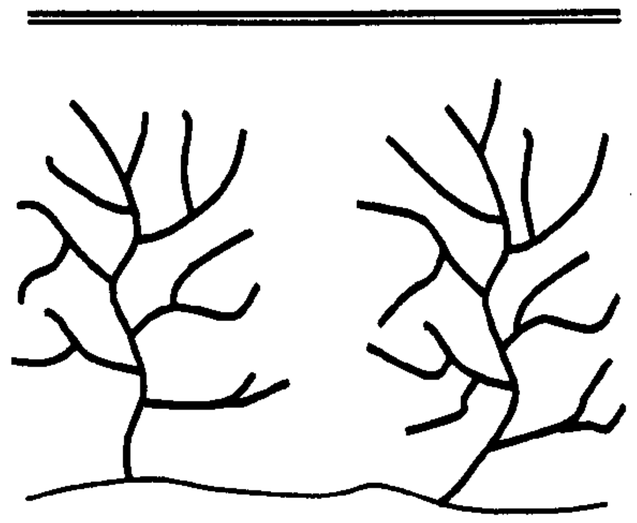	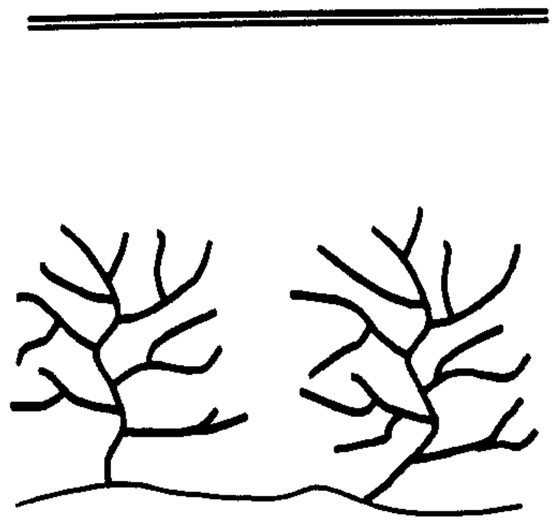
River Duddon	Isle of Walney	Isle of Walney
River Ribble	River Leven	River Dovey
Burry Inlet	River Dovey	Severn Estuary
River Beaulieu	River Carew	Stour Estuary
Pagham Harbour	River Loughor	The Swale
Maplin Sands	Severn Estuary	Saltfleet marshes
River Roach	Keyhaven, The Solent	
River Crouch	Lymington	
Dengie Peninsula	Stour Estuary	
River Colne	River Blackwater	
River Orwell	Hamford Water	
Brancaster Harbour	Stiffkey marshes	
Holbeach (The Wash)	Scolt Head Island	
Butterwick (The Wash)	Saltfleet marshes	

Table 3.2 Occurrence of space filling saltmarsh channel formations and unconfined networks that may be sub-extended and/or underdeveloped.

following assessment of the performance and characteristics of area-based measures of D,$\%C$ and F as descriptors of network texture and pattern. In anticipation of subsequent phases of statistical analysis requiring a near-normal behaviour, the frequency distribution of A_{min}, A_{eq} and A_{max} datasets was assessed with a formal test of skewness (Norcliffe, 1977). Statistically significant (α=.05) levels of skew (see Table 6.1) indicate that all three series exhibit non-normal behaviour. The degree of departure from normality was improved to an acceptable level by the application of a logarithmic transformation.

3.4.2 Intra-site variability

The extensive phase of this analysis employs a single representative network from each study site, under the premise that the morphologic properties of all formations at the particular locality are similarly adjusted to and characteristic of local boundary conditions. Providing this is a reasonable assumption, intra-site variability in optimal morphometric indicators should be minimal relative to inter-site variations.

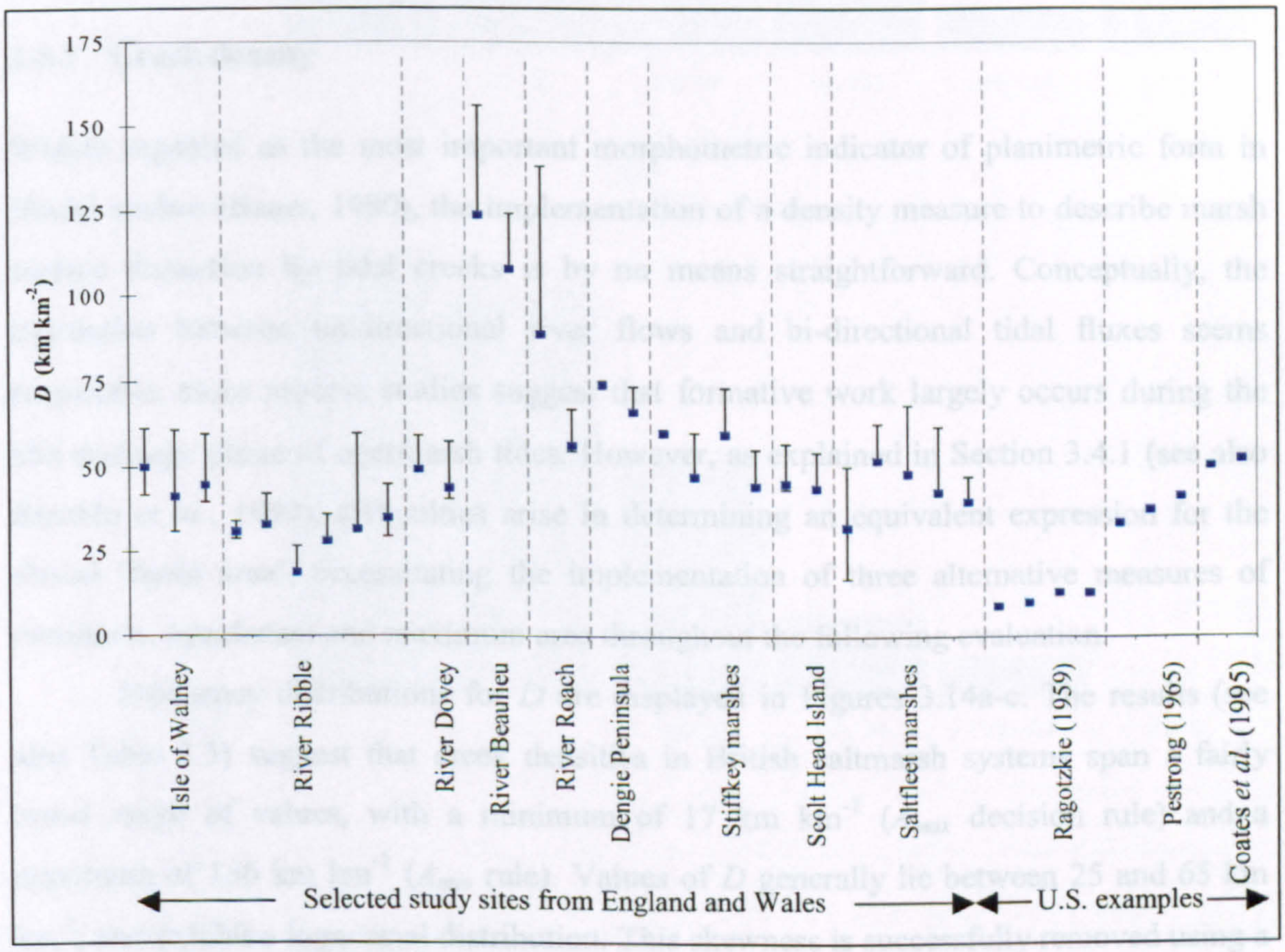

Figure 3.13 Intra-site variability in *D* at selected UK study sites and from US examples documented in the literature. Error bars reflect differences in *A* computed according to minimum, equidistant and maximum decision rules.

To confirm that this is indeed the case, creek densities were computed for sites displaying a number of adjacent, yet independent networks. The results (Figure 3.13) indicate that within site variability is limited compared with variation between the localities. Although, the generally small sample size precludes the analysis of variance to establish a statistical expression of variation between the localities, it may be concluded that the use of a 'representative' network for morphologic characterisation is appropriate.

Patterns of response for D are similar to those identified by Ragotzkie (1959), Pestrong (1965) and Coates *et al.* (1995) for creek densities in the U.S. (Figure 3.13), inasmuch that the dominance of inter- over intra-site variability is a ubiquitous finding. However, an isolated departure from this generalisation is apparent in the present results, whereby variance between the density of adjacent networks at Devil's Reach and The Middleway on the River Roach is exceptionally high. In the absence of an obvious explanation, the decision was made to include both networks in subsequent stages of the extensive analysis.

3.4.3 Creek density

Widely regarded as the most important morphometric indicator of planimetric form in fluvial studies (Bauer, 1980), the implementation of a density measure to describe marsh surface dissection by tidal creeks is by no means straightforward. Conceptually, the translation between unidirectional river flows and bi-directional tidal fluxes seems reasonable, since process studies suggest that formative work largely occurs during the ebb *drainage* phase of overmarsh tides. However, as explained in Section 3.4.1 (see also Rinaldo *et al.*, 1999), difficulties arise in determining an equivalent expression for the fluvial 'basin area', necessitating the implementation of three alternative measures of minimum, equidistant and maximum area throughout the following evaluation.

Frequency distributions for D are displayed in Figures 3.14a-c. The results (see also Table 3.3) suggest that creek densities in British saltmarsh systems span a fairly broad range of values, with a minimum of 17 km km^{-2} (A_{max} decision rule) and a maximum of 156 km km^{-2} (A_{min} rule). Values of D generally lie between 25 and 65 km km^{-2}, and exhibit a lognormal distribution. This skewness is successfully removed using a logarithmic transformation.

Wide geographic variability is apparent in D, when displayed in sequential order around the British coastline (Figure 3.15). At this stage of the analysis it is useful to distinguish several broad classes of density measure. Concentrating on values defined according to the A_{eq} decision rule, which are represented by the symbol ■ (definitions based on A_{min} and A_{max} form the upper and lower whiskers), densities of $0 < D < 45$ km km^{-2} may be classified as low or *coarse* (see also Pestrong, 1965), intermediate densities of $45 < D < 65$ km km^{-2} as *medium*, and high densities of $D > 65$ km km^{-2} as *fine* textured.

The sensitivity of creek density to the method used in computing A is considerable. The division between space-filling and unconfined systems observed in

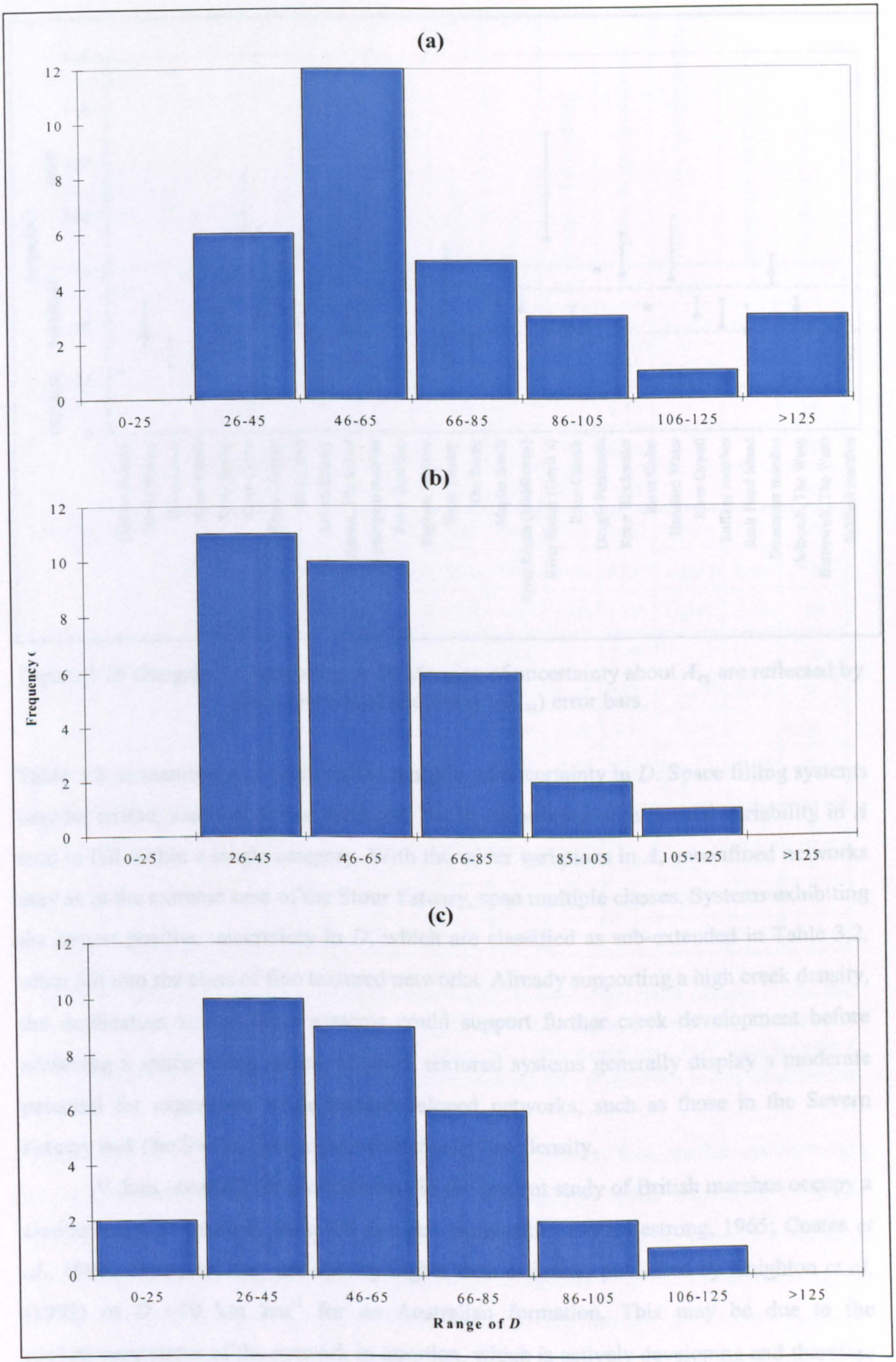

Figure 3.14 Frequency distribution of D computed using: (a) A_{min}; (b) A_{eq}; and (c) A_{max} decision rules.

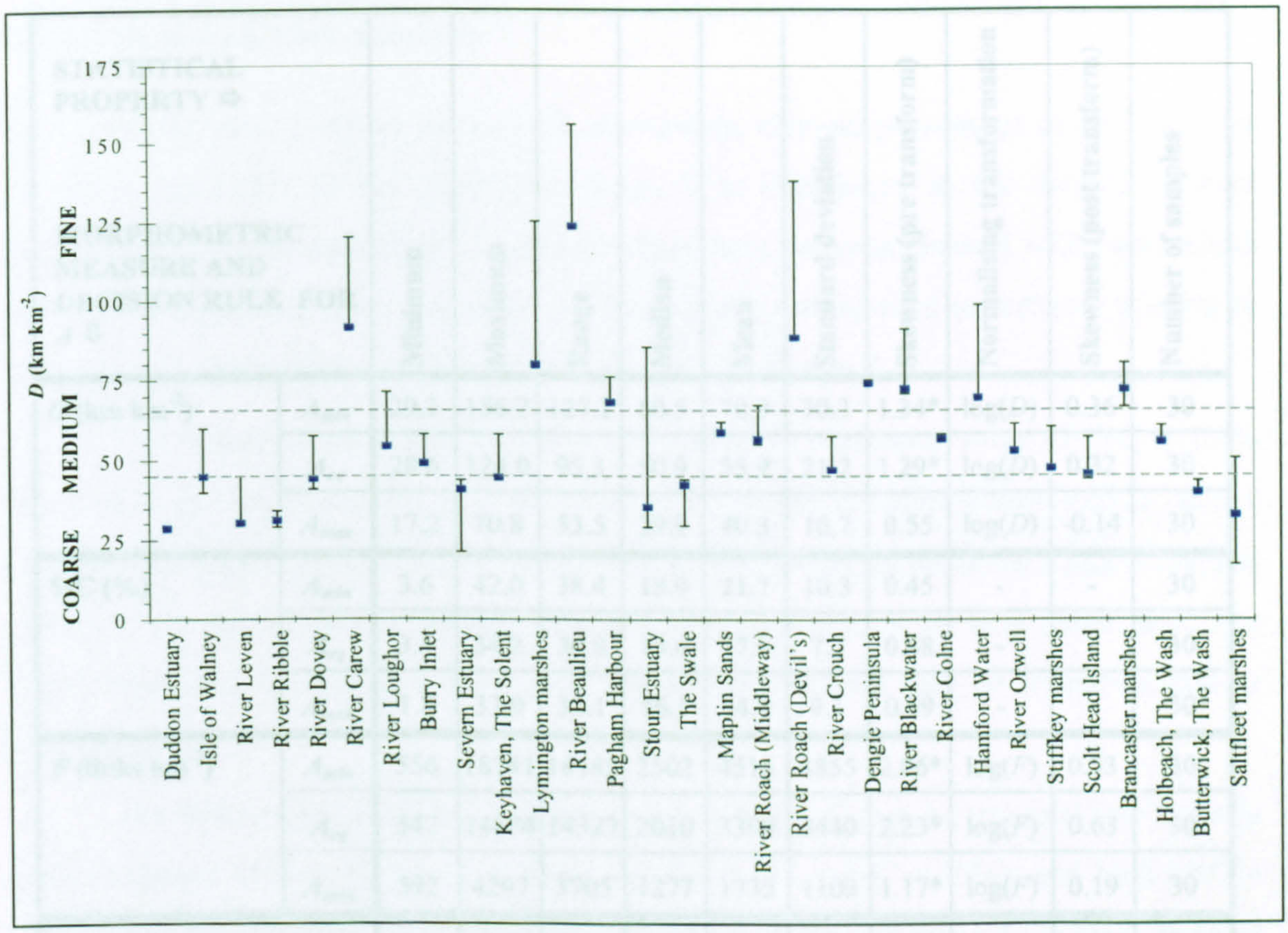

Figure 3.15 Geographic variability in D. Margins of uncertainty about A_{eq} are reflected by the upper (A_{min}) and lower (A_{max}) error bars.

Table 3.2, is manifest as widely varied margins of uncertainty in D. Space filling systems may be coarse, medium or fine textured, but in accordance with limited variability in A tend to fall within a single category. With the wider variations in A, unconfined networks may as in the extreme case of the Stour Estuary, span multiple classes. Systems exhibiting the largest positive uncertainty in D, which are classified as sub-extended in Table 3.2, often fall into the class of fine textured networks. Already supporting a high creek density, the implication is that these systems could support further creek development before achieving a space-filling status. Medium textured systems generally display a moderate potential for expansion, while underdeveloped networks, such as those in the Severn Estuary and The Swale, have a characteristically low density.

Values obtained for creek density in the present study of British marshes occupy a similar range as readings from US systems (Ragotzkie, 1959; Pestrong, 1965; Coates *et al.*, 1995). However, they are notably higher than estimates published by Knighton *et al.* (1992) of D ~10 km km^{-2} for an Australian formation. This may be due to the evolutionary status of the network in question, which is actively developing and therefore unlikely to have reached a stage that reflects adjustment with local boundary conditions.

STATISTICAL PROPERTY ⇨ / MORPHOMETRIC MEASURE AND DECISION RULE FOR A ⇩		Minimum	Maximum	Range	Median	Mean	Standard deviation	Skewness (pre transform)	Normalising transformation	Skewness (post transform)	Number of samples
D (km km^{-2})	A_{min}	29.1	156.2	127.1	60.5	70.9	30.3	1.34*	log(D)	0.36	30
	A_{eq}	28.6	124.0	95.3	50.9	55.9	21.2	1.29*	log(D)	0.32	30
	A_{max}	17.2	70.8	53.5	39.9	40.3	16.7	0.55	log(D)	-0.14	30
$\%C$ (%)	A_{min}	3.6	42.0	38.4	18.9	21.7	10.3	0.45	-	-	30
	A_{eq}	3.4	34.2	30.8	15.6	17.0	7.7	0.48	-	-	30
	A_{max}	1.8	33.9	32.1	16.1	14.9	9.1	0.39	-	-	30
F (links km^{-2})	A_{min}	556	18741	18185	2502	4516	4855	2.06*	log(F)	0.53	30
	A_{eq}	547	14874	14327	2010	3390	3440	2.23*	log(F)	0.63	30
	A_{max}	592	4297	3705	1277	1735	1109	1.17*	log(F)	0.19	30
L (m)		6.7	52.3	45.5	24.9	24.6	11.4	0.44	-	-	30
L_{EXT} (m)		7.1	56.3	49.2	21.8	23.3	12.4	0.98*	$L_{EXT}^{1/2}$	0.33	30
L_{INT} (m)		5.1	53.2	48.1	26.3	25.9	11.9	0.33	-	-	30
L_{EXT}/L_{INT}		0.39	1.64	1.26	0.89	0.93	0.29	0.70*	$\frac{L_{EXT}^{1/2}}{L_{INT}}$	0.18	30
S		1.06	3.01	1.95	1.32	1.49	0.46	1.77*	$-(S^{-2})$	0.26	30
S_N		1.01	2.09	1.08	1.15	1.28	0.29	1.37*	$-(S_N^{-2})$	0.48	30
S_A		1.00	1.15	1.15	1.01	1.02	0.03	3.76*	$-(S_A^{-2})$	3.34*	30
S_T		1.03	1.40	1.40	1.09	1.13	0.09	1.57*	$-(S_T^{-2})$	0.95*	30

Table 3.3 Statistical characteristics for area-based measures of: creek density D (for the population as a whole and divided according to scale dependence into small, intermediate and large formations); percentage channel cover $\%C$; link-based texture F; link lengths L; and principal channel sinuosity S. * symbolises statistically significant levels of skewness.

In absolute terms, dissection is also higher in tidal systems than fluvial environments, where density rarely exceeds 20 km km^{-2} (Gardiner *et al.*, 1977; Pethick, 1984). Of further interest is the disparity between the value of $8 < D < 11$ km km^{-2} obtained by Shi *et al.* (1995) for marshes bordering the River Dovey, compared with the substantially higher result of $D \sim 45$ km km^{-2} reported in Figure 3.15. In this instance, the contrast in results may be traced to differences between the temporal and spatial resolution of the photographic media, the method of data collection and the definition of contributing area.

3.4.4 Percentage channel cover

As a morphometric measure of network planimetry, channel percentage cover (*%C*) has no direct equivalent in the fluvial literature. It is introduced in the context of tidal networks as an index reflecting the mutual adjustment between channel width and length within a 'contributing area'. As such, *%C* is subject to margins of uncertainty relating to the minimum, equivalent and maximum definitions in Figure 3.5.

The statistical properties in Table 3.3, reveal a minimum value of *%C* = 1.8% (computed according to the A_{max} decision rule), which is synonymous with a sparse channel coverage. From the upper limit of *%C* = 42% (obtained using the A_{min}), it appears that the creek system may in extreme cases occupy nearly half of the total marsh area. The distribution of *%C* (Figure 3.16) is only moderately skewed, and no transformation is warranted.

The frequency distribution further suggests that *%C* may be grouped into broadly defined classes of: low ($0 < \%C < 10\%$); moderate ($11 < \%C < 30\%$); and high ($\%C > 30\%$). The class of networks displaying a moderate degree of channel coverage is most populous. From a graphical representation of site specific variations in *%C* (Figure 3.17), localities falling outside this envelope, which exhibit extreme levels of network coverage, include: the River Carew; River Orwell; River Roach; and Lymington and Keyhaven marshes bordering The Solent. Study sites with particularly limited network development are found in: the River Leven; Severn Estuary; Stour Estuary; The Swale; and at Saltfleet. The obvious distinction between these two groups is in terms of width adjustment. Systems exhibiting a high coverage are characterised by central reaches that appear '*over-widened*', while reaches in the latter networks maintain a narrow width.

The morphologic characteristic of over-widening is not an entirely new discovery, since Pethick (1992) identifies the presence of localised flaring around the mouth of networks on the Dengie Peninsula. However, the finding of extreme adjustment in width *throughout* the master channels of a network is somewhat unusual. Pethick (1992, p.55) draws a parallel between the disproportionate increase in width and the form of larger tidal estuaries, suggesting that widening is *'a response to tidal energy dissipation'*. In contrast, Marshall (1962) claims that widening is attributable to marine erosion. Clearly a subject of some dispute, the causal factors responsible for this phenomenon are examined further in Chapter 6.

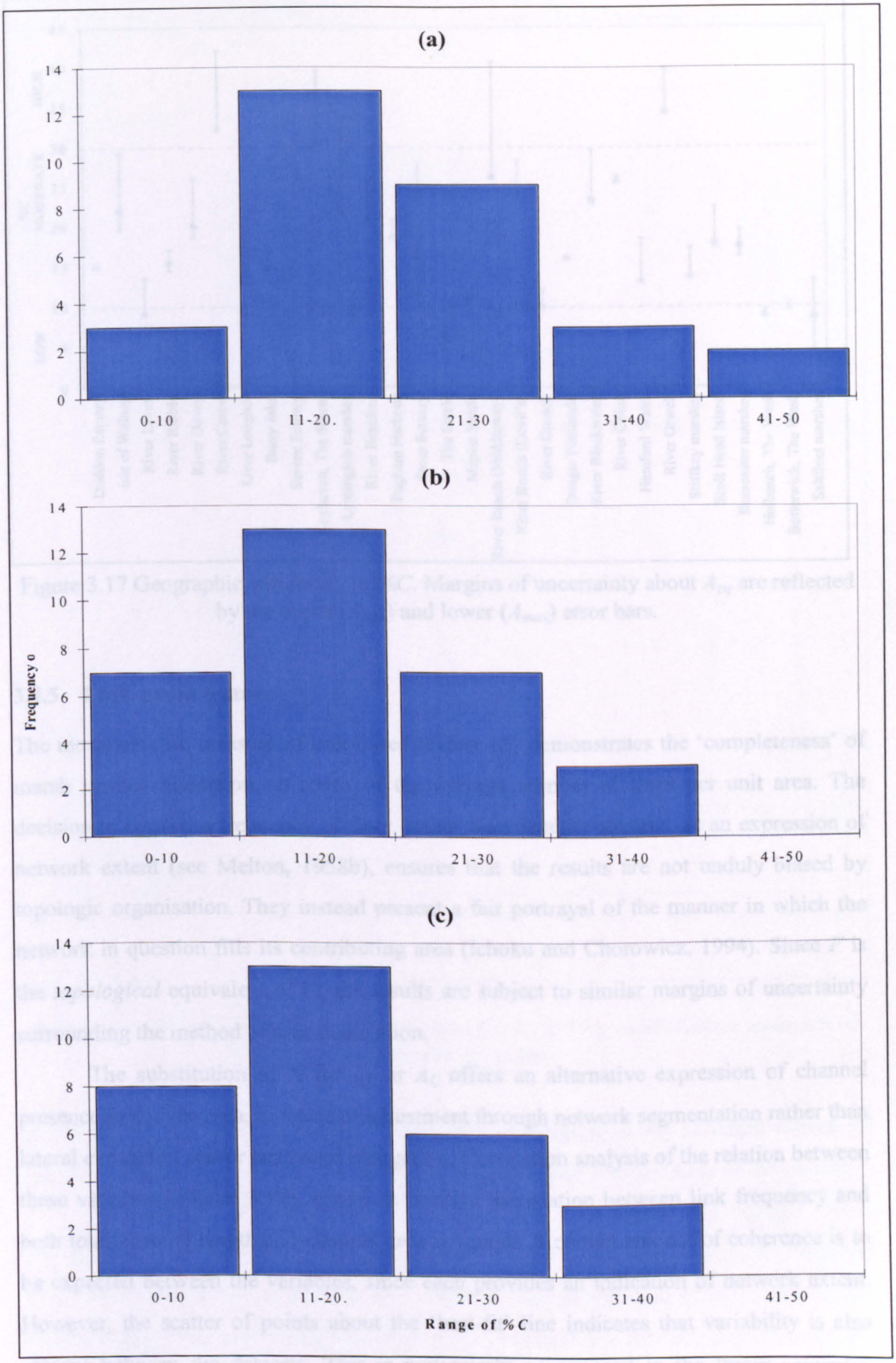

Figure 3.16 Frequency distribution of *%C* computed using: (a) A_{min}; (b) A_{eq}; and (c) A_{max} decision rules.

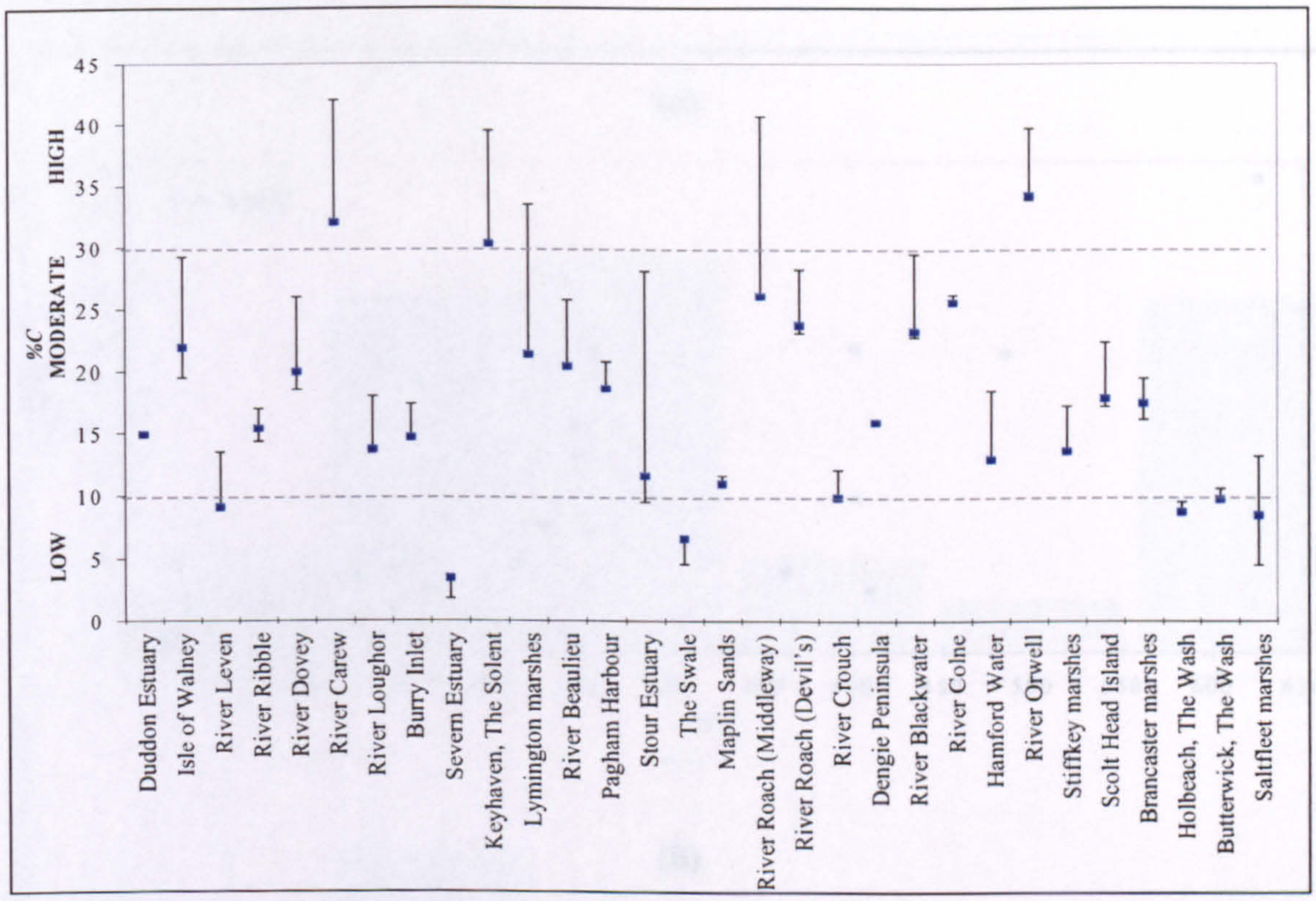

Figure 3.17 Geographic variability in *%C*. Margins of uncertainty about A_{eq} are reflected by the upper (A_{min}) and lower (A_{max}) error bars.

3.4.5 Link-based texture

The morphometric measure of link-based texture (F) demonstrates the 'completeness' of marsh surface dissection, in terms of the average number of links per unit area. The decision to employ a frequency of *links,* rather than Strahler streams, as an expression of network extent (see Melton, 1958b), ensures that the results are not unduly biased by topologic organisation. They instead present a fair portrayal of the manner in which the network in question fills its contributing area (Ichoku and Chorowicz, 1994). Since F is the *topological* equivalent of D, the results are subject to similar margins of uncertainty surrounding the method of area delineation.

The substitution of N for L_T or A_C offers an alternative expression of channel presence in a given area, in terms of adjustment through network segmentation rather than lateral expansion and/or headward elongation. Correlation analysis of the relation between these variables (Figure 3.18), reveals a positive association between link frequency and both total channel length and channel area coverage. A certain amount of coherence is to be expected between the variables, since each provides an indication of network extent. However, the scatter of points about the 'best-fit' line indicates that variability is also present between the datasets. This is particularly pronounced in the larger networks, which comprise a higher number of links, length or area coverage. It may therefore be

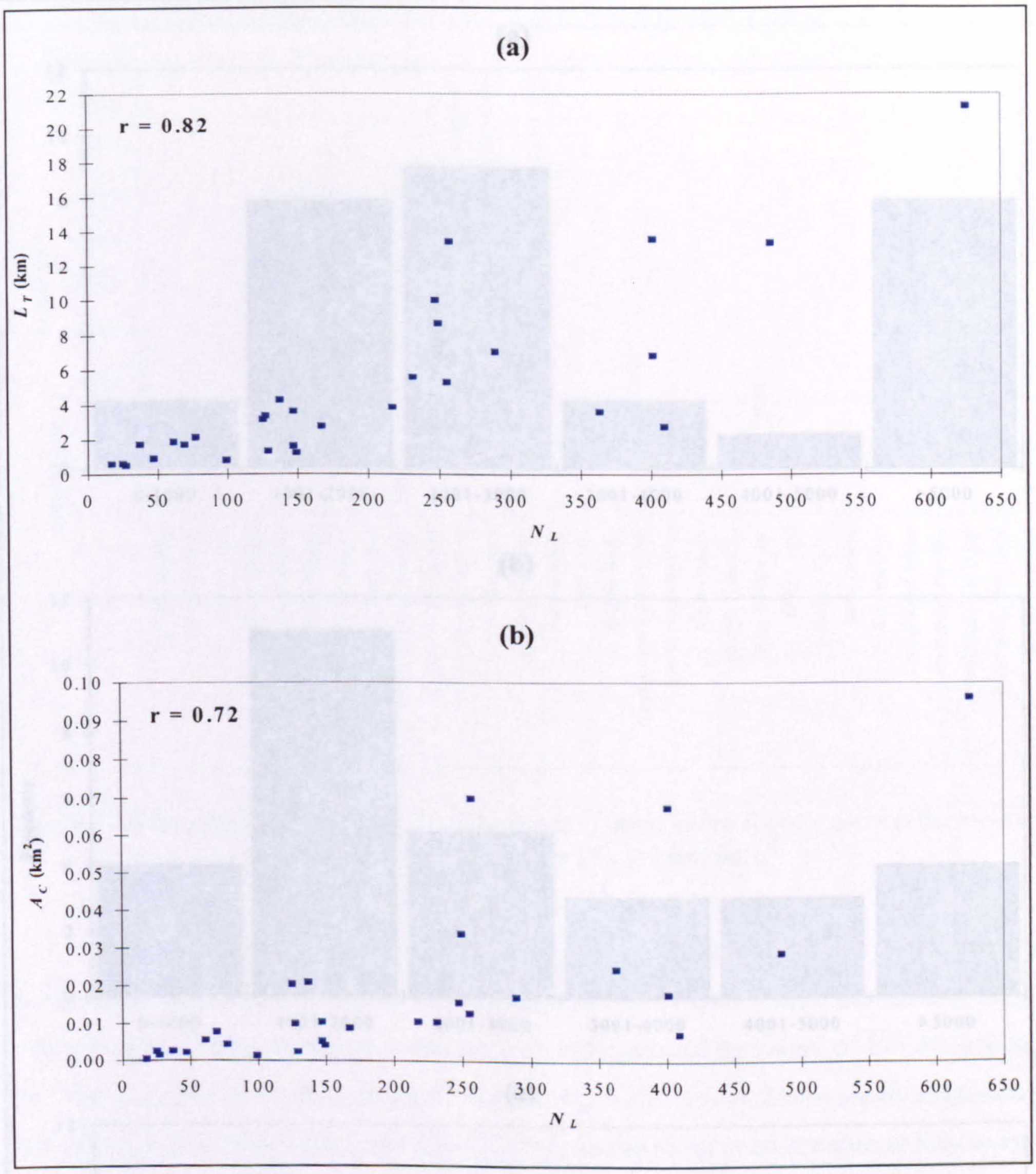

Figure 3.18 Relations between: (a) L_T, N_L; and (b) A_C and N_L, as alternative measures of channel network extent.

surmised that topologic and geometric measures distinguish subtly different aspects of planimetric adjustment, which become increasingly distinct with the scale of the system.

Values of F (Table 3.3) span an exceptionally wide range, with extreme values extending from $F = 547$ links km^{-2} (employing the A_{eq} decision rule) to a highly dissected $F = 18741$ links km^{-2} (under the A_{min} criteria). The distribution of responses in the corresponding frequency histogram (Figure 3.19) indicates a concentration towards the lower end of the scale, between $1000 < F < 3000$ links km^{-2}. This skewness is successfully removed using a logarithmic transformation.

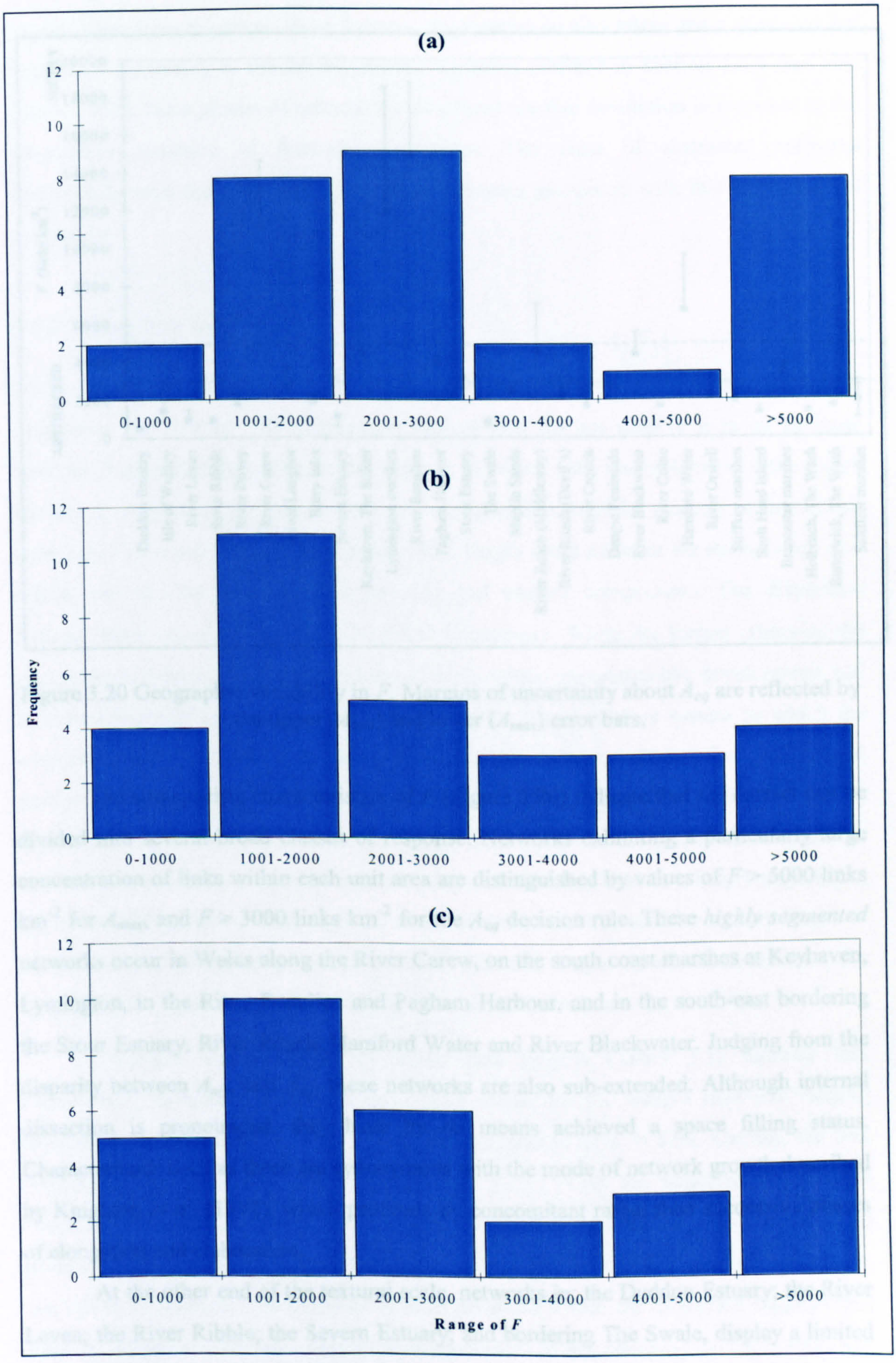

Figure 3.19 Frequency distribution of F computed using: (a) A_{min}; (b) A_{eq}; and (c) A_{max} decision rules.

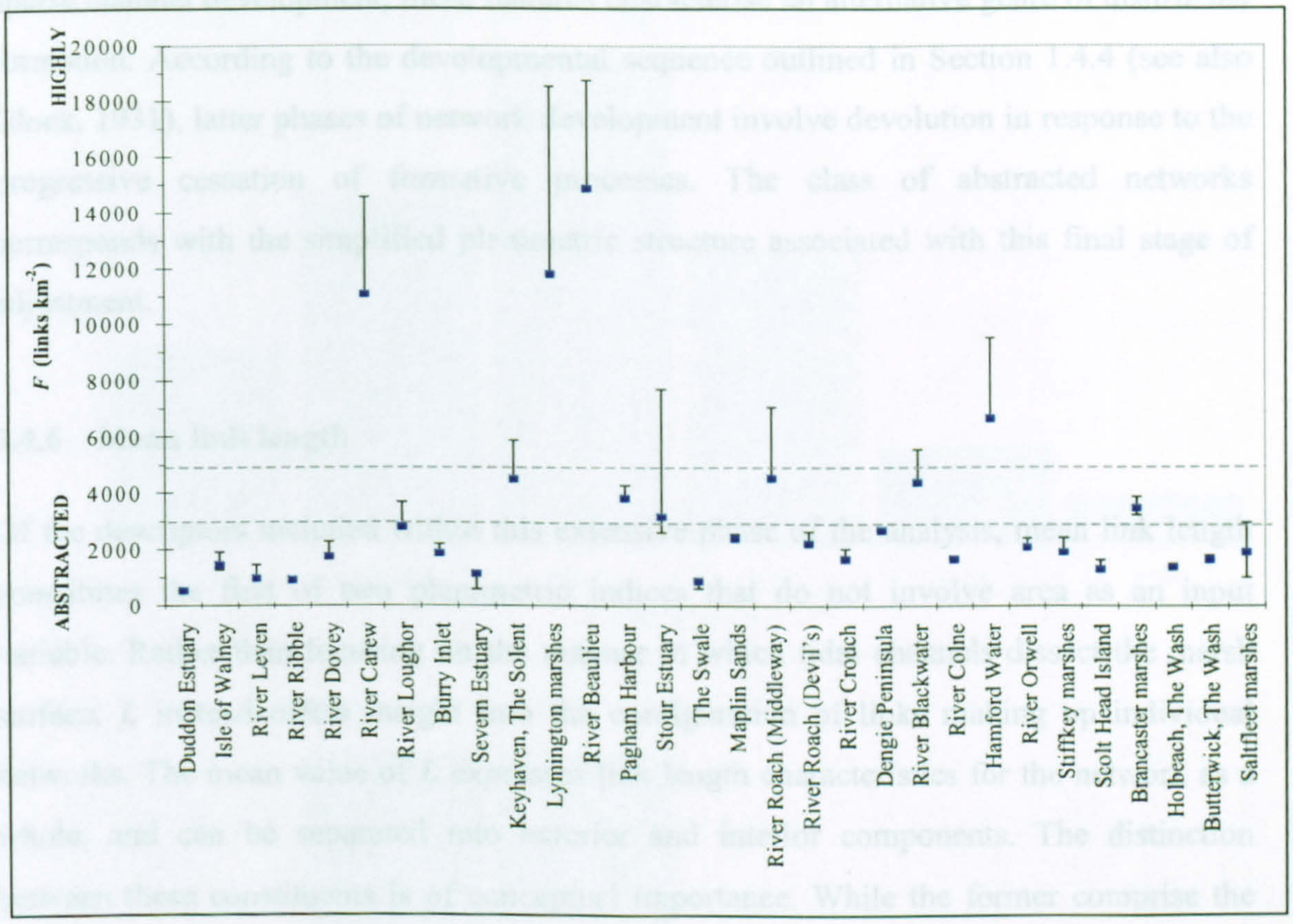

Figure 3.20 Geographic variability in F. Margins of uncertainty about A_{eq} are reflected by the upper (A_{min}) and lower (A_{max}) error bars.

The site-specific characteristics of F (Figure 3.20) indicate that the dataset can be divided into several broad classes of response. Networks exhibiting a particularly large concentration of links within each unit area are distinguished by values of $F > 5000$ links km^{-2} for A_{max}, and $F > 3000$ links km^{-2} for the A_{eq} decision rule. These *highly segmented* networks occur in Wales along the River Carew, on the south coast marshes at Keyhaven, Lymington, in the River Beaulieu and Pagham Harbour, and in the south-east bordering the Stour Estuary, River Roach, Hamford Water and River Blackwater. Judging from the disparity between A_{min} and A_{eq}, these networks are also sub-extended. Although internal dissection is pronounced, they have by no means achieved a space filling status. Characteristics such as these are synonymous with the mode of network growth described by Knighton *et al.* (1992), which proceeds by concomitant rather than successive phases of elongation and elaboration.

At the other end of the textural scale, networks in: the Duddon Estuary; the River Leven; the River Ribble; the Severn Estuary; and bordering The Swale, display a limited number of links per unit area. From the narrow margins of uncertainty surrounding A_{eq} at these localities (Figure 3.12a), network development is space filling. Combined with

sparse channel development, these features characterise an alternative genre of *abstracted* formation. According to the developmental sequence outlined in Section 1.4.4 (see also Glock, 1931), latter phases of network development involve devolution in response to the progressive cessation of formative processes. The class of abstracted networks corresponds with the simplified planimetric structure associated with this final stage of adjustment.

3.4.6 Mean link length

Of the descriptors included within this extensive phase of the analysis, mean link length constitutes the first of two planimetric indices that do not involve area as an input variable. Rather than focusing on the manner in which tidal channels dissect the marsh surface, L instead offers insight into the configuration of links making up individual networks. The mean value of L expresses link length characteristics for the network as a whole, and can be separated into exterior and interior components. The distinction between these constituents is of conceptual importance. While the former comprise the extremities of the system, and medium through which morphometric development and evolution proceed most readily, the latter constitute the circulatory system by which the sources are connected and maintained. In recognition of their disparate functions, fluvial studies have treated exterior and interior links as discrete populations (Shreve, 1967; Abrahams, 1984). However, the absence of previous work on tidal systems means that the statistical characteristics of these sub-sets, together with the total link length population, are essentially unknown. Although the mode of data collection enables a mean length to be derived for the sub-populations in each network, frequency distributions (see, for example, James and Krumbein, 1969) of the constituent links are not available.

Statistical characteristics of mean link lengths (Table 3.3) indicate that considerable variability is present in L, with values for the sample networks ranging between a minimum extent of L = 6.7m to a maximum of L = 52m. Overall, the link lengths are near-normally distributed (Figure 3.21a), with the majority of networks comprising links of $21 < L < 30$m. However, the frequency distribution also identifies two groups of sites supporting particularly high and low values, which stand apart from the rest of the population. The presence of such divisions within the histogram suggests that network formations fall into categories of *short* ($L < 20$ m), *medium* ($20 < L < 40$m) and *long* ($L > 40$ m) links.

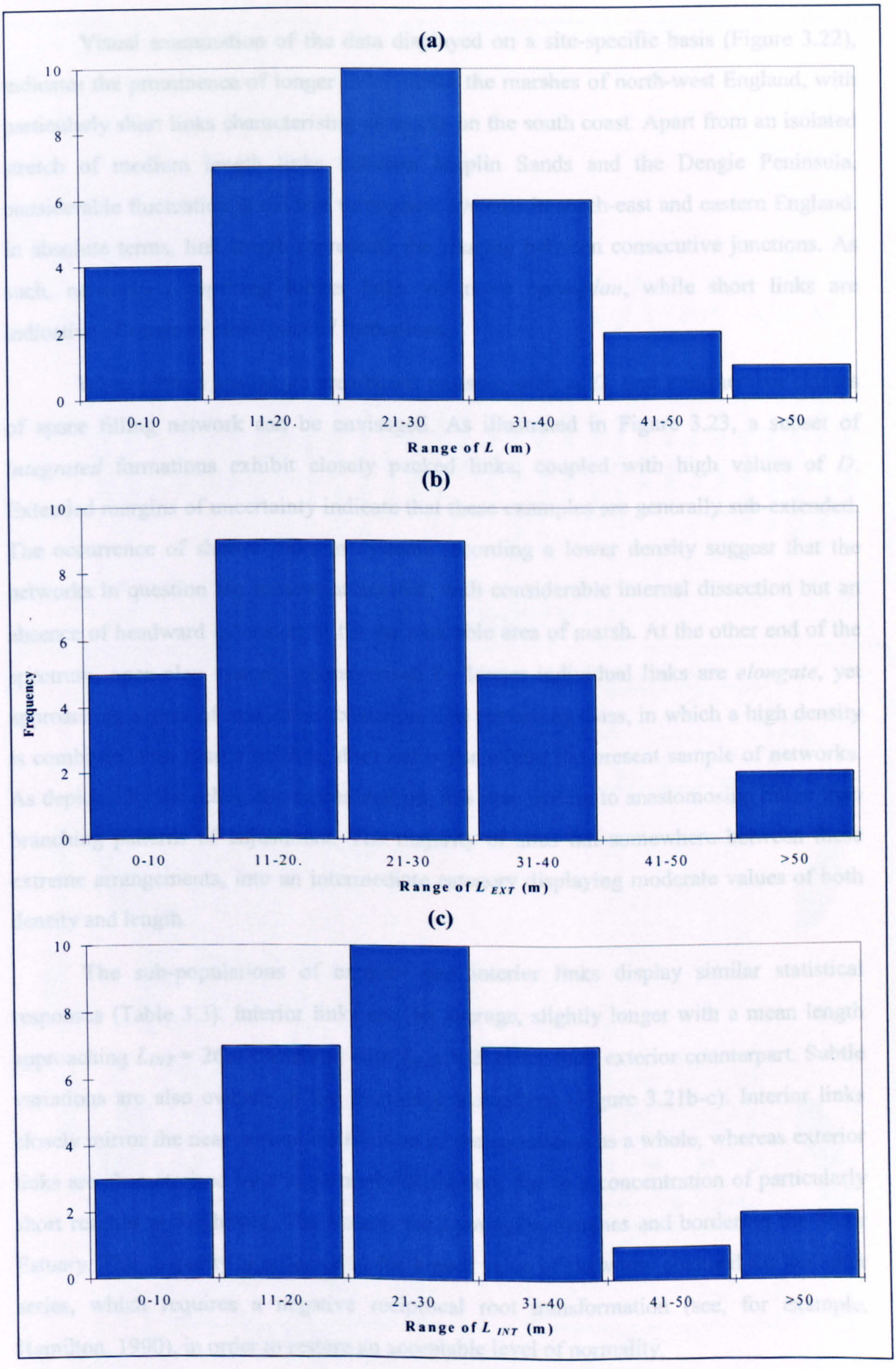

Figure 3.21 Frequency distribution of mean lengths for: (a) the sample population; (b) exterior; and (c) interior links.

Visual examination of the data displayed on a site-specific basis (Figure 3.22), indicates the prominence of longer links within the marshes of north-west England, with particularly short links characterising networks on the south coast. Apart from an isolated stretch of medium length links between Maplin Sands and the Dengie Peninsula, considerable fluctuation is evident throughout systems in south-east and eastern England. In absolute terms, link length represents the *spacing* between consecutive junctions. As such, networks comprising longer links are more *open-plan*, while short links are indicative of dense or *close-packed* formations.

When plotted against an area-based measure such as *D*, four end-member classes of space filling network can be envisaged. As illustrated in Figure 3.23, a subset of *integrated* formations exhibit closely packed links, coupled with high values of *D*. Extended margins of uncertainty indicate that these examples are generally sub-extended. The occurrence of shorter links in systems recording a lower density suggest that the networks in question are somewhat *stunted*, with considerable internal dissection but an absence of headward extension to fill the available area of marsh. At the other end of the spectrum, open-plan systems characterised by longer individual links are *elongate*, yet approaching a state of maximum extension. The remaining class, in which a high density is combined with longer reaches, does not occur within the present sample of networks. As depicted by the schematic representation, this may pertain to anastomosing rather than branching patterns of adjustment. The majority of sites fall somewhere between these extreme arrangements, into an intermediate category displaying moderate values of both density and length.

The sub-populations of exterior and interior links display similar statistical responses (Table 3.3). Interior links are, on average, slightly longer with a mean length approaching L_{INT} = 26m compared with L_{EXT} = 23m for their exterior counterpart. Subtle variations are also evident in the frequency histograms (Figure 3.21b-c). Interior links closely mirror the near-normal distribution of the population as a whole, whereas exterior links are characterised by a lognormal distribution, due to a concentration of particularly short reaches at Keyhaven, The Solent, the Lymington marshes and bordering the Stour Estuary. This disparity is reflected in the higher value of skewness obtained for the latter series, which requires a negative reciprocal root transformation (see, for example, Hamilton, 1990), in order to restore an acceptable level of normality.

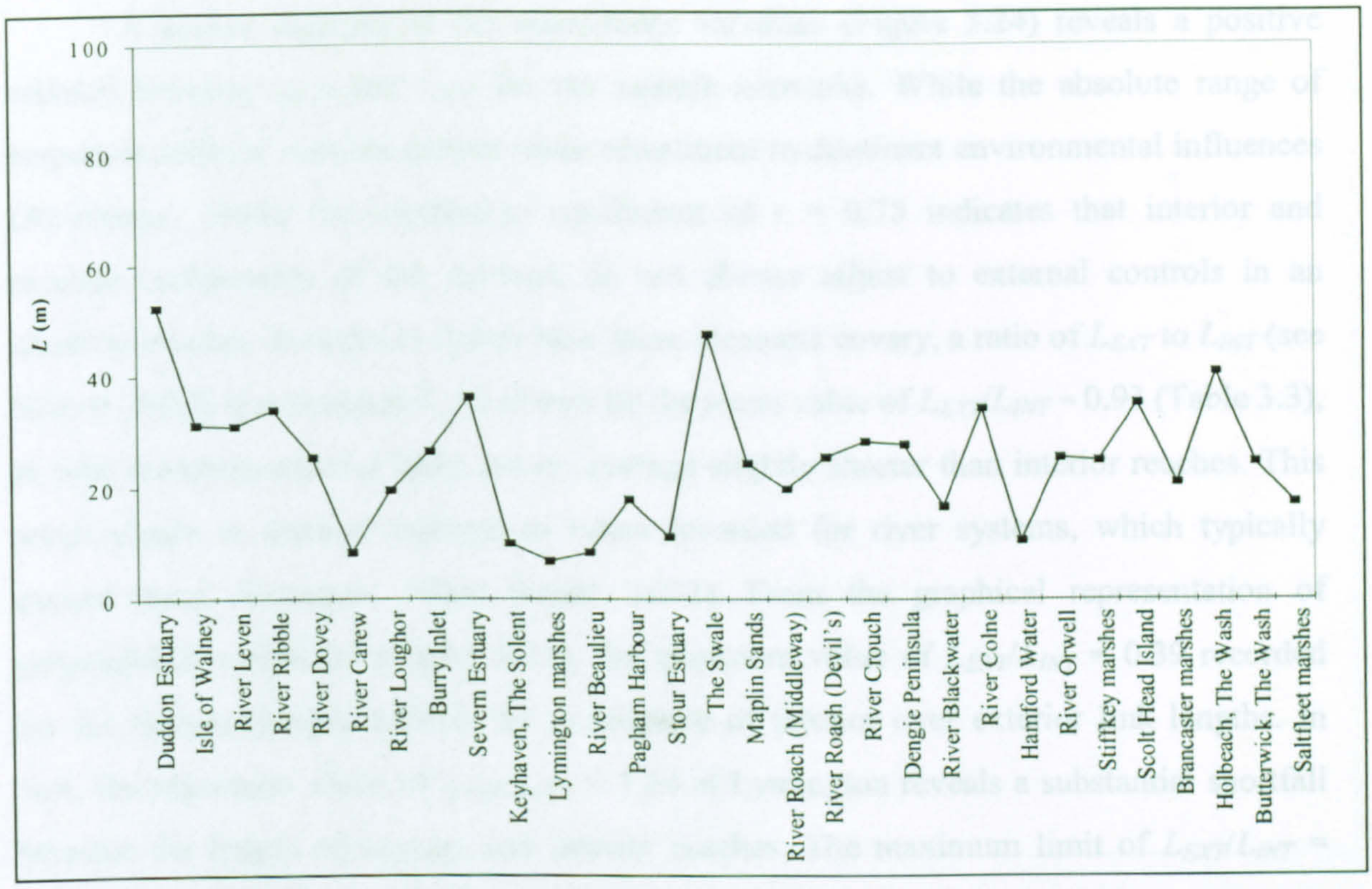

Figure 3.22 Geographic variability in *L*.

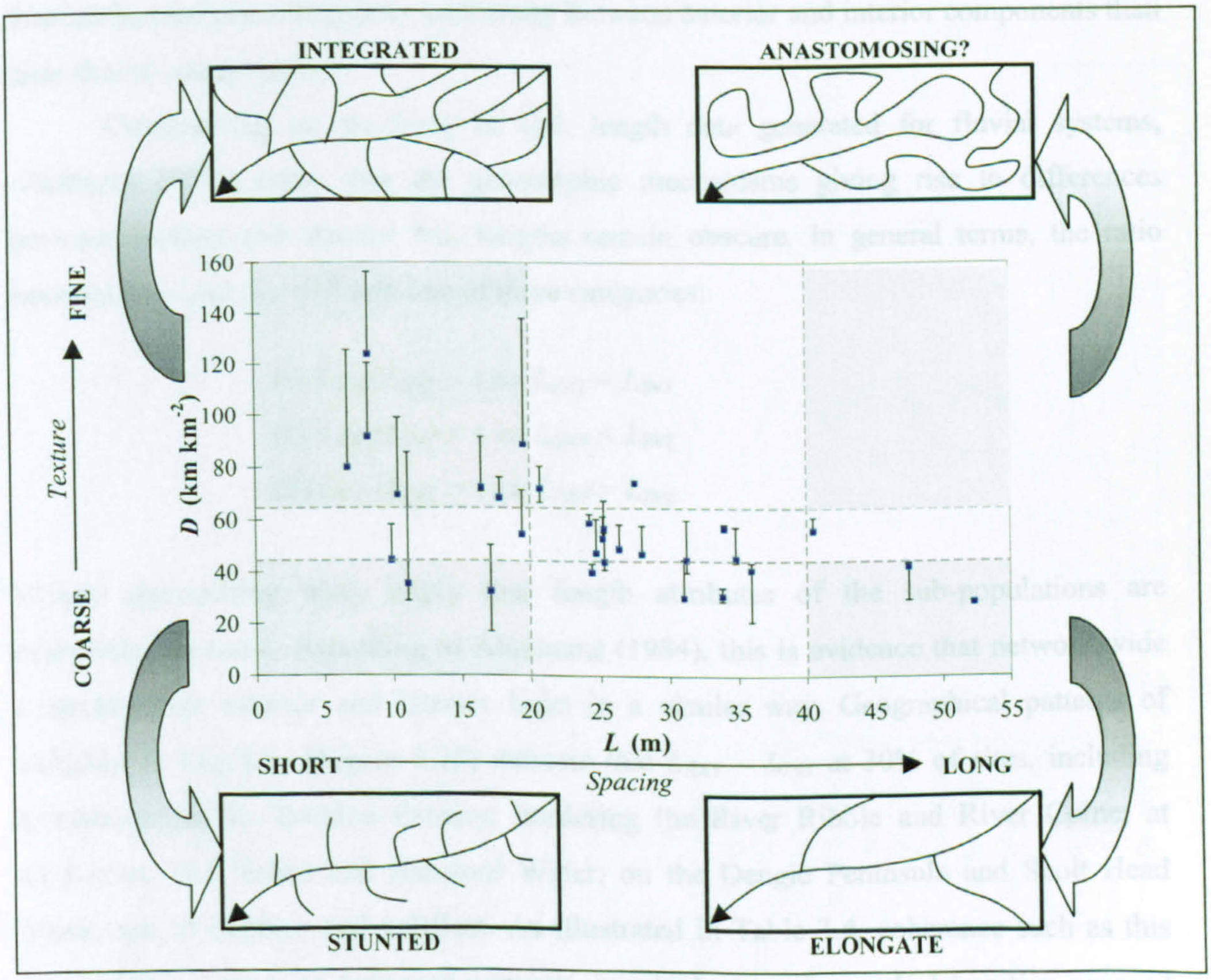

Figure 3.23 Schematic representation of variations in mean link length (L) with creek density (D_{eq}). Error bars reflect uncertainty in D relating to A_{min} and A_{max} decision rules.

A scatter diagram of the constituent variables (Figure 3.24) reveals a positive relation between L_{EXT} and L_{INT} for the sample networks. While the absolute range of responses reflects variable system-wide adjustment to dominant environmental influences (Abrahams, 1984), the correlation coefficient of r = 0.75 indicates that interior and exterior components of the network do not always adjust to external controls in an identical manner. In order to clarify how these elements covary, a ratio of L_{EXT} to L_{INT} (see Shreve, 1967) was computed. As shown by the mean value of $L_{EXT}/L_{INT} = 0.93$ (Table 3.3), in tidal networks exterior links are on average slightly shorter than interior reaches. This result stands in marked contrast to ratios recorded for river systems, which typically exceed unity (Schumm, 1956; Smart, 1972). From the graphical representation of geographical variability (Figure 3.25), the minimum value of $L_{EXT}/L_{INT} = 0.39$ recorded for the Severn Estuary reflects the dominance of interior over exterior link lengths. In turn, the maximum value of $L_{EXT}/L_{INT} = 1.64$ at Lymington reveals a substantial shortfall between the length of sources and interior reaches. The maximum limit of $L_{EXT}/L_{INT} = 2.60$ obtained by Smart (1972) is significantly higher, the implication being that tidal formations tend towards greater uniformity between exterior and interior components than their fluvial counterparts.

Commenting on the body of link length data generated for fluvial systems, Abrahams (1984) notes that the geomorphic mechanisms giving rise to differences between exterior and interior link lengths remain obscure. In general terms, the ratio between L_{EXT} and L_{INT} fall into one of three categories:

(1) $L_{EXT}/L_{INT} \sim 1 \Rightarrow L_{EXT} \sim L_{INT}$

(2) $L_{EXT}/L_{INT} < 1 \Rightarrow L_{EXT} < L_{INT}$

(3) $L_{EXT}/L_{INT} > 1 \Rightarrow L_{EXT} > L_{INT}$

Values approaching unity imply that length attributes of the sub-populations are essentially the same. According to Abrahams (1984), this is evidence that network-wide controls affect exterior and interior links in a similar way. Geographical patterns of variation in L_{EXT}/L_{INT} (Figure 3.25) indicate that $L_{EXT} \sim L_{INT}$ at 30% of sites, including formations: in the Duddon Estuary; bordering the River Ribble and River Colne; at Keyhaven, The Solent and Hamford Water; on the Dengie Peninsula and Scolt Head Island; and at Stiffkey and Saltfleet. As illustrated in Table 3.4, coherence such as this characterises a class of *balanced* network, in which extension and elaboration proceed concomitantly. Although associated mean link lengths span a wide range of values

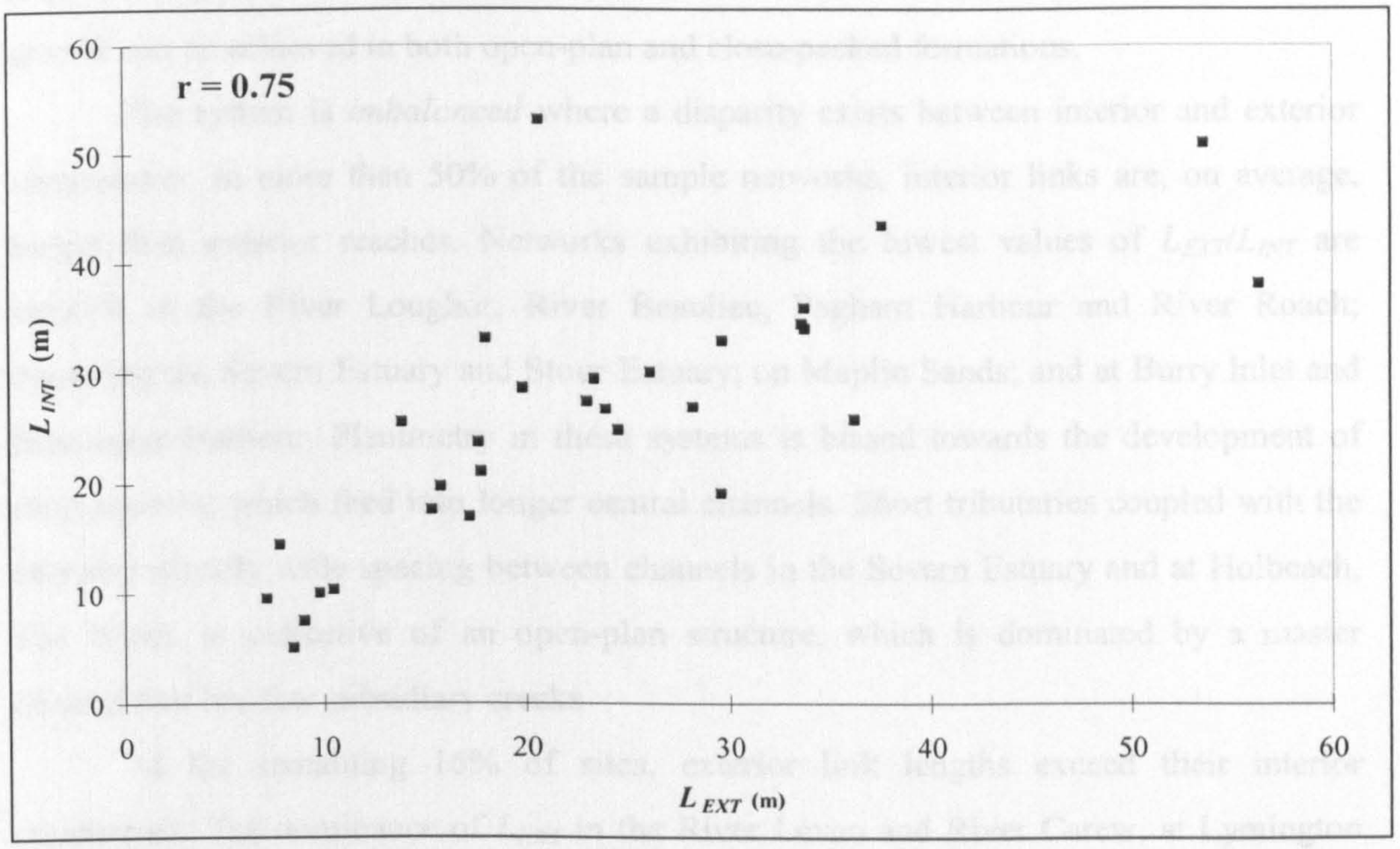

Figure 3.24 Scatter plot showing the degree of association between average exterior and interior link lengths.

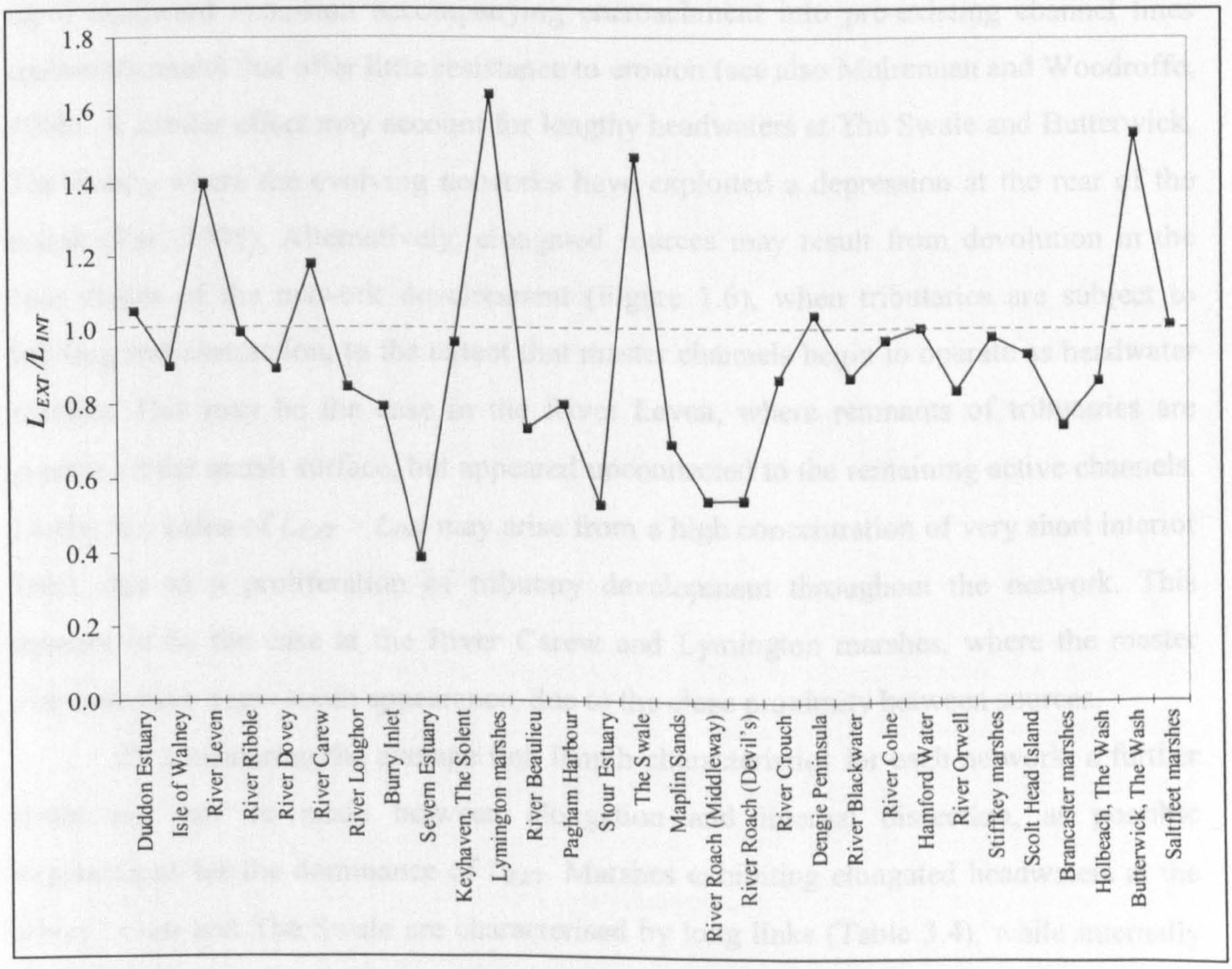

Figure 3.25 Geographic variability in L_{EXT}/L_{INT}.

(Figure 3.22), the indication is that a balance between headward extension and tributary growth can be achieved in both open-plan and close-packed formations.

The system is *imbalanced* where a disparity exists between interior and exterior components. In more than 50% of the sample networks, interior links are, on average, longer than exterior reaches. Networks exhibiting the lowest values of L_{EXT}/L_{INT} are located: in the River Loughor, River Beaulieu, Pagham Harbour and River Roach; bordering the Severn Estuary and Stour Estuary; on Maplin Sands; and at Burry Inlet and Brancaster Harbour. Planimetry in these systems is biased towards the development of short sources, which feed into longer central channels. Short tributaries coupled with the characteristically wide spacing between channels in the Severn Estuary and at Holbeach, The Wash, is indicative of an open-plan structure, which is dominated by a master channel that has few subsidiary creeks

At the remaining 16% of sites, exterior link lengths exceed their interior counterpart. The dominance of L_{EXT} in the River Leven and River Carew, at Lymington and Butterwick, The Wash, and bordering The Swale, has several possible explanations. Knighton *et al.* (1992) attribute particularly elongated sources in Australian marshes to rapid headward extension accompanying encroachment into pre-existing channel lines (palaeochannels) that offer little resistance to erosion (see also Mulrennan and Woodroffe, 1998). A similar effect may account for lengthy headwaters at The Swale and Butterwick, The Wash, where the evolving networks have exploited a depression at the rear of the marsh (Pye, 1995). Alternatively, elongated sources may result from devolution in the later stages of the network development (Figure 1.6), when tributaries are subject to infilling and abstraction, to the extent that master channels begin to operate as headwater reaches. This may be the case in the River Leven, where remnants of tributaries are present on the marsh surface, but appeared unconnected to the remaining active channels. Lastly, the status of $L_{EXT} > L_{INT}$ may arise from a high concentration of very short interior links, due to a proliferation of tributary development throughout the network. This appears to be the case at the River Carew and Lymington marshes, where the master channels have a saw-tooth appearance, due to the close proximity between sources.

By considering the average link length characteristics for each network, a further distinction can be made between elongation and internal dissection, as possible explanations for the dominance of L_{EXT}. Marshes exhibiting elongated headwaters at the River Leven and The Swale are characterised by long links (Table 3.4), while internally dissected marshes at Lymington and the River Carew comprise much shorter reaches.

CHANNEL SPACING	BALANCED	IMBALANCED	
	 $L_{EXT} \sim L_{INT}$	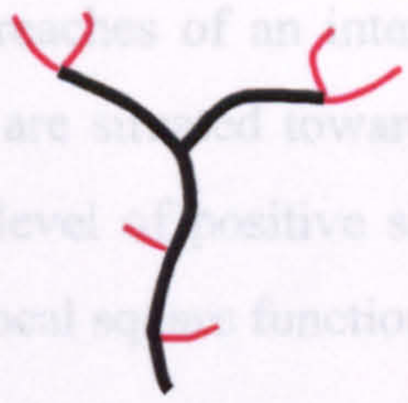 $L_{EXT} < L_{INT}$	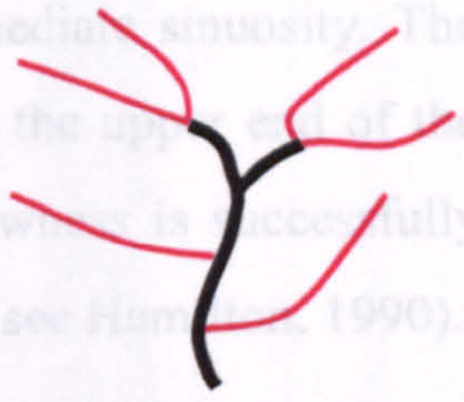 $L_{EXT} > L_{INT}$
OPEN-PLAN CLOSE-PACKED	Duddon Estuary Scolt Head Island River Ribble River Colne Dengie Peninsula Stiffkey marshes Saltfleet marshes Hamford Water Keyhaven, The Solent	Holbeach, The Wash Severn Estuary Isle of Walney River Crouch Burry Inlet River Dovey River Orwell River Roach Maplin Sands Brancaster Harbour River Roach River Loughor Pagham Harbour River Blackwater Stour Estuary River Beaulieu	The Swale River Leven Butterwick, The Wash River Carew Lymington marshes

Table 3.4 Categories of balanced and imbalanced link lengths, with study localities arranged according to mean channel spacing.

3.4.7 Sinuosity of the principal channel

Inclusion of a sinuosity measure, as a basis for distinguishing between the planimetric characteristics of channel networks, is desirable because it serves as a good initial delineation of major stream types (Rosgen, 1994). Leopold *et al.* (1964) distinguish between fluvial patterns on the basis of sinuosity values, whereby *straight* channels are characterised by a value of $S < 1.5$, *sinuous* channels by $S \sim 1.5$ and *meandering* reaches by $S > 1.5$. The frequency histogram in Figure 3.26a indicates that similar groupings are present in the tidal formations. Although results span the range $1.06 < S < 3.01$, the

majority of values are concentrated at the lower end of the scale ($S < 1.25$). While these readings are characteristic of comparatively straight reaches, a second group of responses clustered around S ~ 1.5 are consistent with reaches of an intermediate sinuosity. The least populous group of meandering networks are situated towards the upper end of the scale, with values of S > 1.75. A significant level of positive skewness is successfully removed by the application of a negative reciprocal square function (see Hamilton, 1990).

When organised in decreasing order of magnitude (Figure 3.27), the values obtained for *S* reveal considerable geographical variability in the degree of meandering. The study sites range from highly sinuous networks in the River Blackwater and at Butterwick, the Wash, through moderately sinuous Welsh systems, to linearised formations at the Isle of Walney and Stour Estuary. Stepped transitions are evident in the otherwise continuous series, occurring around sinuosity levels of 1.75, 1.50 and 1.25. These thresholds mark the division between straight, moderately sinuous and meandering systems.

Explaining the distinction between these contrasting levels of sinuosity is by no means straightforward. In designing the methodological procedure, it has already been acknowledged that *S* is an *ensemble* measure, reflecting the composite signal of network- and reach-scale adjustment. Unpacking the constituent signals is a logical step towards a more comprehensive interpretation of the results obtained. From the graphical representation in Figure 3.28, a large proportion of the ensemble sinuosity is accounted for by the network-scale signal, which spans the widest range of $1.01 < S_N < 2.09$ (see also Table 3.3). Tortuosity makes a modest contribution with $S_T < 1.40$, while meander asymmetry accounts for a marginal amount of the total sinuous adjustment with $S_A < 1.2$.

The positively skewed frequency distribution exhibited by *S* is mirrored by histograms for the partial measures (Figure 3.26b-d), indicating that non-normal behaviour transcends network- and reach-scale adjustment. Normality can in part be restored by applying a non-linear transformation. Post-transformation statistics (Table 3.3) indicate that a negative reciprocal square function provides an effective correction for S_N, reducing skewness to a level that supports parametric methods of statistical analysis. Due to deviant observations towards the upper end of the scale, S_A and S_T continue to exhibit an unacceptable level of skew. Since there are insufficient grounds for eliminating these outliers, the skewness is accepted as a limitation of the dataset, which is accommodated through implementing non-parametric statistical tests.

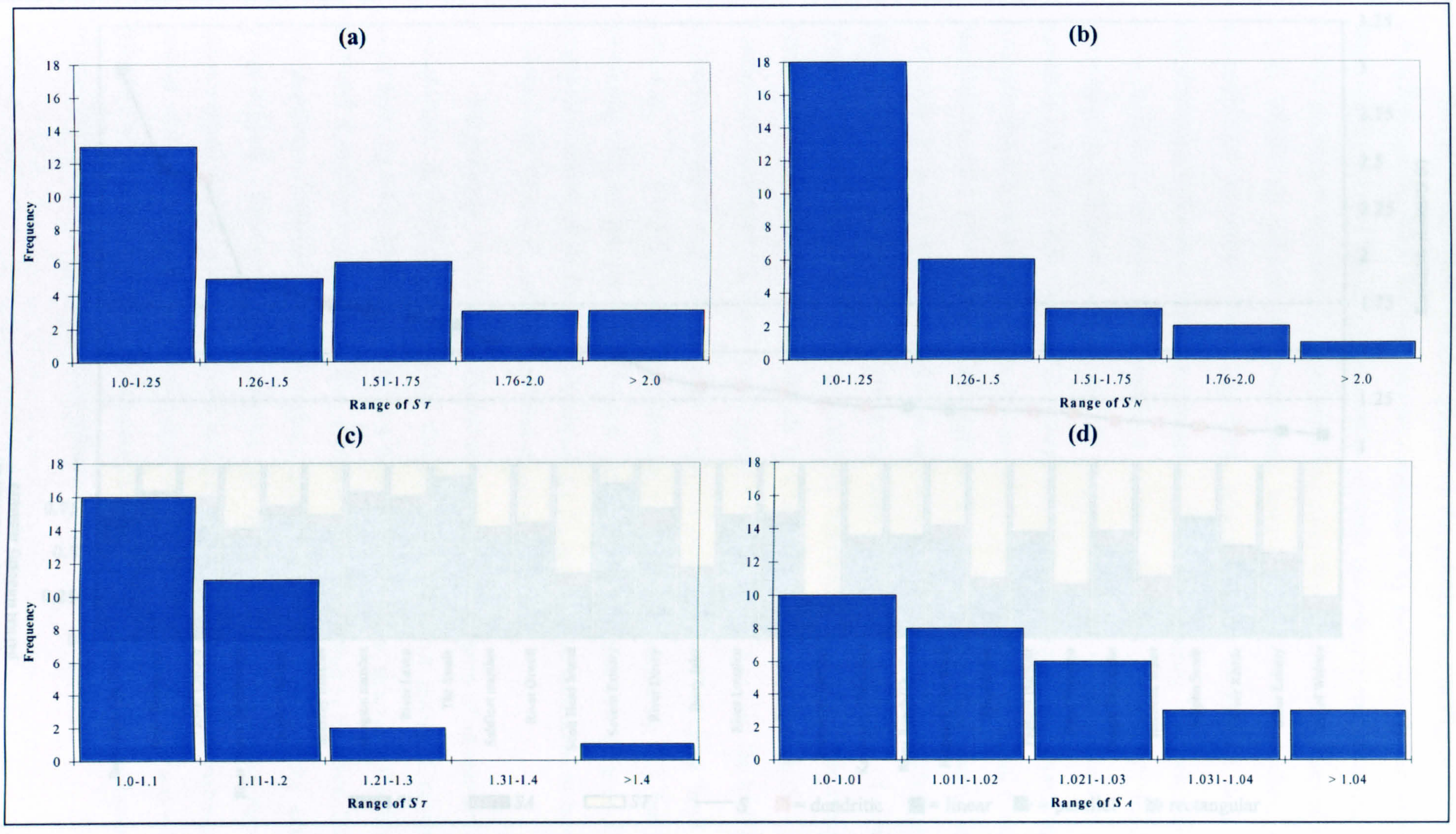

Figure 3.26 Frequency distribution of values obtained for: (a) principal channel sinuosity (S), and partial measures of: (b) network-scale sinuosity (S_N); (c) tortuosity (S_T); and (d) meander asymmetry (S_A).

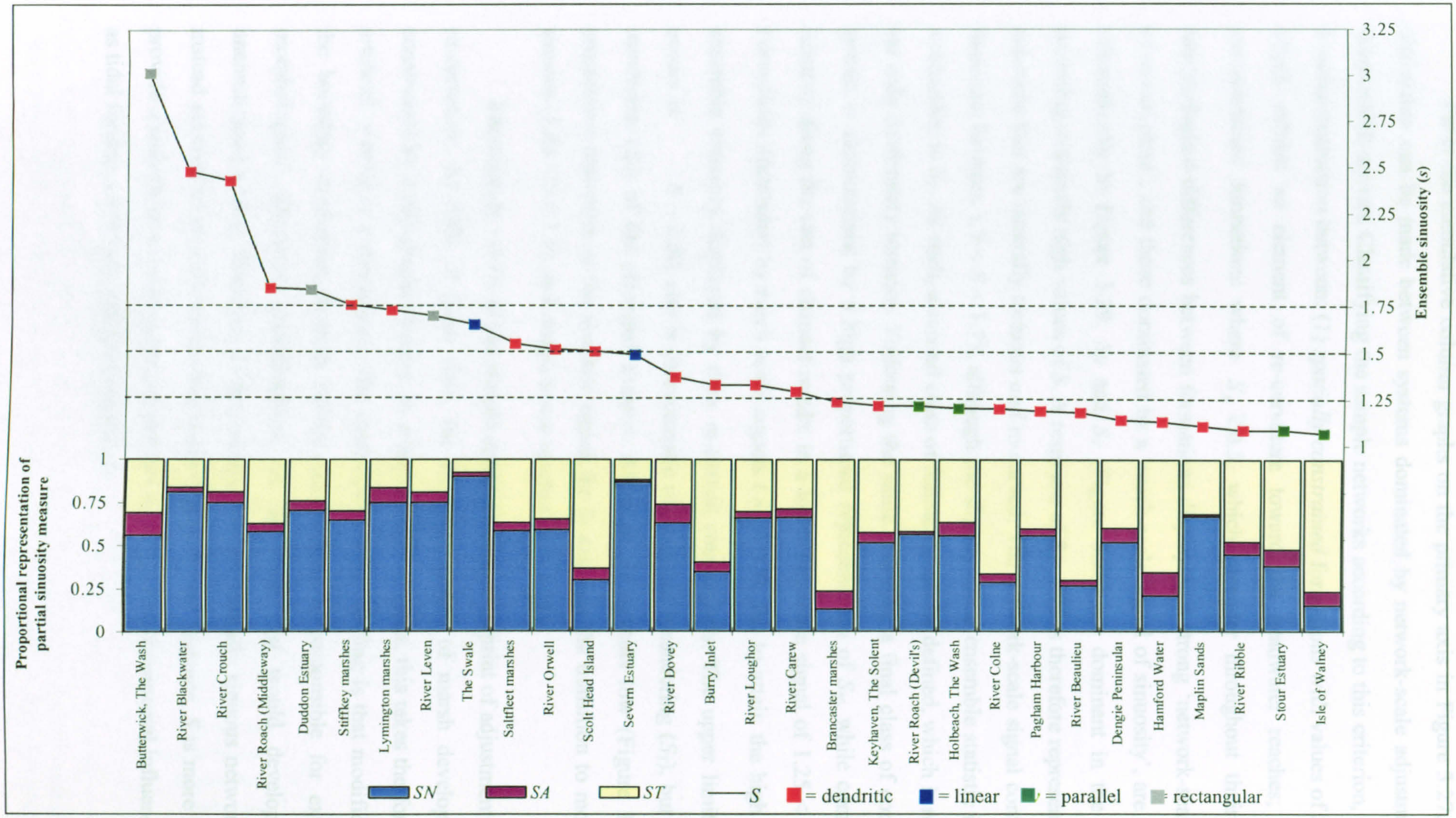

Figure 3.27 Proportional representation of asymmetric meandering (S_A) tortuosity (S_T) and network-scale (S_N) sinuosity terms (primary axis), with ensemble sinuosity (S) organised in decreasing order of magnitude (secondary axis). Threshold values suggested by Leopold *et al.* (1964) are marked, together with supplementary divisions identified during the present analysis.

From the cumulative column graphs on the primary axis in Figure 3.27, a broad distinction can be made between systems dominated by network-scale adjustment, and those which are not. Classifying the sample networks according to this criterion, provides a useful distinction between: (1) *spatially constrained* formations with values of $S_N > 0.5$, which exhibit an element of re-curvature toward the headwater reaches; and (2) *unconstrained* formations where $S_N \lesssim 0.5$, which meander throughout their course. Morphological differences between formations displaying a strong 'network-scale signal of re-curvature', and those dominated by a 'reach-scale signal of sinuosity', are depicted schematically in Figure 3.29. S_N and S_T (Figure 3.28) are dominant in the systems recording extremely high values of S. A response of $S > 1.75$ is therefore representative of networks that are naturally tortuous *and* re-curved. The network-scale signal continues to dominate between $1.5 < S < 1.75$, although the slightly lower ensemble statistic indicates a reduction in S_T. As such, a second class of formation can be defined, which is re-curved yet only moderately tortuous. Following the same principle, a final class of constrained system is characterised by a high proportional representation of S_N, while comparative linearity along the rest of channel results in a lower ensemble signal of $1.25 < S < 1.5$. Formations dominated by reach scale signals ($S_N \lesssim 0.5$), fail to attain the high level of ensemble sinuosity displayed by their re-curved counterparts. The upper limit instead occurs at $S \sim 1.50$, and is characteristic of sustained meandering (S_T), but reduced wandering (S_A) of the principal channel. Although S_N remains low (Figure 3.28c), a progressive reduction in the absolute signal for S_T explains the transition to moderately sinuous ($1.25 < S < 1.5$), and simple linear reaches ($S < 1.25$).

Interestingly, ~45% of the sample networks bare an imprint of adjustment through re-curvature. At 93% of these sites, the landward extent of marsh development is constrained by a topographic barrier. In a further 91% of cases, this takes the form of an artificial seawall or embankment. The implication of this finding is that modification to the boundary conditions, through human intervention, is responsible for extraneous morphological adjustment superimposed on the form that would develop in an unconstrained setting. Members of the second class of naturally sinuous networks have instead evolved in an intervention-free environment. In this instance, S is more likely to provide a realistic representation of adjustment to physical environmental influences such as tidal forcing, erodibility and gradient effects.

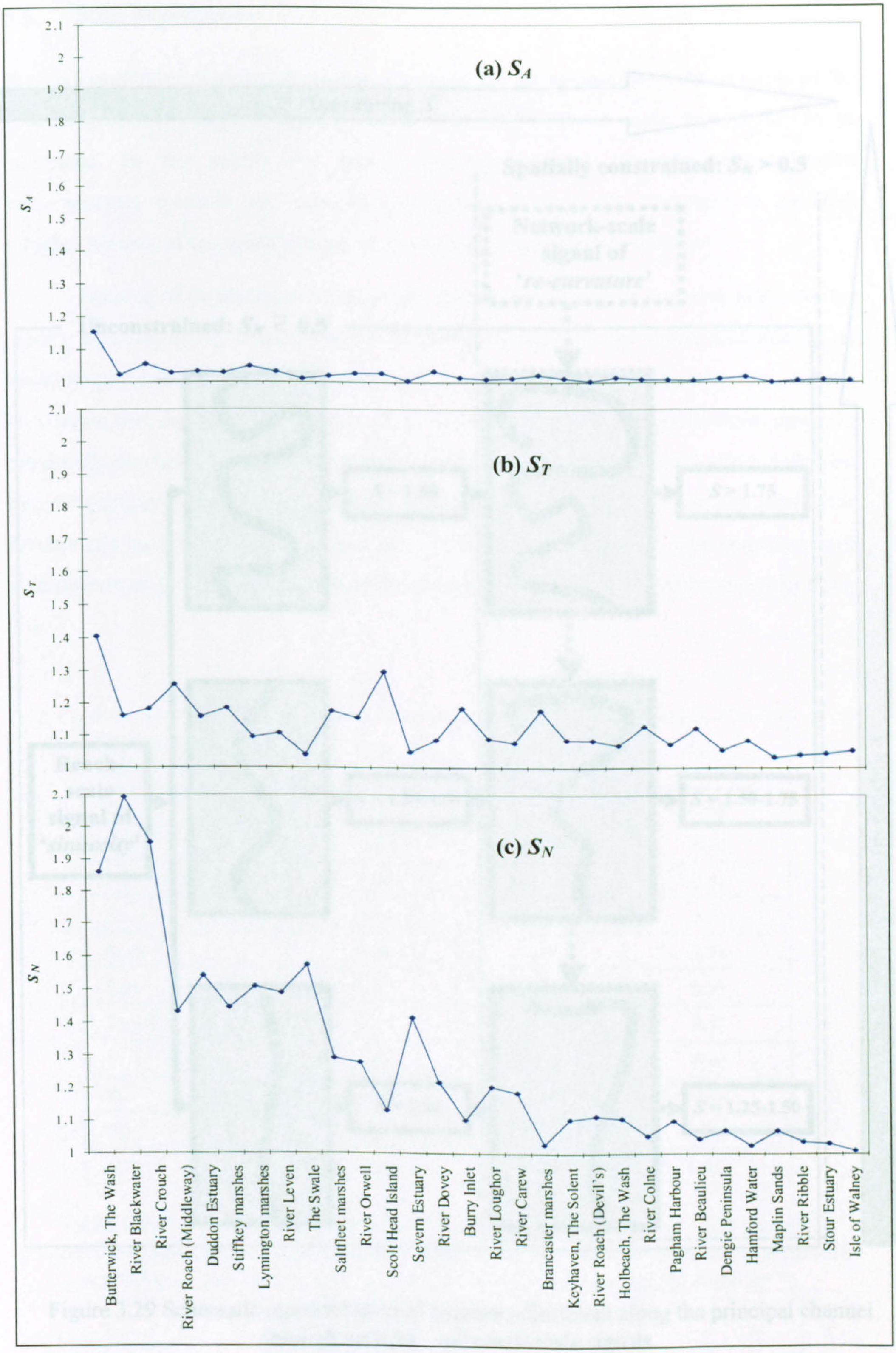

Figure 3.28 Measures of: (a) asymmetric meandering (S_A); (b) tortuosity (S_T); and (c) network-scale sinuosity (S_N). Data are organised in decreasing magnitude of ensemble sinuosity (S)

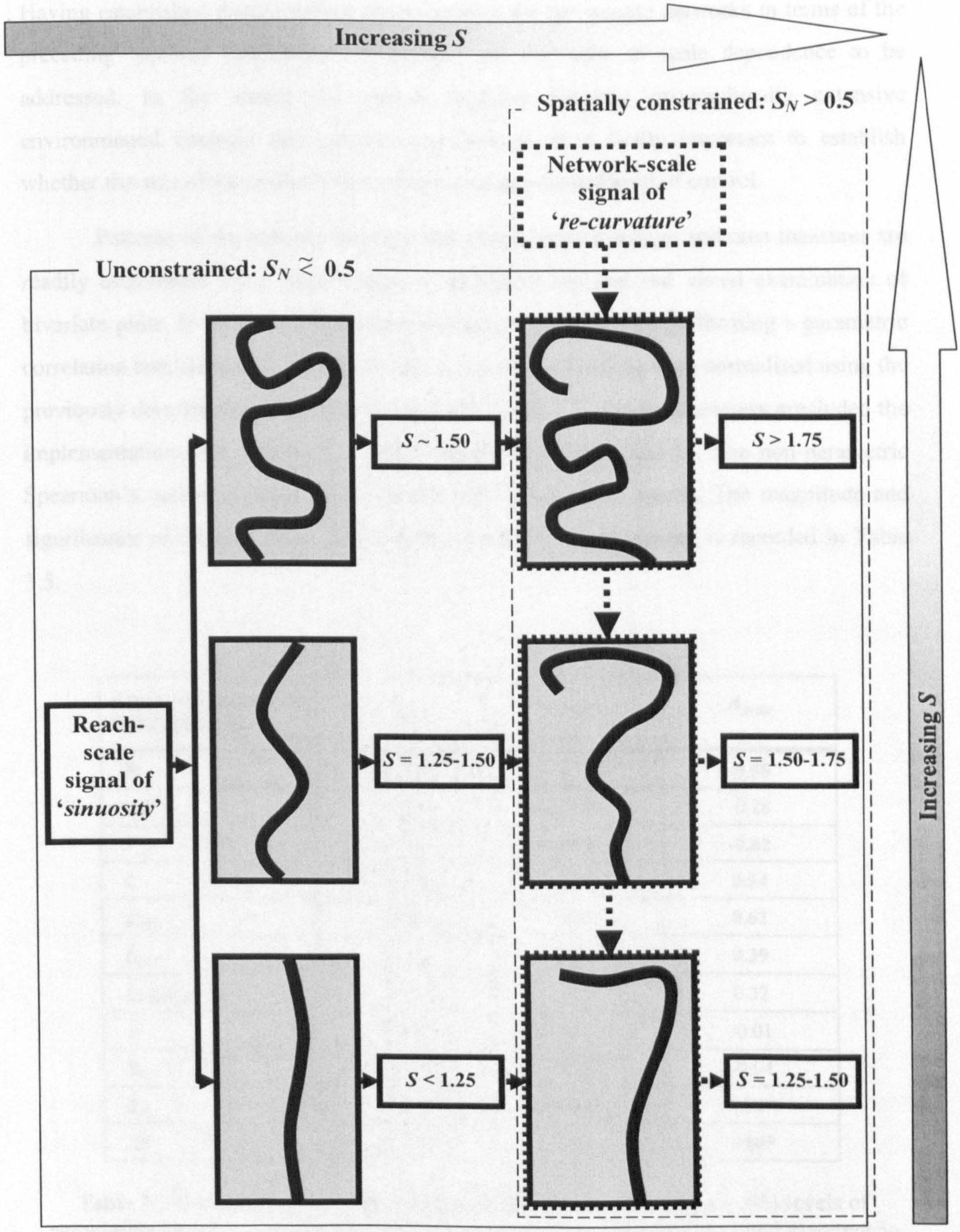

Figure 3.29 Schematic representation of sinuous adjustment along the principal channel through network- and reach-scale signals.

3.5 Scale dependence

Having established distinguishing characteristics for the sample networks in terms of the preceding 'optimal descriptors', it remains for the issue of scale dependence to be addressed. In the search for causal relations between geographically extensive environmental controls and network morphology, it is firstly important to establish whether the size of the system exerts an overriding *internal* level of control.

Patterns of dependence between the morphometric indices and area measures are readily established, by a combination of statistical analysis and visual examination of bivariate plots. In order to achieve the conditions necessary for performing a parametric correlation test, datasets for A, D, $\%C$, F, L, L_{EXT}/L_{INT}, S and S_N were normalised using the previously described transformations (see also Table 3.3). Severe skewness precluded the implementation of a Pearson's product moment test for S_T and S_A. The non-parametric Spearman's rank test (Shaw and Wheeler, 1997) was used instead. The magnitude and significance of the correlation coefficient recorded for each pairing is recorded in Table 3.5.

AREA MEASURE ⇨ DESCRIPTOR ⇩	A_{min}	A_{eq}	A_{max}
D	**-0.71**	**-0.58**	**-0.55**
$\%C$	-0.36	-0.20	-0.28
F	**-0.66**	**-0.61**	**-0.62**
L	**0.57**	**0.52**	**0.54**
L_{EXT}	**0.66**	**0.62**	**0.62**
L_{INT}	**0.42**	0.36	**0.39**
L_{EXT}/L_{INT}	0.35	0.35	0.32
S	0.00	-0.02	-0.01
S_N	-0.04	-0.06	-0.04
S_A	-0.12*	0.11*	0.09*
ST	0.06*	0.07*	0.04*

Table 3.5 Correlation matrix showing **statistically significant** ($\alpha = .05$) levels of association between appropriately transformed measures of marsh area and planimetric descriptors (Spearman's rank correlation coefficients are distinguished by *).

Results suggest that D, F, L, L_{EXT} and L_{INT} exhibit a statistically significant level of scale dependence, irrespective of the decision rule employed in area delineation. Negative associations for D (Figure 3.30a) and F (Figure 3.30b) imply that the degree of surface dissection systematically decreases as the scale of the marsh system increases. The similarity in responses obtained for these indices was perhaps to be expected, since link-based texture is the topological equivalent of creek density. The positive associations recorded for link lengths (Figure 3.30c-e) suggest that the interval between junctions increases with area cover. In view of the high photographic resolution (Appendix 1), this finding is unlikely to reflect errors of interpretation (see Shi *et al.* 1995), and instead indicates that branching characteristics change according to the scale of the system. Associations for the remaining measures of link length ratio and sinuosity are not significant at the designated critical threshold, the implication being that these series are essentially scale free.

The issue of scale dependence has previously been addressed for the fluvial measure of drainage density (Pethick, 1975; Gardiner *et al.*, 1977; Pethick, 1978). The comparable mode of derivation means that the same concerns apply to tidal systems, inasmuch that an underlying relation to marsh area could mask important causal associations with external controlling elements. As stated by Ferguson (1978, p.351) '*the real importance of the scale effect lies in its implication for what is surely the main geomorphological question about drainage density, namely how it varies with environmental conditions*'. Several lines of reasoning have been put forward to explain the systematic pattern of response between D and A. Strahler (1964, p.52) originally observed that where geometrical similarity exists between two networks, '*their drainage densities will be related in the same ratio as the inverse of the linear scale ratio*'. In simple terms, this means that where the ratio of total channel length to marsh area maintains a roughly similar form as network coverage increases, values for D will always decrease. A plot of $\sum L$ against A (Figure 3.31a) reveals that total channel length is strongly related to A. Variance about the regression line suggests that the sample networks may be categorised into three fairly distinct groups according to size. *Large* systems in the Duddon Estuary, River Ribble and River Colne, occupy $A > 0.35$ km^2. Formations covering an *intermediate* area of $0.12 < A < 0.25$ km^2 occur at Dengie Peninsula, Scolt Head Island, sites fringing The Wash, and the Saltfleet marshes. The remaining 22 *small* systems occupy an area of $A < 0.12$ km^2. These findings stand in marked contrast to the observation made by Pethick (1992), that the total extent of creek development is

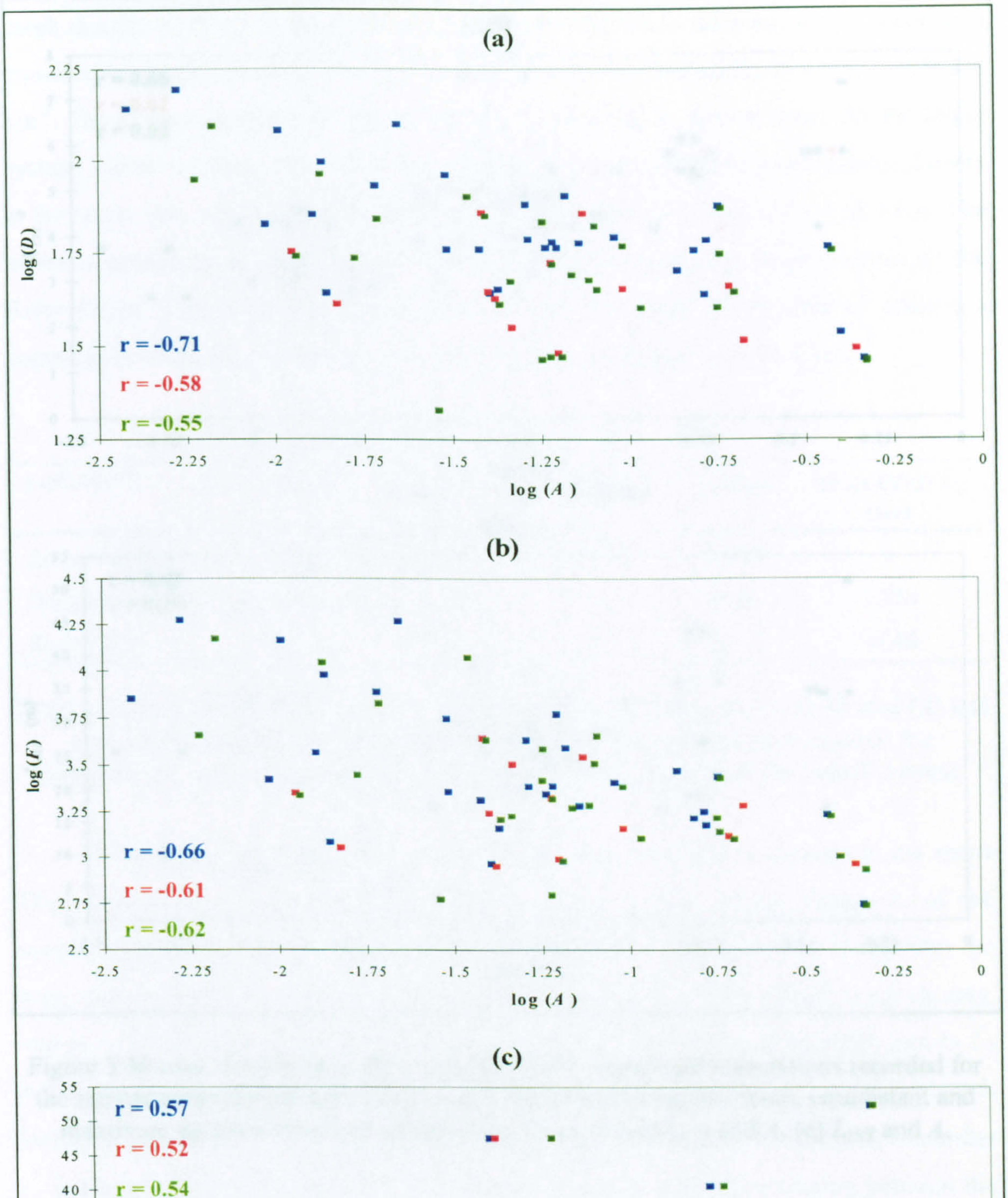

Figure 3.30 Scatter plots showing statistically significant associations recorded for the sample networks between: (a) D and A (computed using minimum, equidistant and maximum decision rules); (b) F and A; (c) L and A; (d) L_{EXT} and A; (e) L_{INT} and A.

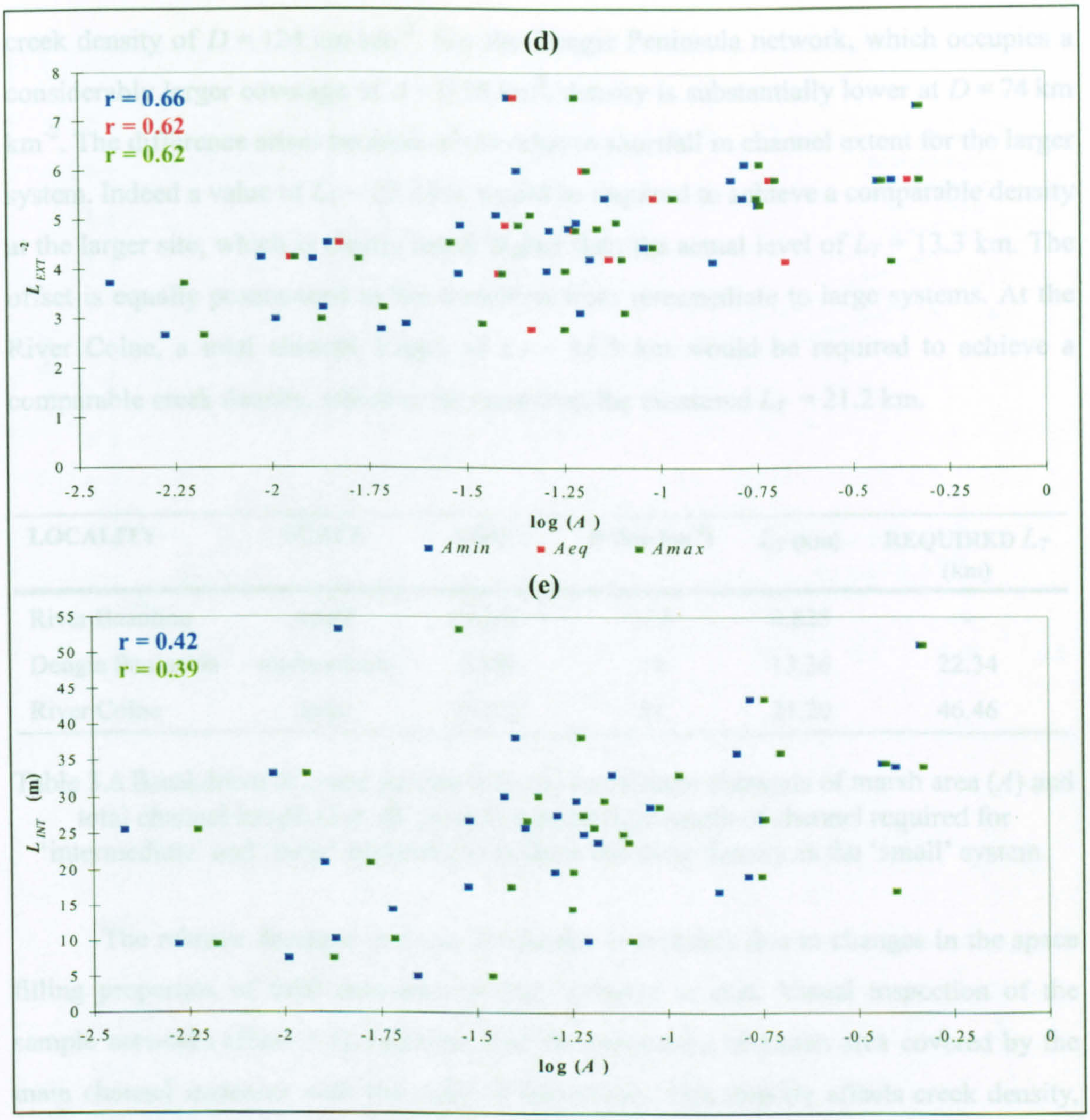

Figure 3.30 cont. Scatter plots showing statistically significant associations recorded for the sample networks between: (a) D and A (computed using minimum, equidistant and maximum decision rules); (b) F and A; (c) L and A; (d) L_{EXT} and A; (e) L_{INT} and A.

independent of marsh area coverage. If this were the case, the narrow clustering of points about the trendline would be replaced by an essentially random scatter.

Smart (1978, p.155) goes on to note that, '*a negative correlation* [between D and A] *is to be expected unless the numerator....increases in at least a linear fashion with area*'. In line with Gregory and Walling (1973), the present length-area relation takes the form of a power rather than a linear function. The implication of area increasing more rapidly with scale than channel extent is usefully illustrated with reference to selected examples from the present study. As shown in Table 3.6, the balance between L_T and A for a small system spanning an area of $A = 0.007$ km^2 at the River Beaulieu, results in a

creek density of $D = 124$ km km^{-2}. For the Dengie Peninsula network, which occupies a considerably larger coverage of $A = 0.18$ km^2, density is substantially lower at $D = 74$ km km^{-2}. The difference arises because of the relative shortfall in channel extent for the larger system. Indeed a value of $L_T \sim 22.4$ km would be required to achieve a comparable density at the larger site, which is clearly much higher than the actual level of $L_T = 13.3$ km. The offset is equally pronounced in the transition from intermediate to large systems. At the River Colne, a total channel length of $L_T \sim 46.5$ km would be required to achieve a comparable creek density, which is far more than the measured $L_T = 21.2$ km.

LOCALITY	SCALE	A (km^2)	D (km km^{-2})	L_T (km)	REQUIRED L_T (km)
River Beaulieu	small	0.007	124	0.825	-
Dengie Peninsula	intermediate	0.180	74	13.36	22.34
River Colne	large	0.375	57	21.20	46.46

Table 3.6 Breakdown of creek density (D) into constituent elements of marsh area (A) and total channel length (L_T), showing the theoretical length of channel required for 'intermediate' and 'large' networks to achieve the same density as the 'small' system.

The relative decrease in L_T as A enlarges is probably due to changes in the space filling properties of tidal networks as they increase in size. Visual inspection of the sample networks (Plate 3.1), indicates that the proportion of marsh area covered by the main channel increases with the scale of the system. This directly affects creek density, because a single wide channel in the lower reaches of the system contributes less to L_T than would an equivalent sector dissected by numerous narrow tributaries. Since creek density is a network-wide measure, it may be expected that systems displaying a number of dominant creeks will display a lower value of D, due to spatial averaging between the lower density master channels and the higher density tributaries. This idea is expressed schematically in Figure 3.32a. Homogeneity in L_T is seen to diminish with increasing marsh coverage, with spatial averaging explaining the lower values of D compared with a small network where L_T is consistently high.

Percentage channel cover is a dimensionless alternative to creek density, which avoids the pitfall of scale related spatial averaging (Table 3.5). The positive association between $\%C$ and A (Figure 3.31b) is best approximated by a linear function, the implication being that the *rate* of growth in channel coverage exhibits greater consistency with increasing area than extent alone. As explained in Figure 3.32b, the addition of a

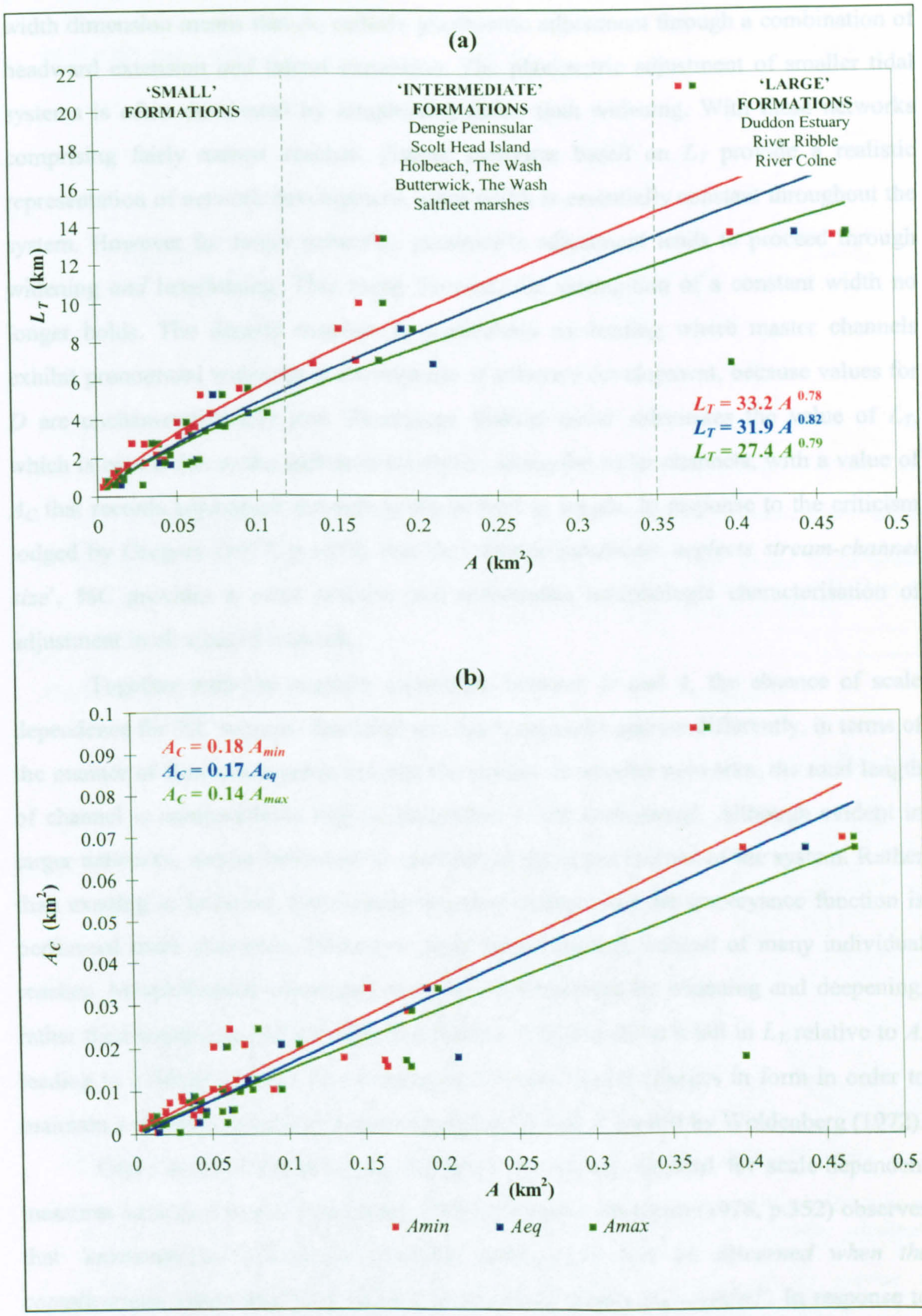

Figure 3.31 Scatter plot showing relations between: (a) L_T and A (computed using minimum, equidistant and maximum decision rules); and (b) A_C and A.

width dimension means that A_C reflects planimetric adjustment through a combination of headward extension *and* lateral expansion. The planimetric adjustment of smaller tidal systems is often dominated by lengthening rather than widening. With these networks comprising fairly narrow reaches, density measures based on L_T provide a realistic representation of network development, since width is essentially constant throughout the system. However for larger networks, planimetric adjustment tends to proceed through widening *and* lengthening. This being the case, the assumption of a constant width no longer holds. The density measure is particularly misleading where master channels exhibit pronounced widening at the expense of tributary development, because values for D are uncharacteristically low. Percentage channel cover substitutes the value of L_T, which is biased due to the deficit of tributaries along the wider channels, with a value of A_C that records adjustment through width as well as length. In response to the criticism lodged by Gregory (1977, p.1075) that the *'density parameter neglects stream-channel size'*, *%C* provides a more realistic and comparable morphologic characterisation of adjustment in all sizes of network.

Together with the negative correlation between D and A, the absence of scale dependence for *%C* suggests that large and small networks operate differently, in terms of the manner of flow conveyance through the system. In smaller networks, the total length of channel is comparatively high in proportion to the area served. Although evident in larger networks, similar behaviour is confined to the upper reaches of the system. Rather than existing in isolation, these outer tributaries merge, and the conveyance function is performed more efficiently through a single larger channel, instead of many individual reaches. Morphological adjustment is therefore dominated by widening and deepening, rather than lengthening of the principal channel. This results in a fall in L_T relative to A, leading to a decrease in D. The occurrence of scale-related changes in form in order to maintain a constant function, has been alluded to in a tidal context by Woldenberg (1972).

Other external controls may influence the values recorded for scale-dependent measures such as F and D (see Bauer, 1980). However, Ferguson (1978, p.352) observes that *'environmental effects on drainage density can best be discerned when the complications introduced by downstream and scale effects are avoided'*. In response to further comments that densities should be compared for separate areas of the same size, the distinction between small, intermediate and large formations was tested as a means of alleviating the effect of scale. Results indicate that an element of scaling persists

(a) Progressive reduction in D with increasing A

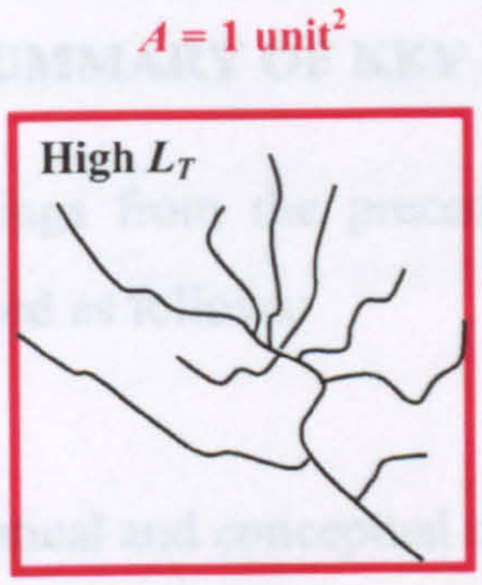

EXAMPLE 1: THE **SMALL** NETWORK

- L_T is high throughout the contributing area (A=1) of the network.
- This results in a high value of D

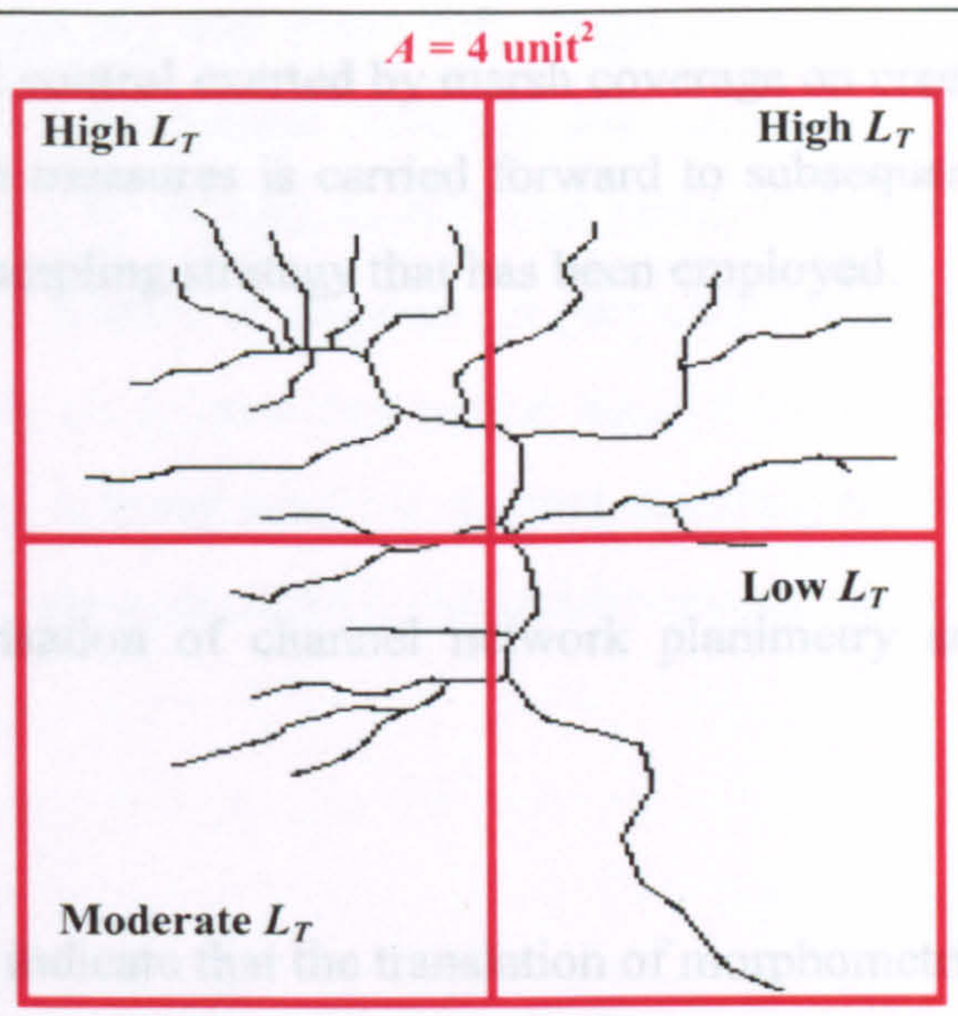

EXAMPLE 2: THE **LARGE** NETWORK

- As A increases, L_T varies considerably between the unit contributing areas.
- Since D provides an average density for the network as a whole, an intermediate value results from the combination of high, moderate and low L_T.

(b) Scale-free behaviour of $\%C$

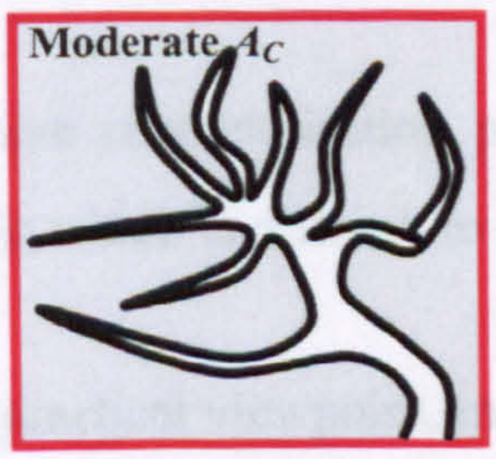

EXAMPLE 1: THE **SMALL** NETWORK

- For smaller networks, planimetry is dominated by adjustment through lengthening.
- Creeks are consistently narrow and width adjustment contributes little to the overall value of A_C.
- A_C and L_T are highly correlated, with either providing a realistic expression of network development.

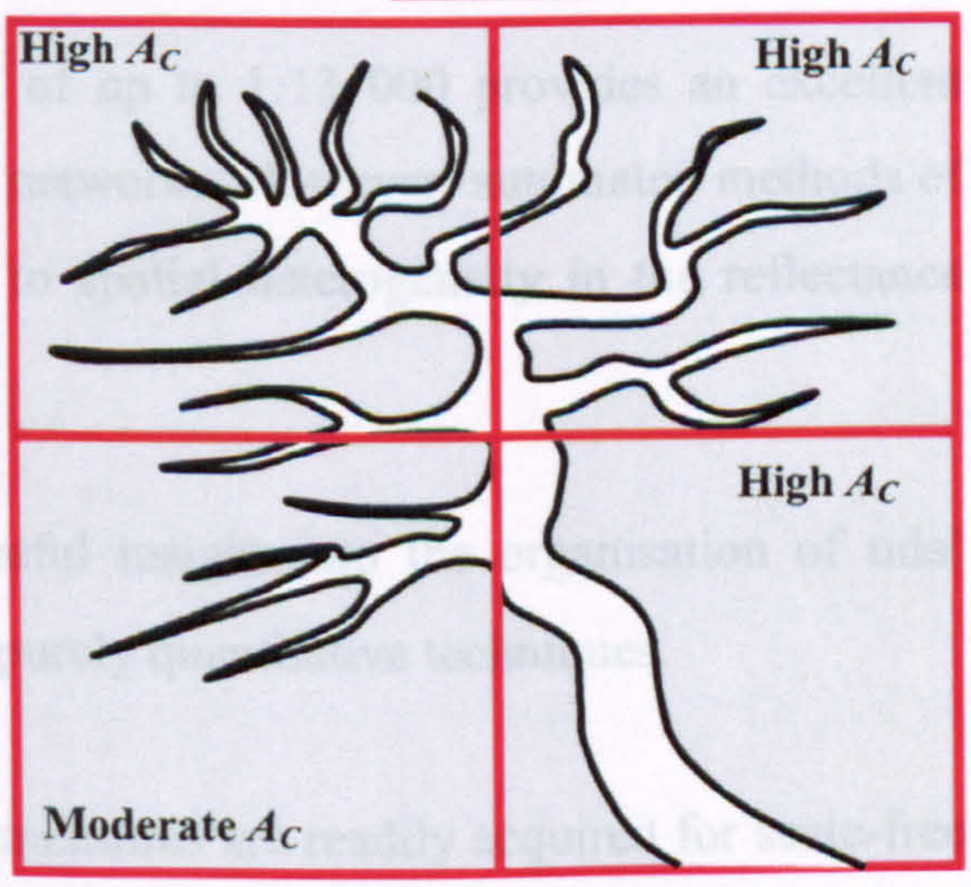

EXAMPLE 2: THE **LARGE** NETWORK

- Channel widening replaces tributary development as the principal mode of planimetric adjustment towards the mouth of larger systems.
- Density measures based on L_T provide an uncharacteristic representation of textural form.
- A_C reflects mutual adjustment through both channel width and length and is less highly correlated with L_T than in smaller networks.
- Scale dependent spatial averaging is alleviated by $\%C$.

Figure 3.32 Schematic diagram showing: (a) progressive reduction in D with increasing marsh area due to the influence of master channels; and (b) scale-free behaviour of $\%C$.

within these sub-groups. As such, the internal control exerted by marsh coverage on creek density, link-based frequency and link length measures is carried forward to subsequent phases of the analysis, as a limitation of the sampling strategy that has been employed.

3.6 SUMMARY OF KEY FINDINGS

Key findings from the preceding characterisation of channel network planimetry are summarised as follows:

- Theoretical and conceptual considerations indicate that the translation of morphometric descriptors from a fluvial to a tidal context is a reasonable undertaking. The extreme velocities, which are capable of performing erosive work and occur during the ebb phase of overmarsh tides, are comparable with the dominant discharges identified for river networks. Although the frequency with which these fluxes occur differs markedly between the two environments, the shared drainage function provides grounds for employing a similar analytical approach.

- Aerial photography at a spatial resolution of up to 1:13 000 provides an excellent source of planimetric data for tidal channel networks. However, automated methods of feature extraction are of limited use, due to spatial heterogeneity in the reflectance characteristics of creek bed and banks

- Descriptive characterisation provides a useful insight into the organisation of tidal networks, which is difficult to assess using purely quantitative techniques.

- From a practical viewpoint, morphometric measures are readily acquired for scale-free indices such as mean link length and sinuosity. In the case of area-based indices, the measurement of a contributing area is subject to uncertainty due to the difficulty of delimiting topographic boundaries, and uncertainty concerning the pathways followed by overmarsh flows.

- Geographical variations in the planimetric characteristics of tidal channels throughout England and Wales generally exceeds intra-site variability between adjacent networks.

- Measures of creek density, link-based frequency and mean link length exhibit scale-dependence that is absent from expressions of channel coverage and sinuosity. This stands in marked contrast to the observation by Pethick (1992) that network extent is independent of marsh area. The systematic pattern of response in part arises from the changing manner in which tidal flows are accommodated as the size of the system increases. In small formations, adjustment is dominated by channel lengthening. For larger systems, flows are more efficiently accommodated by channel convergence and adjustment through widening.

4. LONGITUDINAL CHARACTERISATION

4.1 INTRODUCTION

While recognised as being of primary importance in the study fluvial channel networks (Knighton, 1998), the longitudinal characteristics of tidal formations have received surprisingly little attention. The few observations that have been made regarding downstream adjustments in channel bed elevation (Pestrong, 1965; Myrick and Leopold, 1963; Allen, 1985a; Collins *et al.*, 1987; French and Stoddart, 1992; Ayles and Lapointe, 1996) offer conflicting insights into profile form, ranging from: straight to upwardly concave; and smooth to highly irregular. The application of morphometric expressions and models to describe and predict profile form is similarly limited, an isolated attempt being made by Collins *et al.* (1987) to analyse channel gradients. It remains for a comprehensive characterisation to be undertaken, in order to qualify and quantify the manner in which the longitudinal form of saltmarsh creeks adjusts to accommodate imposed boundary conditions.

In the present study, an extensive methodological approach (Section 2.1) is used to establish common and distinguishing features of the longitudinal profile for saltmarsh localities throughout England and Wales. Following details of data acquisition (Section 4.2), an exploratory analysis of profile form is undertaken (Section 4.3), providing an insight into morphological regularities and spatially discontinuous behaviour displayed at both 'network-wide' and 'downstream' scales. In Section 4.4, a selection of morphometric descriptors are employed to provide quantitative bases for comparing and contrasting the various modes of longitudinal adjustment displayed by the population of study sites. Finally, in order to establish whether marsh area exerts an internal level of control over longitudinal adjustment, the issue of scale dependence is addressed (Section 4.5).

4.2 DATA ACQUISITION

Defined in a fluvial context as *'the gradient of a stream at the reach and longitudinal scales'* (Knighton, 1998, p.156), an equivalent longitudinal profile in tidal networks involves the expression of channel bed elevation as a function of distance along the channel. Field surveying is the optimal source of primary data for the characterisation undertaken here (see Figure 2.1). In the case of river networks, longitudinal profiles are

often derived from topographic maps (Rosgen, 1994). However, corresponding intertidal elevation data are scarce, with poor hydrographic coverage and only mean high and mean low water marks consistently depicted on Ordnance Survey sheets. As noted in Section 2.2, airborne lidar altimetry (Hill *et al.*, 2000) may prove useful in future creek mapping exercises, but is presently unavailable for many of the study sites.

With the sole exception of Landimore marsh bordering Burry Inlet (which proved inaccessible at the time of survey), the suite of localities identified in Figure 2.5 were included to ensure a geographically diverse sample of networks. Longitudinal characterisation was carried out along a single reach corresponding with the principal channel of each system (see Figures 3.6-3.9; for decision rules see Figure 3.7). The principal creek was selected as the basis for analysis, since it is most likely to reflect morphological adjustment throughout the developmental sequence (Figure 1.6). The inclusion of tributary reaches is inappropriate, since these reflect a shorter period of adjustment, while the composite profile defined by Strahler (1964) and utilised by Yang (1971) is based on Hortonian ordering and subject to the limitations outlined in Figure 2.6. Where possible, sample reaches were selected with 'dead-end' rather than 'through flowing' headwaters (Plate 4.1), since hydrodynamic studies (see Ashley and Zeff, 1988) suggest that these contrasting morphologies experience markedly different flow regimes. In the field, the upper limit of the profile was identified as the channel head, defined in a fluvial context by Dietrich and Dunne (1993, p.179) as '*the upstream boundary of concentrated water flow... between definable banks*'. In accordance with fundamental contrasts between the process regime of vegetated saltmarsh and fronting tidal flats, the lower limit of the principal channel is here defined by the boundary of halophytic colonisation.

In line with methodological procedures employed by Collins *et al.* (1987) and Ayles and Lapointe (1996), field surveys (Figure 4.1) were undertaken during June-July 1999 along the selected reach at each study locality. Following the basic principles outlined by Anderson and Mikhail (1985), Electronic Distance Measuring (EDM) equipment comprising a Topcon GTS 300 with a Psion II logger running NSS software (NSS, 1992) and extendable pole with reflecting prism, was used to record elevation data as a sequence of point samples.

A purposive sampling strategy (Norcliffe, 1977) was used to inform data acquisition. Sample frequency was high towards the headwaters, commensurate with the occurrence of breaks in slope. Progressing along the sinuous course of the network,

(a)

(b)

Plate 4.1 Contrasting morphological characteristics displayed by: (a) a 'dead-end' reach, Isle of Walney; and (b) 'through-flowing' headwaters, Hamford Water.

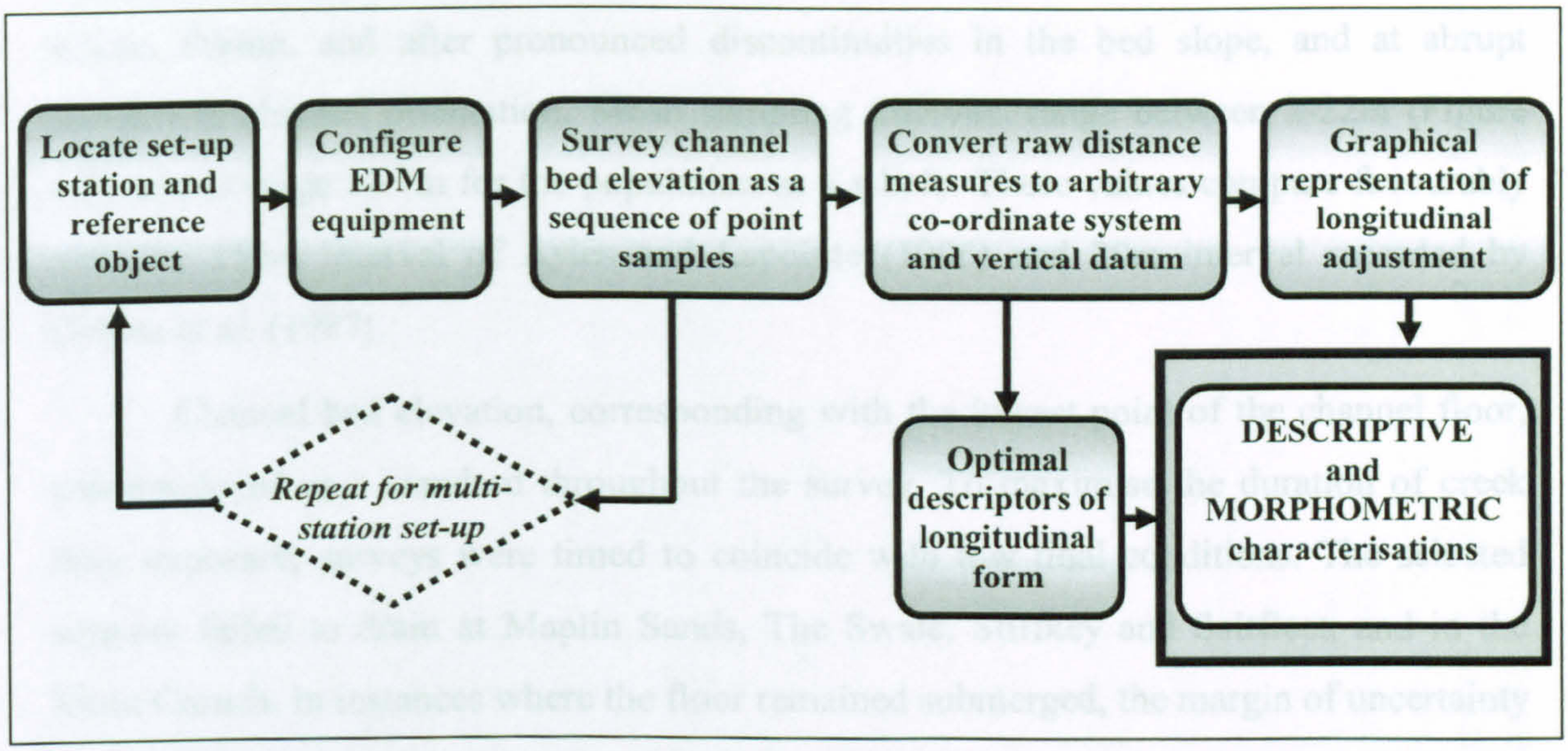

Figure 4.1 Schematic representation of the methodological procedure employed to produce data for the descriptive and morphometric characterisation of longitudinal adjustment.

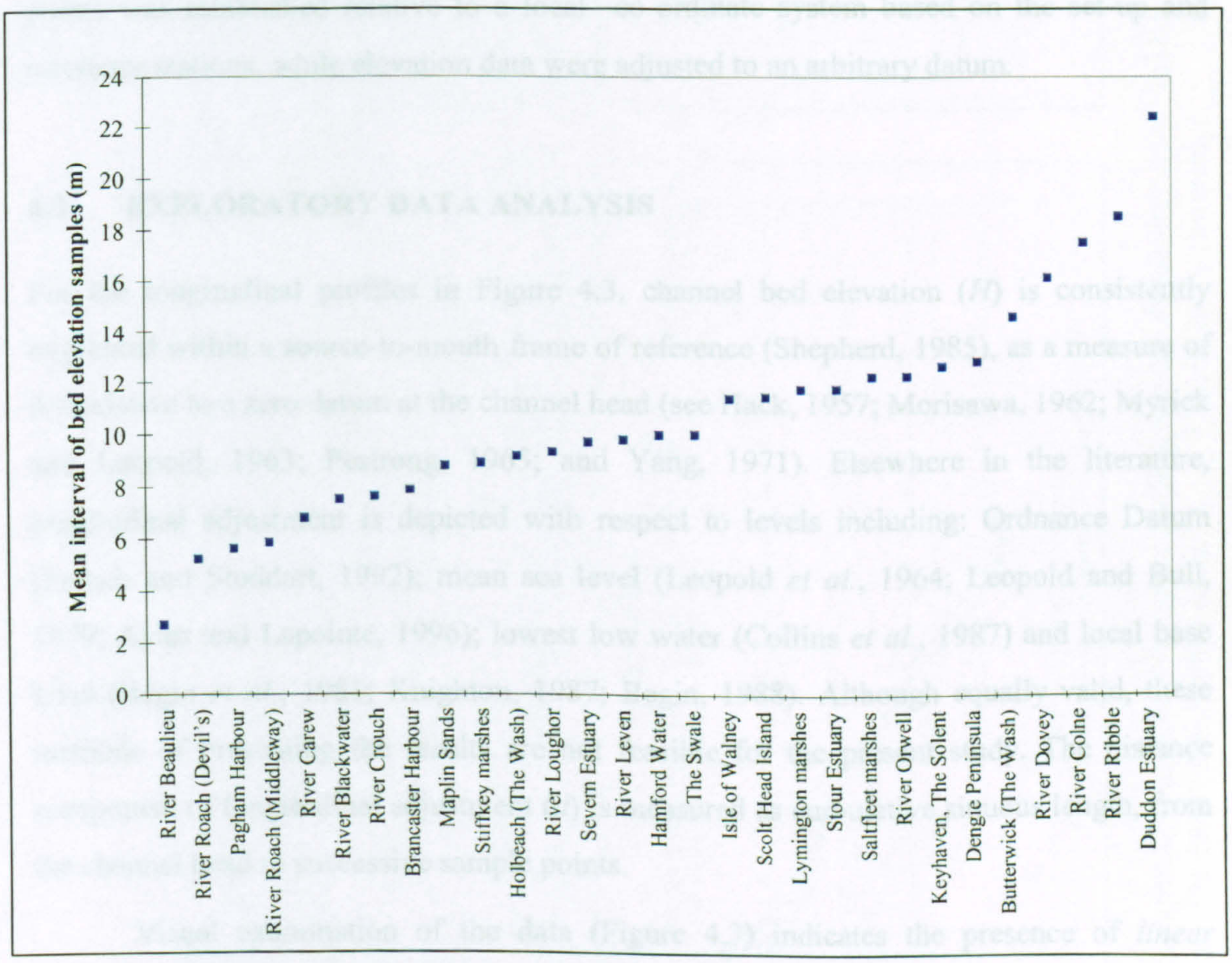

Figure 4.2 Mean sampling interval for channel bed elevation data at study localities.

readings were taken at the mid point of each link, at accessible intermediate junctions, before, during, and after pronounced discontinuities in the bed slope, and at abrupt changes in channel orientation. Mean sampling intervals range between 2-22m (Figure 4.2), and average 10.7m for the population as a whole. These values compare favourably with the 150m interval of Ayles and Lapointe (1996) and 20m interval recorded by Collins *et al.* (1987).

Channel bed elevation, corresponding with the lowest point of the channel floor, was employed as a standard throughout the survey. To maximise the duration of creek floor exposure, surveys were timed to coincide with low tidal conditions. The selected network failed to drain at Maplin Sands, The Swale, Stiffkey and Saltfleet, and in the River Crouch. In instances where the floor remained submerged, the margin of uncertainty introduced to the reading was minimised, by employing an average elevation for points recorded at several intervals across the creek. Raw survey data were converted to position and elevation statistics using NSS Survpro software (NSS, 1992). The location of survey points was established relative to a local co-ordinate system based on the set-up and reference stations, while elevation data were adjusted to an arbitrary datum.

4.3 EXPLORATORY DATA ANALYSIS

For the longitudinal profiles in Figure 4.3, channel bed elevation (H) is consistently expressed within a source-to-mouth frame of reference (Shepherd, 1985), as a measure of fall relative to a zero datum at the channel head (see Hack, 1957; Morisawa, 1962; Myrick and Leopold, 1963; Pestrong, 1965; and Yang, 1971). Elsewhere in the literature, longitudinal adjustment is depicted with respect to levels including: Ordnance Datum (French and Stoddart, 1992); mean sea level (Leopold *et al.*, 1964; Leopold and Bull, 1979; Ayles and Lapointe, 1996); lowest low water (Collins *et al.*, 1987) and local base level (Begin *et al.*, 1981; Knighton, 1987; Begin, 1988). Although equally valid, these methods of presenting the results are not feasible for the present study. The distance component of longitudinal adjustment (d) is measured as cumulative sinuous length, from the channel head to successive sample points.

Visual examination of the data (Figure 4.3) indicates the presence of *linear* (Pestrong, 1965; French and Stoddart, 1992), *upwardly concave* (Collins *et al.*, 1987; Ayles and Lapointe, 1996), and *composite* profiles within the sample population.

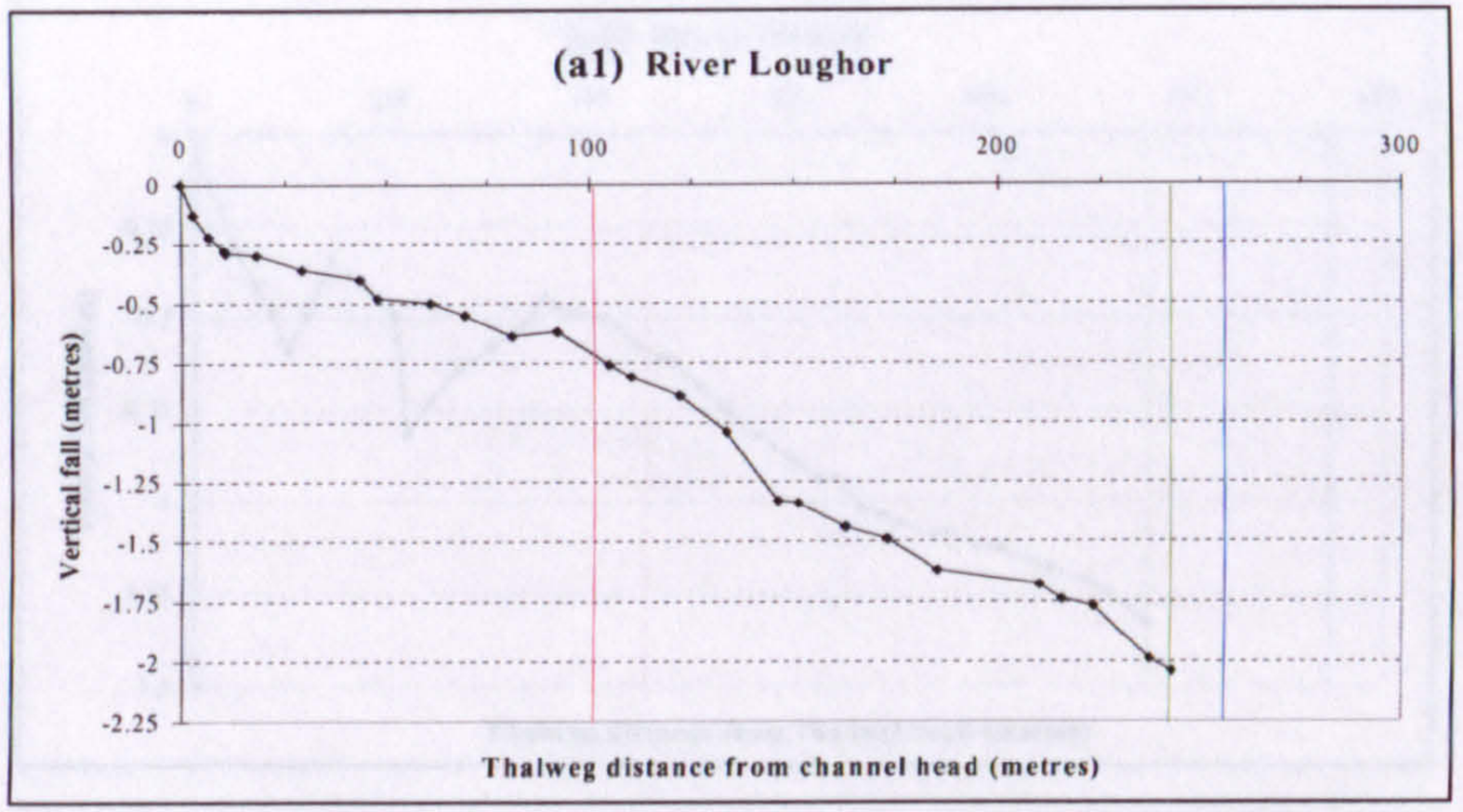

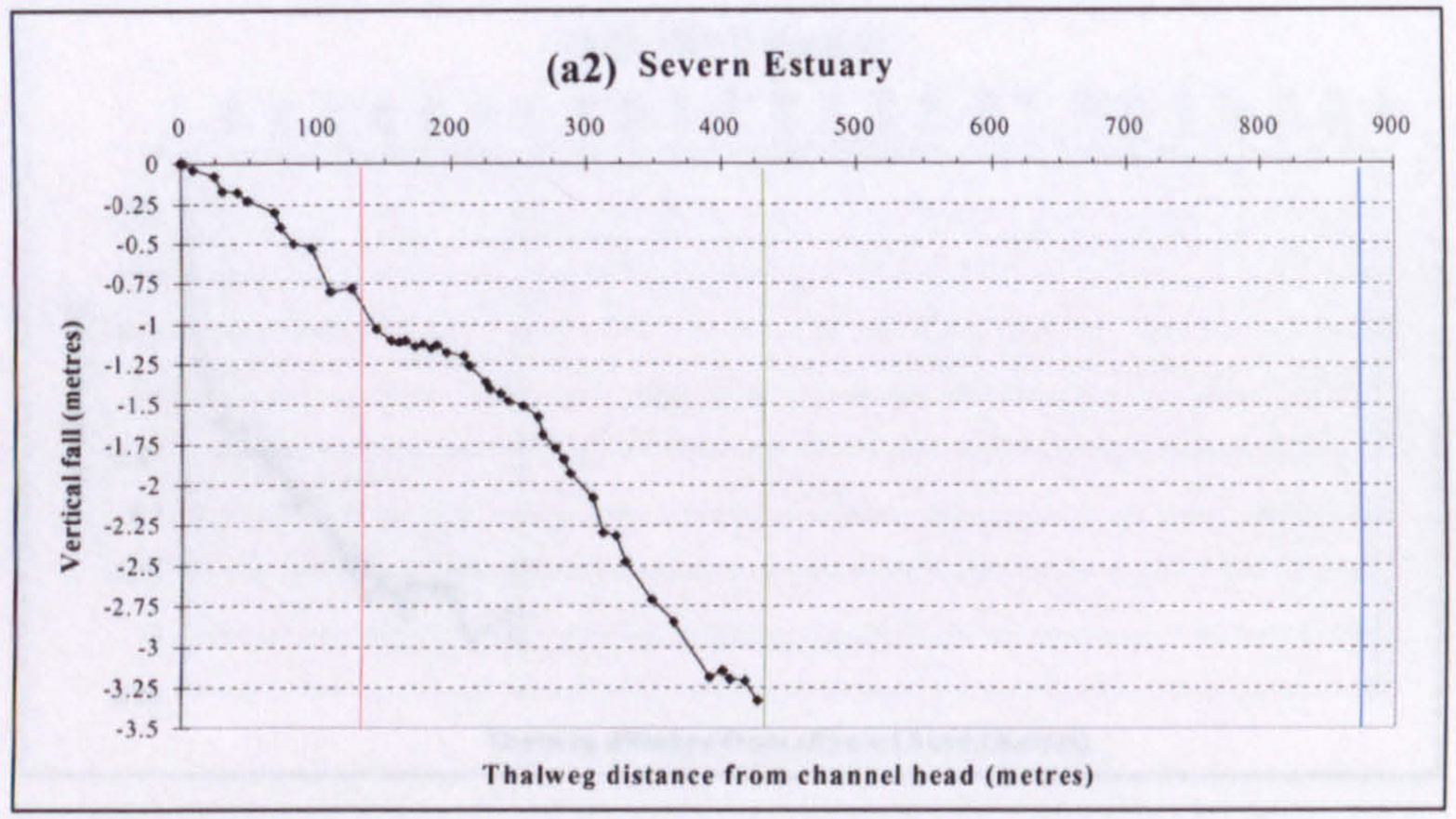

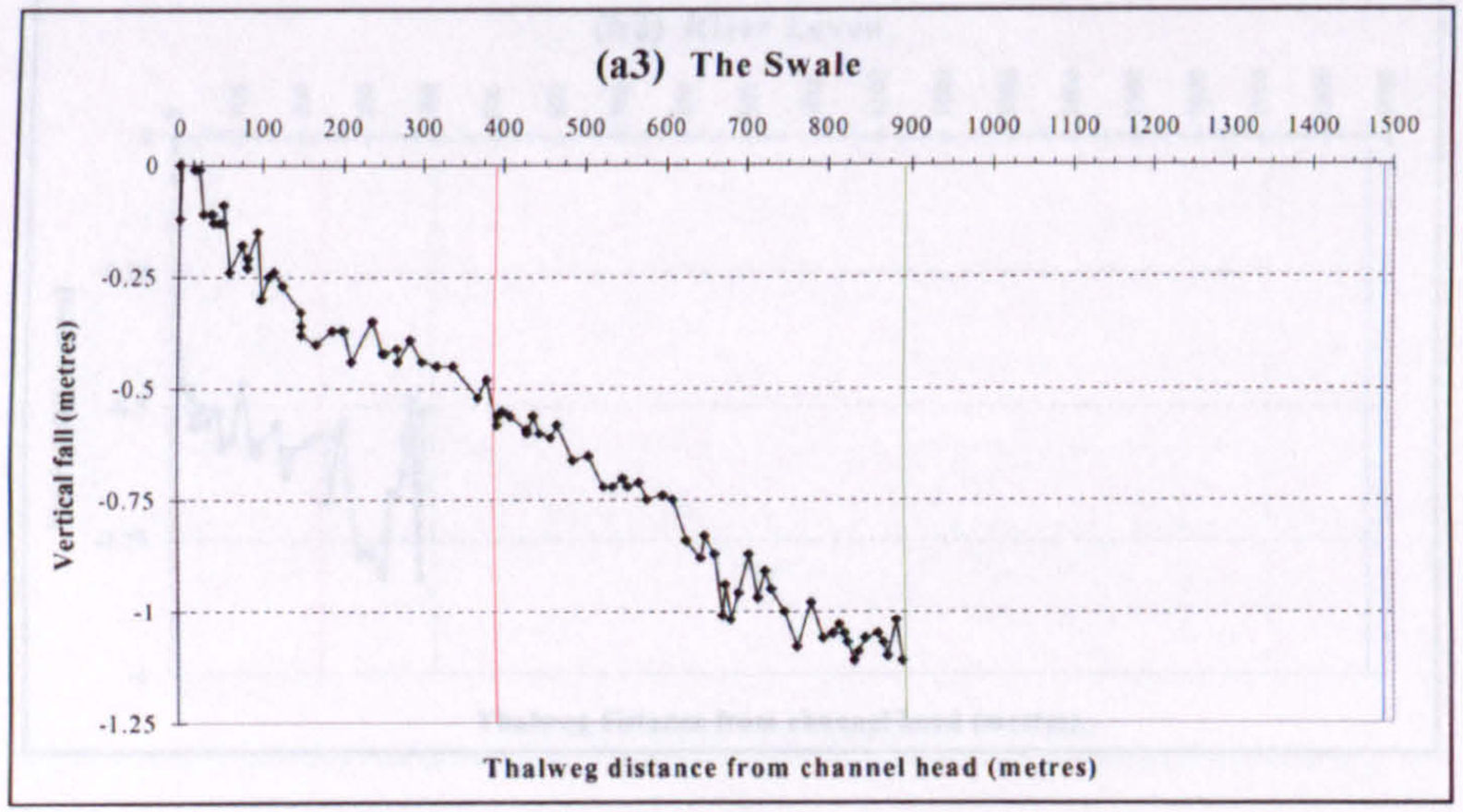

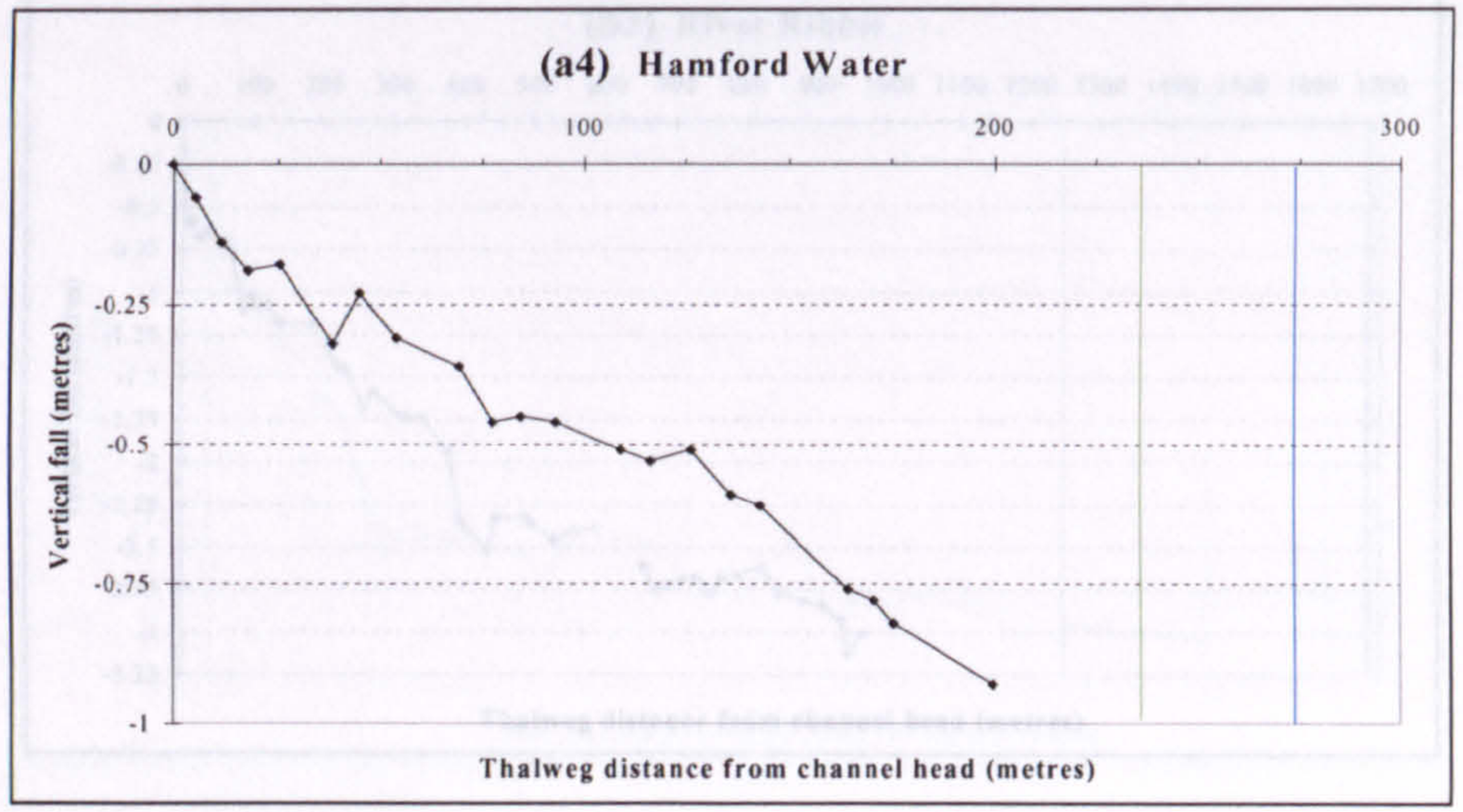

Figure 4.3 Longitudinal profiles grouped according to those displaying: *linear* (a1-a5) *upwardly concave* (b1-b14); and *composite* (c1-c10) patterns of descent. The limit of vegetative cover (___), mean low water mark (___), and loci of re-curvature (___) provide a frame of reference.

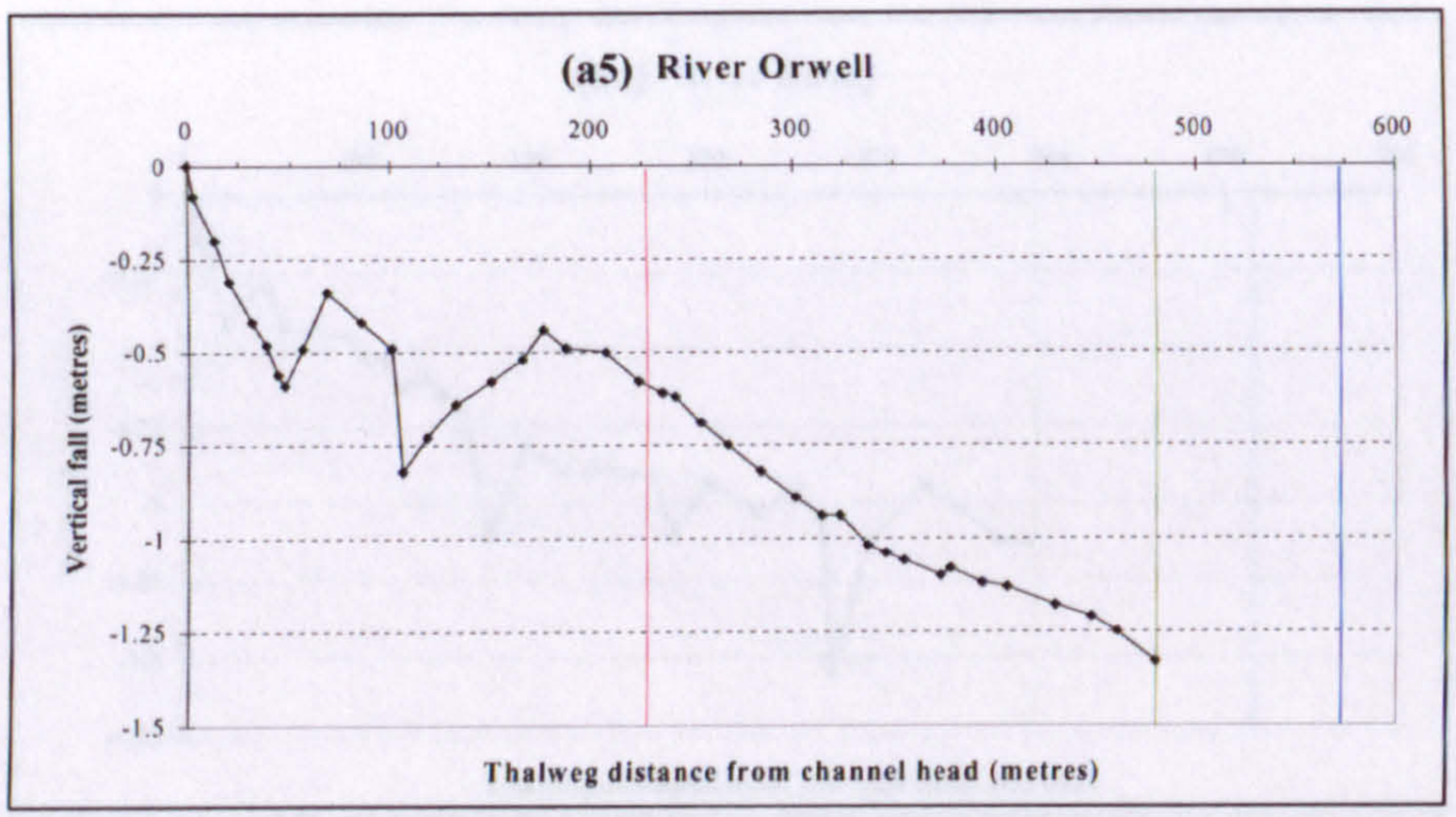

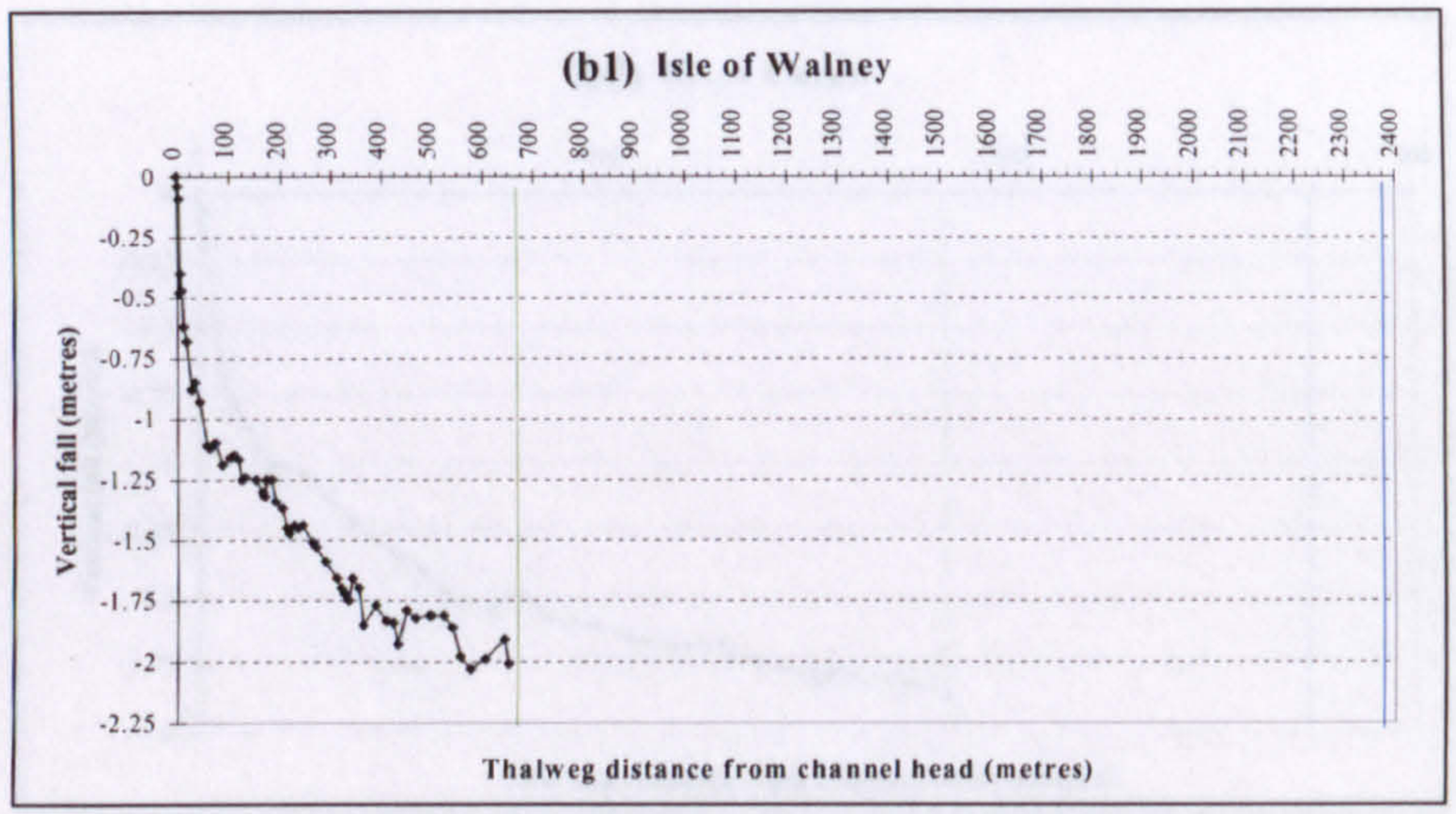

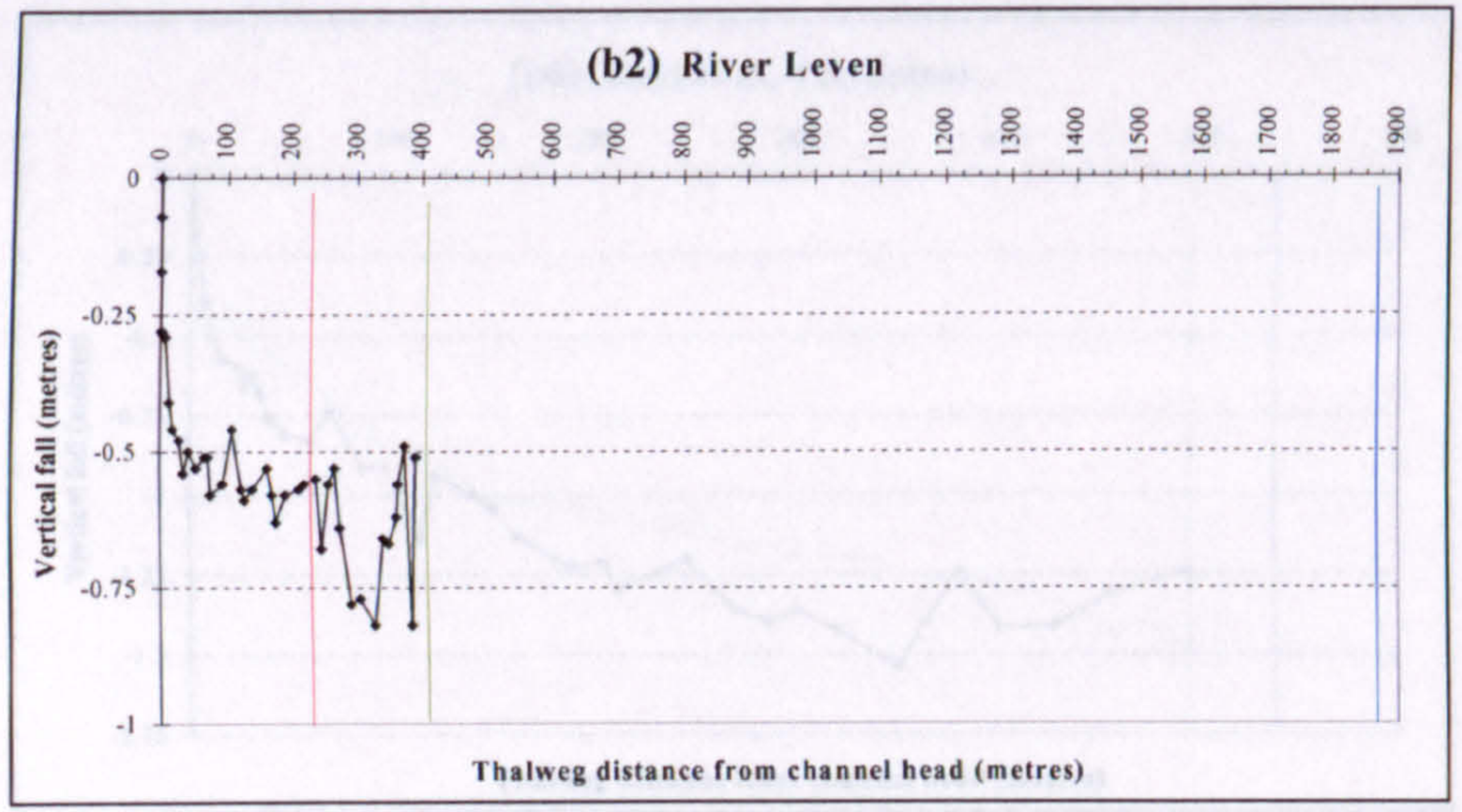

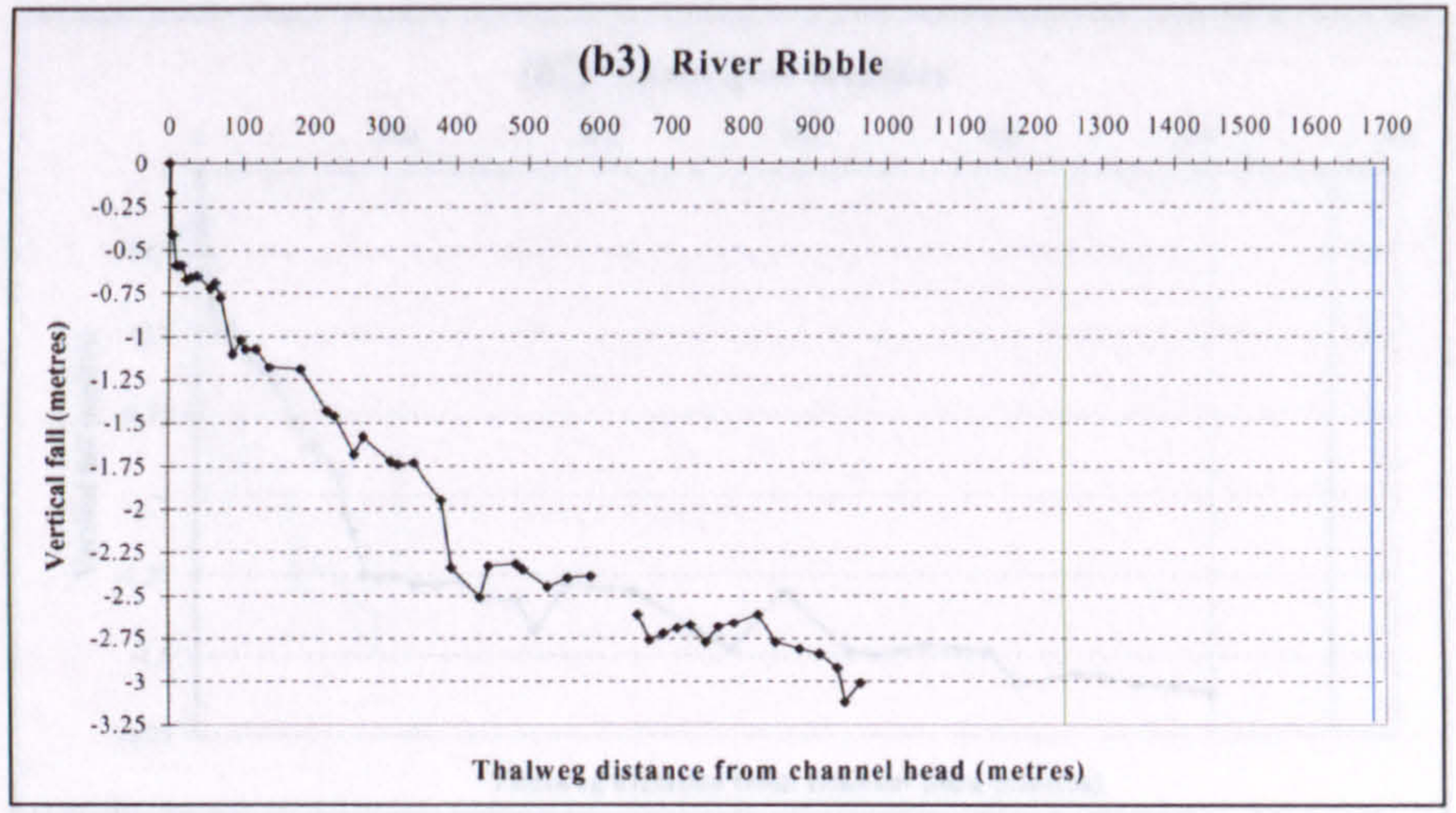

Figure 4.3 (cont.) Longitudinal profiles grouped according to those displaying: *linear* (a1-a5) *upwardly concave* (b1-b14); and *composite* (c1-c10) patterns of descent. The limit of vegetative cover (___), mean low water mark (___), and loci of re-curvature (___) provide a frame of reference.

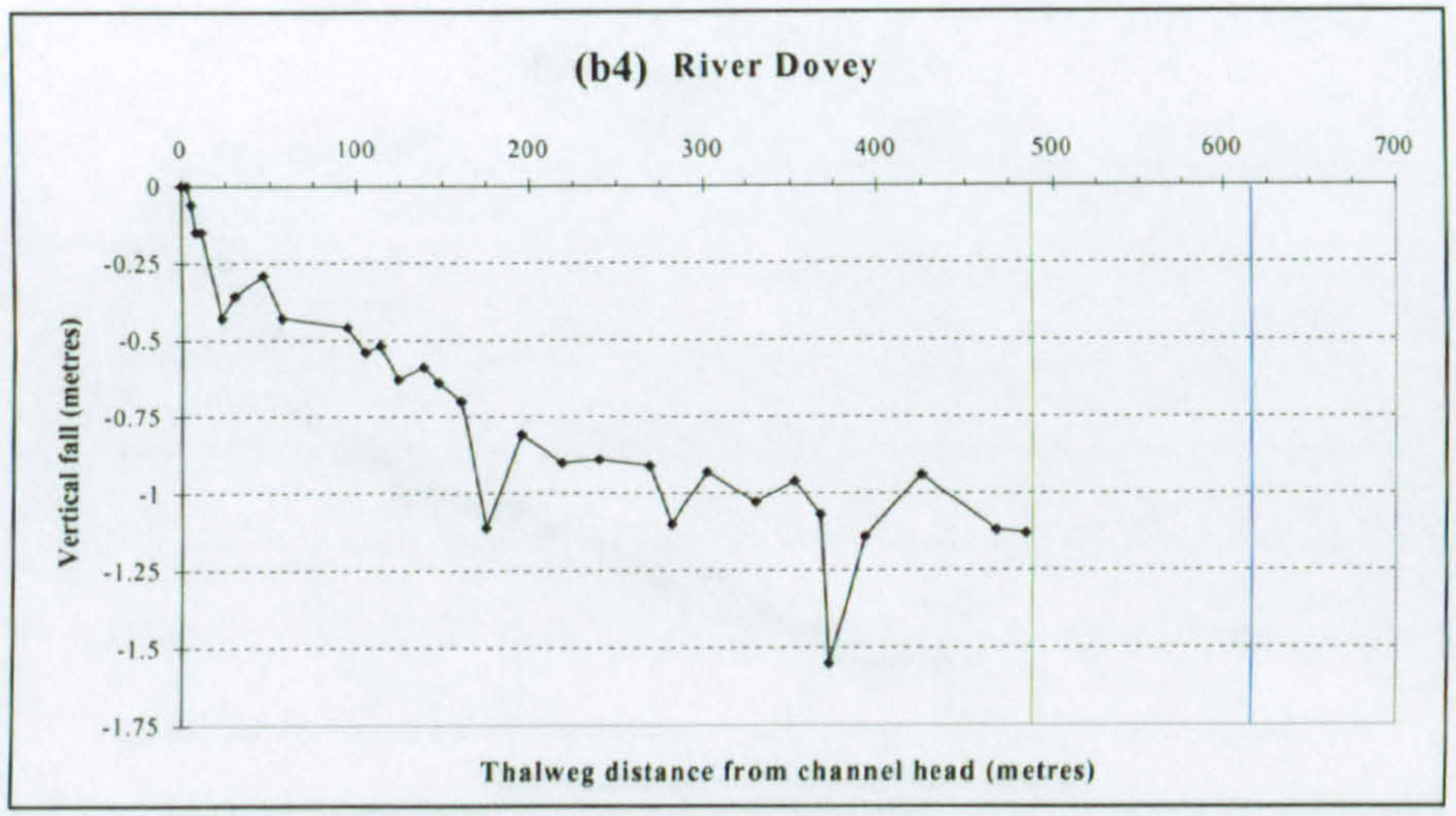

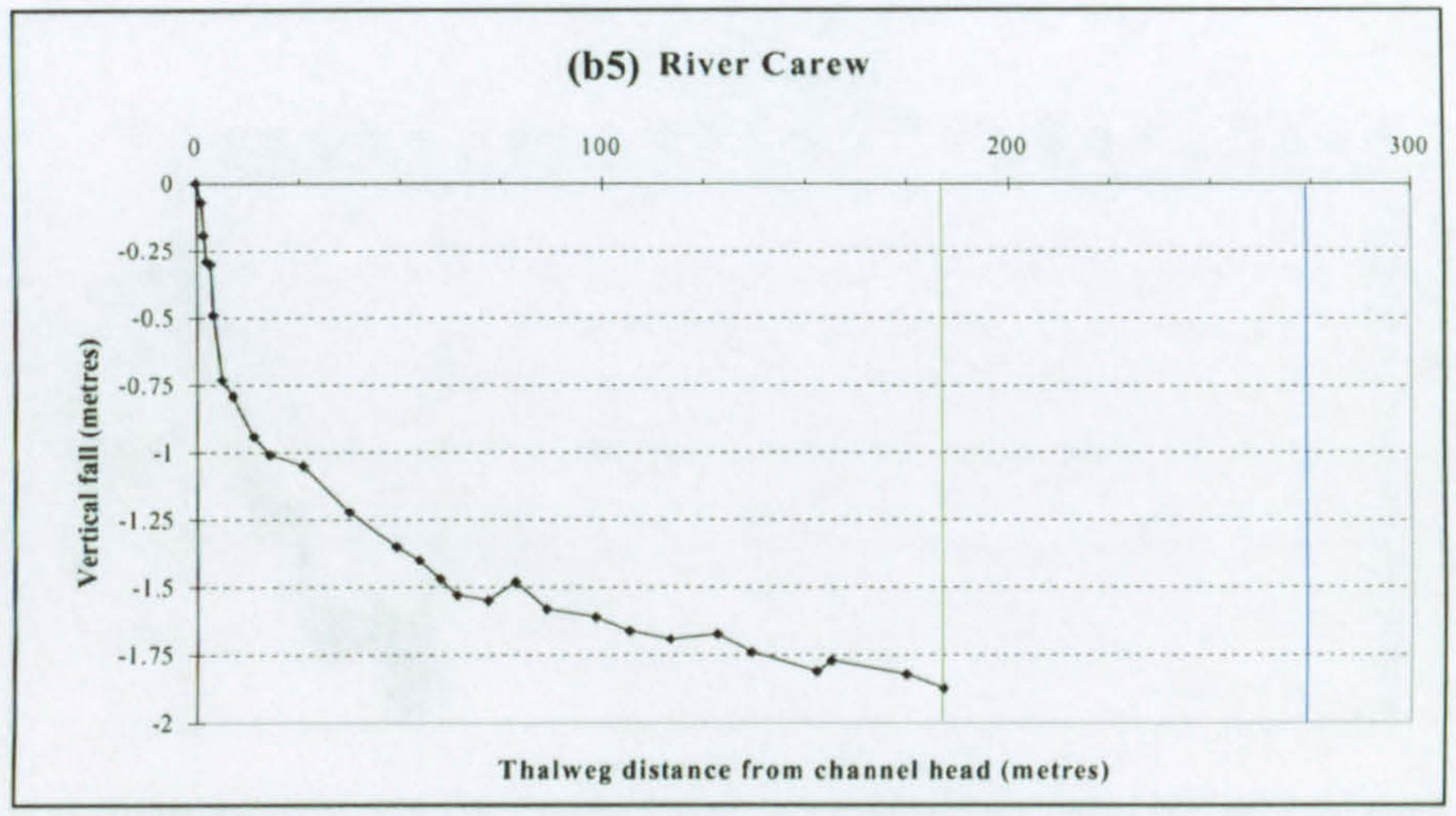

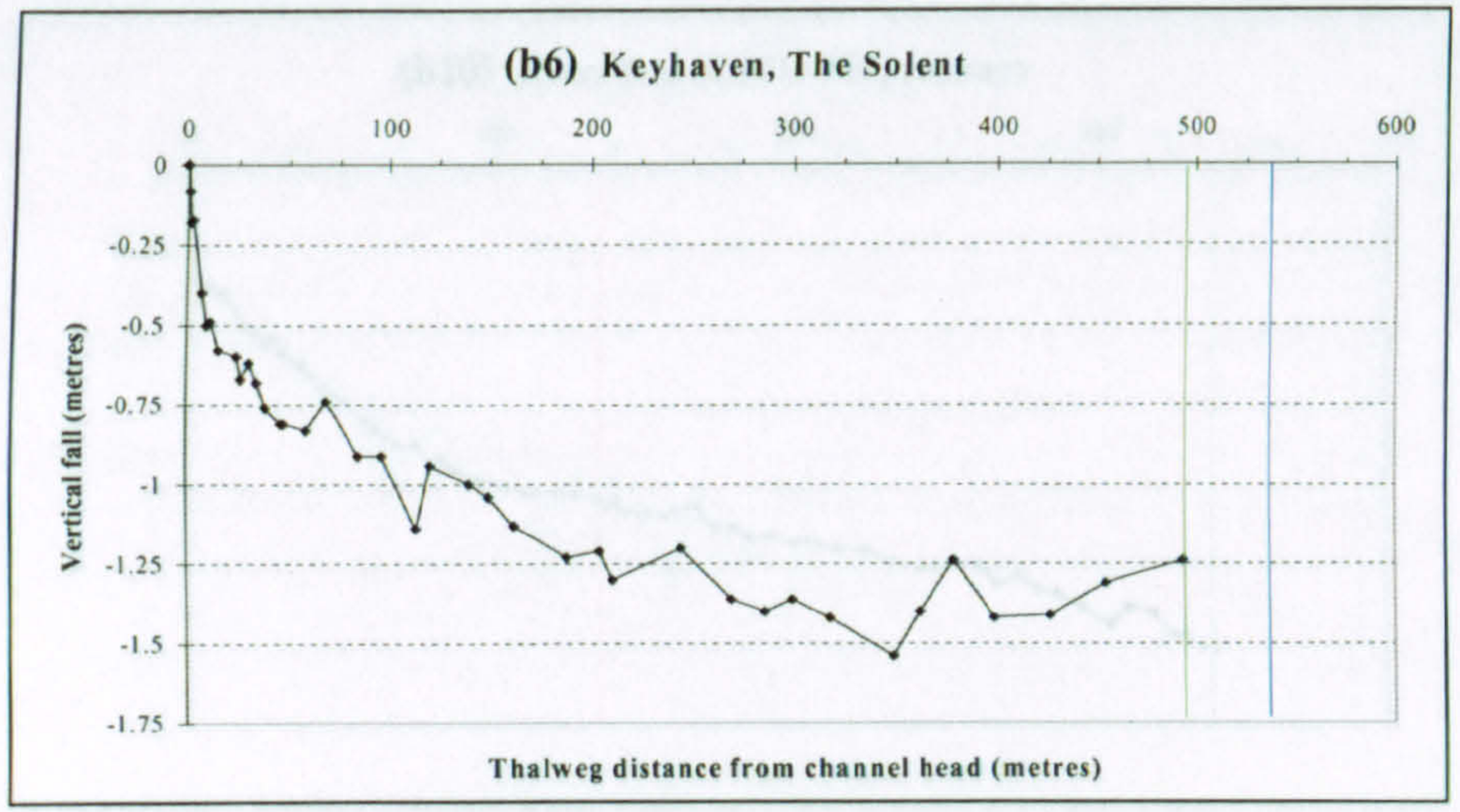

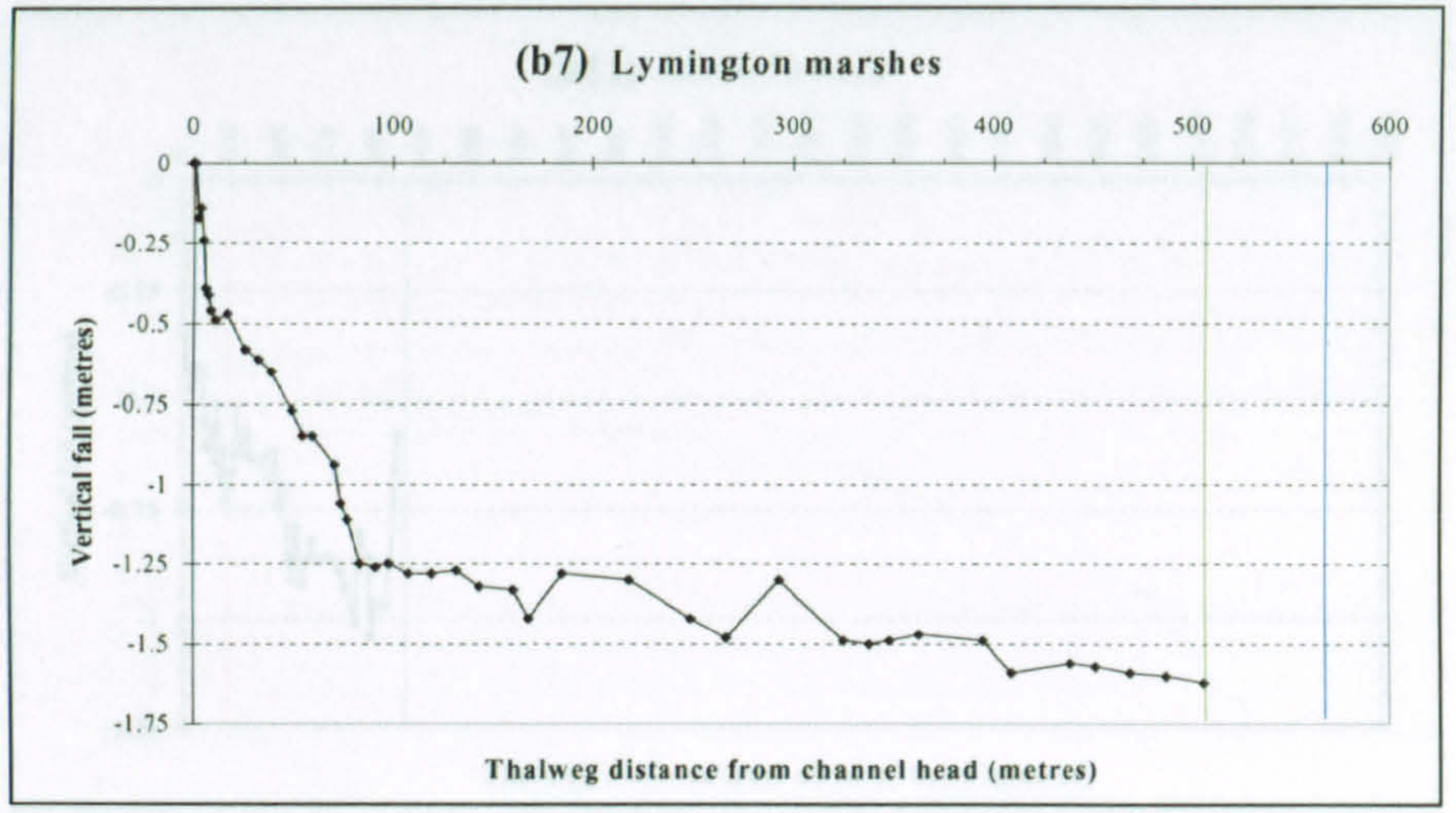

Figure 4.3 (cont.) Longitudinal profiles grouped according to those displaying: *linear* (a1-a5) *upwardly concave* (b1-b14); and *composite* (c1-c10) patterns of descent. The limit of vegetative cover (___), mean low water mark (___), and loci of re-curvature (___) provide a frame of reference.

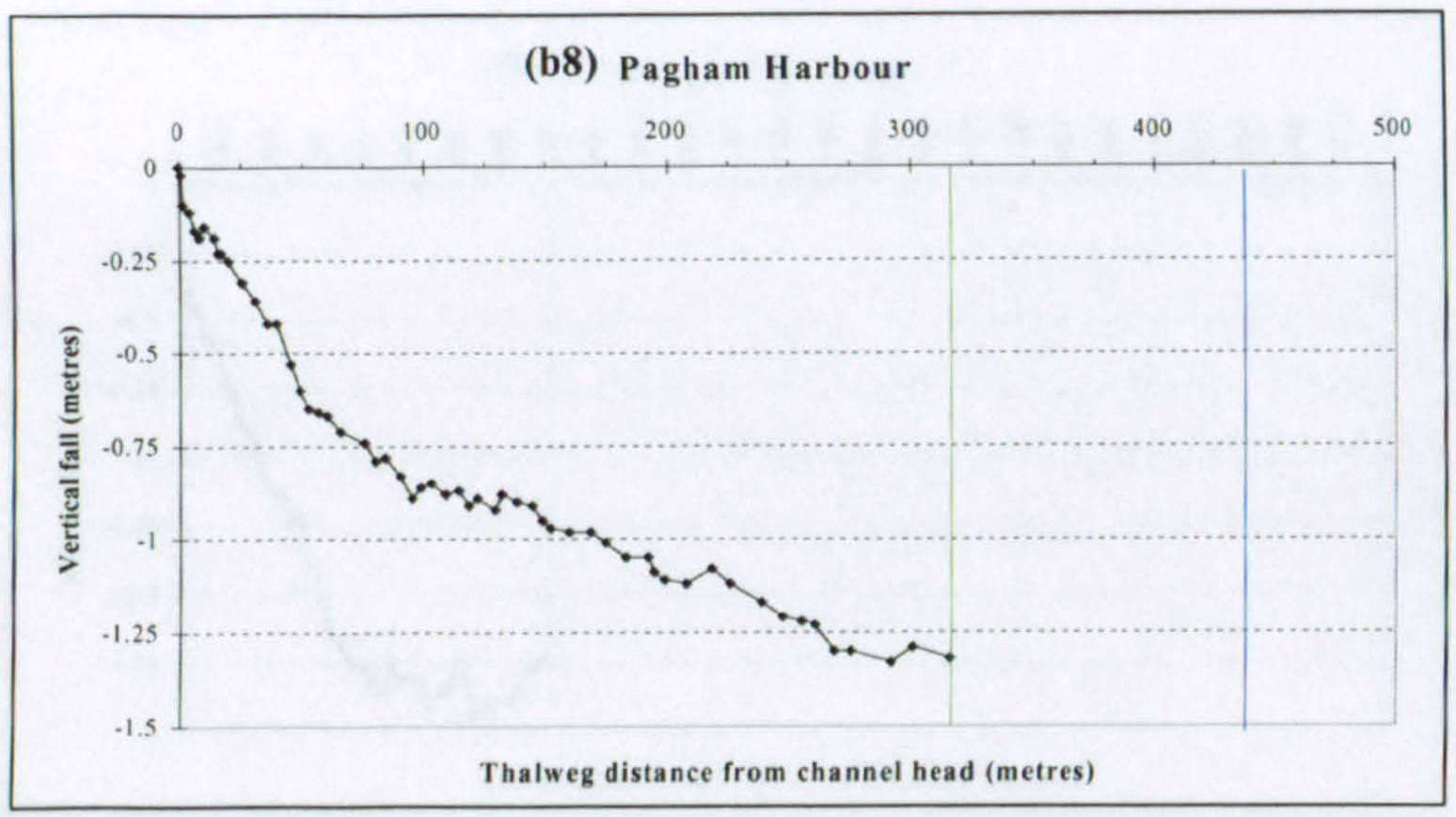

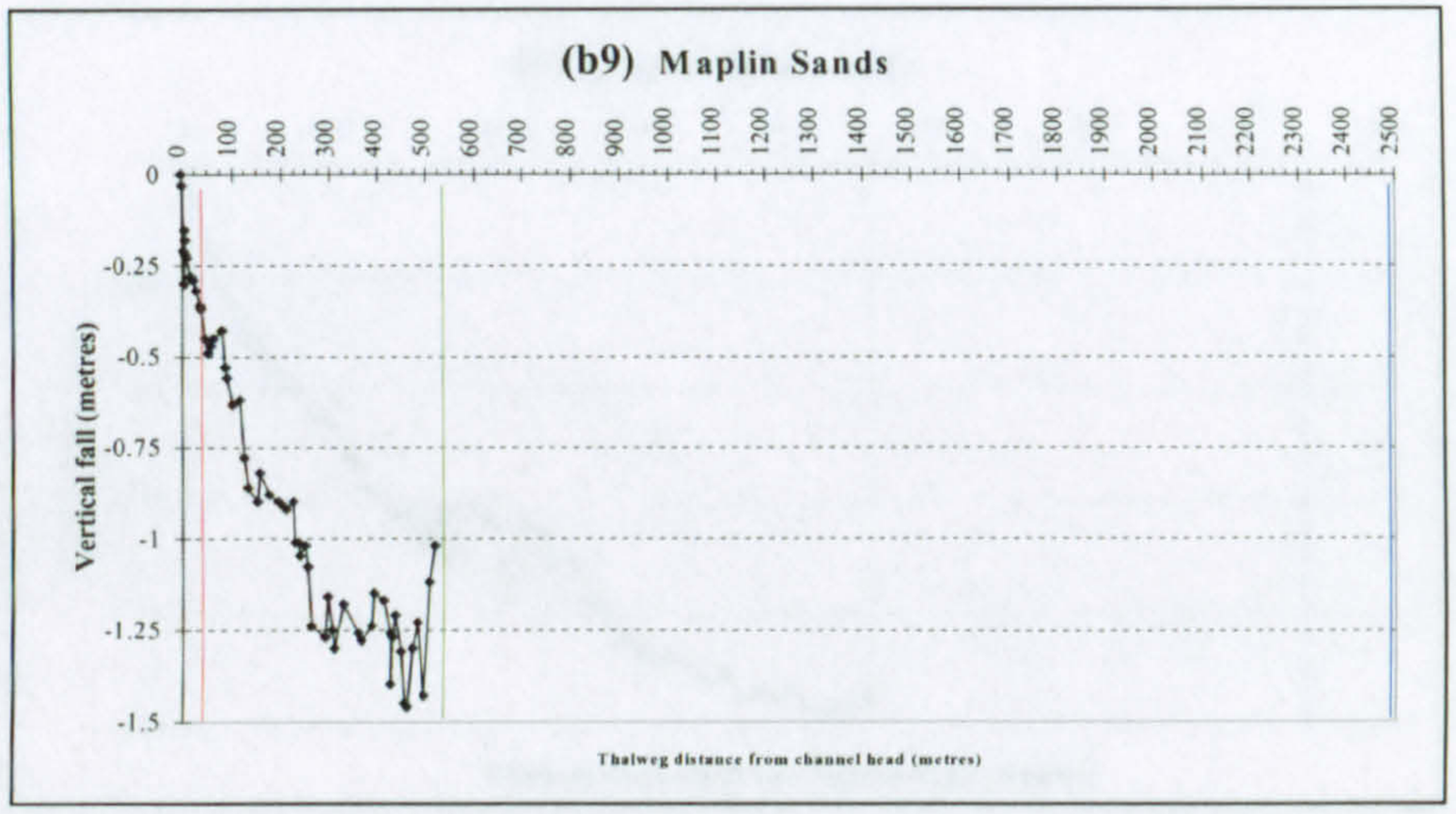

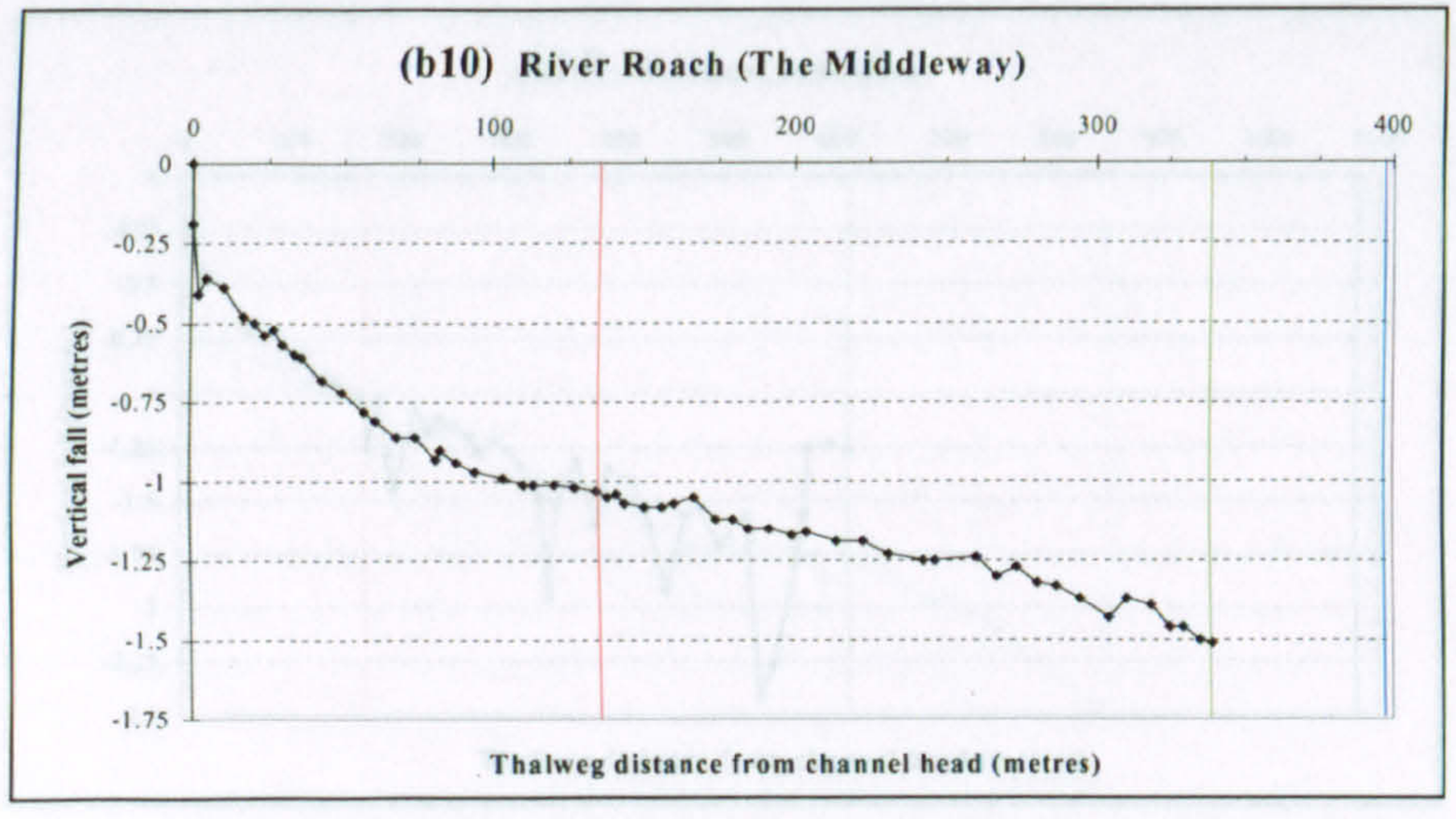

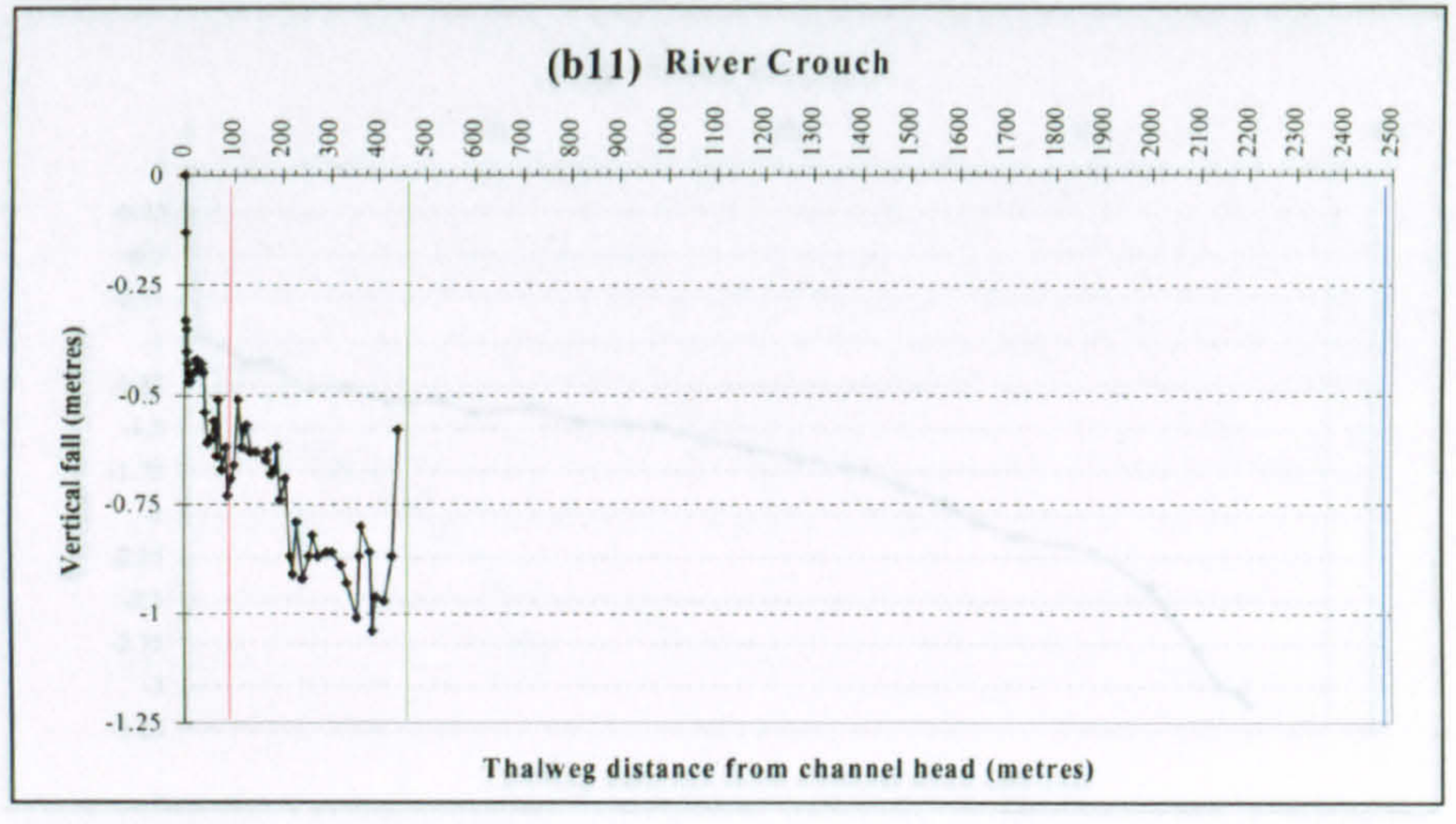

Figure 4.3 (cont.) Longitudinal profiles grouped according to those displaying: *linear* (a1-a5) *upwardly concave* (b1-b14); and *composite* (c1-c10) patterns of descent. The limit of vegetative cover (___), mean low water mark (___), and loci of re-curvature (___) provide a frame of reference.

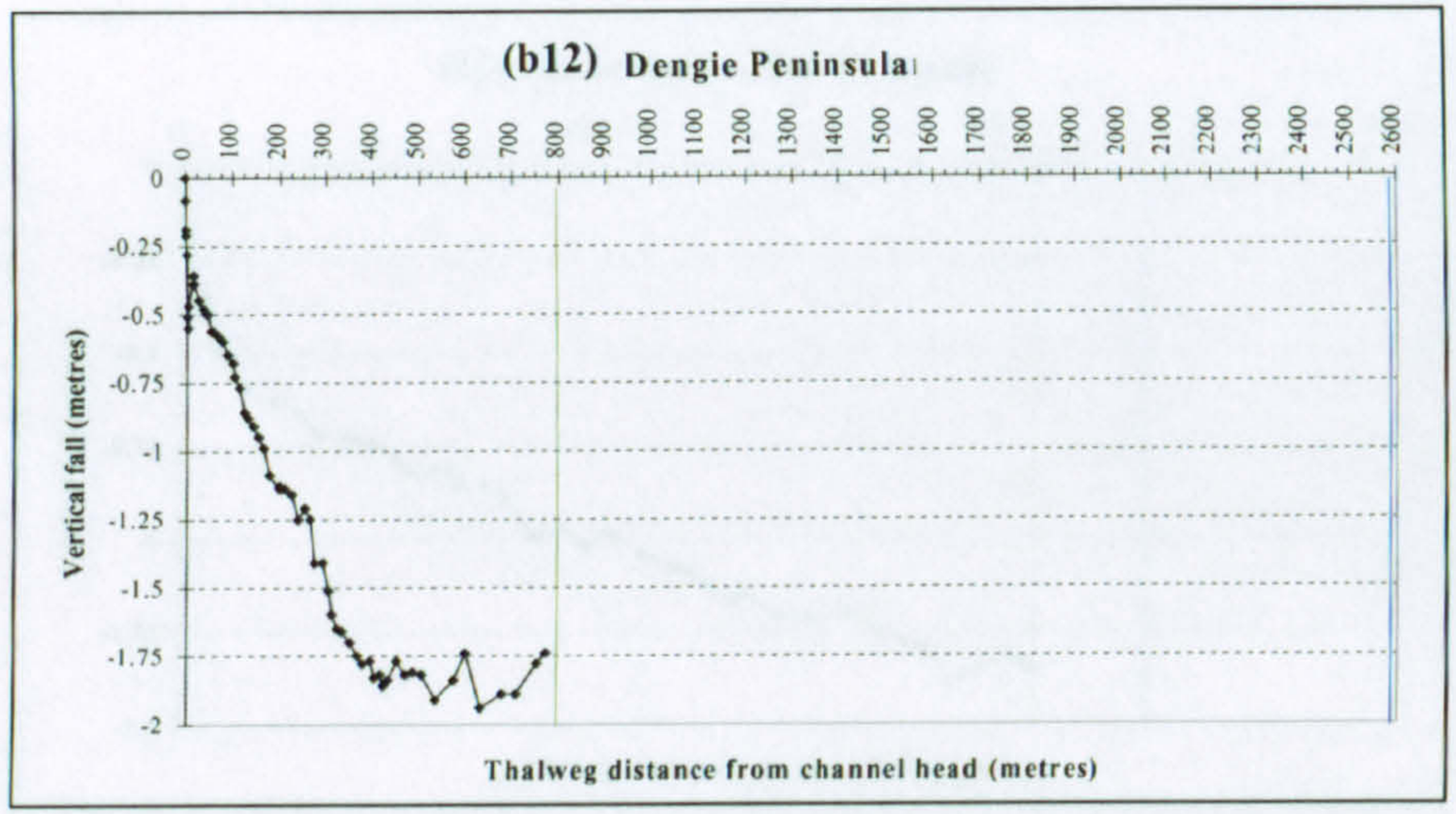

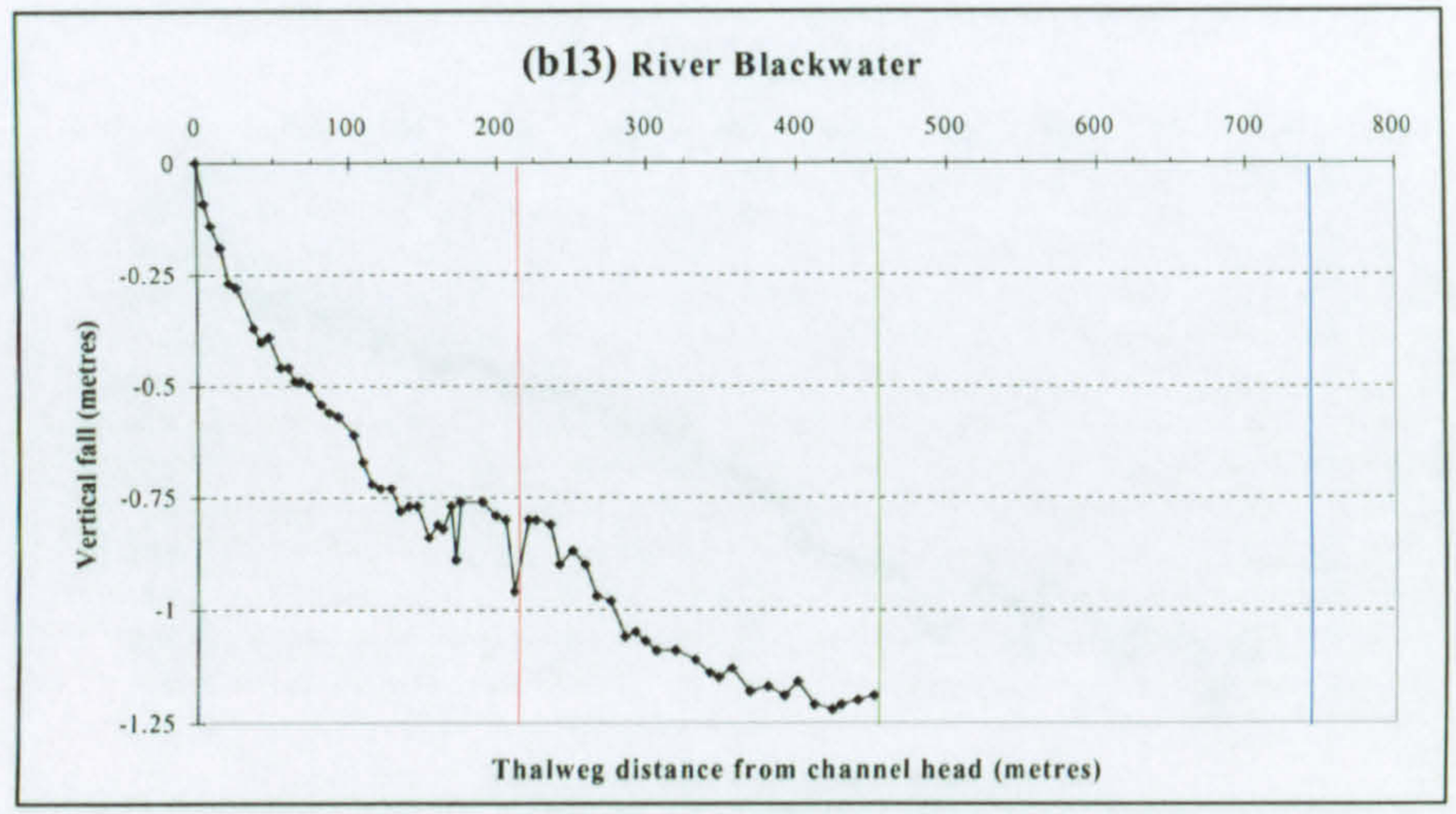

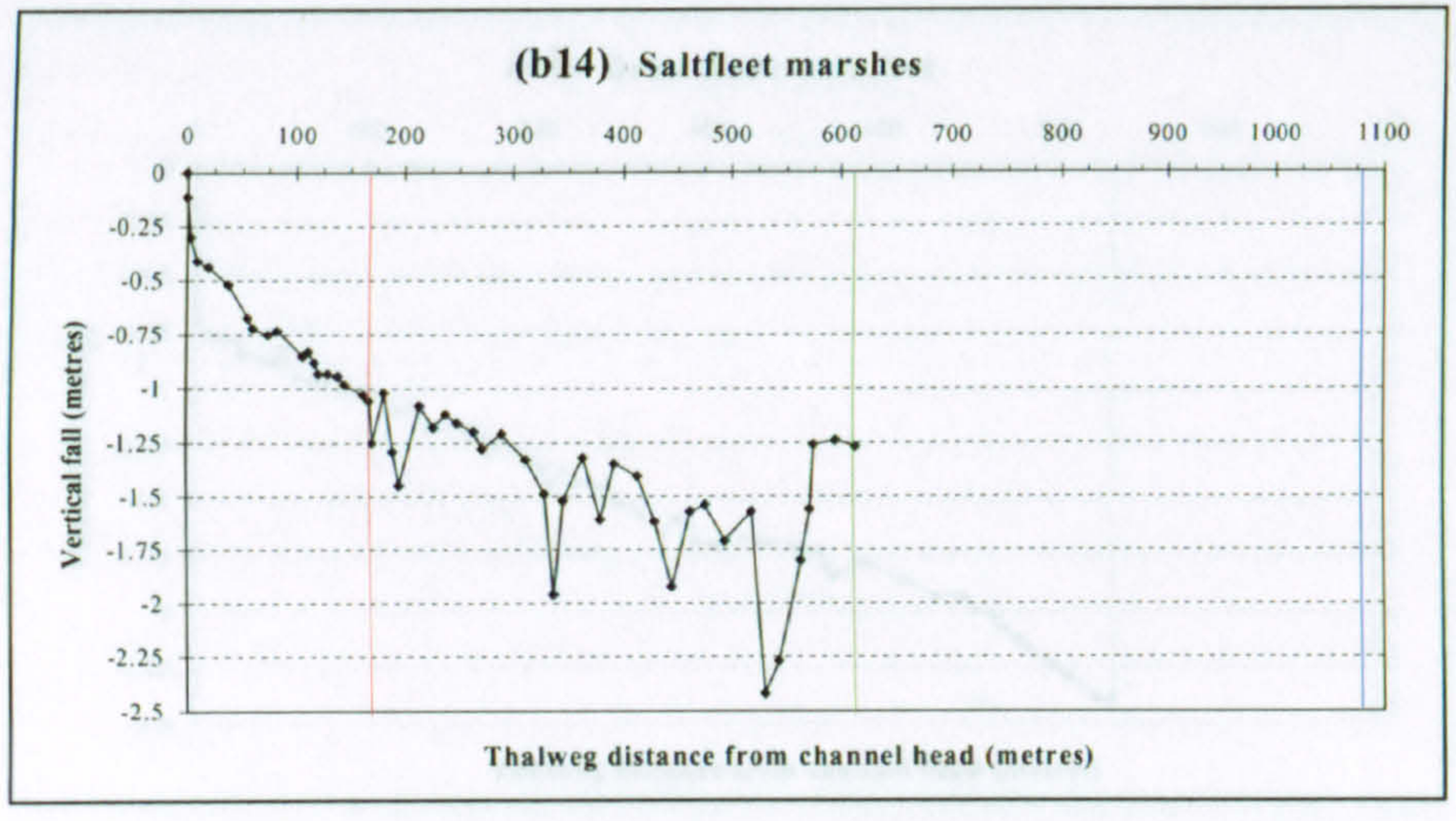

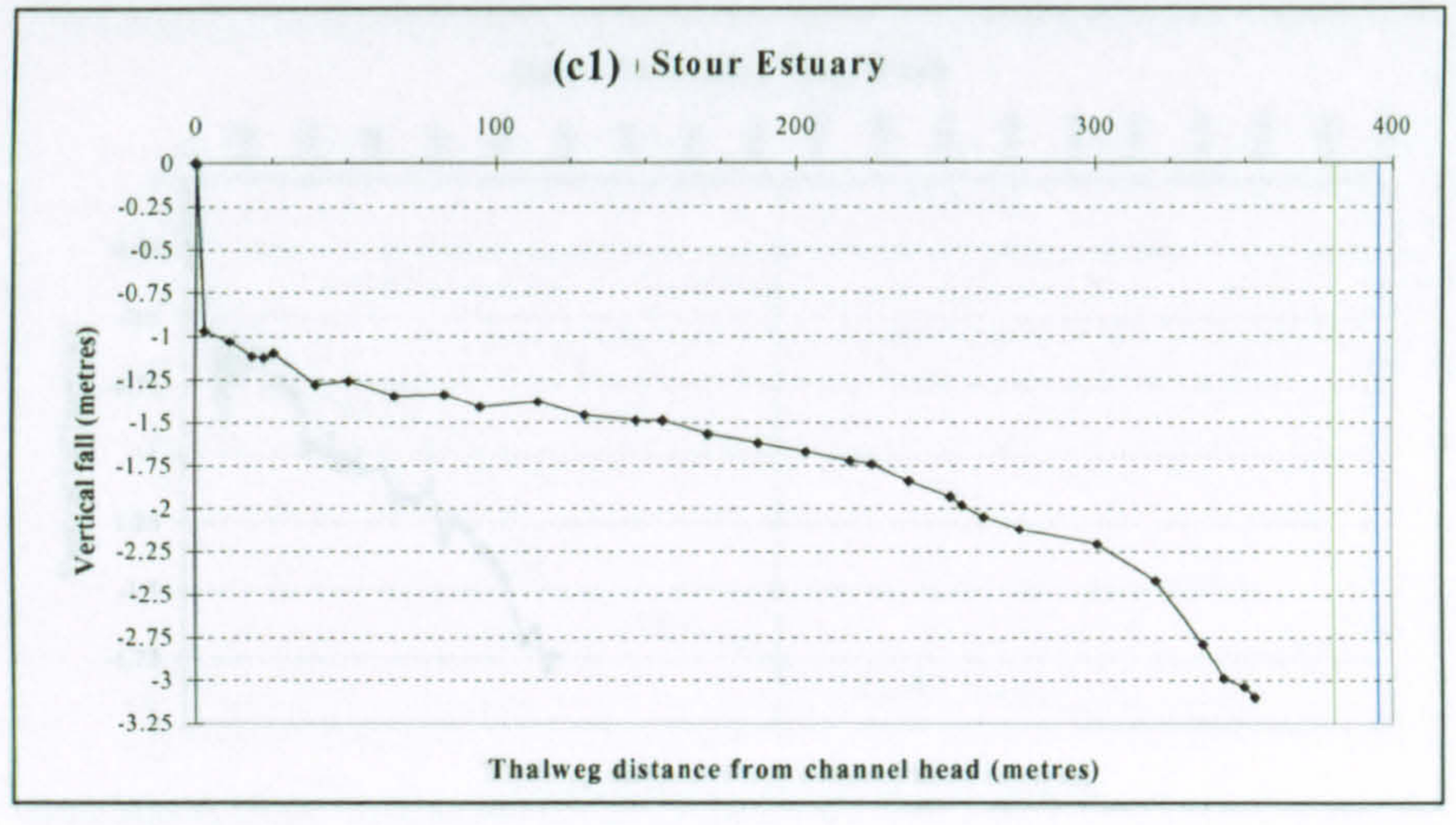

Figure 4.3 (cont.) Longitudinal profiles grouped according to those displaying: *linear* (a1-a5) *upwardly concave* (b1-b14); and *composite* (c1-c10) patterns of descent. The limit of vegetative cover (___), mean low water mark (___), and loci of re-curvature (___) provide a frame of reference.

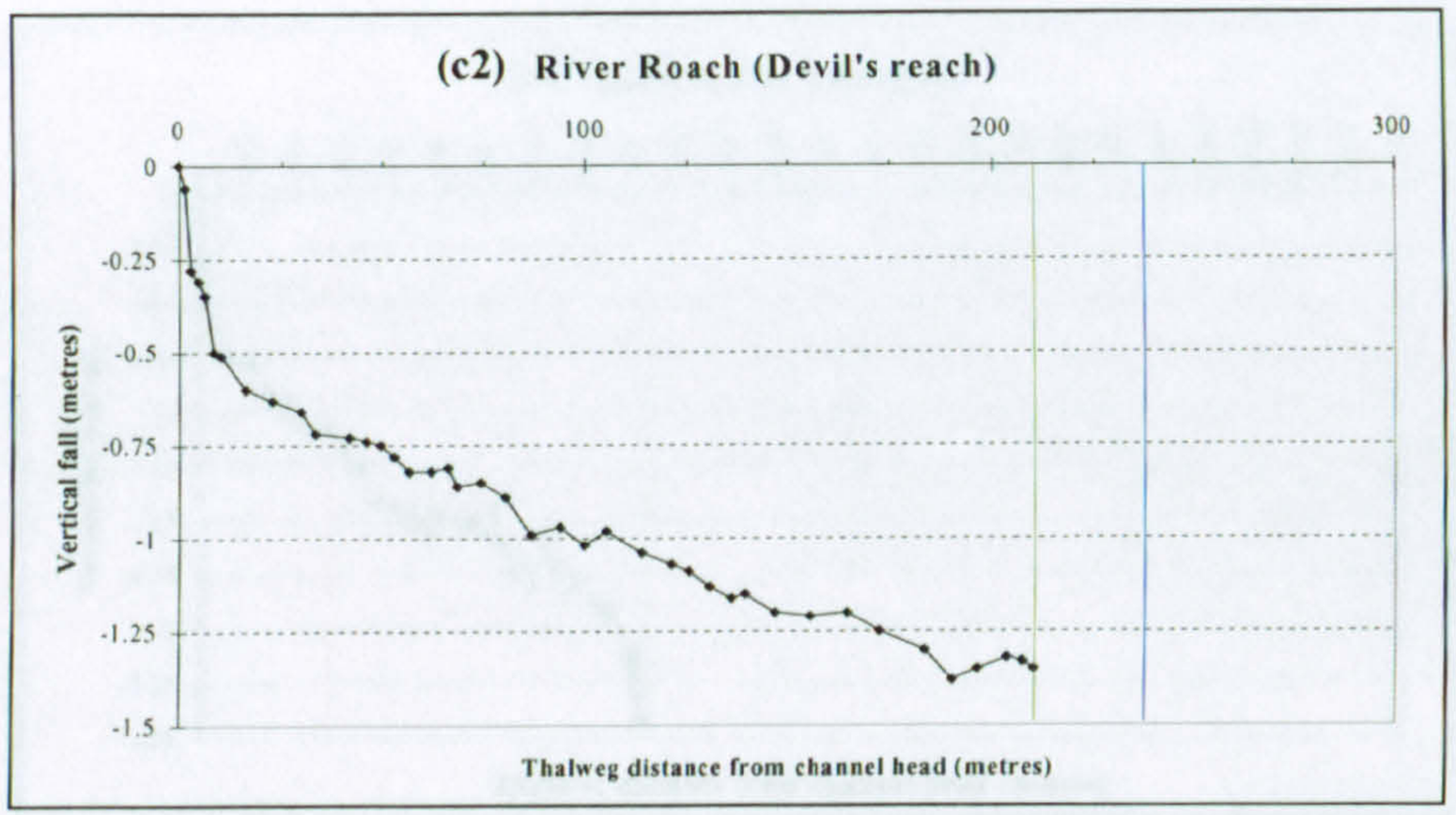

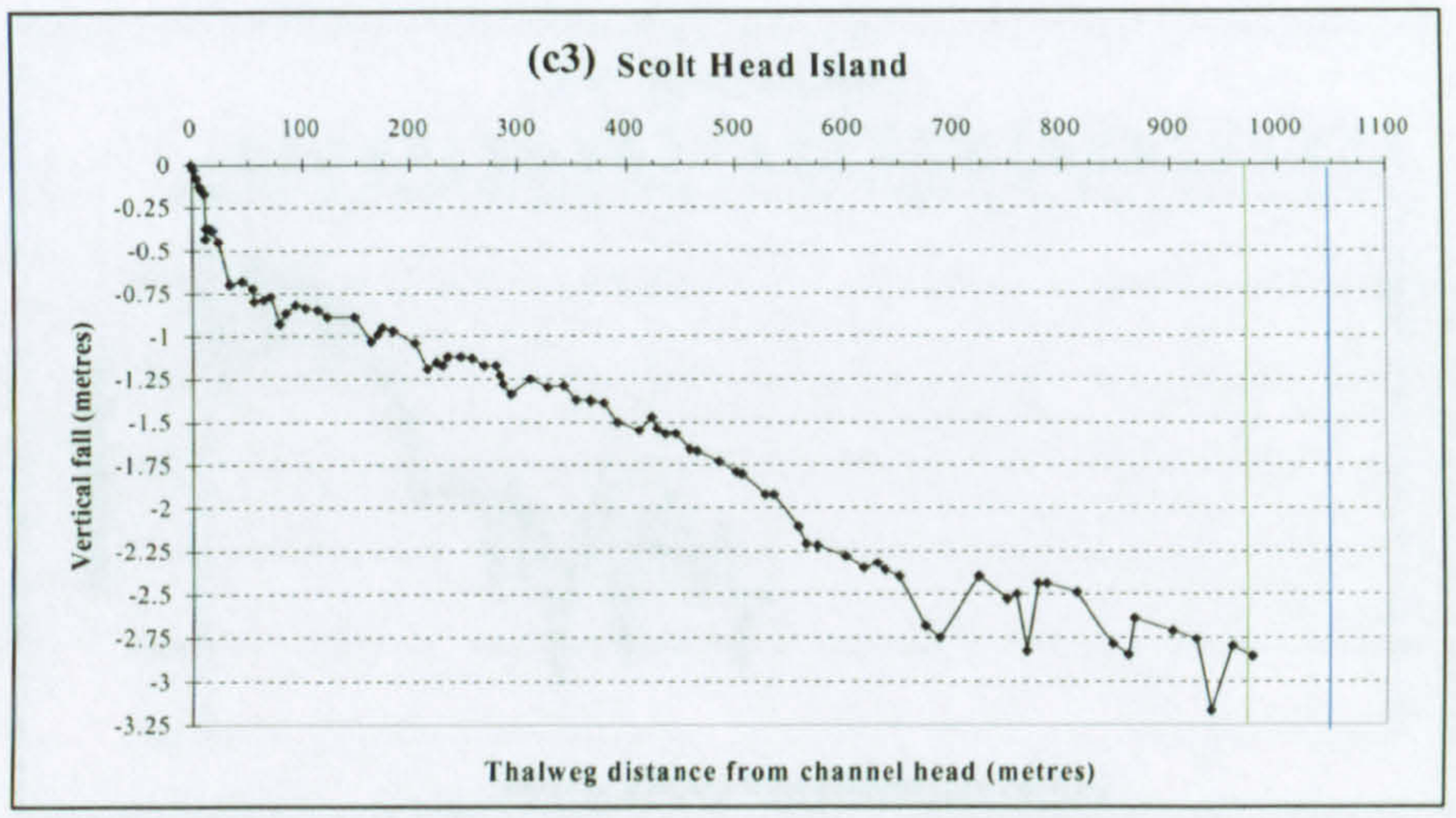

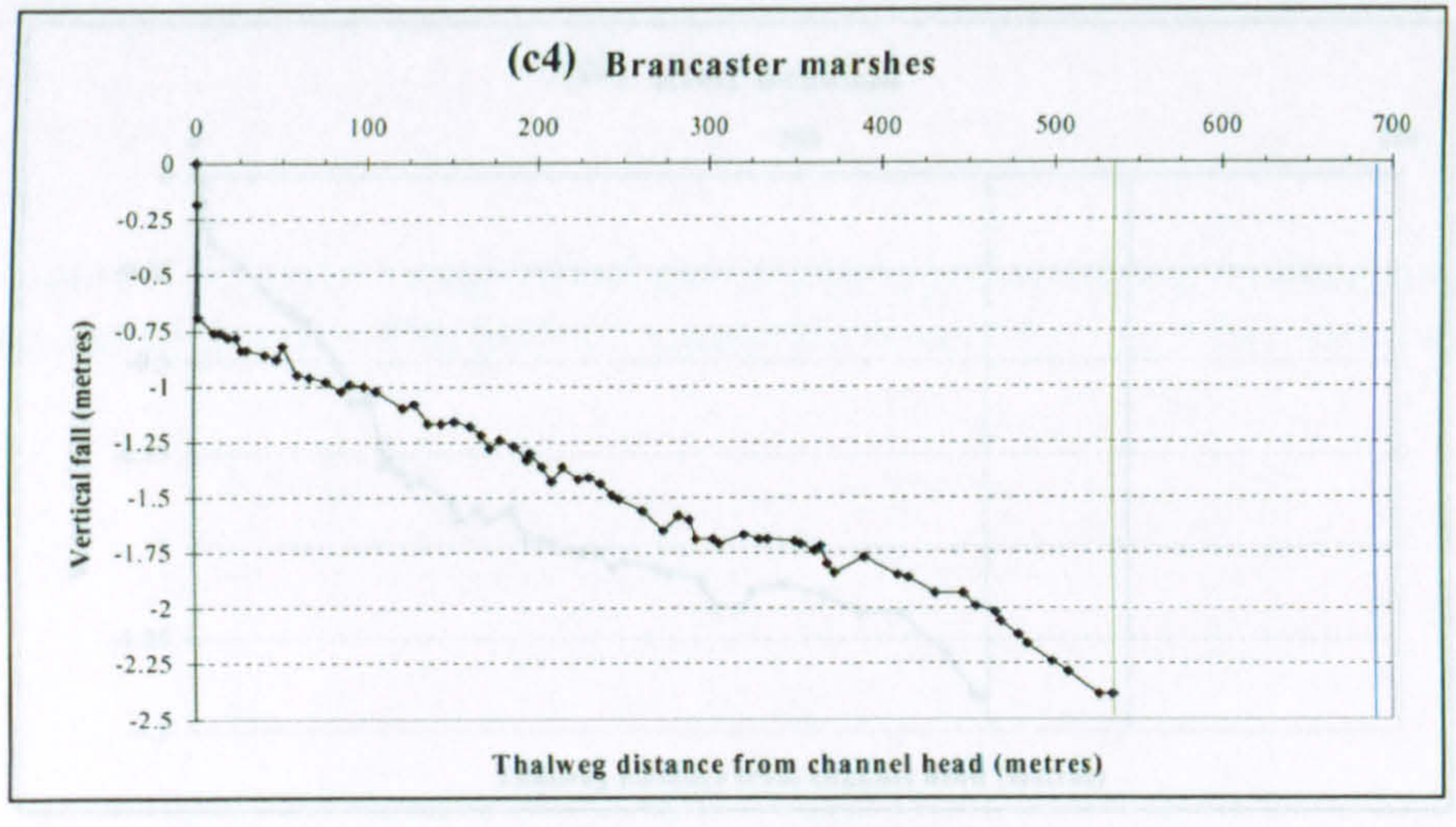

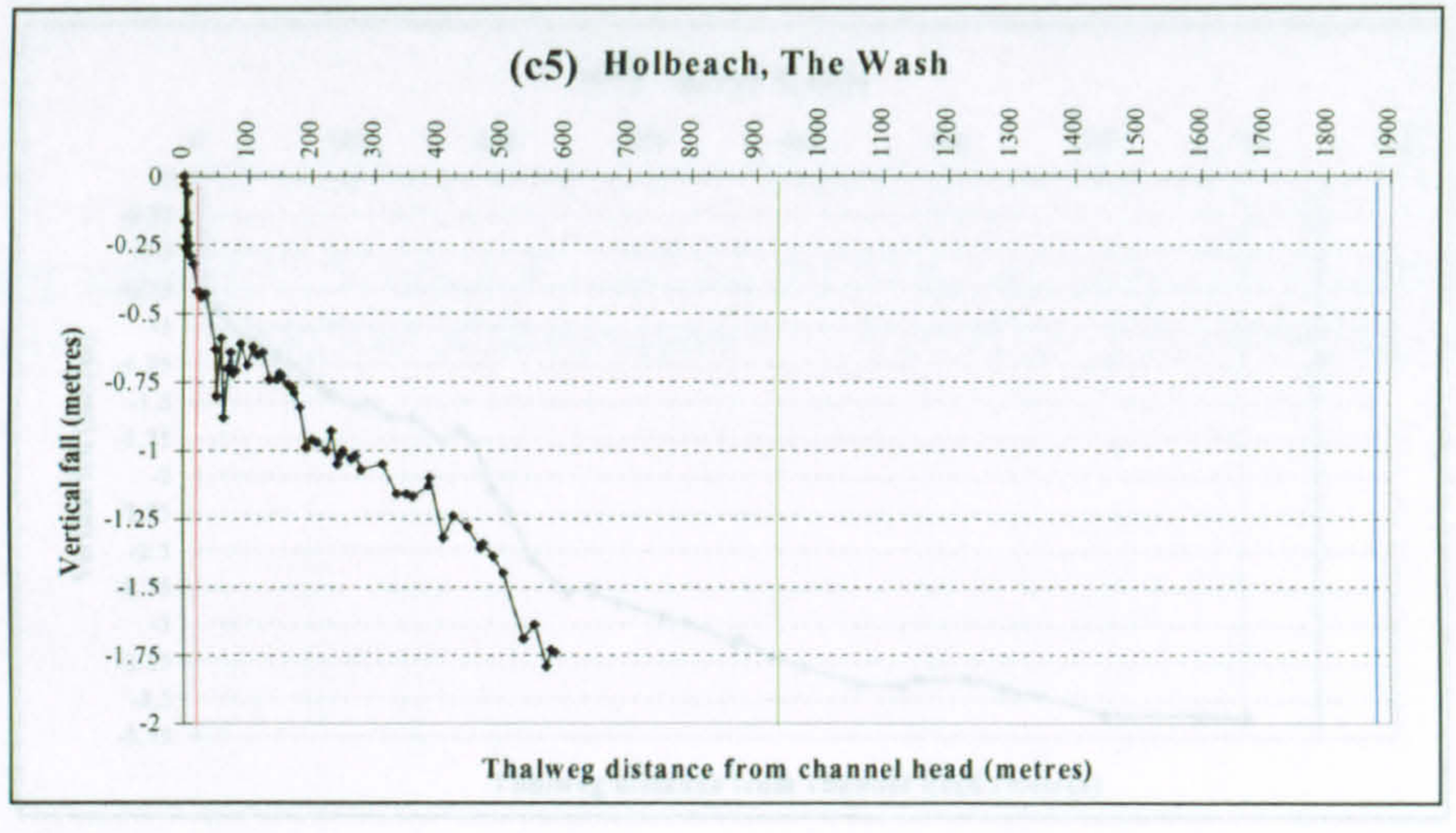

Figure 4.3 (cont.) Longitudinal profiles grouped according to those displaying: *linear* (a1-a5) *upwardly concave* (b1-b14); and *composite* (c1-c10) patterns of descent. The limit of vegetative cover (___), mean low water mark (___), and loci of re-curvature (___) provide a frame of reference.

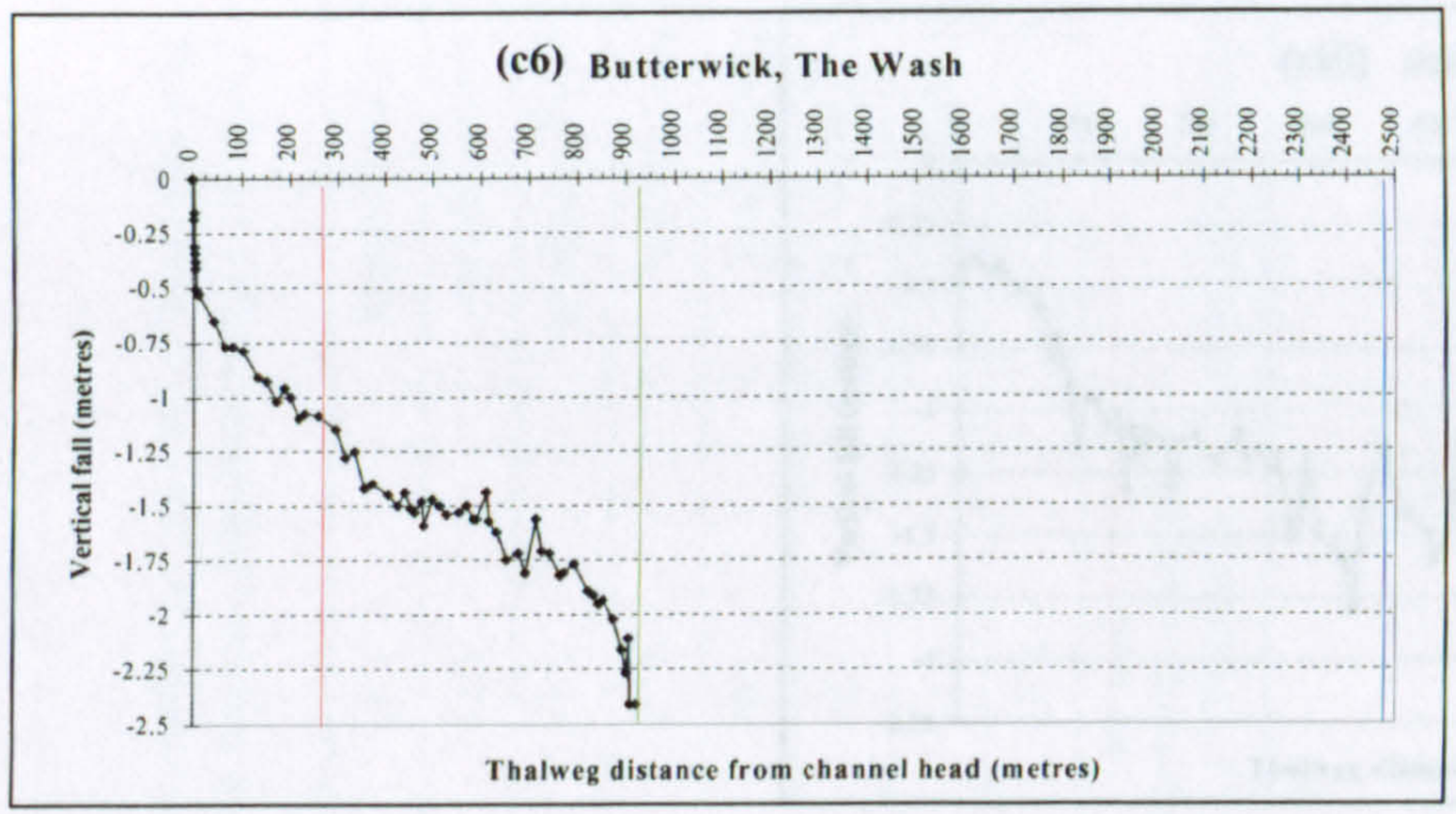

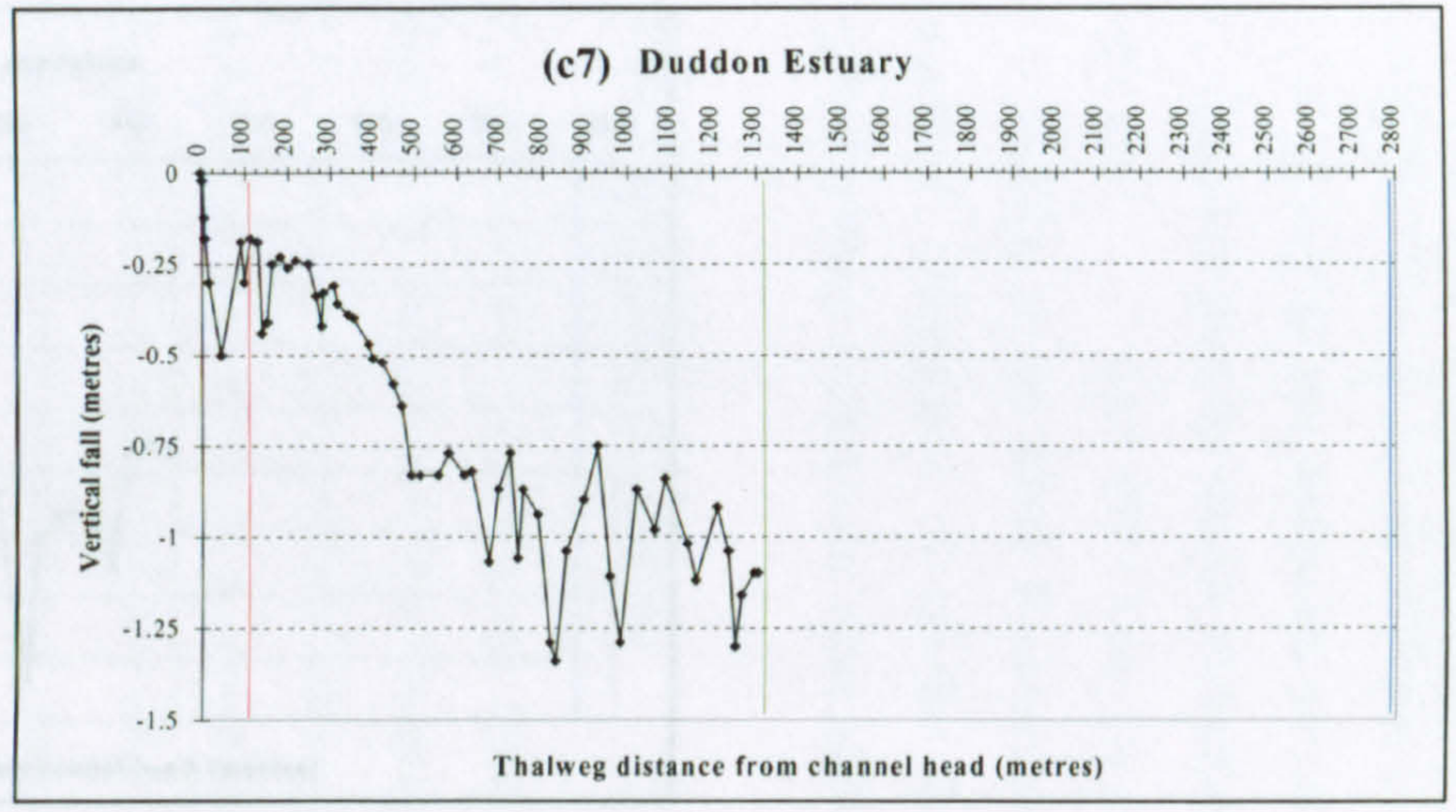

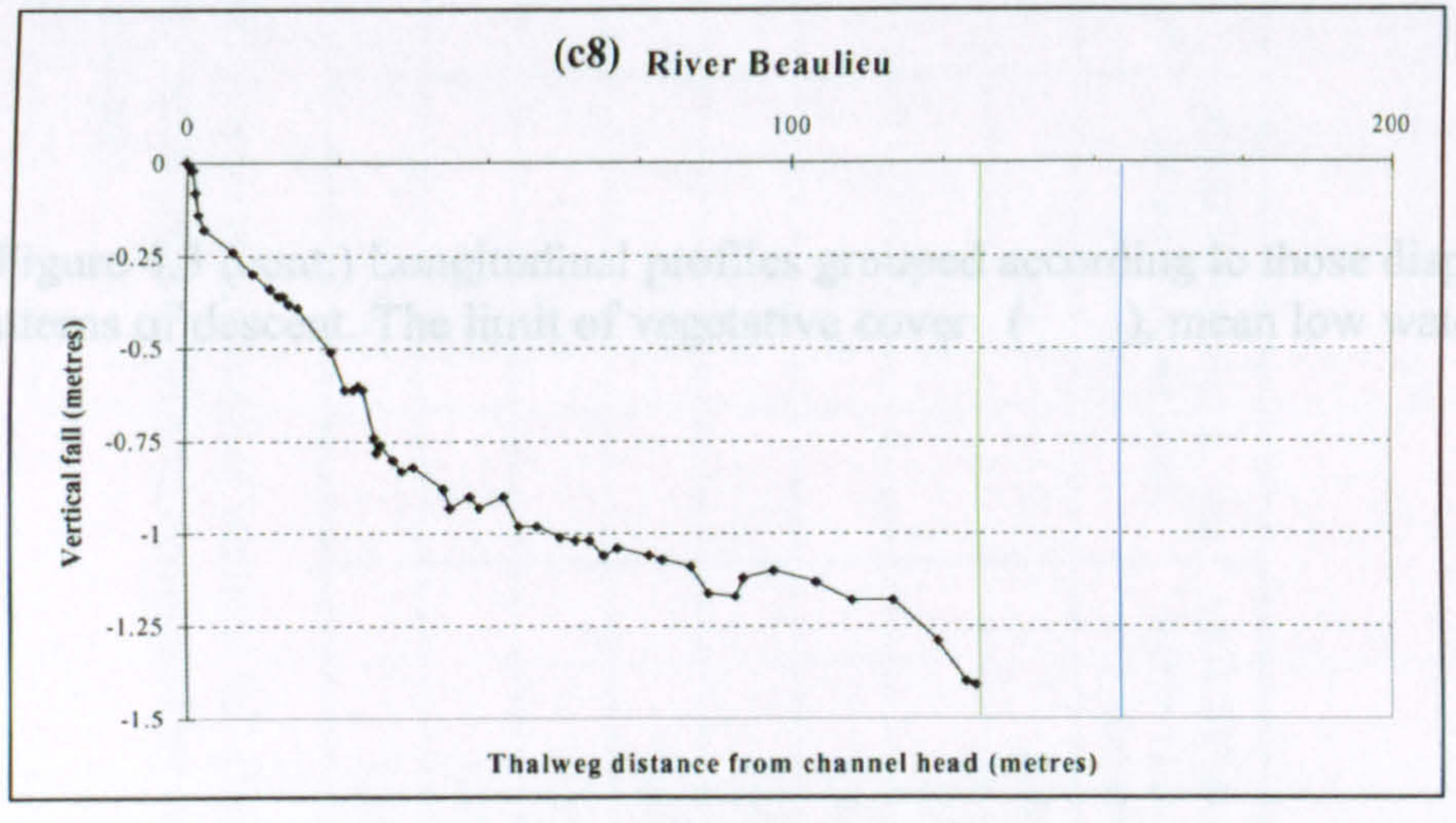

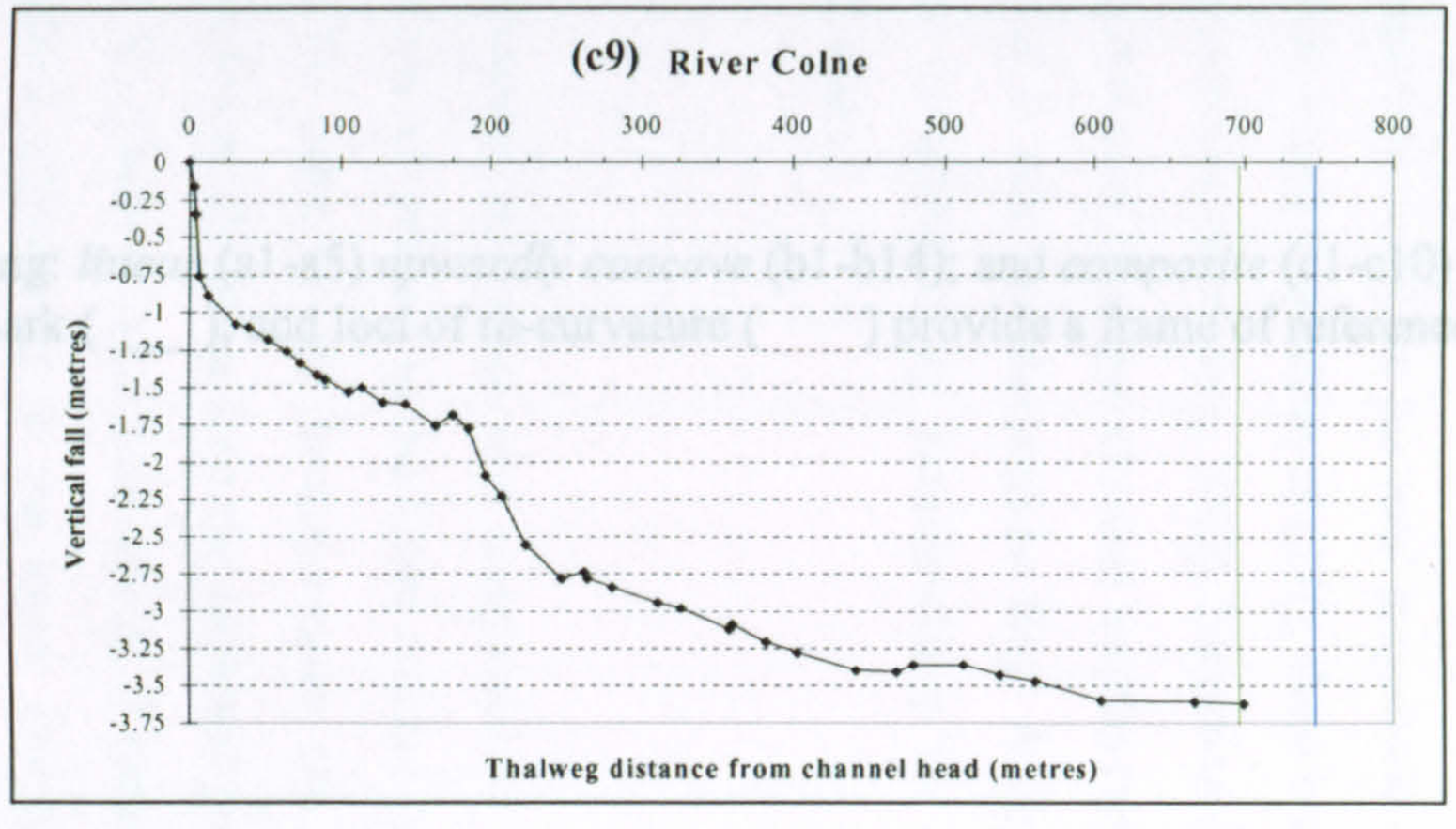

Figure 4.3 (cont.) Longitudinal profiles grouped according to those displaying: *linear* (a1-a5) *upwardly concave* (b1-b14); and *composite* (c1-c10) patterns of descent. The limit of vegetative cover (___), mean low water mark (___), and loci of re-curvature (___) provide a frame of reference.

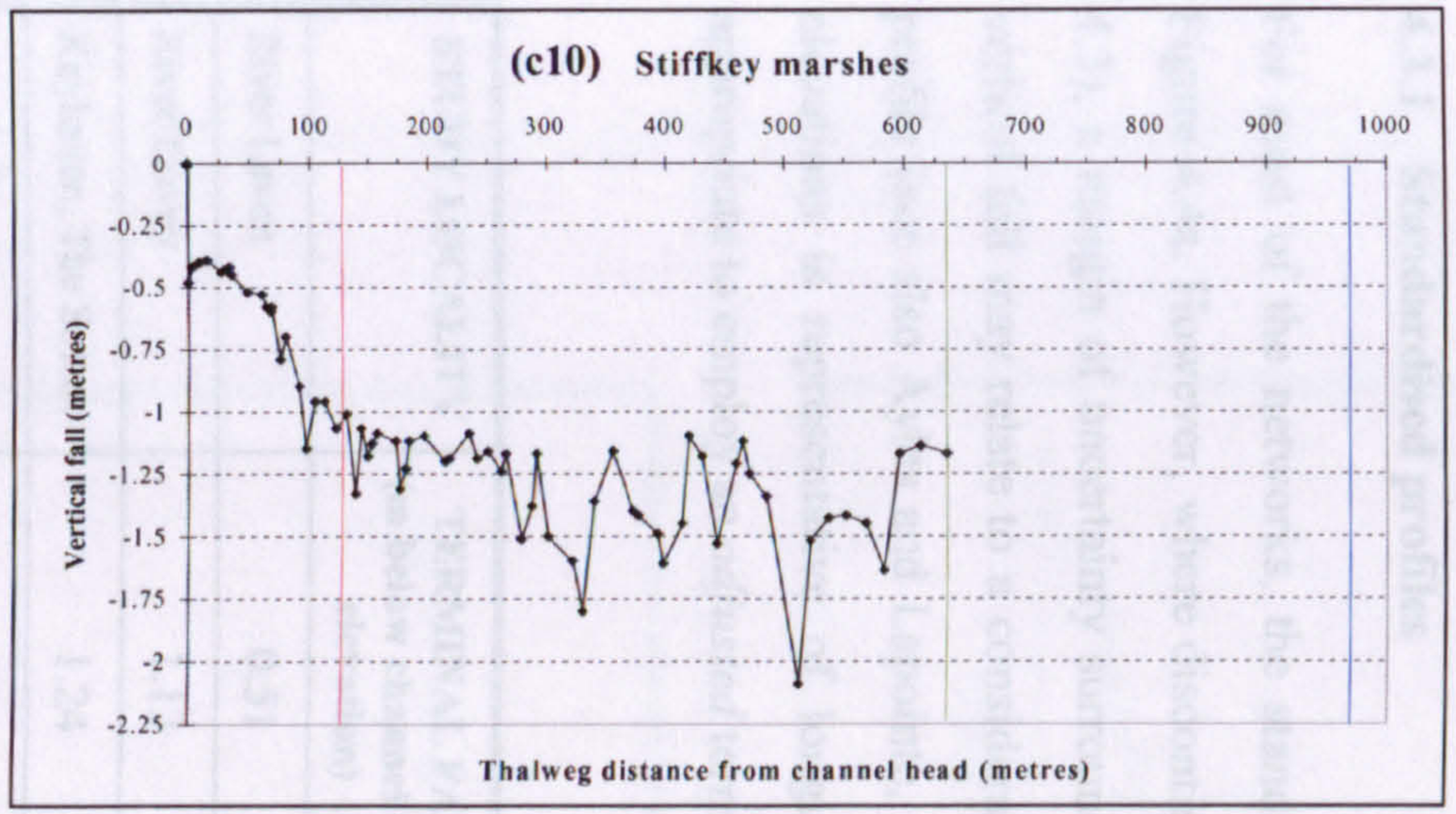

Figure 4.3 (cont.) Longitudinal profiles grouped according to those displaying: *linear* (a1-a5) *upwardly concave* (b1-b14); and *composite* (c1-c10) patterns of descent. The limit of vegetative cover (___), mean low water mark (___), and loci of re-curvature (___) provide a frame of reference.

However, basic fall-distance plots do not best reveal the differences between these categories. The results are difficult to superimpose, since the total magnitude of vertical adjustment (Σd), and horizontal extent over which it is achieved (ΣH), show considerable variation between the sample formations (see also Morisawa, 1962). Elevation changes of between $0.6 < \Sigma H < 3.6$m are depicted over principal channel lengths ranging from Σd < 200m at the River Beaulieu to Σd > 1km in Morecambe Bay. A significantly improved comparison of profile shape is afforded by *standardising* the graphical representations according to a normalised scale.

4.3.1 Standardised profiles

For most of the networks, the standardisation procedure was completed as shown in Figure 4.4a. However, where discontinuities are present in the lower reaches (see Figure 4.3), a margin of uncertainty surrounds the value of ΣH. In these cases, the *maximum* vertical fall may relate to a considerably lower elevation than the *terminal* point of the profile (see also Ayles and Lapointe, 1996). Since it is unclear which, if either of these elevations is representative of longitudinal adjustment at the lower boundary, it is appropriate to employ an *adjusted* terminal elevation.

STUDY LOCALITY	TERMINAL FALL (m below channel head elevation)	MAXIMUM FALL (m below channel head elevation)	ADJUSTED FALL (m below channel head elevation)
River Leven	0.51	0.82	0.64
River Dovey	1.13	1.55	1.23
Keyhaven, The Solent	1.24	1.54	1.36
Maplin Sands	1.02	1.46	1.27
River Crouch	0.58	1.04	0.88
Dengie Peninsula	1.74	1.94	1.83
Stiffkey marshes	1.17	2.09	1.39
Saltfleet marshes	1.27	2.42	1.66

Table 4.1 Offset recorded between the maximum magnitude of vertical fall and channel bed elevation at the limit of vegetative cover. Adjusted fall was computed by regression analysis.

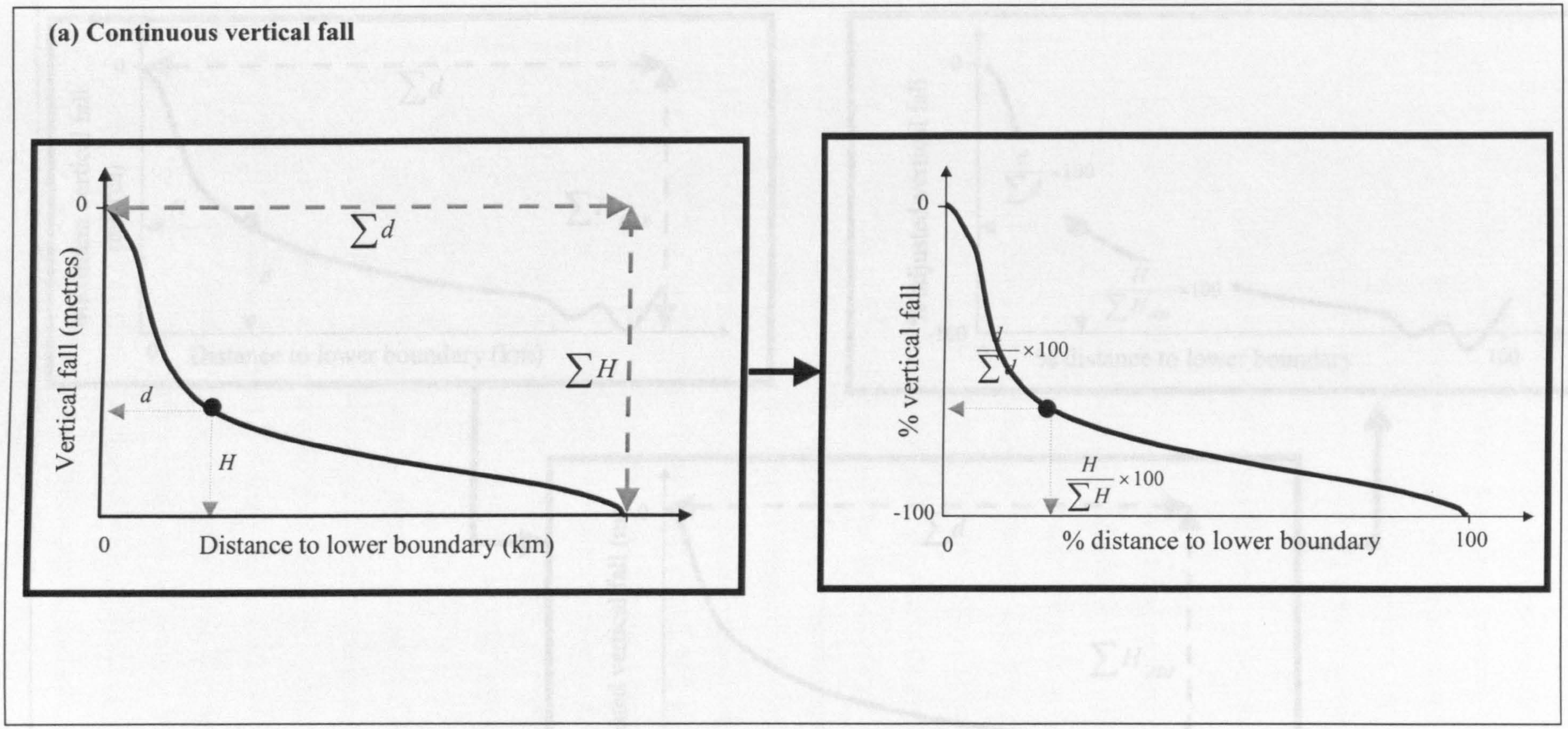

Figure 4.4 Schematic representation of the method employed for converting survey results to standardised longitudinal profiles for: (a) continuous; and (b) discontinuous patterns of vertical fall. Channel bed elevation is expressed as a function of total vertical fall and distance from the channel head as a % of total distance to the lower measurement boundary.

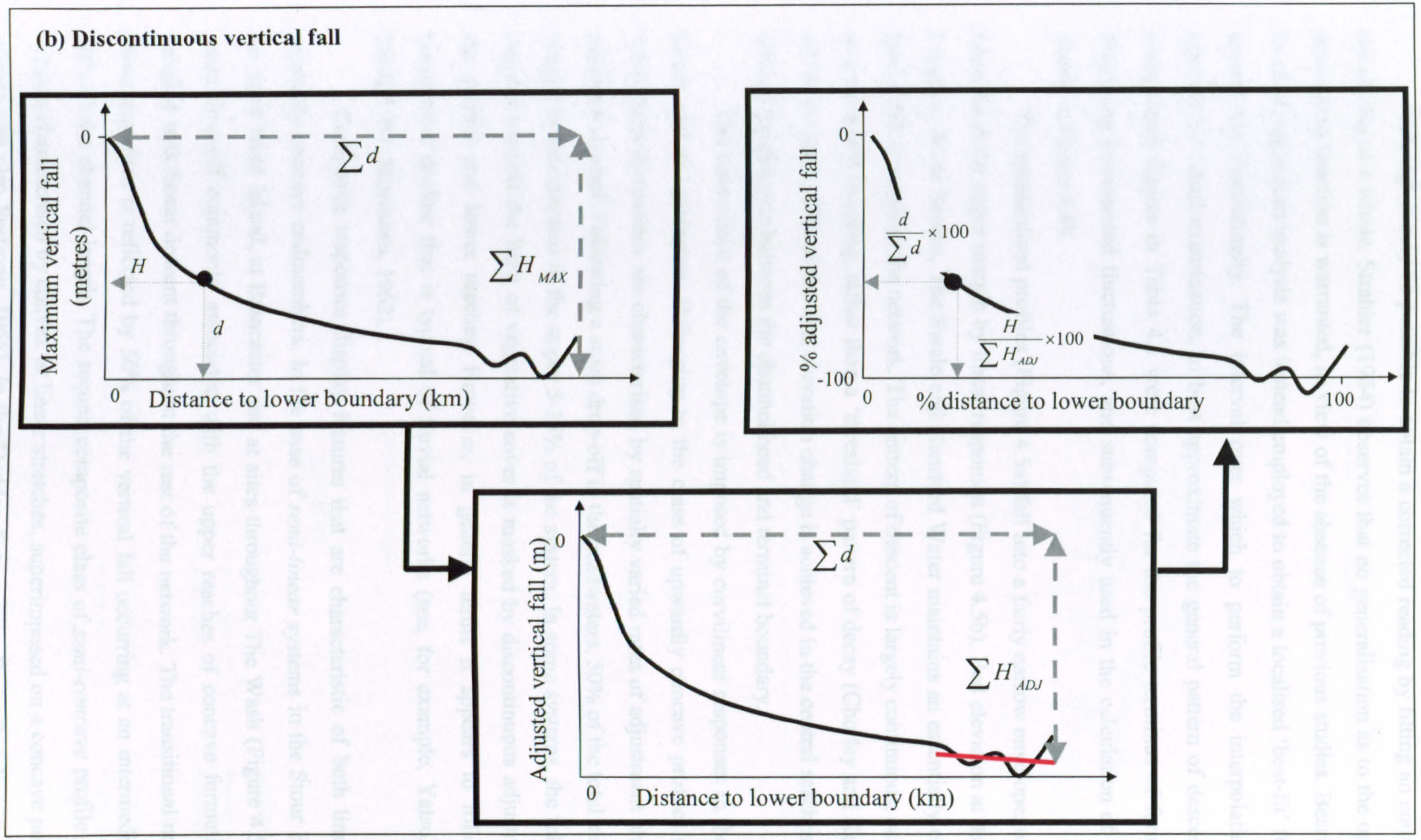

Figure 4.4 cont. Schematic representation of the method employed for converting survey results to standardised longitudinal profiles for: (a) continuous; and (b) discontinuous patterns of vertical fall. Channel bed elevation is expressed as a function of total vertical fall and distance from the channel head as a % of total distance to the lower measurement boundary.

Although it may be possible to obtain a corrected reading by fitting an equation to the profile as a whole, Strahler (1964) observes that no generalisation as to the optimum descriptive function is warranted, in view of the absence of previous studies. Bearing this in mind, regression analysis was instead employed to obtain a localised 'best-fit' function around the discontinuity. The interval over which to perform the interpolation was selected by visual examination, to best approximate the general pattern of descent. The interpolated figures in Table 4.1 were computed for the profile terminus of formations displaying pronounced fluctuations, and subsequently used in the calculation of ΣH, as shown in Figure 4.4b.

The standardised profiles (Figure 4.5a) fall into a fairly narrow envelope, which is bounded at the upper margin by linear responses (Figure 4.5b). Bed elevation at the River Loughor, River Severn, The Swale and Hamford Water maintains an essentially constant rate of fall *throughout* the network. The pattern of descent is largely continuous, occurring as a sustained lowering, rather than a 'threshold' pattern of decay (Chorley and Kennedy, 1971). As such, 50% of the total elevation change is achieved in the central reaches, at 45-65% of the distance between the channel head and terminal boundary.

The lower limit of the envelope is imposed by curvilinear responses in the River Leven and at Lymington. Belonging to the class of upwardly concave profiles (Figure 4.5c), these formations are characterised by spatially varied rates of adjustment along the principal channel. Following a steep drop-off in the headwaters, 50% of the total elevation change is concentrated in the upper 5-25% of the system. In some systems, the following descent towards the limit of vegetative cover is masked by discontinuous adjustment in the central and lower reaches. However, in general terms it appears to follow the progressive decline that is typical of fluvial networks (see, for example, Yatsu, 1955; Hack, 1957; Morisawa, 1962).

Composite responses display features that are characteristic of both linear and upwardly concave endmembers. In the case of *semi-linear* systems in the Stour Estuary, on Scolt Head Island, at Brancaster and at sites throughout The Wash (Figure 4.5d), the steep drop-off commonly associated with the upper reaches of concave formations, is coupled with linear descent throughout the rest of the network. The transitional nature of these responses is reflected by 50% of the vertical fall occurring at an intermediate 30-50% of the channel length. The second composite class of *semi-concave* profile (Figure 4.5e) is characterised by convex or linear stretches, superimposed on a concave pattern of decent (see also Pestrong, 1965). In the Duddon Estuary, the River Beaulieu, the River

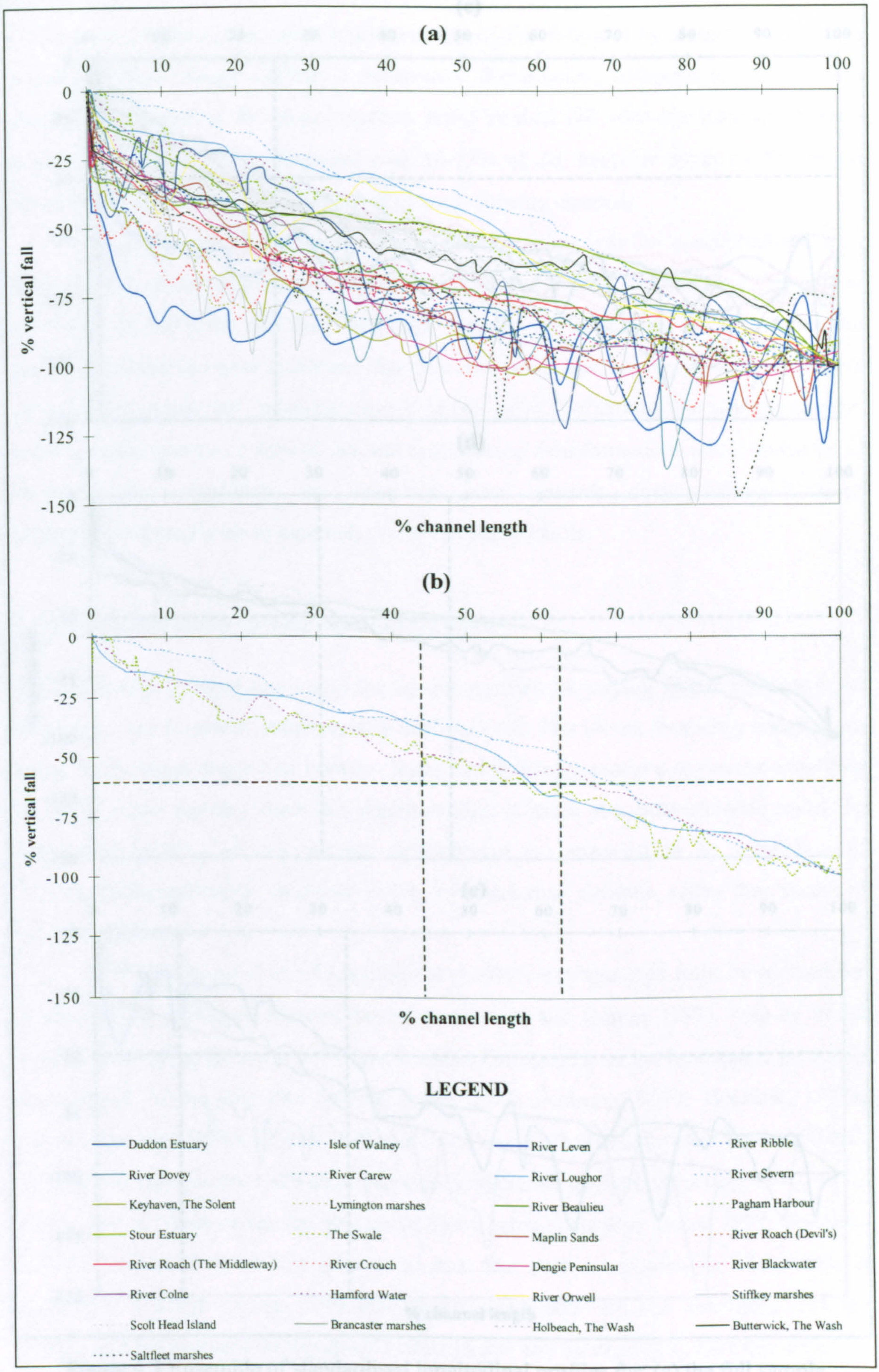

Figure 4.5 Ensemble of standardised longitudinal profiles for: (a) the full sample population; (b) linear responses; (c) upwardly concave reaches; (d) linear reaches coupled with headwater drop-off; and (e) composite responses.

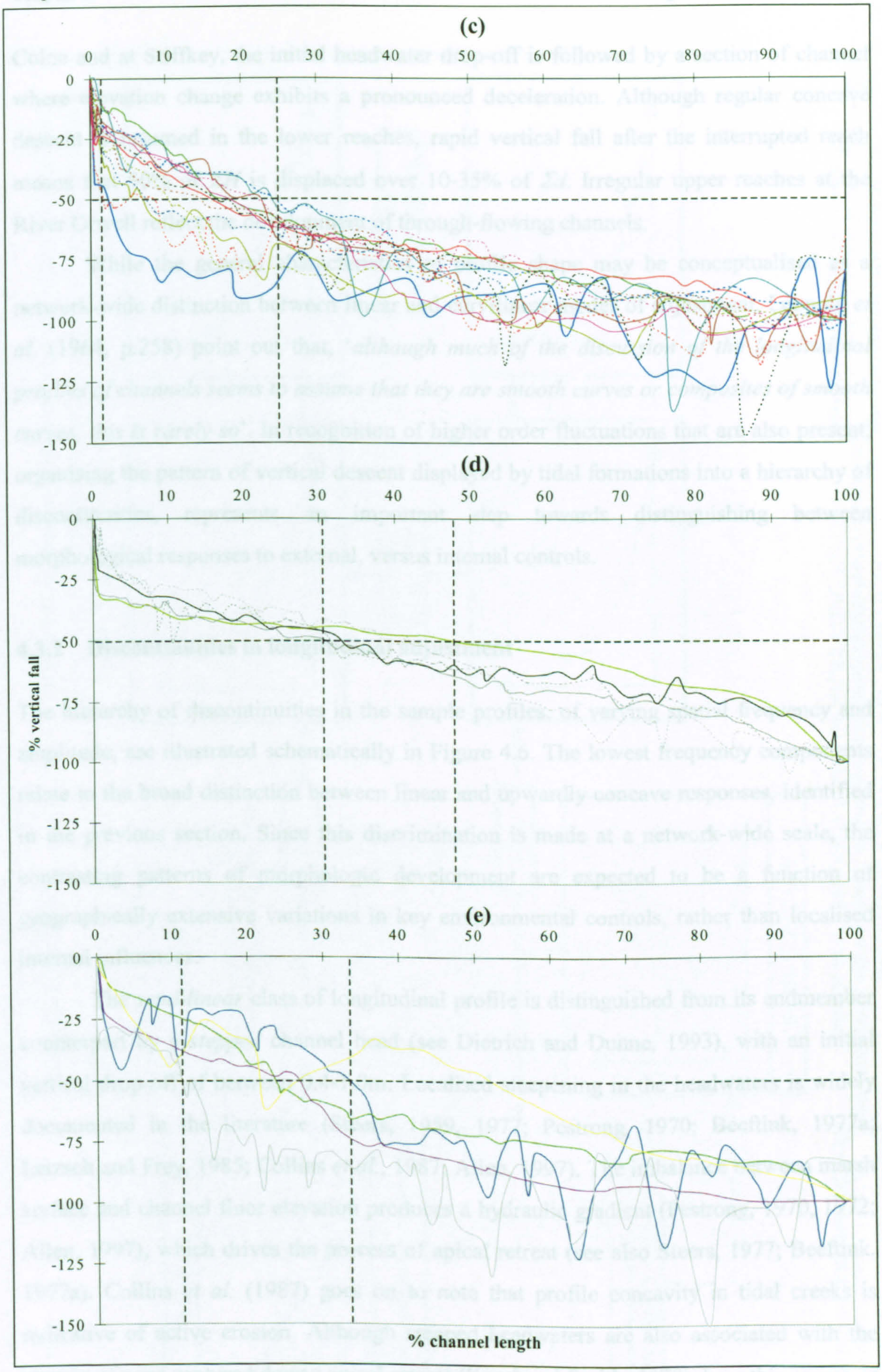

Figure 4.5 Ensemble of standardised longitudinal profiles for: (a) the full sample population; (b) linear responses; (c) upwardly concave reaches; (d) linear reaches coupled with headwater drop-off; and (e) composite responses.

Colne and at Stiffkey, the initial headwater drop-off is followed by a section of channel where elevation change exhibits a pronounced deceleration. Although regular concave descent is resumed in the lower reaches, rapid vertical fall after the interrupted reach means that 50% of ΣH is displaced over 10-35% of Σd. Irregular upper reaches at the River Orwell reflect the development of through-flowing channels.

While the general characteristics of profile shape may be conceptualised as a network-wide distinction between linear and curvilinear modes of adjustment, Leopold *et al.* (1964, p.258) point out that, '*although much of the discussion of the longitudinal profiles of channels seems to assume that they are smooth curves or composites of smooth curves, this is rarely so*'. In recognition of higher order fluctuations that are also present, organising the pattern of vertical descent displayed by tidal formations into a hierarchy of discontinuities, represents an important step towards distinguishing between morphological responses to external, versus internal controls.

4.3.2 Discontinuities in longitudinal adjustment

The hierarchy of discontinuities in the sample profiles, of varying spatial frequency and amplitude, are illustrated schematically in Figure 4.6. The lowest frequency components relate to the broad distinction between linear and upwardly concave responses, identified in the previous section. Since this discrimination is made at a network-wide scale, the contrasting patterns of morphologic development are expected to be a function of geographically extensive variations in key environmental controls, rather than localised internal influences.

The *semi-linear* class of longitudinal profile is distinguished from its endmember counterpart by a *stepped* channel head (see Dietrich and Dunne, 1993), with an initial vertical drop-off of between 0.4-1.0m. Localised steepening in the headwaters is widely documented in the literature (Steers, 1959, 1977; Pestrong, 1970; Beeftink, 1977a; Letzsch and Frey, 1985; Collins *et al.*, 1987; Allen, 1997). The imbalance between marsh surface and channel floor elevation produces a hydraulic gradient (Pestrong, 1970, 1972; Allen, 1997), which drives the process of apical retreat (see also Steers, 1977; Beeftink, 1977a). Collins *et al.* (1987) goes on to note that profile concavity in tidal creeks is indicative of active erosion. Although stepped headwaters are also associated with the margin of pans captured during apical retreat (Kesel and Smith, 1978), here this source of accelerated fall has only been observed at Stiffkey.

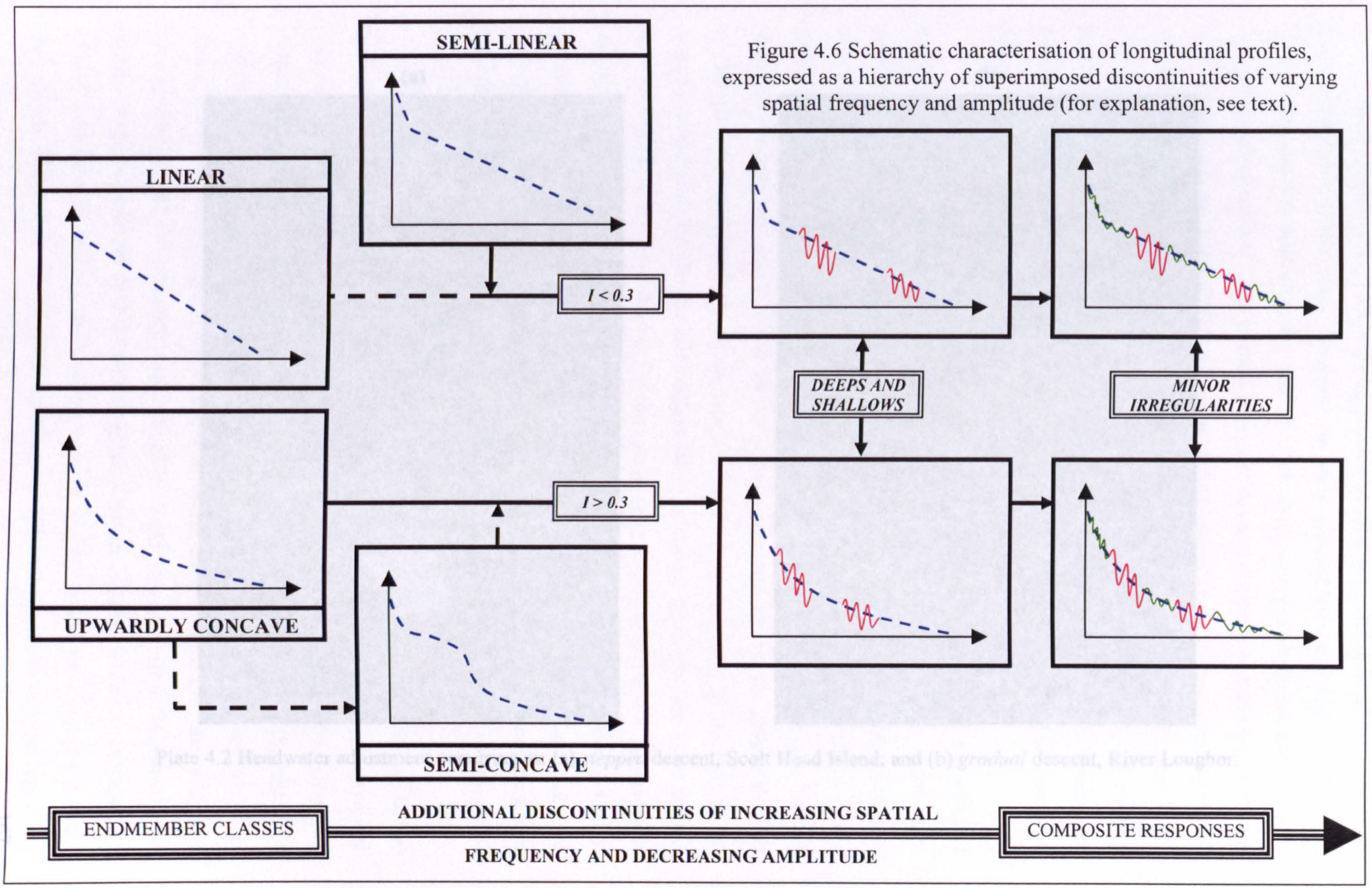

Figure 4.6 Schematic characterisation of longitudinal profiles, expressed as a hierarchy of superimposed discontinuities of varying spatial frequency and amplitude (for explanation, see text).

(a)

(b)

Plate 4.2 Headwater adjustment occurring as: (a) *stepped* descent, Scolt Head Island; and (b) *gradual* descent, River Loughor.

Headward erosion is an ongoing process at sites with cliffed headwaters, such as Scolt Head Island (Plate 4.2a). However, an early account by Carey and Oliver (1918, p.167) observes that tidal channels may also *'get shallower and shallower until they die out on the marsh surface'*. The gradual pattern of descent (Dietrich and Dunne, 1993) that this describes, is commensurate with a significant reduction in hydraulic gradient, and effective cessation in the erosive potential of morphologically active ebb tidal flows. Marshall (1962) likens apical erosion to a type of 'waterfall' retreat which, by analogy with fluvial systems, may proceed until the rate of energy expenditure is minimised. Following this line of reasoning, it seems that the nature of channel head adjustment may reflect the stage of network development (Figure 1.6).

Progressive rather than stepped headwater adjustment is recorded in a number of networks (Figure 4.5b), the implication being that a minimum rate of energy expenditure has been achieved. In the case of the River Loughor (Plate 4.2b), equilibrium adjustment has been achieved through opportunistic channel extension (see also Knighton *et al.*, 1992) along a natural depression running along the rear of the marsh, rather than through progressive headward retreat. While through-flowing reaches explain the progressive fall at Hamford Water, channel extension along a line of least resistance at the rear of the marsh is responsible for the gradual descent along re-curved reaches in the River Severn and The Swale. A 0.5-1.1m drop-off at the loci of re-curvature (see Table 4.2) represents the disparity between marsh surface and channel bed elevation on encountering a topographic barrier at the rear of the intertidal zone. Channelisation has proceeded along a re-curved course at these sites, driven by the tendency towards a balance between resistive and erosive forces. Notably, this headward retreat has substantially reduced the height of drop-off at the channel head, when compared with the loci of re-curvature.

The present results suggest that a stable equilibrium form can be attained by re-curvature along a line of least resistance. However, in the absence of an extended temporal record, they are unable to confirm that stepped channel heads evolve towards a gradual pattern of descent. The analysis of cross-sectional morphology (Section 5.3) suggests that the central and upper reaches of formations in the Duddon Estuary, the River Leven, the River Ribble, and at Holbeach, The Wash, have reached the latter stages of development. If the evolutionary model applies, these 'mature' networks should also display gradual descent in the headwater reaches. Despite evidence of retrogression (Plate 4.3a-b) as vegetation bridges the creeks (Yapp *et al.*, 1917) and colonises the channel floor (Kesel and Smith, 1978), the longitudinal profiles (Figure 4.3) suggest that fairly

STUDY LOCALITY	CHANNEL HEAD STEP (metres)	DROP-OFF (metres)	NATURE OF OBSTRUCTION
Duddon Estuary	0.12	0.19	embankment
River Leven	0.29	0.56	concrete seawall
River Loughor	-	0.76	sand dune
River Severn	-	1.03	embankment
The Swale	-	0.56	embankment
Maplin Sands	0.21	0.29	concrete seawall
River Roach (Middleway)	0.28	1.07	embankment
River Crouch	0.33	0.66	concrete seawall
River Blackwater	-	0.80	embankment
River Orwell	-	0.61	higher terrain
Stiffkey marshes	0.48	1.07	embankment
Holbeach, The Wash	0.26	0.59	embankment
Butterwick, The Wash	0.31	1.28	embankment
Saltfleet marshes	0.30	1.02	higher terrain

Table 4.2 Height of stepped channel head and vertical drop-off between zero datum and channel bed elevation at the loci of re-curvature, for channel reaches encountering various forms of topographic obstruction at the rear of the marsh.

rapid descent is sustained in the upper reaches. It therefore appears that the processes driving apical retreat do not necessarily result in gradual headwater descent (see, for example, Figure 4.5b), before becoming ineffective. As a function of the re-curvature process, rather than an expression of equilibrium adjustment, progressive fall around the channel head should be viewed as a distinctive morphological response to irregular boundary conditions, instead of an endmember state. As such, the classification can be simplified to a three-way distinction between linear, concave and semi-concave responses.

In line with observations by Snow and Slingerland (1987) concerning spatial discontinuities in fluvial profiles, extraneous convexity within the *semi-concave* responses, and high frequency noise within the sample population as a whole, can be traced to *local* influences. The substantially reduced bed slope in the upper course of profiles from the Duddon Estuary and the Stiffkey marshes corresponds with a re-curved tract at the rear of the marsh. Irregular behaviour in central stretches at the River Colne and the River Beaulieu coincides with interruptions in the normal pattern of flow, along a captured reach (Greensmith and Tucker, 1966; Collins *et al.*, 1987) and around a major confluence.

(a)

(b)

Plate 4.3 Headwaters devolving through: (a) bridging over, Holbeach, The Wash; and (b) grassing in, River Leven.

Higher frequency discontinuities superimposed on the basic profiles range from shallows and deeps of moderate amplitude, to comparatively minor bedforms. Their relative importance in the sample formations is somewhat masked in Figure 4.3, by the ranges of sampling interval (Figure 4.2) and total vertical fall. Although broad differences can be identified between regular patterns of descent bordering the Stour Estuary and the highly irregular profile form at Stiffkey, the first order derivative (see Hack, 1957; Strahler, 1964) provides a better impression of rugosity (Shepherd, 1985).

Slope-distance plots (Figure 4.7; see also Flint, 1976) reveal distant amplitudes of response. At a subset of the study sites (a1-a17), minor fluctuations of $\pm$0-30 x10^{-3} were observed to be a function of: bedforms (Plate 4.4a); crossing points forged by livestock (Plate 4.4b); and temporary obstructions to the channel bed (Plate 4.4c) caused by bank-fall debris (Plate 4.4d). Additional higher amplitude discontinuities (see profiles b1-b12), are reflected by local slopes ranging from $\pm$30-100 x10^{-3}. While occasional irregularities in central reaches at the River Orwell (Plate 4.4e) and River Blackwater correspond with disrupted flow patterns arising from channel capture, periodic interruptions are prevalent in the lower reaches of trunk channels. Noted by Pestrong (1965) to be a function of bi-directional flows, ponding in networks at Scolt Head Island and the River Leven results from the reworking of sedimentary material (see Ranwell, 1972; also Myrick and Leopold, 1963). Severe disruption to longitudinal descent in the Stiffkey and Saltfleet marshes, at Maplin Sands and in the River Crouch (Plate 4.4f-g), can be traced to the migration of a sand or shell ridge across the mouth of the network (see, for example, Greensmith and Tucker, 1965, 1966; Hartnall, 1984). These networks fail to drain at low water and a deep *collecting pool* is formed. Where the system is no longer flushed by tidal action, sedimentation is enhanced, and bed material remains unconsolidated.

Comparing the location of discontinuities with changes in link frequency (Figure 4.7), suggests that depressions in the channel floor often occur around junctions. Interruptions to regular patterns of fall at: the River Dovey (Plate 4.4h); River Ribble; River Beaulieu; and sites bordering The Wash, coincide with confluences, the implication being that the reworking of bed material by convergent flows promotes the development of localised discontinuities.

High frequency adjustments in channel bed elevation to localised influences constitute a distinctive and ubiquitous characteristic of the profiles. However, the underlying *low* frequency harmonics are ultimately diagnostic of the network-wide response to key environmental controls, which is the focus of this extensive analysis.

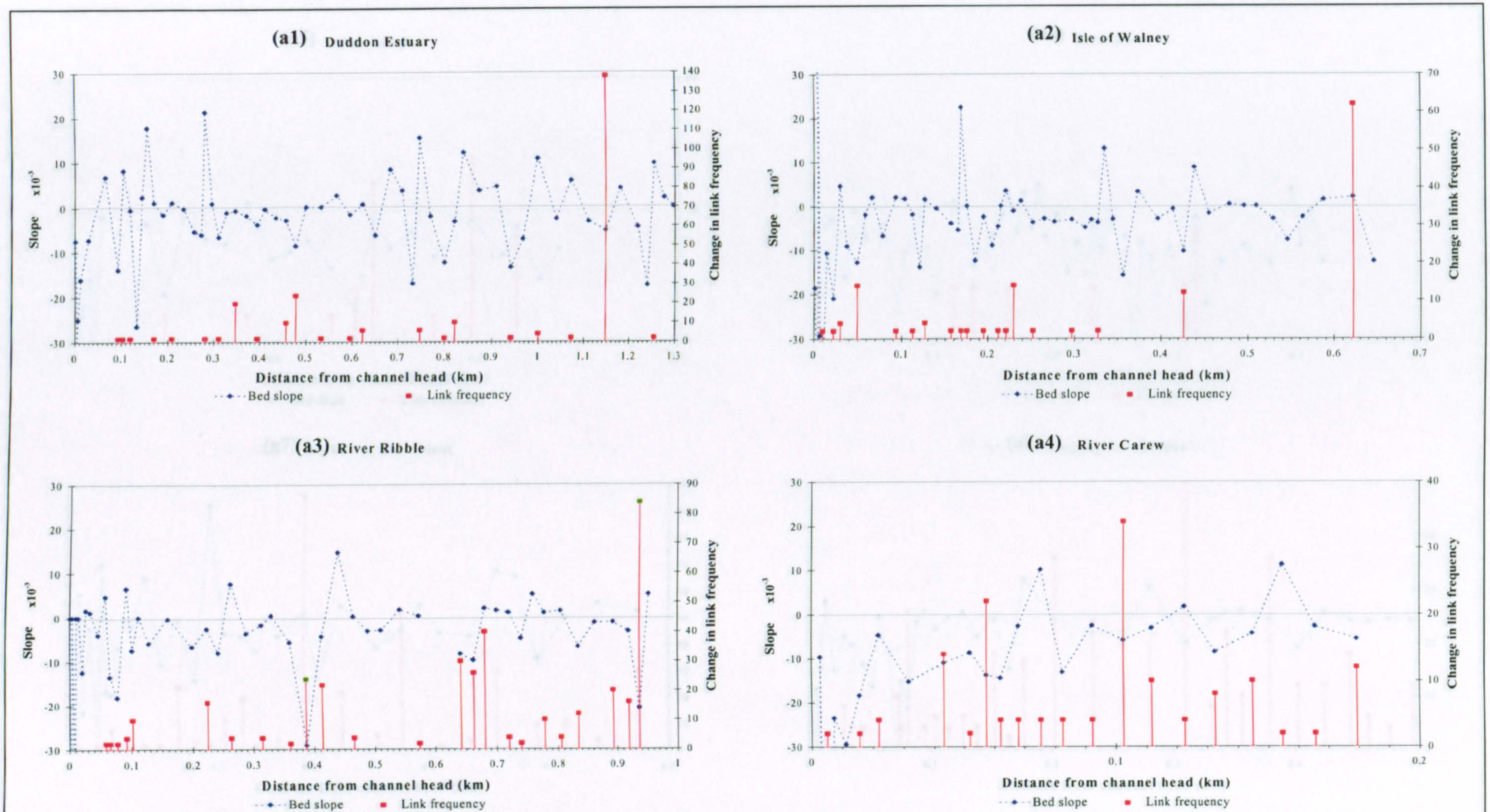

Figure 4.7 Relation of local bed slope to distance from the channel head for the subset of profiles exhibiting: minor irregularities (a1-a17); and high amplitude fluctuations (b1-b12). The location of major tributaries along the principal channel is recorded by substantial changes in link frequency.

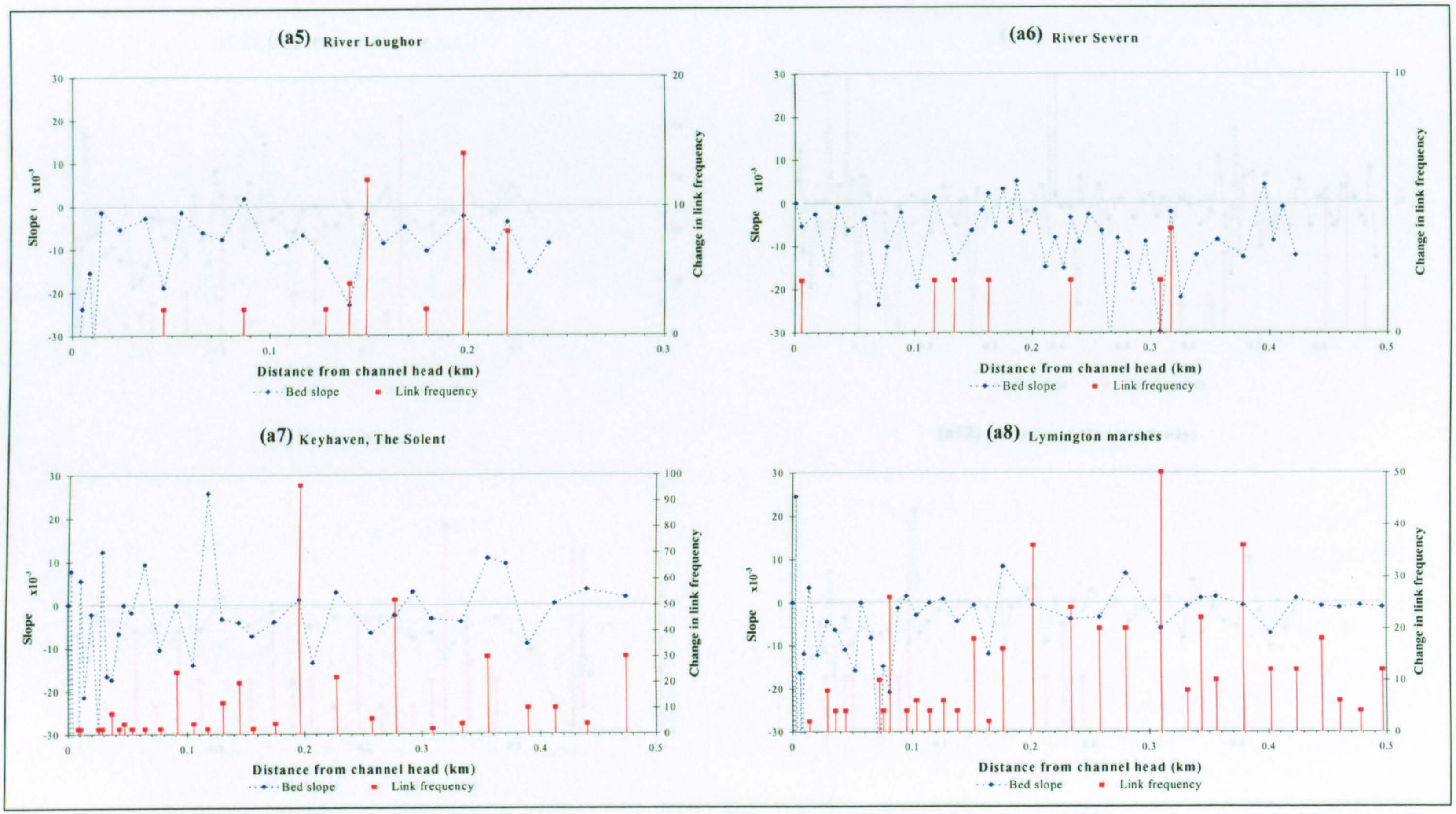

Figure 4.7 (cont.) Relation of local bed slope to distance from the channel head for the subset of profiles exhibiting: minor irregularities (a1-a17); and high amplitude fluctuations (b1-b12). The location of major tributaries along the principal channel is recorded by substantial changes in link frequency.

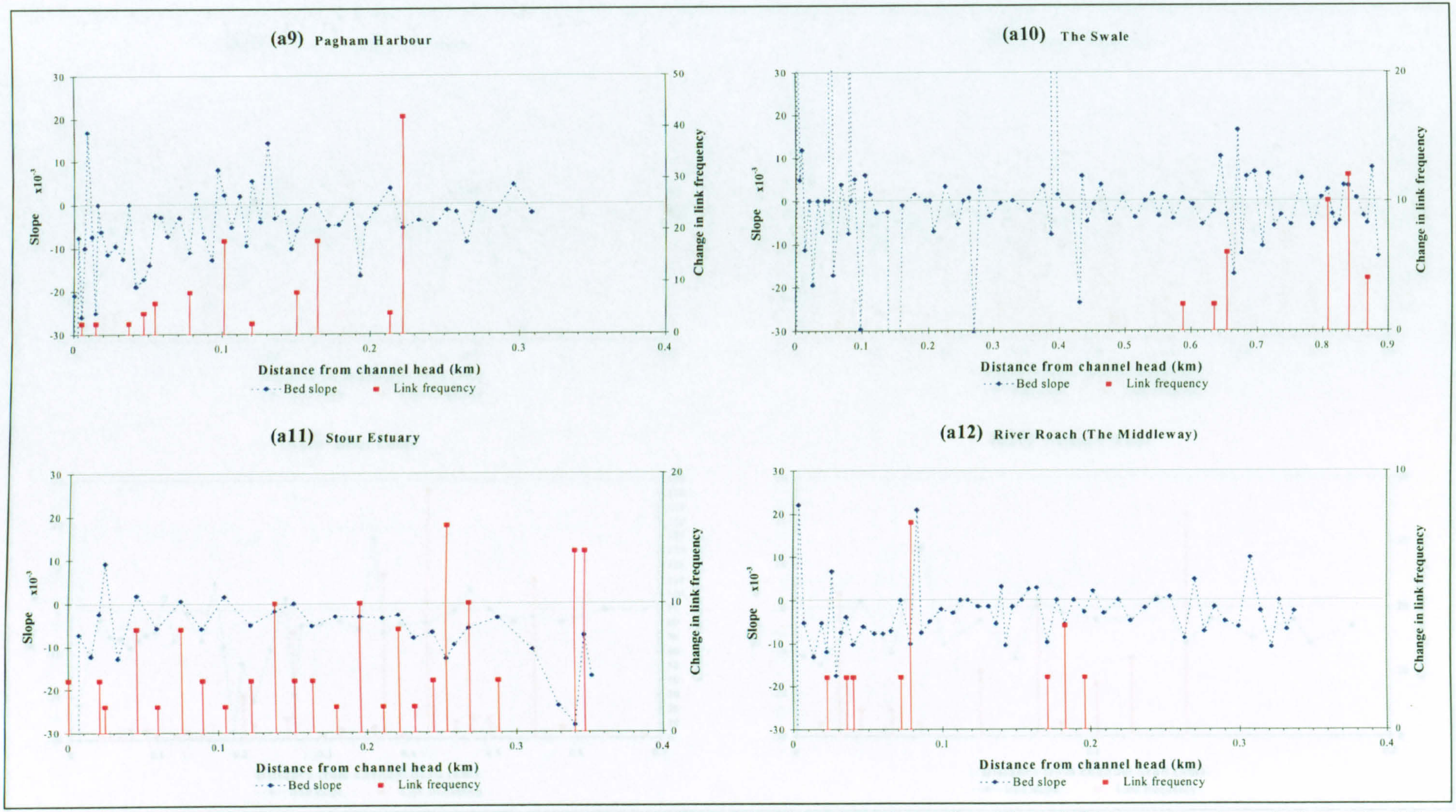

Figure 4.7 (cont.) Relation of local bed slope to distance from the channel head for the subset of profiles exhibiting: minor irregularities (a1-a17); and high amplitude fluctuations (b1-b12). The location of major tributaries along the principal channel is recorded by substantial changes in link frequency.

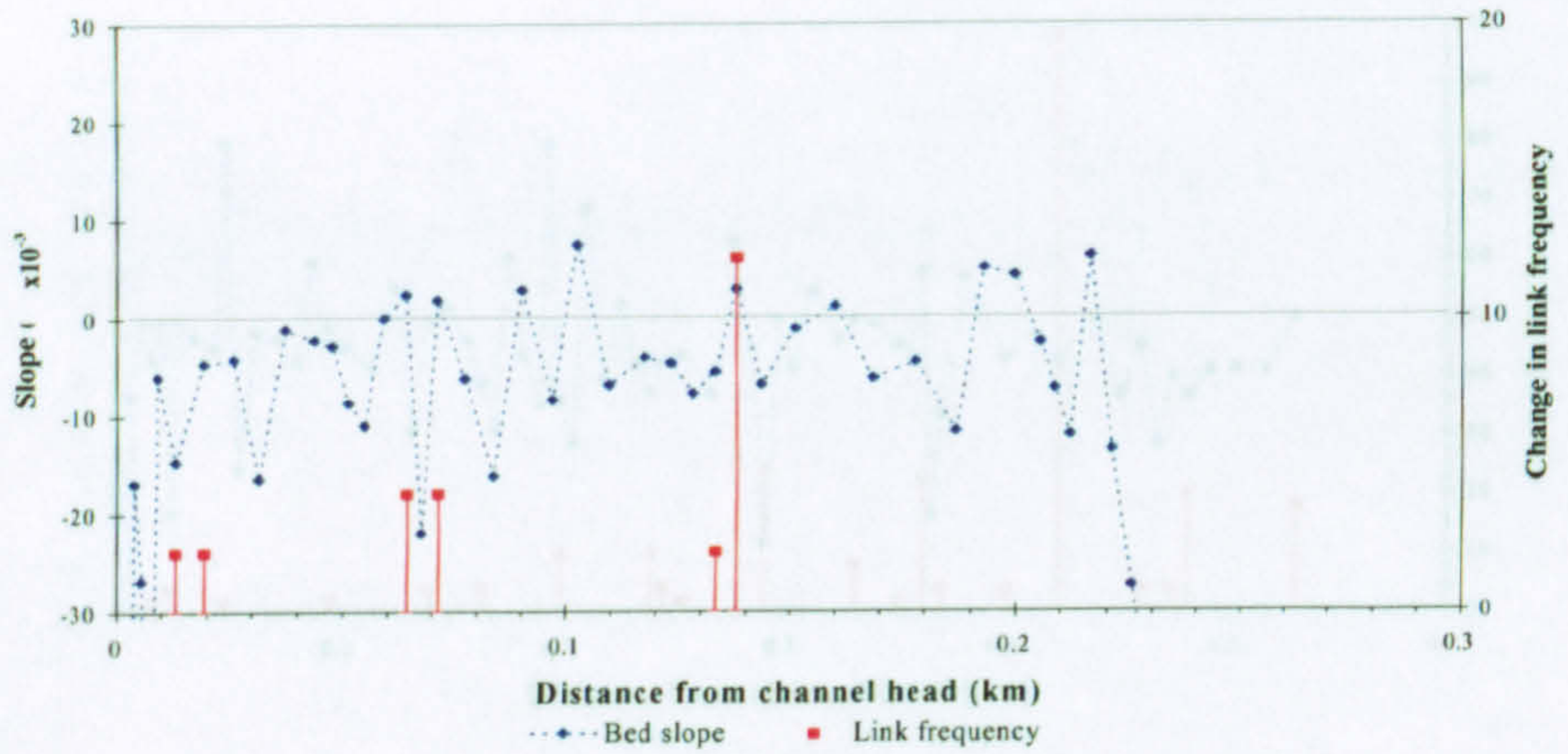

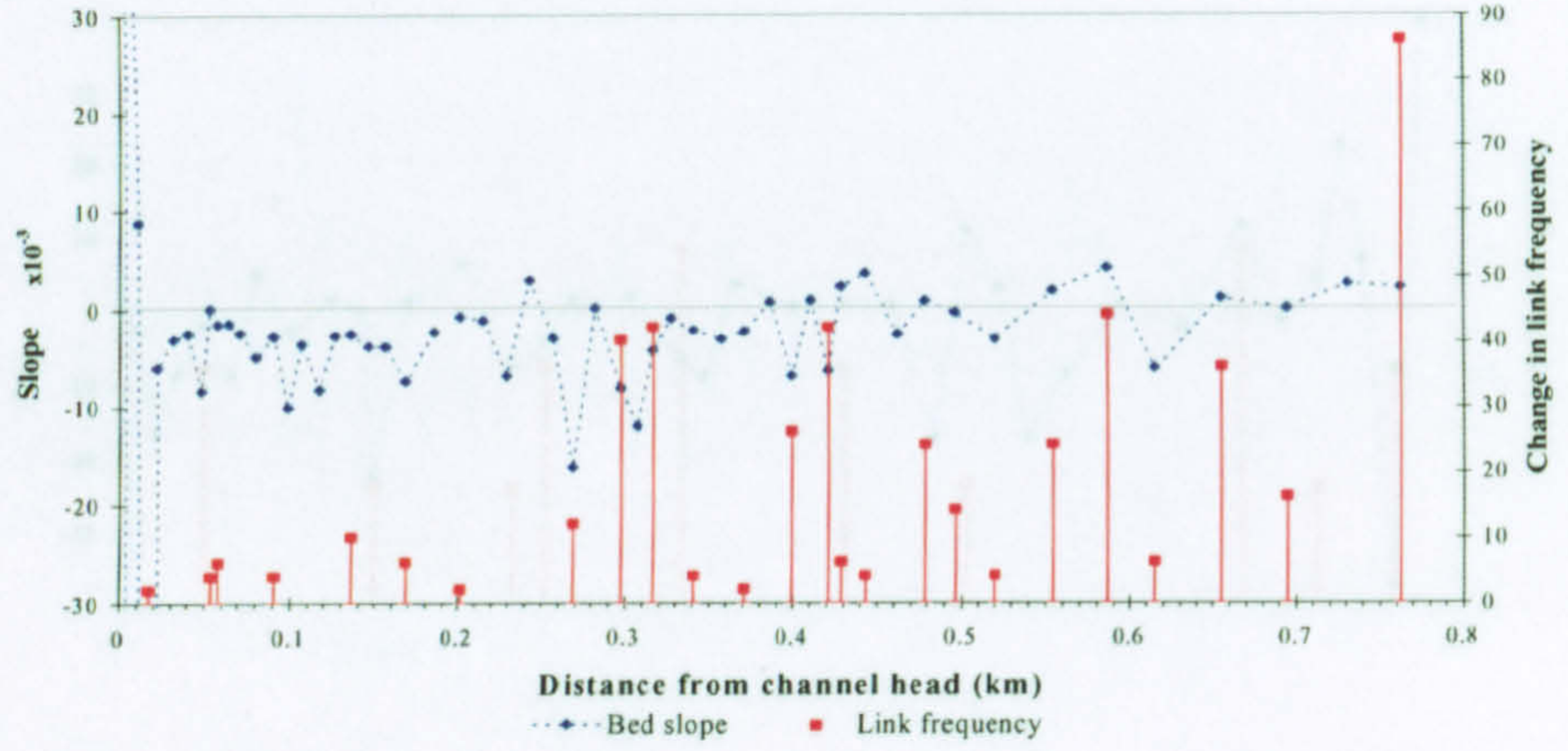

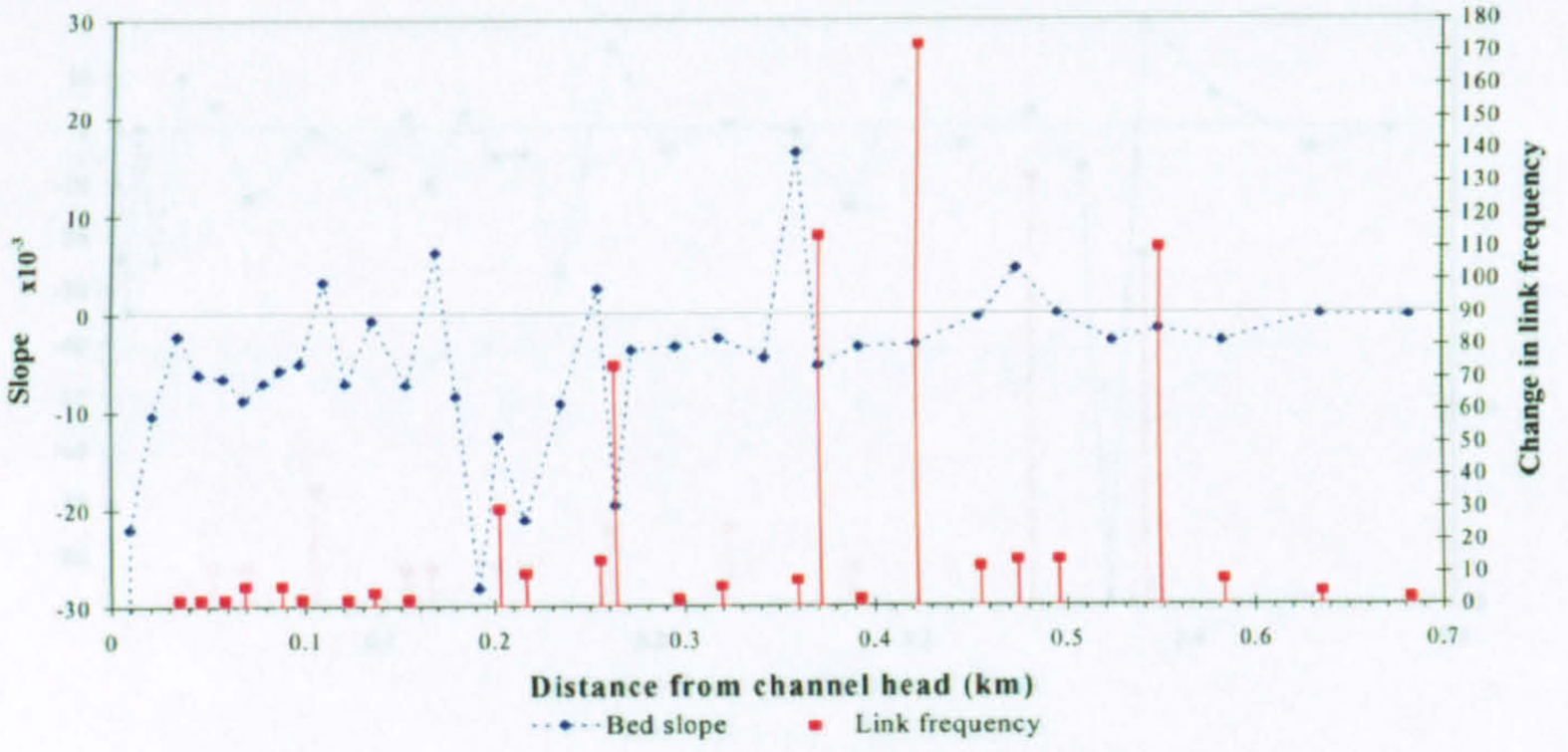

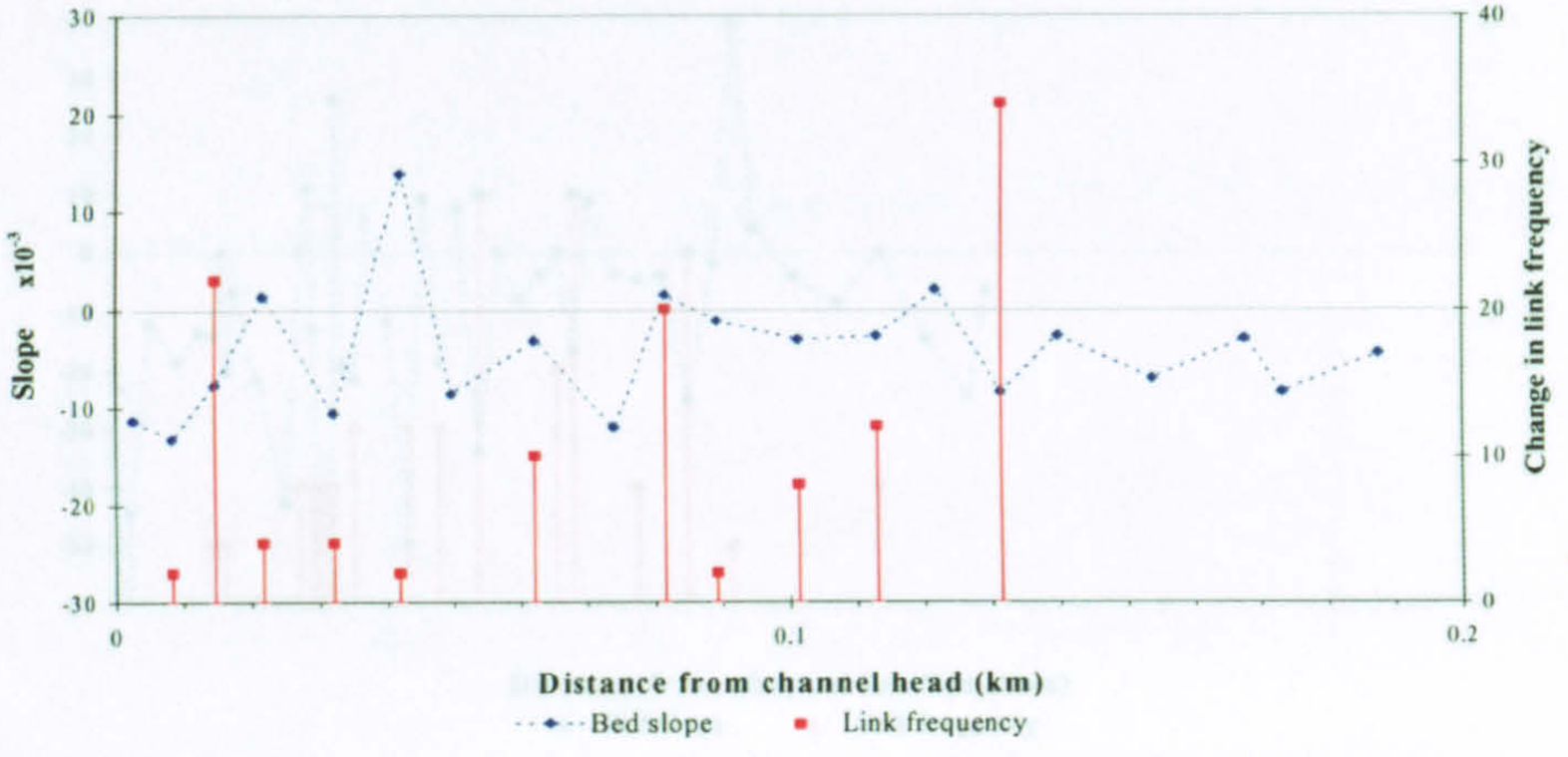

Figure 4.7 (cont.) Relation of local bed slope to distance from the channel head for the subset of profiles exhibiting: minor irregularities (a1-a17); and high amplitude fluctuations (b1-b12). The location of major tributaries along the principal channel is recorded by substantial changes in link frequency.

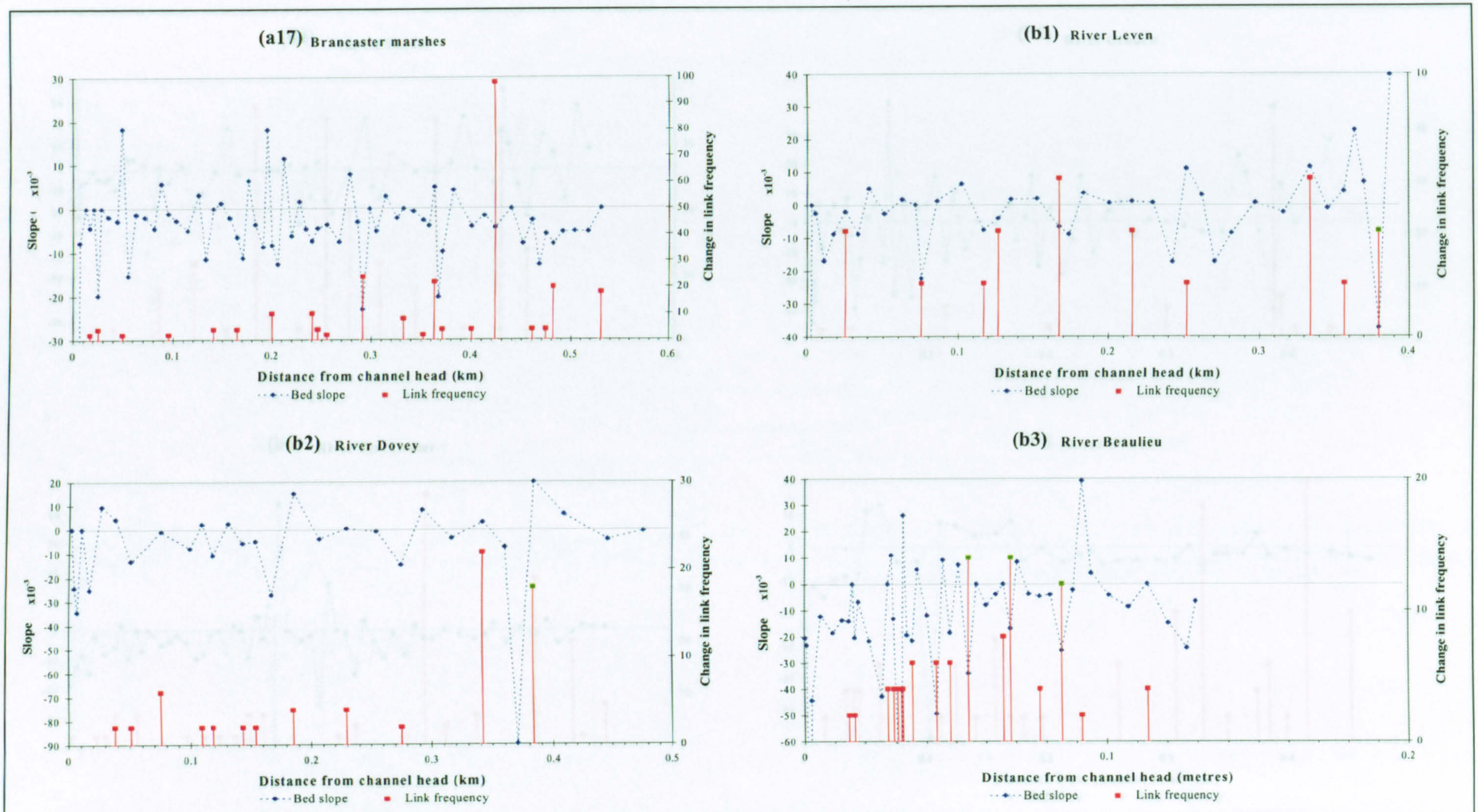

Figure 4.7 (cont.) Relation of local bed slope to distance from the channel head for the subset of profiles exhibiting: minor irregularities (a1-a17); and high amplitude fluctuations (b1-b12). The location of major tributaries along the principal channel is recorded by substantial changes in link frequency.

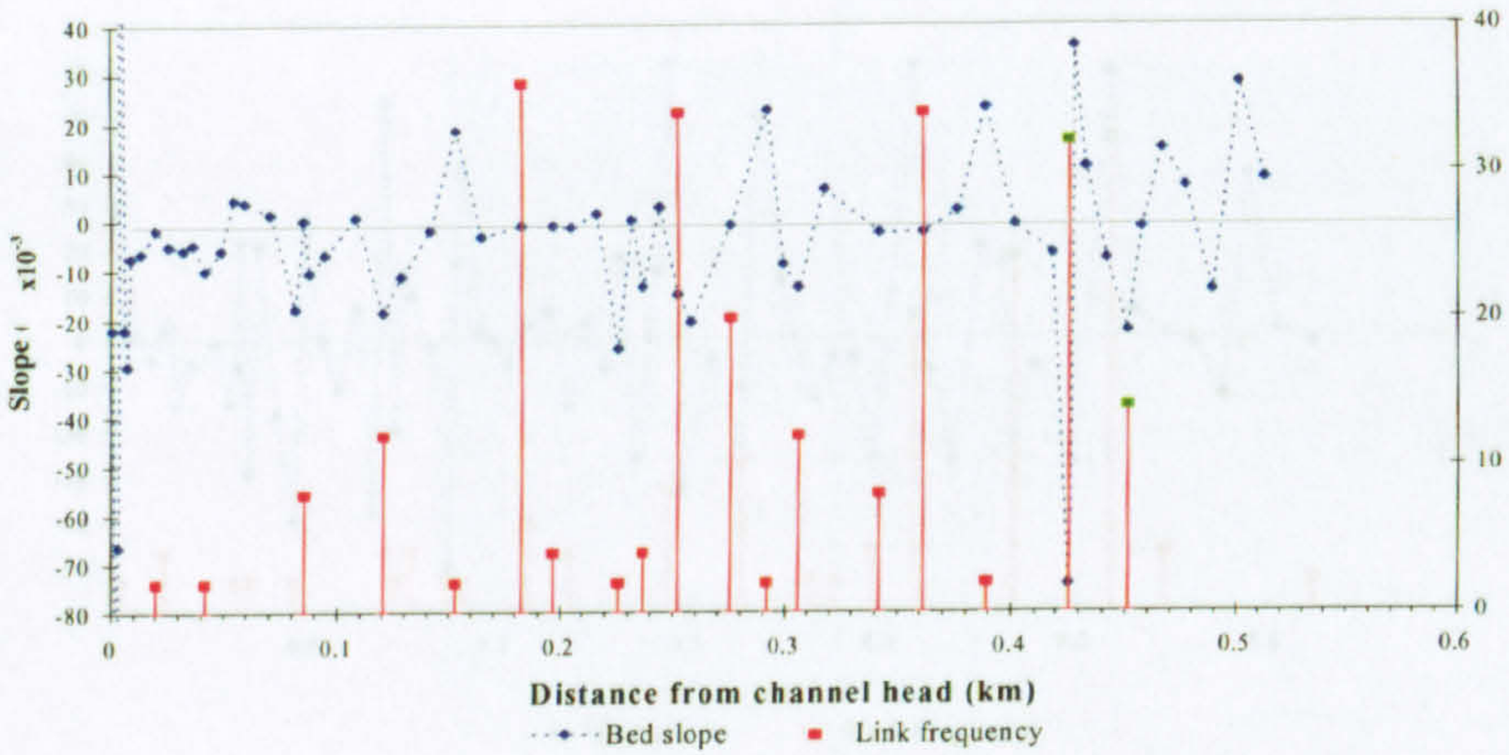

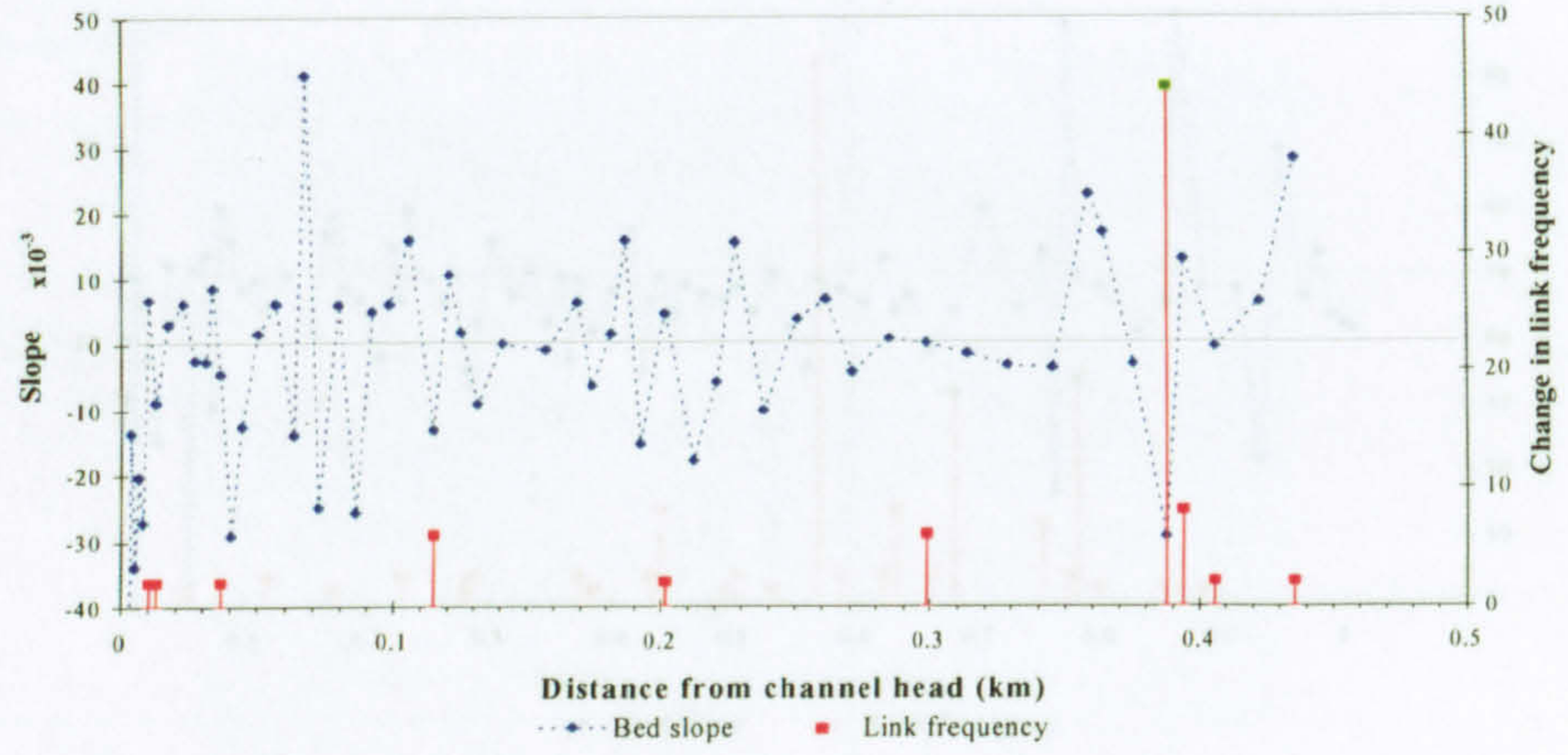

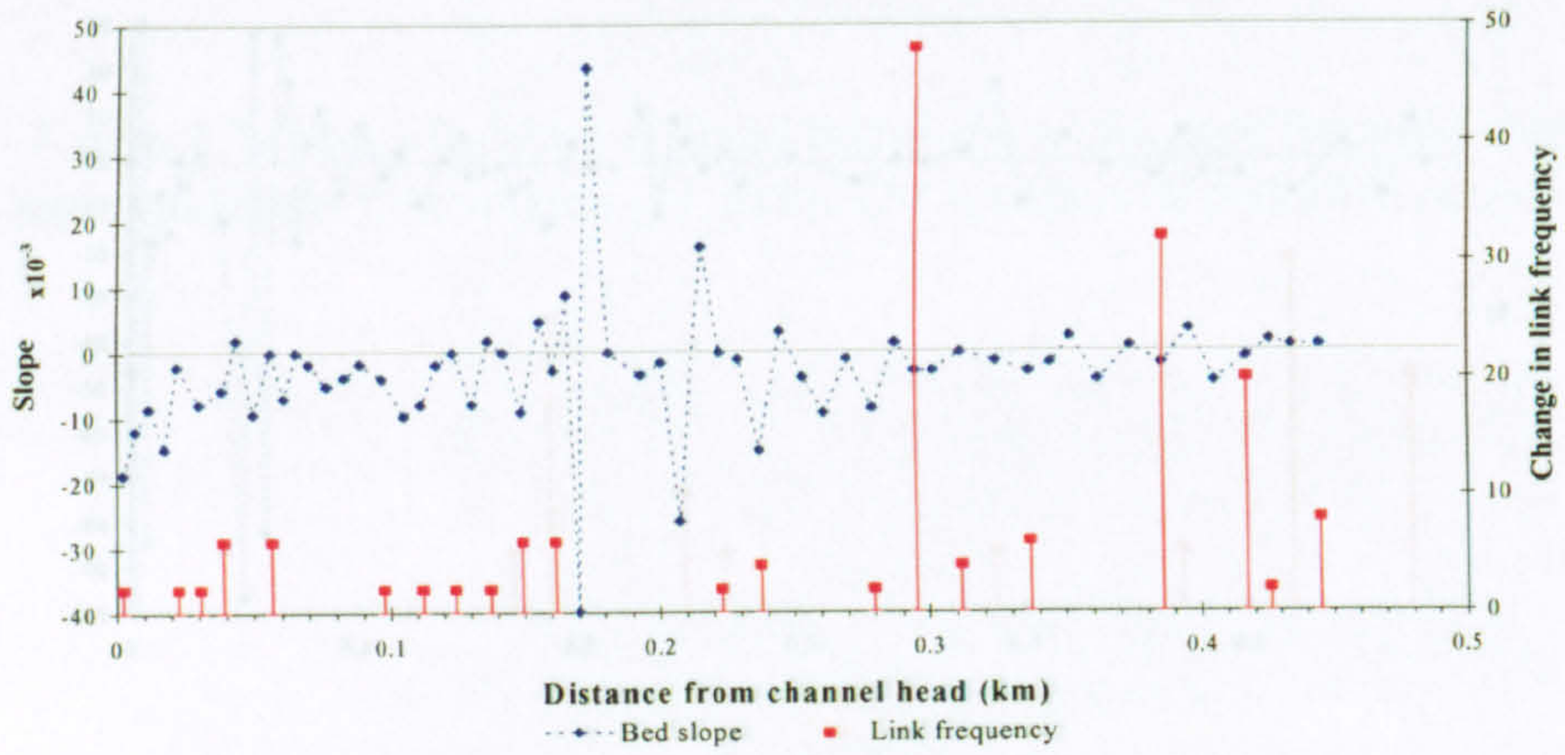

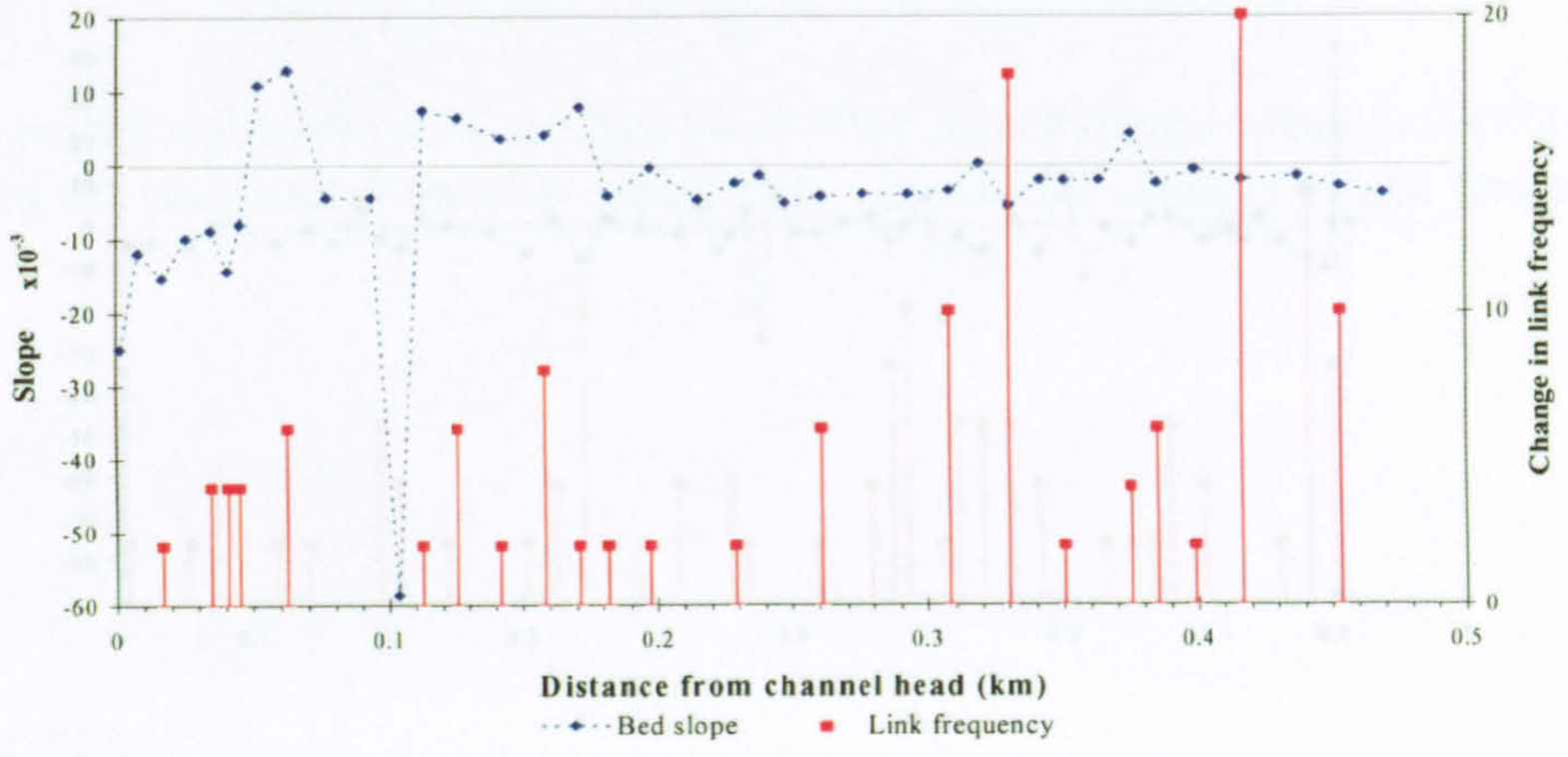

Figure 4.7 (cont.) Relation of local bed slope to distance from the channel head for the subset of profiles exhibiting: minor irregularities (a1-a17); and high amplitude fluctuations (b1-b12). The location of major tributaries along the principal channel is recorded by substantial changes in link frequency.

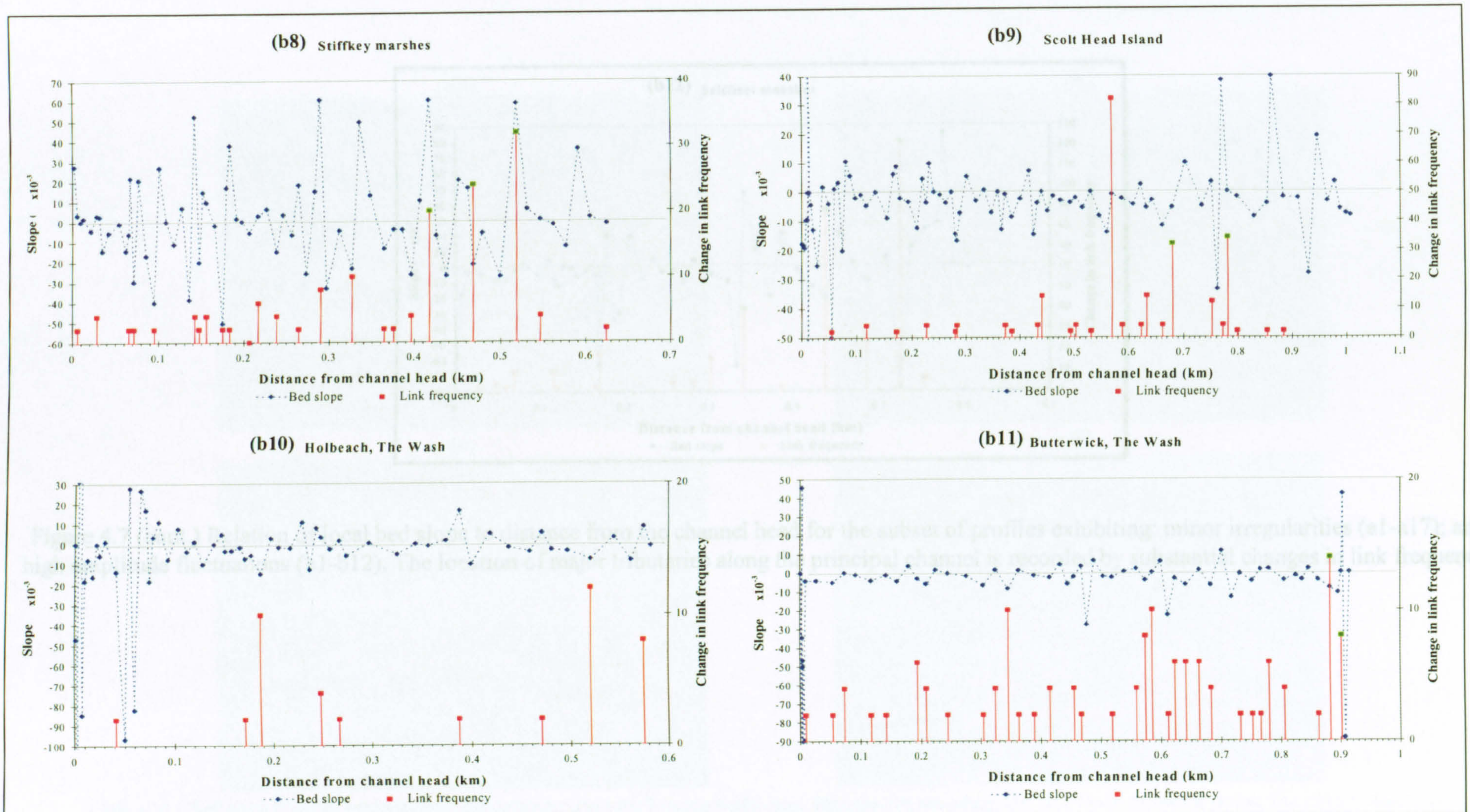

Figure 4.7 (cont.) Relation of local bed slope to distance from the channel head for the subset of profiles exhibiting: minor irregularities (a1-a17); and high amplitude fluctuations (b1-b12). The location of major tributaries along the principal channel is recorded by substantial changes in link frequency.

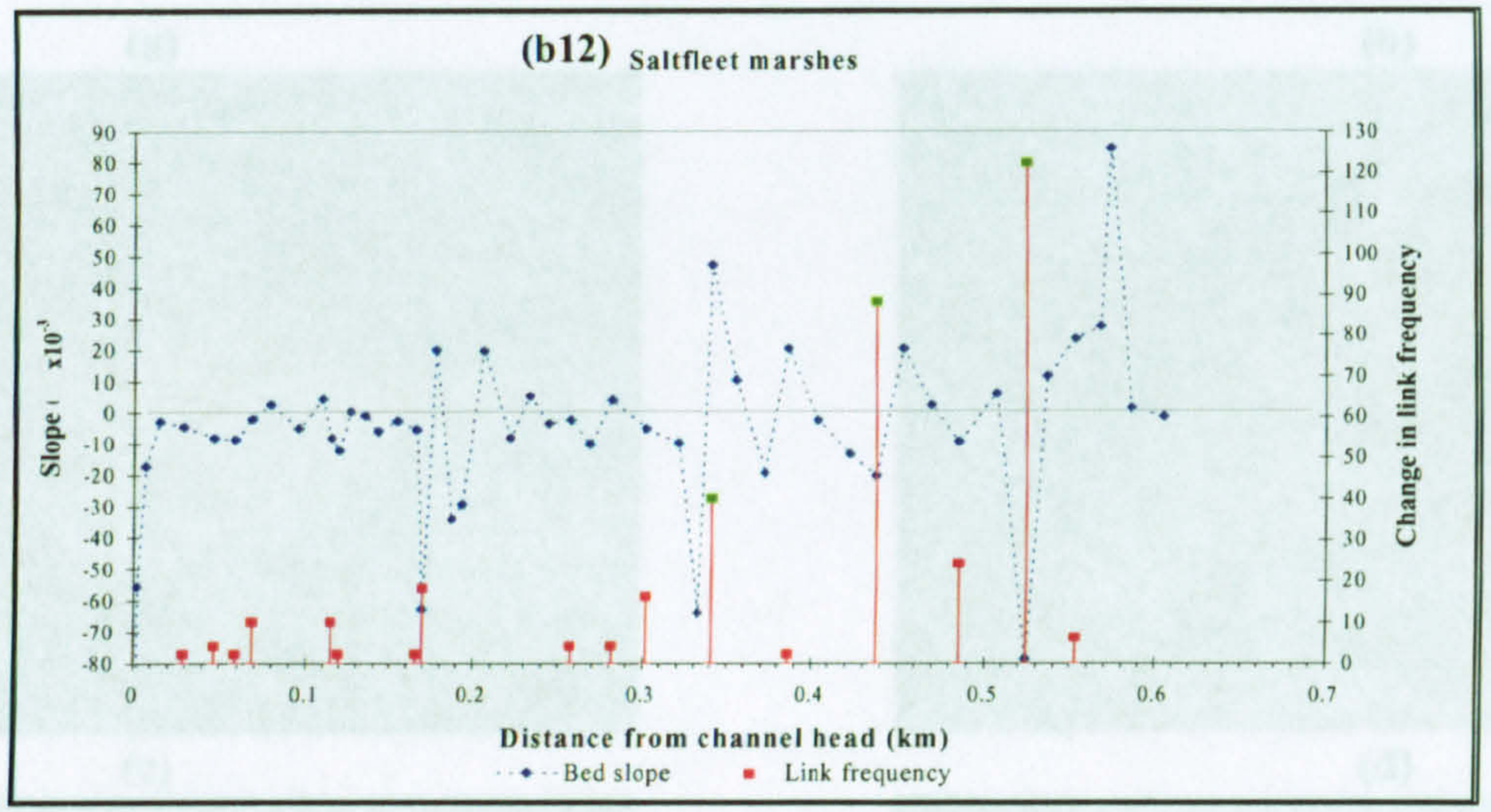

Figure 4.7 (cont.) Relation of local bed slope to distance from the channel head for the subset of profiles exhibiting: minor irregularities (a1-a17); and high amplitude fluctuations (b1-b12). The location of major tributaries along the principal channel is recorded by substantial changes in link frequency.

(a)

(b)

(c)

(d)

Plate 4.4 Discontinuities in longitudinal adjustment: (a) small-scale bedforms, Brancaster marshes; (b) livestock crossing point, Duddon Estuary; (c) thalweg obstruction, Lymington; (d) local obstruction by bank fall debris, River Ribble; (e) through-flowing reaches arising from channel capture, River Orwell; (f) collecting pool caused by migration of a sand bank across the channel mouth, Maplin Sands; (g) shell ridge blocking channel outflow, River Crouch; and (h) channel bed depression around a major junction, River Dovey

(e)

(f)

(g)

(h)

Plate 4.4 cont. Discontinuities in longitudinal adjustment: (a) small-scale bedforms, Brancaster marshes; (b) livestock crossing point, Duddon Estuary; (c) thalweg obstruction, Lymington; (d) local obstruction by bank fall debris, River Ribble; (e) through-flowing reaches arising from channel capture, River Orwell; (f) collecting pool caused by migration of a sand bank across the channel mouth, Maplin Sands; (g) shell ridge blocking channel outflow, River Crouch; and (h) channel bed depression around a major junction, River Dovey.

Although progress has been made in identifying distinctive categories of morphological adjustment, it remains for these classes to be expressed in morphometric terms, which can be more readily implemented in a statistical analysis, than a nominal classificatory scheme.

4.4 MORPHOMETRIC EXPRESSIONS OF LONGITUDINAL ADJUSTMENT

In the same manner that 'optimal' morphometric descriptors (Gardiner, 1978) were employed in the evaluation of planimetric morphology, to complement and build upon the descriptive results, quantitative expressions of longitudinal adjustment promise additional insight into the ways in which profile shapes relate to geographically diverse boundary conditions. Indices may be divided into two groups according to whether they: (1) quantify the pattern of descent in *absolute* terms; or (2) describe the *shape* of the longitudinal profile.

The most basic and commonly applied measure of longitudinal adjustment is channel gradient. Although widely associated with reach-scale adjustment (Rosgen, 1994), a network gradient (G_N) may be computed according to Equation 4.1. Where discontinuities were present in the lower reaches of the profile, an adjusted terminal elevation was employed in the computation of ΣH.

$$G_N = \frac{\sum H}{\sum d} \qquad [4.1]$$

Although G_N provides a useful comparative statistic at a network-wide scale, the computation makes limiting assumptions concerning the pattern of descent. As an average term, the rate of fall is assumed to be constant between the channel head and limit of vegetative cover. However, the analysis in Section 4.3 (see also Pestrong, 1965 and Collins *et al.*, 1987) indicates that this is not always the case. Profiles are typically steeper in the headwaters, and often display a concave pattern of descent in the central and lower reaches. It is therefore appropriate to employ an additional index, which represents curvilinear responses more accurately.

A range of techniques is documented for comparing curved profile forms (Hack, 1957; Strahler, 1964; Shepherd, 1985). Approximating the long profile of a channel network by a single curve is noted by Hack (1957, p.70) to be particularly valuable, since *'it permits comparisons of the profiles or parts of the profiles of two different streams, or their numerical expression by one or two constants'*. Strahler (1964) describes the

statistical regression of channel bed elevation against distance using a selection of simple equations. Linear, polynomial, exponential, logarithmic and power functions have all been used in fluvial networks (see, for example, Hack, 1957; Snow and Slingerland, 1987; Morris and Williams, 1997; Knighton, 1999). However, Shepherd (1985) observes a number of serious problems in the curve-fitting procedure, arising from the undue influence exerted by the datum against which elevation and distance are measured. Strahler (1964) and Snow and Slingerland (1987) propose various solutions. However, preliminary analysis of the present dataset suggests that curve-fitting is of limited value, because: (1) empirical functions proved highly sensitive to the method used in manipulating the basic profile data; (2) no single curve could be identified as an optimal descriptor for all profiles; (3) best-fit responses were unduly influenced by the asymptotic tendency of the upper and lower reaches towards the primary axes; and (4) interpretation of the relative magnitudes of coefficients obtained for profiles fitted by the same curvilinear function was unclear.

An easily interpreted measure proposed by Langbein (1964), instead provides a useful comparative measure of the degree of curvature displayed by the longitudinal profiles. Originally implemented in fluvial systems (see Langbein, 1964; also Leopold *et al.*, 1964), the Index of Concavity (I) records the distribution of vertical fall about the mid-point of either a regular or standardised profile.

$$I = \frac{2\Delta H_{50}}{\sum H} \qquad [4.2]$$

The index is simple to compute and readily translated to tidal networks. As shown in Equation 4.2, and depicted schematically in Figure 4.8a, the measurement is calculated as a ratio between the height difference from the profile at mid-distance to a straight line joining the start and end nodes (ΔH_{50}), and the total vertical fall. For discontinuous profiles (Figure 4.8b), the computation was carried out using the adjusted terminal elevation (Table 4.1).

4.4.1 Network gradient

The morphometric measure of network gradient provides a useful indication of the length of tidal channel required to accommodate differing magnitudes of total elevation change. Values of G_N define a fairly wide envelope of responses, ranging across an order of magnitude (Table 4.3) from a maximum of 10.8 $x10^{-3}$ in the River Beaulieu, to a

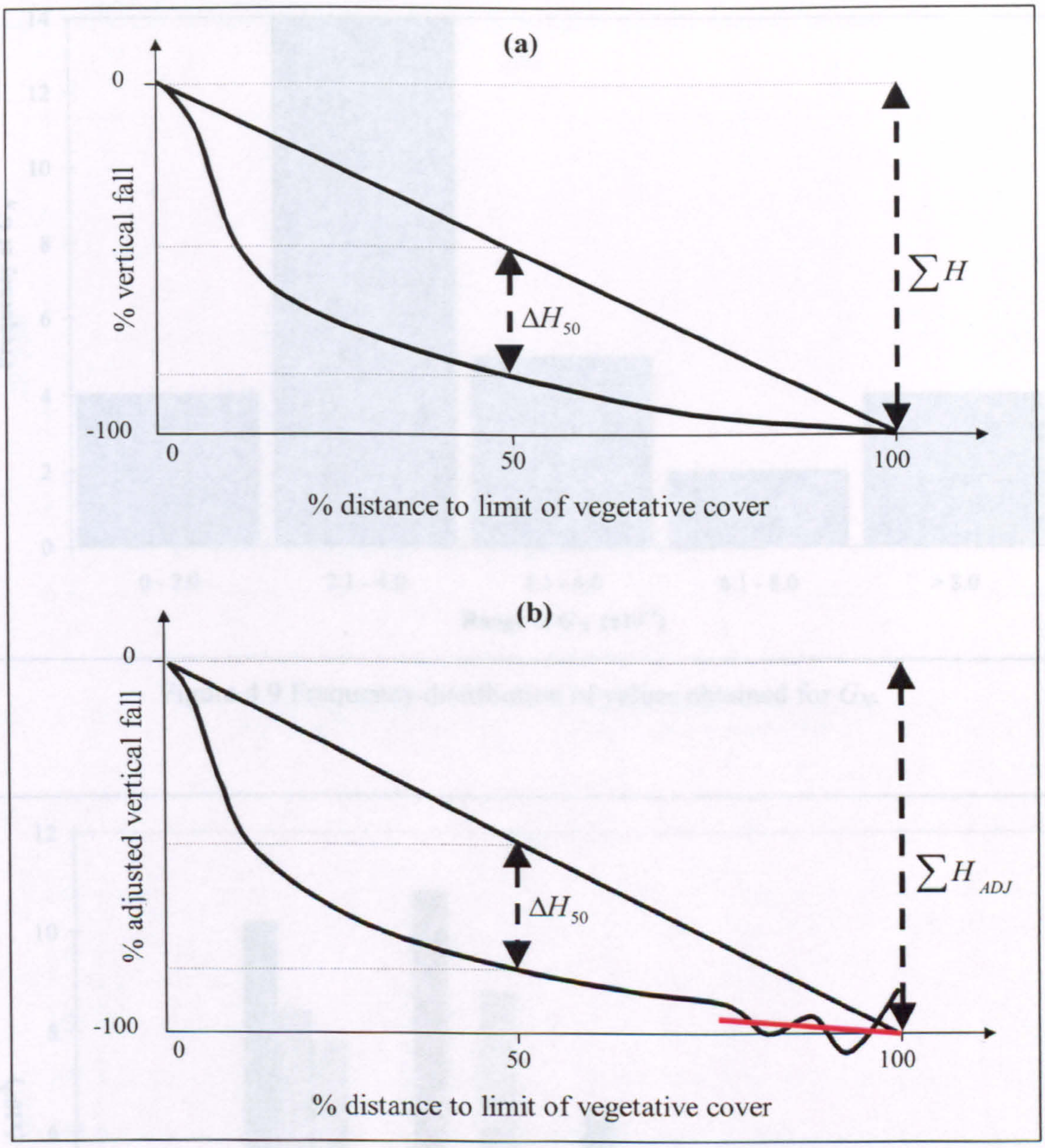

Figure 4.8 Definition sketch for computing the Index of Concavity for: (a) continuous and (b) discontinuous sample profiles.

minimum of 0.8 x10^{-3} in the Duddon Estuary. The frequency distribution recorded in Figure 4.9 exhibits a positive departure from normal behaviour, commensurate with a cluster of responses in the range of $2.1 < G_N < 4.0$ x10^{-3}. A statistically significant level of skewness (skew = 1.2) is evident (Figure 4.9), although this is effectively removed by performing a logarithmic transformation.

By comparing Figure 4.10 with Figure 4.11a, the distribution and range of G_N is in line with values computed from data that has been published by Pestrong (1965) and French and Stoddart (1992). Readings are also of a comparable magnitude to fluvial

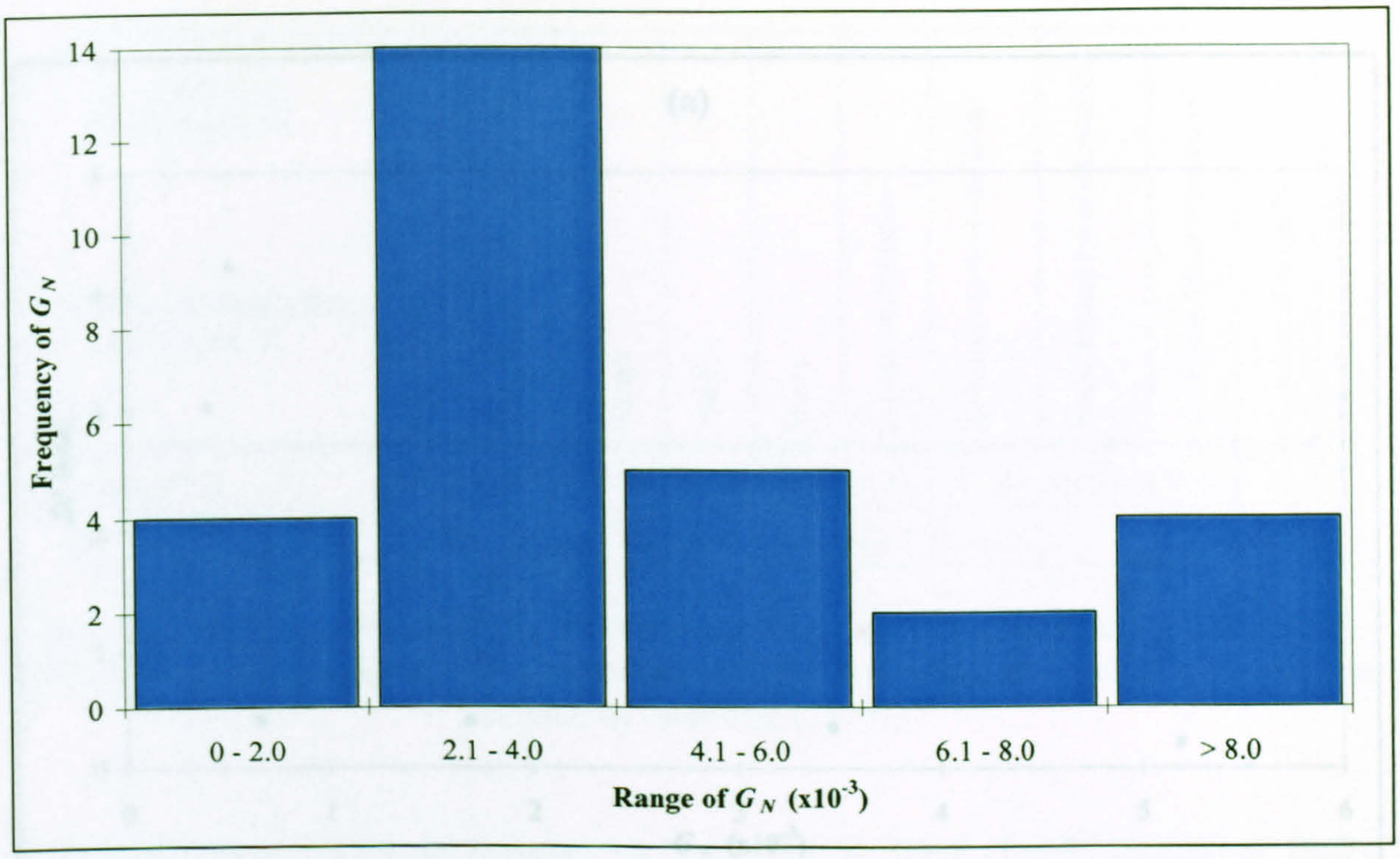

Figure 4.9 Frequency distribution of values obtained for G_N.

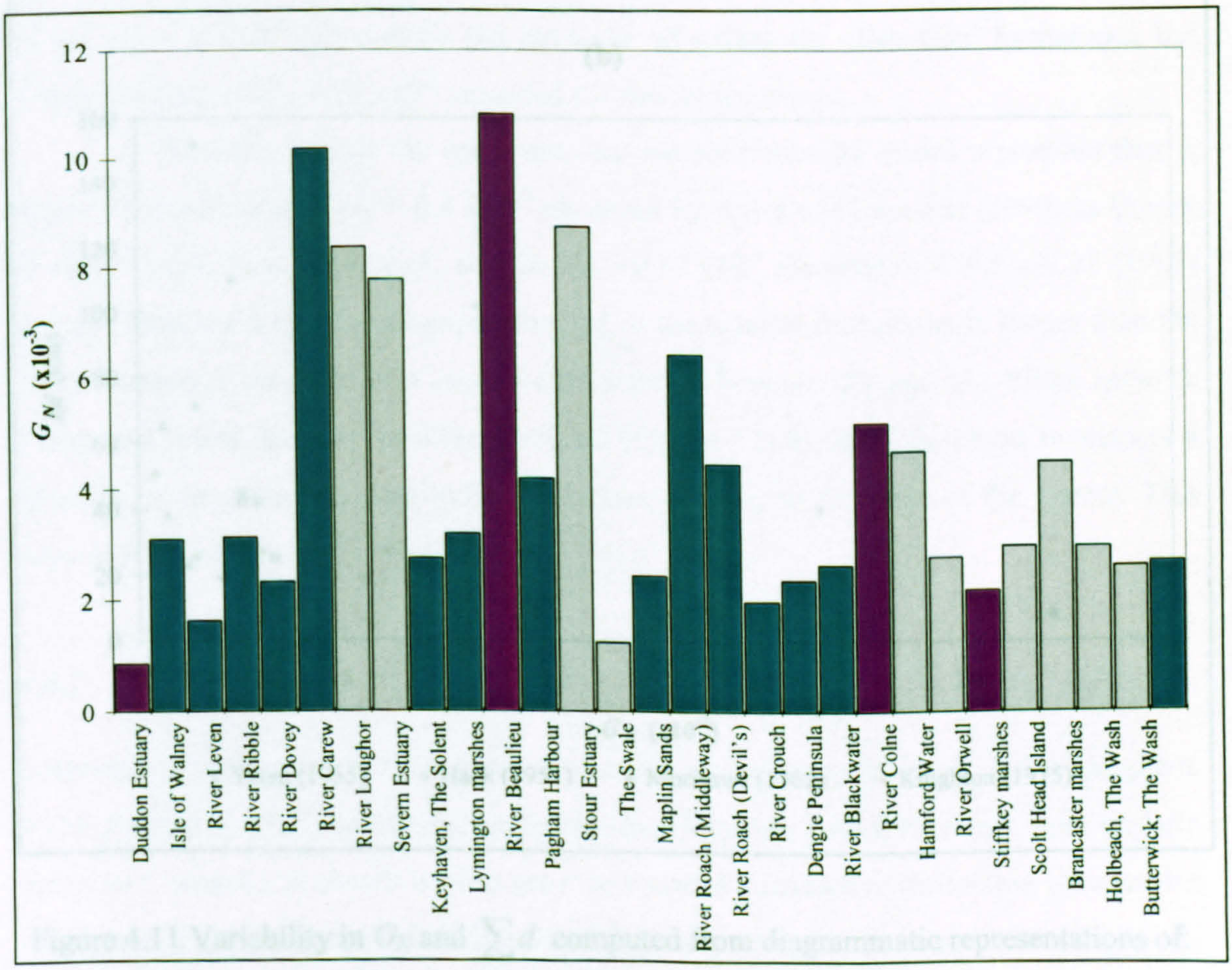

Figure 4.10 Geographic variability in G_N, computed for: ■ = linear / semi-linear; ■ = upwardly concave; and ■ = semi-concave profile shapes.

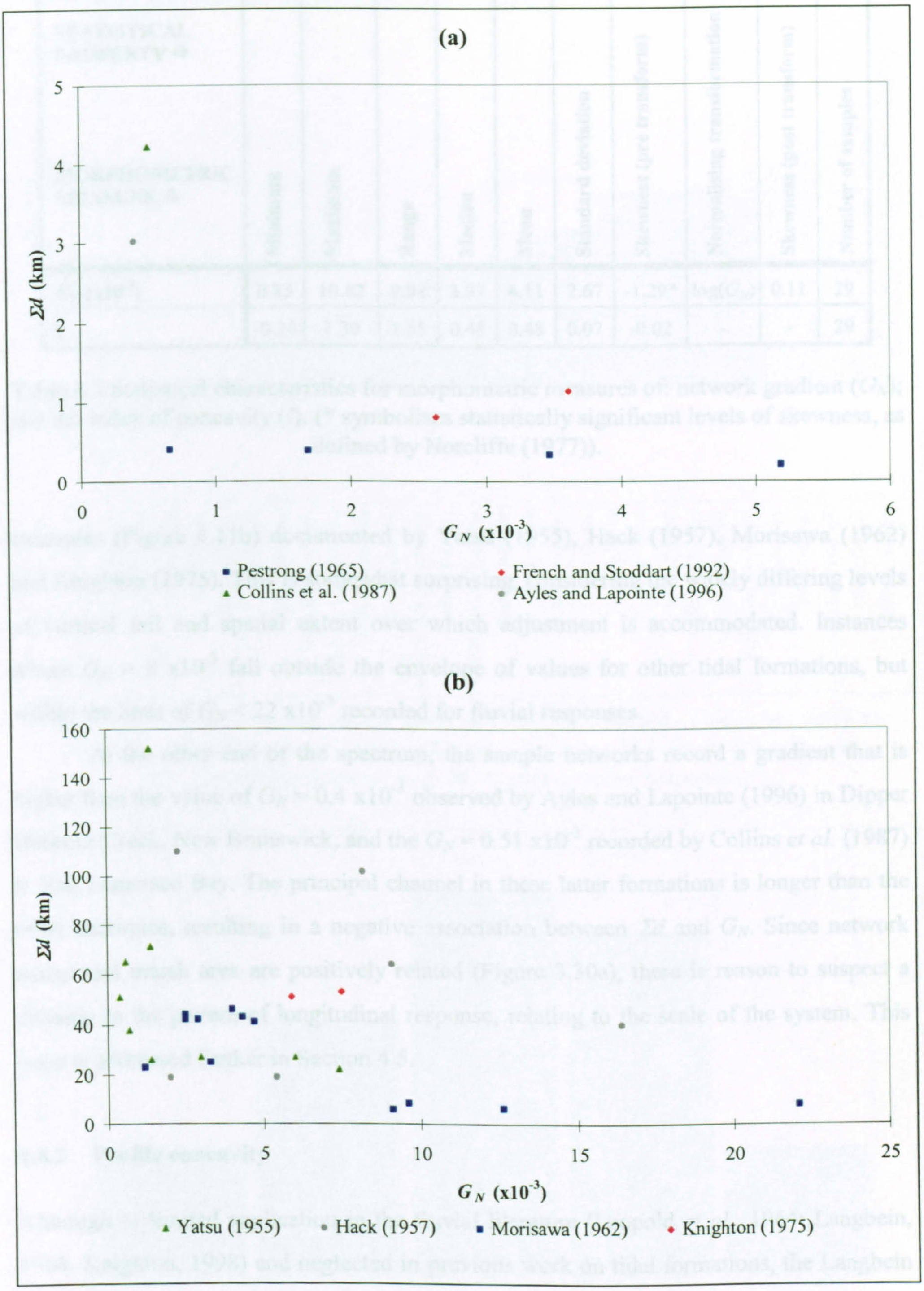

Figure 4.11 Variability in G_N and $\sum d$ computed from diagrammatic representations of: (a) tidal; and (b) fluvial longitudinal profiles documented in the literature (names of individual networks are recorded in an abbreviated form).

STATISTICAL PROPERTY ⇨ / MORPHOMETRIC MEASURE ⇩	Minimum	Maximum	Range	Median	Mean	Standard deviation	Skewness (pre transform)	Normalising transformation	Skewness (post transform)	Number of samples
G_N (x10^{-3})	0.85	10.82	9.98	2.97	4.11	2.67	-1.29*	log(G_N)	0.11	29
I	-0.24	1.30	1.55	0.48	0.48	0.07	-0.02	-	-	29

Table 4.3 Statistical characteristics for morphometric measures of: network gradient (G_N); and the Index of concavity (I). (* symbolises statistically significant levels of skewness, as defined by Norcliffe (1977)).

examples (Figure 4.11b) documented by Yatsu (1955), Hack (1957), Morisawa (1962) and Knighton (1975). This is somewhat surprising, considering the widely differing levels of vertical fall and spatial extent over which adjustment is accommodated. Instances where $G_N > 8$ x10^{-3} fall outside the envelope of values for other tidal formations, but within the limit of $G_N < 22$ x10^{-3} recorded for fluvial responses.

At the other end of the spectrum, the sample networks record a gradient that is higher than the value of $G_N = 0.4$ x10^{-3} observed by Ayles and Lapointe (1996) in Dipper Harbour Creek, New Brunswick, and the $G_N = 0.51$ x10^{-3} recorded by Collins *et al.* (1987) in San Francisco Bay. The principal channel in these latter formations is longer than the other examples, resulting in a negative association between Σd and G_N. Since network extent and marsh area are positively related (Figure 3.30a), there is reason to suspect a division in the pattern of longitudinal response, relating to the scale of the system. This issue is addressed further in Section 4.5.

4.4.2 Profile concavity

Although of limited application in the fluvial literature (Leopold *et al.*, 1964; Langbein, 1964; Knighton, 1998) and neglected in previous work on tidal formations, the Langbein Index of Concavity is shown here to provide a useful quantitative distinction between the basic profile shapes identified during the exploratory analysis. Arranged according to the generic classes in Figure 4.12, the boundary between formations exhibiting linear and upwardly concave patterns of descent is demarcated by a value of $I = 0.3$.

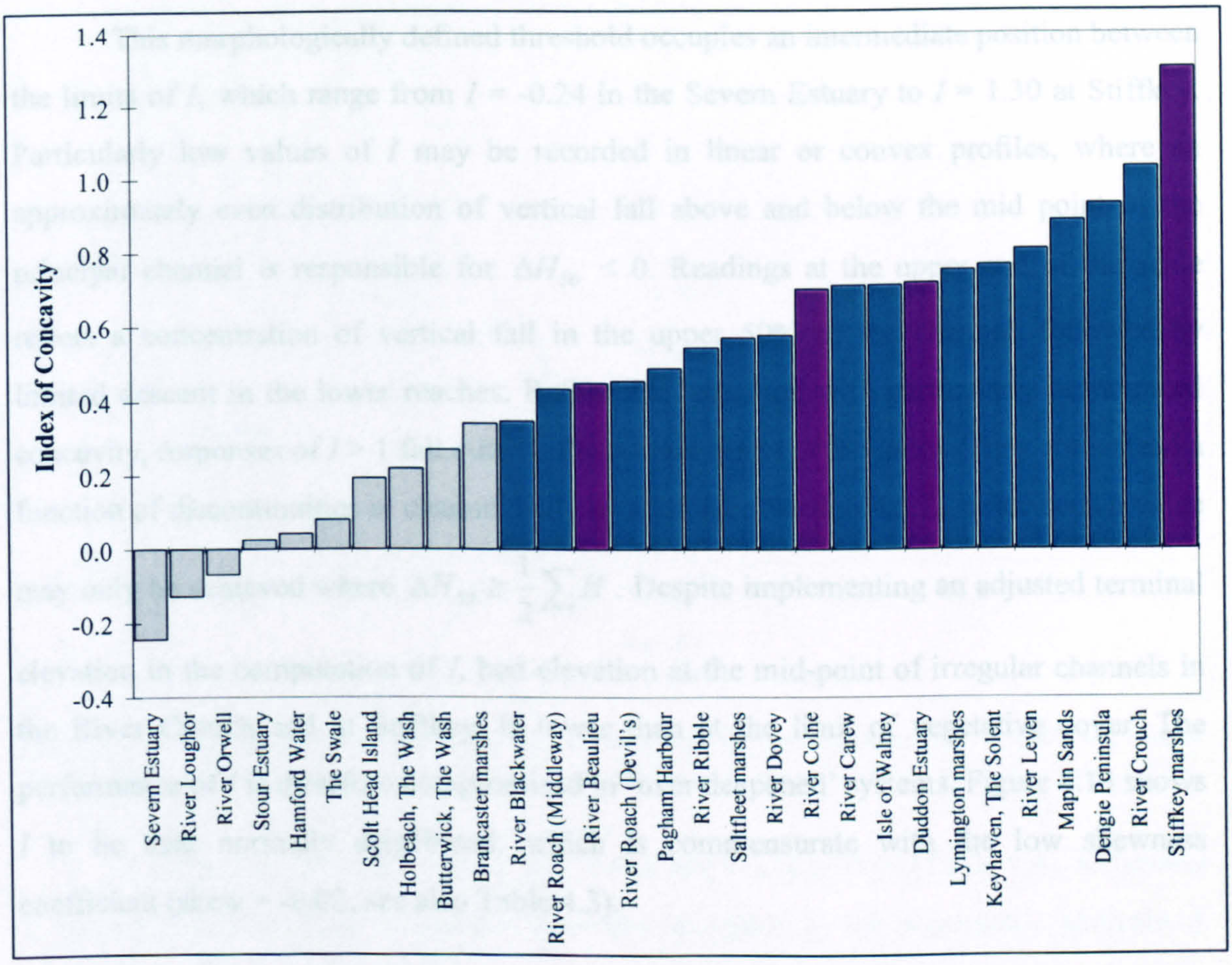

Figure 4.12 Values obtained for the Index of Concavity, ranked in ascending order to reflect the relation between *I* and profile shapes, where ■ = linear / semi-linear; ■ = upwardly concave; and ■ = semi-concave responses.

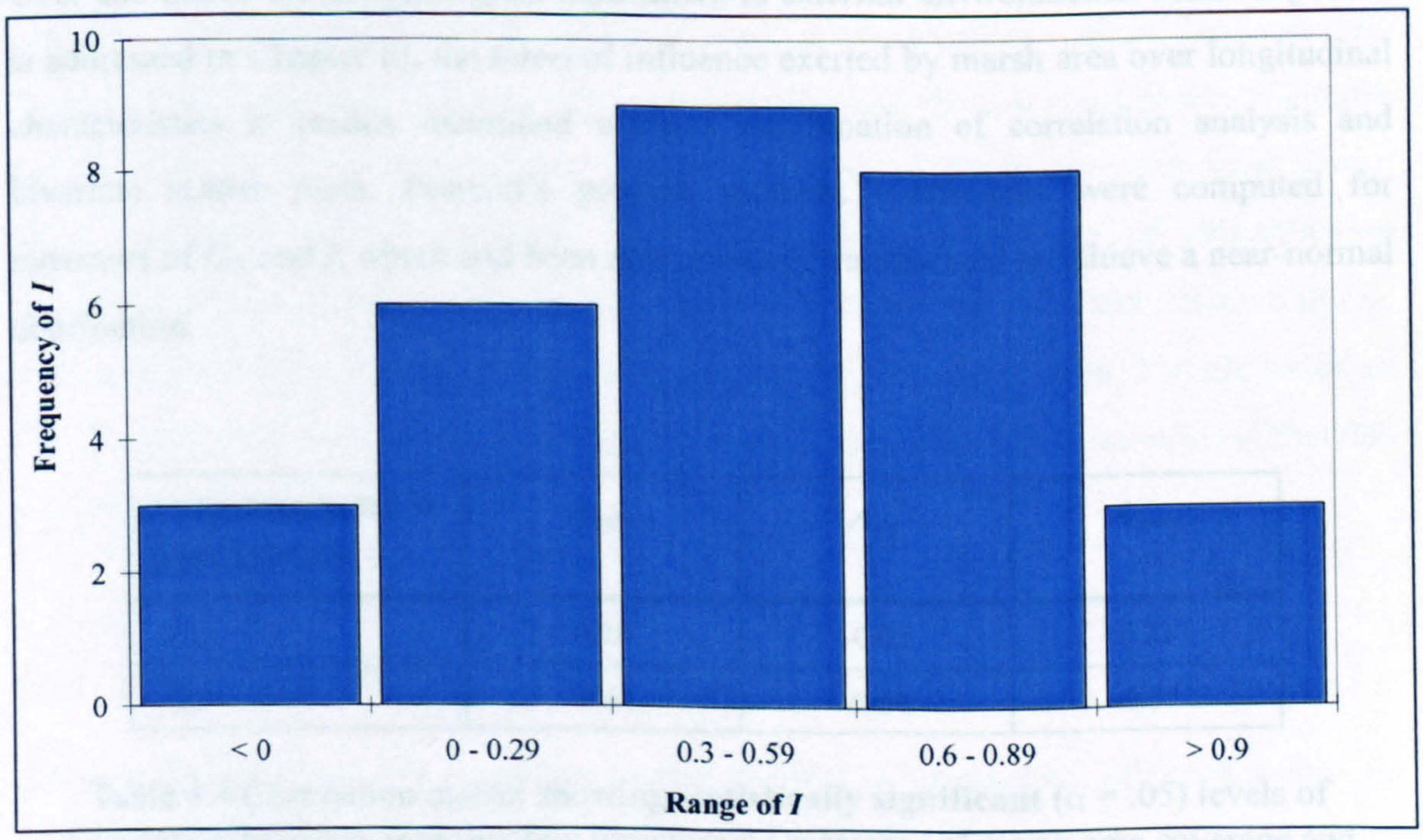

Figure 4.13 Frequency distribution of the Index of Concavity (*I*).

This morphologically defined threshold occupies an intermediate position between the limits of I, which range from I = -0.24 in the Severn Estuary to I = 1.30 at Stiffkey. Particularly low values of I may be recorded in linear or convex profiles, where an approximately even distribution of vertical fall above and below the mid point of the principal channel is responsible for $\Delta H_{50} < 0$. Readings at the upper end of the scale reflect a concentration of vertical fall in the upper 50% of the channel, followed by limited descent in the lower reaches. Rather than equating with particularly pronounced concavity, responses of $I > 1$ fall outside the normal limits of the index. They are instead a function of discontinuities in channel bed elevation (see Section 4.3.2), since such a value may only be achieved where $\Delta H_{50} \geq \frac{1}{2}\sum H$. Despite implementing an adjusted terminal elevation in the computation of I, bed elevation at the mid-point of irregular channels in the River Crouch and at Stiffkey, is lower than at the limit of vegetative cover. The performance of I is therefore compromised in 'over deepened' systems. Figure 4.13 shows I to be near normally distributed, which is commensurate with the low skewness coefficient (skew = -0.02; see also Table 4.3).

4.5 SCALE DEPENDENCE

Over and above the morphological adjustment to *external* environmental controls (which is addressed in Chapter 6), the *internal* influence exerted by marsh area over longitudinal characteristics is readily examined using a combination of correlation analysis and bivariate scatter plots. Pearson's product moment coefficients were computed for measures of G_N and I, which had been appropriately transformed to achieve a near-normal distribution.

AREA MEASURE ⇨ DESCRIPTOR ⇩	A_{min}	A_{eq}	A_{max}
I	0.28	-0.02	0.23
G_N	**-0.61**	**-0.59**	**-0.57**

Table 4.4 Correlation matrix showing **statistically significant** (α = .05) levels of association between appropriately transformed measures of marsh area coverage and morphometric descriptors.

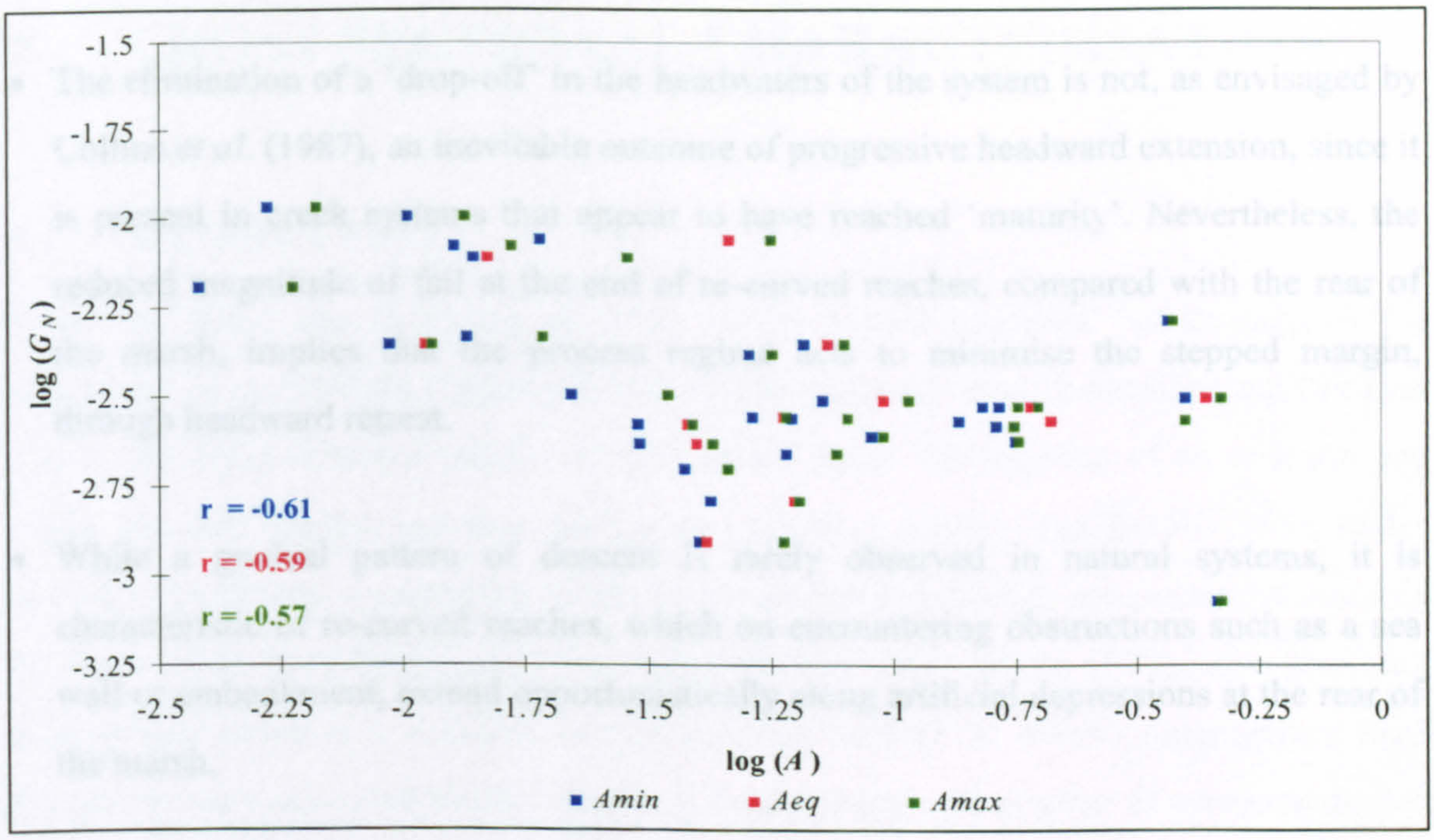

Figure 4.14 Scatter plot showing the statistically significant association between G_N and A (computed using minimum, equidistant and maximum decision rules from Section 3.2.5).

A strong negative association between A and G_N is evident (Table 4.4). Returning to the three-way division of sample networks identified in the planimetric analysis of creek density (Section 3.5), Figure 4.14 suggests that the highest network gradients correspond with 'small' formations in Wales and along the south coast. Since the lateral extent of marsh development and associated length of channel is limited at these localities, vertical adjustment is achieved over a comparatively short distance. The 'intermediate' and 'large' systems of Morecambe Bay and the east coast generally exhibit lower values of G_N. In this instance, a similar amount of fall is accommodated over a more extensive tract of saltmarsh. The corresponding coefficient of determination suggests that scale dependence accounts for up to 37% of the statistical variance in G_N, with a residual 63% of the variance attributable to alternative factors. For the Index of Concavity, the coefficients are consistently non-significant, the implication being that this measure is essentially scale-free.

4.6 SUMMARY OF KEY FINDINGS

The key findings from the preceding characterisation of longitudinal adjustment may be summarised as follows:

- Descriptive characterisation indicates that longitudinal profiles fall into two basic categories, exhibiting linear and upwardly concave patterns of descent.

- The elimination of a 'drop-off' in the headwaters of the system is not, as envisaged by Collins *et al.* (1987), an inevitable outcome of progressive headward extension, since it is present in creek systems that appear to have reached 'maturity'. Nevertheless, the reduced magnitude of fall at the end of re-curved reaches, compared with the rear of the marsh, implies that the process regime acts to minimise the stepped margin, through headward retreat.

- While a gradual pattern of descent is rarely observed in natural systems, it is characteristic of re-curved reaches, which on encountering obstructions such as a sea wall or embankment, extend opportunistically along artificial depressions at the rear of the marsh.

- Measures of network gradient and profile concavity are useful quantitative expressions for the shape and rate of longitudinal descent across the intertidal zone. G_N exhibits a strong element of scale dependence, which arises because the range of vertical fall within the sample networks exhibits less variation than the distance over which it occurs.

5. CROSS-SECTIONAL CHARACTERISATION

5.1 INTRODUCTION

From the initial channelisation of flows across a bare intertidal flat through to the attainment of equilibrium adjustment in the latter stages of network development (Section 1.4.4), the cross-sectional profile of tidal creeks bears the imprints of an evolutionary battle between locally operative motive and resistive forces (Van Eerdt, 1985), under boundary conditions imposed by a suite of geographically diverse environmental controls (Section 1.1.1). In addition to a strong aspect of inheritance (Allen, 1997), cross-sectional morphology provides a valuable insight into the manner in which contemporary tidal fluxes are accommodated within saltmarsh creek systems. A number of previous studies address reach-scale cross-sectional characteristics (Pestrong, 1965, 1970, 1972), where a range of qualitative expressions (Collins *et al.*, 1987; Wells *et al.*, 1990; Leopold *et al.*, 1993; Coates *et al.* 1995; Zeff, 1999) and a number of quantitative terms (Johnson, 1973; Wright *et al.*, 1973; Bridges and Leeder, 1976; Zeff, 1988; Hume, 1991; Allen, 1997) have been employed to describe the boundary shape and capacity of tidal channels. Although providing a useful framework for establishing patterns of morphological adjustment, the application of descriptive terminology and morphometric descriptors at a spatially *extensive* scale is limited. Observations by Collins *et al.* (1987) and Coates *et al.* (1995) suggest the presence of network-wide variability in cross-sectional adjustment. However, the comparative analysis has yet to be extended to consider inter-site variations (Chapman, 1974; Steers, 1977) and the broader conditions that underpin them.

The following analysis characterises cross-sectional behaviour and defines the range of spatial variability in adjustment displayed by British saltmarsh channel networks. Following details of the methods of data acquisition in Section 5.2, an initial descriptive evaluation is undertaken (Section 5.3). Section 5.4 considers the performance of various morphometric descriptors as means of quantifying network-wide trends in cross-sectional form. As before, the issue of scale dependence is also addressed (Section 5.5), and key findings are summarised in Section 5.6.

5.2 DATA ACQUISITION

Channel width and depth are widely regarded as the basic dimensional parameters quantifying cross-sectional *size* (see, for example, Hume, 1991; Knighton *et al.*, 1992;

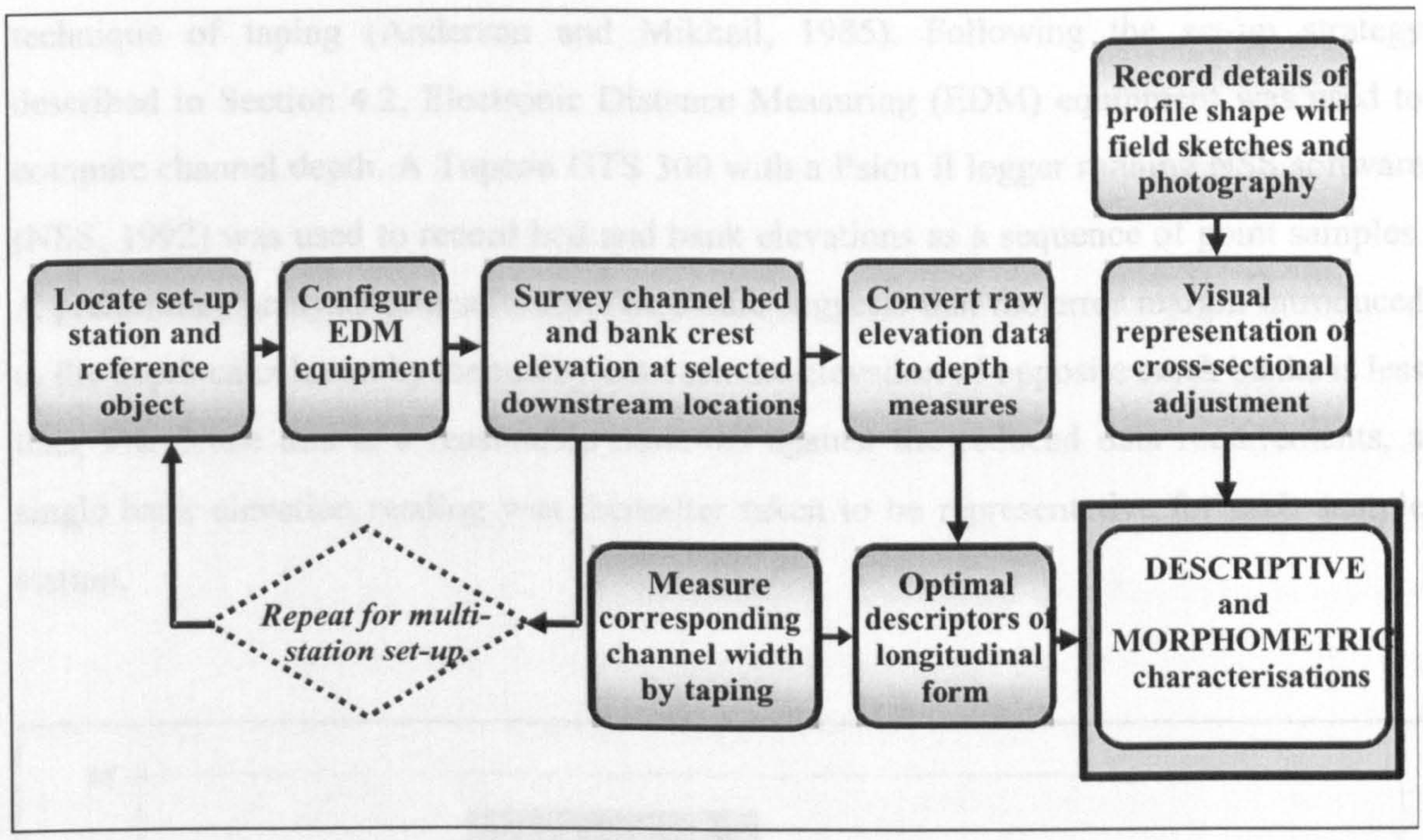

Figure 5.1 Schematic representation of the methodological procedure used to acquire data for the descriptive and morphometric characterisation of cross-sectional adjustment.

Coates *et al.*, 1995). In the present analysis, bankfull width is defined as the distance between the upper creek margins at a particular cross-section, and is comparable with bankfull capacity in an estuarine (Myrick and Leopold, 1963) or fluvial system (Knighton, 1998). As such, this measure represents the degree of lateral adjustment required to accommodate formative flow events. In line with the characterisation of U.S. tidal network morphology by Haltiner and Williams (1987), vertical adjustment is recorded as the maximum depth between the elevation of the channel bank and bed. To avoid undue influence from adjacent levee features (Ragotzkie, 1959; Steers, 1959; Marshall, 1962; Letzsch and Frey, 1980a, 1980b; Hartnall, 1984; Collins *et al.*, 1987; Zeff, 1988; Esselink *et al.*, 1998), bank elevation was taken at the crest of the upper creek margin. In some localities, a relic step feature was present above the active facet. In these cases, readings for channel width and depth were recorded at both the upper and incised margin. Following the procedure employed in longitudinal characterisation, bed elevation corresponds with the lowest point of the channel floor.

With the sole exception of Landimore Marsh bordering Burry Inlet (which proved inaccessible during the period of data acquisition from June-July 1999), cross-sectional characterisation was carried out along the principal channel (as defined in Section 3.2.4) of each formation. As summarised in Figure 5.1, channel width was surveyed using the

technique of taping (Anderson and Mikhail, 1985). Following the set-up strategy described in Section 4.2, Electronic Distance Measuring (EDM) equipment was used to compute channel depth. A Topcon GTS 300 with a Psion II logger running NSS software (NSS, 1992) was used to record bed and bank elevations as a sequence of point samples. A preliminary analysis of results for The Swale suggests that the error margin introduced to the depth calculation by inequality between the elevation of opposite creek banks is less than 5%. Since this is a reasonable trade-off against the reduced data requirements, a single bank elevation reading was thereafter taken to be representative for each sample station.

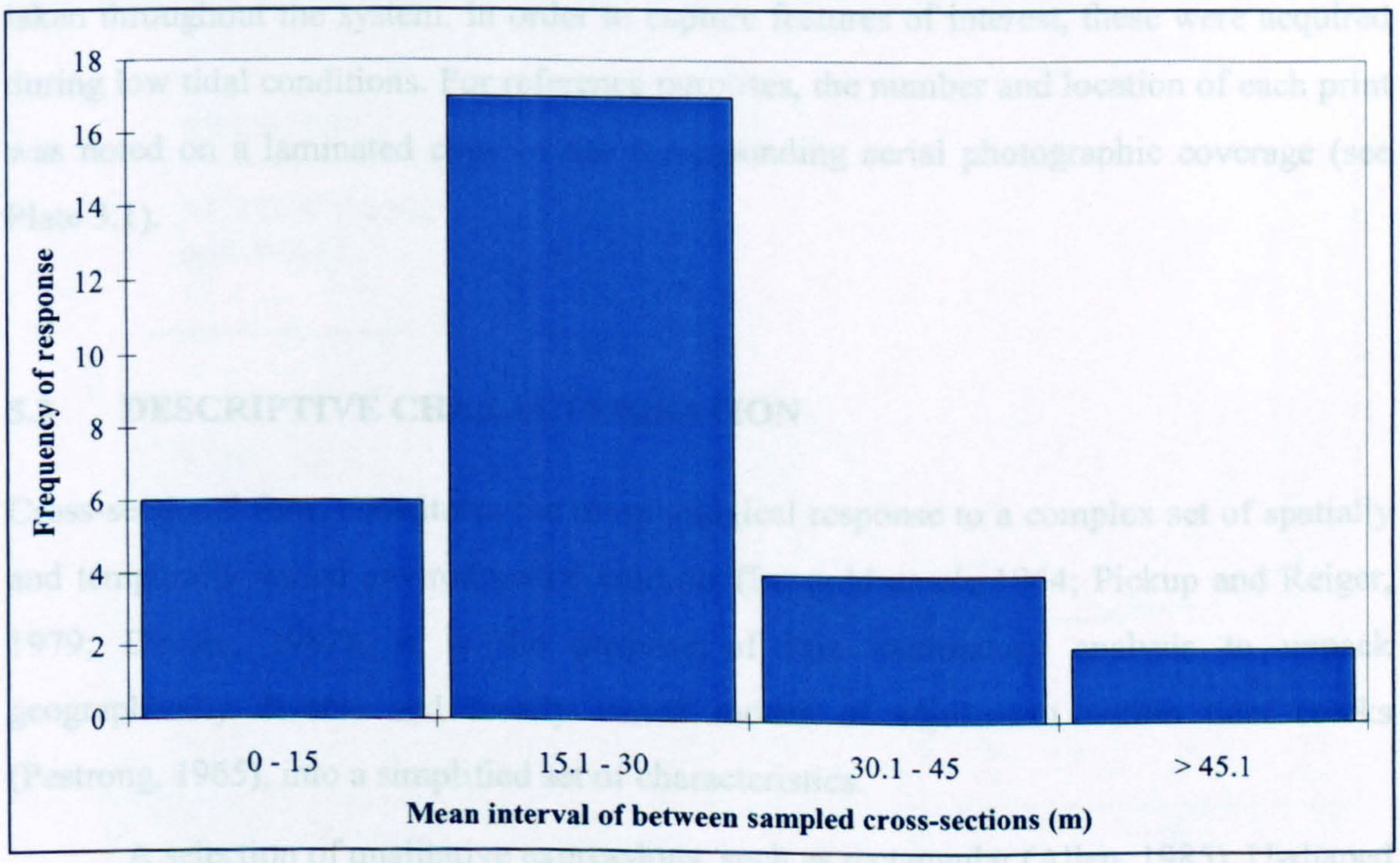

Figure 5.2 Frequency histogram showing the mean sampling interval between cross-sections at each study locality.

From an initial section in the channelised headwaters, cross-sectional form was surveyed at a series of sections up to the limit of saltmarsh development (see, for example, Pestrong, 1965, 1970, 1972), which was taken to correspond with boundary of vegetative cover. Progressing along the course of the network, readings were obtained between major junctions, around pronounced changes in form, and at abrupt deviations in channel orientation. The position of each section was measured relative to the channel head, according to the sinuous distances defined during the longitudinal characterisation. From Figure 5.2, the sampling frequency at 80% of the study localities falls within the

range of 0-30m. This result compares favourably with studies by Collins *et al.* (1987) and Knighton *et al.* (1992). Owing to equipment failure at the River Colne, problems of accessibility at the River Orwell and a general absence of tributary reaches along The Swale, sparser surveys were conducted.

Visual records are consistently employed throughout the literature to provide a detailed representation of cross-sectional *shape* (Pestrong, 1965, 1970, 1972; Myrick and Leopold, 1963; and Collins *et al.*, 1987). In accordance with the exploratory nature of the present study, characterisation was undertaken using field-sketches and photographic records, rather than through the lengthy mapping procedure that has been employed elsewhere (see Gregory, 1977). Sketches were made at each station, and photographs were taken throughout the system. In order to capture features of interest, these were acquired during low tidal conditions. For reference purposes, the number and location of each print was noted on a laminated copy of the corresponding aerial photographic coverage (see Plate 3.1).

5.3 DESCRIPTIVE CHARACTERISATION

Cross-sectional form constitutes the morphological response to a complex set of spatially and temporally varied environmental controls (Leopold *et al.*, 1964; Pickup and Reiger, 1979; Davies, 1987). It is the purpose of this exploratory analysis to unpack geographically diverse and locally varied modes of adjustment within tidal creeks (Pestrong, 1965), into a simplified set of characteristics.

A selection of qualitative expressions, such as rectangular (Allen, 1985), U-shaped (Wells *et al.*, 1990), parabolic (Coates *et al.*, 1995), trapezoidal (Leopold and Maddock, 1953); triangular (Collins *et al.*, 1987; Leopold *et al.*, 1993) and v-shaped (Coates *et al.*, 1995; Zeff, 1999), have been used to distinguish between the different modes adjustment. Although valuable as a means of summarising general characteristics, Coates *et al.* (1995) point out that cross-sectional form is in fact more complex, since tidal channels comprise a number of morphologically distinct segments or facets. Viewing each cross-section as a function of these constituent elements provides an improved understanding of the factors controlling adjustment, together with a more rigorous and versatile classificatory scheme than would be supported by all encompassing, descriptive terminology.

5.3.1 Cross-sectional facets

As a framework for establishing systematic regularities and differences between boundary shapes, the cross-sections of saltmarsh creeks can usefully be separated into a number of basic segments that may be present individually or in combination. In a study of U.S. tidal networks, Coates *et al.* (1995) distinguish between: (1) the channel *wall*; and (2) the channel *toe*. As illustrated in Figure 5.3, results from the present analysis reveal the widespread occurrence of an additional (3) *floor* facet, together with the occasional presence of (4) a *relic step* above the active channel bank.

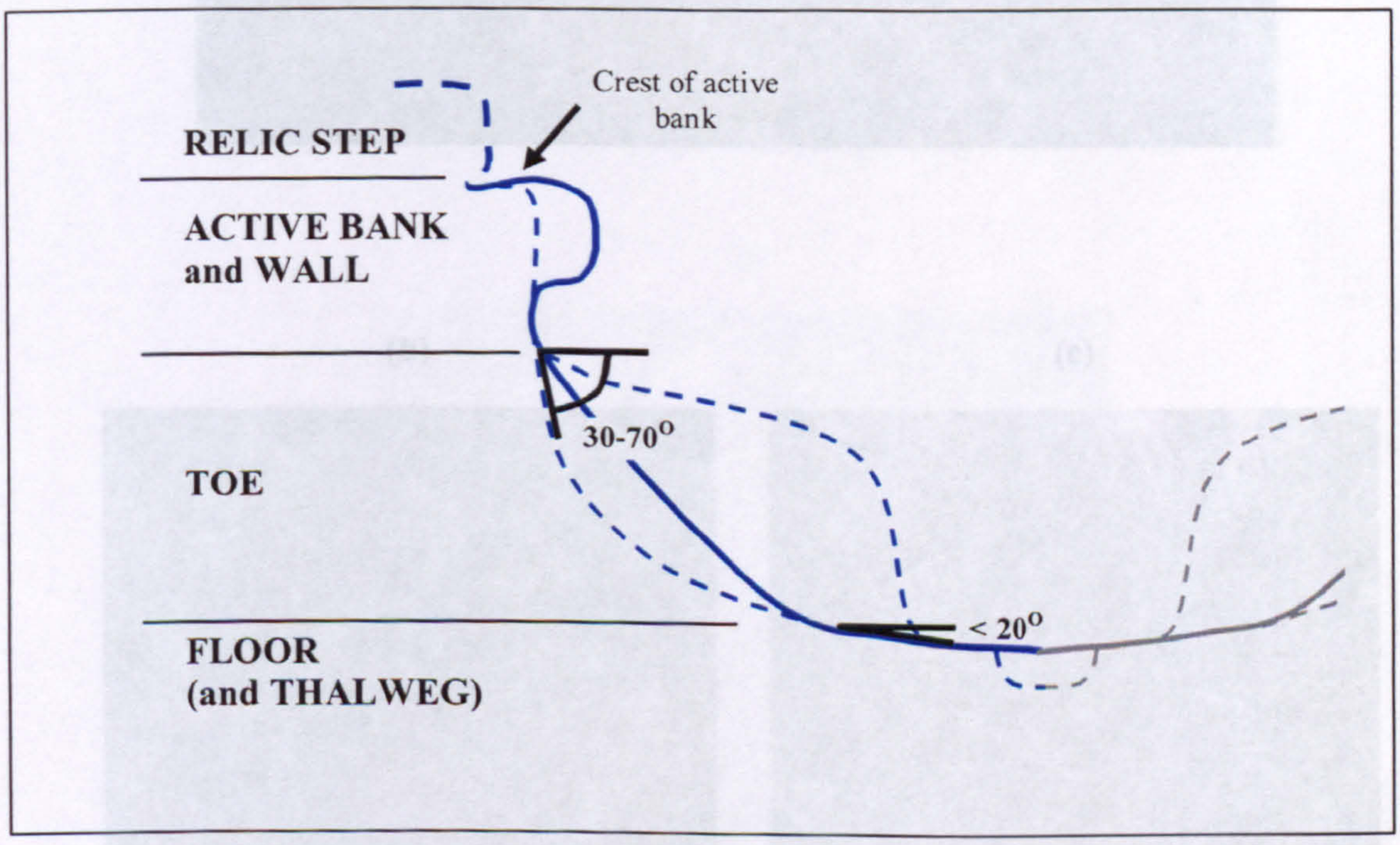

Figure 5.3 Definition diagram showing the cross-sectional facets that may be present in tidal creeks. (-------) represents the envelope of variability observed for each component.

The bank and wall together comprise the active upper limit of cross-sectional profiles. The banks of a tidal creek extend from the channel margin towards the marsh interior. The envelope of variability surrounding the mean response (Figure 5.3), indicates that the banks may be subtly convex or concave (see also Steers, 1959) and, as observed in Section 5.2, usually occur at a similar elevation. Creek banks are generally colonised by halophytic species, the range of which (Pestrong, 1965) is conditioned by tidal hydrodynamics and edaphic controls (Ranwell, 1972; Burd, 1989). However, vegetative cover may be virtually absent (Plate 5.1a) at sites experiencing die-back

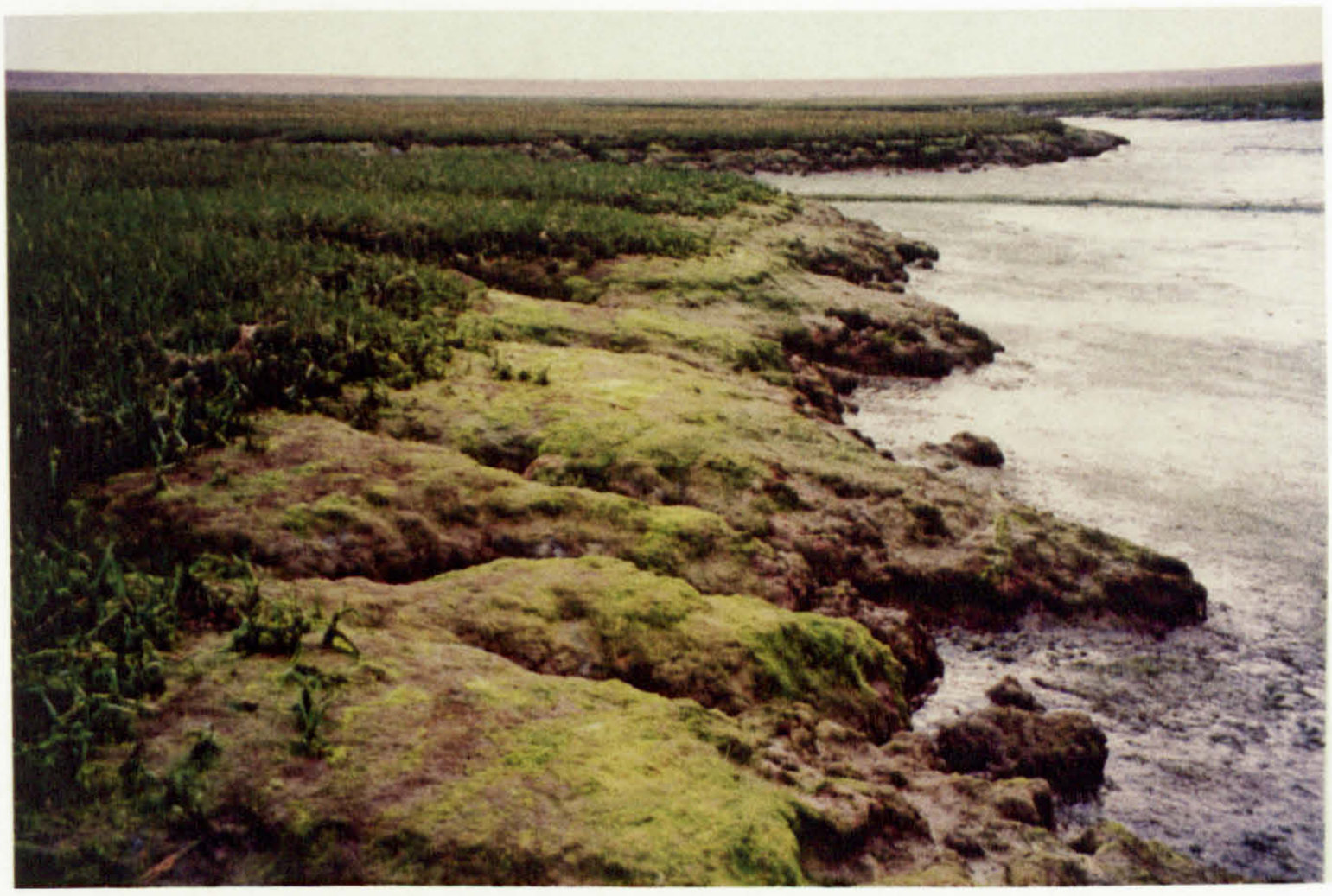

Plate 5.1 Bank/wall facet of cross-sectional profiles displaying: (a) die back, Keyhaven, The Solent; (b) overhanging vegetation, Holbeach, The Wash; (c) vertical wall, Stiffkey; (d) minor undercut, River Dovey; and (e) substantial undercut, River Crouch.

(d)

(e)

Plate 5.1 cont. Bank/wall facet of cross-sectional profiles displaying: (a) die back, Keyhaven, The Solent; (b) overhanging vegetation, Holbeach, The Wash; (c) vertical wall, Stiffkey; (d) minor undercut, River Dovey; (e) substantial undercut, River Crouch.

(Goodman, 1960, 1961; Lambert, 1964; Sivansen and Manners, 1972). Although often obscured by a cap of overhanging vegetation (see Plate 5.1b), the wall descends steeply from the crest of the channel bank (Allen, 1985a; Tubbs, 1999). Its near vertical form is sustained by the binding action of the root layer (Plate 5.1c), which at the present study sites was consistently found to extend over 0.3-0.4m.

The lower limit of the bank/wall segment is typically undercut (see, for example, Pestrong, 1965). This feature varies from a minor lip (Plate 5.1d) to a substantial horizontal incision (Plate 5.1e). The toe facet, which extends below the vertical limit of root binding action, adopts a variety of forms in its descent to the channel floor. At its simplest, the toe is smoothly concave. An initially steep side angle of up to 70° progressively diminishes with distance from the undercut (Plate 5.2a). At the other end of the morphological spectrum, the toe appears as a convex bench (Plate 5.2b), which protrudes towards the centre of the channel. According to Pestrong (1965, p.32), the presence of this bench feature is '*related to stages of maximum current velocities within the channels*'. Since the development of internal terraces is instead observed by Carey and Oliver (1918), Beeftink (1977a), Shi *et al.* (1995) and Allen (1997) to proceed by infilling, the geomorphological processes underlying their formation remains a subject of debate.

Differing degrees of halophytic colonisation may be evident on an active bench, depending on the frequency and intensity of tidal flushing. Although a surface veneer of green filamentous algae is common (Plate 5.2c), vegetative cover is generally sparse due to high velocities and the prolonged period of submergence. While mixed swards temporarily persist on collapsed blocks (Redfield, 1972, Zeff, 1988), pioneer colonisation of the profile toe (Plate 5.2d) is limited to reaches that experience a reduction in flow intensity (see, for example, Greensmith and Tucker, 1966; Collins *et al.*, 1987). Increasingly extensive colonisation of this lower facet (Plate 5.2e) is associated with the latter stages of network development (see Section 1.4.4).

The channel floor is situated at the base of the toe. It can be distinguished by the comparatively subdued angle of descent, which in the present study localities was measured at less than 20°. As Steers (1959) notes, the floor may be part of the substratum. Where this is the case, the composition of sedimentary material exhibits a conspicuous contrast with the adjacent toe (Plate 5.3a). Along the course of a channel, the floor often alternates between featureless free-flowing reaches (Wells *et al.*, 1990), and sections obstructed by depositional material and debris from collapsed blocks (Plate 4.4c-d).

(a)

(b) **(c)**

Plate 5.2 Toe facet of cross-sectional profiles displaying: (a) smoothly concave descent, The Middleway, River Roach; (b) prominent active bench, The Swale; (c) algal colonisation, River Beaulieu; (d) pioneer colonisation, Butterwick, The Wash; (e) densely vegetated inactive bench, River Leven.

(d)

(e)

Plate 5.2 cont. Toe facet of cross-sectional profiles displaying: (a) smoothly concave descent, The Middleway, River Roach; (b) prominent active bench, The Swale; (c) algal colonisation, River Beaulieu; (d) pioneer colonisation, Butterwick, The Wash; (e) densely vegetated inactive bench, River Leven.

(a)

(b)

(c)

(d)

Plate 5.3 Floor facet of cross-sectional profiles displaying: (a) abrupt transition between a sandy floor segment and silty toe facet, Scolt Head Island; (b) algal colonisation, River Carew; (c) confined lateral development, Maplin Sands; (d) extensive lateral development, River Ribble; (e) freely meandering thalweg feature, Isle of Walney; (f) minor thalweg development, Brancaster marshes; and (g) deeply incised thalweg, Lymington marshes.

(e)

(f)

(g)

Plate 5.3 cont. Floor facet of cross-sectional profiles displaying: (a) abrupt transition between a sandy floor segment and silty toe facet, Scolt Head Island; (b) algal colonisation, River Carew; (c) confined lateral development, Maplin Sands; (d) extensive lateral development, River Ribble; (e) freely meandering thalweg feature, Isle of Walney; (f) minor thalweg development, Brancaster marshes; and (g) deeply incised thalweg, Lymington marshes.

Although halophytic colonisation is largely absent, under conditions of limited tidal flushing the floor may be covered by a veneer of algae (see Plate 5.3b; also Coates *et al.*, 1995). The width of the floor varies according to position within the network. In the central reaches (Plate 5.3c), the floor segment appears narrowly confined between prominent toe features. In the lower reaches (Plate 5.3d), the floor occupies a considerably wider tract.

In accordance with observations by Ashley and Zeff (1988), Zeff (1988) and Wells *et al.* (1990), a marked thalweg is often present in the channel floor. Incised below the general level of the creek bed, the thalweg does not necessarily occupy a central position. Instead, it may meander freely between limits imposed by adjoining toe segments (plate 5.3e). As the degree of incision varies from an almost imperceptible depression (Plate 5.3f) to comparatively deep channelisation (Plate 5.3g), the thalweg plays an increasingly significant role in the conveyance of low stage tidal flows. While it may be envisaged that gravity driven dewatering during the latter stages of the ebb tide carves and maintains this incised basal facet, it is uncertain whether fluxes at the onset of the flood contribute to thalweg formation.

In addition to active cross-sectional facets, relic step features were identified at a number of sites. Occupying a set-back position along the upper margin, steps usually occur in pairs, and bare a strong morphological resemblance to the bank/wall segment above which they are situated. The elevation of the relic bank corresponds closely with the marsh interior (Plate 5.4a), and it is typically colonised by a more mature sward than the fronting facet. A near-vertical wall (Figure 5.4b) separates the active and relic banks, the displacement between which was found to vary between 0.18-0.64m. Previous studies identify this relic feature as the active margin of an earlier phase of channelisation, which has subsequently been abandoned through episodic (see Kestner, 1962; Gray, 1972; Chapman, 1974) or progressive changes (Allen, 1997) in local boundary conditions. Another possible explanation is upstream knick-point migration (see, for example, Pringle, 1995), whereby gravity-driven downcutting creates a deep central incision as subsidiary channels adjust to the base level downstream.

5.3.2 Conceptualising spatial scales of morphologic variability

Morphological variability in cross-sectional adjustment is summarised in Figure 5.4. This conceptual model was compiled by examining an extensive library of photographs and field sketches from 690 sample stations. To distinguish 'at-a-station' from 'downstream'

(a)

(b)

Plate 5.4 Relic step facet of cross-sectional profiles displaying: (a) lateral offset and contrasting halophytic colonisation between upper and lower margins, Holbeach, The Wash; and (b) abandoned channel wall transcending a vertical offset of ~0.4 m between upper and lower banks, Duddon Estuary.

(Leopold and Maddock, 1953; Leopold *et al.*, 1964)) patterns of response, the records were sorted according to position within the network. Each system was divided into four *spatial sectors* (see Section 4.3.1), defined by the standardised distance of each sample point relative to the channel head. Stations in the upper 0-5% of the channel were designated *headwater* reaches, while those in the following 5-25% were allocated to the *upper* class. *Central* reaches comprise stations at 25-75% of the total distance along the principal creek, whereas the *lower* category falls between 75-100%. In evaluating the model, sequential numbering (1-4) of these sectors provides the structure for establishing downstream changes in cross-sectional characteristics, which are superimposed on the range of morphological adjustment observed at comparable positions within the networks.

1. Headwaters: Cross-sections within the headwater reaches consistently display a *rectangular* form. Sparsely colonised, convex banks and near-vertical walls descend directly to a flat and featureless floor, notably in the absence of an appreciable toe facet. The degree of vertical adjustment is primarily controlled by vegetative binding action, and remains fairly constant throughout the study localities. In contrast, the extent of the floor segment exhibits substantial variation. Over-widened reaches in re-curved headwaters at the River Loughor (Plate 5.5a) are at one end of the scale, with an opposing tendency towards adjustment through deepening (see Pethick, 1992) arising where width is relatively constrained. This latter condition is represented in the dataset by incised sections, such as those at the River Carew (Plate 5.5b). Cross-sections exhibiting a comparatively balanced pattern of adjustment are depicted as intermediate between these endmember responses (Figure 5.4).

2a. Symmetrical upper reaches: In line with Coates *et al.* (1995), profiles in the upper reaches exhibit a *triangular* or *v-shaped* form, which is roughly symmetrical (see also Allen, 1985; Collins *et al.*, 1987). While the bank/wall facet is widely stabilised by a cap of halophytic material, relic steps are evident in: the Duddon Estuary; the River Leven; the River Ribble; the Severn Estuary; The Swale; and at Butterwick and Holbeach, The Wash. A steep sided toe facet is usually present below the characteristic undercut of the active upper segment. The adjoining floor remains flat and featureless, with low stage flows occupying most of its width, rather than a confined thalweg. Comparing Plates 5.6a-b demonstrates how the degree of constraint on width and depth varies within the networks. While the wall and toe segments maintain a consistent pattern of adjustment, contrasts in boundary shape reflect the differing extent of the floor facet.

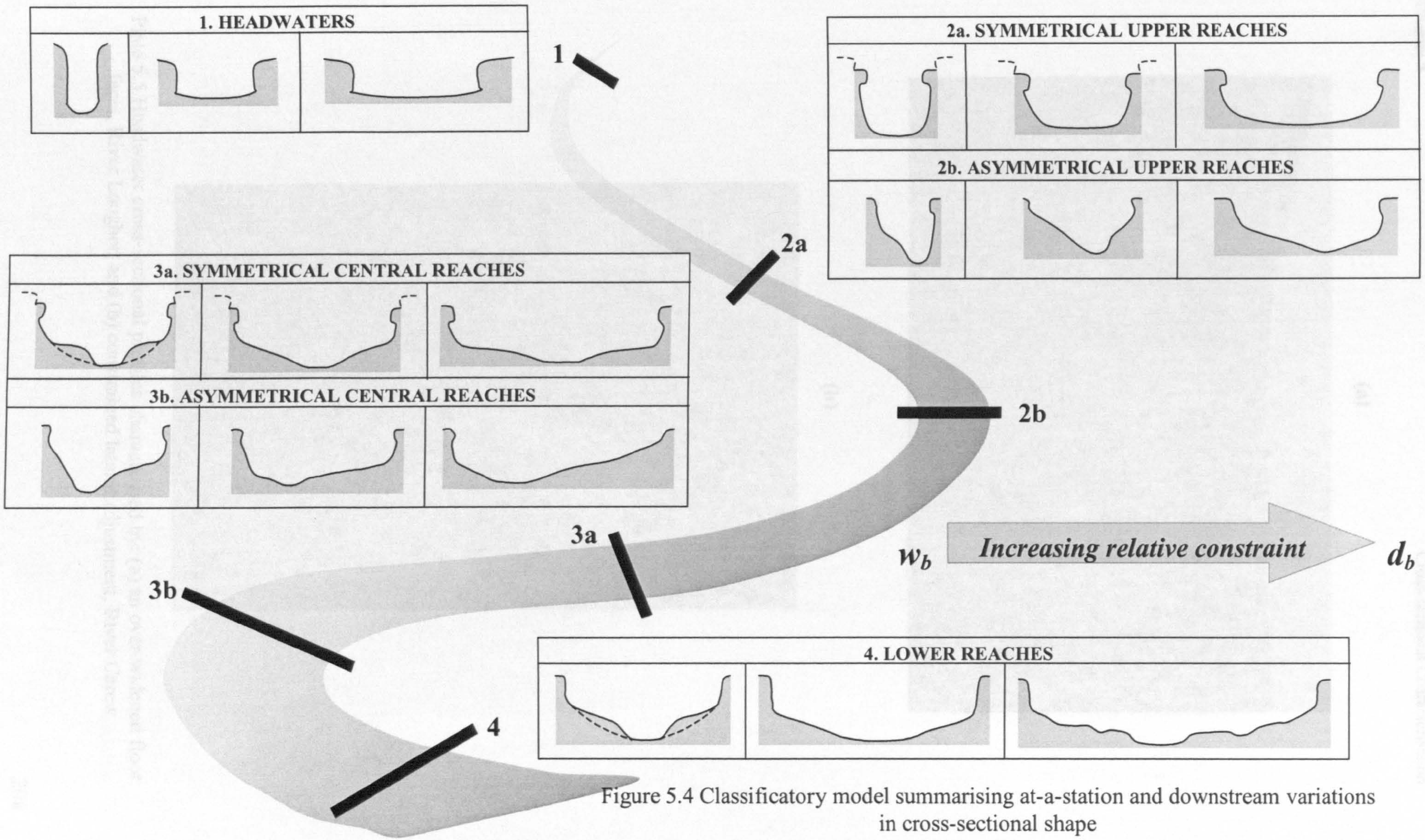

Figure 5.4 Classificatory model summarising at-a-station and downstream variations in cross-sectional shape

(a)

(b)

Plate 5.5 Headwater cross-sectional profiles characterised by: (a) an over-widened floor facet, River Loughor; and (b) constrained lateral adjustment, River Carew.

(a)

(b)

Plate 5.6 Cross-sectional profiles in the upper reaches, displaying: (a) symmetrical triangular adjustment, The Ribble; (b) an extended floor facet, Pagham Harbour; (c) asymmetrical toe protrusion with offset floor, Maplin Sands; and (d) persistence of relic steps, River Leven.

(c)

(d)

Plate 5.6 cont. Cross-sectional profiles in the upper reaches, displaying: (a) symmetrical triangular adjustment, The Ribble; (b) an extended floor facet, Pagham Harbour; (c) asymmetrical toe protrusion with offset floor, Maplin Sands; and (d) persistence of relic steps, River Leven.

2b. Asymmetrical upper reaches: Asymmetrical responses which were predominantly observed in meandering rather than 'crossing' (Pestrong, 1965) sections of the upper reaches, exhibit pronounced distortion within the toe and floor facets. On the outside of a bend, incision below the channel wall is amplified and the pattern of descent through the toe is consistently concave. The undercut is substantially reduced on the inside margin, where the toe feature often exhibits a convex bench-like protrusion. This descends gradually to a narrow floor, with a low point that is characteristically displaced from the centreline, towards the outer apex. Constraints on channel width and depth are manifest in a similar manner to symmetrical reaches, although toe distortion and offset in the position of the floor are exacerbated (see Plate 5.6c) as width adjustment is constrained relative to depth. Evidence from the River Leven (Figure 5.6d) shows how relic steps persist throughout asymmetrical upper reaches, occupying a set-back position on both the inner and outer banks of a bend.

3a. Symmetrical central reaches: Channel capacity visibly increases towards the central reaches of the sample networks, where a transition is made from narrow, angular sections to a more open and curved pattern of cross-sectional adjustment. Referred to by a number of authors (see Coates *et al.*, 1995) as *parabolic*, cross-sectional shape is dominated by exaggerated toe and floor facets. Varying degrees of protrusion are evident below the bank/wall segment, which retains the characteristic form of upper reaches. It is evident from the envelope of variability (Figure 5.4) that steep, concave side slopes are sustained at some localities. However, illustrative examples such as the River Roach (Plate 5.7a) are comparatively scarce. Paired benches (Pethick, 1992) are far more widespread throughout the networks. Depending on the degree of width constraint, the floor segment may appear deeply incised, or wide and unconfined. Low stage flows are commonly channelised along a thalweg feature. Although the thalweg occupies a narrow range of positions within confined reaches such as the Severn Estuary (Plate 5.7b), its location is increasingly indeterminate as the floor segment enlarges (see Plate 5.7c).

3b. Asymmetrical central reaches: Deflection of the thalweg is also a characteristic of asymmetric profiles in the central reaches of the networks. The extent to which the upper bank/wall and toe facets are influenced by channel meandering varies according to the relative importance of widening or deepening. The basic morphological differences between symmetrical and asymmetrical upper reaches, persist in the

(a)

(b)

(c)

Plate 5.7 Cross-sectional adjustment in the central reaches, displaying: (a) sustained toe concavity, Devil's Reach, River Roach; (b) confined floor and thalweg feature, Severn Estuary; and (c) shortened toe facet and offset floor on the outside apex of a bend, Lymington marshes.

central sector of formations exhibiting a high or intermediate level of width constraint. In unconfined profiles, the upper bank/wall facet at the outside apex appears largely unaffected by changes in channel orientation, while the active bench is merely shortened rather than eliminated by thalweg displacement (Plate 5.7c).

4. Lower reaches: An open parabolic form is sustained throughout the enlarged lower reaches of the networks. Where width adjustment is relatively unconstrained, wall and toe facets occupy an outer margin, with boundary shape instead dominated by an extended floor segment. Sedimentary material often accumulates on the creek floor (Plate 5.8a; see also Tubbs, 1999), and may be dissected by incised flow lines. Although a series of quasi-parallel lines are often present in wide reaches (see also Zeff, 1999), a single, dominant thalweg can usually be identified. In laterally confined reaches, the toe facet continues to play a significant role, with the floor facet remaining incised between paired benches. The undercut, which characterises stretches of the upper and central sectors, is often absent in the lower reaches of the network. Sparse halophytic colonisation and the convex form of the upper bank/wall facet indicate that root binding is less influential in this sector than elsewhere in the system (Plate 5.8b). Evidence of erosion is also widespread throughout the study localities, where it has disrupted normal patterns of toe and wall development (see, for example, Plate 5.8c).

The generic classificatory model proposed here successfully summarises the variations in cross-sectional shape displayed by the present sample of tidal networks. However, the categories into which each study site falls, both at-a-station and in a downstream direction, have yet to be addressed. Networks in the Duddon Estuary, the River Dovey, the River Colne, the River Orwell, on the Isle of Walney, and at Keyhaven and Lymington, are characterised by preferential cross-sectional adjustment through widening rather than deepening, along the entire course of the principal channel (Figure 5.5). This stands in marked contrast to channels bordering The Swale and at Butterwick, The Wash, where adjustment through widening is consistently constrained. Width adjustment is similarly limited throughout central and lower reaches in the River Leven, the River Beaulieu, the River Roach, the River Crouch, the Stour Estuary, at Hamford Water, and at Holbeach, The Wash.

(a)

(b)

(c)

Plate 5.8 Cross-sectional adjustment in the lower reaches, displaying: (a) dominant thalweg with adjacent incised flow lines, River Colne; (b) amplified bank convexity arising from the diminished influence of root binding, Butterwick, The Wash; and (c) toe facet degraded by erosive action, River Blackwater.

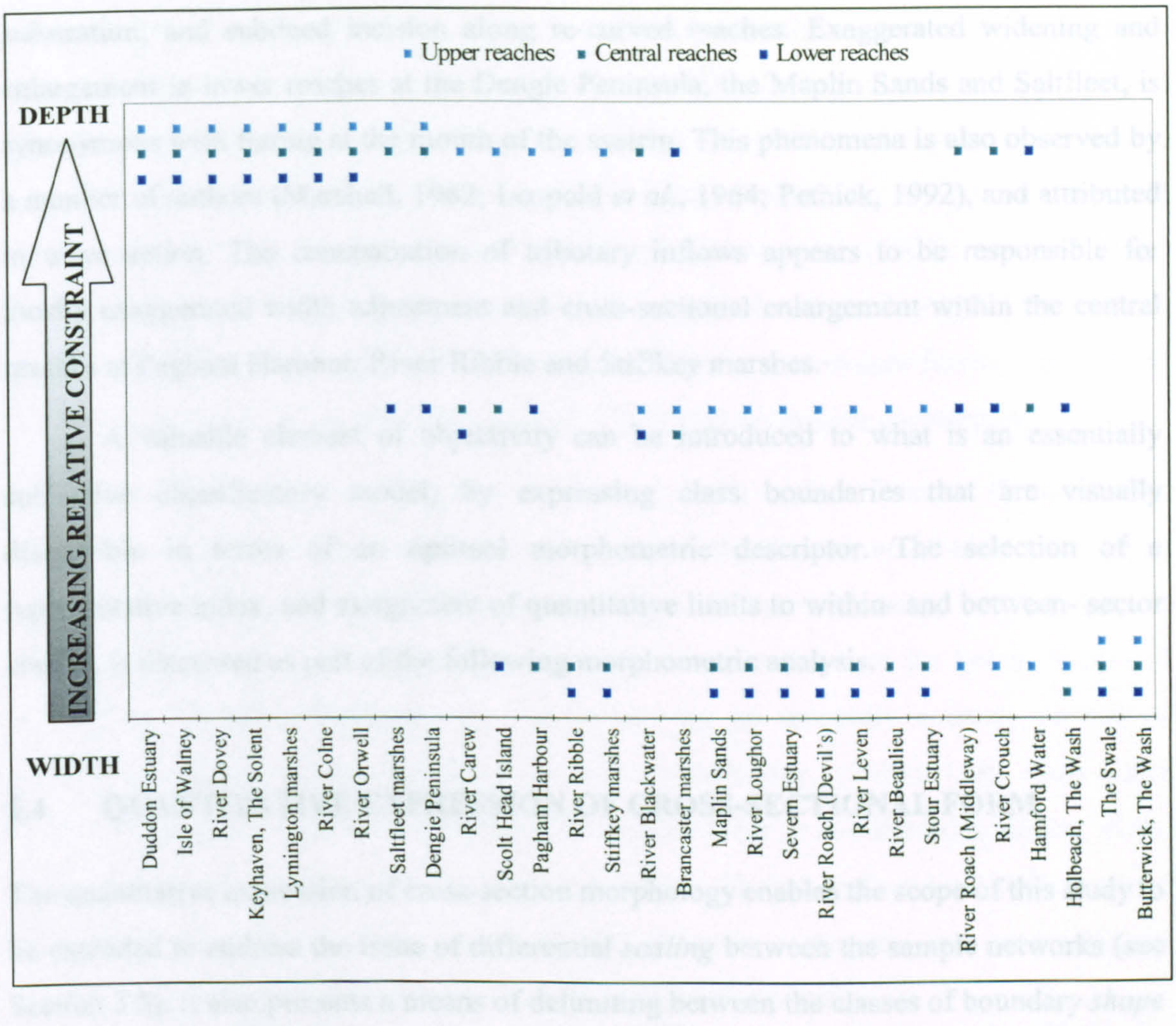

Figure 5.5 Application of the classificatory model for cross-sectional adjustment to the suite of sample networks. Responses observed in the upper, central and lower sectors are expressed on a three-tier scale of increasing constraint in depth relative to width, ranging from 'laterally constrained', to 'balanced' and 'over-widened'.

Such fundamental and systematic differences in the manner through which formative flows are accommodated by cross-sectional adjustment are likely to reflect network-scale influences, as well as broad diversity in external environmental controls. Local variations in internal controls are instead reflected by inconsistencies *within* individual networks. Cross-sectional adjustment switches between the different 'classes of constraint' along the course of several networks. Categories are frequently transcended between the upper and central reaches of the systems, with greater consistency in the central and lower sectors. At sites including: the River Blackwater; the River Loughor; the Severn Estuary; Devil's Reach at the River Roach; and Brancaster Marsh, adjustment through widening in the headwaters is replaced by balanced or laterally constrained cross-sections. Changes in boundary conditions coinciding with this transition include: disruption of the flow regime by channel capture; exacerbated depth constraint by the

substratum; and subdued incision along re-curved reaches. Exaggerated widening and enlargement in lower reaches at the Dengie Peninsula, the Maplin Sands and Saltfleet, is synonymous with flaring at the mouth of the system. This phenomena is also observed by a number of authors (Marshall, 1962; Leopold *et al.*, 1964; Pethick, 1992), and attributed to wave action. The concentration of tributary inflows appears to be responsible for locally exaggerated width adjustment and cross-sectional enlargement within the central reaches at Pagham Harbour, River Ribble and Stiffkey marshes.

A valuable element of objectivity can be introduced to what is an essentially subjective classificatory model, by expressing class boundaries that are visually discernible in terms of an optimal morphometric descriptor. The selection of a representative index, and assignment of quantitative limits to within- and between- sector classes, is discussed as part of the following morphometric analysis.

5.4 QUANTITATIVE EXPRESSION OF CROSS-SECTIONAL FORM

The quantitative expression of cross-section morphology enables the scope of this study to be extended to address the issue of differential *scaling* between the sample networks (see Section 3.5). It also presents a means of delimiting between the classes of boundary *shape* identified by the preceding visually-based analysis. Working with the rudimentary measures of bankfull width and depth, the performances of the derived morphometric indices: (1) width:depth ratio and (2) cross-sectional area (see Doornkamp and King, 1971; Gardiner and Park, 1978) are evaluated, in a bid to identify optimal descriptors of network-wide profile adjustment.

5.4.1 Constituent variables

As a precursor to the evaluation of derived morphometric measures, an appreciation of spatial variability in the constituent variables is desirable. The graphical representation of bankfull width (w_b) as a function of sinuous distance from the channel head (Figure 5.6a) reveals fundamental differences in the magnitude of this basic geometric measure within the sample of networks. Adjustment through widening is constrained along the course of formations such as The Swale, which are situated towards the lower margin of the envelope of responses. At the upper margin, extreme lateral adjustment is present at localities including the River Colne and Keyhaven, The Solent. Interestingly, the principal

channel transcends a comparable length of the foreshore in these systems, the implication being that factors other than scale dependence determine the degree of relative constraint. The range of values recorded for channel width ($0.5 < w_b < 49.2$ m) is in line with results obtained for the central and upper reaches of tidal networks by Myrick and Leopold (1963), Zeff (1988), Ashley and Zeff (1988), Knighton *et al.* (1992), and Ayles and Lapointe (1996). However, the marked shortfall compared with the lower reaches of these systems, which attain a width of 200m, suggests that the conveyance function performed by British networks is small in relation to their U.S. and Australian counterparts.

A standardised representation of channel width against distance (Figure 5.6b), provides a better indication of progressive change along the course of each system than the equivalent dimensional plot. The results (Figure 5.7) reveal a range of responses. At ~50% of the sites, adjustment through widening is concentrated in the lower reaches of the system. These formations are characterised by an upwardly concave pattern of adjustment (Figure 5.7a). The linear or convex responses, exhibited by many other localities (Figure 5.7b), are commensurate with consistent or accelerated widening in the upper and central reaches. Considerable irregularity is likely to reflect localised variations in boundary conditions, which are superimposed on the systematic and geographically extensive controls responsible for the overall pattern of response.

Previous studies (Leopold *et al.*, 1964; Wright *et al.*, 1973; French and Stoddart, 1992; Pethick, 1992; Knighton *et al.*, 1992) suggest that an empirically-based model of downstream width adjustment provides a useful starting point for translating qualitative trends into quantitative expressions. In each of the above examples, exponential rates of increase in channel width with distance were recorded. To determine if this generalisation could be extended to the present study localities, a best-fit function was identified (see also Rinaldo *et al.*, 1999). Sites displaying a concave pattern of response (Figure 5.7a) generally conform to the exponential model. However, in only a limited number of cases did the model provide a realistic representation along the entire course of channel. In most instances, the curve is unduly influenced by asymptotic behaviour towards the origin (channel head), which often bears limited resemblance to adjustment in the central and lower reaches (see Section 5.3.2). Since conformity is also poor in the formations displaying linearised or convex responses, the suitability of an exponential model to quantify and distinguish between the various patterns of width adjustment is clearly limited.

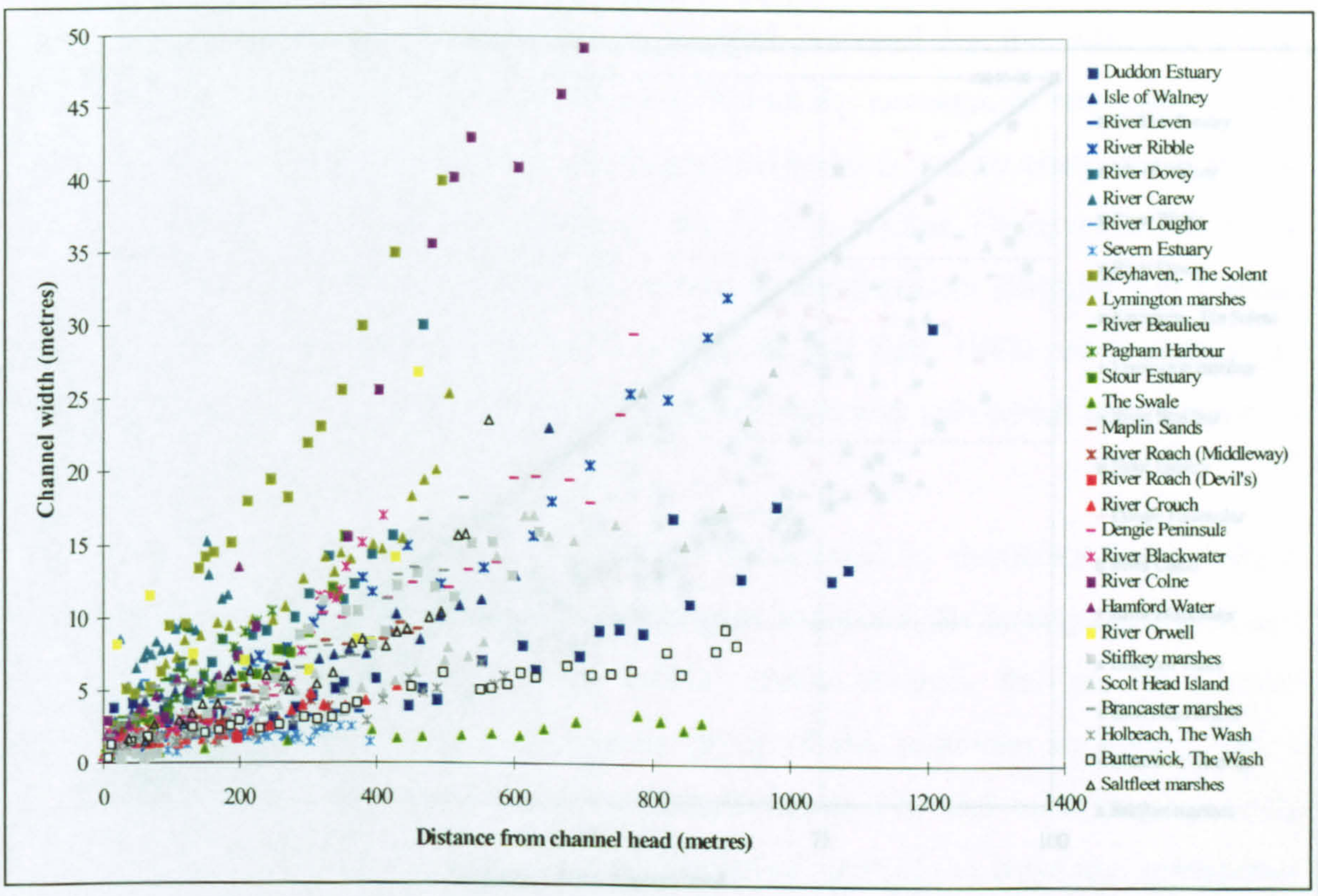

Figure 5.6 (a) Dimensional and (b) standardised plots showing w_b as a function of distance along the course of the principal channel for the population of study localities.

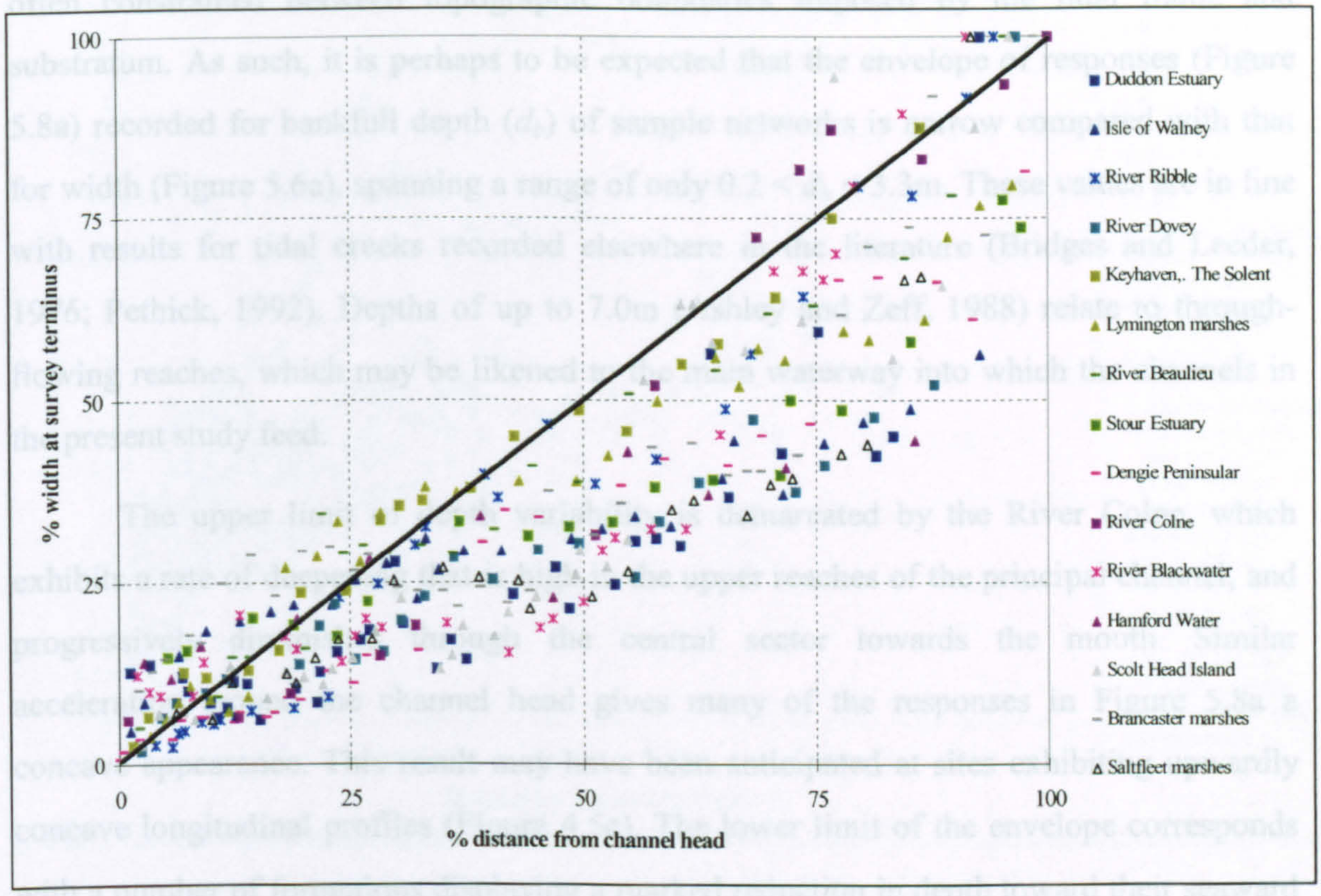

Figure 5.7 Study localities displaying: (a) concave; and (b) convex or irregular patterns of downstream width adjustment.

The degree of cross-sectional adjustment achieved through channel deepening is often constrained between topographic boundaries imposed by the tidal frame and substratum. As such, it is perhaps to be expected that the envelope of responses (Figure 5.8a) recorded for bankfull depth (d_b) of sample networks is narrow compared with that for width (Figure 5.6a), spanning a range of only $0.2 < d_b < 3.3$m. These values are in line with results for tidal creeks recorded elsewhere in the literature (Bridges and Leeder, 1976; Pethick, 1992). Depths of up to 7.0m (Ashley and Zeff, 1988) relate to through-flowing reaches, which may be likened to the main waterway into which the channels in the present study feed.

The upper limit of depth variability is demarcated by the River Colne, which exhibits a rate of deepening that is high in the upper reaches of the principal channel, and progressively diminishes through the central sector towards the mouth. Similar acceleration around the channel head gives many of the responses in Figure 5.8a a concave appearance. This result may have been anticipated at sites exhibiting upwardly concave longitudinal profiles (Figure 4.5c). The lower limit of the envelope corresponds with a number of formations displaying a marked reduction in depth toward their seaward boundary. Irregular shallows in the lower reaches are more readily distinguished from a standardised plot (Figure 5.8b), where channel depth is adjusted relative to the maximum value recorded within the system. The discontinuities in longitudinal adjustment described in Section 4.4.3, explain fluctuations in the lower reaches of networks in the Duddon Estuary, the River Leven and the River Crouch, and at Keyhaven, The Solent and Saltfleet. However, they are unable to account for the *sustained* fall in d_b at sites including The Swale, the River Carew and the Isle of Walney. Since the longitudinal characteristics of these formations have already been established as linear or upwardly concave (Figure 4.5), bank elevation is the remaining factor that could explain the unusual reduction in depth towards the mouth of the system.

Plotting bank elevation as a function of distance from the channel head (Figure 5.9a) indicates that values tend to be near constant (see also Marshall, 1962; Ranwell, 1972; Pethick, 1992; Pringle, 1995), or to subtly increase in a seaward direction (Collins *et al.*, 1987). A pronounced fall in elevation towards the limit of vegetative cover (Kestner, 1962; Dalby, 1970) is evident at a subset of formations (Figure 5.9b). An exaggerated drop-off in the Severn Estuary and at the Isle of Walney is at least in part a function of the coastal setting, which borders a deep tidal channel. However, surface

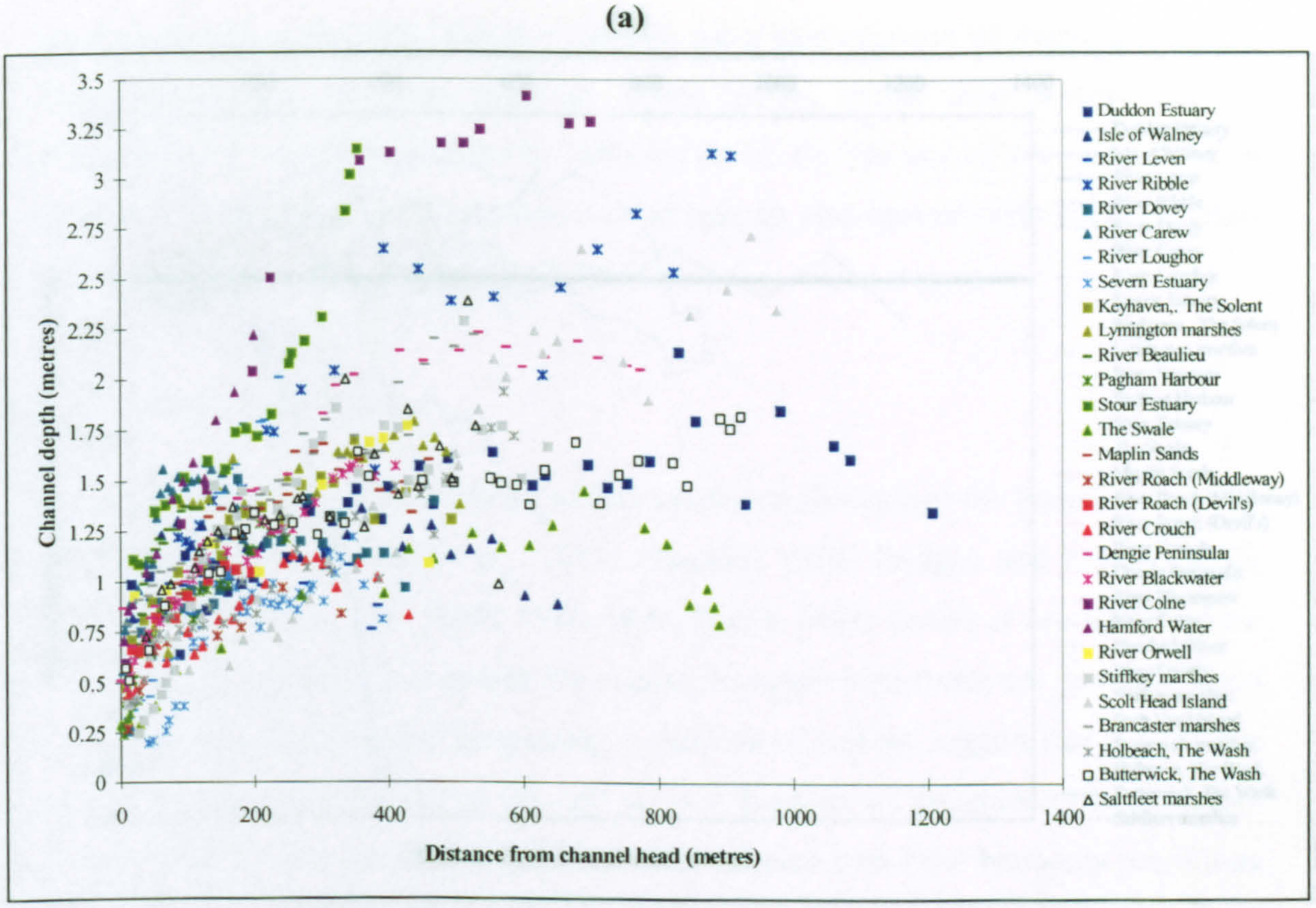

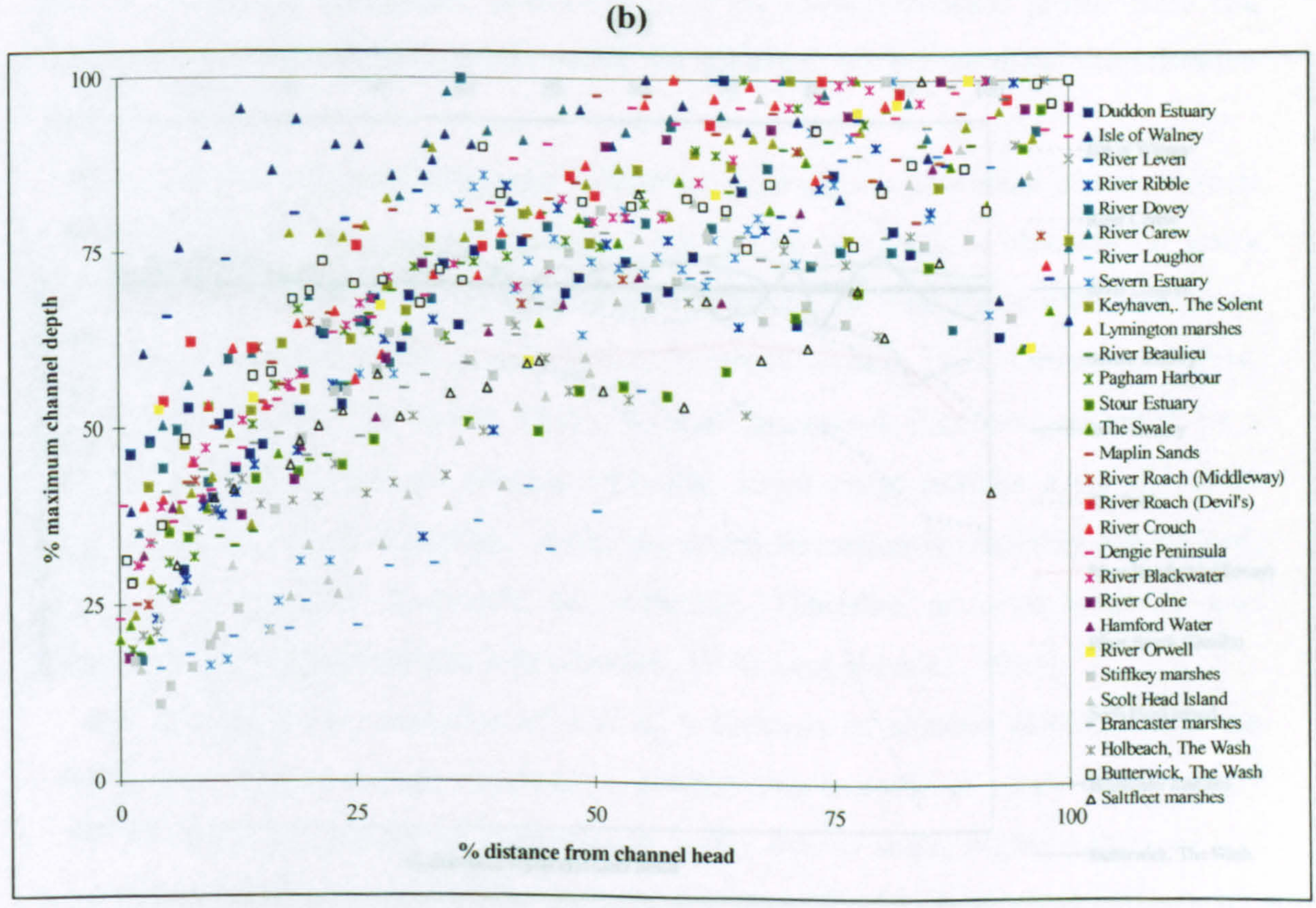

Figure 5.8 (a) Dimensional and (b) standardised plots showing d_b as a function of distance along the course of the principal channel for the population of study localities.

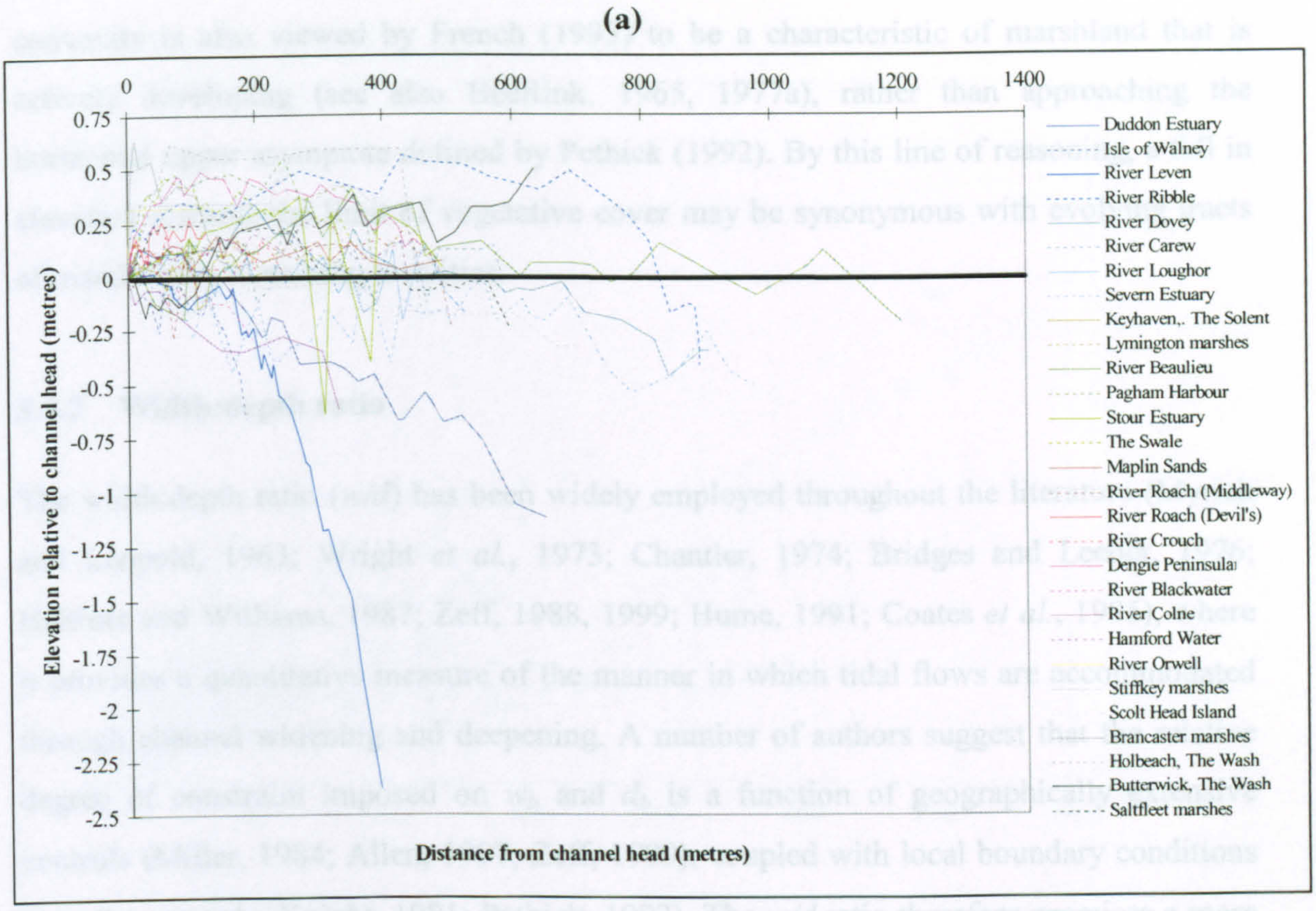

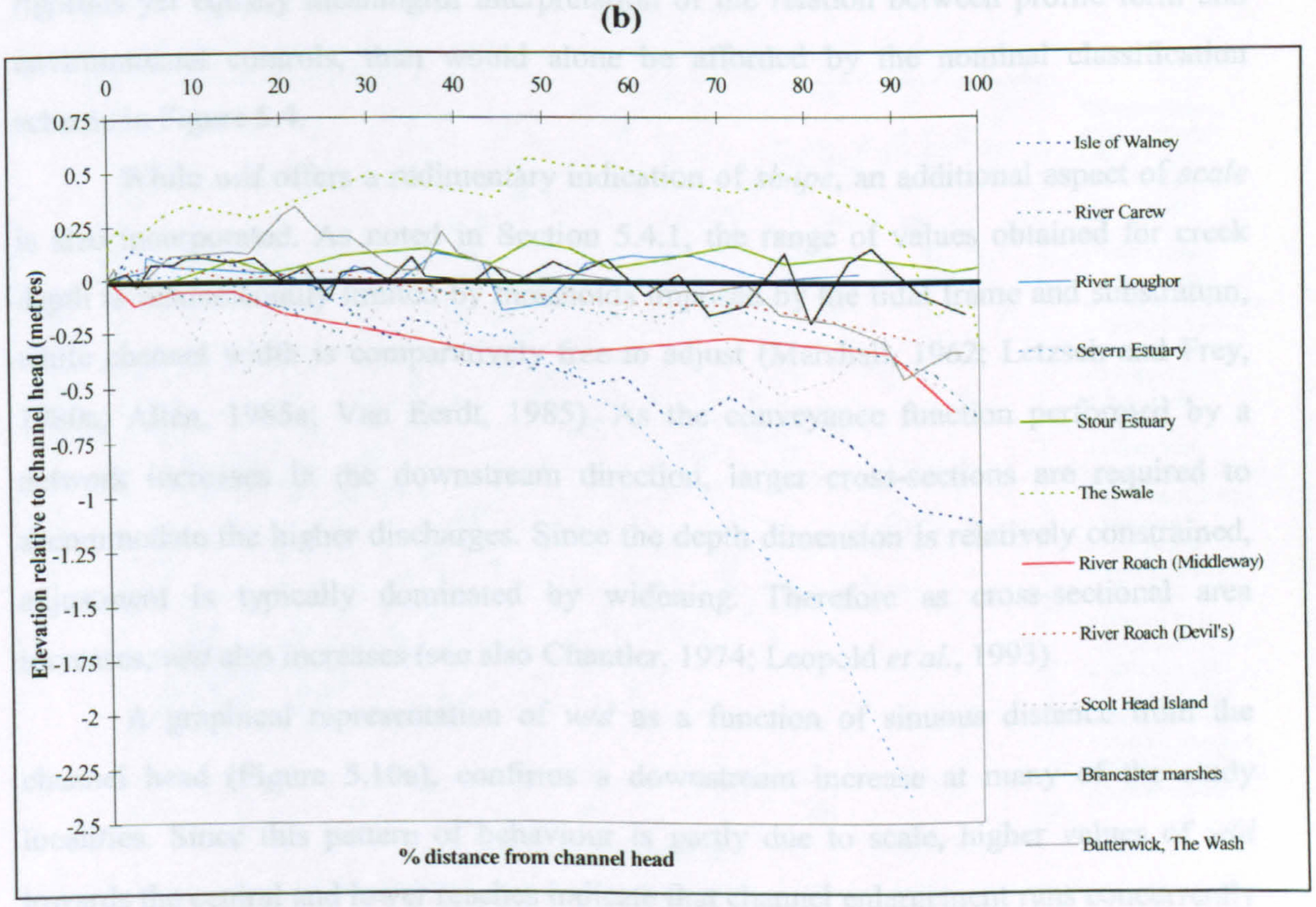

Figure 5.9 Bank elevation expressed as: (a) a function of distance for the population of study sites; and (b) standardised distance for selected localities exhibiting a fall towards the seaward margin.

convexity is also viewed by French (1993) to be a characteristic of marshland that is actively developing (see also Beeftink, 1965, 1977a), rather than approaching the horizontal upper asymptote defined by Pethick (1992). By this line of reasoning, a fall in elevation towards the limit of vegetative cover may be synonymous with evolving tracts of marsh at the remaining localities.

5.4.2 Width:depth ratio

The width:depth ratio (*w/d*) has been widely employed throughout the literature (Myrick and Leopold, 1963; Wright *et al.*, 1973; Chantler, 1974; Bridges and Leeder, 1976; Haltiner and Williams, 1987; Zeff, 1988, 1999; Hume, 1991; Coates *et al.*, 1995), where it provides a quantitative measure of the manner in which tidal flows are accommodated through channel widening and deepening. A number of authors suggest that the relative degree of constraint imposed on w_b and d_b is a function of geographically extensive controls (Miller, 1984; Allen, 1997; Zeff, 1999), coupled with local boundary conditions (see, for example, Knight, 1981; Pethick, 1992). The *w/d* ratio therefore promises a more rigorous yet equally meaningful interpretation of the relation between profile form and environmental controls, than would alone be afforded by the nominal classification scheme in Figure 5.4.

While *w/d* offers a rudimentary indication of *shape*, an additional aspect of *scale* is also incorporated. As noted in Section 5.4.1, the range of values obtained for creek depth is fundamentally limited by thresholds imposed by the tidal frame and substratum, while channel width is comparatively free to adjust (Marshall, 1962; Letzsch and Frey, 1980a; Allen, 1985a; Van Eerdt, 1985). As the conveyance function performed by a network increases in the downstream direction, larger cross-sections are required to accommodate the higher discharges. Since the depth dimension is relatively constrained, adjustment is typically dominated by widening. Therefore as cross-sectional area increases, *w/d* also increases (see also Chantler, 1974; Leopold *et al.*, 1993).

A graphical representation of *w/d* as a function of sinuous distance from the channel head (Figure 5.10a), confirms a downstream increase at many of the study localities. Since this pattern of behaviour is partly due to scale, higher values of *w/d* towards the central and lower reaches indicate that channel enlargement runs concurrently with widening through extension of the toe and floor facets (see Section 5.3.2). A similar pattern of change in *w/d* noted by Bridges and Leeder (1976) and Zeff (1988, 1999),

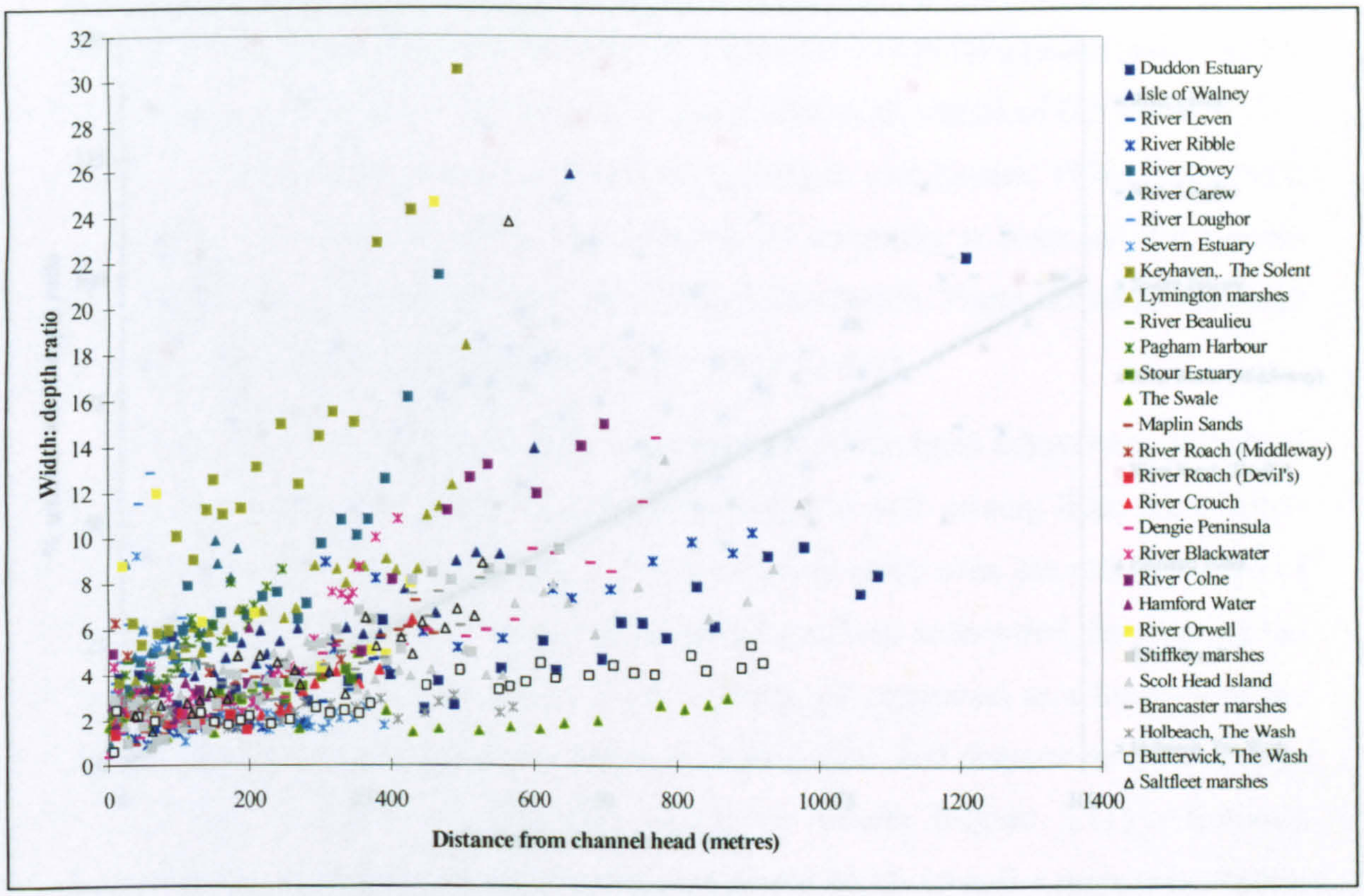

Figure 5.10 (a) Dimensional and (b) standardised plots showing *w/d* as a function of distance along the course of the principal channel for the population of study localities.

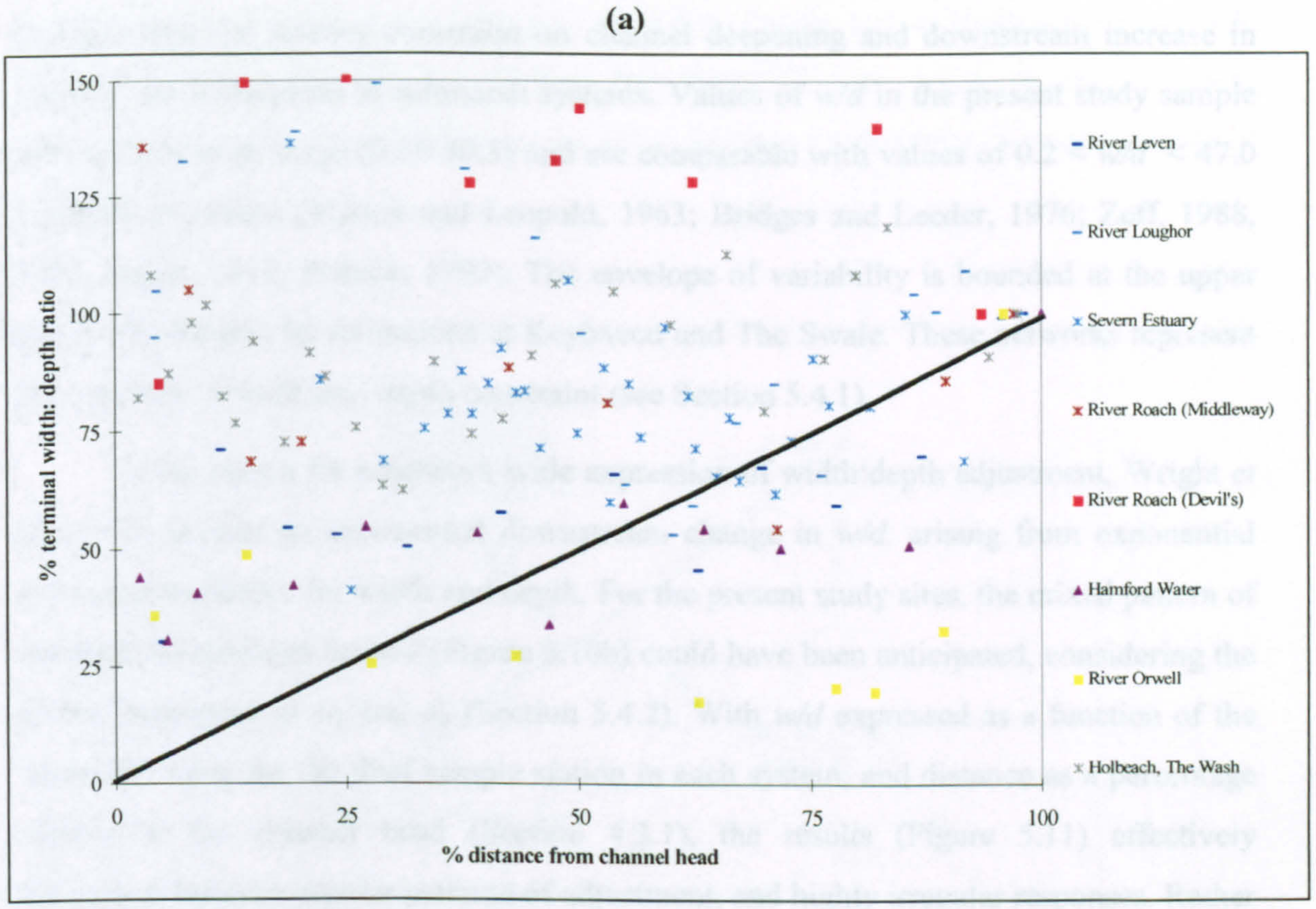

Figure 5.11 Study localities displaying: (a) irregular adjustment in *w/d* along the course of the network; and (b) regular convex, concave and linear patterns of increase in *w/d*.

confirms that the relative constraint on channel deepening and downstream increase in capacity are widespread in saltmarsh systems. Values of *w/d* in the present study sample span a fairly large range (0.39-30.5) and are comparable with values of $0.2 < w/d < 47.0$ recorded elsewhere (Myrick and Leopold, 1963; Bridges and Leeder, 1976; Zeff, 1988, 1999; Hume, 1991; Pethick, 1992). The envelope of variability is bounded at the upper and lower margins by formations at Keyhaven and The Swale. These networks represent the extremes of width and depth constraint (see Section 5.4.1).

In the search for a network-wide expression of width:depth adjustment, Wright *et al.* (1973) predict an exponential downstream change in *w/d,* arising from exponential individual responses for width and depth. For the present study sites, the mixed pattern of standardised readings for *w/d* (Figure 5.10b) could have been anticipated, considering the diverse behaviour of w_b and d_b (Section 5.4.2). With *w/d* expressed as a function of the 'terminal' value for the final sample station in each system, and distance as a percentage relative to the channel head (Section 4.3.1), the results (Figure 5.11) effectively distinguish between regular patterns of adjustment, and highly irregular responses. Rather than a downstream increase in *w/d*, standardised values exceeding 100% in the River Loughor, the Severn Estuary, the River Roach, and at Holbeach, The Wash (Figure 5.11a), indicate that *w/d* decreases towards the mouth of the system. This anomalous behaviour either arises from undue constraint on channel width at the terminal station, or else reflects exaggerated widening within the upper reaches of re-curved formations. In the River Leven, the River Orwell and at Hamford Water, downstream width adjustment is matched by depth, resulting in near-constant values for *w/d* throughout the central sector of these networks.

The distribution of *w/d* (Figure 5.11b) may be viewed as continuum, where the position of individual formations along this scale reflects the relative degree of constraint on channel width and depth throughout the course of the principal channel. Networks that fall below the line of constant *w/d* in the Duddon Estuary, the Isle of Walney, the River Dovey, on the Dengie Peninsula and at Saltfleet, exhibit accelerated width adjustment in the central and lower sectors. A concave pattern of adjustment is commensurate with exaggerated widening towards the mouth of the system, and equates with seaward flaring (see Section 5.3.2). As shown in Figure 5.12, such a response corresponds with 'estuarine behaviour', of the nature identified by Wright *et al.* (1973). In the absence of flaring, adjustment in *w/d* is more evenly distributed throughout localities including Keyhaven, The Solent and the River Colne, that fall linearly about the marker. Convex responses for

the Severn Estuary, the River Loughor, the River Roach, and at Holbeach, The Wash, instead relate to 'laterally constrained behaviour' (Figure 5.12). In this instance, adjustment in *w/d* is limited following an initial increase in the upper or central sectors of the system.

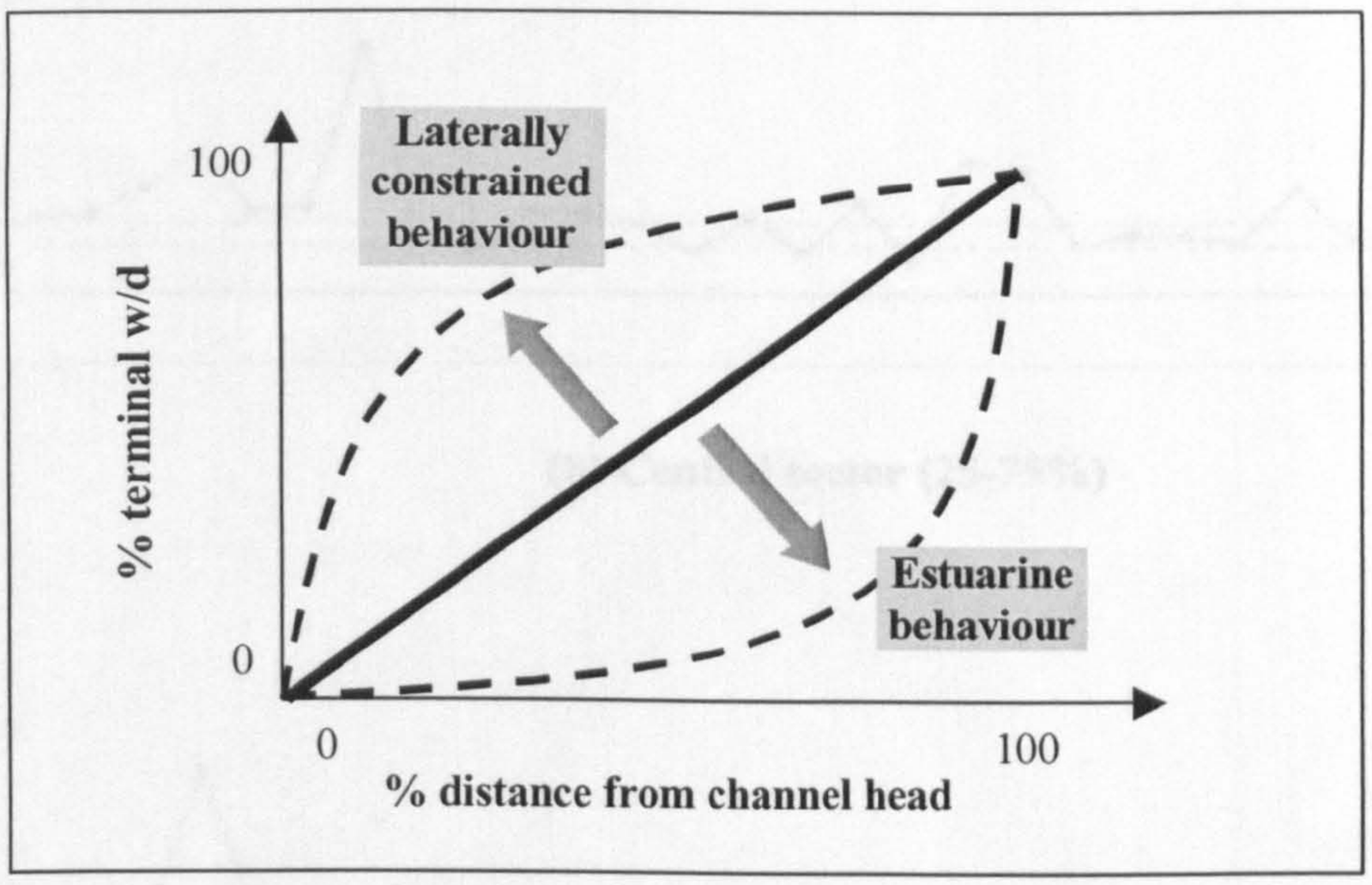

Figure 5.12 Schematic representation of the continuum in *w/d* adjustment for the sample networks. Endmember responses correspond with extreme 'estuarine' and 'laterally constrained' behaviour.

Considering the widely varying responses for *w/d*, no single function can be ascribed as a representative model for comparing and contrasting downstream modes of behaviour. However, alternative descriptors may be obtained by segmenting sample networks into the constituent sectors that were introduced in Section 5.3.2. The result of computing an average *w/d* statistic for stations in the upper, central and lower reaches of each formation is shown in Figure 5.13.

By comparing these responses with the visually determined classes in Figure 5.4, a series of thresholds can be identified for *w/d* (see ----- in Figure 5.13). These provide a quantitative scale for the original conceptual model. With the study localities organised according to the descriptive classification in Figure 5.5, a strong resemblance is evident between the average *w/d* and the nominal scale of laterally constrained, balanced and over-widened responses. In the upper sector (Figure 5.13a), the generic categorisation is mirrored by the distinction between: (1) formations with high values of *w/d* such as Keyhaven, The Solent, the River Orwell, the River Loughor, and the Severn Estuary;

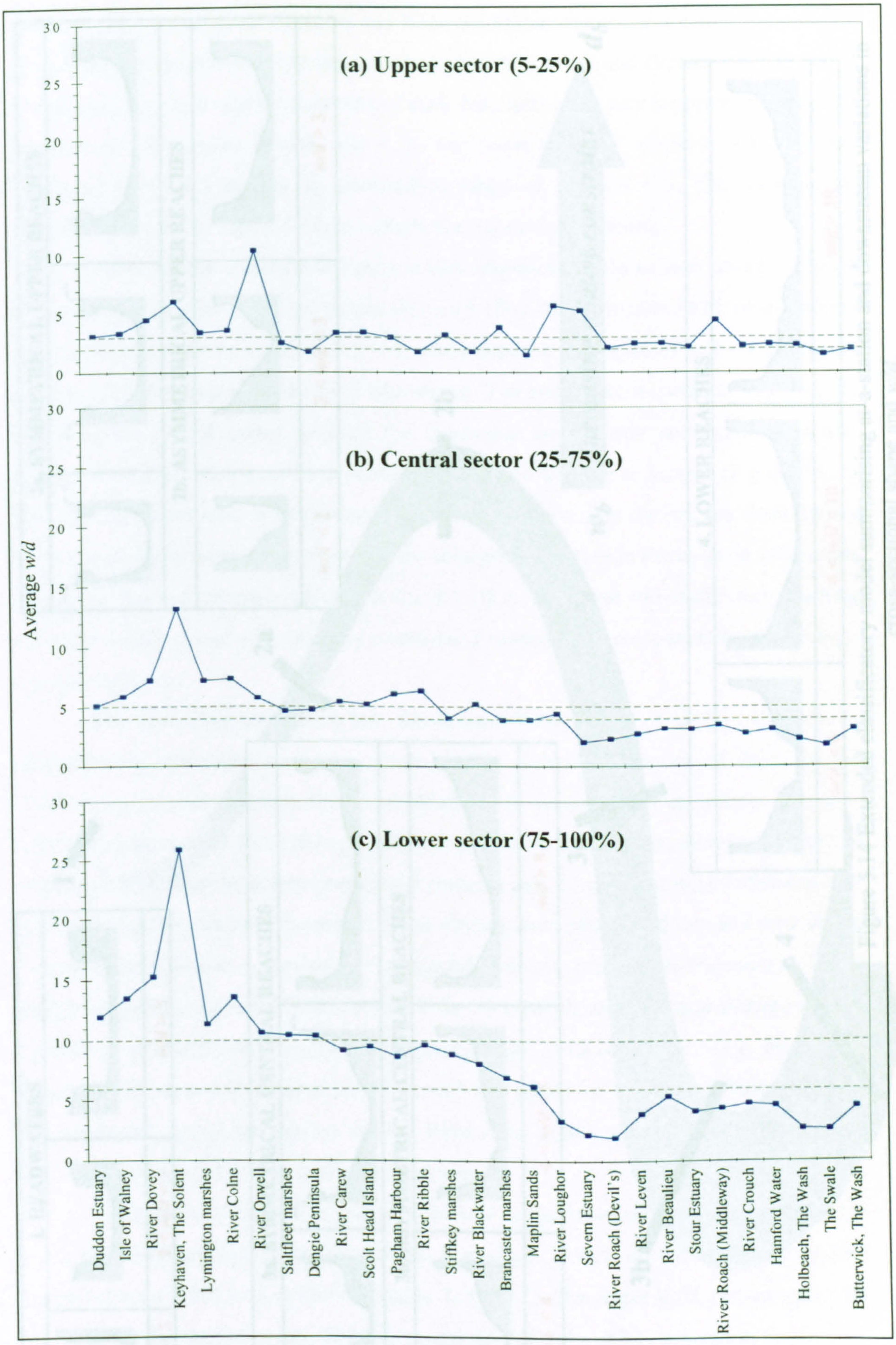

Figure 5.13 Average *w/d* for: (a) upper; (b) central; and (c) lower sectors of the principal channel at each study locality. Quantitative limits for the descriptive classes are given by (-----).

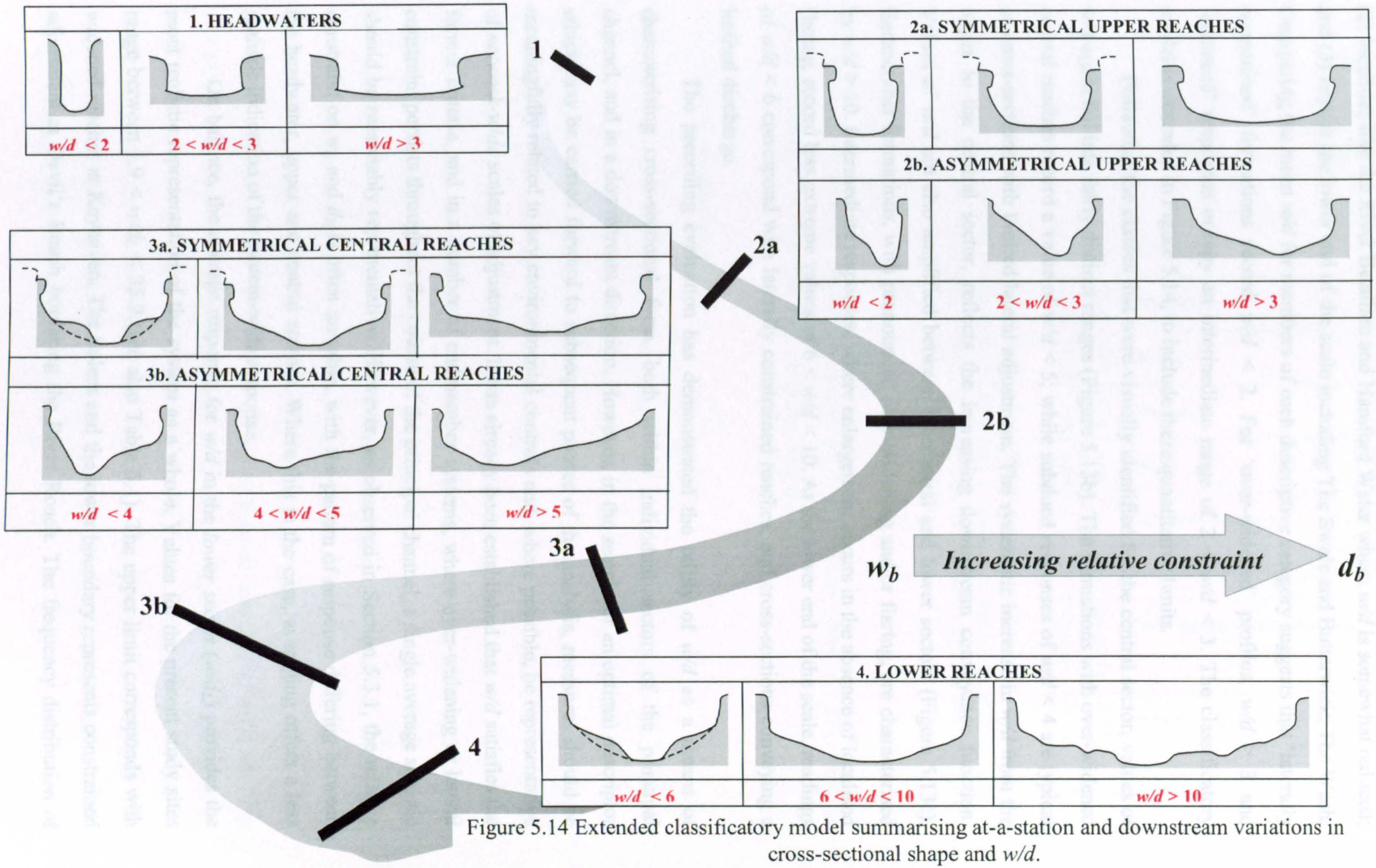

Figure 5.14 Extended classificatory model summarising at-a-station and downstream variations in cross-sectional shape and *w/d*.

(2) localities like the River Beaulieu and Hamford Water where *w/d* is somewhat reduced; and (3) sites at the lower end of the scale including The Swale and Butterwick, The Wash. Comparing the mean *w/d* for members of each descriptive category suggests that 'laterally constrained' formations record $w/d < 2$. For 'over-widened' profiles, $w/d > 3$ and 'balanced' responses occupy an intermediate range of $2 < w/d < 3$. The classificatory model is extended in Figure 5.14, to include these quantitative limits.

Following the classes that were visually identified for the central sector, values of *w/d* again fall into fairly distinct ranges (Figure 5.13b). The formations with over-widened central reaches record a value of $w/d < 5$, while subdued responses of $w/d < 4$ are typical of cross-sections with limited lateral adjustment. The systematic increase in *w/d* from the upper to the central sector, reflects the increasing downstream conveyance function. Values of *w/d* are also amplified between the central and lower sectors (Figure 5.13c). Endmember formations, with pronounced over-widening and/or flaring, are characterised by $w/d > 10$. Intermediate responses, where enlargement occurs in the absence of localised flaring, record less extreme values of $6 < w/d < 10$. At the lower end of the scale, readings of $w/d < 6$ correspond with laterally constrained reaches, and cross-sections conveying a limited discharge.

The preceding evaluation has demonstrated the utility of *w/d* as a means of characterising cross-sectional form, both within individual sectors of the principal channel, and in a downstream direction. However, in the search for an optimal descriptor which may be carried forward to subsequent phases of the analysis, measures should be meaningfully related to key environmental controls and, where possible, be representative of *network-wide* scales of adjustment. It has already been established that *w/d* satisfies the former criteria, and in a number of endmember systems, where over-widening or lateral constraint persists throughout the course of the principal channel, a single average statistic should be reasonably representative. However, as observed in Section 5.3.1, the relative constraint on w_b and d_b is often unstable, with the pattern of response differing between the headwater, upper and central sectors. Where this is the case, averaging offers a less realistic indication of the system-wide response.

On balance, the average response for *w/d* in the *lower* sector (w/d_L) provides the most realistic representation of the system as a whole. Values for the present study sites range between $1.9 < w/d_L < 25.9$ (see also Table 5.1). The upper limit corresponds with widened reaches at Keyhaven, The Solent and the lower boundary represents constrained adjustment at Devil's Reach bordering the River Roach. The frequency distribution of

STATISTICAL PROPERTY ⇨ / MORPHOMETRIC MEASURE ⇩	Minimum	Maximum	Range	Median	Mean	Standard deviation	Skewness (pre transform)	Normalising transformation	Skewness (post transform)	Number of samples
w/d_L	1.94	25.9	23.9	8.09	8.06	5.10	1.53*	log (w/d_L)	-0.19	29
A_{SL}	2.16	145.5	143.3	17.10	25.27	29.11	2.90*	log (A_{SL})	-0.13	29

Table 5.1 Statistical characteristics for cross-sectional measures of: average width:depth ratio (w/d_L); and median cross-sectional area (A_{SL}) recorded in the lower sector of the principal channel at each study locality. (* symbolises statistically significant levels of skew as defined by Norcliffe, 1977).

w/d_L exhibits a statistically significant level of positive skewness (skew = 1.53), which is effectively removed by logarithmically transforming the data.

5.4.3 Cross-sectional area

Although it has been shown that downstream increases in w/d incorporate an aspect of scale (Section 5.4.2), a more explicit expression of channel *size* is provided by cross-sectional area (A_S). The magnitude of A_S at any station along a network is seen to reflect the conveyance function that is performed (Gardner and Bohn, 1980; Allen, 1997). A_S has been extensively employed as an approximation for channel capacity, where an equilibrium relation with key hydraulic controls such as tidal prism (Gao and Collins, 1994) and discharge (Chantler, 1974; Friedrichs, 1995), has rendered it a crucial parameter in modelling (Johnson, 1973) and designing (Hume, 1991) stable profile forms.

For the present study, A_S is defined as the product of bankfull width and channel depth. Plotting A_S as a function of distance from the channel head (Figure 5.15a) indicates that the envelope of variability for the composite measure is considerably narrower than that recorded for either w_b (Figure 5.6a) or d_b (Figure 5.8a) in isolation. Although in absolute terms readings span a fairly wide range of $0.1 < A_S < 162.1\text{m}^2$, the spread of values is concentrated towards the lower boundary, where formations including The Swale exhibit a limited capacity. Towards the upper boundary, capacious reaches at the River Colne stand apart from the other results.

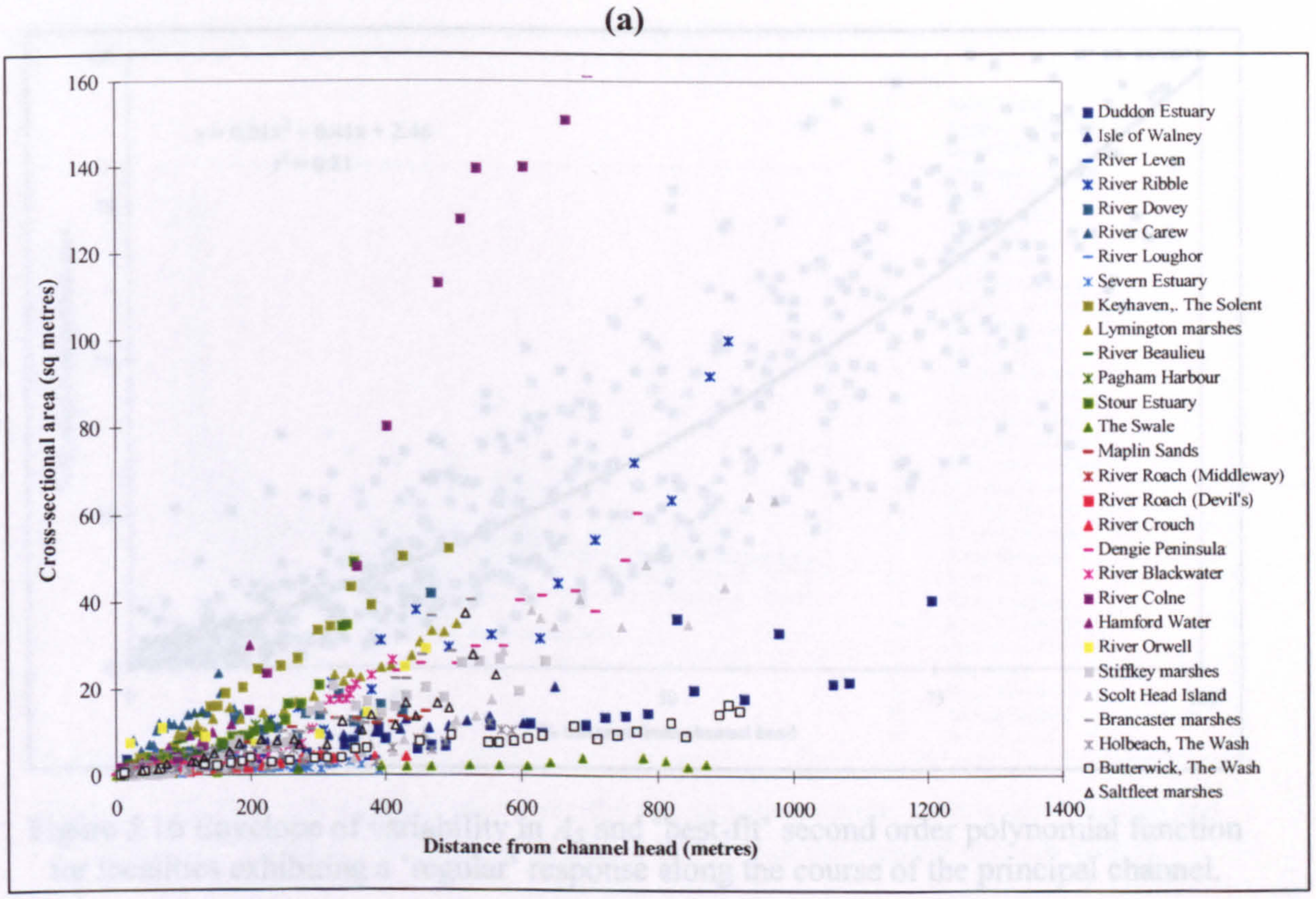

Figure 5.15 (a) Dimensional and (b) standardised plots showing A_S as a function of distance along the course of the principal channel for the population of study localities.

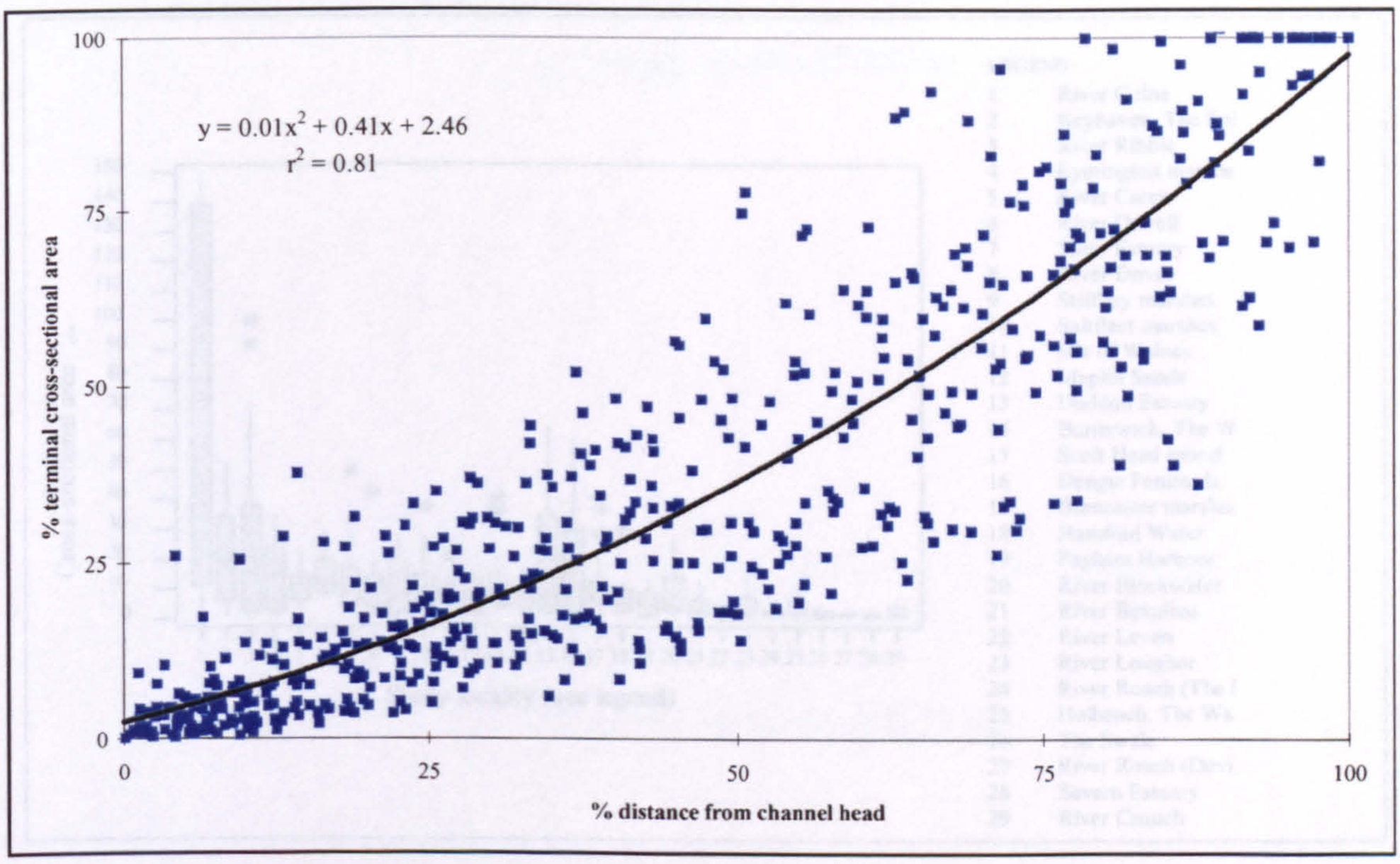

Figure 5.16 Envelope of variability in A_S and 'best-fit' second order polynomial function for localities exhibiting a 'regular' response along the course of the principal channel.

A general increase in A_S is evident from the channel head towards the central and lower sectors of the standardised responses (Figure 5.15b). While most of the series approximate to a linear or upwardly concave pattern, scattered outliers above the regular trend relate to erratic responses in the River Leven, the River Carew, the Severn Estuary, The Swale, the River Roach, the River Crouch, and at Saltfleet. At first sight, unusually high values of A_S in the upper reaches of these systems suggest that profile capacity experiences minimal further adjustment following an initial increase around the channel head. Such consistency in the conveyance function could be explained by the distribution of tributaries adjoining the principal channel, with for example, a concentration of inflow in the upper reaches and limited additional inputs in the central or lower sectors. However, the anomalous pattern of change is also likely to reflect shallowing towards the limit of vegetative cover, as bank elevation falls (see Section 5.4.1). Where a reduction is observed in d_b, the terminal value for A_S is effectively lowered. This in turn introduces a degree of irregularity to the standardised measures.

The effect of removing irregular responses on the distribution of values for A_S is recorded in Figure 5.16. The remaining 'regular' responses comprise a narrow envelope, the lower and upper limits of which are best fitted by upwardly convex or linear functions.

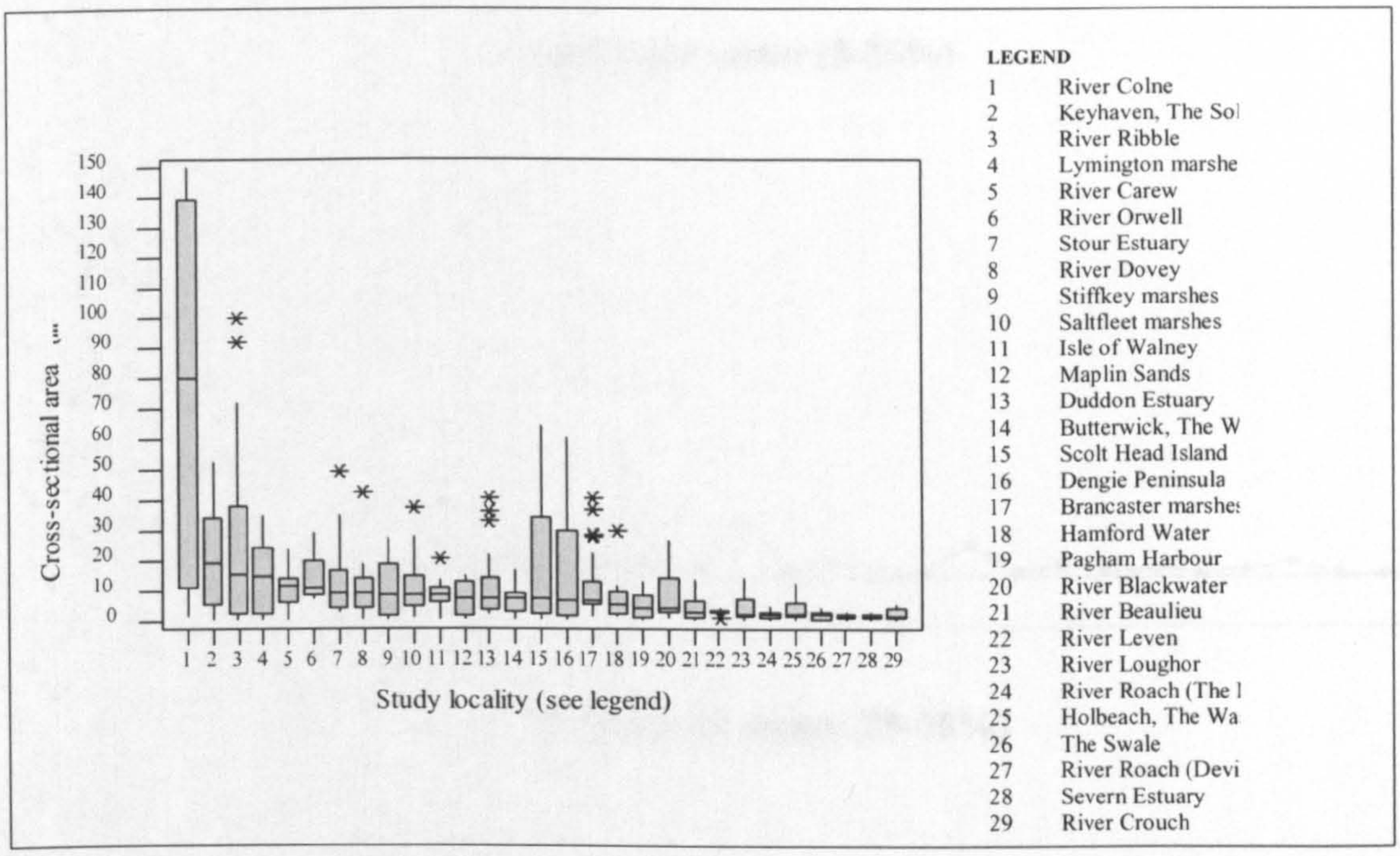

Figure 5.17 Box and whisker plot showing the sample median, interquartile range and outliers (*) of A_S. Localities are ranked in order of decreasing median values.

This suggests that downstream increases in A_S fall somewhere between accelerated enlargement towards the lower reaches, and a constant rate of change throughout the system. While a curvilinear function nicely summarises behaviour of the population as a whole, the clustering of values towards the origin means that standard exponential, power, and logarithmic curves provide a poor empirical model in the central and lower sectors. As shown, a second order polynomial instead offers a reasonable fit.

In the search for an optimal descriptor, French and Stoddart (1992) observe an exponential change in A_S at Scolt Head Island. However, no single function adequately represents the varied downstream responses of the present study localities. A central measure of tendency for A_S could be used to represent adjustment throughout the course of the principal channel. However, the box and whisker plots in Figure 5.17 reveal considerable variability in the magnitude, and substantial skew in the distribution of A_S, between the channel head and limit of vegetative cover. The sample median, which is recorded on the figure, provides a reasonable distinction between systems with a large capacity, such as the River Colne, Keyhaven, The Solent and the River Ribble. However, for channels with a smaller capacity, many of the median values for A_S fall into a narrow range. In these cases, the distinguishing power of this measure is limited.

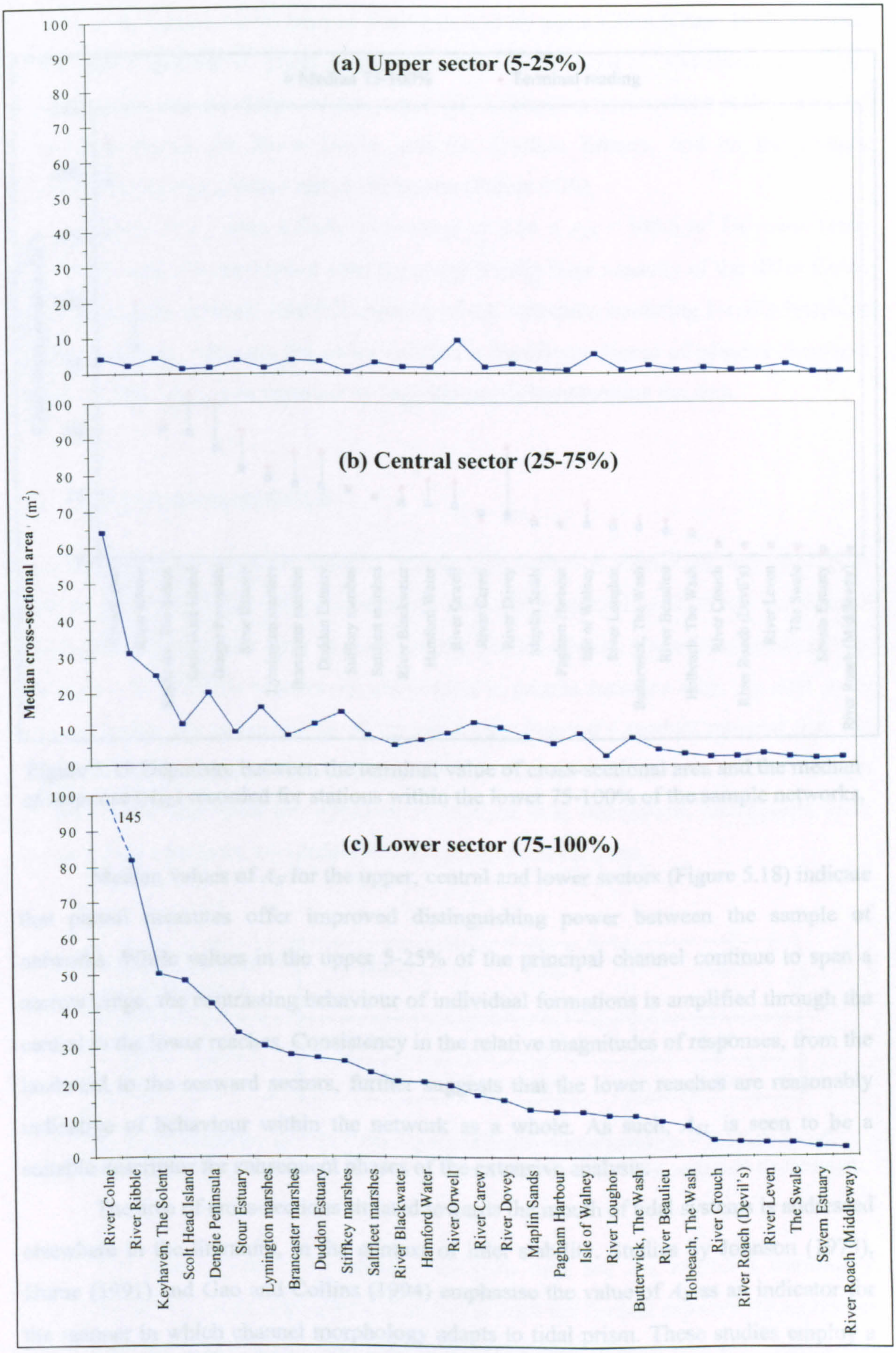

Figure 5.18 Median cross-sectional area computed for: (a) upper; (b) central; and (c) lower sectors of the principal channel at each study locality.

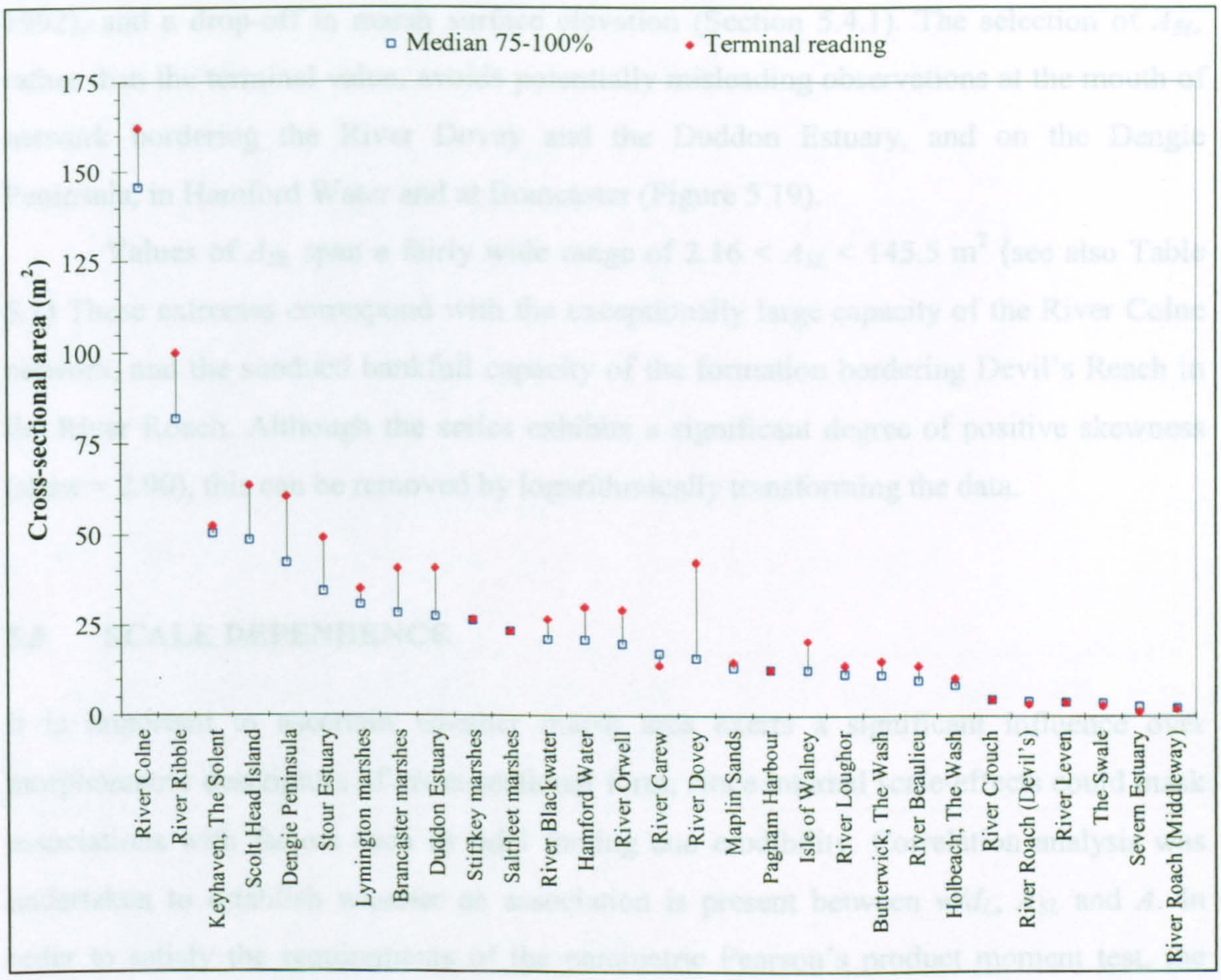

Figure 5.19 Departure between the terminal value of cross-sectional area and the median of response (A_{SL}) recorded for stations within the lower 75-100% of the sample networks.

Median values of A_S for the upper, central and lower sectors (Figure 5.18) indicate that partial measures offer improved distinguishing power between the sample of networks. While values in the upper 5-25% of the principal channel continue to span a narrow range, the contrasting behaviour of individual formations is amplified through the central to the lower reaches. Consistency in the relative magnitudes of responses, from the landward to the seaward sectors, further suggests that the lower reaches are reasonably indicative of behaviour within the network as a whole. As such, A_{SL} is seen to be a suitable descriptor for subsequent phases of the extensive analysis.

The area of cross-sections situated towards the mouth of tidal systems is addressed elsewhere in the literature, in the context of inlet stability. Studies by Johnson (1973), Hume (1991) and Gao and Collins (1994) emphasise the value of A_S as an indicator for the manner in which channel morphology adapts to tidal prism. These studies employ a 'representative' section corresponding with the mouth of the system. However, it has been established that for the present study localities, the 'terminal' value is often distorted by

end-effects (Chantler, 1974) such as flaring caused by wave action (Gray, 1972; Pethick, 1992), and a drop-off in marsh surface elevation (Section 5.4.1). The selection of A_{SL}, rather than the terminal value, avoids potentially misleading observations at the mouth of network bordering the River Dovey and the Duddon Estuary, and on the Dengie Peninsula, in Hamford Water and at Brancaster (Figure 5.19).

Values of A_{SL} span a fairly wide range of $2.16 < A_{SL} < 145.5$ m^2 (see also Table 5.1) These extremes correspond with the exceptionally large capacity of the River Colne network, and the subdued bankfull capacity of the formation bordering Devil's Reach in the River Roach. Although the series exhibits a significant degree of positive skewness (skew = 2.90), this can be removed by logarithmically transforming the data.

5.5 SCALE DEPENDENCE

It is important to ascertain whether marsh area exerts a significant influence over morphometric descriptors of cross-sectional form, since internal scale-effects could mask associations with factors such as tidal forcing and erodibility. Correlation analysis was undertaken to establish whether an association is present between w/d_L, A_{SL} and A. In order to satisfy the requirements of the parametric Pearson's product moment test, the data were subject to transformations described in the preceding sections. Since a margin of uncertainty surrounds the optimum method of area delineation, coefficients were computed for minimum, equidistant and maximum decision rules.

AREA MEASURE ⇨ DESCRIPTOR ⇩	A_{min}	A_{eq}	A_{max}
w/d_L	**0.43**	**0.45**	**0.42**
A_{SL}	**0.57**	**0.61**	**0.57**

Table 5.2 Correlation matrix showing **statistically significant** ($\alpha = .05$) levels of association between transformed measures of marsh area and cross-sectional descriptors.

The results (Table 5.2) indicate that both w/d_L and A_{SL} exhibit a statistically significant level of scale dependence. The coefficients for channel capacity are somewhat higher than for channel shape. This reflects differing levels of sensitivity to A recorded by a measure that is dominated by scaling effects such as A_{SL}, compared with measure like

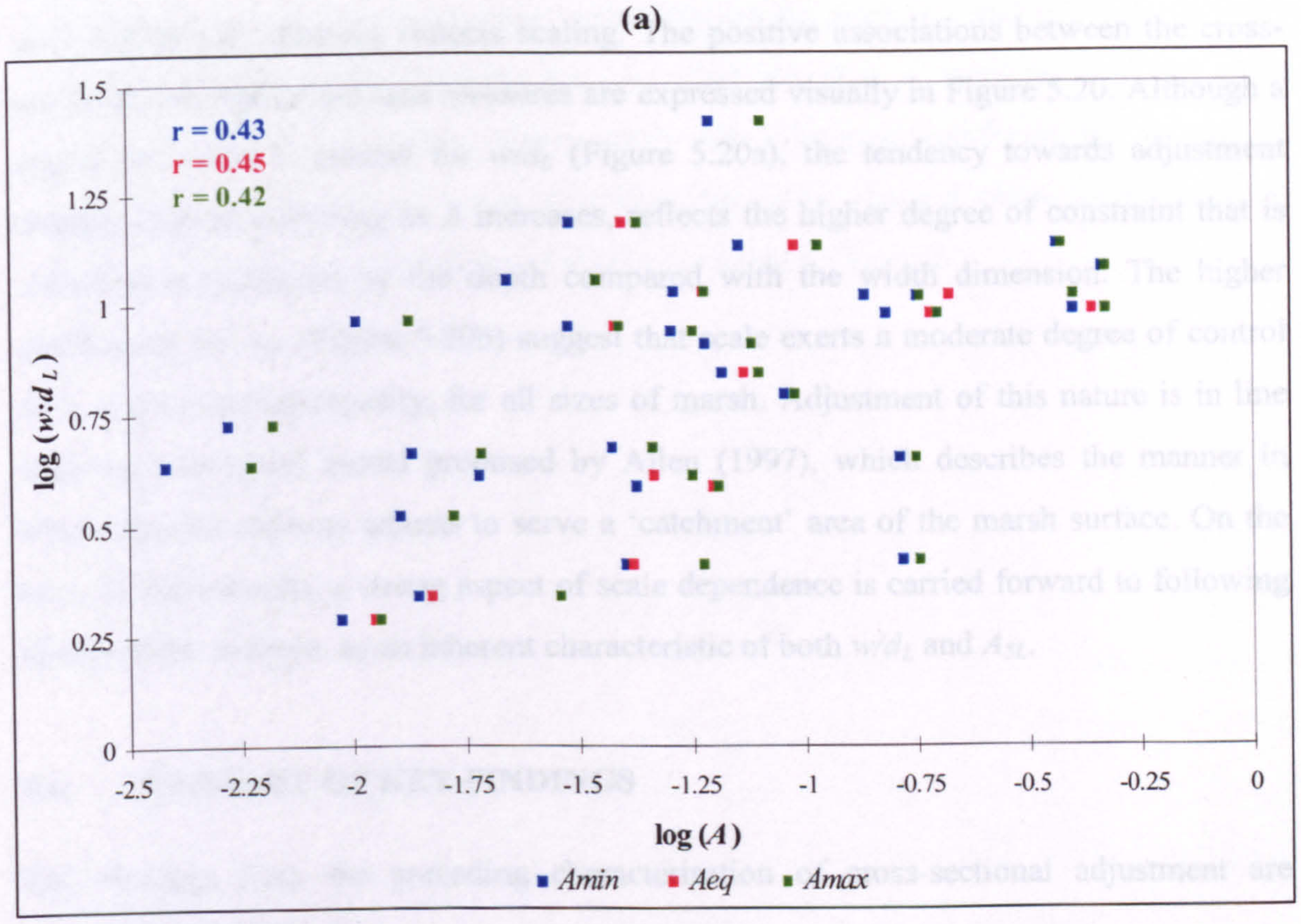

Figure 5.20 Scatter plots showing statistically significant levels of scale dependence for: (a) width:depth ratio ($w{:}d_L$); and (b) cross-sectional area (A_{SL}).

w/d_L, which only partially reflects scaling. The positive associations between the cross-sectional descriptors and area measures are expressed visually in Figure 5.20. Although a degree of scatter is present for w/d_L (Figure 5.20a), the tendency towards adjustment through channel widening as A increases, reflects the higher degree of constraint that is ultimately experienced by the depth compared with the width dimension. The higher coefficients for A_{SL} (Figure 5.20b) suggest that scale exerts a moderate degree of control over cross-sectional capacity, for all sizes of marsh. Adjustment of this nature is in line with the conceptual model proposed by Allen (1997), which describes the manner in which channel capacity adjusts to serve a 'catchment' area of the marsh surface. On the basis of these results, a strong aspect of scale dependence is carried forward to following phases of the analysis, as an inherent characteristic of both w/d_L and A_{SL}.

5.6 SUMMARY OF KEY FINDINGS

Key findings from the preceding characterisation of cross-sectional adjustment are summarised as follows:

- For the characterisation procedure, field-based survey is the most appropriate source of quantitative data, with photographic evidence and sketches yielding important information concerning cross-sectional shape. However, additional measurements, more appropriate to an intensive mode of study, are required to elucidate the processes behind the development of internal features such as benches.

- Systematic downstream patterns in cross-sectional form are evident throughout the sample networks. Dividing the system into upper, central and lower sectors provides a convenient framework for summarising these patterns of variability. Networks tend to maintain a similar pattern of adjustment from the central reaches through to the limit of vegetative cover. However, changing cross-sectional characteristics between the upper and central/lower sectors probably reflects spatial variations in the dominant physical controls.

- For comparative purposes, w/d_L and A_{SL} provide the greatest discriminating power between networks from England and Wales. Regression functions, which might potentially summarise network-wide adjustment, are inappropriate for tidal channels.

- Scale dependence is an important consideration for both A_{SL} and w/d_L. Statistically significant associations indicate that A_{SL} increases with A, implying that the creek system is adjusted to serve a given marsh area. Although significant, the strength of association with w/d_L is lower, indicating that while channel shape incorporates an element of scale, it is also adjusted to other external influences.

6. INTERPRETATION OF CHANNEL NETWORK MORPHOLOGY

6.1 INTRODUCTION

The *interpretation* of saltmarsh channel network morphology undertaken here, seeks to establish 'substantial relations of connection' (Sayer, 1992) between the planimetric, longitudinal and cross-sectional characteristics identified in Chapters 3-5, and a number of broad-scale environmental controls that may exert individual or collective influence over the pattern of adjustment. Although the suggestion has been made by a number of authors (Pestrong, 1965; Ranwell, 1972; Chapman, 1974) that spatial variability in the intensity of certain controlling elements is a source of regional diversity in morphological behaviour, this remains a working hypothesis. While the factors identified in Figure 2.8 are cited as being of *potential* importance, the studies in which they are described make only limited progress in exploring the underlying interactions.

Successful implementation of the extensive methodological procedure (see Section 2.1) to identify and explain causal relations depends on a number of factors, including: (1) selecting variables that are representative of the key external controls (Melton, 1958a; Chorley and Morgan, 1962); and (2) avoiding, where possible, interdependence between these measures (Richards, 1988). Quantitative expression of the chosen indicators is described in Section 6.2, and the issue of multicollinearity is addressed in Section 6.3. Although every effort was made to select conceptually irreducible expressions of planimetric, longitudinal and cross-sectional form, interrelations between descriptors employed for these planes of adjustment are assessed in Section 6.4. In light of findings from this exploratory data analysis, a statistical evaluation of bivariate associations between the control and response variables is undertaken in Section 6.5. The results are developed further in Section 6.6, through the use of multivariate techniques. Key findings are summarised in Section 6.7.

6.2 EXTERNAL CONTROL DATA

The elements controlling the morphological adjustment of tidal channel networks (Figure 2.8) fall into general categories of: (1) tidal forcing; (2) erodibility; (3) gradient effects;

and (4) extraneous considerations. From the list of variables that could be used to quantify these classes, a subset of 'readily observable properties' (Dyer *et al.*, 2000) can be identified, comprising: tidal prism; hydraulic duty; relative sea level change; percentage silt-clay content; vegetative composition; tidal range; intertidal gradient; coastal setting; and marsh area. Procedures involved in data acquisition, together with statistical characteristics of the resulting series, are described in the following sections.

6.2.1 Hydraulic duty

Conceptualised by Allen (1997), the *hydraulic duty* performed by tidal channel networks corresponds with the elevation deficit between high water and the marsh surface platform. While of interest from a historical perspective, since the balance between these levels is seen to reflect the evolutionary status of the system (Reed, 1995; Allen, 1997), the depth of tidal inundation is regarded as an important parameter in the emerging realm of network design (see, for example, Coates *et al.*, 1995; Haltiner *et al.*, 1997), through its influence on channel initiation and maintenance.

Myrick and Leopold (1963) observe that effectiveness and frequency are key criteria defining dominant flows in tidal systems. The discharge corresponding with maximum velocity was noted by Langbein (1963) to be of particular importance, and results obtained by French (1989) suggest that channel velocity increases with the depth of over-marsh flow. In terms of tidal forcing, a *maximum* hydraulic duty (H_{max}) can therefore be defined, which in theory has the greatest potential to perform erosive work, and as such may be causally related to the morphological characteristics of tidal channel networks. H_{max} is defined as:

$$H_{max} = HAT - \overline{E} \qquad [6.1]$$

where HAT relates to the highest astronomical tide that is predicted to occur under average meteorological conditions (Hydrographic Office, 1997), and $\overline{E}$ corresponds with the mean marsh surface elevation (see Figure 6.1). At several localities (Figure 5.9b), bank elevation falls towards the seaward limit of vegetative cover. However, in the absence of detailed terrain models for the sample systems, a spatially averaged statistic (see, for example, French, 1993) corresponding with an idealised horizontal marsh surface platform (Woolnough *et al.*, 1995), is the most realistic data currently available. Due to a lack of benchmarks in proximity to the study localities, elevation data (corrected to

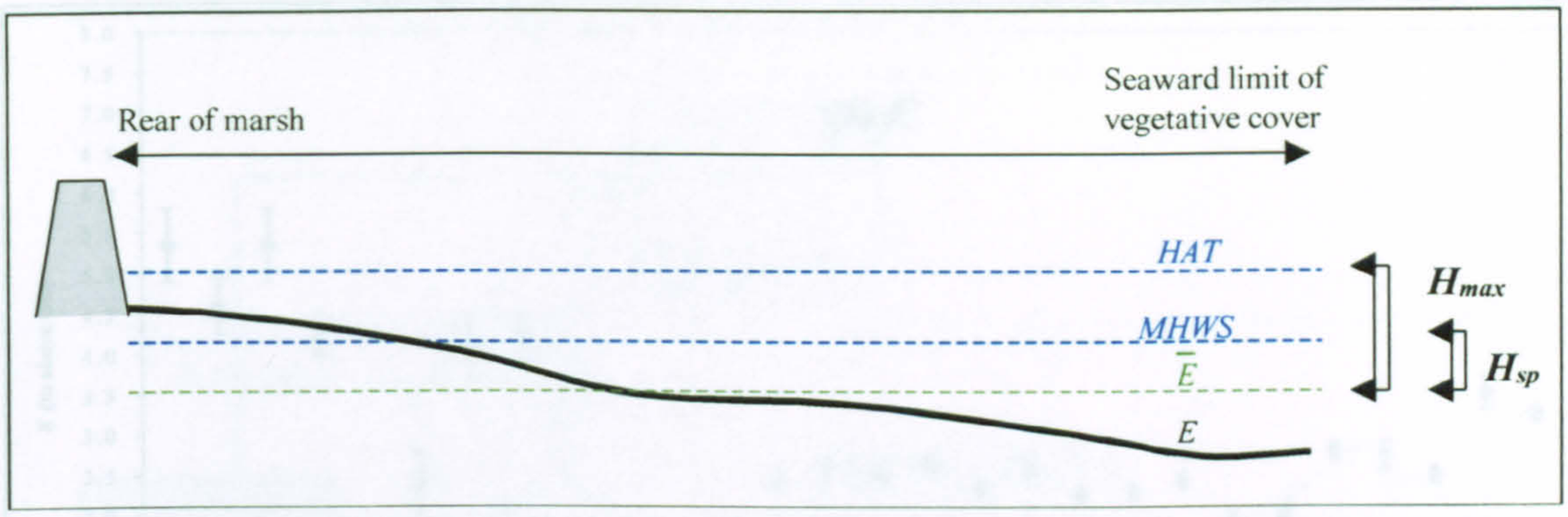

Figure 6.1 Definition diagram for the calculation of hydraulic duty.

Ordnance Datum (OD)) were obtained from a range of secondary sources, rather than through field survey. With the exception of Brancaster Marsh, for which airborne lidar altimetry was available (see Section 2.4.3), Environment Agency (EA) shore profiles were used to extract terrain information for sites throughout south-east and eastern England. Photogrammetric maps and derived profiles were acquired from the EA Southern division, for localities along the south coast. The high quality of these data is reflected by error margins of <5% surrounding values of $\overline{E}$ (Figure 6.2a). These uncertainties relate to fluctuations along the course of the profile, and allow for surface curvature, together with a degree of spatial offset between the sample sites and nearest transect. The absence of similarly reliable data for Wales and north-west England, is apparent from the increase in uncertainty to ~10% accompanying the use of data extracted from reports by Pye and French (1993) and Clarke *et al.* (1993). Elevation data proved unattainable for the marshes at Burry Inlet.

HAT was computed from Admiralty Tide Tables (Hydrographic Office, 1997) for a standard or secondary port in close proximity to each site. Details of the methodological procedure are summarised in Figure 6.3. A best-fit value was interpolated between ports for Brancaster Marsh, Scolt Head Island, the Stiffkey marshes, the River Orwell, and the River Ribble, which are situated some distance from any one data source. While the amplified error bars in Figure 6.2b reflect this element of uncertainty, the readings are otherwise considered accurate to within 3%.

Although *HAT* represents the most *effective* tidal conditions for performing erosive work, such a level of inundation will not necessarily be reached every year (Hydrographic Office, 1997). French and Stoddart (1992, p.235) observe that *'the marsh surface acts as a topographic threshold separating the depositional regime of below-marsh tides from the erosional (ebb dominated) regime of over-marsh tides'*. Following

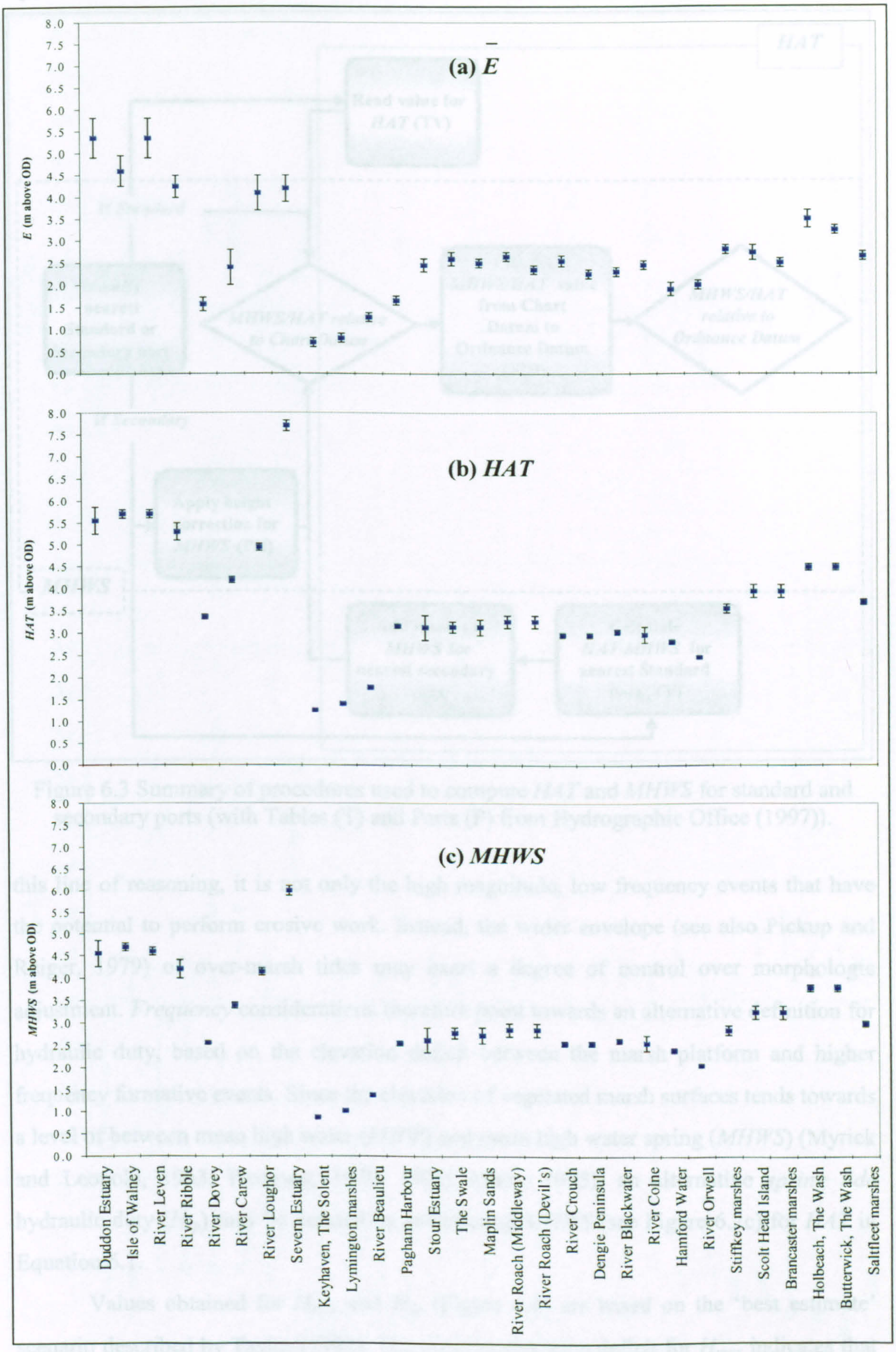

Figure 6.2 Statistical characteristics of input series for the calculation of hydraulic duty: (a) mean marsh surface elevation ($\bar{E}$); (b) Highest Astronomical Tide (*HAT*); and (c) Mean High Water Spring (*MHWS*). Margins of uncertainty about the best estimate are expressed by error bars.

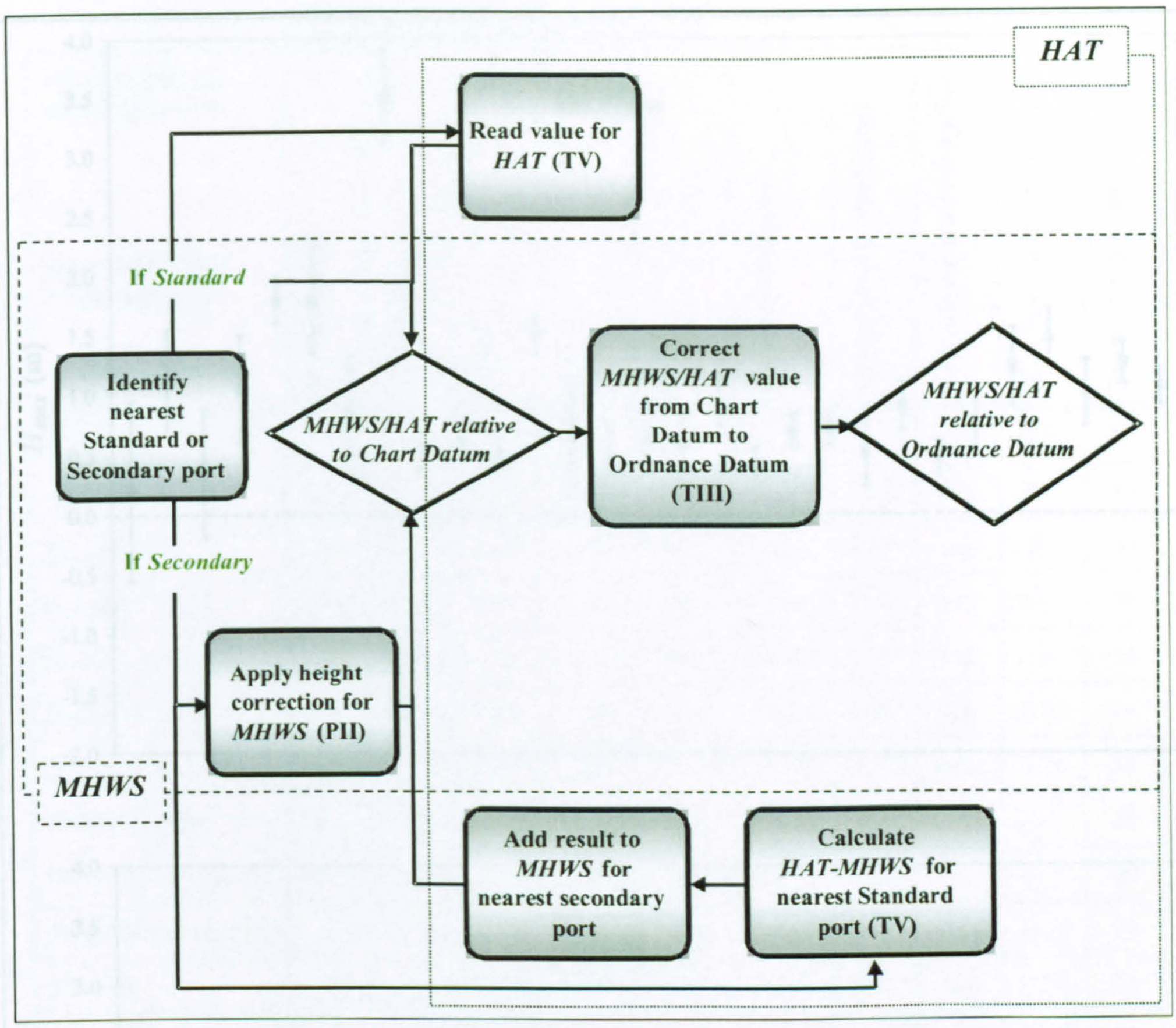

Figure 6.3 Summary of procedures used to compute *HAT* and *MHWS* for standard and secondary ports (with Tables (T) and Parts (P) from Hydrographic Office (1997)).

this line of reasoning, it is not only the high magnitude, low frequency events that have the potential to perform erosive work. Instead, the wider envelope (see also Pickup and Reiger, 1979) of over-marsh tides may exert a degree of control over morphologic adjustment. *Frequency* considerations therefore point towards an alternative definition for hydraulic duty, based on the elevation deficit between the marsh platform and higher frequency formative events. Since the elevation of vegetated marsh surfaces tends towards a level of between mean high water (*MHW*) and mean high water spring (*MHWS*) (Myrick and Leopold, 1963; Pestrong, 1970, 1972; Amos, 1995), an alternative *spring tide* hydraulic duty (H_{sp}) may be defined by substituting *MHWS* (see Figure 6.2c) for *HAT* in Equation 6.1.

Values obtained for H_{max} and H_{sp} (Figure 6.4) are based on the 'best estimate' scenario described by Taylor (1982). The positive elevation deficit for H_{max} indicates that all of the study sites experience a degree of tidal inundation during the course of the year. As such, they have yet to reach supratidal status (Amos, 1995; Allen, 1997), when

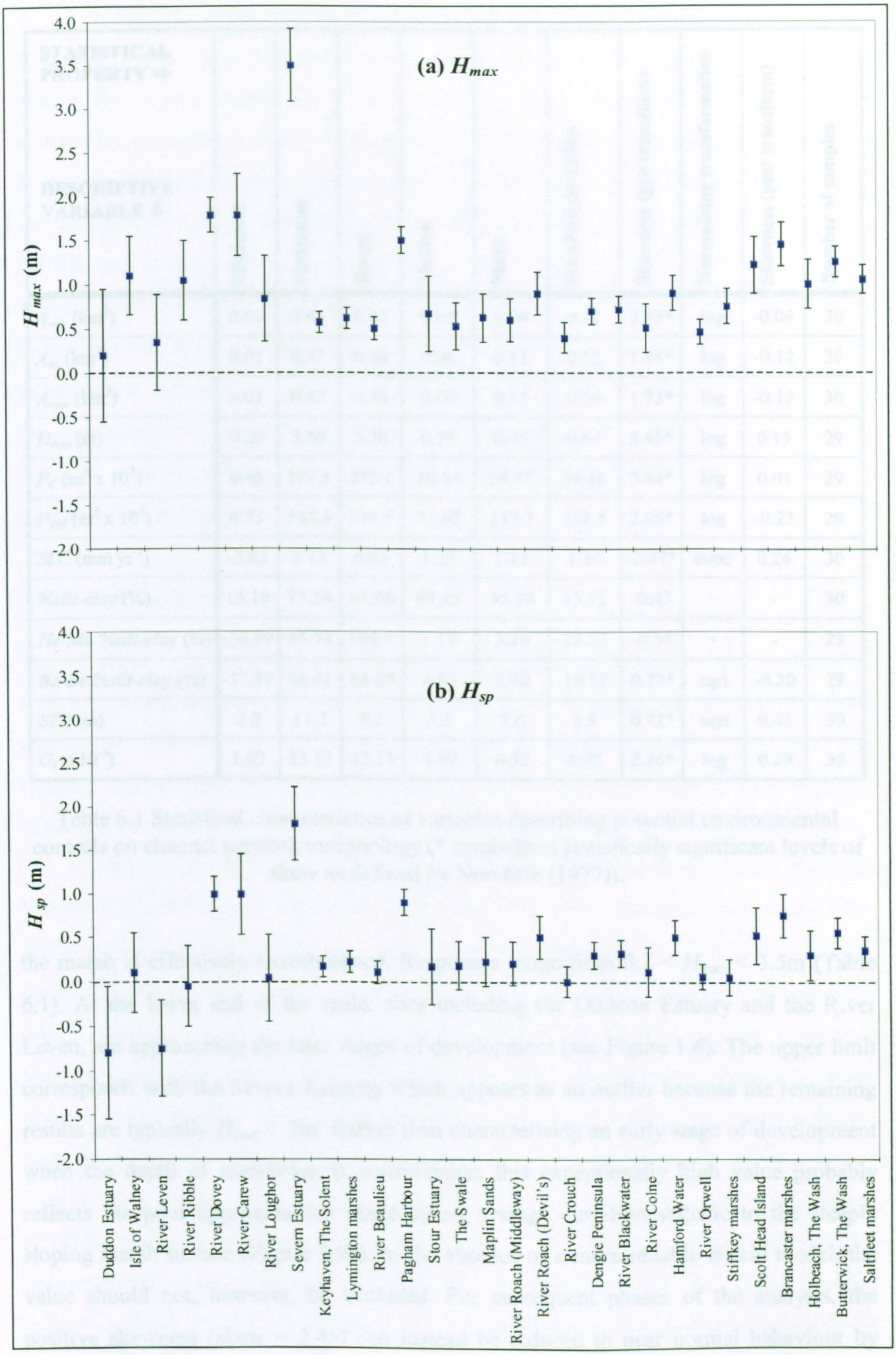

Figure 6.4 (a) Maximum hydraulic duty (H_{max}); and (b) spring hydraulic duty (H_{sp}), with margins of uncertainty about the best estimate expressed by error bars.

STATISTICAL PROPERTY ⇨ / DESCRIPTIVE VARIABLE ⇩	Minimum	Maximum	Range	Median	Mean	Standard deviation	Skewness (pre transform)	Normalising transformation	Skewness (post transform)	Number of samples
A_{min} (km^2)	0.01	0.46	0.46	0.05	0.09	0.11	2.05*	log	-0.04	30
A_{eq} (km^2)	0.01	0.47	0.46	0.06	0.11	0.12	1.88*	log	-0.12	30
A_{max} (km^2)	0.01	0.47	0.46	0.06	0.12	0.14	1.73*	log	-0.13	30
H_{max} (m)	0.20	3.50	3.30	0.75	0.95	0.64	2.45*	log	0.15	29
P_C (m^3 x 10^3)	0.45	273.5	273.1	10.53	29.42	54.58	3.64*	log	0.01	29
P_{TM} (m^3 x 10^3)	4.73	584.3	579.5	71.82	117.3	138.5	2.05*	log	-0.23	29
SLC (mm yr^{-1})	-3.82	3.13	6.95	1.28	1.15	1.30	-2.47*	cube	0.26	30
%silt-clay (%)	15.19	77.26	62.06	49.25	45.18	15.71	-0.43	-	-	30
He-Mo %silt-clay (%)	-56.99	45.74	102.7	1.19	3.16	23.37	-0.54	-	-	29
Ba-Be %silt-clay (%)	-17.19	46.91	64.09	4.88	8.90	16.37	0.77*	sqrt	-0.20	29
STR (m)	2.0	11.2	9.2	5.1	5.6	1.9	0.72*	sqrt	0.03	30
G_I (x10^{-3})	1.03	33.17	32.13	4.69	6.95	6.95	2.26*	log	0.29	30

Table 6.1 Statistical characteristics of variables describing potential environmental controls on channel network morphology (* symbolises statistically significant levels of skew as defined by Norcliffe (1977)).

the marsh is effectively terrestrialised. Responses range from 0.2 < H_{max} < 3.5m (Table 6.1). At the lower end of the scale, sites including the Duddon Estuary and the River Leven, are approaching the later stages of development (see Figure 1.6). The upper limit corresponds with the Severn Estuary, which appears as an outlier because the remaining results are typically H_{max} < 2m. Rather than characterising an early stage of development when the depth of inundation is considerable, this exceptionally high value probably reflects the poor approximation made by an average elevation statistic to the steeply sloping marsh surface (Figure 5.9b). In the absence of a more reliable terrain model, the value should not, however, be excluded. For subsequent phases of the analysis, the positive skewness (skew = 2.45) can instead be reduced to near normal behaviour by performing a logarithmic transformation.

In absolute terms, the elevation deficit of $-0.8 < H_{sp} < 1.8$m is small compared with $H_{max.}$. From Figure 6.4b, marsh surface elevation is approaching *MHWS* in the River Ribble, the River Loughor, the River Crouch, the River Orwell and at Stiffkey. These systems have reached a more advanced stage of development than marshes in the River Dovey, the River Carew and Pagham Harbour, where H_{sp} is substantial. Negative values for the Duddon Estuary and River Leven indicate that the marsh platform rises above *MHWS*, and is inundated by only the highest tides. As the transition is made from an actively evolving to a 'mature' system, the envelope of tidal fluxes received by these formations has been progressively truncated. Since the formative phases of channel initiation and extension occurred some time ago, it is unlikely that the current H_{sp} reflects the conditions to which creek morphology is adjusted. In general terms, H_{max} therefore provides a more realistic representation of effective tidal forcing than H_{sp}, which is considered no further in the analysis.

6.2.2 Tidal prism

The influence of *tidal prism* on network morphology has received considerable attention in the literature, through: (1) research concerning the geometric adjustment of channel reaches to dominant hydraulic fluxes (Myrick and Leopold, 1963; Chantler, 1974; Haltiner and Williams, 1987; Knighton *et al.*, 1992; Fenies and Faugeres, 1998), and (2) in the context of tidal inlet stability (Johnson, 1973; Hume, 1991; Gao and Collins, 1994).

Although a number of definitions are recorded in the literature (see, for example, Wright *et al.*, 1973; Dyer, 1997), the interpretation of tidal prism by Coates *et al.* (1995, p.17) as *'the volume of water in a marsh system contained between two defined tidal datums'* is particularly pertinent to this study. A range of datums has been employed in the prism calculation, which encapsulate varying degrees of physical realism. Computed between mean high water (*MHW*) and mean low water (*MLW*) levels, mean tidal prism (Coates *et al.*, 1995) excludes the overmarsh component of the tidal flux, which is known from process studies (French and Stoddart, 1992) to be an important driving force behind erosive work. With vertical limits comprising *MHWS* and mean low water spring (*MLWS*), spring tidal prism (Hume, 1991; Coates *et al.*, 1995) is not best suited to the present investigation, considering the negative values recorded for H_{sp} in the Duddon Estuary and the River Leven (Figure 6.4b). An alternative *maximum tidal prism* (P_{TM}) avoids this limitation, and incorporates both marsh surface and channelised flows (Figure 6.5).

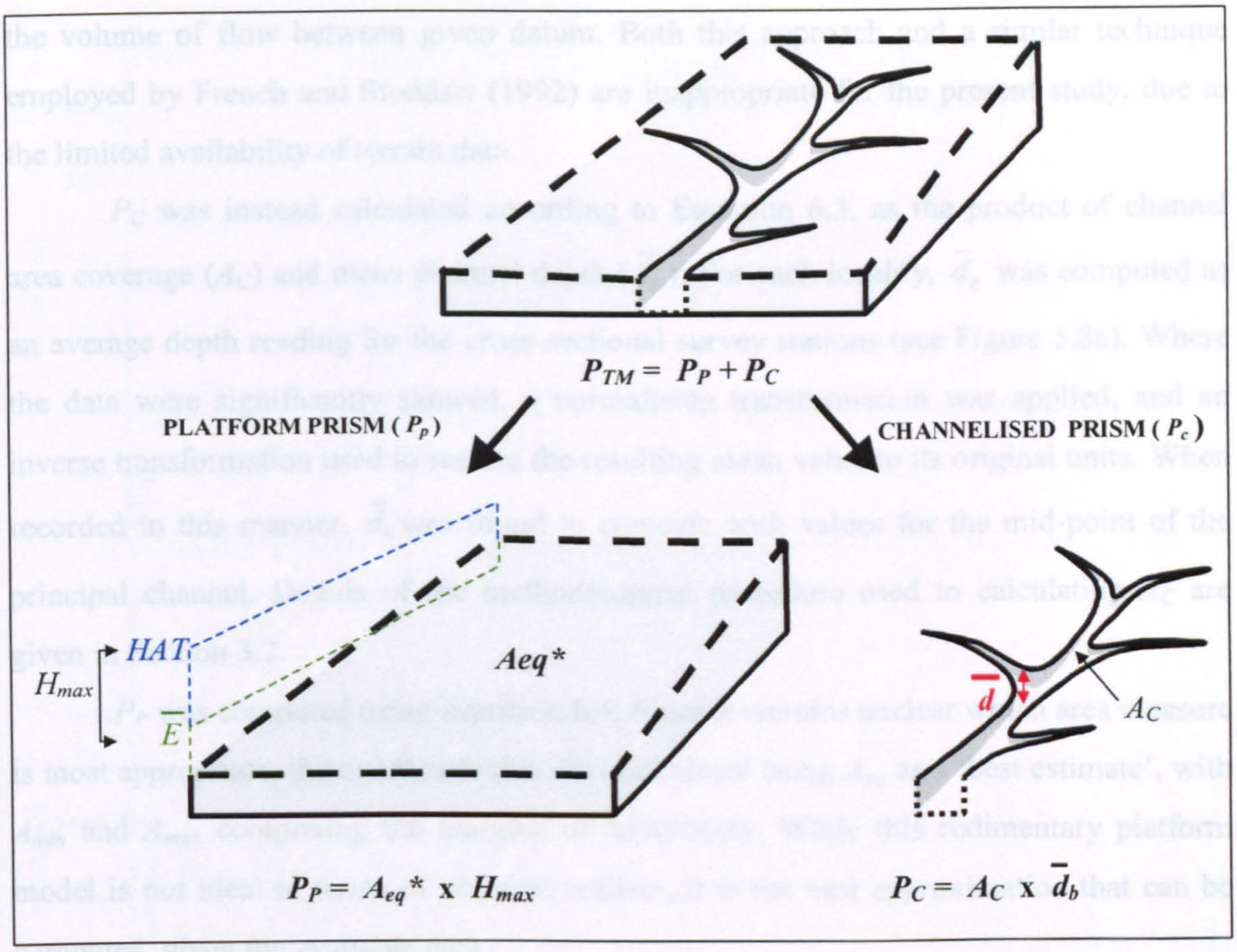

Figure 6.5 Definition diagram showing input measures involved in the computation of maximum total tidal prism (P_{TM}) from channelised (P_C) and platform (P_P) components, for an idealised tidal network.

$$P_{TM} = P_C + P_P \quad [6.2]$$

To simplify the calculation of P_{TM}, tidal prism can be divided into a channelised portion (P_C), and overmarsh or platform (P_P) flux (Equation 6.2). A number of procedures were considered for computing P_C. Gregory (1977) calculates a comparable measure of network volume, by integrating a downstream power function, where channel capacity is the dependent and total stream length the independent variable. However, this method was rejected in view of pronounced inaccuracies observed by Ferguson (1979). Coates *et al.* (1995) compute the volume between sequential cross-sections using the formula for a cone frustum. In this instance, the technique is inappropriate, because cross-sectional data were solely obtained along the principal channel. Introduced in a fluvial context by Strahler (1962), and implemented by Boon (1975), Pethick (1980), and Boon and Bryne (1981) in the study of tidal systems, hypsometric analysis may also be used to compute

the volume of flow between given datum. Both this approach and a similar technique employed by French and Stoddart (1992) are inappropriate for the present study, due to the limited availability of terrain data.

P_C was instead calculated according to Equation 6.3, as the product of channel area coverage (A_C) and mean channel depth ($\bar{d}_b$). For each locality, $\bar{d}_b$ was computed as an average depth reading for the cross-sectional survey stations (see Figure 5.8a). Where the data were significantly skewed, a normalising transformation was applied, and an inverse transformation used to restore the resulting mean value to its original units. When recorded in this manner, $\bar{d}_b$ was found to coincide with values for the mid-point of the principal channel. Details of the methodological procedure used to calculating A_C are given in Section 3.2.

P_P was computed using Equation 6.4. Since it remains unclear which area measure is most appropriate, the overmarsh flux was calculated using A_{eq} as a 'best estimate', with A_{min} and A_{max} comprising the margins of uncertainty. While this rudimentary platform model is not ideal in terms of physical realism, it is the best approximation that can be computed, given the available data.

$$P_C = A_C \; x \; d_b \qquad [6.3]$$

$$P_P = A_{eq}^{*} \; x \; H_{max} \qquad [6.4]$$

Values for P_C (Figure 6.6a) range between $0.45 < P_C < 273.5\text{m}^3 \text{ x}10^3$. Results for the River Colne fall at the upper end of the scale. Network volume is also considerable in the Duddon Estuary and the River Ribble. This subset of localities corresponds with the group of 'large' formations, identified during the analysis of scale dependence (Section 3.5). Formations bordering the Isle of Walney and the Dengie Peninsula, at Keyhaven, The Solent, in the River Orwell, and on Scolt Head Island, exhibit an intermediate capacity. At the lower end of the scale, reduced volumes in the River Dovey, the River Carew, and the River Beaulieu, may in part be explained by their state of development. The substantial hydraulic duty (Figure 6.4a) suggests that these marshes are actively developing, and it is likely that the channel system has yet to reach its maximum extent. Where the duty is lower in the River Leven, the River Loughor, the River Crouch, and bordering The Swale, values of $P_C < 10\text{m}^3 \text{ x}10^3$ cannot be explained by their developmental status, and instead point towards a systematic relation between marsh area and network volume.

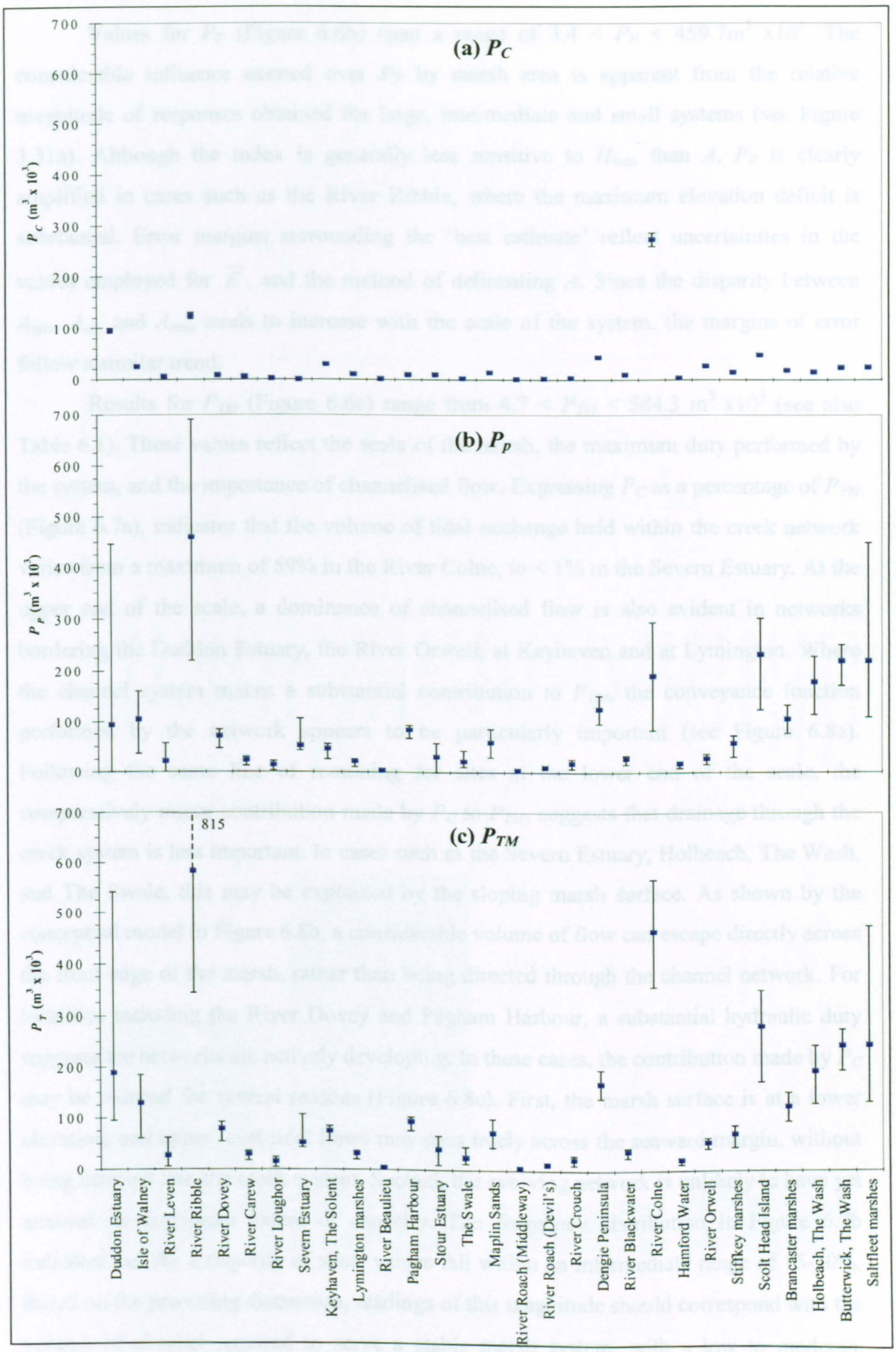

Figure 6.6 (a) Channelised (P_C) and (b) platform (P_P) components of (c) maximum tidal prism (P_{TM}), with margins of uncertainty about the best estimate expressed by error bars.

Values for P_P (Figure 6.6b) span a range of $3.4 < P_P < 459.7 m^3 \times 10^3$. The considerable influence exerted over P_P by marsh area is apparent from the relative magnitude of responses obtained for large, intermediate and small systems (see Figure 3.31a). Although the index is generally less sensitive to H_{max} than A, P_P is clearly amplified in cases such as the River Ribble, where the maximum elevation deficit is substantial. Error margins surrounding the 'best estimate' reflect uncertainties in the values employed for $\overline{E}$, and the method of delineating A. Since the disparity between A_{min}, A_{eq}, and A_{max} tends to increase with the scale of the system, the margins of error follow a similar trend.

Results for P_{TM} (Figure 6.6c) range from $4.7 < P_{TM} < 584.3\ m^3 \times 10^3$ (see also Table 6.1). These values reflect the scale of the marsh, the maximum duty performed by the system, and the importance of channelised flow. Expressing P_C as a percentage of P_{TM} (Figure 6.7a), indicates that the volume of tidal exchange held within the creek network varies from a maximum of 59% in the River Colne, to < 1% in the Severn Estuary. At the upper end of the scale, a dominance of channelised flow is also evident in networks bordering the Duddon Estuary, the River Orwell, at Keyhaven and at Lymington. Where the channel system makes a substantial contribution to P_{TM}, the conveyance function performed by the network appears to be particularly important (see Figure 6.8a). Following the same line of reasoning for sites at the lower end of the scale, the comparatively minor contribution made by P_C to P_{TM}, suggests that drainage through the creek system is less important. In cases such as the Severn Estuary, Holbeach, The Wash, and The Swale, this may be explained by the sloping marsh surface. As shown by the conceptual model in Figure 6.8b, a considerable volume of flow can escape directly across the front edge of the marsh, rather than being directed through the channel network. For localities including the River Dovey and Pagham Harbour, a substantial hydraulic duty suggests the networks are actively developing. In these cases, the contribution made by P_C may be reduced for several reasons (Figure 6.8c). First, the marsh surface is at a lower elevation, and upper level tidal flows may pass freely across the seaward margin, without being directed into the creek system. Second, the evolving network is unlikely to have yet attained its maximum extent or capacity. The frequency distribution in Figure 6.7b indicates that for a majority of sites, values fall within an intermediate range of 15-30%. Based on the preceding discussion, readings of this magnitude should correspond with the volume of channel required to serve a stable marsh system, with a low to moderate surface gradient (Figure 6.8d).

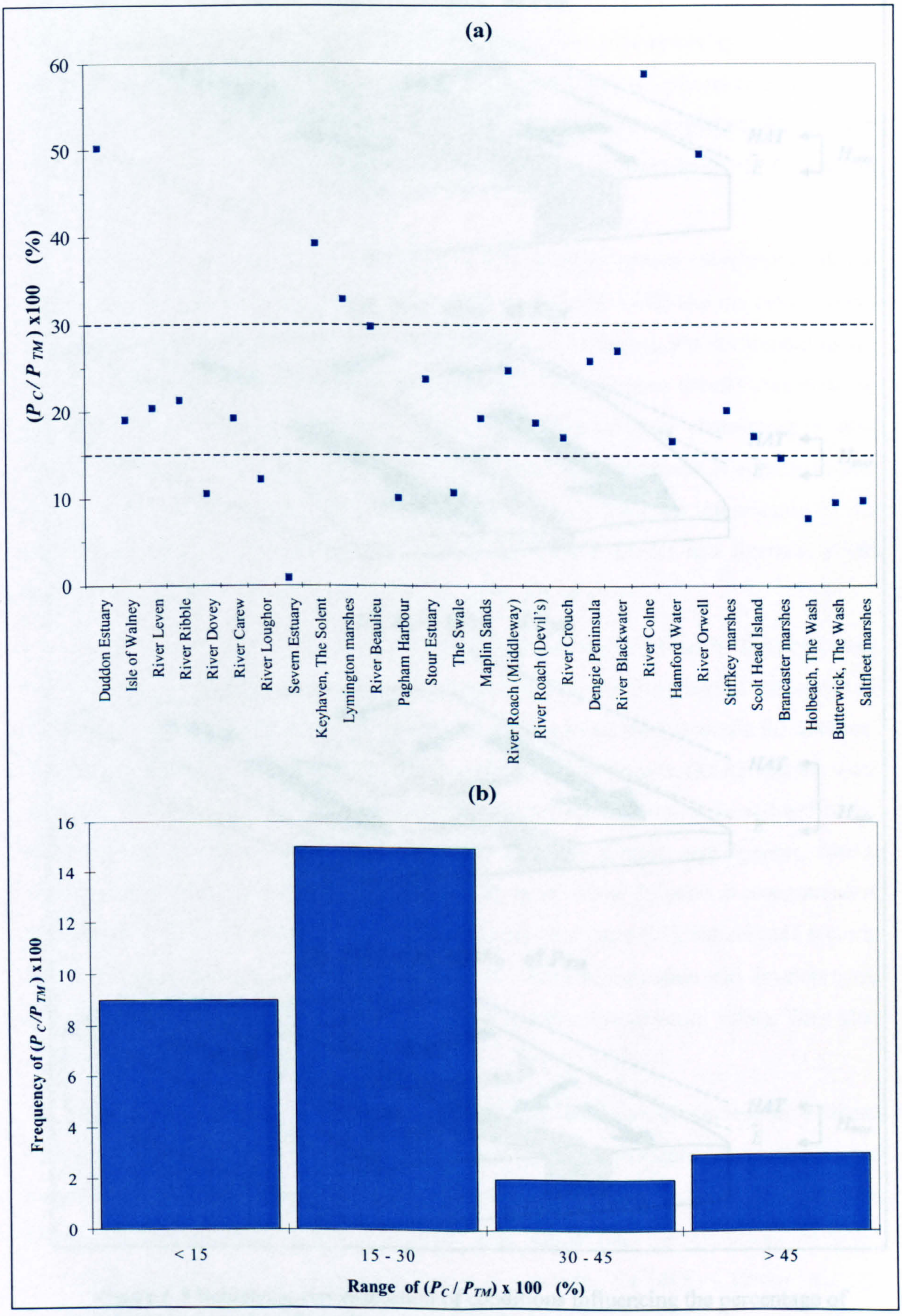

Figure 6.7 (a) Geographical distribution of channelised prism (P_C) expressed as a percentage of the total maximum tidal prism (P_{TM}); and (b) the frequency distribution of values obtained.

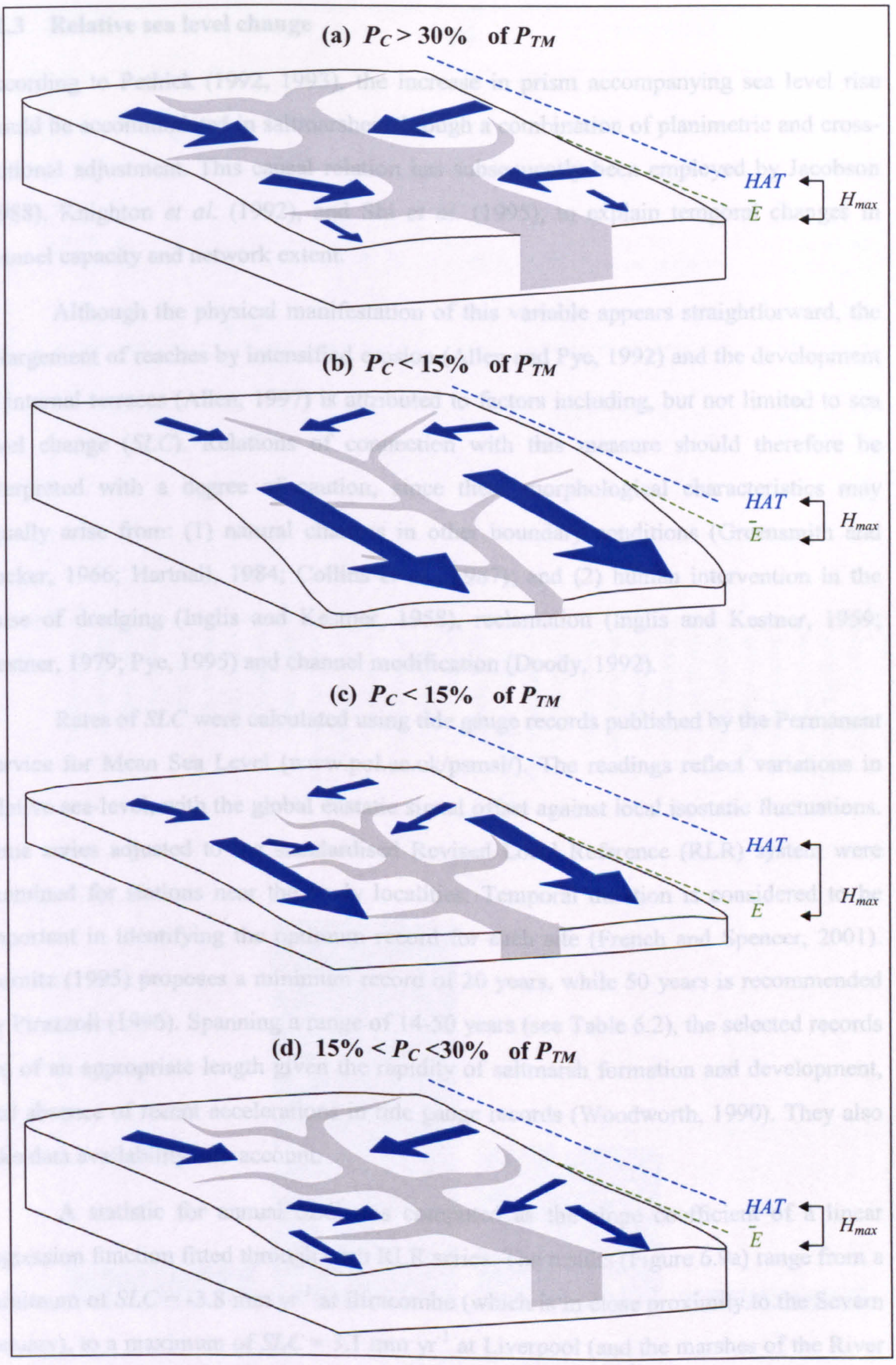

Figure 6.8 Schematic representation of conditions influencing the percentage of total maximum tidal prism (P_{TM}) accounted for by the channelised component (P_C) (see text for explanation).

6.2.3 Relative sea level change

According to Pethick (1992, 1993), the increase in prism accompanying sea level rise should be accommodated in saltmarshes, through a combination of planimetric and cross-sectional adjustment. This causal relation has subsequently been employed by Jacobson (1988), Knighton *et al.* (1992), and Shi *et al.* (1995), to explain temporal changes in channel capacity and network extent.

Although the physical manifestation of this variable appears straightforward, the enlargement of reaches by intensified erosion (Allen and Pye, 1992) and the development of internal terraces (Allen, 1997) is attributed to factors including, but not limited to sea level change (*SLC*). Relations of connection with this measure should therefore be interpreted with a degree of caution, since these morphological characteristics may equally arise from: (1) natural changes in other boundary conditions (Greensmith and Tucker, 1966; Hartnall, 1984; Collins *et al.*, 1987); and (2) human intervention in the guise of dredging (Inglis and Kestner, 1958), reclamation (Inglis and Kestner, 1959; Kestner, 1979; Pye, 1995) and channel modification (Doody, 1992).

Rates of *SLC* were calculated using tide gauge records published by the Permanent Service for Mean Sea Level (www.pol.ac.uk/psmsl/). The readings reflect variations in relative sea-level, with the global eustatic signal offset against local isostatic fluctuations. Time series adjusted to the standardised Revised Local Reference (RLR) system were examined for stations near the study localities. Temporal duration is considered to be important in identifying the optimum record for each site (French and Spencer, 2001). Gornitz (1995) proposes a minimum record of 20 years, while 50 years is recommended by Pirazzoli (1996). Spanning a range of 14-50 years (see Table 6.2), the selected records are of an appropriate length given the rapidity of saltmarsh formation and development, and absence of recent accelerations in tide gauge records (Woodworth, 1990). They also take data availability into account.

A statistic for annual *SLC* was computed as the slope coefficient of a linear regression function fitted through each RLR series. The results (Figure 6.9a) range from a minimum of $SLC = -3.8$ mm yr^{-1} at Ilfracombe (which is in close proximity to the Severn Estuary), to a maximum of $SLC = 3.1$ mm yr^{-1} at Liverpool (and the marshes of the River Ribble). Although a fall in relative sea level was computed for Milford Haven (and the River Carew network), the frequency distribution in Figure 6.9b shows that most

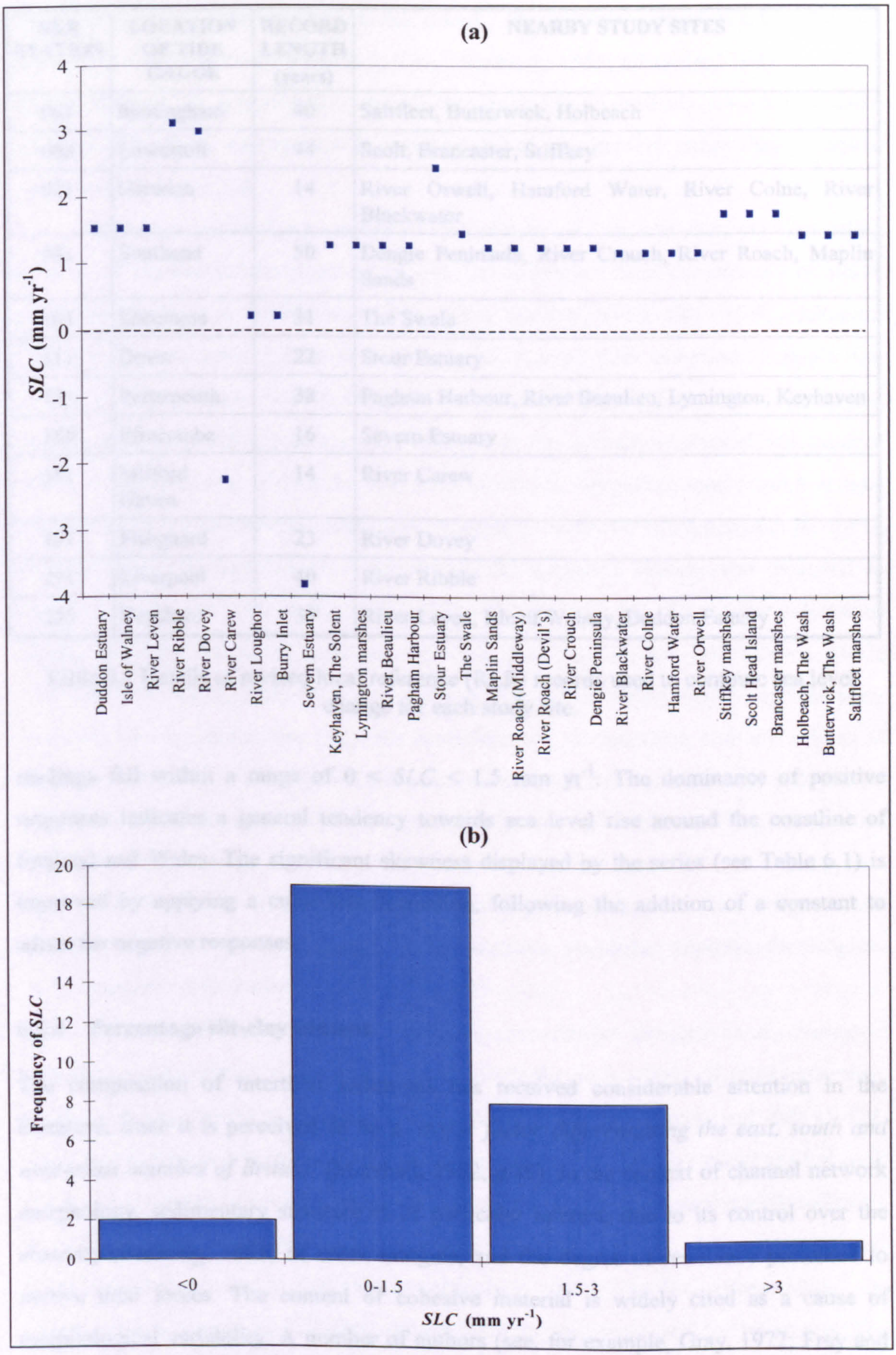

Figure 6.9 (a) Geographical distribution of sea level change (*SLC*); and (b) the frequency distribution of values obtained.

RLR STATION	LOCATION OF TIDE GAUGE	RECORD LENGTH (years)	NEARBY STUDY SITES
061	Immingham	40	Saltfleet, Butterwick, Holbeach
068	Lowestoft	44	Scolt, Brancaster, Stiffkey
071	Harwich	14	River Orwell, Hamford Water, River Colne, River Blackwater
081	Southend	50	Dengie Peninsula, River Crouch, River Roach, Maplin Sands
101	Sheerness	31	The Swale
111	Dover	22	Stour Estuary
131	Portsmouth	38	Pagham Harbour, River Beaulieu, Lymington, Keyhaven
166	Ilfracombe	16	Severn Estuary
181	Milford Haven	14	River Carew
191	Fishguard	23	River Dovey
211	Liverpool	40	River Ribble
225	Heysham	39	River Leven, Isle of Walney, Duddon Estuary

Table 6.2 Details of revised local reference (RLR) records used to compute sea level change for each study site.

readings fall within a range of $0 < SLC < 1.5$ mm yr^{-1}. The dominance of positive responses indicates a general tendency towards sea level rise around the coastline of England and Wales. The significant skewness displayed by the series (see Table 6.1) is improved by applying a cubic transformation, following the addition of a constant to adjust for negative responses.

6.2.4 Percentage silt-clay content

The composition of intertidal sediments has received considerable attention in the literature, since it is perceived to be a *'major factor differentiating the east, south and west-coast marshes of Britain'* (Marshall, 1962, p.89). In the context of channel network morphology, sedimentary structure is of particular interest, due to its control over the erosivity (Pestrong, 1965) of creek margins, and the degree of resistance presented to motive tidal forces. The content of cohesive material is widely cited as a cause of morphological variability. A number of authors (see, for example, Gray, 1972; Frey and Bassan, 1985; Jacobsen, 1988; Adam, 1990; Allen, 1992) concur with the observation by Chapman (cited in Ragotzkie, 1959, p.28) that '*you get a different type of creek system on*

a very sandy marsh compared to a muddy marsh'. The moisture content of tidal substrates is also an influential factor (Marshall, 1962; Pestrong, 1965; Chapman, 1974; Coates *et al.*, 1995). However, quantifying a variable that is temporally unsteady poses considerable practical difficulties, and as such is better suited to an intensive rather than extensive methodological approach.

While the results from studies of fluvial networks suggest that: (1) contrasting patterns of planimetric development reflect the different infiltration capacity of sandy versus silty substrates (Morisawa, 1962, 1964; Strahler, 1964; Day, 1980; Schumm, 1997); (2) cross-sectional form is a function of channel bank cohesion (Leopold and Maddock, 1953; Thorne and Tovey, 1981; Pizzuto, 1984); and (3) the shape of the longitudinal profile reflects downstream changes in the strength of channel bed material (Hack, 1957; Shepherd, 1985), the operation of similar controlling mechansims in tidal systems has yet to be formally established. In order to assess the influence of erosivity on all three planes of morphological adjustment, the sampling strategy was designed to record variations both at-a-station and in a downstream direction. To register patterns of change along the course of each network (see also Van Straaten and Kuenen, 1957; Pestrong, 1970, 1972; Zeff, 1988; and Ayles and Lapointe, 1996), sample stations were established in the headwaters (He), the central/middle reaches (Mi), and at the limit of vegetative cover or mouth (Mo) of the principal channel. To investigate the presence of intra-reach variability (see also Pestrong, 1965; Steers, 1977; Hume, 1991; and Miller, 1991), separate readings were acquired for active channel bank and floor facets (see Figure 5.3). In order to mitigate the influence of vegetative material, bank samples were taken below the limit of root binding. The thalweg was avoided to minimise the transient load contained within the bed sample.

Although Pizzuto (1984) successfully uses tensile strength as an indicator, sedimentary composition of the channel perimeter is the more widely reported parameter. In line with the procedure employed by Haynes and Dobson (1969) and Zeff (1988), samples of the surface sediment (extending to a depth of ~0.05m) were collected at each station. On returning to the laboratory, the composition of the material was analysed using the wet sieving technique (Courtney and Trudgill, 1976). Since proportional representation of cohesive material is particularly relevant to the present study, the substrate was separated into silt/clay and sand/gravel components, and the percentage silt-clay content (*%silt-clay*) computed.

For each network, results from the tiered sampling of sedimentary characteristics

may be analysed at: (1) regional; (2) downstream; and (3) reach spatial scales. *Regional* patterns of response are recorded by the average statistics in Figure 6.10a. Broad geographical diversity is evident, of the nature identified in U.S. marshes by Pestrong (1965), and their British counterparts by Marshall (1962) and Chapman (1974). The *%silt-clay* is consistently low in north-west England and Wales, with a minimum of *%silt-clay* < 20% recorded in networks bordering the Duddon Estuary and the River Dovey. The Severn Estuary forms a boundary between these predominantly sandy systems, and the more cohesive constituents of marshes along the south coast, and throughout south-east England. Values of *%silt-clay* peak at Hamford Water, before rapidly decreasing in the Norfolk marshes and remaining formations of eastern England. On average (see Table 6.1), responses tend towards an intermediate level of *%silt-clay* = 45%, which corresponds closely with the distinction by Pye and Crooks (1995) between cohesive and non-cohesive substrates. With readings fairly evenly distributed about this value, it is not necessary to apply a normalising transformation to the series.

Downstream patterns of response (see, for example, Van Straaten and Kuenen, 1957; Ayles and Lapointe, 1996) are represented in Figure 6.10b, as the average of bed and bank readings for stations in the upper, central and lower reaches of each system. Systematic headward fining is present in more than half of the study sites. According to the model proposed by Pestrong (1970, 1972), this spatial gradient of sediment texture may be expected where the channel network performs a normal dispersive function. Irregular distributions at the remaining localities suggest that a different set of factors control the nature of substrate material. The concentration of cohesive sediment towards the seaward limit of marsh development at Keyhaven and Saltfleet, and bordering the River Beaulieu and The Swale, may be attributable to the reworking of substrates. Alternatively, it could reflect changes in the source material, or be related to alterations in the tidal flow regime.

Intra-reach variations are recorded in Figure 6.10c, as the average downstream reading for the channel bed, and also the channel bank. Results indicate that the content of cohesive material is consistently higher along the creek margin than on the floor. Several mechanisms have been proposed, which may explain this disparity. Steers (1959, p.75) notes that in the case of Norfolk marshes, the bottoms of creeks '*are part of the substratum*', the implication being that differences in bed and bank material are an inherent characteristic of the wider coastal setting in which the saltmarsh has developed. In contrast, French and Stoddart (1992), observe that the dispersal of fine material across

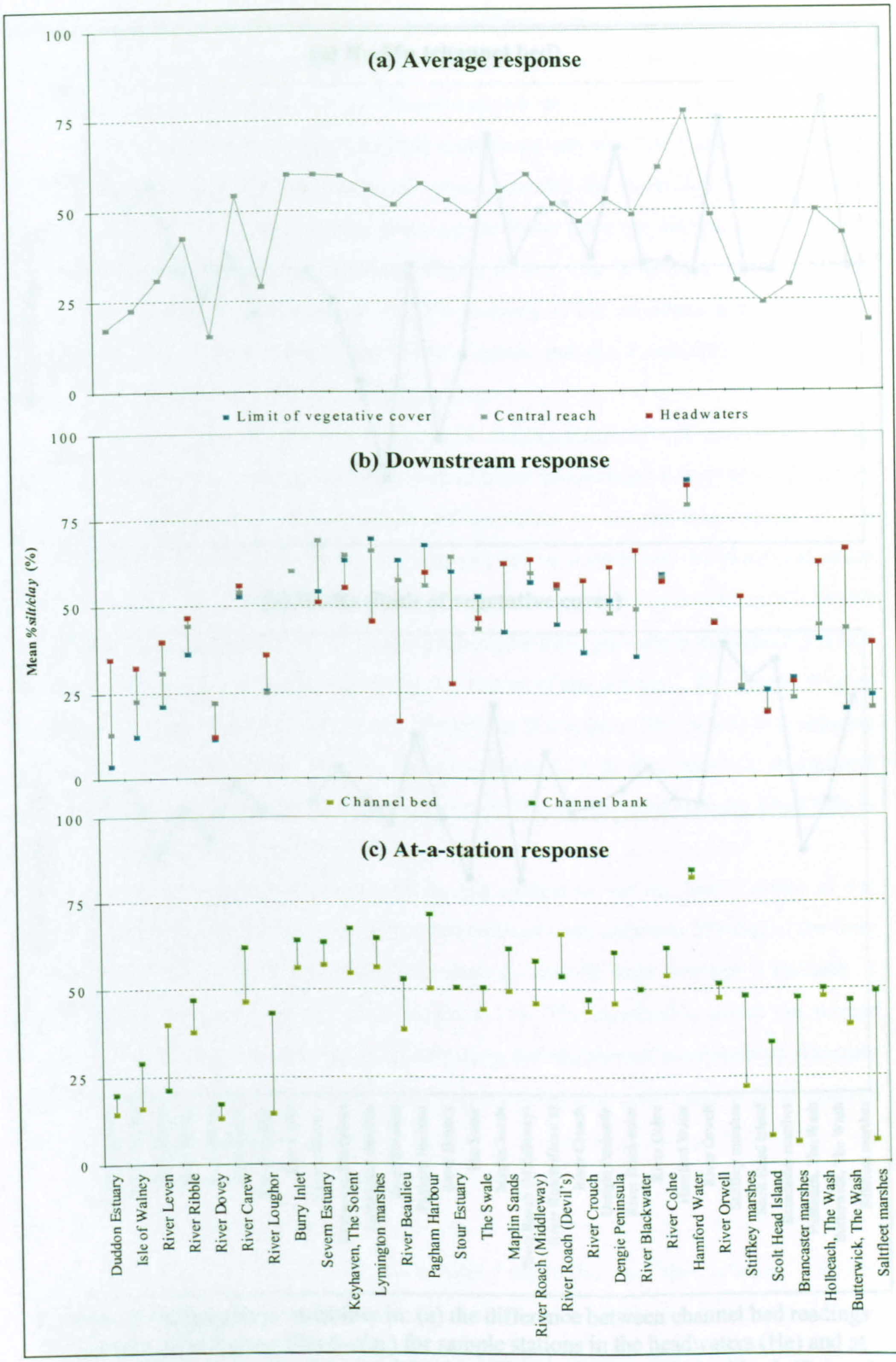

Figure 6.10 Geographical variability in: (a) average; (b) downstream; and (c) at-a-station readings of sediment cohesiveness (*%silt-clay*).

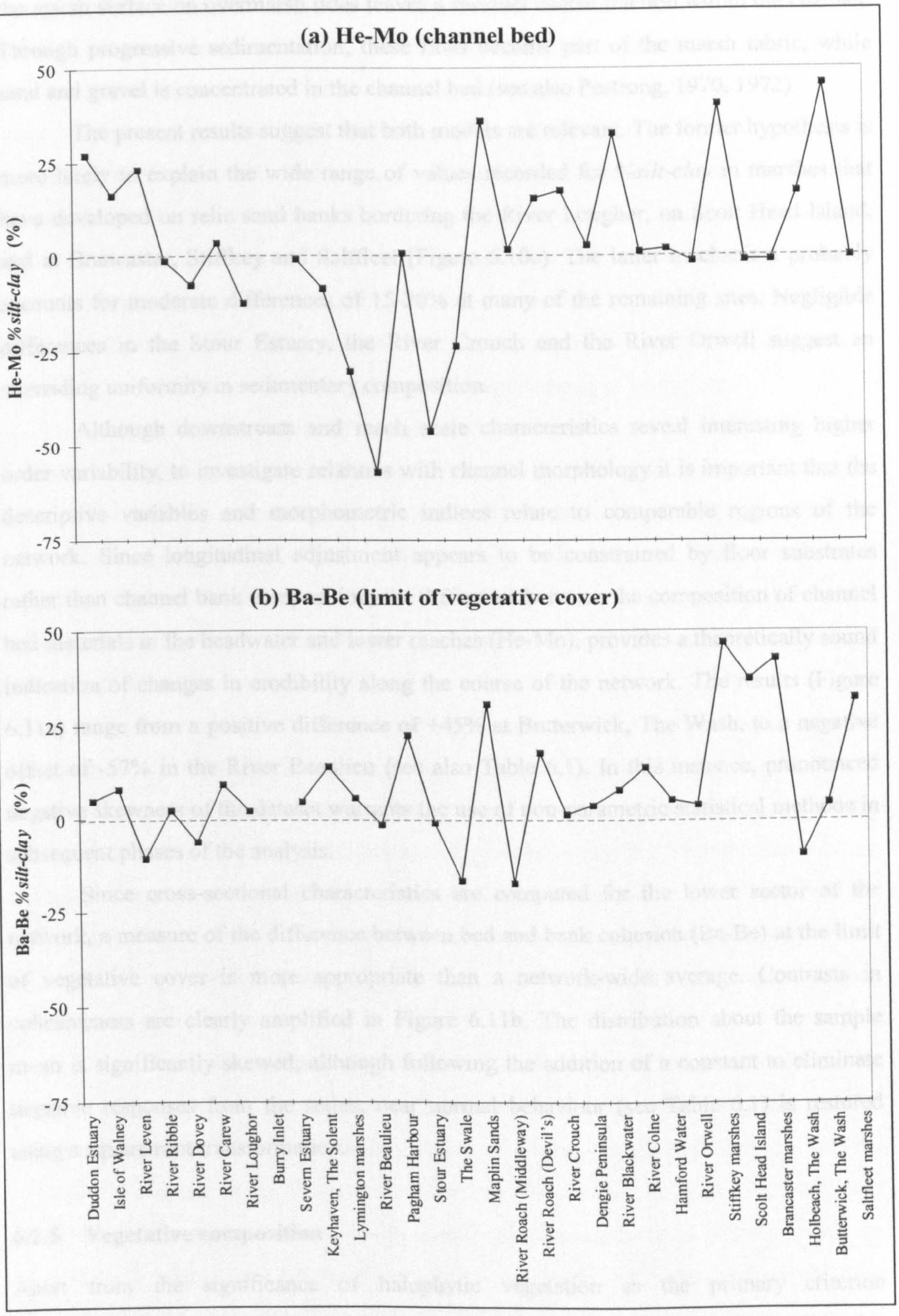

Figure 6.11 Geographical variability in: (a) the difference between channel bed readings of sediment cohesiveness (*%silt-clay*) for sample stations in the headwaters (He) and at the limit of vegetative cover (Mo); and (b) the difference between channel bank (Ba) and bed (Be) readings at the limit of vegetative cover.

the marsh surface on overmarsh tides leaves a residual coarse fraction within the channel. Through progressive sedimentation, these fines become part of the marsh fabric, while sand and gravel is concentrated in the channel bed (see also Pestrong, 1970, 1972).

The present results suggest that both models are relevant. The former hypothesis is more likely to explain the wide range of values recorded for *%silt-clay* in marshes that have developed on relic sand banks bordering the River Loughor, on Scolt Head Island, and at Brancaster, Stiffkey and Saltfleet (Figure 6.10c). The latter mechanism probably accounts for moderate differences of 15-20% at many of the remaining sites. Negligible differences in the Stour Estuary, the River Crouch and the River Orwell suggest an overriding uniformity in sedimentary composition.

Although downstream and reach scale characteristics reveal interesting higher order variability, to investigate relations with channel morphology it is important that the descriptive variables and morphometric indices relate to comparable regions of the network. Since longitudinal adjustment appears to be constrained by floor substrates rather than channel bank composition, the difference between the composition of channel bed materials in the headwater and lower reaches (He-Mo), provides a theoretically sound indication of changes in erodibility along the course of the network. The results (Figure 6.11a) range from a positive difference of +45% at Butterwick, The Wash, to a negative offset of -57% in the River Beaulieu (see also Table 6.1). In this instance, pronounced negative skewness of the dataset warrants the use of non-parametric statistical methods in subsequent phases of the analysis.

Since cross-sectional characteristics are computed for the lower sector of the network, a measure of the difference between bed and bank cohesion (Ba-Be) at the limit of vegetative cover is more appropriate than a network-wide average. Contrasts in cohesiveness are clearly amplified in Figure 6.11b. The distribution about the sample mean is significantly skewed, although following the addition of a constant to eliminate negative responses from the series, near normal behaviour (see Table 6.1) is restored using a square root transformation.

6.2.5 Vegetative composition

Apart from the significance of halophytic vegetation as the primary criterion distinguishing saltmarsh from other intertidal zones (Pestrong, 1965), vegetative composition exerts an important control over channel network morphology, through the degree of resistance to erosion presented by colonised creek margins (Pestrong, 1965;

Steers, 1977; Williams and Harvey, 1983; Van Eerdt, 1985; Coates *et al.*, 1995). Following the early stages of channel initiation (Section 1.4.4), when pioneer species are seen to enhance planimetric development (Frey and Bassan, 1985), the binding action of more mature communities limits further elaboration (Shi *et al.*, 1995; Fenies and Faugeres, 1998), and in the latter stages may accelerate devolution (see, for example, Yapp *et al.*, 1917; Collins *et al.*, 1987). The species composition is therefore an important degree of freedom in the envelope of controlling elements, through its potential influence on erodibility. It also provides insight into the developmental status of the selected marsh localities (Ranwell, 1972; Chapman, 1974), and can be used alongside hydraulic duty to assess whether the sample networks are at a comparable stage of evolution.

Classificatory procedures of varying complexity are documented in the literature. The detailed mapping undertaken by Adam (1981) in producing the National Vegetation Classification (NVC) is superfluous, given the extensive nature of the present analysis. While maintaining a general distinction between low, mid and upper floristic zones, the simplified classes employed by Burd (1989) are more appropriate here. The correspondence between nominal classes, a generic framework, and the NVC categories is shown in Table 6.3.

For each locality, the composition of marsh surface vegetation was recorded during June-July 1999, by field observation along a transect between the landward and seaward limit of halophytic colonisation. A single dominant class was subsequently identified, characterising the marsh system as a whole. While it is appropriate to use an average measure at most localities, horizontal zonation (see Dalby, 1970; and Ranwell, 1972; Zedler et al., 1999) was observed where the marsh platform is more steeply inclined, in the Severn Estuary, The Swale, and at Holbeach and Butterwick (see Plate 6.1a-b).

From Table 6.3, a broad distinction is in order between systems dominated by pioneer, mid, and upper marsh species. The majority of study sites (53%) fall into the mid-marsh category, due to a predominance of diagnostic species such as *Atriplex portulacoides* (Plate 6.2a), *Puccinellia maritima* and *Limonium vulgare* (Plate 6.2b). These formations have reached a stable state of development (see Figure 1.6), and are most likely to be in a state of equilibrium with contemporary environmental controls (see also Pickup and Reiger, 1979). Diagnostic pioneer species such as *Salicornia spp.* and *Spartina spp.* (Plate 6.2c) were particularly abundant at 17% of the study localities, the implication being that these sites are actively evolving. Comparison with the values

CLASS	COMMUNITY*	NVC** COMMUNITIES	DIAGNOSTIC SPECIES	STUDY LOCALITIES	
1	**Pioneer / low marsh**	SM 4-9 SM 11-12	*Spartina spp.* *Salicornia spp.* *Suaeda maritima* *Aster tripolium*	Isle of Walney River Carew Keyhaven, The Solent	Lymington Pagham Harbour
2	**Mid marsh**	SM 10 SM 13-14	*Atriplex portulacoides* *Puccinellia maritima* *Limonium vulgare*	River Dovey River Loughor River Beaulieu Stour Estuary Maplin Sands River Roach Dengie Peninsula River Blackwater	River Colne Hamford Water River Orwell Scolt Head Island Brancaster Harbour Butterwick, The Wash Saltfleet marshes
3	**Upper marsh**	SM 15-18 SM 24 SM 28	*Elytrigia spp.* *Atriplex prostrata* *Armeria maritima* *Juncus spp.* *Festuca rubra*	Duddon Estuary River Leven River Ribble Burry Inlet Severn Estuary	The Swale River Crouch Stiffkey marshes Holbeach, The Wash

Table 6.3 Classification scheme used to establish the dominant vegetative community at each site, based on previous studies by **Adam (1981) and *Burd (1989).

obtained for hydraulic duty (Figure 6.4a) confirm a considerable elevation deficit at the Isle of Walney, Pagham Harbour, and in the River Carew. The marginal offset at Keyhaven and Lymington may be explained by the reduced tidal range (see Section 6.2.6). While these systems are by no means poorly adjusted to current external influences, channel network morphology may be underdeveloped or sub-extended (see Table 3.2), since it clearly has the potential to elaborate further before the system attains a 'mature' developmental status (Figure 1.6). The remaining localities are characterised by upper marsh species. In north-west England, grazed swards (Plate 6.2e) fringing the River Leven and the Duddon Estuary are dominated by *Armeria maritima* and *Festuca rubra*. Elsewhere, grasses such as *Elytrigia spp.* (Plate 6.2d) are diagnostic of systems in the later stages of development. While differences in developmental status are likely to introduce an additional element of noise into relations between control and response variables (Haltiner and Williams, 1987), the intensity of key environmental influences is unlikely to have changed to the extent that a Type I error (Shaw and Wheeler, 1997) is made.

(a)

(b)

Plate 6.1 Horizontal zonation observed between: (a) mid-marsh species at the landward boundary; and (b) pioneer species at the seaward limit of vegetative colonisation, Butterwick, The Wash.

(a)

(b)

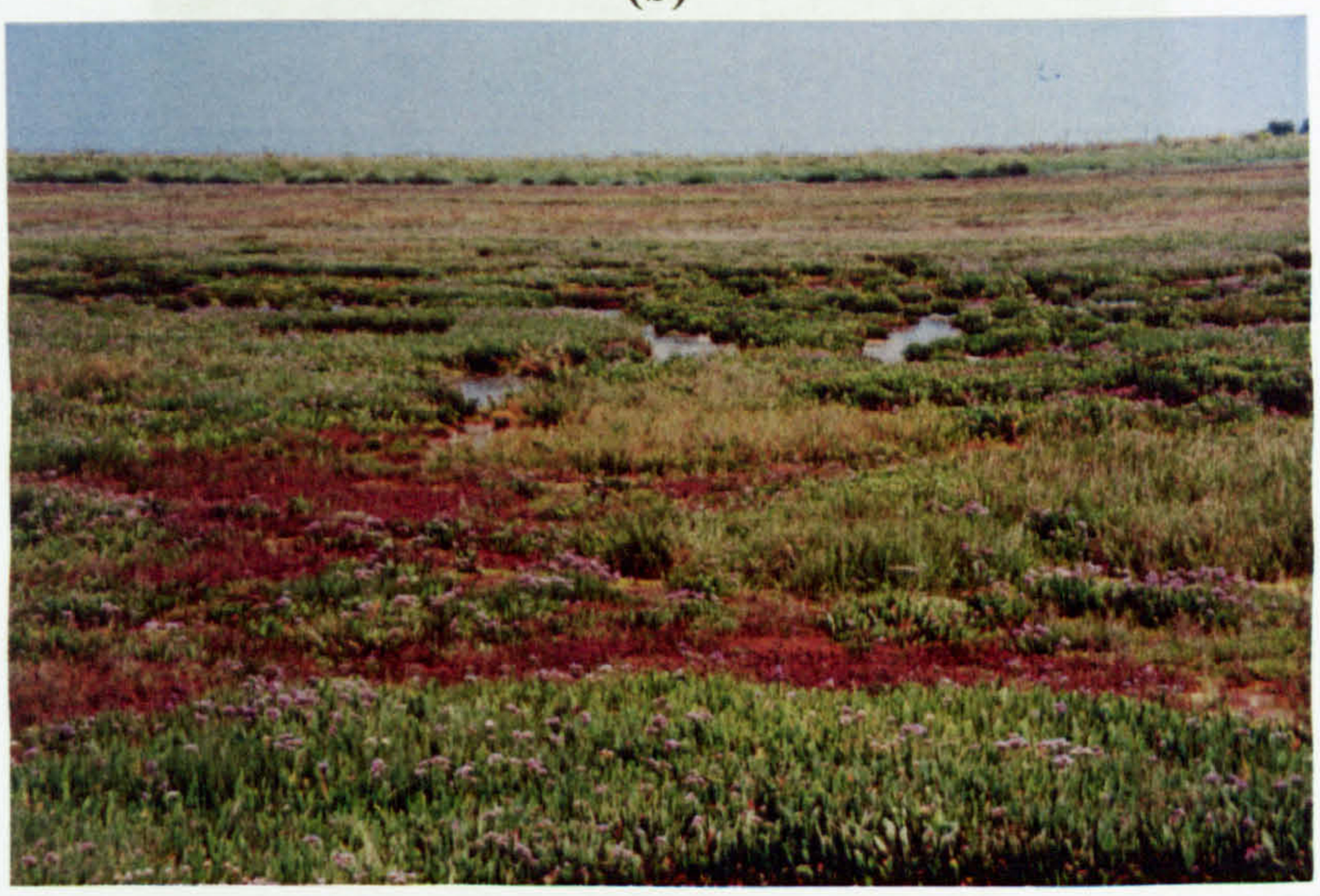

(c)

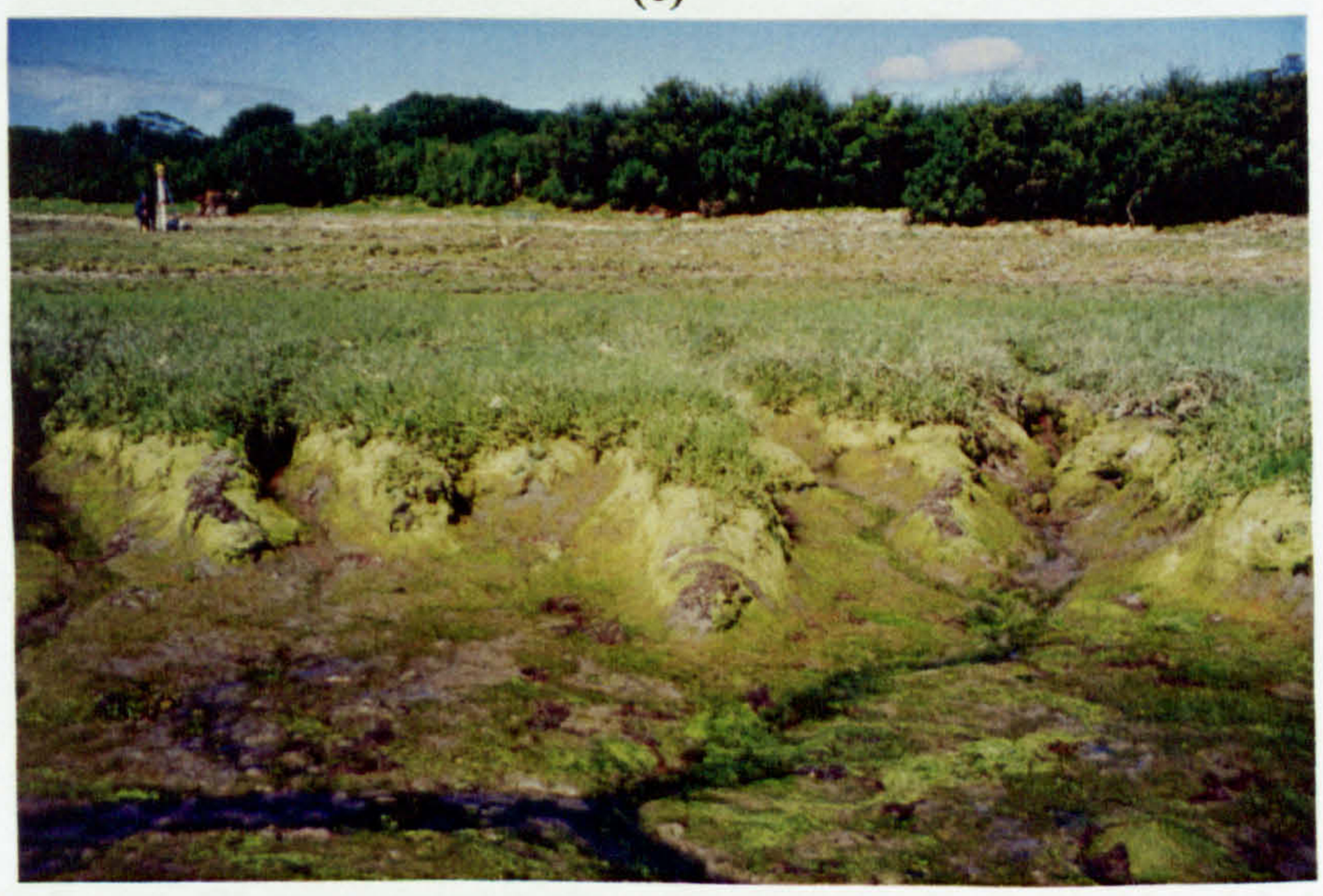

Plate 6.2 Classes of vegetative composition dominated by: (a) *Atriplex portulacoides*, Saltfleet marshes; and (b) *Limonium vulgare* and *Puccinellia maritima*, River Colne; (c) *Spartina spp.*, River Carew; (d) *Elytrigia spp.*, Holbeach, The Wash; and (e) *Festuca rubra* and *Armeria maritima*, Duddon Estuary.

(d)

(e)

Plate 6.2 cont. Classes of vegetative composition dominated by: (a) *Atriplex portulacoides*, Saltfleet marshes; and (b) *Limonium vulgare* and *Puccinellia maritima*, River Colne; (c) *Spartina spp.*, River Carew; (d) *Elytrigia spp.*, Holbeach, The Wash; and (e) *Festuca rubra* and *Armeria maritima*, Duddon Estuary.

6.2.6 Tidal range

According to Davies (1964, p.137) the importance of *tidal range* is two-fold, since it determines '*not only the range of daily variation in water level but also the efficiency of tidal streams*'. The degree of variation in water level has already been referred to through its control over the altitudinal limits between which halophytic species may colonise, and as such the area available for saltmarsh development (Section 1.1.1). However, in terms of channel network morphology, the influence exerted by tidal range over the efficiency of flows, is of greater interest for the present study.

Relations between tidal range and the morphological characteristics of saltmarsh creeks have been alluded to by a number of authors (see, for example, Collins *et al.*, 1987; Adam, 1990; also Allen, 1992). However, Ranwell (1972, p.28) specifically hypothesises that contrasting planimetric formations emerge as a result of spatial variations in tidal exchange, whereby marshes within a large range tend to have *'sharper drainage systems normal to the shore'* and lower ranges support *'a more complex network of winding and much-branched creeks'*. The distinction between these formations is made on the premise that different driving forces dominate the process of network development under contrasting ranges of tidal exchange. Following the observation by Lincoln and Fitzgerald (1988) that tidal range affects the dominance of flood and ebb tides, it may be envisaged that the velocities attained during formative phases of overmarsh events are at least in part a function of the offset between high and low water levels (see also Bridges and Leeder, 1976). Where the range is high, a considerable depth of flow has to be exchanged over a single tidal period. As such, the water surface slope that develops during the retreating ebb tide (Knight, 1981; Green *et al.*, 1986; French and Stoddart, 1992; Leopold *et al.*, 1993) is likely to be comparatively steep, and the potential energy available to perform erosive work considerable. 'Sharper' planimetric adjustment may therefore result from the higher velocities and enhanced downcutting ability associated with a steep hydraulic gradient. The same line of reasoning can explain a lack of structure in networks developing under a reduced tidal range. Where a lower volume of flow is to be exchanged, the hydraulic gradient is much reduced. Other more random influences, such as the pattern of vegetative colonisation, may instead influence network behaviour.

Spring Tidal Range (*STR*) was selected as a convenient and representative surrogate for the intensity of hydraulic gradient. Where study sites were situated at an intermediate position between ports (see Hydrographic Office, 1997), an average statistic

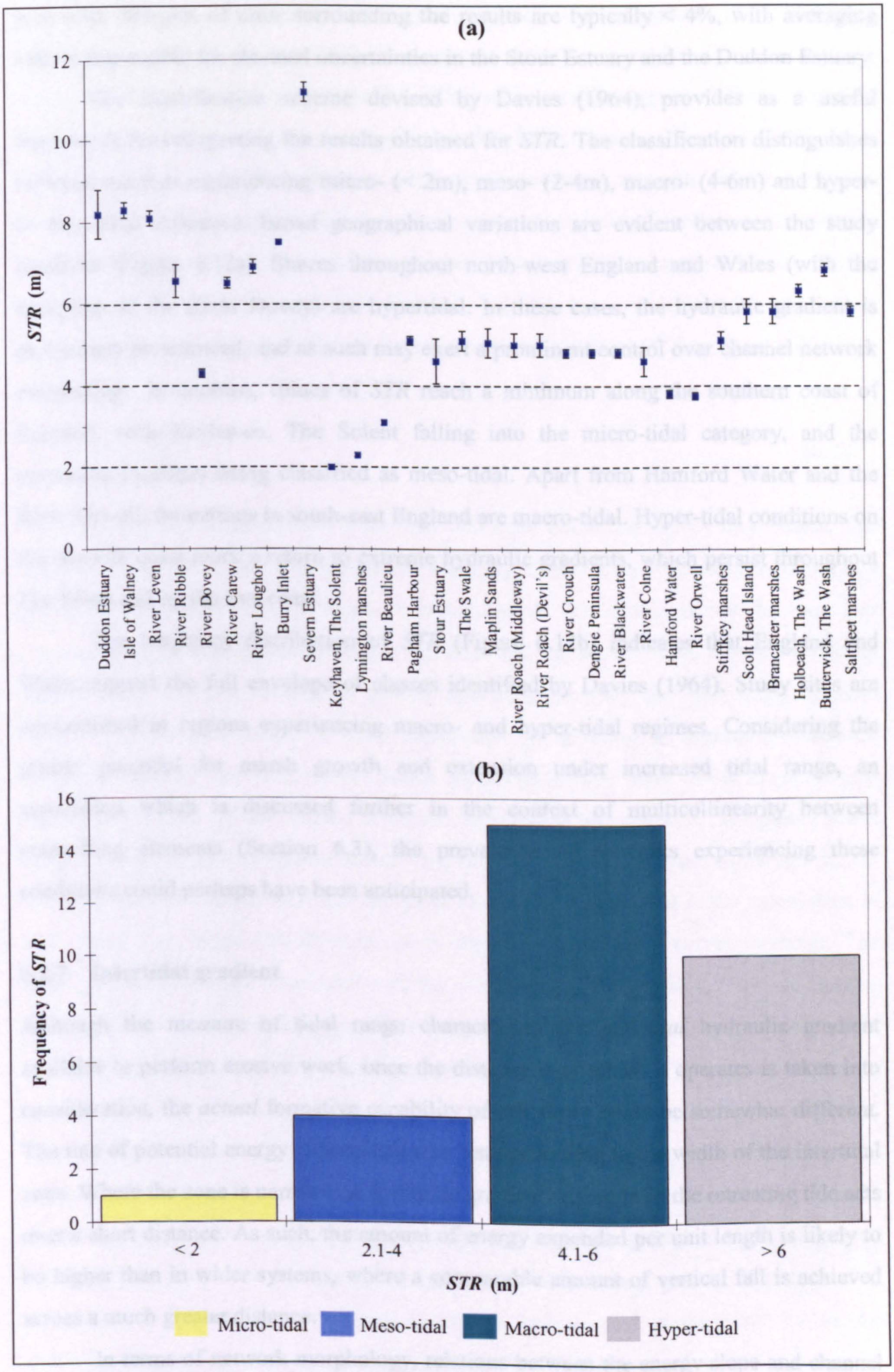

Figure 6.12 (a) Geographical distribution of spring tidal range (*STR*); and (b) the frequency distribution of responses, organised into classes specified by Davies (1964).

was used. Margins of error surrounding the results are typically < 4%, with averaging effects responsible for elevated uncertainties in the Stour Estuary and the Duddon Estuary.

The classification scheme devised by Davies (1964), provides as a useful framework for interpreting the results obtained for *STR*. The classification distinguishes between marshes experiencing micro- (< 2m), meso- (2-4m), macro- (4-6m) and hyper- (> 6m) tidal influence. Broad geographical variations are evident between the study localities (Figure 6.12a). Shores throughout north-west England and Wales (with the exception of the River Dovey) are hypertidal. In these cases, the hydraulic gradient is particularly pronounced, and as such may exert a prominent control over channel network morphology. In contrast, values of *STR* reach a minimum along the southern coast of England, with Keyhaven, The Solent falling into the micro-tidal category, and the remaining localities being classified as meso-tidal. Apart from Hamford Water and the River Orwell, formations in south-east England are macro-tidal. Hyper-tidal conditions on the Norfolk coast mark a return to extreme hydraulic gradients, which persist throughout The Wash and up the east coast.

The frequency distribution of *STR* (Figure 6.12b) indicates that England and Wales support the full envelope of classes identified by Davies (1964). Study sites are concentrated in regions experiencing macro- and hyper-tidal regimes. Considering the greater potential for marsh growth and extension under increased tidal range, an association which is discussed further in the context of multicollinearity between controlling elements (Section 6.3), the prevalence of networks experiencing these conditions could perhaps have been anticipated.

6.2.7 Intertidal gradient

Although the measure of tidal range characterises the *potential* hydraulic gradient available to perform erosive work, once the distance over which it operates is taken into consideration, the *actual* formative capability of ebb flows could be somewhat different. The rate of potential energy expenditure may vary according to the width of the intertidal zone. Where the zone is narrow, the hydraulic gradient arising from the retreating tide acts over a short distance. As such, the amount of energy expended per unit length is likely to be higher than in wider systems, where a comparable amount of vertical fall is achieved across a much greater distance.

In terms of network morphology, relations between the energy slope and channel development are widely cited in the fluvial literature (Zernitz, 1932; Schumm, 1956;

Strahler, 1958, 1964; Morisawa, 1962, 1964; Howard, 1967; Ferguson, 1975; Bannister and Arbor, 1980; Abrahams, 1984). However, in a tidal context, the equivalent balance between tidal range and width of the foreshore, which may be expressed more succinctly as intertidal gradient (G_I), has received somewhat less attention. Chapman (1974, p.32) initially suggested that G_I influences planimetric development, with dendritic systems arising on *'virginal mudflats that have a steady seaward slope'*, and tortuous systems ascribed to *'ground lacking any distinct slope'*. However, subsequent studies employing the slope parameter (see, for example, Dyer *et al.*, 2000), have overlooked this interaction. G_I was computed for each study locality (Equation 6.5), where *MTR* is mean tidal range and L_I is the width of the intertidal zone.

$$G_I = \frac{MTR}{L_I} \qquad [6.5]$$

L_I was measured directly from 1:25 000 scale Ordnance Survey map sheets. The landward limit of saltmarsh development is readily identified in systems terminating at a natural topographic barrier, seawall or embankment. Where this is not the case (for example in the River Ribble, the Stour Estuary, and the River Colne, which are instead backed by an adjacent network or gradual landward gradient), the most likely terminal point was established based on field experience. In selecting an appropriate seaward boundary, Leopold and Bull (1979) define a theoretical base level as the lower vertical limit below which a stream cannot downcut. However in this instance, the optimal lower limit is determined by pragmatic rather than theoretical considerations. Although *MLWS* has already been used to represent the point of zero hydraulic head in the calculation of *STR*, Mean Low Water (*MLW*) is the level depicted on Ordnance survey coverage. The slightly elevated reading associated with this statistic (see, for example, Frey and Bassan, 1985) may not represent absolute base level, but nevertheless provides a reasonable indication of horizontal extent. Ambiguity in the position of either boundary is reflected by higher margins of uncertainty surrounding 'best estimate' (Taylor, 1982) values of G_I.

For reasons of consistency, *MLW* was designated as the lower vertical boundary. Calculated as the average of low water spring and neap tides, data were obtained from the Admiralty Tide Tables (Hydrographic Office, 1997; see also Figure 6.3). *MHW* was similarly derived for the corresponding upper vertical boundary, and *MTR* computed as the difference between these readings. In mature marshes such as the River Leven, the *MHW* line depicted on O.S. coverage is situated towards the seaward marsh boundary. In systems such as these, which are situated high in the intertidal profile, the upper

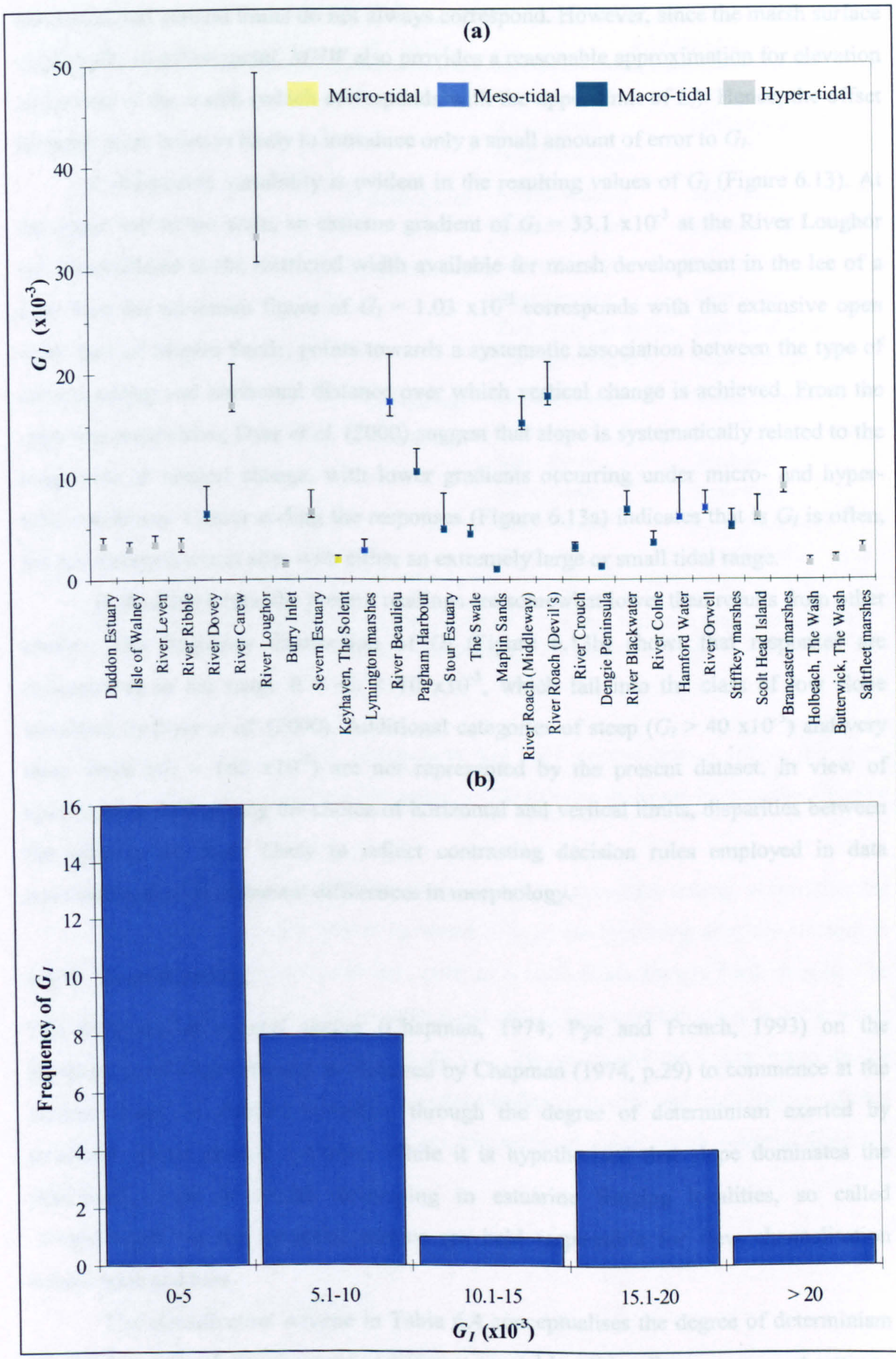

Figure 6.13 (a) Geographical distribution of values recorded for intertidal gradient (G_I) which are grouped into classes of tidal range (Davies, 1964); and (b) the frequency distribution of responses.

horizontal and vertical limits do not always correspond. However, since the marsh surface is generally near-horizontal, *MHW* also provides a reasonable approximation for elevation at the rear of the marsh (which corresponds with the upper limit of L_l). Hence, the offset between these limits is likely to introduce only a small amount of error to G_l.

Considerable variability is evident in the resulting values of G_l (Figure 6.13). At the upper end of the scale, an extreme gradient of $G_l = 33.1 \times 10^{-3}$ at the River Loughor can be attributed to the restricted width available for marsh development in the lee of a spit. That the minimum figure of $G_l = 1.03 \times 10^{-3}$ corresponds with the extensive open coast flats of Maplin Sands, points towards a systematic association between the type of coastal setting and horizontal distance over which vertical change is achieved. From the opposing perspective, Dyer *et al.* (2000) suggest that slope is systematically related to the magnitude of vertical change, with lower gradients occurring under micro- and hyper-tidal conditions. Colour coding the responses (Figure 6.13a) indicates that is G_l is often, but not always lower at sites with either an extremely large or small tidal range.

In absolute terms, the present readings are somewhat lower than results from other studies. The frequency distribution of G_l (Figure 6.13b) shows that responses are concentrated in the range $0 < G_l < 10 \times 10^{-3}$, which fall into the class of low slope identified by Dyer *et al.* (2000). Additional categories of steep ($G_l > 40 \times 10^{-3}$) and very steep slope ($G_l \sim 160 \times 10^{-3}$) are not represented by the present dataset. In view of uncertainties surrounding the choice of horizontal and vertical limits, disparities between the datasets are more likely to reflect contrasting decision rules employed in data acquisition, than fundamental differences in morphology.

6.2.8 Coastal setting

The influence of *coastal setting* (Chapman, 1974; Pye and French, 1993) on the morphology of tidal networks is observed by Chapman (1974, p.29) to commence at the earliest stages of channel initiation, through the degree of determinism exerted by structural versus random controls. While it is hypothesised that slope dominates the planimetric form of creeks developing in estuarine fringing localities, so called *'irregularities'* in the intertidal surface are held responsible for flow channelisation behind spits and bars.

The classification scheme in Table 6.4 conceptualises the degree of determinism involved in network development at different coastal localities. From open coast settings, where marsh will only form if the intertidal profile is sufficiently subdued to mitigate

CONTROL	NOMINAL CLASS	SETTING	EXAMPLES	
Random	**1**	**Open coast**	Maplin Sands	Stiffkey marshes
			River Crouch	Saltfleet marshes
			Dengie Peninsula	
	2	**Embayment**	Pagham Harbour	Butterwick, The Wash
			Hamford Water	Holbeach, The Wash
	3	**Back-barrier**	Isle of Walney	River Beaulieu
			River Loughor	River Colne
			Keyhaven, The Solent	Scolt Head Island
			Lymington marshes	Brancaster marshes
Structural	**4**	**Estuarine fringing**	Duddon Estuary	Severn Estuary
			River Leven	Stour Estuary
			River Ribble	The Swale
			River Dovey	River Roach
			River Carew	River Blackwater
			Burry Inlet	River Orwell

Table 6.4 Classification expressing the degree of 'random' versus 'structural' control exerted over network morphology by coastal setting.

wave energy (Chapman, 1974), embayment and back barrier classes reflect the more pronounced influence of gradient. This effect is likely to be strongest in estuarine fringing localities.

Estuarine fringing is the most populous class of coastal setting, accounting for 43% of the study localities (Table 6.4). Some 27% of the remaining sites are situated in the lee of natural topographic barriers, such as a sand dune, shingle bank or spit. The frequency of sample networks in an open coast setting is somewhat lower at 17%, while 13% of sites border an embayment. If the selected study sites are taken to be representative of the population of coastal saltmarshes, estuaries and back-barrier settings appear to be particularly favourable for the formation of stable marsh systems, dissected by a tidal channel network.

6.3 MULTICOLLINEARITY

The issue of multicollinearity is addressed from the outset, since it in part determines the success of subsequent phases of statistical analysis, and if ignored may fundamentally

alter the results obtained. Defined by Shaw and Wheeler (1997, p.256) as the *'situation in which high correlations exist between independent variables'*, multicollinearity is seen as a major cause of ambiguity in interpreting the influence of controlling elements over network morphology (see also Hauser, 1974). A number of approaches have been employed to firstly recognise, and then adjust for multicollinearity. Correlation analysis is the most widely documented (Hauser, 1974; Mosley, 1981; Dyer *et al.*, 2000), whereby the significant statistical association between a pair of control variables, or alternatively the close correspondence between bivariate (zero order) and multiple correlation statistics (Shaw and Wheeler, 1997), is taken as a sign of interdependence.

Balanced against the merits of avoiding high statistical intercorrelations, is the possibility of incorrectly discarding important variables. In response, Hauser (1974) presents a number of solutions including: (1) obtaining new data on the designated element; (2) including the full variable set and accepting data redundancy; (3) identifying an irreducible set of combined variables; and (4) excluding all but one of the collinear variables. While the first option is impractical since there is often no other means of measurement and the second does nothing to alleviate the problem at hand, the third approach has been implemented through the use of principal components analysis (see, for example, Gardiner, 1978). However, the difficulties that are encountered when interpreting the resulting orthogonal variables, precludes the use of this technique. The final option is deemed appropriate for the present study, since it is most likely to result in a set of apposite yet uncorrelated predictors.

The dependence of each environmental measure (see Figure 2.8) on other members of the variable set, was investigated using appropriate statistical tests. Pearson's product-moment correlation coefficient (r) was computed for series at an interval or ratio scale, which display near-normal behaviour (Hauser, 1974; Mosley, 1981; Dyer *et al.*, 2000). For lower order data (Melton, 1958), or where transformation failed to restore an acceptable level of normality, the Spearman's rank statistic (r_s) was employed. To minimise the probability of making a Type II error (Shaw and Wheeler, 1997), a significance level of $\alpha = .05$ was used to test the null hypothesis of 'no association'. In the absence of a suitable equivalent for nominal classes, the Kruskal-Wallis test was used to decide whether groups of responses could be drawn from the same population, or if they are instead associated with different intensities of environmental control.

The matrix of correlation coefficients (Table 6.5) indicates that scale dependence is an important source of multicollinearity within the set of control variables. By

CONTROL ⇨	TIDAL FORCING				ERODIBILITY			GRADIENT		SCALE DEPENDENCE		
DESCRIPTIVE VARIABLE ⇩	H_{max}	P_C	P_{TM}	*SLC*	*%silt-clay*	*He-Mo %silt-clay*	*Ba-Be %silt-clay*	*STR*	G_I	A_{min}	A_{eq}	A_{max}
H_{max}		-0.23	0.19	0.07	-0.09*	0.01*	0.26	0.32	0.22	-0.16	-0.18	-0.12
P_C			**0.84**	**0.37**	-0.26*	0.14*	**0.38**	-0.08	**-0.54**	**0.80**	**0.90**	**0.86**
P_{TM}				**0.43**	-0.30*	0.16*	**0.42**	0.26	**-0.59**	**0.92**	**0.92**	**0.93**
SLC					**-0.64***	-0.09*	-0.05	0.08	-0.18	**0.40**	**0.44**	**0.38**
%silt-clay						-0.09*	-0.01*	-0.35*	-0.03*	-0.31*	-0.34*	-0.36*
He-Mo %silt-clay							0.22*	**0.40***	-0.31*	0.31*	0.27*	0.25*
Ba-Be %silt-clay								-0.04	-0.06	0.31	0.31	0.31
STR									-0.01	0.20	0.18	0.23
G_I										**-0.67**	**-0.68**	**-0.68**
A_{min}											**0.99**	**0.98**
A_{eq}												**0.99**
A_{max}												

Table 6.5 Correlation matrix showing **statistically significant** ($\alpha = .05$) levels of multicollinearity between appropriately transformed variables describing potential controlling elements (Spearman's rank correlation coefficients are distinguished by *).

employing the threshold of r > 0.8 recommended by Hooke (1979), it appears that serious collinearity is present between A and P_{TM}. This may be explained through the inclusion of A_{eq} in the calculation of P_P (Equation 6.4), which is in turn a component of P_{TM}. However, the significant positive relation between A and P_C (r = 0.90) is attributable to other factors, because area is not directly involved in the calculation. This correlation is instead likely to arise as a morphological response to the conveyance function that the system performs during overmarsh tides.

Although the level of explanation is weaker, correlation coefficients between A, SLC and G_I are nevertheless significant. The prevalence of larger marshes at localities experiencing amplified levels of SLC, implies that surface accretion is able to keep pace with rising sea levels. The positive relation therefore justifies the cautionary observation by Allen and Pye (1992, p.12) that it is *'by no means established with certainty that increased marsh erosion...* [resulting in a smaller area coverage] *is associated with changing sea level'*. Of the parameters involved in computing G_I, tidal range is not correlated with marsh area. The negative association between G_I and A therefore suggests that marsh extent is related to the remaining parameter, L_I. It is hardly surprising that larger marshes tend to form where the width of the intertidal zone is substantial, given the increased tract of foreshore across which sediment may accumulate. However, the coefficient of r = -0.68 indicates that there is noise about the trend. This is likely to reflect extraneous influences over the pattern of marsh growth, such as shape of the intertidal profile and the frequency of high magnitude erosive events.

As noted by Norcliffe (1977) and Kirkby *et al.* (1987), statistical associations between pairs of variables may occur for reasons other than direct causality. A significant correlation may also arise where variables are dependent on a common parameter. Mutual dependence on area may be responsible for statistically significant relations between G_I, P_{TM} and SLC. However, the remaining associations are less obviously linked through A. For the negative correspondence between *%silt-clay* and SLC, a causal explanation is not immediately apparent. However, this relation is of particular interest, since it appears that tidal forcing amplified by sea-level rise coincides with sandy systems where marsh substrates are comparatively mobile. Resulting instability may be linked to the sequential periods of marsh advance and retreat observed by Pringle (1995), and reflected by the discordant course followed by rectangular creeks in the Duddon Estuary and the River Leven. Correlations between at-a-station sedimentary composition and P_{TM}, and

downstream changes in *%silt-clay* with *STR* are also difficult to justify from existing knowledge of geomorphological processes. In view of the weak coefficients, which are only just significant at the designated level, it may be that these associations have arisen by chance.

In general, the nominal measures of vegetative cover and coastal setting show a limited association with higher order descriptive variables. After running the Kruskal-Wallis test on all possible pairings, the null hypothesis was accepted in all but two instances. As shown by the box-whisker plot in Figure 6.14a, significant grouping was identified between *STR* and classes of vegetative cover. Upper marsh communities dominate the marsh platform of formations experiencing a high *STR*, while pioneer species tend to occur where the range is lower. These patterns of response suggest that marsh surface accretion is more successful where the tidal range is higher. The association between G_I and geomorphic setting (Figure 6.14b) supports the suggestion made in Section 6.2.8, that coastal localities experience different intensities of structural determinism. Higher slopes in estuarine fringing and back-barrier settings indicate that hydraulic effects are likely to play a significant role in determining the course of tidal creeks. Consistently low values of G_I at open coast sites, point towards reduced efficiency of the energy gradient.

Based on the preceding assessment of intercorrelation, a refined set of descriptive variables may be carried forward to subsequent phases of the analysis. Since scale dependence has already proved to be an important consideration in responses for a number of morphometric indices, it is necessary to retain an expression of marsh area. However, problems of multicollinearity, arising from the strong associations between measures acquired according to minimum, equidistant and maximum decision rules, can be moderated by using A_{eq} as a 'best-estimate'. P_C is more than just another surrogate measure, expressing the scale of the system. Together with *SLC*, the geomorphological significance and independent mode of derivation employed for these parameters, have already been established. As such, they are both retained for further study. With the knowledge that it encompasses both A and P_C, P_{TM} is also included on conceptual grounds, due to its importance as a summary measure for the total force driving channel development. Less serious collinearity between A and G_I warrants its inclusion. Following the same line of reasoning, average, downstream and at-a-station measures of *%silt-clay* are retained, since they explain only some common variance.

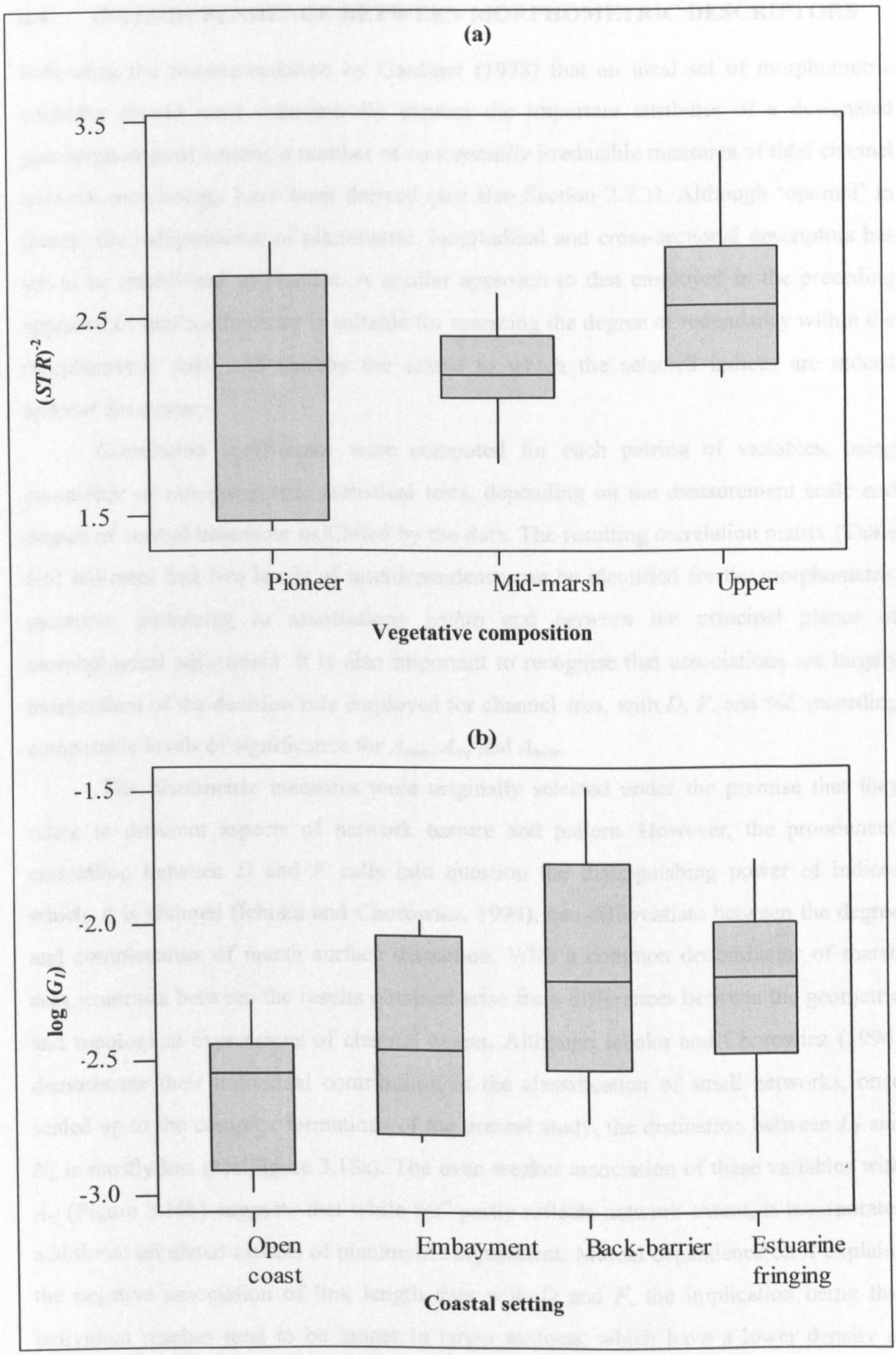

Figure 6.14 'Box-whisker' plots showing associations between: (a) class of vegetative cover and spring tidal range (*STR*); and (b) type of coastal setting and intertidal gradient (G_I).

6.4 INTERDEPENDENCE BETWEEN MORPHOMETRIC DESCRIPTORS

Following the recommendation by Gardiner (1978) that an ideal set of morphometric variables should most economically express the important attributes of a designated geomorphological system, a number of *conceptually* irreducible measures of tidal channel network morphology have been derived (see also Section 2.2.3). Although 'optimal' in theory, the independence of planimetric, longitudinal and cross-sectional descriptors has yet to be established in practise. A similar approach to that employed in the preceding appraisal of multicollinearity is suitable for assessing the degree of redundancy within the morphometric data, and thereby the extent to which the selected indices are indeed *optimal descriptors*.

Correlation coefficients were computed for each pairing of variables, using parametric or non-parametric statistical tests, depending on the measurement scale and degree of normal behaviour exhibited by the data. The resulting correlation matrix (Table 6.6) indicates that two levels of interdependence can be identified for the morphometric measures, pertaining to associations *within* and *between* the principal planes of morphological adjustment. It is also important to recognise that associations are largely independent of the decision rule employed for channel area, with D, F, and $\%C$ recording comparable levels of significance for A_{min}, A_{eq} and A_{max}.

The planimetric measures were originally selected under the premise that they relate to different aspects of network texture and pattern. However, the pronounced correlation between D and F calls into question the distinguishing power of indices which, it is claimed (Ichoku and Chorowicz, 1994), can differentiate between the degree and completeness of marsh surface dissection. With a common denominator of marsh area, contrasts between the results obtained arise from differences between the geometric and topological expressions of channel extent. Although Ichoku and Chorowicz (1994) demonstrate their individual contribution in the classification of small networks, once scaled up to the complex formations of the present study, the distinction between L_T and N_L is mostly lost (see Figure 3.18a). The even weaker association of these variables with A_C (Figure 3.18b) suggests that while $\%C$ partly reflects network extent, it incorporates additional unrelated aspects of planimetric adjustment. Mutual dependence on A explains the negative association of link length data with D and F, the implication being that individual reaches tend to be longer in larger systems, which have a lower density or frequency of channels. Shorter links are in turn associated with systems of a higher density, which generally occupy smaller areas. This finding suggests that the interval

PLANE OF → ADJUSTMENT / MEASURE ↓		PLANIMETRIC																		LONGITUDINAL		CROSS-SECTIONAL	
		D			*%C*			*F*			*L*	L_{EXT}	L_{INT}	L_E/L_I	*S*	S_N	S_T	S_A	G_N	*I*	$w{:}d_L$	A_{SL}
		A_{min}	A_{eq}	A_{max}	A_{min}	A_{eq}	A_{max}	A_{min}	A_{eq}	A_{max}													
D	A_{min}		**0.89**	**0.81**	**0.59**	**0.45**	**0.46**	**0.92**	**0.92**	**0.91**	**-0.77**	**-0.79**	**-0.68**	-0.17	-0.27	-0.28	-0.11*	-0.26*	**0.65**	-0.02	-0.03	-0.03
	A_{eq}			**0.94**	**0.45**	**0.47**	**0.50**	**0.74**	**0.83**	**0.85**	**-0.56**	**-0.58**	**-0.48**	-0.14	-0.23	-0.26	-0.01*	-0.23*	**0.54**	0.02	-0.02	-0.05
	A_{max}				**0.50**	**0.55**	**0.61**	**0.68**	**0.76**	**0.84**	**-0.51**	**-0.48**	**-0.48**	-0.04	-0.21	-0.26	-0.01*	-0.17*	**0.40**	0.15	0.08	0.05
%C	A_{min}					**0.93**	**0.91**	**0.61**	**0.59**	**0.62**	**-0.56**	**-0.55**	**-0.52**	-0.08	-0.18	-0.22	0.09*	-0.05*	**0.40**	0.15	**0.47**	0.05
	A_{eq}						**0.99**	**0.44**	**0.48**	**0.54**	**-0.40**	**-0.38**	**-0.37**	-0.04	-0.14	-0.21	0.14*	-0.06*	0.25	0.13	**0.55**	0.32
	A_{max}							**0.45**	**0.49**	**0.57**	**-0.39**	**-0.37**	**-0.37**	-0.02	-0.13	-0.19	0.17*	-0.04*	0.24	0.16	**0.52**	0.31
F	A_{min}								**0.98**	**0.95**	**-0.93**	**-0.92**	**-0.87**	-0.05	-0.23	-0.24	-0.01*	-0.15*	**0.63**	0.01	0.11	0.09
	A_{eq}									**0.98**	**-0.90**	**-0.88**	**-0.84**	-0.03	-0.23	-0.24	-0.07*	-0.17*	**0.62**	0.03	0.13	0.10
	A_{max}										**-0.86**	**-0.83**	**-0.83**	0.01	-0.23	-0.25	-0.01*	-0.15*	**0.56**	0.10	0.17	0.14
L												**0.95**	**0.93**	0.06	0.19	0.21	-0.04*	0.05*	**-0.59**	-0.04	-0.19	-0.15
L_{EXT}													**0.78**	0.31	0.26	0.26	0.04*	0.22*	**-0.71**	0.07	-0.08	-0.06
L_{INT}														-0.27	0.11	0.13	-0.08*	-0.07*	**-0.38**	-0.14	-0.28	-0.24
L_{EXT}/L_{INT}															0.34	0.35	0.09*	**0.48***	**-0.50**	0.30	0.28	0.23
S																**0.95**	**0.69***	**0.78***	**-0.44**	0.05	-0.18	-0.34
S_N																	**0.43***	**0.64***	**-0.46**	0.08	-0.23	-0.36
S_T																		**0.70***	-0.18*	0.06*	0.09*	0.05*
S_A																			**-0.53***	0.18*	0.14*	0.05*
G_N																				**-0.39**	-0.24	-0.03
I																					**0.48**	0.22
$w{:}d_L$																						**0.75**
A_{SL}																						

Table 6.6 Correlation matrix showing **statistically significant** ($\alpha = .05$) levels of association between appropriately transformed morphometric descriptors (Spearman's rank correlation coefficients are distinguished by *).

between junctions increases with the scale of the network. Significant associations involving L_{EXT}/L_{INT} and sinuosity measures are limited. Apart from intercorrelations between the expressions of sinuosity, relations are restricted to the negative association of S_A with L_{EXT}/L_{INT}. The dominance of interior link lengths in networks supporting higher values of S_A is not unusual, since both series relate to meandering or asymmetry of the principal channel. The significant association between cross-sectional indices confirms that both w/d_L and A_{SL} reflect an element of scale. Interrelations between the longitudinal measures are barely significant, indicating that they relate to essentially independent aspects of morphological adjustment.

Mutual dependence on scale explains significant correlations between the various measures of planimetric extent and G_N. Interpreted literally, the results suggest that steep network gradients are associated with a high creek density and link frequency, and low mean link length. It is likely that these systematic trends in fact arise from the indirect relation between A and the total length of the principal channel. This is because D, F and L are strongly influenced by area (Section 3.5), and results for G_N are dominated by the distance component (Section 4.4.1) rather than the vertical offset, which remains comparatively uniform between the study localities.

Factors other than scale dependence explain the remaining associations. In the case of L_{EXT}/L_{INT}, it appears that imbalanced networks (see Table 3.4) characterised by elongated exterior links, tend to occur on lower gradients. While balanced systems coincide with intermediate slopes, the dominance of short exterior links in systems with a high gradient, suggests that flow convergence leads to increased branching. Unpacking the negative correlation of sinuosity measures with G_N is problematic because of the similarity between denominators used in the original calculations. Although L_S and $\sum d$ were acquired by entirely different means, the former through digitising and the later from field measurements, they both express length of the principal channel. Rather than the straightforward occurrence of amplified sinuosities at localities with a lower network gradient, the association between G_N and S reflects differences between the respective numerators, namely meander pathlength and vertical offset. Finally, pronounced associations between $\%C$ and w/d_L are attributable to the sensitivity of both indices to the relative degree of constraint on channel widening and deepening. While higher values of w/d_L have already been shown to occur where the conveyance function is accommodated through channel widening rather than deepening (Section 5.4.2), intercorrelation indicates that $\%C$ encapsulates elements of the same phenomena, only at a network-wide scale.

Performing a Kruskal-Wallis test on possible pairings between nominal planimetric classes and the higher order series, produces a significant ($\alpha = .05$) result for: *D*, *F*, *%C* and the set of sinuosity measures. 'Box-whisker' plots (Figure 6.15) provide a schematic representation of the responses for linear, parallel, rectangular and dendritic formations. Values recorded for *D* are generally higher in parallel and dendritic formations, than in their linear and rectangular counterparts (Figure 6.15a). A lower level of marsh surface dissection is to be expected in linear formations, where creek development is by definition (Table 3.1) sparse beyond the master channel. However, the subdued responses obtained for rectangular systems are somewhat surprising, given their extensive area (see Plate 3.1). Of the formations falling into this category, the paucity of tributary development on the Butterwick marshes may be due to the fairly recent reclamation (Pye, 1995) of reaches which used to comprise the central and upper sectors of the network (Kestner, 1979). Indeed, the substantial hydraulic duty (Figure 6.4a) and mid-marsh vegetative composition (Table 6.3) suggest that this particular system has yet to attain maximum extension under the modified regime. In contrast, a much reduced hydraulic duty and a dominance of mature halophytic species, implies that degenerate processes are responsible for abstracted formations in the Duddon Estuary and the River Leven. In the case of *%C* (Figure 6.15b), the planimetric groups display a systematic increase from linear through to dendritic. The moderated shortfall in rectangular systems reaffirms the importance of incorporating elements of both network extent and coverage in subsequent stages of the analysis. Since results for *F* (Figure 6.15c) mirror the response obtained for *D*, these measures are essentially interchangeable in terms of distinguishing power. Interestingly, there is a marked correspondence between the magnitude of *D* (and thereby *F*) recorded for dendritic and parallel formations. Since the dissecting creeks are similarly spaced, it appears that a comparable conveyance function is performed by networks displaying contrasting configurations. This suggests that the *amount* of channel development is a more important consideration than its *organisation*, with differences in layout reflecting extraneous influences such as the degree of structural determinism, rather than basic functional differences.

As shown in Figure 6.15d, sinuosity measures offer a rudimentary basis for distinguishing between networks with a straight or meandering morphology. Defined in Table 3.1 as having a highly sinuous appearance and a prevalence of re-curved headward

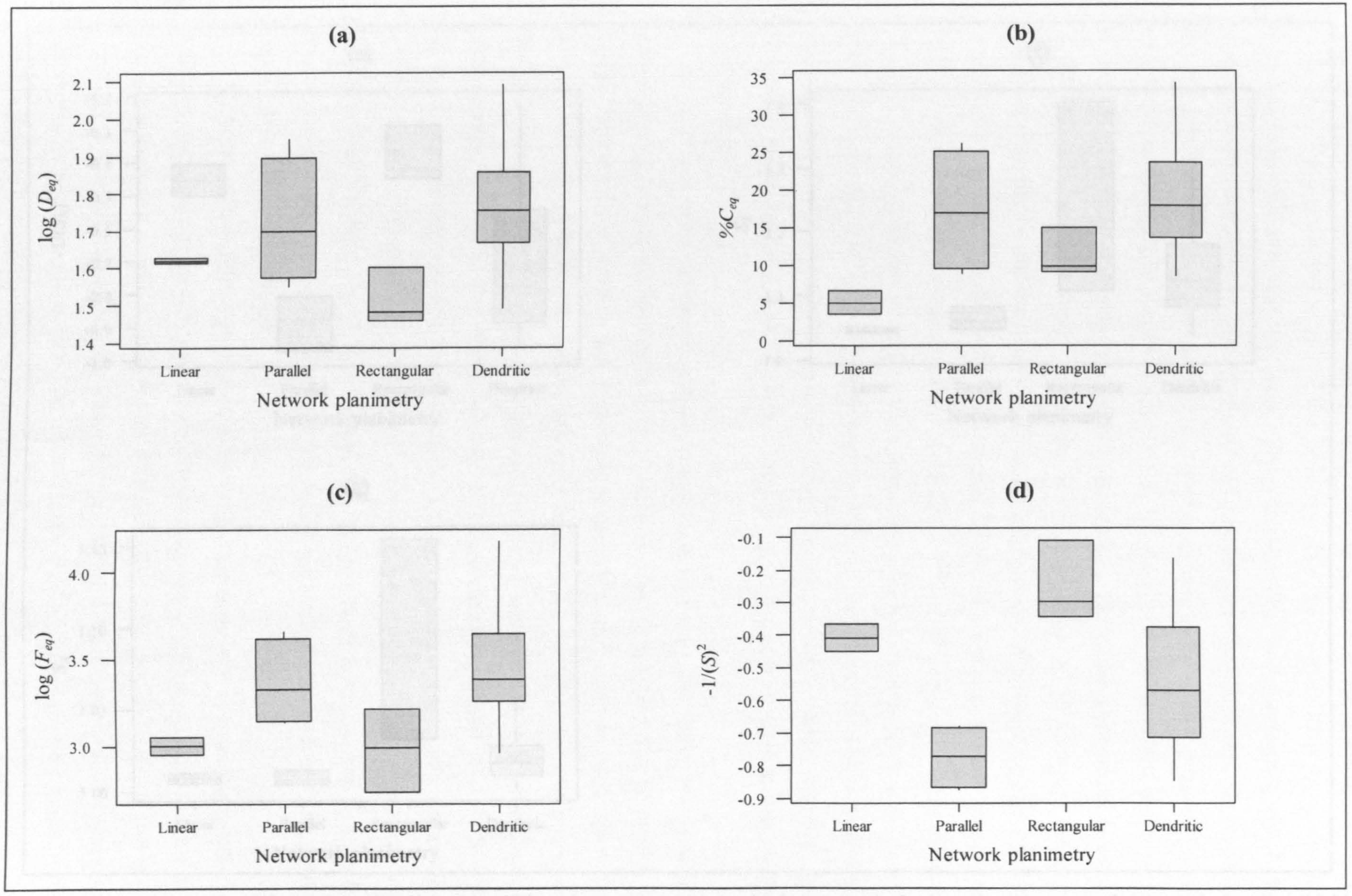

Figure 6.15 'Box-whisker' plots showing associations between network planimetry and planimetric measures of: (a) creek density; (b) % channel cover; (c) link-based texture; (d) principal channel sinuosity; (e) network-scale sinuosity; (f) tortuosity; and (e) meander asymmetry.

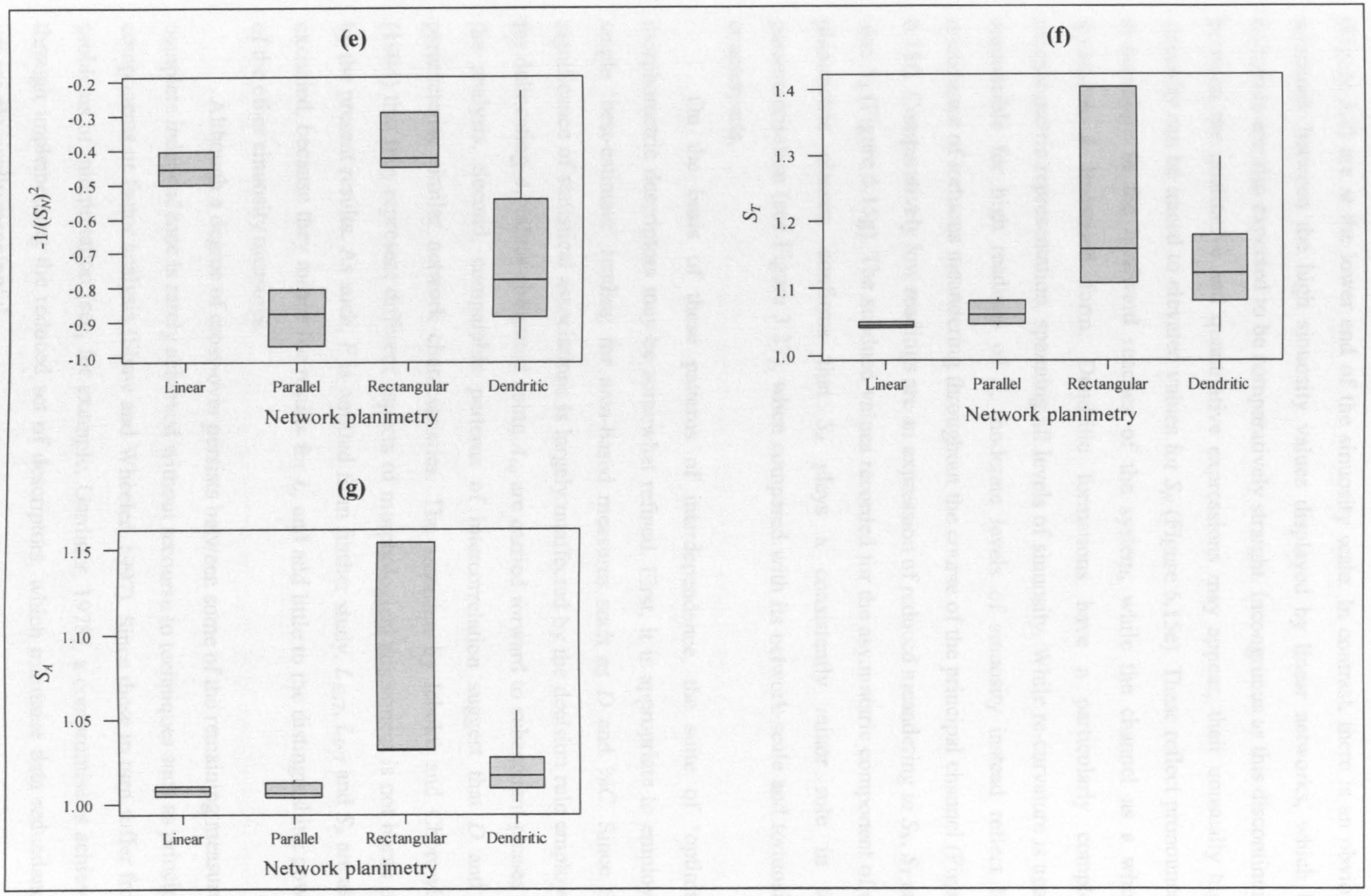

Figure 6.15 cont. 'Box-whisker' plots showing associations between network planimetry and planimetric measures of: (a) creek density; (b) % channel cover; (c) link-based texture; (d) principal channel sinuosity; (e) network-scale sinuosity; (f) tortuosity; and (e) meander asymmetry.

reaches, rectangular systems (see also Figure 3.7) rightly fall towards the upper end of the sinuosity scale. As expected, the straight master creeks associated with parallel formations (Figure 3.8) are at the lower end of the sinuosity scale. In contrast, there is an obvious mismatch between the high sinuosity values displayed by linear networks, which by definition are also expected to be comparatively straight. Incongruous as this discontinuity between the qualitative and quantitative expressions may appear, their unusually high sinuosity can be traced to elevated values for S_N (Figure 6.15e). These reflect pronounced re-curvature in the headward reaches of the system, while the channel as a whole maintains a linearised form. Dendritic formations have a particularly complex morphometric representation, spanning all levels of sinuosity. While re-curvature is again responsible for high readings of S, moderate levels of sinuosity instead reflect the dominance of tortuous meandering throughout the course of the principal channel (Figure 6.15f). Comparatively low readings are an expression of reduced meandering in S_N, S_T and also S_A (Figure 6.15g). The subdued values recorded for the asymmetric component of all planimetric classes, confirms that S_A plays a consistently minor role in the parameterisation (see Figure 3.27), when compared with its network-scale and tortuosity counterparts.

On the basis of these patterns of interdependence, the suite of 'optimal' morphometric descriptors may be somewhat refined. First, it is appropriate to employ a single 'best-estimate' reading for area-based measures such as D and $\%C$. Since the significance of statistical associations is largely unaffected by the decision rule employed for delineating A, values computed using A_{eq} are carried forward to subsequent phases of the analysis. Second, comparable patterns of intercorrelation suggest that D and F parameterise similar network characteristics. The assertion by Ichoku and Chorowicz (1994) that they represent different aspects of morphological adjustment is not borne out by the present results. As such, F is omitted from further study. L_{EXT}, L_{INT} and S_A are also excluded, because they mirror the results for L, and add little to the distinguishing power of the other sinuosity measures.

Although a degree of cross-over persists between some of the remaining measures, complete independence is rarely achieved without recourse to techniques such as principal components or factor analysis (Shaw and Wheeler, 1997). Since these in turn suffer from problems of interpretation (see, for example, Gardiner, 1978), a compromise is achieved through implementing the reduced set of descriptors, which minimise data redundancy, yet are physically meaningful.

6.5 BIVARIATE ASSOCIATIONS

This interpretative phase of the study seeks to establish relations of connection between controlling elements and optimal morphometric descriptors of tidal channel network morphology (see Figure 2.1). Following the call made by Melton (1958a, p.443) for *'a method of handling data obtained on the many elements pertinent to a general study...that will furnish insight into the relations of each of these elements to all others'*, a two stage analysis involving bivariate and multivariate techniques is appropriate. Described in the following sections, the initial phase employs correlation analysis to identify significant associations between the refined sets of control and response variables (see also Morisawa, 1962). Bivariate scatter plots are used to visualise the results obtained (see, for example, Johnson, 1973; Hume, 1991; Gao and Collins, 1994; Coates *et al.*, 1995; Friedrichs, 1995). Focusing attention in this manner on measures with the highest level of explanatory power, serves to justify the selection of input parameters for the subsequent phase of analysis (Section 6.6), where a multivariate approach is used to investigate the collective importance of these key controls in determining morphological adjustment.

In line with approaches employed during the preceding assessments of multicollinearity and interdependence, statistically significant (α = .05) levels of association between pairings of variables were identified, using a combination of parametric and non-parametric tests. Responses exceeding the critical values ascribed to Pearson's product-moment and Spearman's rank correlation coefficients, are highlighted in Table 6.7. Results suggest that the multiplicity of environmental elements exert a significant level of control over: D_{eq}; $\%C$; L; G_N; I; w/d_L; and A_{SL}, but exhibit a marked shortfall in explanatory power for L_{EXT}/L_{INT} and the sinuosity measures. Statistically significant coefficients range from the lower critical limit of r = 0.37 to a maximum of r = 0.82. Between these extremes, a concentration of coefficients around r = $\pm$0.5 indicates that, in general, the environmental variables make a moderate *individual* contribution to the level of explanation. Interestingly, the patterns of association recorded by P_{TM} mirror those of A. As these measures appear to be interchangeable, in terms of control exerted over the morphometric descriptors, there is no need to consider both terms. P_{TM} is preferentially retained on the basis of its conceptual importance and the fact that it acts as a surrogate for scale.

A number of the morphometric indices record significant associations with several controls. Where this is the case, partial correlation coefficients are depicted alongside the zero order statistics (Table 6.7). A slight reduction in the magnitude of many partial

CONTROL ⇨		TIDAL FORCING				ERODIBILITY			GRADIENT		SCALE
MORPHOMETRIC MEASURE ⇩		H_{max}	P_C	P_{TM}	SLC	*%silt-clay*	*He-Mo %silt-clay*	*Ba-Be %silt-clay*	STR	G_I	A_{eq}
PLANIMETRIC	D_{eq}	0.11	-0.34	**-0.50** -0.01	-0.36	**0.49*** **0.41**	-0.04*	-0.01	**-0.45** **-0.36**	**0.41** **0.37**	**-0.58**
	$\%C_{eq}$	-0.01	0.21	-0.14	-0.06	0.18*	-0.18*	0.09	**-0.48**	0.33	-0.20
	L	-0.18	0.27	**0.43** 0.35	0.13	-0.29*	0.25*	-0.21	**0.57** **0.53**	-0.30	**0.52**
	L_{EXT}/L_{INT}	-0.27	0.35	0.24	0.12	-0.26*	0.17*	-0.11	-0.16	-0.33	0.36
	S	-0.18	-0.14	-0.11	-0.12	-0.32*	0.29*	0.01	0.10	0.04	-0.02
	S_N	-0.20	-0.22	-0.16	-0.18	-0.26*	0.29*	-0.13	0.12	-0.01	-0.06
	S_T	-0.08	0.14	0.04	-0.01	-0.29*	0.25*	0.18	-0.01	0.10	0.08
LONGITUDINAL	G_N	**0.47** **0.59**	**-0.42** 0.28	**-0.38** -0.21	-0.35	**0.47*** **0.50**	**-0.45*** **-0.40**	0.03	-0.05	**0.61** **0.46**	**-0.59**
	I	-0.34	0.35	-0.15	0.18	-0.08*	**0.42*** 0.26	0.27	-0.19	**-0.40** -0.31	0.28
CROSS-SECTIONAL	$w:d_L$	-0.20	**0.68** **0.42**	**0.47** -0.31	0.28	-0.18*	-0.10*	0.36	**-0.37** -0.33	-0.28	**0.45**
	A_{SL}	-0.08	**0.82** **0.69**	**0.63** -0.24	0.36	-0.02*	-0.20*	**0.44** 0.29	-0.33	-0.28	**0.61**

Table 6.7 Correlation matrix showing **statistically significant** ($\alpha = .05$) levels of association between appropriately transformed environmental control and morphometric response variables (Spearman's rank correlation coefficients are distinguished by *). Partial correlation coefficients are also recorded for significant zero order associations.

coefficients, compared with their bivariate counterpart, reflects interdependence between the subset of controls. Where the margin of fall is more acute, the measures account for a greater proportion of shared variance. While pairings such as: D_{eq} and G_I; G_N and P_C; and w/d_L with P_{TM}, no longer record such a high probability of significance, associations continuing to exceed the critical threshold exhibit the best explanatory potential. Doornkamp and King (1971, p.90) observe that *'the most interesting differences between the correlation coefficient and the partial correlation coefficient are those where there is a change in the sign'*, the implication being that the true nature of interaction is masked by interdependence with other variables. For the present study, this effect is held to a minimum, since partial correlations tend to follow the zero order coefficient. A change of sign is limited to associations between: G_N and P_C; w/d_L and P_{TM}; and A_{SL} with P_{TM}. In the former instance, the switch to a positive association indicates that G_N increases with P_C when all other controls are held constant. In the later cases, the negative coefficient reveals an unexpected tendency for A_{SL} and w/d_L to decline when P_{TM} increases. That these measures do not exhibit a straightforward increase with the partial coefficient for P_{TM}, highlights the complex nature of interactions determining the portion of overmarsh flux involved in channel adjustment.

In recognition of the differing degrees of inherent multicollinearity and shared explanatory power exhibited by the controlling variables, the bivariate relations can be divided (see also Doornkamp and King, 1971) into: (1) 'apparent' associations arising from *mutual dependence* on a another factor, or several intermediary variables, to form a causative chain; and (2) 'genetic' effects that are more probably connected by a *causal* relation.

6.5.1 Mutual dependence on an intermediary variable

Although the influence of marsh area has already been assessed, first in the context of scale dependence, and second as a cause of multicollinearity, a number of variables displaying a degree of association with A were retained for this stage of the study, due to their conceptual importance. Scale dependence must therefore be considered in relations involving the control variables: P_C; G_I; and SLC, and response measures of: D; L; G_N; w/d_L; and A_{SL}.

Since A is employed in the computation of both D_{eq} and P_{TM}, the significant correlation in Figure 6.16a is expected. A is indirectly involved in the association between D_{eq} and G_I (Figure 6.16b), through its relation to width of the foreshore (see Section

6.2.7). The positive coefficient suggests a tendency for higher creek densities to evolve in systems experiencing an amplified energy gradient, in a similar manner to that observed in fluvial systems by Morisawa (1962) and Strahler (1964). Systematic changes in L, G_N, w/d_L, and A_{SL} with P_{TM}, demonstrate that other network characteristics alter with the scale of the system. Networks conveying a greater P_{TM} typically exhibit longer reaches, a reduced gradient along the principal channel and enlarged cross-sections. Of these relations, the highest coefficient is recorded for A_{SL}, where the value of r = 0.63 reveals that the total volume of flow explains some 40% of the variation in creek capacity. The strength of this association was perhaps to be expected, given the widespread implementation of tidal prism as a key criteria in channel design (see Johnson, 1973; Mehta *et al.*, 1976; Hume, 1991; Gao and Collins, 1994; Friedrichs, 1995; Haltiner *et al.*, 1997), and its use as a surrogate for tidal discharge in studies involving hydraulic geometry (Leopold and Maddock, 1953; Chantler, 1974; Zeff, 1999). It also accounts for the increase in capacity, which is seen by Greensmith and Tucker (1966), Gardner and Bohn (1980), Collins *et al.* (1987) and Knighton *et al.* (1992), to accompany changes in the magnitude of flow.

A reduction in explanatory power occurs when a platform component is included in the prism calculation. When considered alone, P_C accounts for a higher proportion (67%) of total variance in A_{SL} (see also Figure 6.16g). However, the importance of overmarsh flow, in terms of its potential to perform erosive work, has already been widely established through process studies (see, for example, Bayliss-Smith *et al.*, 1979; French and Stoddart, 1992). These seemingly paradoxical findings, which are mirrored by associations with w/d_L (Figure 6.16h) and G_N (Figure 6.16i), may be attributed to the parameterisation of the platform component. The physical realism of the method used to calculate P_P is limited. Although current levels of understanding have progressed since Haltiner and Williams (1987, p.298) observed that *'the effect of* [over-marsh flows] *on channel formation/maintenance is unknown'*, uncertainty still surrounds the contribution which they make to channelised tidal exchange. The general lack of understanding concerning flow pathways across the marsh surface (see, for example, Pestrong, 1965) is a likely source of ambiguity. Although it is generally perceived that tidal channel networks serve a finite area of marsh (Knighton *et al.*, 1992), and that microtopography acts to focus overmarsh flows (Collins *et al.*, 1987; Leonard, 1997), these assertions have yet to be verified in a way that leads to an improved definition for P_P. Losses across the seaward margin of the marsh are noted by Allen (1997) to be a further consideration, with

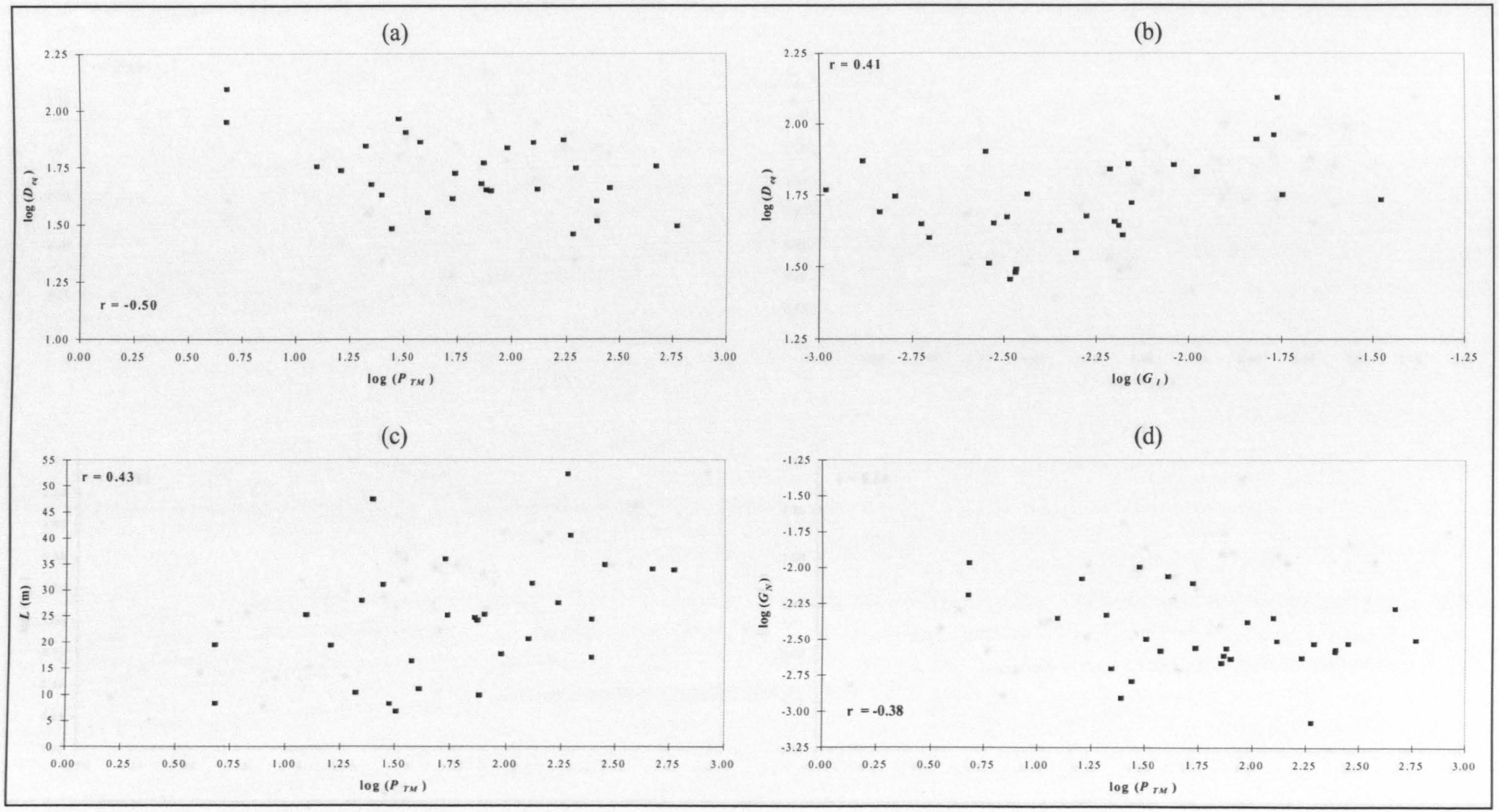

Figure 6.16 Scatter plots showing statistically significant ($\alpha = .05$) associations which are in part attributable to mutual dependence on marsh area cover, between: (a) creek density (D_{eq}) and total prism (P_{TM}); (b) D_{eq} and intertidal gradient (G_I); (c) mean link length ($\overline{L}$) and P_{TM}; (d) network gradient (G_N) and P_{TM}; (e) width:depth ratio ($w{:}d_L$) and P_{TM}; (f) cross-sectional area (A_{SL}) and P_{TM}; (g) A_{SL} and channelised prism (P_C); (h) $w{:}d_L$ and P_C; (i) G_N and P_C; and (j) G_N and G_I.

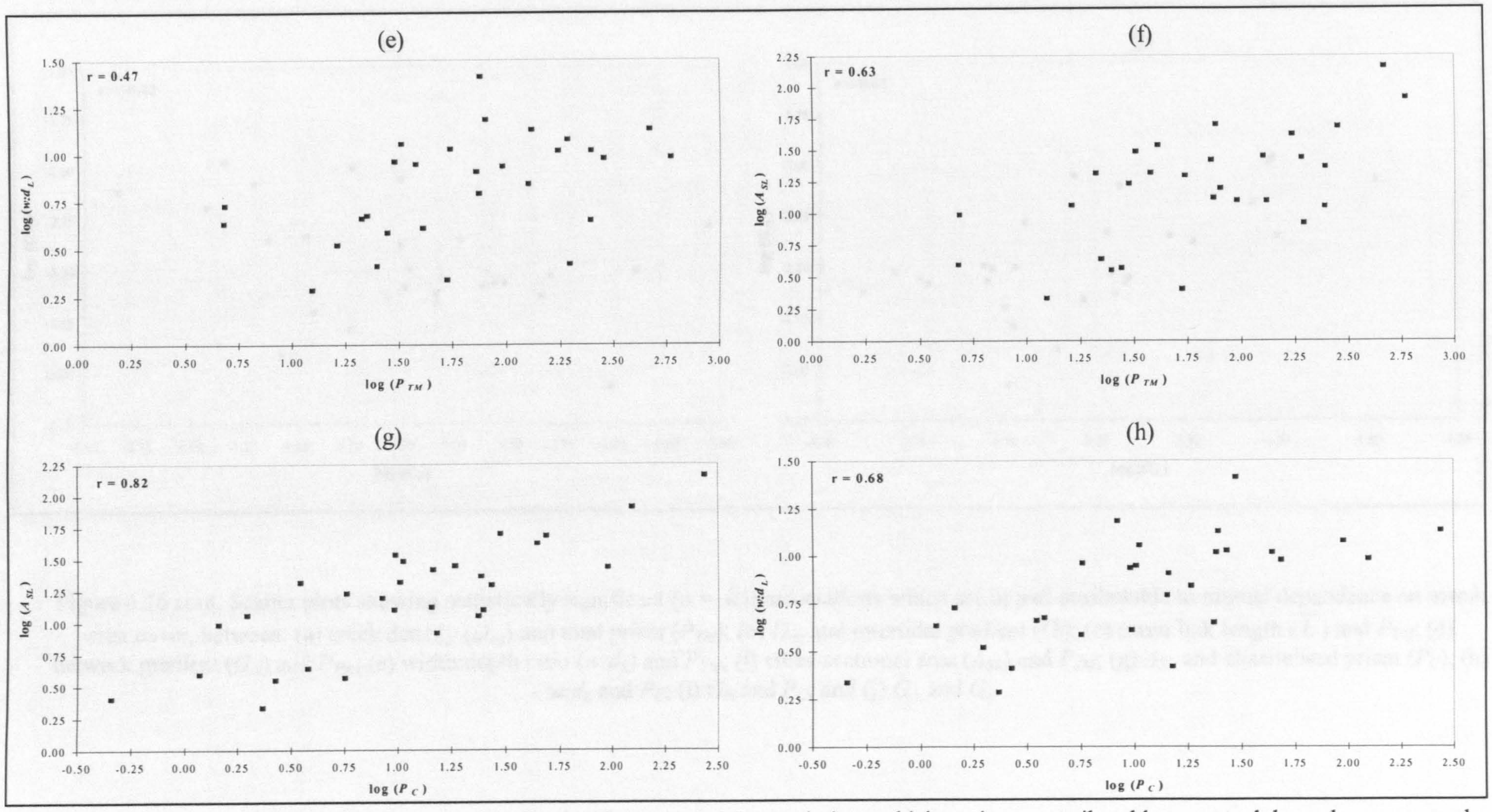

Figure 6.16 cont. Scatter plots showing statistically significant ($\alpha = .05$) associations which are in part attributable to mutual dependence on marsh area cover, between: (a) creek density (D_{eq}) and total prism (P_{TM}); (b) D_{eq} and intertidal gradient (G_I); (c) mean link length ($\bar{L}$) and P_{TM}; (d) network gradient (G_N) and P_{TM}; (e) width:depth ratio ($w{:}d_L$) and P_{TM}; (f) cross-sectional area (A_{SL}) and P_{TM}; (g) A_{SL} and channelised prism (P_C); (h) $w{:}d_L$ and P_C; (i) G_N and P_C; and (j) G_N and G_I.

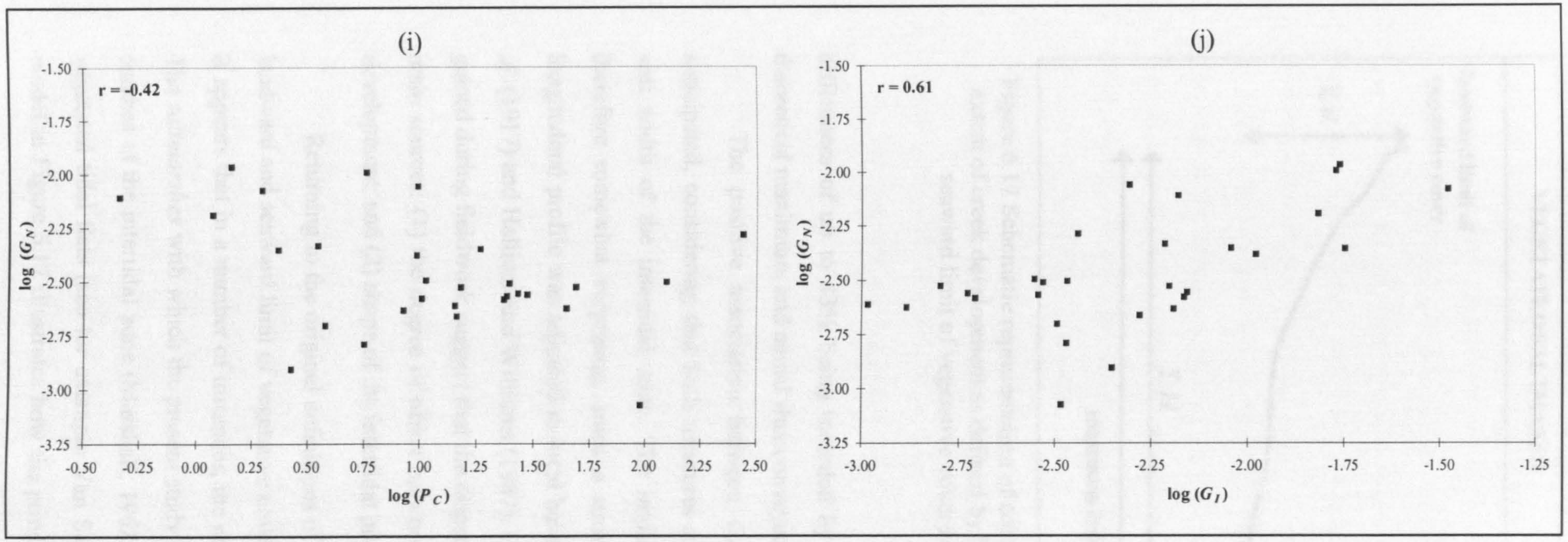

Figure 6.16 cont. Scatter plots showing statistically significant ($\alpha = .05$) associations which are in part attributable to mutual dependence on marsh area cover, between: (a) creek density (D_{eq}) and total prism (P_{TM}); (b) D_{eq} and intertidal gradient (G_I); (c) mean link length ($\overline{L}$) and P_{TM}; (d) network gradient (G_N) and P_{TM}; (e) width:depth ratio ($w{:}d_L$) and P_{TM}; (f) cross-sectional area (A_{SL}) and P_{TM}; (g) A_{SL} and channelised prism (P_C); (h) $w{:}d_L$ and P_C; (i) G_N and P_C; and (j) G_N and G_I.

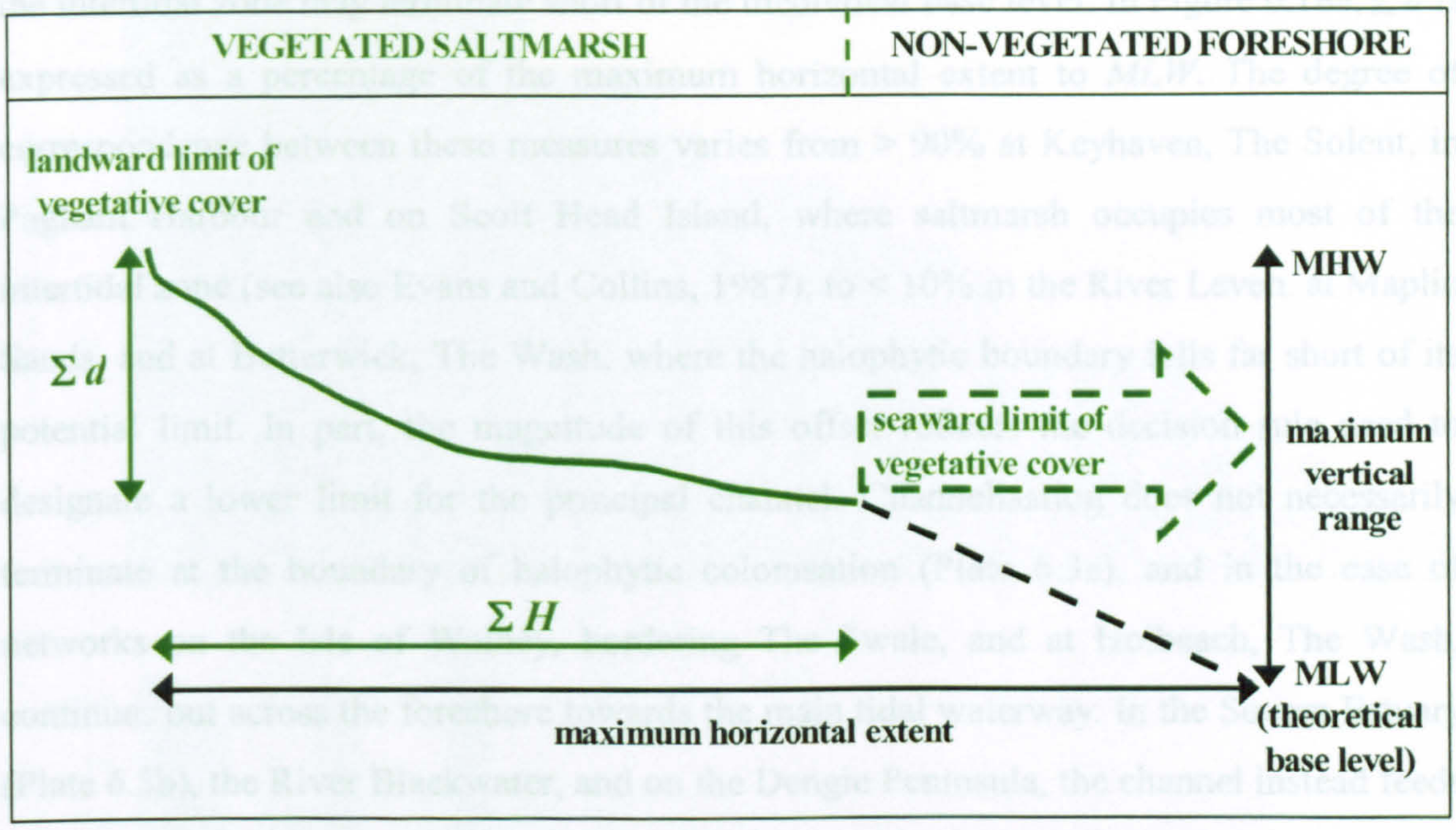

Figure 6.17 Schematic representation of coherence between the maximum theoretical extent of creek development as defined by base level, and the varied position of the seaward limit of vegetative cover recorded at the sample networks.

differences of up to 43% being recorded by French and Stoddart (1992) between the theoretical maximum, and actual flux conveyed through the creek system.

The positive association between G_N and G_I (Figure 6.16j) may have been anticipated, considering that both measures express the amount of vertical fall across a unit width of the intertidal zone. The imperfect nature of the relation ($r = 0.61$) is therefore somewhat surprising, since a stronger correlation could be expected if the longitudinal profile was adjusted to local base level in the manner envisaged by Yapp *et al.* (1917) and Haltiner and Williams (1987). Examination of the literature and experience gained during fieldwork suggest that the disparity between G_N and G_I can be traced to two main sources: (1) the degree of offset between theoretical and actual limits of saltmarsh development; and (2) shape of the intertidal profile.

Returning to the original definitions of G_N and G_I, the former extends between the landward and seaward limit of vegetative cover and the latter ranges from *MHW* to *MLW*. It appears that in a number of instances, the respective lower boundaries do not coincide. The *saltmarshes* with which the present study is concerned, are often perched in the upper reaches of the intertidal zone (Marshall, 1962; Chapman, 1974), and are fronted by non-vegetated tidal flats (see for example Van Straaten and Kuenen, 1957). The conceptual model in Figure 6.17 illustrates how the principal channel within the vegetated region of

the intertidal zone may terminate short of the theoretical base level. In Figure 6.18a, $\sum d$ is expressed as a percentage of the maximum horizontal extent to *MLW*. The degree of correspondence between these measures varies from > 90% at Keyhaven, The Solent, in Pagham Harbour and on Scolt Head Island, where saltmarsh occupies most of the intertidal zone (see also Evans and Collins, 1987), to < 10% in the River Leven, at Maplin Sands, and at Butterwick, The Wash, where the halophytic boundary falls far short of its potential limit. In part, the magnitude of this offset reflects the decision rule used to designate a lower limit for the principal channel. Channelisation does not necessarily terminate at the boundary of halophytic colonisation (Plate 6.3a), and in the case of networks on the Isle of Walney, bordering The Swale, and at Holbeach, The Wash, continues out across the foreshore towards the main tidal waterway. In the Severn Estuary (Plate 6.3b), the River Blackwater, and on the Dengie Peninsula, the channel instead feeds into a zone of mudmounds (see also Greensmith and Tucker, 1966). Elsewhere, the creek system terminates abruptly at the limit of vegetative colonisation, although an incised thalweg may extend towards the adjacent river channel (Plate 6.3c).

The shape of the intertidal profile is a second source of variation between G_N and G_I. If the foreshore exhibited a linear rate of descent between upper and lower boundaries, values for G_N and G_I would remain constant, irrespective of any horizontal shortfall. However, expressing Σd as a percentage of the vertical range between *MHW* and *MLW* (see Figure 6.17), indicates that this is not the case. At the majority of sites (Figure 6.18b), the percentage elevation change is very different from the corresponding lateral offset. The exponent of $b = 0.46$ for the trendline in Figure 6.18c, suggests that adjustment is far from evenly distributed across the intertidal zone, where a value of unity would denote a linear relation between the horizontal and vertical results. The subdued coefficient of determination ($r^2 = 0.38$) indicates that considerable noise is present about the regression line. This is particularly concentrated towards the upper end of the percentage scale, where scenarios range from near complete adjustment, to a pronounced vertical shortfall. In the former case, progressive adjustment throughout the system means that limited descent occurs beyond the boundary of halophytic colonisation. In the latter instance, the remaining offset is achieved through rapid descent across a lower convex margin, like that found at the River Roach (Plate 6.4a). Similar convexity on the lower mudflats bordering the main channel of the Severn Estuary, is responsible for an enhanced gradient. As shown by the aerial photographic coverage in Plate 6.4b, this effect has given rise to an array of proto-creeks (see also Van Straaten and Kuenen, 1957; Allen, 1985).

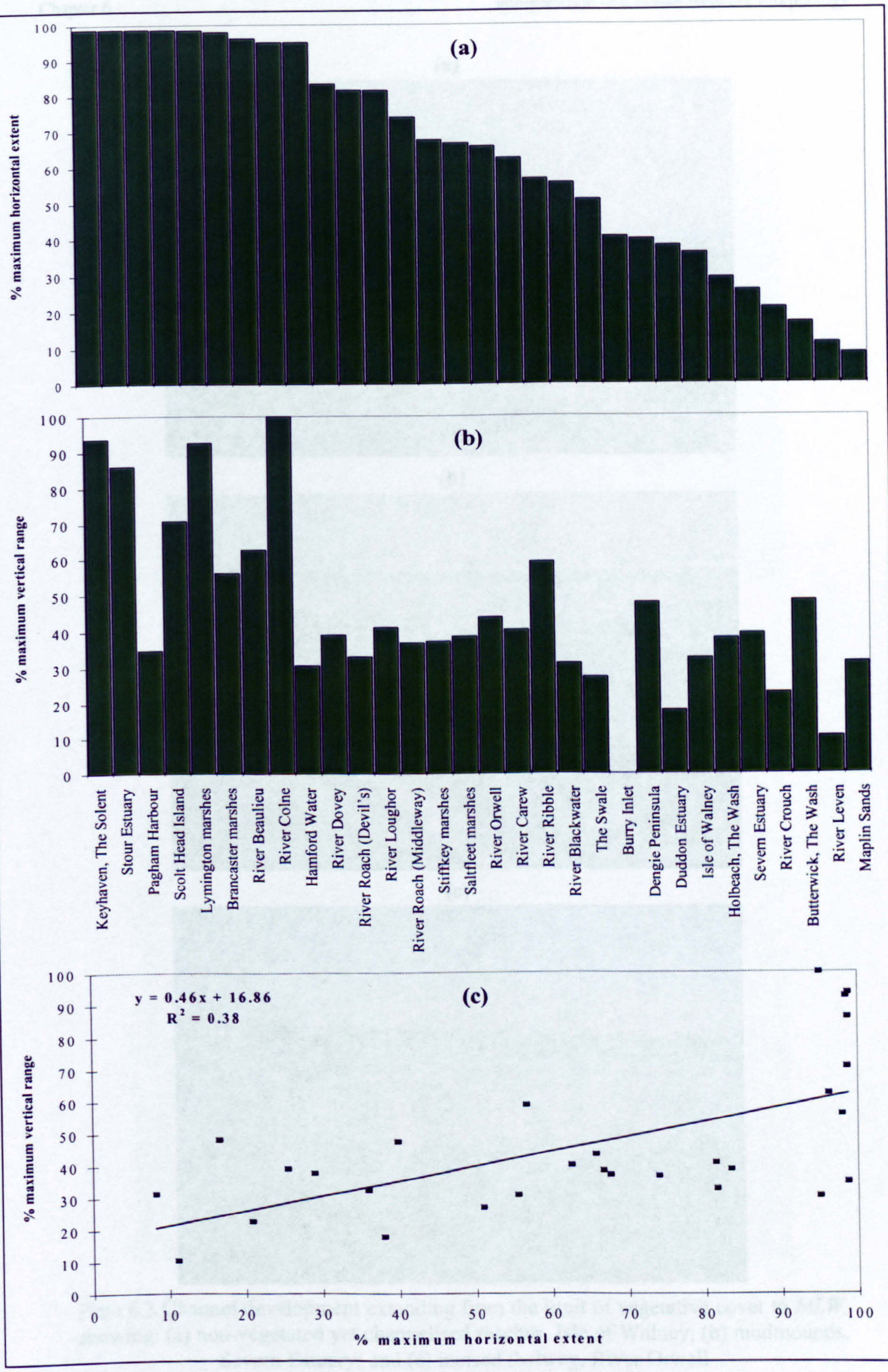

Figure 6.18 (a) Percentage offset between the limit of vegetative cover and maximum horizontal extent of saltmarsh development defined by *MLW*; (b) percentage offset between total elevation change ($\sum H$) along the principal channel and the maximum vertical range defined by *MTR*; and (c) scatter plot showing the relation between horizontal and vertical

(a)

(b)

(c)

Plate 6.3 Channel development extending from the limit of vegetative cover to *MLW,* showing: (a) non-vegetated yet channelised reaches, Isle of Walney; (b) mudmounds, Severn Estuary; and (c) incised thalweg, River Orwell

(a)

(b)

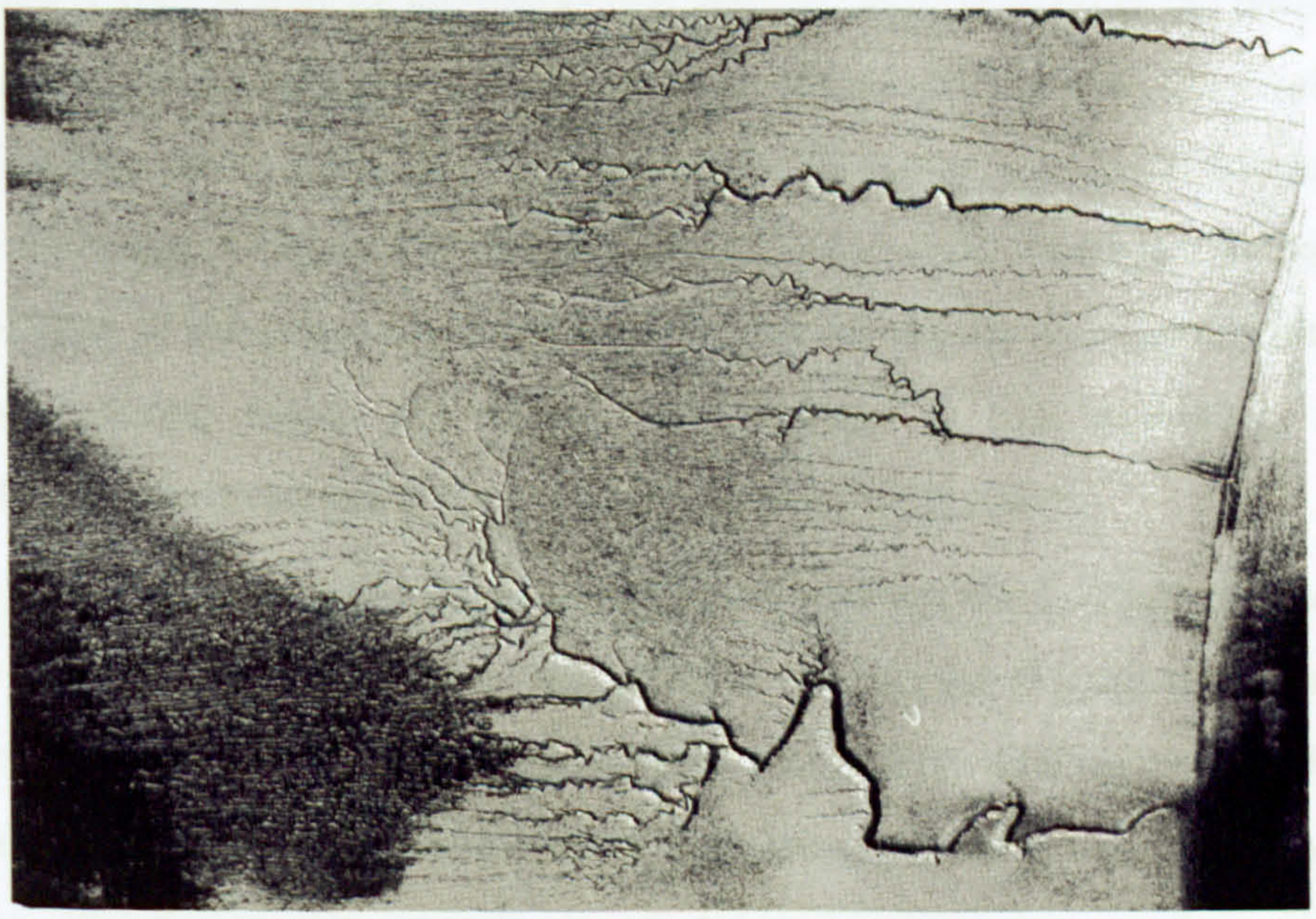

Plate 6.4 Convex descent to base-level across: (a) a narrow non-vegetated margin at the River Roach; and (b) mudflats bordering the main channel of the Severn Estuary.

6.5.2 Causal effects

In the absence of obvious mutual dependencies, the remaining significant associations (Table 6.7) are likely to reflect causal relations. The most widely alluded to association between network morphology and environmental controls, concerns the influence of sedimentary composition on network complexity (Chapman, 1974; Frey and Bassan, 1985; Allen, 1992). The positive correlation between *%silt-clay* and D_{eq} (Figure 6.19a) indicates that a lower density of creeks is needed to serve marshes situated on sandy materials compared with their silty counterparts. Morisawa (1964) suggests that the degree of channel development reflects the relative importance of different flow pathways. On impermeable soils with a high *%silt-clay*, the drainage of overmarsh flows should, in theory, be accomplished by surface runoff and channelised discharge. However, sub-surface flows are able to play an increasingly important role as the infiltration capacity of the marsh platform increases.

Several authors go on propose a link between D_{eq} and *STR* (Adam, 1990; Allen, 1992). The negative association in Figure 6.19b, indicates that marshes experiencing a large tidal range tend to support simple networks, while the density of creeks is higher under micro- and meso-tidal conditions. With a comparable level of association recorded for *%C* (Figure 6.19c), it may be envisaged that vertical range influences the proportion of tidal flux discharged through the channel network. Where *STR* is low, the creek system provides an efficient flow. As such, it tends to cover a higher proportion of the total marsh area. Where the range is higher, the marsh surface is more often sloping. Consequently, a greater proportion of the prism can be exchanged directly across the seaward limit of the system. The reduced extent of channel development is not surprising, since in proportional terms the conveyance function to be performed is lower.

STR achieves a maximum level of explanatory power for *L*, where it accounts for 32% of the total statistical variance. The positive correlation (Figure 6.19d) reveals a tendency towards the development of longer links under high tidal ranges. As the length of individual reaches reflects the frequency of branching, this systematic response may be attributed to changes in the importance of deterministic versus random influences. Opportunities for flow convergence, through channel meandering, are clearly enhanced where stochastic factors dominate during the early phases of network development (Section 1.4.4). Elongated reaches instead materialise when the controlling factors are

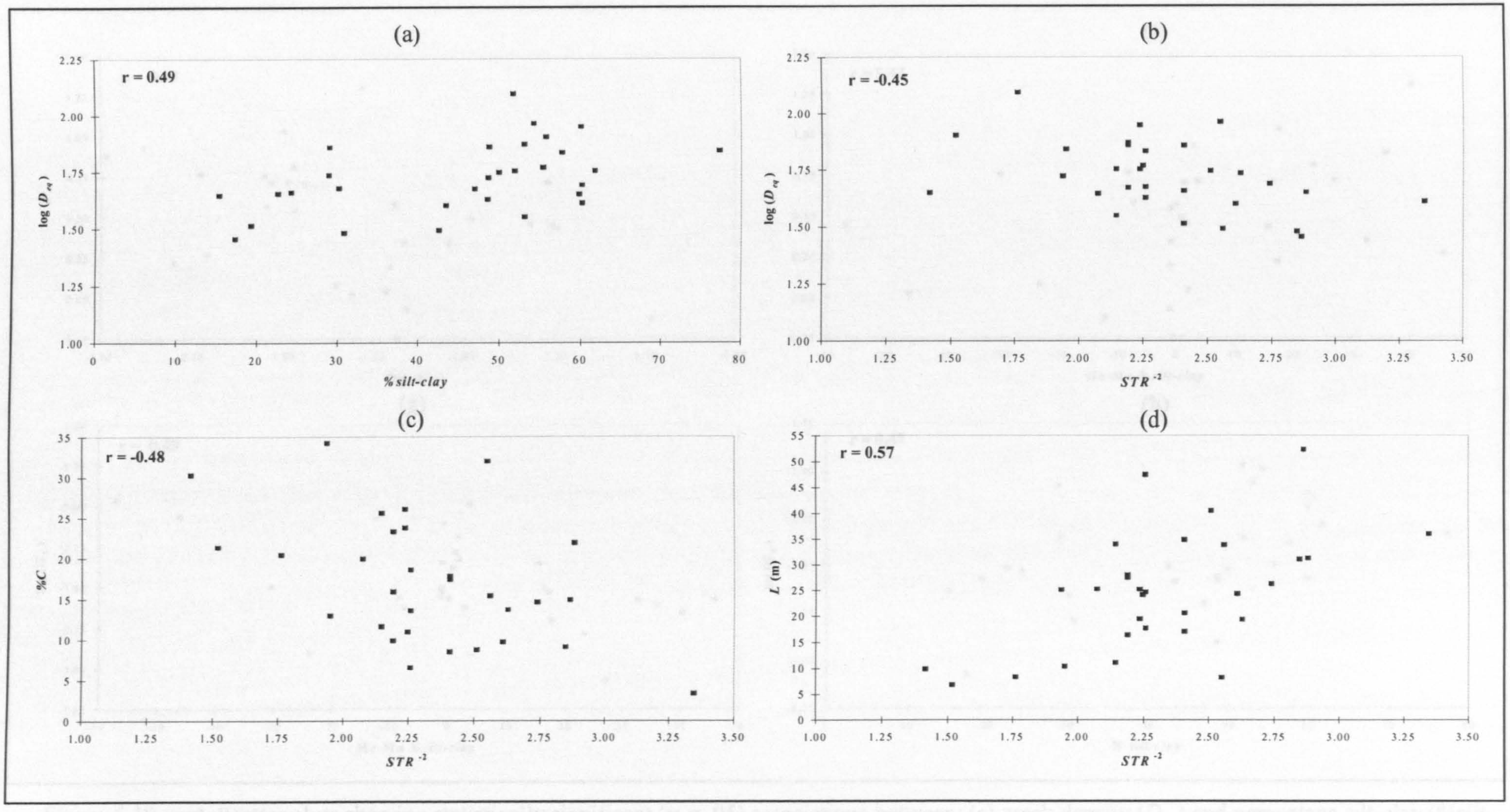

Figure 6.19 Scatter plots showing statistically significant ($\alpha = .05$) associations between: (a) creek density (D_{eq}) and percentage silt-clay (*%silt-clay*); (b) D_{eq} and spring tidal range (*STR*); (c) percentage channel cover (*%C*) and *STR*; (d) mean link length ($\bar{L}$) and *STR* (e) profile concavity (*I*) and intertidal gradient (G_I); (f) *I* and He-Mo *%silt-clay*; (g) network gradient (G_N) and He-Mo *%silt-clay*; (h) G_N and *%silt-clay*; (i) G_N and maximum hydraulic duty (H_{max}); (j) width:depth ratio ($w{:}d_L$) and *STR*.

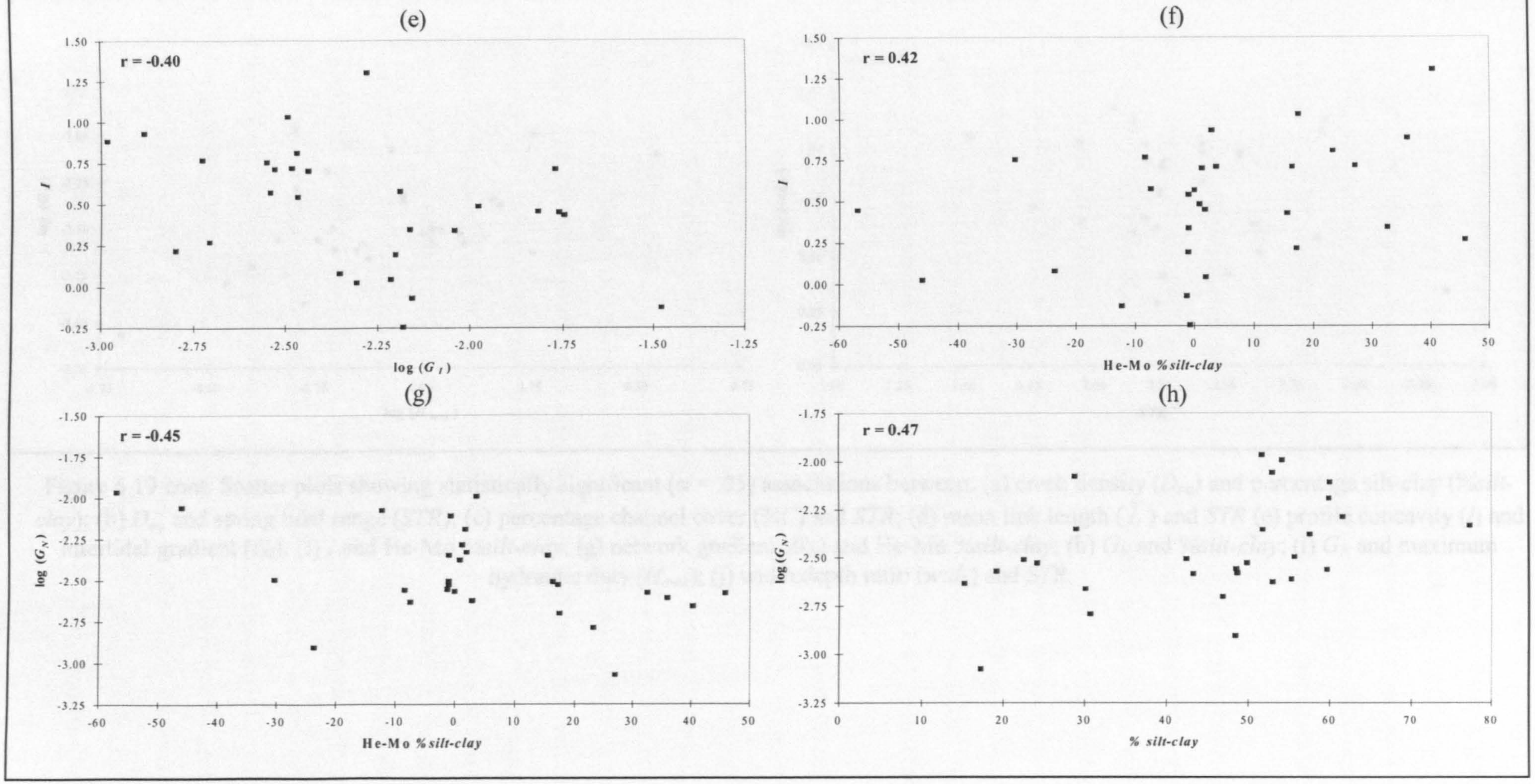

Figure 6.19 cont. Scatter plots showing statistically significant ($\alpha = .05$) associations between: (a) creek density (D_{eq}) and percentage silt-clay (*%silt-clay*); (b) D_{eq} and spring tidal range (*STR*); (c) percentage channel cover (*%C*) and *STR*; (d) mean link length ($\bar{L}$) and *STR* (e) profile concavity (*I*) and intertidal gradient (G_I); (f) *I* and He-Mo *%silt-clay*; (g) network gradient (G_N) and He-Mo *%silt-clay*; (h) G_N and *%silt-clay*; (i) G_N and maximum hydraulic duty (H_{max}); (j) width:depth ratio ($w{:}d_L$) and *STR*.

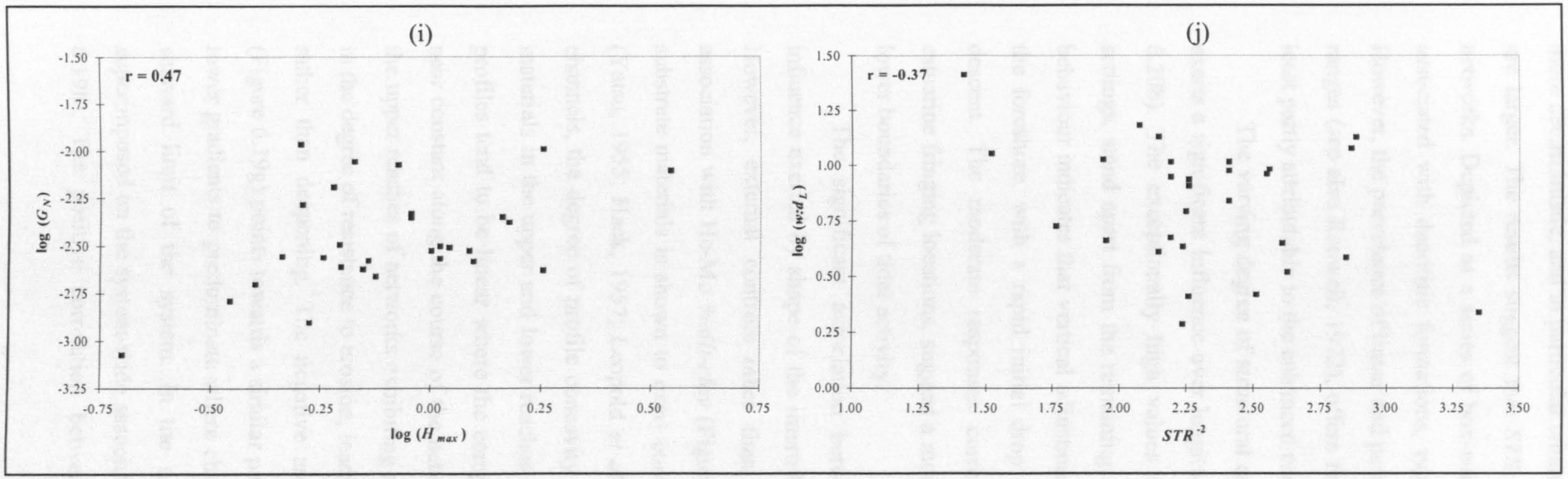

Figure 6.19 cont. Scatter plots showing statistically significant ($\alpha = .05$) associations between: (a) creek density (D_{eq}) and percentage silt-clay (*%silt-clay*); (b) D_{eq} and spring tidal range (*STR*); (c) percentage channel cover (*%C*) and *STR*; (d) mean link length ($\overline{L}$) and *STR* (e) profile concavity (*I*) and intertidal gradient (G_I); (f) *I* and He-Mo *%silt-clay*; (g) network gradient (G_N) and He-Mo *%silt-clay*; (h) G_N and *%silt-clay*; (i) G_N and maximum hydraulic duty (H_{max}); (j) width:depth ratio ($w:d_L$) and *STR*.

more deterministic, and in particular where the tidal range and resulting hydraulic gradient are larger. The results suggest that *STR* also influences the basic organisation of tidal networks. Depicted as a series of box-whisker plots in Figure 6.20a, the shorter reaches associated with dendritic formations, typically develop under subdued vertical ranges. However, the prevalence of linear and parallel formations at localities experiencing higher ranges (see also Ranwell, 1972), offers further confirmation that extended reaches are at least partly attributable to the enhanced energy slope.

The varying degree of structural control associated with different coastal settings, exerts a significant influence over longitudinal as well as planimetric adjustment (Figure 6.20b). The exceptionally high values recorded for profile concavity in open coast settings, stand apart from the remaining classes of response. This distinctive pattern of behaviour indicates that vertical adjustment is concentrated towards the upper reaches of the foreshore, with a rapid initial drop in bed elevation followed by a more gradual descent. The moderate responses corresponding with embayment, back-barrier and estuarine fringing locations, suggest a more evenly distributed fall between the upper and lower boundaries of tidal activity.

The significant association between G_I and I (Figure 6.19e), confirms the influence exerted by shape of the intertidal zone on the pattern of longitudinal descent. However, external controls other than gradient are also shown important, by the association with He-Mo *%silt-clay* (Figure 6.19f). In a fluvial context, the erodibility of substrate materials is shown to exert control over profile shape by a number of authors (Yatsu, 1955; Hack, 1957; Leopold *et al.*, 1964; Morisawa, 1964). In the case of tidal channels, the degree of profile concavity increases with the offset between channel bed materials in the upper and lower reaches of the system. In simple terms, this means that profiles tend to be linear where the composition and erodibility of substrate material is near constant along the course of the network. The concentration of vertical fall towards the upper reaches of networks exhibiting a changing composition, may reflect differences in the degree of resistance to erosion, leading to exaggerated adjustment through widening rather than deepening. The negative association between G_N and He-Mo *%silt-clay* (Figure 6.19g) points towards a similar pattern of constraint, since there is a tendency for lower gradients to predominate where channel bed materials coarsen rapidly towards the seaward limit of the system. In the networks studies, this 'downstream' signal is superimposed on the system-wide association between average *%silt-clay* and G_N (Figure 6.19h). The positive correlation between these variables suggests that longitudinal

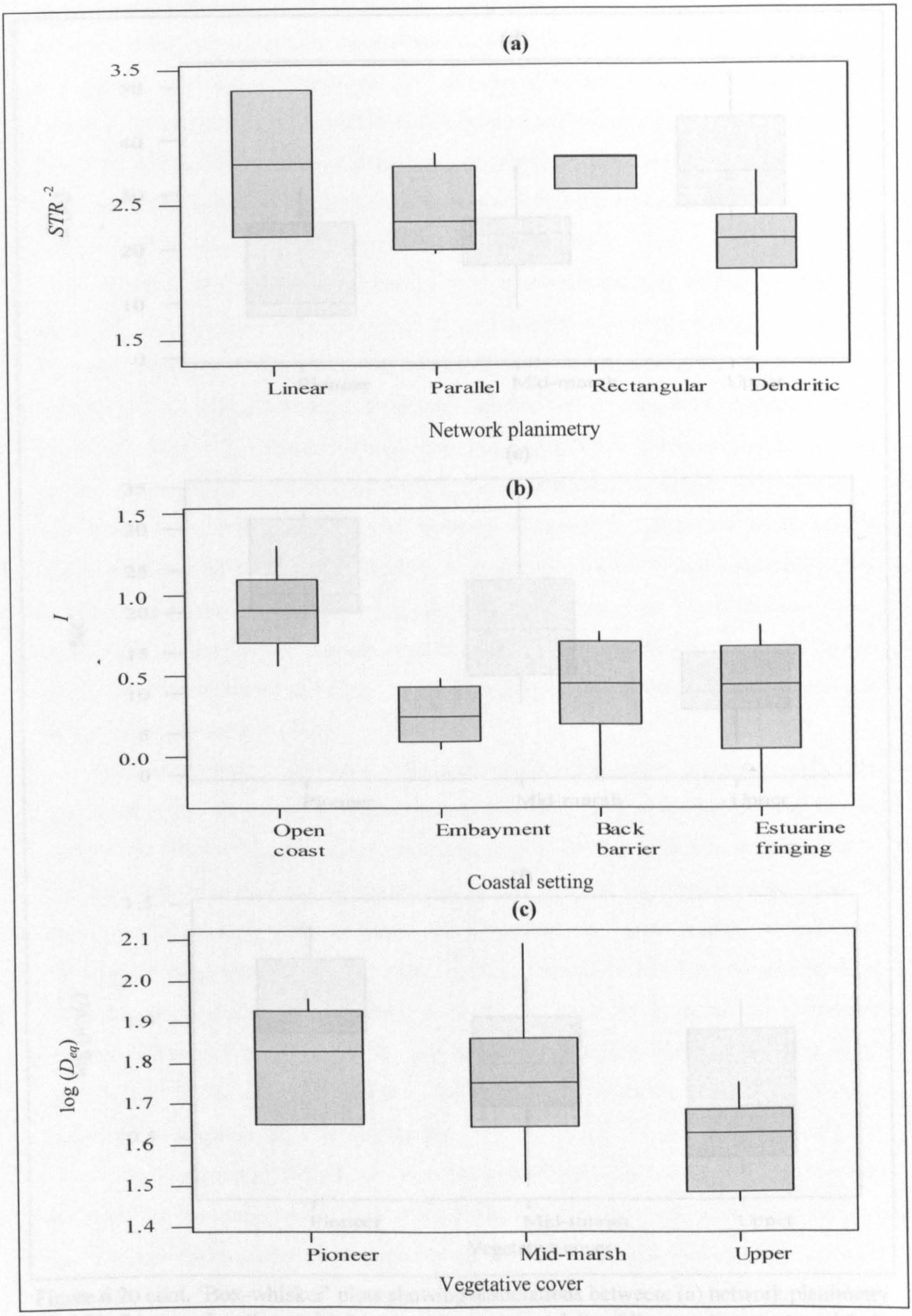

Figure 6.20 'Box-whisker' plots showing associations between: (a) network planimetry and *STR*; (b) coastal setting and *I*; (c) vegetative cover and D_{eq}; (d) vegetative cover and *L*; (e) vegetative cover and *%C*; and (f) vegetative cover and $w{:}d_L$.

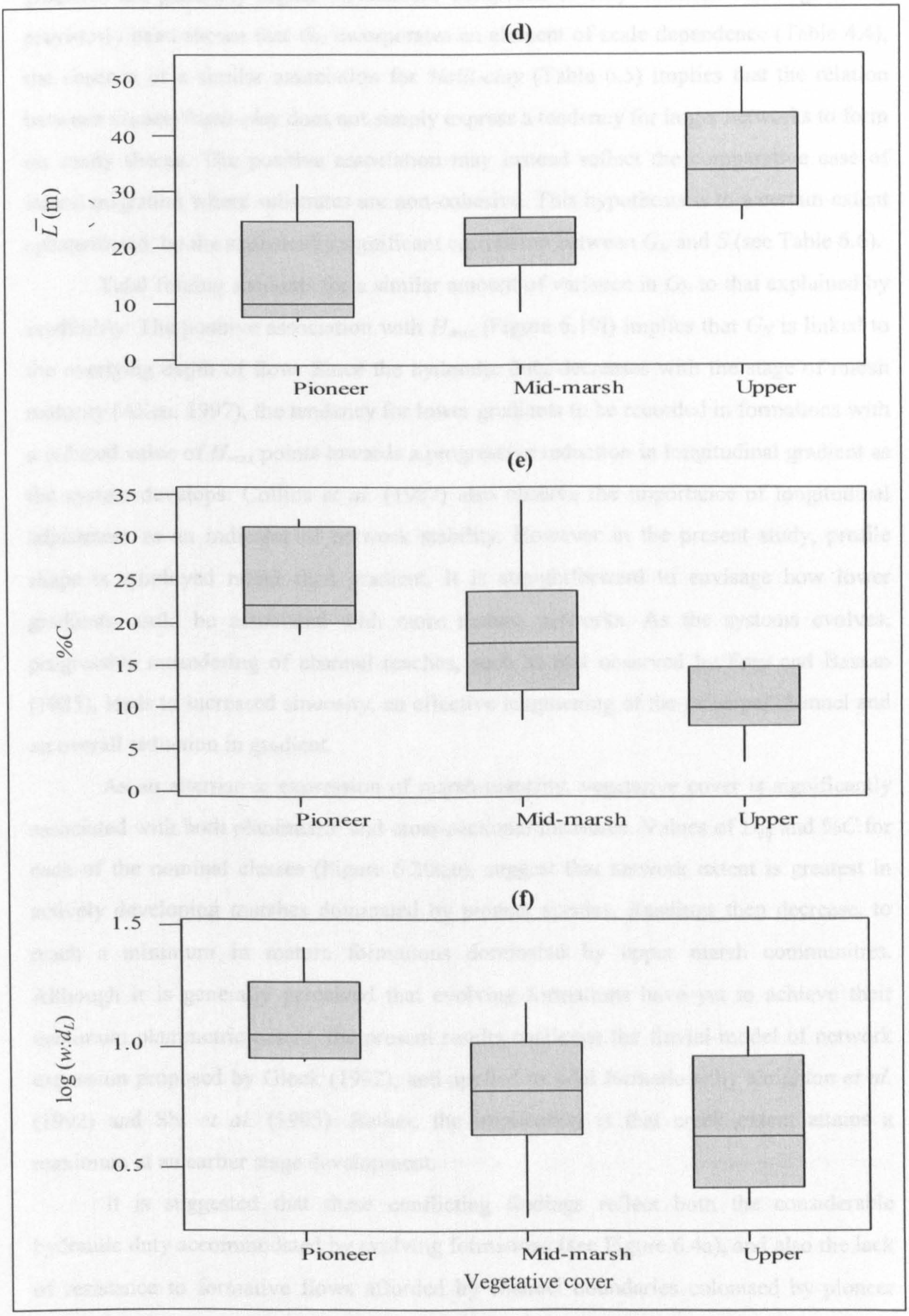

Figure 6.20 cont. 'Box-whisker' plots showing associations between: (a) network planimetry and *STR*; (b) coastal setting and *I*; (c) vegetative cover and D_{eq}; (d) vegetative cover and *L*; (e) vegetative cover and *%C*; and (f) vegetative cover and $w{:}d_L$.

gradients are generally higher on marshes composed of silty material. Although it has previously been shown that G_N incorporates an element of scale dependence (Table 4.4), the absence of a similar association for *%silt-clay* (Table 6.5) implies that the relation between G_N and *%silt-clay* does not simply express a tendency for larger networks to form on sandy shores. The positive association may instead reflect the comparative ease of lateral migration where substrates are non-cohesive. This hypothesis is to a certain extent substantiated, by the statistically significant correlation between G_N and S (see Table 6.6).

Tidal forcing accounts for a similar amount of variance in G_N to that explained by erodibility. The positive association with H_{max} (Figure 6.19i) implies that G_N is linked to the overlying depth of flow. Since the hydraulic duty decreases with the stage of marsh maturity (Allen, 1997), the tendency for lower gradients to be recorded in formations with a reduced value of H_{max} points towards a progressive reduction in longitudinal gradient as the system develops. Collins *et al.* (1987) also observe the importance of longitudinal adjustment as an indicator of network stability. However in the present study, profile shape is employed rather than gradient. It is straightforward to envisage how lower gradients could be associated with more mature networks. As the systems evolves, progressive meandering of channel reaches, such as that observed by Frey and Bassan (1985), leads to increased sinuosity, an effective lengthening of the principal channel and an overall reduction in gradient.

As an alternative expression of marsh maturity, vegetative cover is significantly associated with both planimetric and cross-sectional measures. Values of D_{eq} and $\%C$ for each of the nominal classes (Figure 6.20c,e), suggest that network extent is greatest in actively developing marshes dominated by pioneer species. Readings then decrease, to reach a minimum in mature formations dominated by upper marsh communities. Although it is generally perceived that evolving formations have yet to achieve their maximum planimetric extent, the present results challenge the fluvial model of network expansion proposed by Glock (1932), and applied to tidal formations by Knighton *et al.* (1992) and Shi *et al.* (1995). Rather, the implication is that creek extent attains a maximum at an earlier stage development.

It is suggested that these conflicting findings reflect both the considerable hydraulic duty accommodated by evolving formations (see Figure 6.4a), and also the lack of resistance to formative flows afforded by channel boundaries colonised by pioneer halophytes (Pestrong, 1965; Williams and Harvey, 1983; Coates *et al.*, 1995). From field experience, responses for $\%C$ in the River Carew and at Keyhaven and Lymington, appear

to be exaggerated by *Spartina* die-back (see also Tubbs, 1999). High values for w/d_L (Figure 6.20f), indicate that this effect has lead to considerable widening throughout the network. The marked fall in *%C* for systems colonised by upper-marsh species, is accompanied by a general lengthening of constituent links (Figure 6.20d). As such, the network characteristics of marshes colonised by mature communities adhere more closely to the conventional model of network development (see Frey and Bassan, 1985; also Allen, 1997). In these cases, a progressive reduction in hydraulic duty leads to network abstraction, reflected by an increase in the spacing between junctions along the course of the principal channel.

Of the remaining associations involving cross-sectional measures, the relation between w/d_L and *STR* is barely significant at the designated level. This implies only a weak tendency towards the dominance of adjustment through widening rather than deepening in networks experiencing a lower tidal range. The somewhat stronger positive correlation of A_{SL} with Be-Ba *%silt-clay* suggests that, to a certain extent, channel capacity reflects the relative erodibility of channel bed and banks. However, the tendency for reaches with comparatively cohesive banks to exhibit a larger capacity is unexpected. Other studies have instead found that resistance to erosion increases with the cohesion of constituent materials, thereby constraining the degree of enlargement (see, for example, Morisawa, 1964).

While the previous finding is difficult to explain from a knowledge of geomorphological processes, a number of associations that may have been anticipated on the basis of previous studies, did not prove significant for the present set of results. In terms of planimetric adjustment, additional relations are alluded to involving the sinuosity measures. While both Chapman (1974) and Frey and Bassan (1985) refer to the importance of vegetation as a control on the degree of creek meandering, Ranwell (1972) and Adam (1990) propose a negative association with *STR*. Adam (1990) goes onto cite sedimentary composition as a potential control on sinuosity, a factor which is also seen by Chapman (1974) to affect planimetric organisation. Of the cross-sectional measures, associations between A_{SL}, vegetative composition and sediment erodibility have been observed by Coates *et al.* (1995) in U.S. systems, while a number of authors (see, for example, Leopold *et al.*, 1964; Hume, 1991; Zeff, 1999) suggest that the cohesiveness of substrate materials influences w/d_L. Finally, Ranwell (1972) anticipates an association between G_N and *STR*. The absence of a similar relation for the present sample of networks may be explained by the offset between horizontal and vertical boundaries, which has

already been described (see Figure 6.17). However, in the remaining cases, failure to identify statistically significant associations may be due to other factors including:

- the original statement of relations in the form of hypotheses rather than fact, so that some are likely to be rejected and others are accepted
- the application of morphometric measures such as sinuosity, which were originally developed for fluvial systems and may not be appropriate in a tidal context
- the method employed in parameterising control and response variables may not produce a realistic or representative descriptor
- controls may exert a subtle level of influence, which is masked by other dominant factors at this extensive scale of analysis.

6.6 MULTIVARIATE RELATIONS

From a theoretical viewpoint, the natural complexity of environmental systems demands that the influence exerted by potential controls be addressed in combination. In this case, tidal forcing, erodibility and gradient effects are unlikely to operate in isolation. The transition from a bivariate to a multivariate approach, supports the formulation of empirically-based 'black-box' models (Kirkby *et al.*, 1987), which although closely aligned with the exploratory nature of this extensive phase of the analysis, may yield an improved understanding of interactions between the various controls and response measures.

To gain a coherent impression of the combined explanatory power of the key controlling elements, multiple regression analysis was undertaken using SPSS (Statistical Package for the Social Sciences) software. To act as a standard, the total amount of statistical explanation (r_t) provided by the entire suite of appropriately transformed descriptive variables, was computed for the morphometric indices (with the exception of S_T and S_A which do not satisfy normality requirements). Having thereby established the maximum against which the performance of a subset of measures can be compared, linear regression was repeated using the variables that recorded a significant bivariate association (see Table 6.7). Since the 'independent' controls with greatest explanatory potential have already been pre-selected using an intuitive strategy (Shaw and Wheeler, 1997), the regression was carried out by straightforward entry, rather than a selective stepwise approach (Hauser, 1974). The resulting multiple regression coefficient (r_m), multiple coefficient of explanation (R^2) and partial (b) regression coefficients are recorded

MORPHOMETRIC MEASURE	r_t (R^2)	r_m (R^2)	PRE-SELECTED INDEPENDENT VARIABLES $^{b}_{B}$
D_{eq}	0.81 (0.65)	0.74 (0.55)	***%silt – clay*** $^{0.01}_{0.37}$ ***GI*** $^{0.15}_{0.37}$ ***STR*** $^{-0.11}_{-0.30}$ ***PTM*** $^{-0.03}_{-0.09}$
$\%C_{eq}$	0.97 (0.94)	0.48 (0.23)	***STR*** $^{-9.21}_{-0.48}$
$\overline{L}$	0.86 (0.75)	0.76 (0.58)	***STR*** $^{13.94}_{0.50}$ ***PTM*** $^{6.31}_{0.30}$
G_N	0.91 (0.82)	0.88 (0.77)	***Hmax*** $^{0.50}_{0.47}$ ***GI*** $^{0.15}_{0.37}$ ***%silt – clay*** $^{0.01}_{0.37}$ ***PC*** $^{0.13}_{0.31}$ ***HeMo*** $^{-0.01}_{-0.26}$ ***PTM*** $^{-0.12}_{-0.23}$
I	0.75 (0.57)	0.46 (0.21)	***GI*** $^{0.25}_{-0.31}$ ***HeMo*** $^{0.01}_{0.25}$
w/d_L	0.87 (0.75)	0.80 (0.64)	***PC*** $^{0.31}_{0.70}$ ***STR*** $^{1.03}_{-0.30}$ ***PTM*** $^{-0.03}_{-0.05}$
A_{SL}	0.93 (0.86)	0.88 (0.77)	***PC*** $^{0.69}_{0.97}$ ***PTM*** $^{-0.22}_{-0.27}$ ***BaBe*** $^{0.05}_{0.19}$
L_{INT}/L_{EXT}	0.70 (0.49)	-	-
S	0.39 (0.15)	-	-
S_N	0.76 (0.58)	-	-

Table 6.8 Summary of regression analysis for the morphometric descriptors, using the full set of transformed 'independent' controls (r_t) and the subset comprising measures that were pre-selected on the basis of statistically significant ($\alpha = .05$) bivariate correlations (r_m). The multiple coefficient of determination (R^2) is recorded for each equation, together with partial regression coefficients (b) and beta weights (B) for every variable.

for each model in Table 6.8. The controls are organised in descending order of influence exerted over the response measure, as indicated by the standardised regression coefficients or beta weights (B).

Values of r_t indicate that the total variable set offers different levels of explanatory potential for statistical variance observed in the morphometric descriptors. Taken as a whole, the combined influence of tidal forcing, erodibility, gradient and extraneous effects accounts for >80% of the variation in $\%C_{eq}$, G_N and A_{SL}. While associated F-statistics show these regression models to be highly significant, in other instances the degree of explanation provided by the elemental controls ranges from a moderate level of 65-75% for D_{eq}, w/d_L and L, to a poor result of < 60% for L_{INT}/L_{EXT} and the sinuosity measures. The subdued readings for these latter indices, which are not significant at the designated level (α=.05), were perhaps to be expected given the failure to identify significant associations during the preceding correlation analysis. Taking S as an example, the

present set of variables accounts for only 15% of the total variance. In a bid to justify this substantial shortfall, as well as the more minor offsets, it is necessary to consider a number of possibilities. As previously discussed in a bivariate context, the disparity may be attributable to: (1) additional factors which proved difficult to parameterise; (2) the dominance of random influences; (3) measurement errors; or (4) the dubious translation of a fluvial measure into a tidal context.

Balanced against the objective of achieving a high level of explanatory power is the consideration of data redundancy. There is little point including variables that make only a minor contribution to the overall performance of the regression model. Comparing results for r_t and r_m reveals the extent to which the pre-selected group of indices replicates the total variable set, and thereby the degree of redundancy within the non-significant controls. For D_{eq}, L, G_N, w/d_L and A_{SL} the offset is comparatively small, suggesting that the reduced set of measures provide a reasonable representation of the key geomorphic interactions and the remaining variables are largely redundant. However, the substantial shortfall for I and C_{eq} instead implies that important aspects of adjustment are accounted for by variables that were rejected on the basis of their statistical significance. Although it appears that a Type II error may have been made, it should be remembered that additional factors explaining, for example, a tendency towards amplified cross-sectional adjustment through widening, or the headward concentration of longitudinal fall, could be spread across a number of the variables. Although not individually significant, these may collectively account for a significant proportion of the total variance. An alternative method of parameterisation is clearly required which represents these outstanding interactions more succinctly.

The partial coefficients (Table 6.8) provide a general impression of the relative importance of each control, in terms of how much change in the dependent variable is produced by a standardised change in each independent variable (Shaw and Wheeler, 1997). A marked similarity in values recorded for the controls on D_{eq} and G_N, suggests that *%silt-clay*, G_I, *STR* and P_{TM} exert a comparable degree of influence. In the case of L, *STR* is instead seen to dominate over P_{TM}. The relative magnitude of readings obtained for B follows the bivariate responses (Table 6.7), indicating that the descriptors of cross-sectional form are far more responsive to changes in P_C than the other factors. The relation of w/d_L and A_{SL} with P_C also overshadows the remaining responses in absolute terms, with the strength of association pointing, at least in a statistical sense, towards the importance of this particular interaction.

In light of these findings, the interpretative phase of this study has served its purpose by establishing substantial relations of connection between the morphologic characteristics of tidal channel networks and geographically diverse environmental controls. Although progress has clearly been made through the generation and evaluation of empirical models, the results are fundamentally lacking in true explanatory power. Accordingly, it is appropriate, and indeed necessary, to relinquish the extensive approach, in favour of intensive analytical methods, which promise insight into the interactions underpinning these basic empirical models.

6.7 SUMMARY OF KEY FINDINGS

Key findings from the preceding interpretation of channel network morphology are summarised as follows:

- Although originally defined as a measure of tidal forcing, hydraulic duty provides a useful indication of the developmental status attained by the sample networks. The minimal duty to be performed, implies that formations in the Duddon Estuary, the River Leven, the River Ribble, and at Holbeach, The Wash, are approaching a mature stage of development. The composition of halophytic species is consistent with this finding, and additionally suggests that networks in the River Carew, and at Keyhaven and Lymington, are actively developing. For the remaining sites, which appear to have achieved a stable status, network characteristics are most likely to reflect the contemporary set of environmental controls.

- It is reasonable to employ the limit of vegetative cover as a lower boundary for *saltmarsh* channel network development, on grounds of the contrasting process regimes displayed by vegetated versus non-vegetated sectors of the intertidal zone. However, such a distinction is called into question where channelisation continues seaward across the fronting tidal flats, in the manner envisaged by Yapp *et al.* (1917). The morphological characteristics of these remote, channelised reaches, and the adjoining mudflats, are probably dominated by the process regime of the main tidal waterway.

- In the absence of detailed terrain models and an improved understanding of flow pathways, the methods available for computing an overmarsh tidal prism are limited in terms of their physical realism.

- A set of morphometric descriptors comprising: D, $\%C$, L, G_N, I, w/d_L and A_{SL}, provide a conceptually sound and apposite representation of planimetric, cross-sectional and longitudinal adjustment for tidal channel networks. While measures of F, L_{EXT} and L_{INT}, in theory, encapsulate distinct aspects of morphological behaviour, correlation analysis indicates that they merely mirror the response of other variables.

- Mutual dependence on scale explains statistically significant bivariate associations involving measures of D_{eq}, L, G_N, w/d_L, A_{SL}, P_C, P_{TM}, and G_I. In the case of area-based indices, relations arise from the method of calculation. For cross-sectional descriptors, associations can instead be explained from a knowledge of geomorphological processes. Causal effects are likely to be responsible for the remaining associations of significance between: D_{eq}, G_I and *%silt-clay*; *%C*, L and *STR*; I and G_I; and G_N with H_{max}.

- The lack of explanatory power for the various sinuosity measures suggests that the translation from a fluvial to a tidal context may be inappropriate. The absence of significant associations between measures such as G_N and *STR*, which are documented elsewhere in the literature, may be attributable to the method of parameterisation.

- Multivariate analysis indicates that the set of external controls account for a high proportion of the total statistical variance displayed by D_{eq}, $\%C$, L, G_N, w/d_L and A_{SL}. The poor performance for S and S_N, suggests that other controlling elements may dominate morphological adjustment. The subset of controls, which were pre-selected on the basis of significant bivariate associations, also provide a high level of statistical explanation for variance observed in D_{eq}, L, G_N, w/d_L, and A_{SL}. Gradient effects and erodibility dominate planimetric and longitudinal measures, while cross-sectional measures primarily reflect the magnitude of tidal forcing.

- An extensive methodological approach has proved useful as a means of exploring general patterns of association between the morphological characteristics of tidal channel networks, internal influences and a geographically diverse suite of external environmental controls. Attention has been focused on a number of highly significant associations, which may be further investigated through a more intensive approach.

7. THEORETICAL BASES FOR THE EVALUATION OF PHYSICAL FUNCTION

7.1 INTRODUCTION

The 'extensive' characterisation and interpretation of saltmarsh channel network morphology undertaken in Chapters 3-6 has usefully highlighted 'substantial relations of connection' between optimal morphometric descriptors and a range of environmental controls. In a statistical sense, the findings are dominated by an association between cross-sectional geometry and tidal prism ($r > 0.8$). As such, tidal forcing is seen to be particularly important in the adjustment process, the implication being that creek morphology may predominantly be conditioned to perform a conveyance function. Process studies (see, for example, French and Stoddart, 1992) indicate that formative events occur as the system drains, during the ebb phase of over-marsh tides. However, Pethick (1992, p.54) instead emphasises the importance of excess flood tidal energy as an agent of geomorphic work, and goes on to assert that '*creeks are not a morphological response to drainage of the ebbing tide from the marsh* ...', but instead represent '*... a morphological device to dissipate tidal wave energy'*. Through the implementation of theoretical mathematical models, the following evaluation seeks to clarify the nature of causal relations between form and function, and resolve these differences in emphasis, with a view to producing a unified conceptual model which may constitute the basis of channel network design in saltmarsh restoration schemes.

The transition from an empirical, to a more theoretically-based approach, is necessary to achieve a higher level of explanatory power. This switch in emphasis is in turn consistent with the adoption of an 'intensive' research design (see Figure 2.1). An increase in spatial scale is typically involved, and in this instance the geographically diverse sample of localities is refined to a *Small-N* (*sensu* Richards, 1996) illustrative case study, focusing on Brancaster Marsh, Norfolk (see Section 2.4.2).

Model evaluation is undertaken in two stages. The first (Section 7.2) investigates the utility of a probabilistic approach involving the prediction of network-scale angular geometry on the basis of an optimality principle that seeks to minimise various 'cost' criteria. A deterministic approach is subsequently employed (Section 7.3), to ascertain whether the physically-based concept of stability shear stress provides an explanation for reach-scale cross-sectional adjustment. Key findings are presented in Section 7.4.

7.2 OPTIMAL ANGULAR GEOMETRY

Through analogy with fluvial systems, the dominance of ebb tidal flows in many saltmarshes suggests that their networks may evolve to perform an efficient *drainage* function. While this has seemed intuitively correct to a number of authors based upon observed similarities between the planimetric organisation of river networks and saltmarsh creeks (see, for example, Yapp *et al.*, 1917; Steers and Thomas, 1929; Ragotzkie, 1959; Steers, 1959), others have emphasised the form-process paradox whereby rivers convey uni-directional and tidal channels bi-directional flows (Wright *et al.*, 1973; Pestrong, 1970, 1972; Knighton *et al.*, 1992). The model of optimal angular geometry, which was originally applied to fluvial systems by Roy (1983, 1985) and subsequently implemented in a tidal context by French (1996), provides a formal means of testing whether the branching pattern of these networks evolves in such a way that they perform comparable functions.

Section 7.2.1 outlines the definition of a model of optimal angular geometry for channel confluences. A selection of cost criteria, which may prove to be important in the adjustment process, are then introduced in Section 7.2.2, and their integration into a *generalised* optimal angular geometry model described. Theoretical responses obtained by running this model for a range of input values are discussed in Section 7.2.3. The methods involved in data acquisition are presented in Section 7.2.4., and a simulation focusing on Brancaster Marsh (for a full description of the study site, see Section 2.4.2) performed in Section 7.2.5, to: (1) ascertain whether the optimality principle can be used to predict the angular geometry of natural tidal creeks; and (2) establish if the 'best-fit' model is meaningful in terms of physical function.

7.2.1 Model definition

The non-random nature of channel network angular geometry is recognised in a number of previous studies (Zernitz, 1932; Horton, 1945; Howard, 1964; Lubowe, 1964; Morisawa, 1964; Roy, 1983). The search for insight into factors governing the adjustment process has involved a number of methodological approaches. Direct observation of processes operating at confluences are made by Mosley (1976), Richards (1980) and Best (1988), while the influence of configurational controls, such as topography and lithology, is inferred by Zernitz (1932) and Pestrong (1965). Inferential techniques also play a key role in the formulation of early models by Horton (1945) and Schumm (1956), which

emphasise the importance of local controls, such as gradient, on branching form. More rigorous analyses of channel width, depth and discharge as potential controls, have respectively been undertaken by Roy and Woldenberg (1986), Roy and Roy (1988) and Pieri (1984).

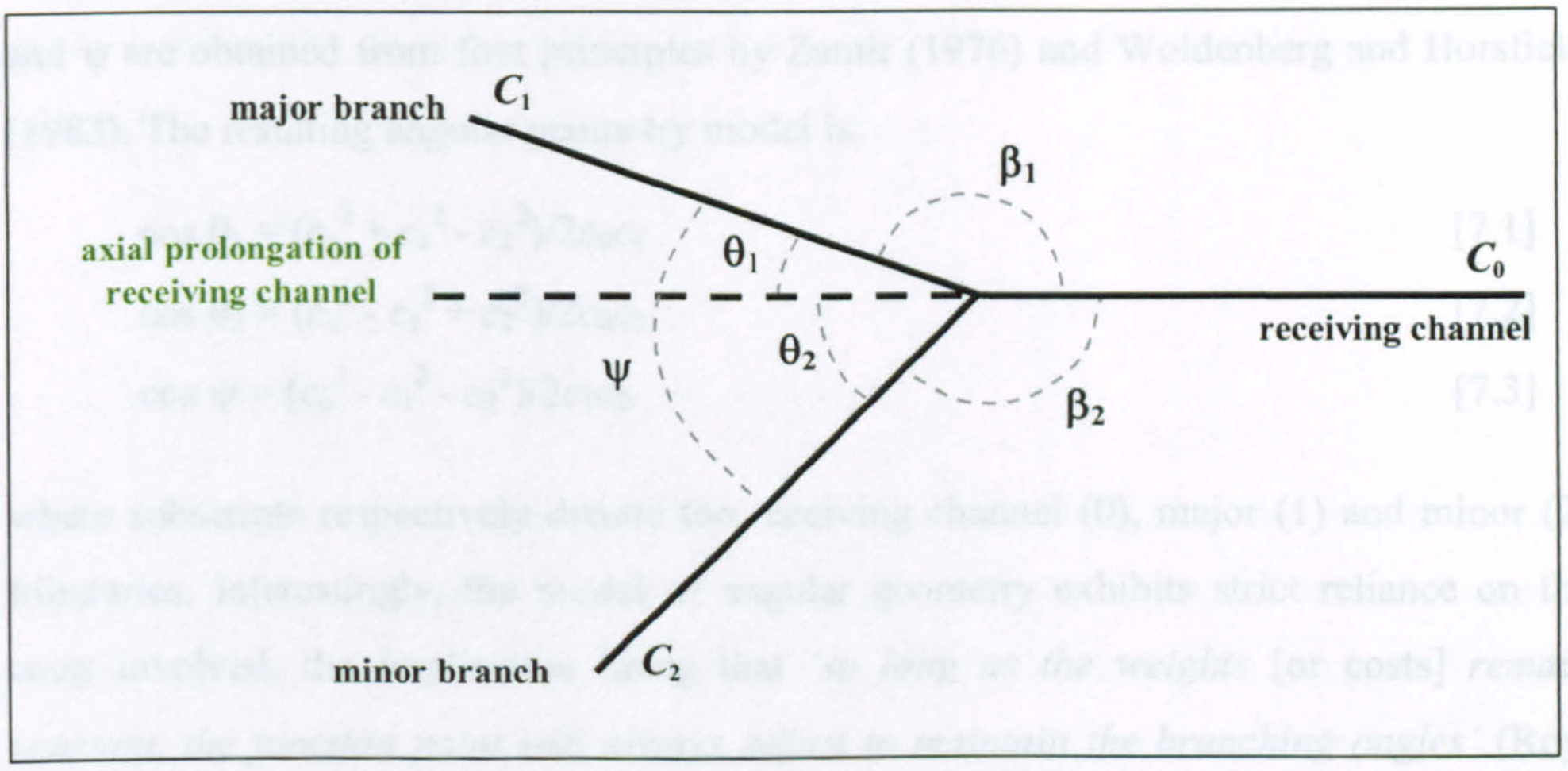

Figure 7.1 Definition diagram showing major (θ_1) and minor (θ_2) branching angles, the junction angle (ψ) and costs (c) for the tributaries and receiving channel (c_0).

Leopold (1971) alternatively suggests that branching structures, such as those viewed in fluvial and tidal networks, are synonymous with an efficient mode of operation, and the optimisation of construction costs (see also Rodriguez-Iturbe *et al.,* 1992). The notion that optimality may constitute a fundamental principle governing system behaviour was first applied in other fields, including the study of transport, communication (Haggett and Chorley, 1969) and biological systems, the structural geometry of organisms and in solid mechanics (see Howard, 1990). In particular, considerable progress has been made towards the definition of optimal junction angles in biological networks (Zamir and Bigelow, 1974; Zamir, 1976, 1986; Roy and Woldenberg, 1982; Woldenberg and Horsfield, 1983, 1986). The basic premise of the *optimality principle* is that optimal branching angles are achieved when a particular 'cost' function (c) is minimised around a junction. The optimal solution is consequently seen as an exercise in locational analysis of the junction point (Roy, 1985).

Following Woldenberg and Horsfield (1983), the angular geometry of any bifurcating junction may, as shown in Figure 7.1, be defined with major (θ_1) and minor (θ_2) branching angles (where $\theta_1 \leq \theta_2$ and $\theta \leq 90^o$) respectively formed between the larger and smaller tributaries and the axial prolongation of the main (receiving) channel. The

junction angle (ψ) is the product ($\theta_1+\theta_2$). Based on the fundamental postulate that a network will perform functions with maximum efficiency so that the costs involved in operation will be minimised, the least cost model has been solved by geographers and regional scientists (see, for example, Miehle, 1956; Wesolowsky, 1973) where it is referred to as the three-point Weber problem. Expressions for the optimal values of θ_1, θ_2, and ψ are obtained from first principles by Zamir (1976) and Woldenberg and Horsfield (1983). The resulting angular geometry model is:

$$\cos\theta_1 = (c_o^2 + c_1^2 - c_2^2)/2c_0c_1 \quad [7.1]$$

$$\cos\theta_2 = (c_o^2 - c_1^2 + c_2^2)/2c_0c_2 \quad [7.2]$$

$$\cos\psi = (c_o^2 - c_1^2 - c_2^2)/2c_1c_2 \quad [7.3]$$

where subscripts respectively denote the receiving channel (0), major (1) and minor (2) tributaries. Interestingly, the model of angular geometry exhibits strict reliance on the costs involved, the implication being that *'so long as the weights* [or costs] *remain constant, the junction point will always adjust to maintain the branching angles'* (Roy, 1985, p.271). As such, the specification of these costs, in terms of viable physical principles, is central to success of this model in explaining the branching characteristics of tidal channel networks.

7.2.2 Cost criteria

A number of cost criteria are documented in the literature. For biological systems, Zamir (1976) suggests that conditions of minimum power (see also Murray, 1926), minimum drag, minimum surface area and minimum volume may govern branching geometry. These expressions are modified by Roy (1983, 1985) for application in fluvial networks, resulting in the identification of possible criteria as: (1) minimum power loss (see also Howard, 1971); (2) minimum total flow resistance; (3) minimum resisting force; and (4) minimum volume. Formula for these principles are given in Equations 7.4 - 7.7, where ρ is fluid density, g is the gravitational constant, Q is dominant discharge, s is energy gradient, w_b is width, d_b is depth and v is velocity of flow.

Minimum power loss:	$c = \rho g Q s$	[7.4]
Minimum total flow resistance:	$c = \rho g w_b d_b s / v^2$	[7.5]
Minimum resisting force:	$c = \rho g w_b d_b s$	[7.6]
Minimum volume:	$c = w_b d_b$	[7.7]

According to Howard (1990) and Molnar and Ramirez (1998a,b), other candidates include minimum shear stress and minimum stream power per unit width. However, these are not considered by the present study due to difficulties in parameterisation.

As depicted in Figure 7.2, Roy (1983) goes on to simplify the cost criteria, using hydraulic geometry relations (Leopold and Maddock, 1953) to express the various physical principles in the common mathematical form of Equation 7.8, where **j** is a constant.

$$c = \mathbf{j}\, Q^{1+\mathbf{k}} \qquad [7.8]$$

$$Q_0 = Q_1 + Q_2 \qquad [7.9]$$

$$\alpha = Q_2 / Q_1 \qquad (\text{where } Q_2 \leq Q_1) \qquad [7.10]$$

Using the continuity equation of flow (Equation 7.9) to define the symmetry ratio (Equation 7.10), which reflects the relative capacities of the major and minor tributaries, general optimal angular geometry models for fluvial and tidal networks can be defined as:

$$\cos\theta_1 = \frac{(1+\alpha)^{2x} + 1 - \alpha^{2x}}{2(1+\alpha)^{x}} \qquad [7.11]$$

$$\cos\theta_2 = \frac{(1+\alpha)^{2x} - 1 + \alpha^{2x}}{2\alpha^{x}(1+\alpha)^{x}} \qquad [7.12]$$

$$\cos\psi = \frac{(1+\alpha)^{2x} - 1 - \alpha^{2x}}{2\alpha^{x}} \qquad [7.13]$$

(for a full derivation see Roy, 1983), where x = 1+**k** and **k** < 0. It is now necessary to establish the sensitivity of Equations 7.11-7.13 to variations in α and x, since this will greatly aid the evaluation of model performance, when 'best' predicted angles are compared with the observed geometric characteristics of natural junctions (Section 7.2.5).

7.2.3 Theoretical responses

Theoretical responses were obtained using the models of optimal angular geometry (Equations 7.11-7.13) for: (a) values of **k** in the range -1.5 < **k** < 0; and (b) values of α in the range $0 < \alpha < 1$.

An analysis of major branching angles (Figure 7.3a), suggests a progressive widening of θ_1 to a maximum of 60° as the exponent **k** tends towards a value of **k** = -1.

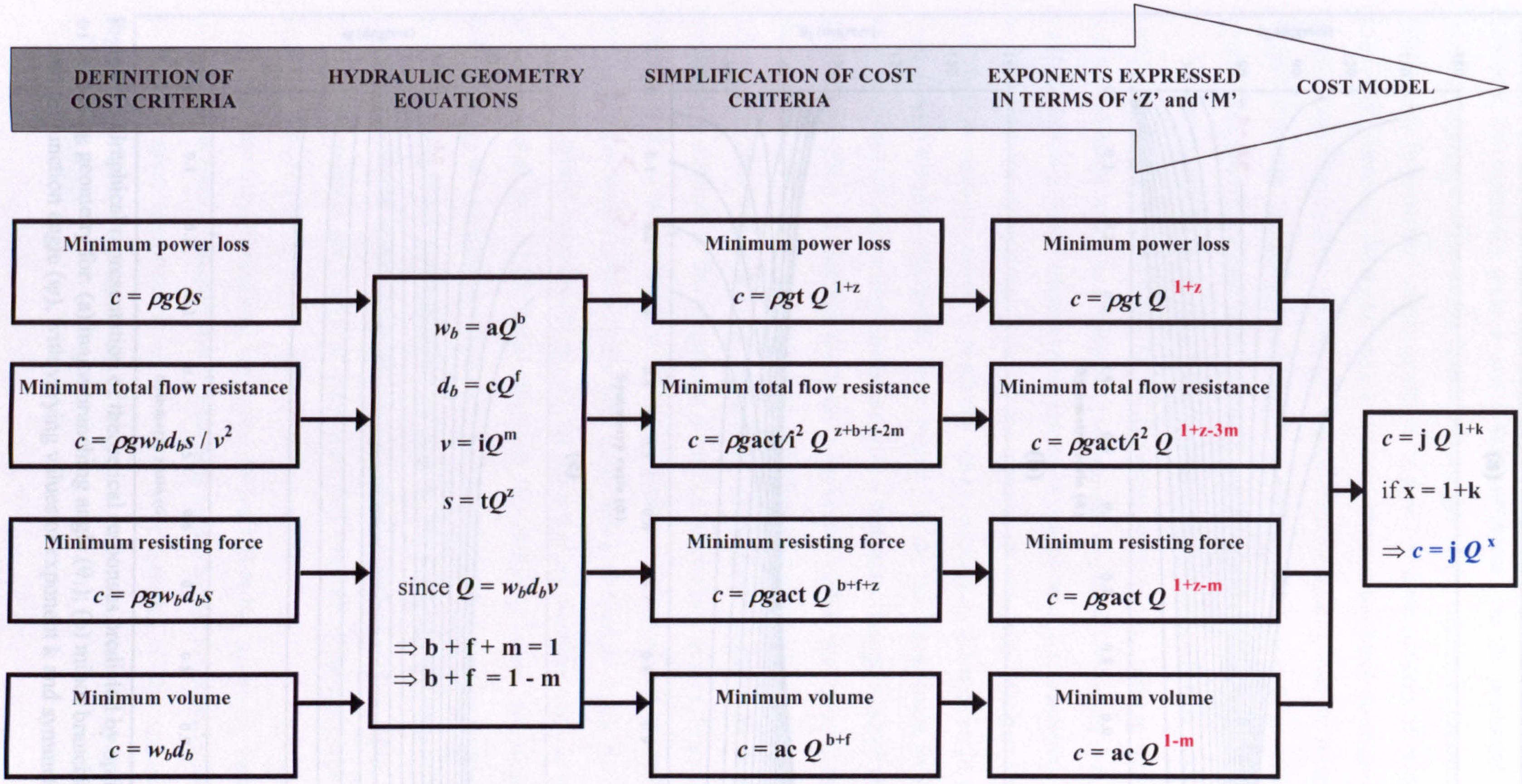

Figure 7.2 Schematic representation of stages involved in the simplification of cost criteria using hydraulic geometry relations.

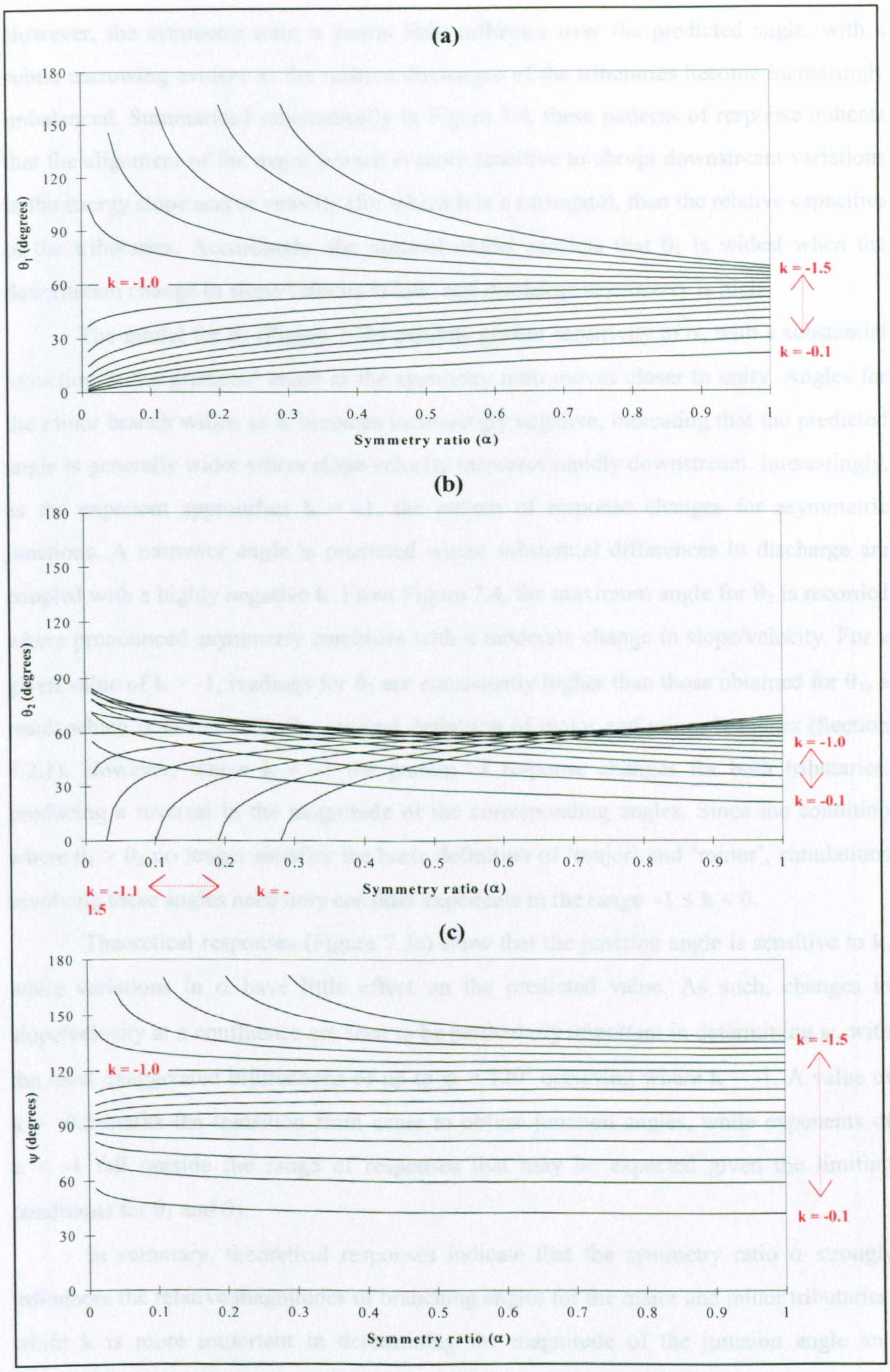

Figure 7.3 Graphical representation of theoretical responses predicted by optimum models of branching geometry for: (a) major branching angle (θ_1); (b) minor branching angle (θ_2) and (c) junction angle (ψ), with varying values of exponent k and symmetry ratio α.

However, the symmetry ratio α exerts little influence over the predicted angle, with a subtle narrowing evident as the relative discharges of the tributaries become increasingly imbalanced. Summarised schematically in Figure 7.4, these patterns of response indicate that the alignment of the major branch is more sensitive to abrupt downstream variations in the energy slope and/or velocity (for which **k** is a surrogate), than the relative capacities of the tributaries. Accordingly, the optimal model predicts that θ_1 is widest when the downstream change in slope/velocity is low, and discharge asymmetry is high.

The model for θ_2 (Figure 7.3b) exhibits greater sensitivity to α, with a substantial reduction in the predicted angle as the symmetry ratio moves closer to unity. Angles for the minor branch widen as **k** becomes increasingly negative, indicating that the predicted angle is generally wider where slope/velocity increases rapidly downstream. Interestingly, as the exponent approaches $\mathbf{k} = -1$, the pattern of response changes for asymmetric junctions. A narrower angle is predicted where substantial differences in discharge are coupled with a highly negative **k**. From Figure 7.4, the maximum angle for θ_2 is recorded where pronounced asymmetry combines with a moderate change in slope/velocity. For a given value of $\mathbf{k} > -1$, readings for θ_2 are consistently higher than those obtained for θ_1, a result which is in line with the original definition of major and minor branches (Section 7.2.1). However, where $\mathbf{k} < -1$ the pattern of response changes for both tributaries, producing a reversal in the magnitude of the corresponding angles. Since the condition where $\theta_1 > \theta_2$ no longer satisfies the basic definition of 'major' and 'minor', simulations involving these angles need only consider exponents in the range $-1 \leq \mathbf{k} < 0$.

Theoretical responses (Figure 7.3c) show that the junction angle is sensitive to **k**, while variations in α have little effect on the predicted value. As such, changes in slope/velocity at a confluence are seen to be particularly important in determining ψ, with the most exaggerated bifurcations of up to $\psi = 120^{\circ}$ occurring where $\mathbf{k} \sim -1$. A value of $\mathbf{k} = -0.5$ marks the transition from acute to obtuse junction angles, while exponents of $\mathbf{k} < -1$ fall outside the range of responses that may be expected given the limiting conditions for θ_1 and θ_2.

In summary, theoretical responses indicate that the symmetry ratio α strongly influences the relative magnitudes of branching angles for the major and minor tributaries, while **k** is more important in determining the magnitude of the junction angle and potentially reflects the importance of downstream changes in exponents for slope (**z**) and/or velocity (**m**).

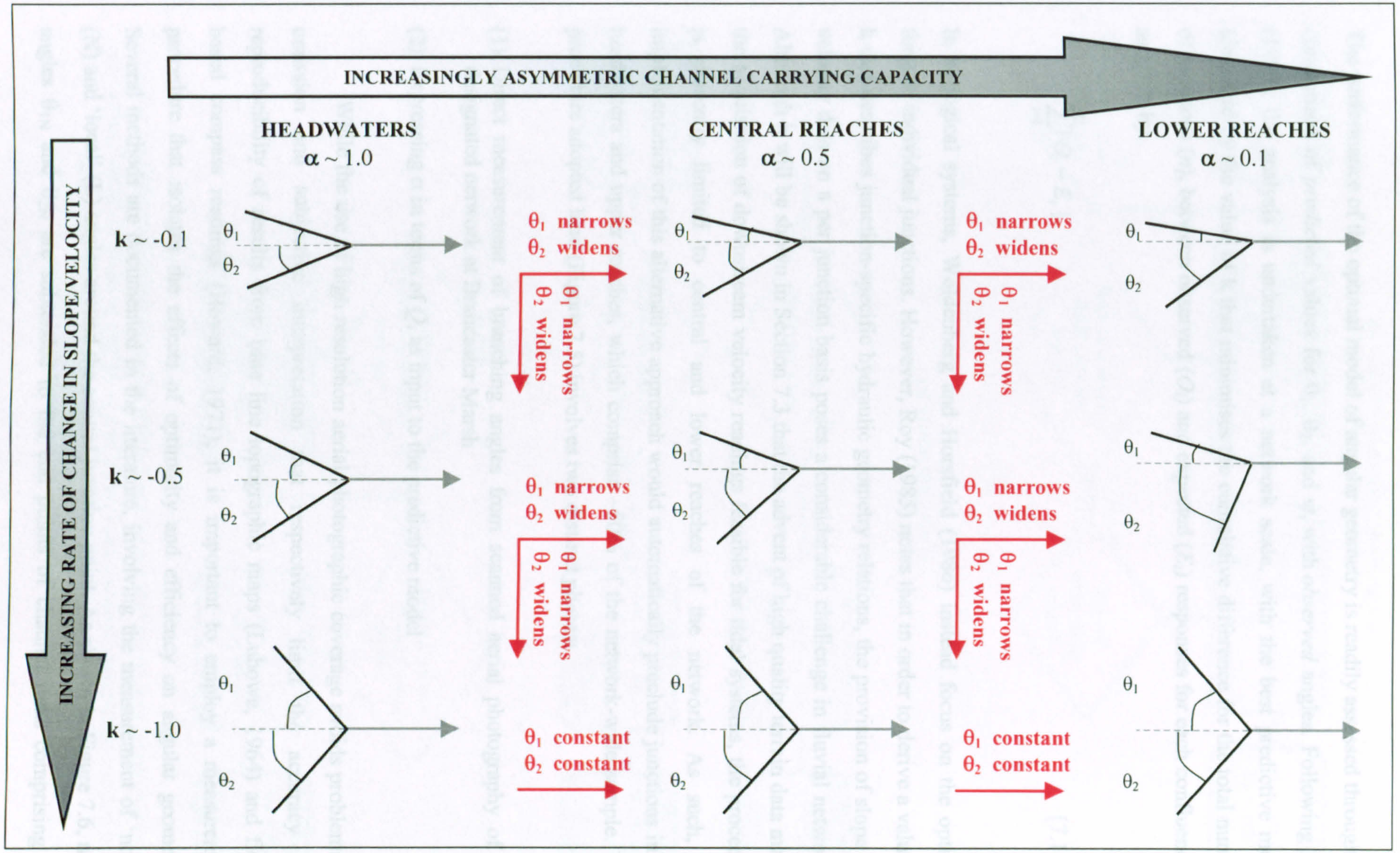

Figure 7.4 Schematic representation of changes in branching angle accompanying downstream increases in slope and/or velocity (exponent **k**) and discharge asymmetry (α).

7.2.4 Data acquisition

The performance of the optimal model of angular geometry is readily assessed through the comparison of *predicted* values for θ_1, θ_2, and ψ, with *observed* angles. Following Roy (1985), the analysis is undertaken at a network scale, with the best predictive model identified by the value of **k** that minimises the cumulative difference for the total number of junctions (n), between observed (O_i) and expected (E_i) responses for each confluence i, as given by

$$\sum_{i=1}^{n} | O_i - E_i | \qquad [7.14]$$

In biological systems, Woldenberg and Horsfield (1986) instead focus on the optimal form of individual junctions. However, Roy (1985) notes that in order to derive a value of **k** that describes junction-specific hydraulic geometry relations, the provision of slope and velocity data on a per junction basis poses a considerable challenge in fluvial networks. Although it will be shown in Section 7.3 that the advent of high quality terrain data makes the acquisition of downstream velocity readings feasible for tidal systems, the procedure is presently limited to central and lower reaches of the network. As such, the implementation of this alternative approach would automatically preclude junctions in the headwaters and upper reaches, which comprise ~50% of the network-wide sample. The procedure adopted here (Figure 7.5) involves two distinct phases:

(1) Direct measurement of branching angles from scanned aerial photography of the designated network at Brancaster Marsh

(2) Expressing α in terms of Q, as input to the predictive model

While the use of high resolution aerial photographic coverage avoids problems of omission and subjective interpretation that respectively limit the accuracy and reproducibility of results from blue line topographic maps (Lubowe, 1964) and field-based compass readings (Howard, 1971), it is important to employ a measurement procedure that isolates the effects of optimality and efficiency on angular geometry. Several methods are documented in the literature, involving the measurement of 'node' (N) and 'local' (L) angles around the central junction point. As shown in Figure 7.6, node angles θ_{1N} and θ_{2N} are subtended to the end points of channel links comprising the

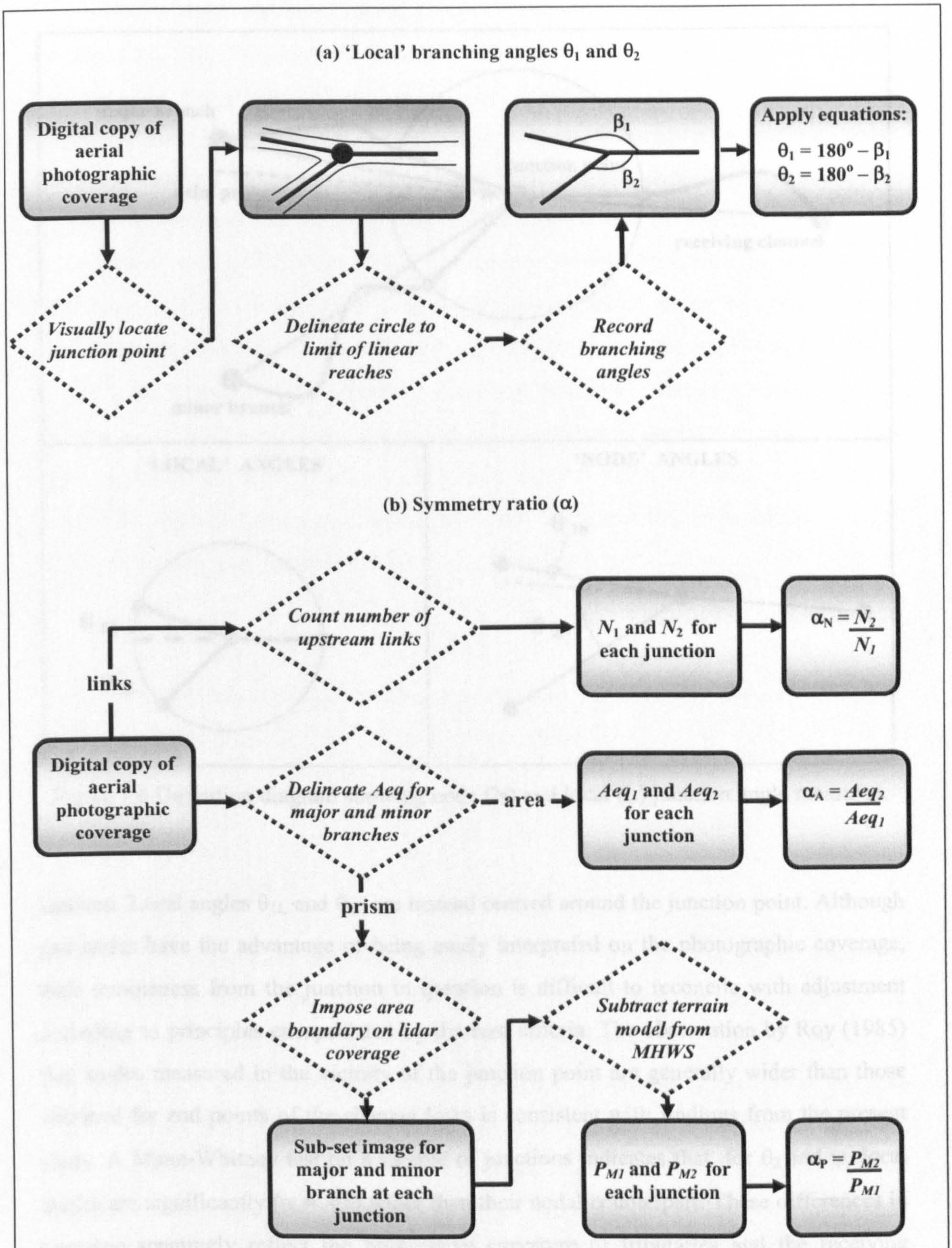

Figure 7.5 Schematic representation of the methodological procedure employed in: (a) measuring 'local' branching angles θ_1 and θ_2; and (b) computing symmetry ratios α_N, α_A and α_P, for evaluation of the optimal model of angular geometry.

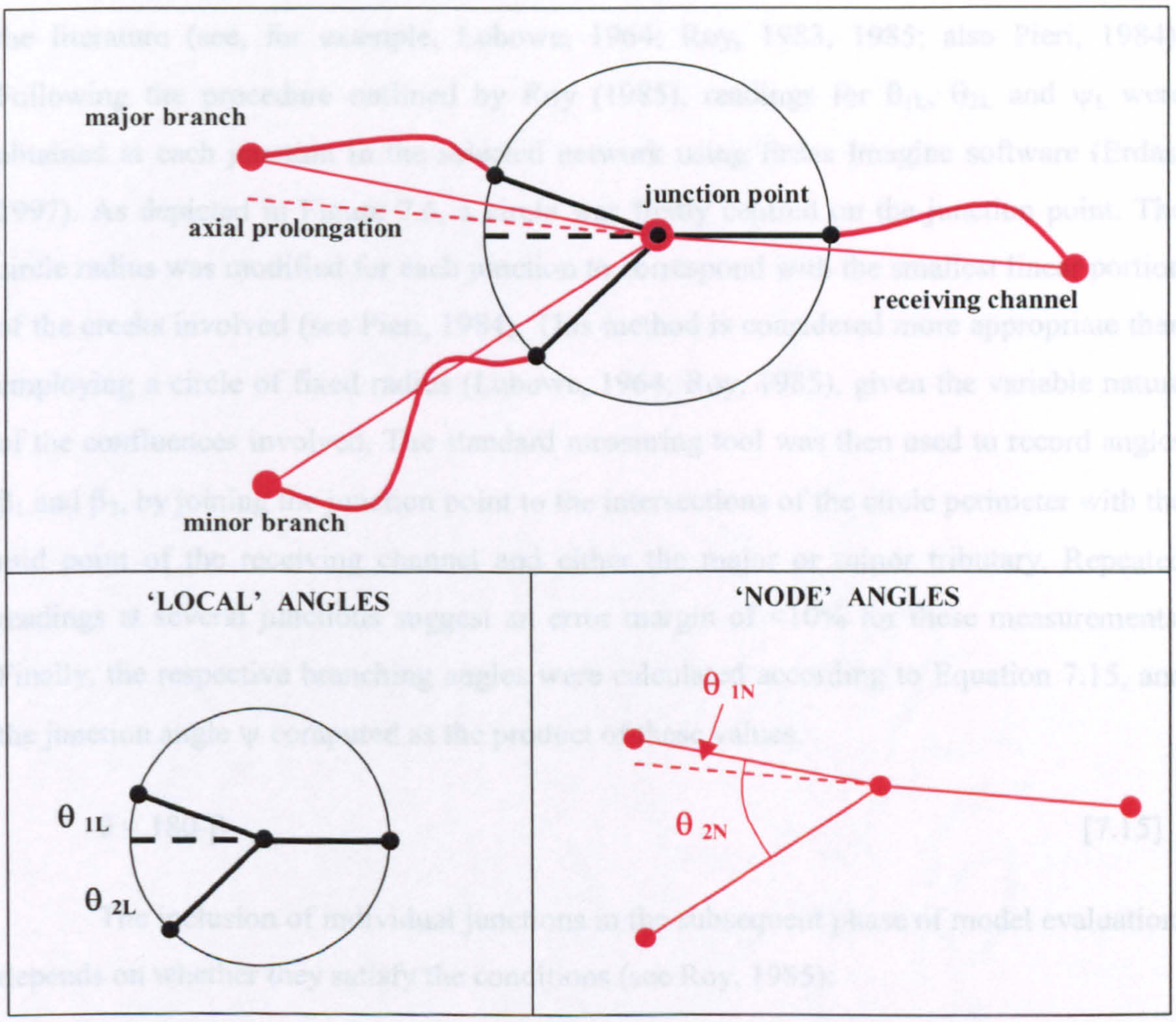

Figure 7.6 Definition diagram showing node (N) and local (L) junction angle measures.

junction. Local angles θ_{1L} and θ_{2L} are instead centred around the junction point. Although end nodes have the advantage of being easily interpreted on the photographic coverage, their remoteness from the junction in question is difficult to reconcile with adjustment according to principles encapsulated by the cost criteria. The observation by Roy (1985) that angles measured in the vicinity of the junction point are generally wider than those obtained for end points of the channel links is consistent with findings from the present study. A Mann-Whitney test on a sample of junctions indicates that, for θ_2 and ψ, local angles are significantly ($\alpha = .05$) wider than their nodal counterpart. These differences in response seemingly reflect the progressive curvature of tributaries and the receiving channel with distance from the junction point. The implication of this finding is that physical environmental controls (Morisawa, 1964) and space filling (Abrahams, 1984) influence the position of the node, while adjustment around the confluence may be solely conditioned by cost minimisation.

Due to their established physical basis, local angles are more widely reported in the literature (see, for example, Lubowe, 1964; Roy, 1983, 1985; also Pieri, 1984). Following the procedure outlined by Roy (1985), readings for θ_{1L}, θ_{2L} and ψ_L were obtained at each junction in the selected network using Erdas Imagine software (Erdas, 1997). As depicted in Figure 7.6, a circle was firstly centred on the junction point. The circle radius was modified for each junction to correspond with the smallest linear portion of the creeks involved (see Pieri, 1984). This method is considered more appropriate than employing a circle of fixed radius (Lubowe, 1964; Roy, 1985), given the variable nature of the confluences involved. The standard measuring tool was then used to record angles β_1 and β_2, by joining the junction point to the intersections of the circle perimeter with the mid point of the receiving channel and either the major or minor tributary. Repeated readings at several junctions suggest an error margin of <10% for these measurements. Finally, the respective branching angles were calculated according to Equation 7.15, and the junction angle ψ computed as the product of these values.

$$\theta = 180-\beta \qquad [7.15]$$

The inclusion of individual junctions in the subsequent phase of model evaluation, depends on whether they satisfy the conditions (see Roy, 1985):

(1) $0^o \leq \theta < 90^o$

(2) $\theta_1 \leq \theta_2$

(3) $0^o \leq \psi < 180^o$

Of the sample population depicted in Figure 7.7, negative branching angles, where the tributary falls on the wrong side of the line of axial prolongation, are recorded at 11 junctions. At the other end of the scale, obtuse branching angles occur at 20 junctions. Rather than conforming to the typical orientation of ebb drainage, reaches are in this case flood-aligned. Discordant behaviour of this nature is predominantly observed at junctions where a low order tributary adjoins a much larger channel. This suggests that although ebb alignment is a characteristic feature of the principal creeks laid down during the early stages of network development, other factors may control the adjustment of tributaries added later through elaboration and extension. The condition outlined by Woldenberg and Horsfield (1983) that θ_1 should be less than θ_2 if an optimality principle is involved, is satisfied at 72% of the junctions. This figure is in line with the 81% statistic recorded by

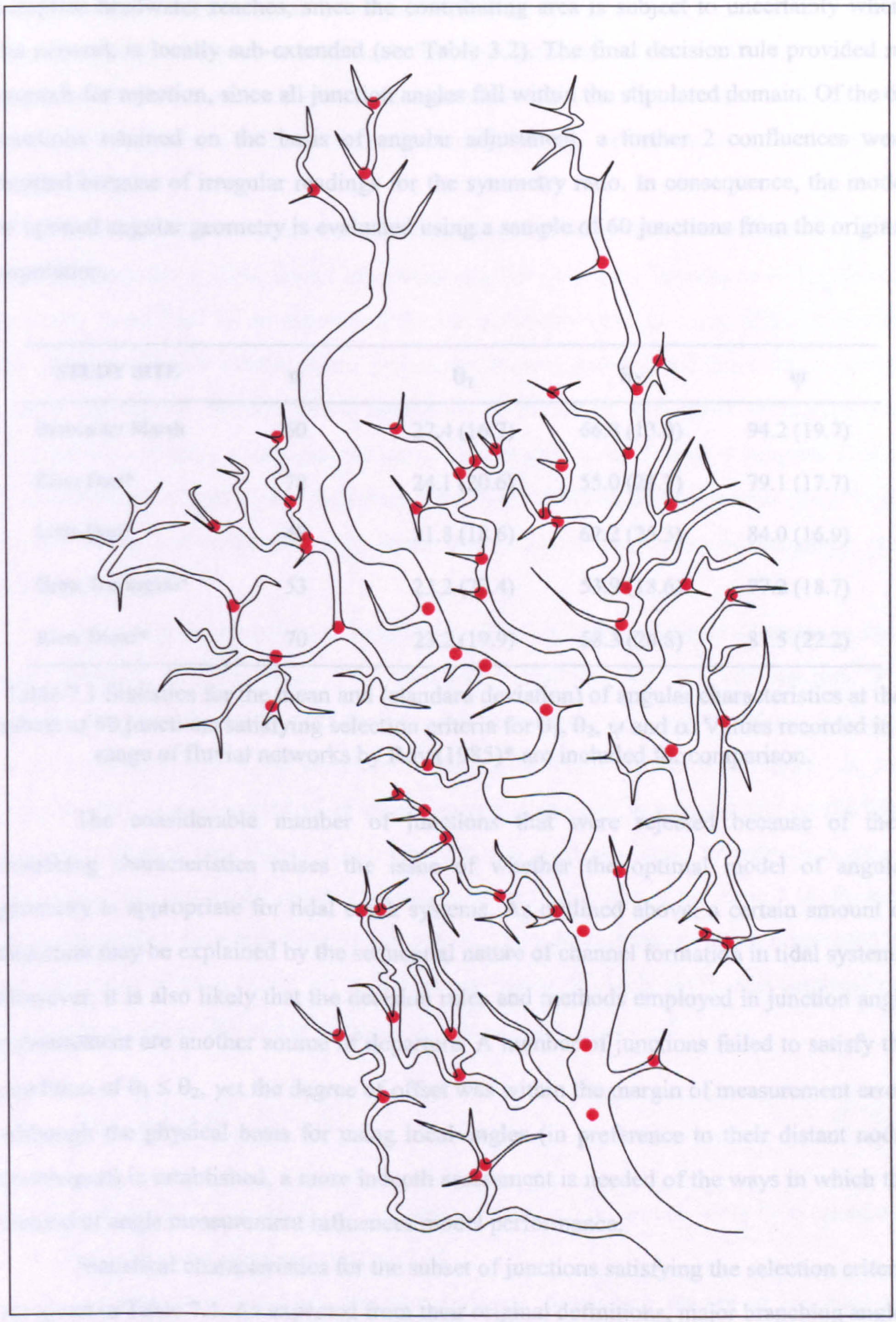

Figure 7.7 Linearised representation of the Brancaster network, highlighting the subset of 60 junctions used to evaluate the performance of the model of optimal angular geometry.

Roy (1985) for fluvial networks. Confluences failing to satisfy this criterion generally comprise headwater reaches, since the contributing area is subject to uncertainty where the network is locally sub-extended (see Table 3.2). The final decision rule provided no grounds for rejection, since all junction angles fall within the stipulated domain. Of the 62 junctions retained on the basis of angular adjustment, a further 2 confluences were omitted because of irregular readings for the symmetry ratio. In consequence, the model of optimal angular geometry is evaluated using a sample of 60 junctions from the original population.

STUDY SITE	n	θ_1	θ_2	ψ
Brancaster Marsh	60	27.4 (16.7)	66.8 (13.0)	94.2 (19.7)
River Dart*	78	24.1 (20.6)	55.0 (21.7)	79.1 (17.7)
Little Dart*	48	21.8 (18.6)	62.2 (25.3)	84.0 (16.9)
Great Torrington*	53	23.2 (22.4)	53.9 (18.6)	77.2 (18.7)
River Duntz*	70	23.2 (19.9)	58.3 (24.8)	81.5 (22.2)

Table 7.1 Statistics for the mean and (standard deviation) of angular characteristics at the subset of 60 junctions satisfying selection criteria for θ_1, θ_2, ψ and α. Values recorded in a range of fluvial networks by Roy (1985)* are included for comparison.

The considerable number of junctions that were rejected because of their branching characteristics raises the issue of whether the optimal model of angular geometry is appropriate for tidal creek systems. As outlined above, a certain amount of departure may be explained by the sequential nature of channel formation in tidal systems. However, it is also likely that the decision rules and methods employed in junction angle measurement are another source of departure. A number of junctions failed to satisfy the condition of $\theta_1 \leq \theta_2$, yet the degree of offset was within the margin of measurement error. Although the physical basis for using local angles (in preference to their distant nodal counterpart) is established, a more indepth assessment is needed of the ways in which the method of angle measurement influences model performance.

Statistical characteristics for the subset of junctions satisfying the selection criteria are given in Table 7.1. As expected from their original definitions, major branching angles are generally more closely aligned with the receiving channel than minor tributaries. Furthermore, comparison with results obtained by Roy (1985) for a selection of river networks in Devon, indicates that mean branching angles are on average wider in tidal

formations than their fluvial counterparts. A similar discrepancy is exhibited by the junction angle, which tends to be obtuse in saltmarsh creeks, while remaining acute in river networks. Although insufficient data are available to ascertain the statistical significance of these differences, their presence nevertheless suggests that the Brancaster network may exhibit a subtly different manner of optimal adjustment compared with the fluvial examples.

The second phase of the methodological procedure involves the computation of α. In simplifying the original model of optimal angular geometry, introduction of hydraulic geometry terms lead to an expression for the symmetry ratio in terms of the dominant discharge. As French (1996) notes, Q is rarely known directly, and since the symmetry ratio is determined by the *relative* magnitude of the major and minor tributaries, it is appropriate to employ a surrogate measure. Consultation of the literature suggests a range of possibilities, of which link frequency (see Pieri, 1984), contributing area (Roy, 1985; French, 1996) and maximum tidal prism were selected for further investigation (see Section 2.4.3).

Following the procedure outlined in Section 3.3.3, the frequency of upstream links was computed for the major (N_1) and minor reaches (N_2) at each junction. For contributing area, the equidistant decision rule (see Figure 3.5) was employed as a basis for delineating A_1 and A_2 on the photographic coverage. As depicted in Figure 7.8, this area boundary was converted to an area of interest (aoi), and in turn overlaid on the lidar altimetry coverage (see Figure 2.11), where it was used as a mask to generate a subset image. The maximum tidal prism (P_M) was computed according to Equation 7.16, for sub-scenes relating to each major and minor branch. H_i represents the elevation (expressed by the DN value) of each 'pixel' (i) in a total population of pixels (n). In this instance, the *HAT* level is 3.95m OD, and every pixel covers an area (A_i) of 4 m^2.

$$P_M = \sum_{i=1}^{n}\left[(HAT - H_i) \times A_i\right] \qquad [7.16]$$

By substituting N, A and P_M for Q, symmetry ratios α_N, α_A and α_P were then calculated for each junction according to Equation 7.10.

In order to avoid data redundancy during subsequent phases of the analysis, Spearman's rank correlation analysis was used to establish the degree of correspondence between symmetry ratios based on the surrogate expressions for Q. The results (Table 7.2) reveal a near perfect correlation ($r^* \sim 0.99$) between α_A and α_P, the implication being that

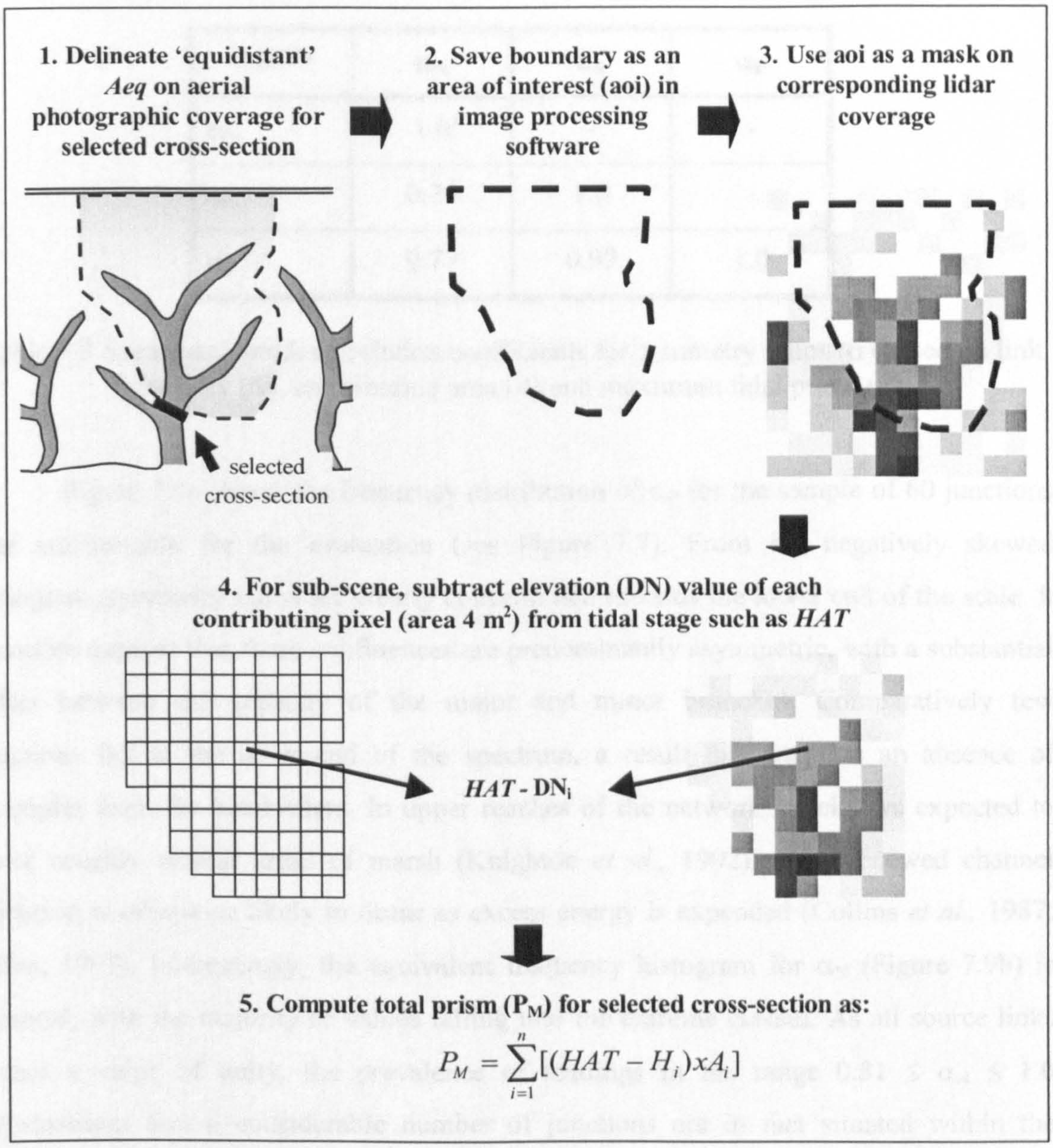

Figure 7.8 Schematic representation of the procedure involved in computing maximum tidal prism (P_M) for a selected cross-section

the area or platform component (see Figure 6.5) dominates values recorded for P_M. In view of the pronounced similarity between these measures, and since prism arguably provides a more realistic representation of Q than area alone, α_P is carried forward to the model evaluation. Reduced levels of association with α_N ($r^* \sim 0.76$) arise because all source links record an identical value of unity on the topological scale. However, the geometric series instead suggest that headwater reaches serve a range of areas. Since the physical realism of the link-based proxy is clearly called into question, it is considered no further in the analysis.

RATIO	α_N	α_A	α_P
α_N	1.0	-	-
α_A	0.75	1.0	-
α_P	0.77	0.99	1.0

Table 7.2 Spearman's rank correlation coefficients for symmetry ratios (α) based on link frequency (N), contributing area (A) and maximum tidal prism (P).

Figure 7.9a shows the frequency distribution of α_P for the sample of 60 junctions that are suitable for the evaluation (see Figure 7.7). From the negatively skewed histogram, symmetry ratios are clearly concentrated towards the lower end of the scale. It therefore appears that these confluences are predominantly asymmetric, with a substantial offset between the capacity of the major and minor branches. Comparatively few junctions fall at the other end of the spectrum, a result that suggests an absence of examples from the headwaters. In upper reaches of the network, creeks are expected to serve roughly similar areas of marsh (Knighton *et al.*, 1992), since renewed channel initiation is otherwise likely to occur as excess energy is expended (Collins *et al.*, 1987; Allen, 1997). Interestingly, the equivalent frequency histogram for α_N (Figure 7.9b) is bimodal, with the majority of values falling into the extreme classes. As all source links record a value of unity, the prevalence of readings in the range $0.81 \leq \alpha_N \leq 1.0$ demonstrates that a considerable number of junctions are in fact situated within the headwaters. The implications of these observations are twofold. First, the discordant nature of responses obtained for link frequency and tidal prism serves to reaffirm the lack of proportionality between topological and geometric surrogates for Q. For tidal networks, it is clearly inappropriate to assume that all sources are of a comparable length or serve an equivalent area. Second, the surprisingly limited number of instances where creeks conveying a similar capacity of flow meet in natural channel networks, points towards the emergence of efficient master creeks that carry a high proportion of the flow, and are adjoined by subordinate sub-networks which perform a lesser conveyance function. This is in line with the model of sequential network development outlined by Glock (1931), whereby the principal drainage lines are established at the outset and subsidiary reaches develop afterwards through processes of extension and elaboration.

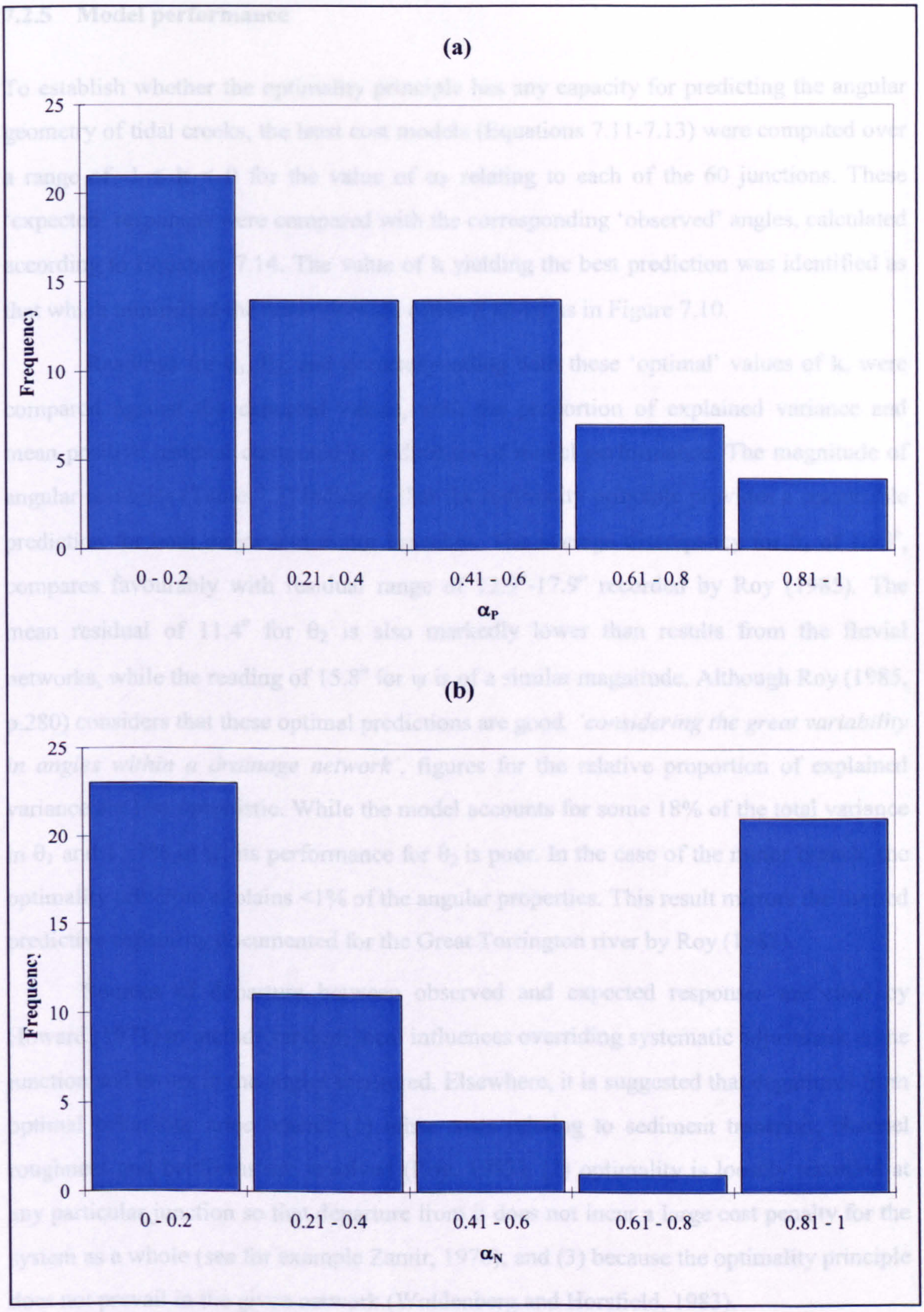

Figure 7.9 Frequency distribution of: (a) α_P ; and (b) α_N, for the sample of 60 junctions employed in evaluating the model of optimal angular geometry.

7.2.5 Model performance

To establish whether the optimality principle has any capacity for predicting the angular geometry of tidal creeks, the least cost models (Equations 7.11-7.13) were computed over a range of $-1 \leq \mathbf{k} < 0$ for the value of α_p relating to each of the 60 junctions. These 'expected' responses were compared with the corresponding 'observed' angles, calculated according to Equation 7.14. The value of **k** yielding the best prediction was identified as that which minimised the network-wide offset Σ |O-E|, as in Figure 7.10.

Readings for θ_1, θ_2, and ψ corresponding with these 'optimal' values of **k**, were compared against the expected values, with the proportion of explained variance and mean positive residual computed as indicators of model performance. The magnitude of angular residuals (Table 7.3) indicates that the optimality principle provides a reasonable prediction for both major and minor branches. The average discrepancy for θ_1 of 12.8°, compares favourably with residual range of 12.9°-17.9° recorded by Roy (1985). The mean residual of 11.4° for θ_2 is also markedly lower than results from the fluvial networks, while the reading of 15.8° for ψ is of a similar magnitude. Although Roy (1985, p.280) considers that these optimal predictions are good, *'considering the great variability in angles within a drainage network'*, figures for the relative proportion of explained variance are less optimistic. While the model accounts for some 18% of the total variance in θ_1 and 11.1% in ψ, its performance for θ_2 is poor. In the case of the minor branch, the optimality principle explains <1% of the angular properties. This result mirrors the limited predictive capability documented for the Great Torrington river by Roy (1985).

Sources of departure between observed and expected responses are cited by Howard (1971) to include random local influences overriding systematic adjustment at the junction and errors in the angles measured. Elsewhere, it is suggested that departures from optimal behaviour arise where: (1) other costs relating to sediment transport, channel roughness and bedforms are involved (Roy, 1983); (2) optimality is loosely recorded at any particular junction so that departure from it does not incur a large cost penalty for the system as a whole (see for example Zamir, 1976); and (3) because the optimality principle does not prevail in the given network (Woldenberg and Horsfield, 1983).

To assess the degree of similarity between angular adjustment in the tidal creeks at Brancaster Marsh and river networks studied by Roy (1985), the respective values recorded for **k** are displayed in Table 7.3. For θ_1, the 'best' response of $\mathbf{k} = -0.42$ falls

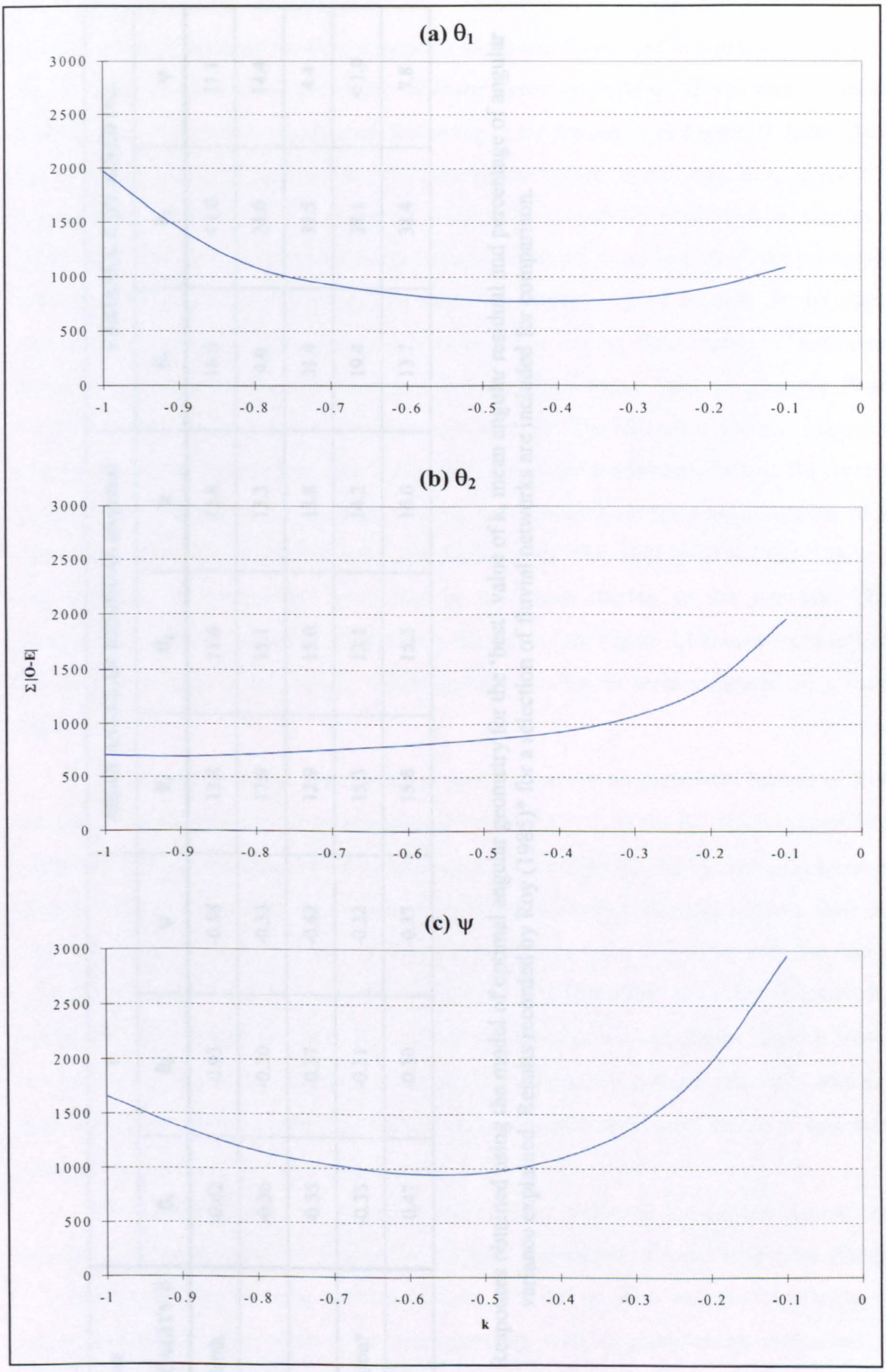

Figure 7.10 Graphical representation of the value for k recording a minimum network-wide offset between observed and expected angles for: (a) θ_1; (b) θ_2 and (c) ψ.

MEASURE ⇒	k			MEAN ANGULAR RESIDUAL (degrees)			VARIANCE EXPLAINED (%)		
STUDY LOCALITY ⇓	θ_1	θ_2	ψ	θ_1	θ_2	ψ	θ_1	θ_2	ψ
Brancaster Marsh	-0.42	-0.93	-0.58	12.8	11.4	15.8	18.0	< 1.0	11.1
River Dart*	-0.36	-0.30	-0.33	17.9	15.1	13.3	4.0	24.0	14.4
Little Dart*	-0.55	-0.37	-0.42	12.9	15.0	13.8	31.4	32.5	4.4
Great Torrington*	-0.33	-0.31	-0.32	15.3	13.1	14.2	19.4	28.1	< 1.0
River Duntz*	-0.47	-0.30	-0.37	15.6	15.5	16.6	13.7	38.4	7.8

Table 7.3 Responses obtained using the model of optimal angular geometry for the 'best' value of k, mean angular residual and percentage of angular variance explained. Results recorded by Roy (1985)* for a selection of fluvial networks are included for comparison.

within the range obtained for fluvial systems in Devon. Expressed in a graphical form by Figure 7.11a, in both cases the major tributary forms an angle of 35-40° with the axial prolongation of the receiving channel. Returning to the frequency histogram (Figure 7.9a), the relatively close alignment with the downstream reach is not surprising given the concentration of asymmetric confluences where a comparatively small channel adjoins a much larger reach. A similar bias towards asymmetric junctions in U.S. rivers prompted Howard (1971) to employ a purposive sampling strategy, which focused on the more symmetrical examples. However, observations made during field visits to Brancaster Marsh suggest that the dominance of asymmetrical confluences (see, for example, Plate 7.1a), is a characteristic feature of this channel network. The efficiency which is achieved through flow convergence (see also Yang, 1971) from the headwaters through the central to the lower reaches of the network, means that junctions comprising tributaries of a similar capacity are comparatively few and far between. The confluence in Plate 7.1b is a rare example of symmetrical behaviour in the lower reaches of the network. The development of this 'expansive' planimetric formation (see Figure 3.10) appears to reflect the boundary shape of the marsh, which serves two distinct areas separated by a sand ridge.

The extent to which asymmetrical junctions are a characteristic feature of this network is highlighted further by the optimal value of $\mathbf{k} = -0.93$ for θ_2, which is amplified compared with results from fluvial systems of $-0.37 \leq \mathbf{k} \leq -0.30$. The theoretical responses (Figure 7.11b) indicate that, on average, minor branches within the tidal network form an angle of 70° with the line of axial prolongation. This is some 20° wider than the figure typically recorded for river networks by Roy (1985). The offset is further reflected by ψ (Figure 7.11c), where the 'best' $\mathbf{k} = -0.58$ is synonymous with an obtuse junction angle, compared with the acute fluvial counterpart. The divergence in these responses concurs with results by French (1996) for a channel system in North Kent, where ψ was also shown to be optimised for $-0.5 \leq \mathbf{k} \leq -0.60$.

The optimal model has therefore successfully replicated the general patterns of angular adjustment identified during the original assessment of mean responses (Table 7.1). However, it has yet to be established if the 'best-fit' model is meaningful in terms of physical function. The value of **k** corresponding with ψ provides an indication of adjustment within the junction as a whole, and is therefore used in preference to constituent responses for θ_1 and θ_2.

(a)

(b)

Plate 7.1 Junctions in the Brancaster network showing: (a) an asymmetrical example from the central reaches where a minor branch adjoins a considerably larger major channel; and (b) a rare example of near-symmetrical branching in the lower reaches.

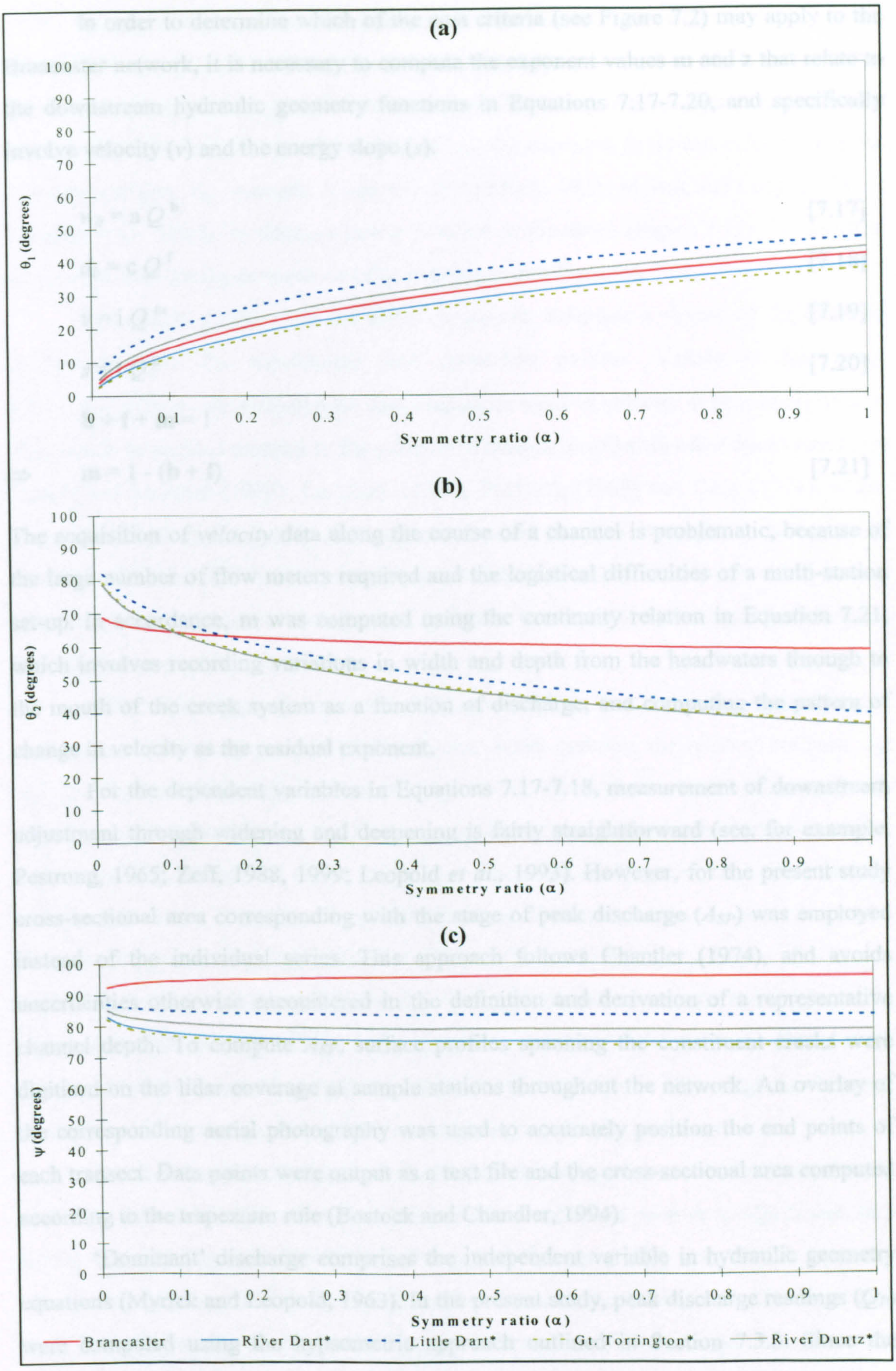

Figure 7.11 Predicted angles for: (a) θ_1; (b) θ_2 and (c) ψ, corresponding with 'best' values of k obtained using the model of optimal angular geometry. Results recorded for fluvial networks by Roy (1985)* are included for comparison.

In order to determine which of the cost criteria (see Figure 7.2) may apply to the Brancaster network, it is necessary to compute the exponent values **m** and **z** that relate to the downstream hydraulic geometry functions in Equations 7.17-7.20, and specifically involve velocity (v) and the energy slope (s).

$$w_b = \mathrm{a}\, Q^{\mathbf{b}} \qquad [7.17]$$

$$d_b = \mathrm{c}\, Q^{\mathbf{f}} \qquad [7.18]$$

$$v = \mathrm{i}\, Q^{\mathbf{m}} \qquad [7.19]$$

$$s = \mathrm{t}\, Q^{\mathbf{z}} \qquad [7.20]$$

$$\mathbf{b} + \mathbf{f} + \mathbf{m} = 1$$

$$\Rightarrow \quad \mathbf{m} = 1 - (\mathbf{b} + \mathbf{f}) \qquad [7.21]$$

The acquisition of *velocity* data along the course of a channel is problematic, because of the large number of flow meters required and the logistical difficulties of a multi-station set-up. In accordance, **m** was computed using the continuity relation in Equation 7.21, which involves recording variations in width and depth from the headwaters through to the mouth of the creek system as a function of discharge, and computing the pattern of change in velocity as the residual exponent.

For the dependent variables in Equations 7.17-7.18, measurement of downstream adjustment through widening and deepening is fairly straightforward (see, for example, Pestrong, 1965; Zeff, 1988, 1999; Leopold *et al.*, 1993). However, for the present study cross-sectional area corresponding with the stage of peak discharge (A_{SP}) was employed instead of the individual series. This approach follows Chantler (1974), and avoids uncertainties otherwise encountered in the definition and derivation of a representative channel depth. To compute A_{SP}, surface profiles spanning the constituent creeks were digitised on the lidar coverage at sample stations throughout the network. An overlay of the corresponding aerial photography was used to accurately position the end points of each transect. Data points were output as a text file and the cross-sectional area computed according to the trapezium rule (Bostock and Chandler, 1994).

'Dominant' discharge comprises the independent variable in hydraulic geometry equations (Myrick and Leopold, 1963). In the present study, peak discharge readings (Q_P) were computed using the hypsometric approach outlined in Section 7.3.3. Since the relative rather than absolute magnitude of downstream changes in Q is of importance, and direct measurement is often seen to be problematic (see Coates *et al.*, 1995; French,

1996), the performance of several proxy measures was also investigated. Results were obtained using a selection of surrogates including: maximum prism (P_M); spring prism (P_S); contributing area (A_{eq}); and link frequency (N). These were computed according to procedures outlined in Section 7.2.4. The composite exponent (b+f) was calculated in the standard way (see, for example, Leopold and Maddock, 1953; Myrick and Leopold, 1963; Leopold *et al.,* 1964), by fitting a power function to the series (Figure 7.12). To compute **m**, data for each surrogate measure of Q were input into Equation 7.21.

The results (Table 7.4) are fairly consistent, although a degree of departure is evident between the topological and geometric proxies. Values in the range $0.30 \leq \mathbf{m} \leq 0.36$ imply a substantial downstream *increase* in velocity at Brancaster Marsh. This stands in marked contrast to the patterns of change recorded in other tidal systems by Myrick and Leopold (1963), Langbein (1964), Pestrong (1965) and Dury (1971), where responses of $\mathbf{m} < 0.1$ imply that velocity is near-constant throughout the network. Although Chantler (1974) observes more pronounced variations in velocity within several U.S. estuaries, the negative value of **m** indicates that current speed actually decreases towards the mouth of these systems.

While this range of responses is likely to reflect the contrasting hydrodynamic regimes experienced by geographically diverse marsh systems, the relation between A_{SP} and Q_P (Figure 7.12a) suggests that the higher velocity exponent for Brancaster Marsh may also be attributable to a divergence in behaviour between the headwaters and central/seaward reaches of the network. For discharge readings in the upper reaches, considerable scatter is evident about the trend line. However, as Q increases, the pattern of response appears to change. Above a value of $Q_P \sim 1.95$ m^3s^{-1}, the degree of scatter is reduced, and the data fall into clusters. This discontinuity coincides with a major junction, which marks the transition from upper to central reaches of the network. The clusters correspond with sectors of the network that are situated between other large confluences, at which point a convergence of flows means that Q_P suddenly increases.

A certain amount of variation is to be expected along the course of natural channel networks, because factors other than Q are likely to influence geometric adjustment. In a fluvial context, Ferguson (1986) and Huang and Warner (1999) note that downstream changes in lithology and bedrock also affect channel form. Hey and Thorne (1986) identify bank vegetation as another degree of freedom. Williams and Harvey (1983) suggest that both of these factors may be important in tidal systems. In view of these spatial variations in the controls exerted over morphological adjustment, Knighton (1987)

SOURCE	LOCALITY	INDEPENDENT VARIABLE	EXPONENT				
			m	b + f	b	f	z
Present study	Brancaster Marsh (all)	Q_P	0.40	0.60	-	-	-0.51
		P_M	0.39	0.61			-0.50
		P_S	0.40	0.60			-0.50
		Aeq	0.40	0.60			-0.51
		N	0.46	0.54			-0.23
	Brancaster Marsh (upper)	Q_P	0.55	0.45			-
	Brancaster Marsh (lower)	Q_P	0.10	0.90			-
Myrick and Leopold (1963)	Potomac River, U.S.	Q	0.05	-	0.71	0.24	-
Langbein (1964)	Potomac River, U.S.	Q	0.05	-	0.72	0.23	-
Pestrong (1965)	San Francisco Bay	Q	0	-	0.70	0.30	-
Dury (1971)	Crooked River, U.S.	Q	-0.02	-	0.78	0.24	-
Chantler (1974)	Thames Estuary	Q	0.06	0.94	-	-	-
	Firth of Forth	Q	0.03	0.97			
	Delaware River, U.S.	Q	0.14	0.86			
	Potomac River, U.S.	Q	0.08	0.92			
	Savannah River, U.S.	Q	-0.33	1.33			
	Potomac River, U.S.	Q	-0.04	1.04			

Table 7.4 Hydraulic exponents computed using a range of independent variables for the selected network at Brancaster Marsh. Results recorded elsewhere in the literature for tidal networks are included for comparison.

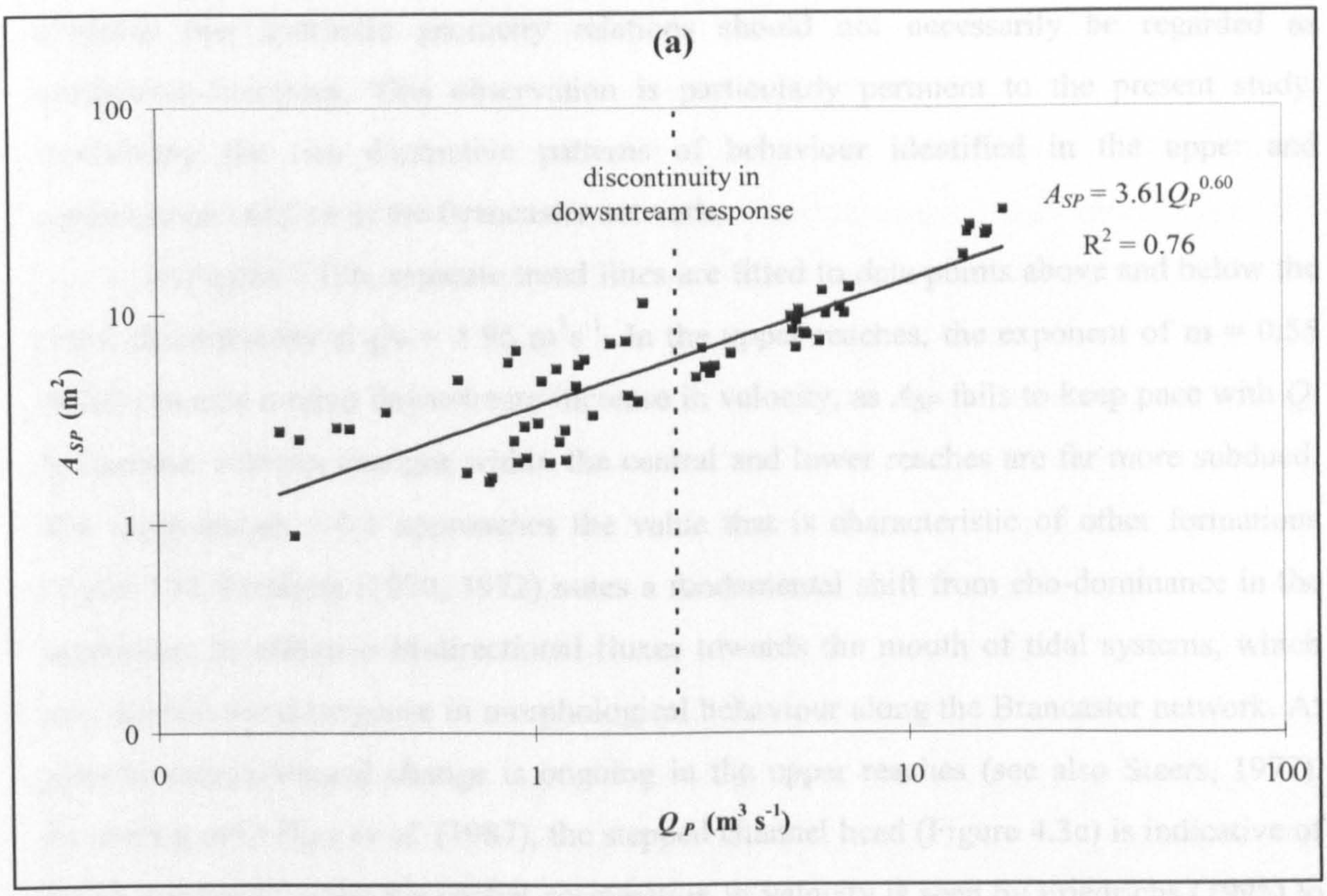

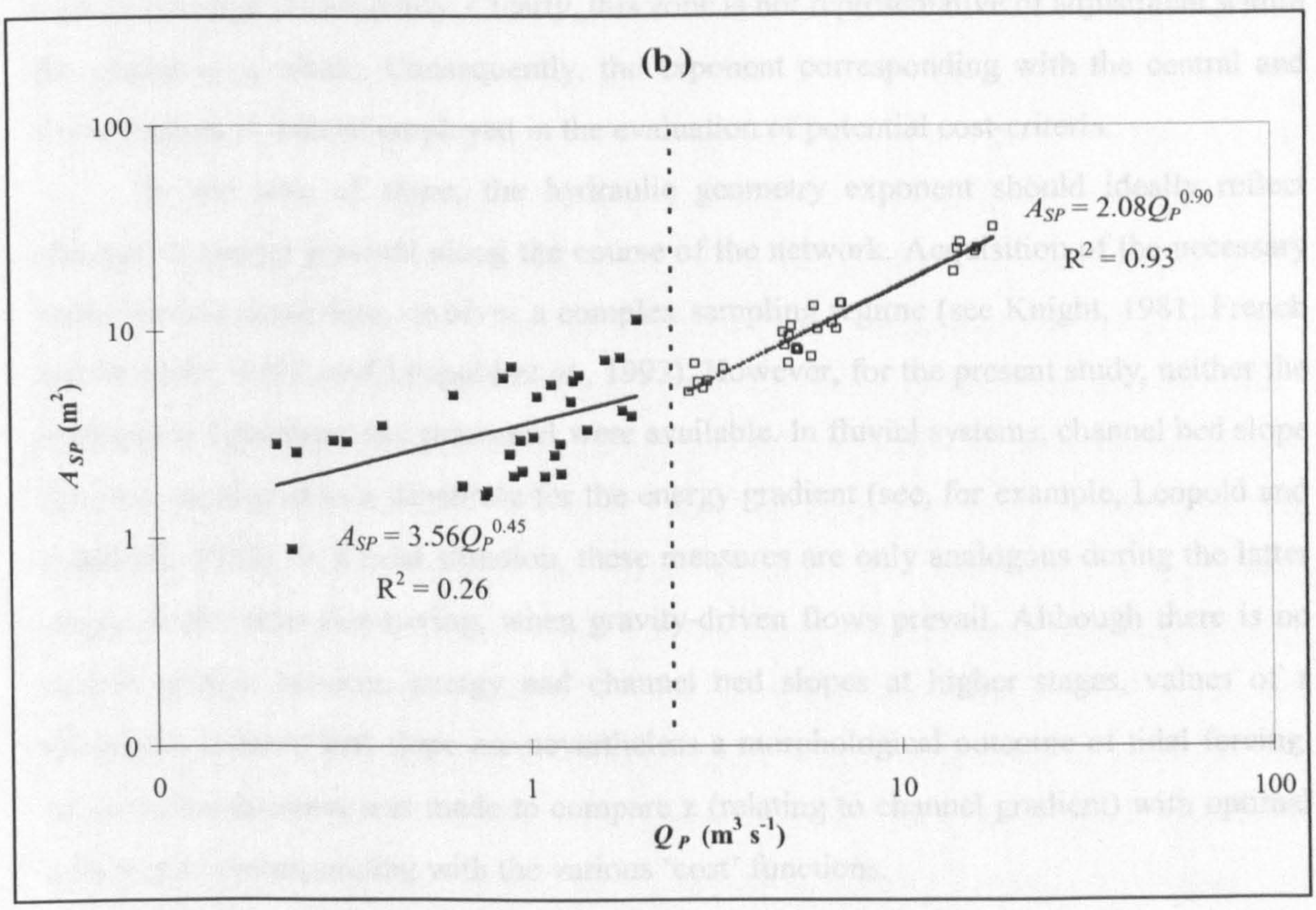

Figure 7.12 Combined hydraulic geometry exponent (b+f) for downstream changes in channel cross-sectional area (A_{SP}) with peak discharge (Q_P), showing: (a) discontinuity in adjustment along the course of the Brancaster network; and (b) separate power functions fitted to the headward reaches and central/lower sectors.

observes that hydraulic geometry relations should not necessarily be regarded as continuous functions. This observation is particularly pertinent to the present study, considering the two distinctive patterns of behaviour identified in the upper and central/lower reaches of the Brancaster network.

In Figure 7.12b, separate trend lines are fitted to data points above and below the major discontinuity at Q_P = 1.95 m^3s^{-1}. In the upper reaches, the exponent of **m** = 0.55 points towards a rapid downstream increase in velocity, as A_{SP} fails to keep pace with Q. In contrast, velocity changes within the central and lower reaches are far more subdued. The exponent **m** = 0.1 approaches the value that is characteristic of other formations (Table 7.4). Pestrong (1970, 1972) notes a fundamental shift from ebb-dominance in the headwaters to effective bi-directional fluxes towards the mouth of tidal systems, which may explain the divergence in morphological behaviour along the Brancaster network. At present, morphological change is ongoing in the upper reaches (see also Steers, 1977). According to Collins *et al.* (1987), the stepped channel head (Figure 4.3c) is indicative of active extension, while the spatial acceleration in velocity is seen by Friedrichs (1995) to be a classic sign of instability. Clearly, this zone is not representative of adjustment within the system as a whole. Consequently, the exponent corresponding with the central and lower reaches is instead employed in the evaluation of potential cost-criteria.

In the case of *slope*, the hydraulic geometry exponent should ideally reflect changes in energy gradient along the course of the network. Acquisition of the necessary water surface slope data, involves a complex sampling regime (see Knight, 1981; French and Stoddart, 1992; and Leopold *et al.*, 1993). However, for the present study, neither the appropriate equipment nor personnel were available. In fluvial systems, channel bed slope has been employed as a substitute for the energy gradient (see, for example, Leopold and Maddock, 1953). In a tidal situation, these measures are only analogous during the latter stages of ebb tidal dewatering, when gravity-driven flows prevail. Although there is no simple relation between energy and channel bed slopes at higher stages, values of **z** relating to channel bed slope are nevertheless a morphological outcome of tidal forcing. As such, the decision was made to compare **z** (relating to channel gradient) with optimal values of **k**, corresponding with the various 'cost' functions.

The **z** exponent for the Brancaster network was obtained in several stages. First, bed elevation was measured at cross-sections throughout the system, using the profile tool of Imagine software (Erdas, 1997). An empirical model was then fitted to a plot of bed elevation against Q. The first derivative was computed as an expression for the

downstream rate of change in bed elevation. Lastly, the exponent **z** was calculated by fitting a power function to the resulting slope-discharge model.

While it is important to reiterate that the physical interpretation of **z** currently defies complete interpretation, and is a subject for further research, the results (Table 7.4) indicate that the downstream exponent for bed slope tends towards a value of $\mathbf{z} \sim -0.5$ in the Brancaster network. This figure is similar in magnitude to responses obtained for fluvial networks by Leopold and Maddock (1953) and Roy (1985), which span a range of $-0.49 \leq \mathbf{z} \leq -0.36$.

Returning to the cost criteria, which are expressed in terms of hydraulic geometry exponents (see Figure 7.2), for the principle of minimum power losses to apply, the 'best' $\mathbf{k} = 0.58$ recorded for ψ should be proportional to **z**. The results in Table 7.4 indicate that **z** is of a similar magnitude. It can therefore be surmised that the network as a whole may be adjusted to this criterion. In terms of minimum total flow resistance, $\mathbf{k} = \mathbf{z} - 3\mathbf{m}$. For this principle to apply under the present conditions of slope, the velocity exponent should tend towards zero. Although the recorded response of $\mathbf{m} = 0.10$ is somewhat larger, this criteria cannot be ruled out. However, it appears more likely that the principle of minimum resisting force applies to the sample network. Given the conditions that $\mathbf{k} = \mathbf{z} + \mathbf{m}$, the velocity exponent is in line with the theoretical value of $\mathbf{m} \sim 0.08$. The final criteria of minimum volume would prove to be operative if $\mathbf{k} = -\mathbf{m}$. For this to be the case, the velocity exponent should be of a similar magnitude to **k**. For the present example, this is clearly not the case, with the much smaller value of **m** suggesting that this principle is least likely to play a role in determining the angular geometry of the Brancaster network.

The performance of various cost criteria within the tidal formation is remarkably similar to that of fluvial systems (see Roy, 1985), the implication being that the branching geometry of saltmarsh creeks and river networks may be similarly optimised. Furthermore, the preceding results indicate that several criteria may be *simultaneously* minimised within the creek system. The morphological characteristics arising from the minimisation of power loss are difficult to isolate from minimum total flow resistance and minimum resisting force, because the combination of hydraulic geometry exponents involved in the specification of cost predict a similar pattern of angular adjustment (see also Roy, 1983). However, a knowledge of geomorphological processes suggests that of the three candidates, the principle of minimum power loss is most likely to guide the morphological behaviour of tidal channels, with the resistance criteria being more obviously associated with the efficient operation of biological systems.

Constituting a simplified case of the minimum rate of energy expenditure, Yang (1971, p.311) explains that the state of minimum stream power arises because '*during the evolution towards its equilibrium condition, a natural stream chooses its course of flow in such a manner that the rate of potential energy expenditure per unit mass of water along this course is a minimum*' (see also Yang *et al.,* 1981). Defined in this way, the theory is applicable to the system as a whole, and includes aspects of morphological adjustment beyond the branching geometry. Elsewhere, minimum power loss is cited as a principle governing the downstream hydraulic geometry of tidal streams (Langbein, 1963), and the planimetric characteristics of simulated networks bearing a close resemblance to river systems (Howard, 1990; Rodriguez-Iturbe *et al.,* 1992; Rigon and Rinaldo, 1993). Based on the analogy between the dominant flows in tidal and fluvial networks, the criteria of minimum power loss could potentially be applied to other aspects of saltmarsh channel network morphology.

Since the envelope of cost criteria are essentially the same for the Brancaster network and rivers analysed by Roy (1985), it is reasonable to suggest that the creek system is similarly optimised to perform a *drainage* function. In natural systems, such as these, the concept of minimum power loss is consistent with efficient drainage. Amplified energy expenditure around discontinuities in the channel bed and bank provides a focus for adjustment, since it acts to remove bankfall debris and restore an equilibrium form. Over time, this tendency leads to the minimisation of change in w_b, d_b, v and s through a particular junction. Huggett (1988, p.46) goes on to note that systems exhibiting adjustment of this kind may also be referred to as '*dissipative structures*'.

A dissipative system, which simultaneously satisfies the criterion of minimum power loss, may be envisaged as one in which the progressive reduction of tidal energy along its course reduces flow velocity to a sub-critical level that is unable to upset the 'nice balance' achieved through power loss minimisation. Under non-dissipative conditions, excess tidal energy at a particular junction would cause a departure from the principle of minimum power loss, and the realignment of tributary reaches so that they were no longer optimised. While Pestrong (1965, p.20) observes how '*the waters simply back up against the channel slopes*' in the upper reaches of U.S. tidal networks, empirical evidence of the gradual, yet progressive, nature of dissipation is provided by Bayliss-Smith *et al.* (1979), Stoddart *et al.* (1989) and French and Stoddart (1992), through the reduction in velocity from the mouth through to the headwaters of British formations. It may therefore be surmised, that although the sample of 60 junctions along the course of

the Brancaster network are not necessarily optimised for maximum dissipation, energy is *sufficiently* dissipated to maintain the condition of minimum power loss.

At this stage, it is important to recognise the distinction between formative processes and the physical functions performed by saltmarsh channel systems. Although creek development is primarily driven by morphologically active forces during the ebb phase of the tidal cycle, and thereafter provides the principal conduit for marsh surface drainage (French and Reed, 2001) and dewatering (Ranwell, 1972), a network that is adjusted to minimise power loss may simultaneously perform a dissipative function, which serves to effectively attenuate flood tidal energy (*sensu* Pethick, 1992). This finding goes some way towards resolving the difference in emphasis between mechanisms envisaged by Pethick (1992), and the results of process studies (see, for example, French and Stoddart, 1992). Tidal creeks that are in a stable state of adjustment can be regarded as a morphological outcome of ebb tidal drainage, *and* as a morphological device that effectively dissipates tidal energy.

7.3 EQUILIBRIUM CROSS-SECTIONAL ADJUSTMENT

Previous observations of an association between channel capacity and morphologically active tidal flows have been made in the context of estuarine environments (Gao and Collins, 1994; Pethick, 1996), tidal inlets (O'Brien, 1931, 1969; Inglis and Kestner, 1958; Johnson, 1973; Jarrett, 1976; Mehta *et al.,* 1976; Fitzgerald and Nummedale, 1983; Hume, 1991) and saltmarsh channel networks (Marshall, 1962; Gardner and Bohn, 1980; Collins *et al.,* 1987; Haltiner and Williams, 1987; Knighton *et al.,* 1992; Coates *et al.,* 1995; Pye, 1995; Allen, 1997; Haltiner *et al.,* 1997; French and Reed, 2001). Although these empirical generalisations highlighted an important 'relation of connection' (Sayer, 1992), they are fundamentally lacking in explanatory power. In order to better understand the physical mechanisms underpinning the adjustment process, Friedrichs (1995) employs a more deterministic approach. The physically-based concept of stability shear stress, provides a basis for establishing the cross-sectional geometry of tidal channels that have attained an equilibrium state of development (Ackers, 1972; Brunsden, 1980; Montgomery, 1989). Although the model was originally applied across a geographically extensive range of systems, it is also a useful tool for evaluating the morphological characteristics of individual networks. The model is applied to Brancaster Marsh (see Section 2.4.2) in this capacity.

In Section 7.3.1, the emergence of stability shear stress as a governing principle for cross-sectional geometry is reviewed. Having thereby established the theoretical basis of the adjustment process, the key equations are introduced (Section 7.3.2). Methods employed in the acquisition of data for the respective input parameters are outlined in Section 7.3.3, together with field-based techniques involved in the collection of measurements for the validation of key series. Model implementation is described in Section 7.3.4, and the extent to which the mechanism of stability shear stress is capable of predicting cross-sectional geometry is assessed.

7.3.1 Stability shear stress criteria

Natural tidal channels exhibit an inherent ability to adjust their morphological characteristics according to the conveyance function that they must perform (Allen, 1997). In simple terms, this adjustment process proceeds through erosion or deposition along the channel margin. However, observations concerning temporal patterns of network development also suggest that creek systems tend towards a state of comparative stability (Letzsch and Frey, 1980, Frey and Bassan, 1985; French and Stoddart, 1992), rather than undergoing continual morphological change. It therefore appears that over time, a balance is struck between the motive and resistive forces that are operating in reaches throughout the system (see Myrick and Leopold, 1963; Davies, 1987; Pethick, 1994, 1996).

Several theoretical explanations have been put forward for the regulating mechanism that has resulted in a large number of formations achieving an equilibrium condition, where cross-sectional geometry is nicely adjusted to tidal forcing (see, for example, Myrick and Leopold, 1963; Chantler, 1974; Hume, 1991; De Jonge, 1992; also Pethick, 1996). As noted by Friedrichs (1995) these 'equilibrium' tidal channels tend to satisfy the condition:

$$A_S \sim Q^{\lambda} \qquad [7.22]$$

with an exponent value of $\lambda \sim 1$ indicating that velocity is near-constant throughout the network (Pethick, 1980). According to Wright *et al.* (1973), such widespread proportionality between A_S and Q occurs because channel morphology progressively adjusts until a state of maximum entropy is achieved. The authors go on to note that where this is the case, networks will exhibit: (1) a uniform distribution of energy

dissipation; and (2) a minimum rate of work in the system as a whole (see also Chang, 1979; Yang *et al.*, 1979). The former aspect has received considerable attention in the literature through the concept of uniform critical velocity. However, the latter extremal hypothesis is not directly connected to the physical equations governing the balance of forces, and the concept of maximum entropy is therefore precluded from further examination.

Uniform critical velocity is forwarded as an alternative explanation for proportionality by Chantler (1974, p.187). The basic premise of the hypothesis is that A_S adjusts through erosion or deposition, resulting in a characteristic cross-sectionally averaged velocity that *'causes a bottom shear stress just capable of dislodging and transporting material from the channel bed and banks'*. If this so called 'critical' velocity (v_C) is consistently less than the peak velocity (v_P) within the channel ($v_P < v_C$), net deposition will decrease the cross-sectional area by infilling. Since the reduction in capacity causes a local increase in v_P, erosion is enhanced and a stable cross-sectional geometry restored. Conversely, where peak velocity exceeds the critical level ($v_P > v_C$), erosion will increase A_S. Enlargement of the cross-section in turn causes a reduction in v_P, and the channel returns to a stable state as sedimentation is promoted. The maintenance of a stable or equilibrium state through these feedback mechanisms is referred to by Friedrichs (1995) as 'critical shear stress theory' (see also Pethick, 1996).

Although the balance between motive and resistive forces has so far been expressed in terms of velocity (see also Bruun, 1967; Pethick, 1996), the shear stress imposed by the flow provides the key dynamic link to entrainment of sediment at the channel margin (Davies, 1987). Following Friedrichs (1995, p.1065), 'stability' shear stress (τ_S) corresponds with '*the total bottom shear stress just necessary to maintain a zero along-channel gradient in net sediment transport*'. From considering the physical properties of the constituent materials, it is possible to define a theoretical critical shear stress (τ_C) which will initiate sediment motion. A lower bound on τ_S may therefore be imposed by the condition that peak shear stress (τ_P) is equal to this critical level.

For a stable system that is 'in regime' (Allen, 1997), the three-way balance between cross-sectional area, motive (represented by τ_P) and resistive forces (represented by τ_S) applies to a particular envelope of flow conditions. Krishnamurthy (1977) suggests that the time-averaged stability shear stress associated with mean velocity is the key determinant (see also Haltiner and Williams, 1987; Coates *et al.*, 1995). However, process studies indicate that formative flows are associated with the peak velocity transients of

over-marsh, rather than under-marsh or bankfull events (Bayliss-Smith *et al.*, 1979; Reed, 1987; French and Stoddart, 1992). Consequently, channel geometry is more likely to be adjusted to the maximum shear stresses occurring during spring tides (see also Hume, 1991), than those experienced during neap tides.

7.3.2 Model definition

According to critical shear stress theory, the balance between motive and restive forces is upset when the peak shear stress imposed by tidal action exceeds a critical level defined by sedimentary composition of the channel margin. Cross-sectional geometry may be related to τ_C through a number of physical equations. In the first step towards forging a connection, velocity is expressed in terms of discharge and cross-sectional area (Equation 7.23). From here v_C, and therefore A_S, can be related to τ_C through several different formulae. Although the log-layer solution outlined by Yalin (1972) is a candidate, Friedrichs (1995) and Van Dongeren and De Vriend (1994) suggest that the Manning-Strickler formula (see Henderson, 1966; Dingman, 1984; Chadwick and Morfett, 1993) provides a more appropriate basis for studying tidal reaches.

$$v_P = \frac{Q_P}{A_{SP}} \qquad [7.23]$$

$$v = \frac{1}{n} R^{\frac{1}{6}} \sqrt{\frac{\tau}{\rho g}} \qquad [7.24]$$

$$R = \frac{A_S}{W} \qquad [7.25]$$

The Manning-Strickler formula (Equation 7.24) has distinct advantages over other associations inasmuch that: (1) it is based on three-dimensional flows; (2) it accommodates the effects of meandering; (3) τ applies to the entire channel bed rather than simply the thalweg; and (4) the equation is successfully implemented by Mehta (1978) in modelling tidal formations. From Equations 7.23-7.25, the cross-sectional geometry at a particular channel reach may, as shown by Equation 7.26, be expressed in terms of peak discharge and critical shear stress.

$$A_{SP} R_P^{\frac{1}{6}} = Q_P n \left(\frac{\rho g}{\tau_C} \right)^{\frac{1}{2}} \qquad [7.26]$$

The performance of stability shear stress, as a physically-based mechanism governing the cross-sectional geometry of tidal channels, can be evaluated by comparing

predicted values (obtained using the right hand side of Equation 7.26) with observed characteristics of A_{SP} and R_P that have been measured from the actual network.

7.3.3 Data acquisition

A combination of strategies is employed to predict and measure variables for evaluating Equation 7.26. While τ_C and n are readily obtained from empirical sources, the remaining parameters were computed using a combination of field-based measurements and data derived from remotely sensed imagery. Finding appropriate values for the critical level of shear stress is more problematic. In implementing the model for an extensive sample of tidal channels, Friedrichs (1995) recognises the influence exerted by variations in sedimentary composition over the results obtained (see also Haltiner and Williams, 1987; Dexter, 1995). In the case of non-cohesive material, τ_C is a function of physical properties such as grain size and bed roughness. Coates *et al.* (1995) indicate that critical shear stress diminishes from a maximum of 0.3 Nm^{-2} for coarse sand particles (~0.50mm), to 0.15 Nm^{-2} for material with a diameter of ~0.05mm (see also Mehta *et al.*, 1976). However, frictional drag associated with the development of bedforms, such as ripples and dunes, is also seen to play a role, increasing the critical level in natural channels by a factor of between 1.4-5.5 (Smith and McLean, 1977; Druery *et al.*, 1984). For cohesive materials (see Pye and Crooks, 1995), the critical shear stress necessary to initiate erosion is primarily determined by the forces of attraction between constituent particles. Readings are generally higher than for sandy materials. Coates *et al.* (1995) record values of $0.02 < \tau_C < 7$ Nm^{-2}, and elsewhere values of up to 60.9 Nm^{-2} have been obtained (Lee *et al.*, 1994, cited in Friedrichs, 1995, p.1068). The material comprising the Brancaster network is non-cohesive (see Figure 6.10a; mean *%silt-clay* = 29%). Following Friedrichs (1995), a value for the total critical bed shear stress of $\tau_C = 0.5$ Nm^{-2} is used here. Error margins of 0.1 Nm^{-2} and 1.1 Nm^{-2} are also employed, to examine the sensitivity of the model to this parameter.

For a U.S. tidal slough, Leopold *et al.* (1993) record considerable variation in the roughness coefficient n, with tidal stage. Values ranging between $0.028 < n < 0.063$ $m^{-1/3}s$ reflect the multiplicity of factors influencing the degree of frictional resistance presented to flow (Leopold *et al.*, 1964). Previous studies suggest that n tends to decline with stage (Knight, 1981), but increases with the degree of meandering, density of bank vegetation, and roughness of the channel margin (Dingman, 1984; Chadwick and Morfett, 1993). For

the present study, a value of n = 0.03 $m^{-1/3}s$ is selected, with an error margin of $\pm$ 0.005 $m^{-1/3}s$ reflecting the departure from other readings employed for tidal systems (see Mehta *et al.*, 1976; Boon and Byrne, 1981).

As depicted in Figure 7.13, the acquisition of discharge readings and measures of cross-sectional geometry for sample stations throughout the sample network, involves integrating a combination of data from remotely sensed imagery and field-based survey. Due to the logistical difficulty of tracking Q_P along the course of a creek system, discharge readings were instead obtained from a hypsometric model (Wright *et al.*, 1973; Boon, 1975; Settlemeyer and Gardner, 1977; Pethick, 1980; Boon and Byrne, 1981; Fitzgerald and Nummedale, 1983; Healey *et al.*, 1981; Hume, 1991) based on high resolution lidar altimetry (see Section 2.4.3). Referred to by Boon and Byrne (1981) as a closed hypsometric representation of basin-storage-volume channel-flow relationships, the model (see Equation 7.26) employs the principle of continuity (Fitzgerald and Nummedale, 1983), that the rate of change of water volume in the marsh equals the discharge through the channel cross-section.

$$Q_E = A_E \frac{dE}{dt} \qquad [7.26]$$

Discharge for a given tidal elevation (E), is therefore expressed as the volumetric product of the area contributing flow (A_E) and the rate of change in stage (dE/dt).

Following the methodological procedure outlined in Figure 7.8, A_{eq} was delineated on the high resolution photographic coverage using Imagine software, for each of the 60 sample stations along the Brancaster network. Although these stations are distributed throughout the upper, central and lower sectors of the system, headwater reaches were avoided because field experience suggests that channel width may be similar to, or less than, the spatial resolution of the imagery. After saving the delineated region as an area of interest (aoi), a sub-scene was created from the lidar coverage using the aoi as a mask. The area contributing to channelised discharge changes with tidal stage, as inundation or emergence becomes increasingly widespread with the rising or falling water level (see Figure 7.14). In order to compute the area corresponding with various stages of the tidal cycle, a simple programming script was composed to count the number of pixels at or below the designated elevation within a particular sub-scene. With each pixel covering an area of $4m^2$, the corresponding figure for A_E was then computed.

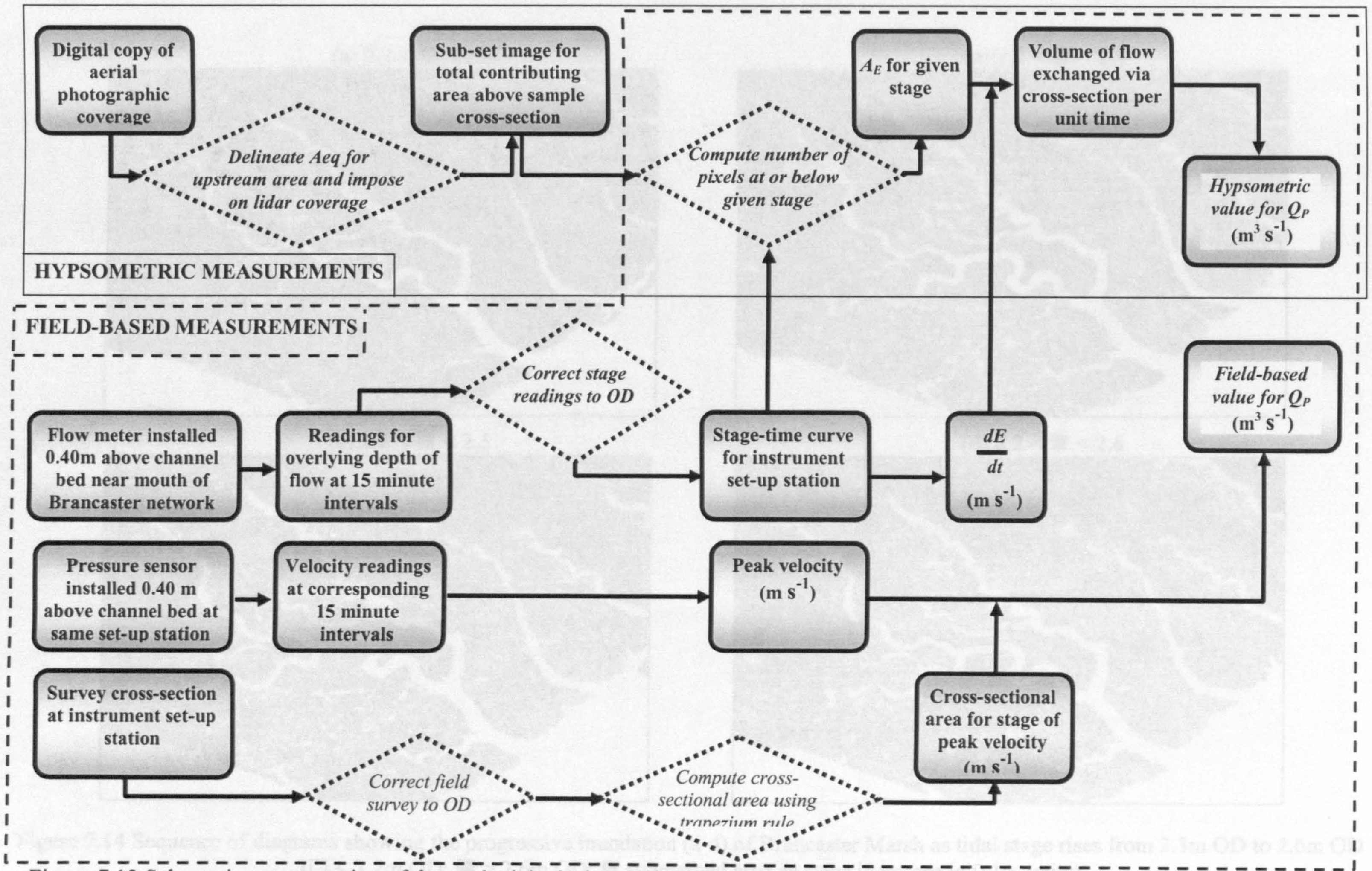

Figure 7.13 Schematic representation of the methodological procedure employed in obtaining predicted and observed measures of peak ebb tidal discharge, for the evaluation of stability shear stress as a principle governing equilibrium cross-sectional geometry.

(a) 2.2 < ■ < 2.3

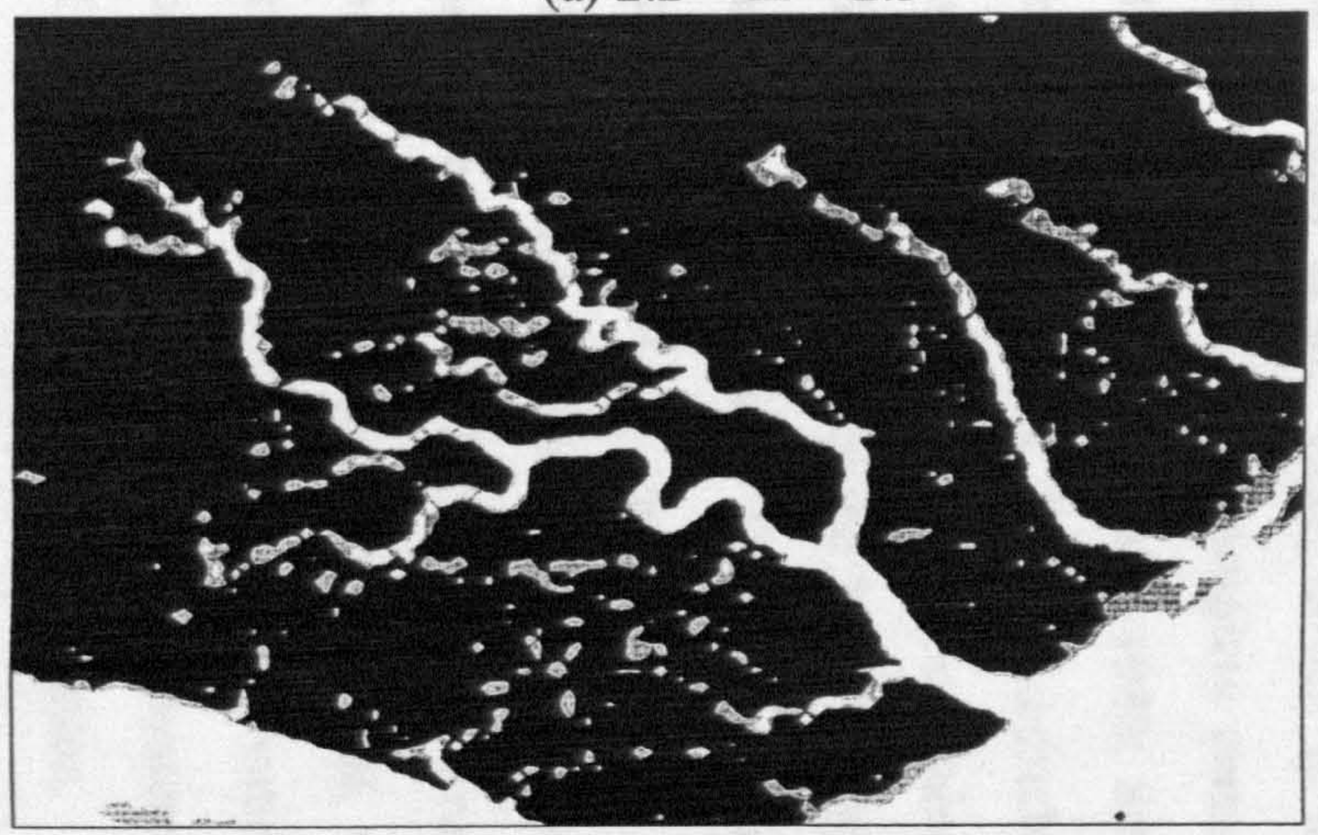

(b) 2.2 < ■ < 2.4

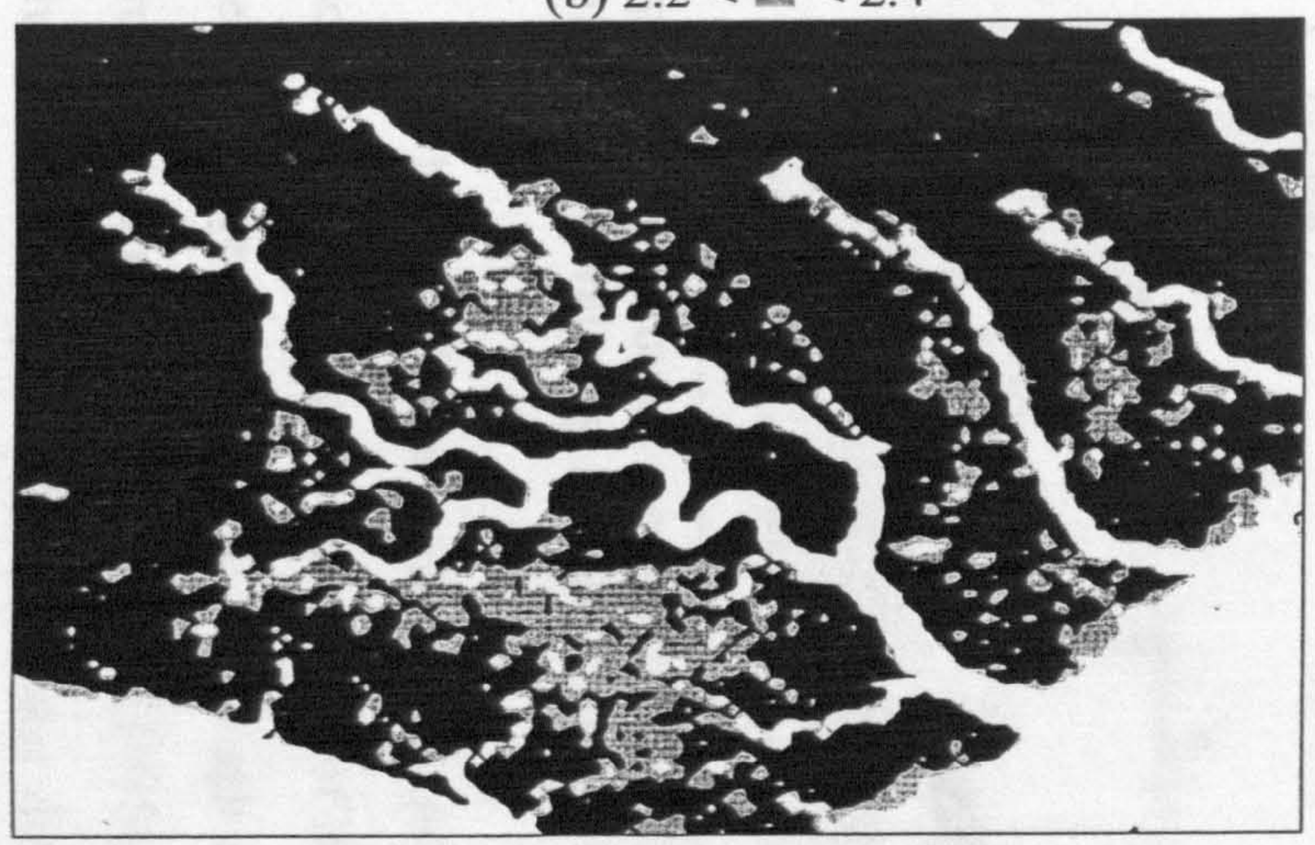

(c) 2.2 < ■ < 2.5

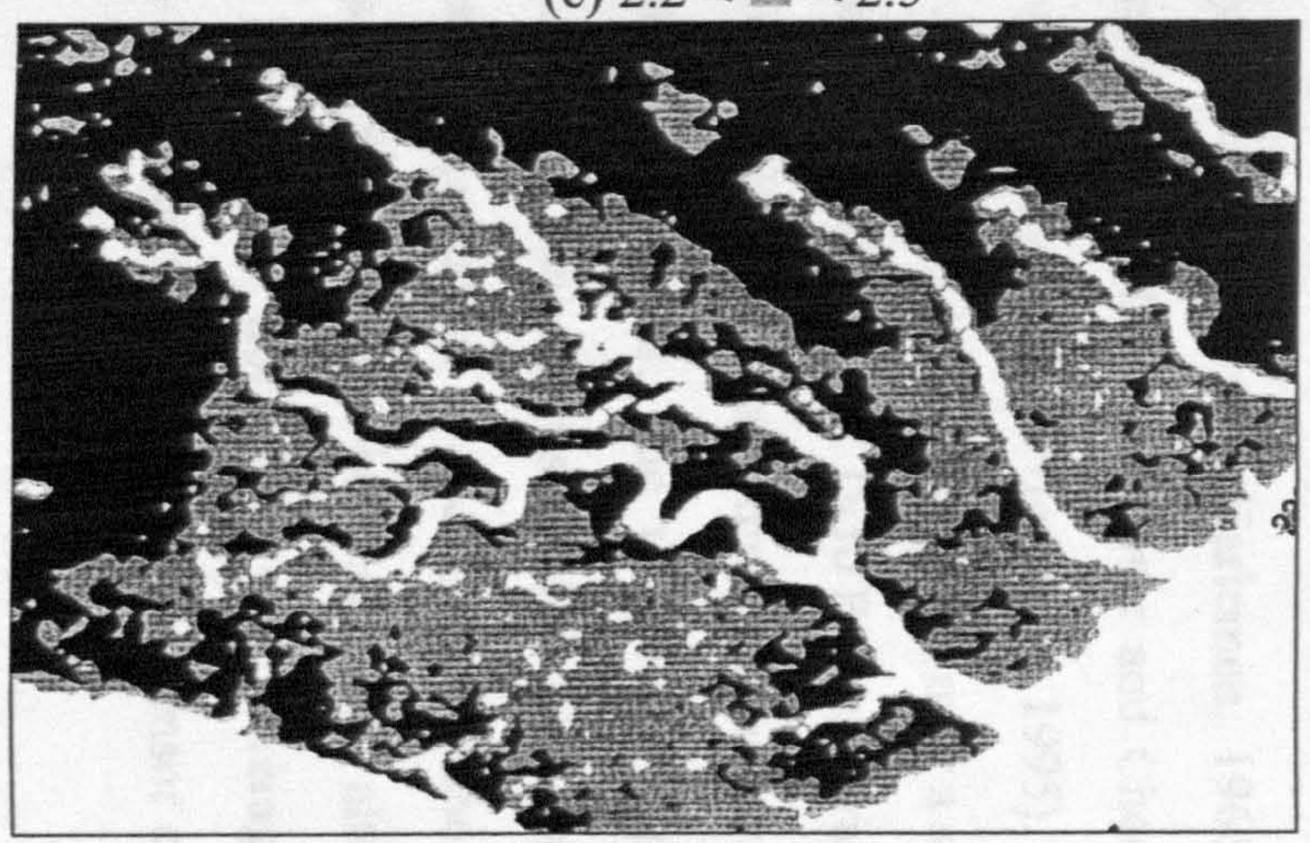

(d) 2.2 < ■ < 2.6

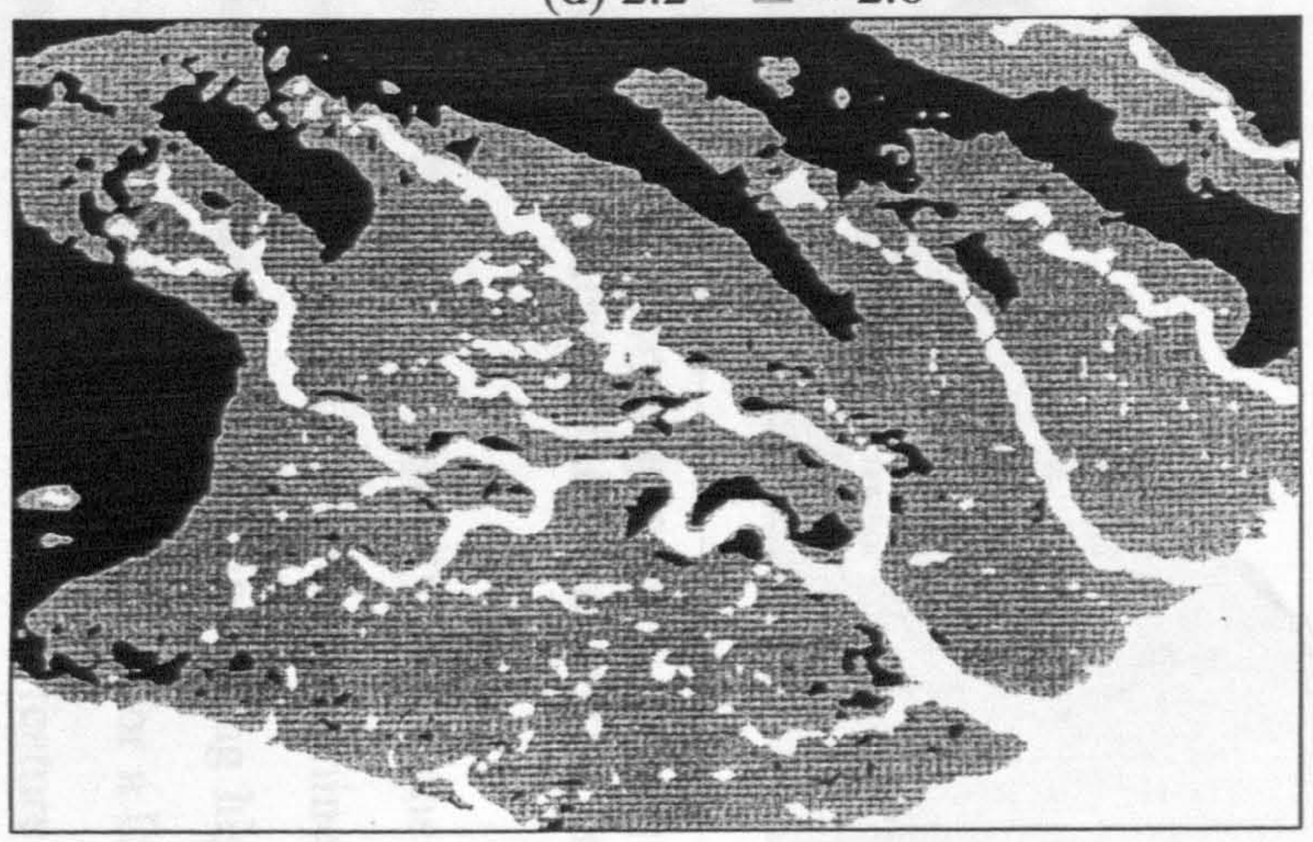

Figure 7.14 Sequence of diagrams showing the progressive inundation (a-d) of Brancaster Marsh as tidal stage rises from 2.3m OD to 2.6m OD (□ < 2.2m OD; ■ > 2.6m OD; ■ submerged area as stage increases in 0.1m units)

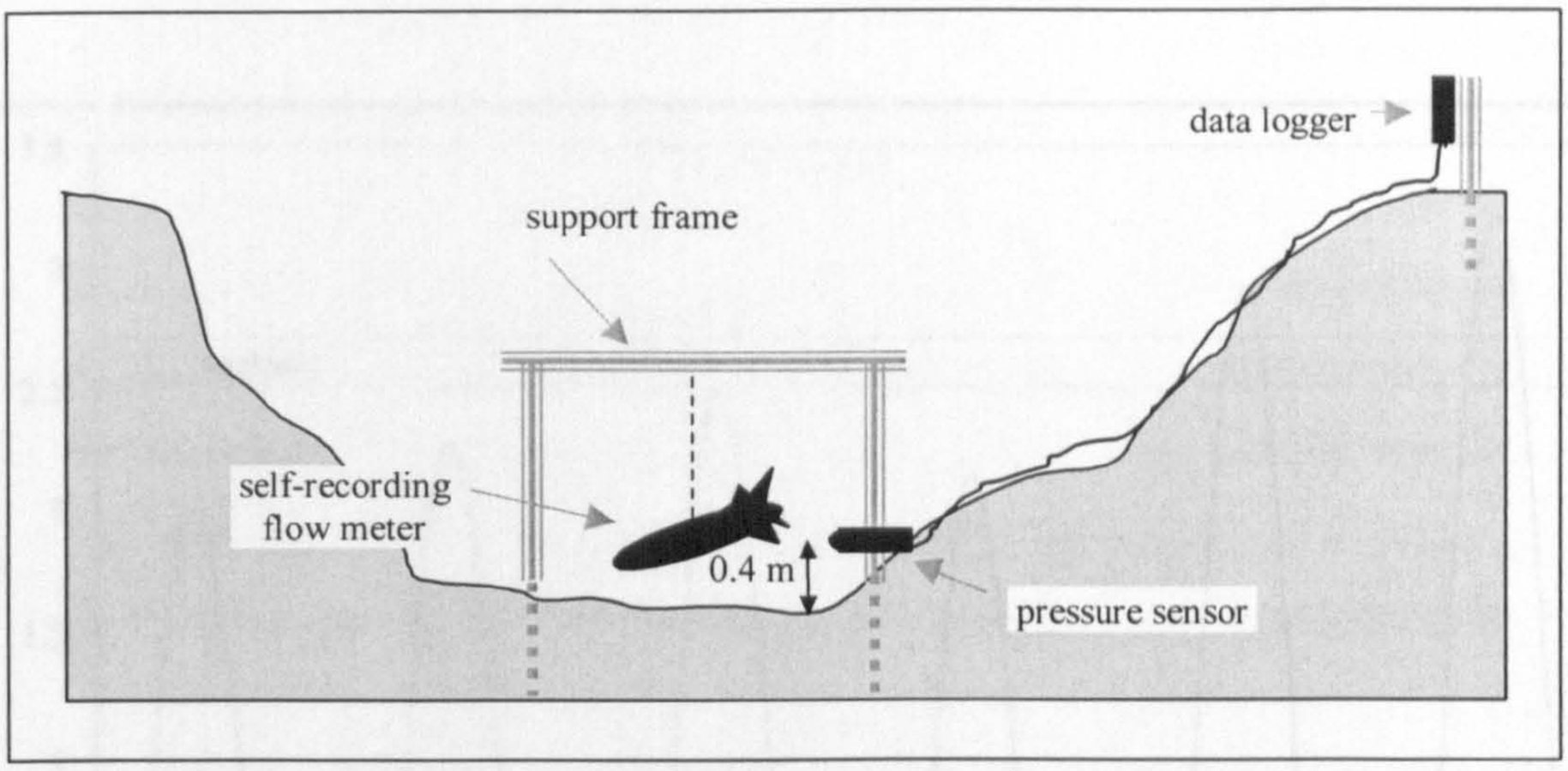

Figure 7.15 Schematic representation of the instrument array employed in the acquisition of stage and velocity data for a section in the lower reaches of the Brancaster network.

While discharge is partially dependent on the storage capacity of the channelised reaches and the platform component of the saltmarsh system, Q_P is also determined by the rate of change in tidal stage. Although a tidal prediction equation, including high order harmonics, is employed by Boon (1975) to simulate the stage-time curve for a U.S. tidal network, the complex shallow water distortions that are a characteristic feature of tidal exchanges in saltmarsh systems (Pestrong, 1965; Bayliss-Smith *et al.,* 1979; Pethick, 1980; Healey *et al.,* 1981; Green *et al.,* 1986; Pringle, 1995; Tubbs, 1999), remain difficult to predict with complete certainty (see, for example, Harlemen, 1966; Pugh, 1987; Lincoln and Fitzgerald, 1988; Schuepfer *et al.,* 1988; Falconer and Chen, 1991; Friedrichs and Madsen, 1992; Friedrichs and Aubrey, 1994; Friedrichs, 1995). For the present study, stage readings were obtained directly at 15 minute intervals over a sequence of 6 tidal cycles between the 23-26th October 2000, using a PTX 1830 Pressure transmitter attached to a Newlog 'Technolog' datalogger. Ideally, stage-time curves would be obtained for each of the 60 sample stations. However, due to limited equipment availability and logistical considerations a single sensor, installed 0.40m above the channel bed (Figure 7.15) at the instrument setup station in the lower reaches of the Brancaster network (see Figure 2.10), was employed as the best available alternative. Control points, for which the elevation was known from the lidar coverage, were established throughout the marsh system, and the height of the pressure sensor corrected to OD with a first order transformation.

Shallow water effects are clearly apparent from the stage-time plots in Figure 7.16. Due to the truncated nature of the stage curves (see also Yapp *et al.*, 1917; Pethick, 1980; Ashley and Zeff, 1988; Lincoln and Fitzgerald, 1988), it is difficult to ascertain if

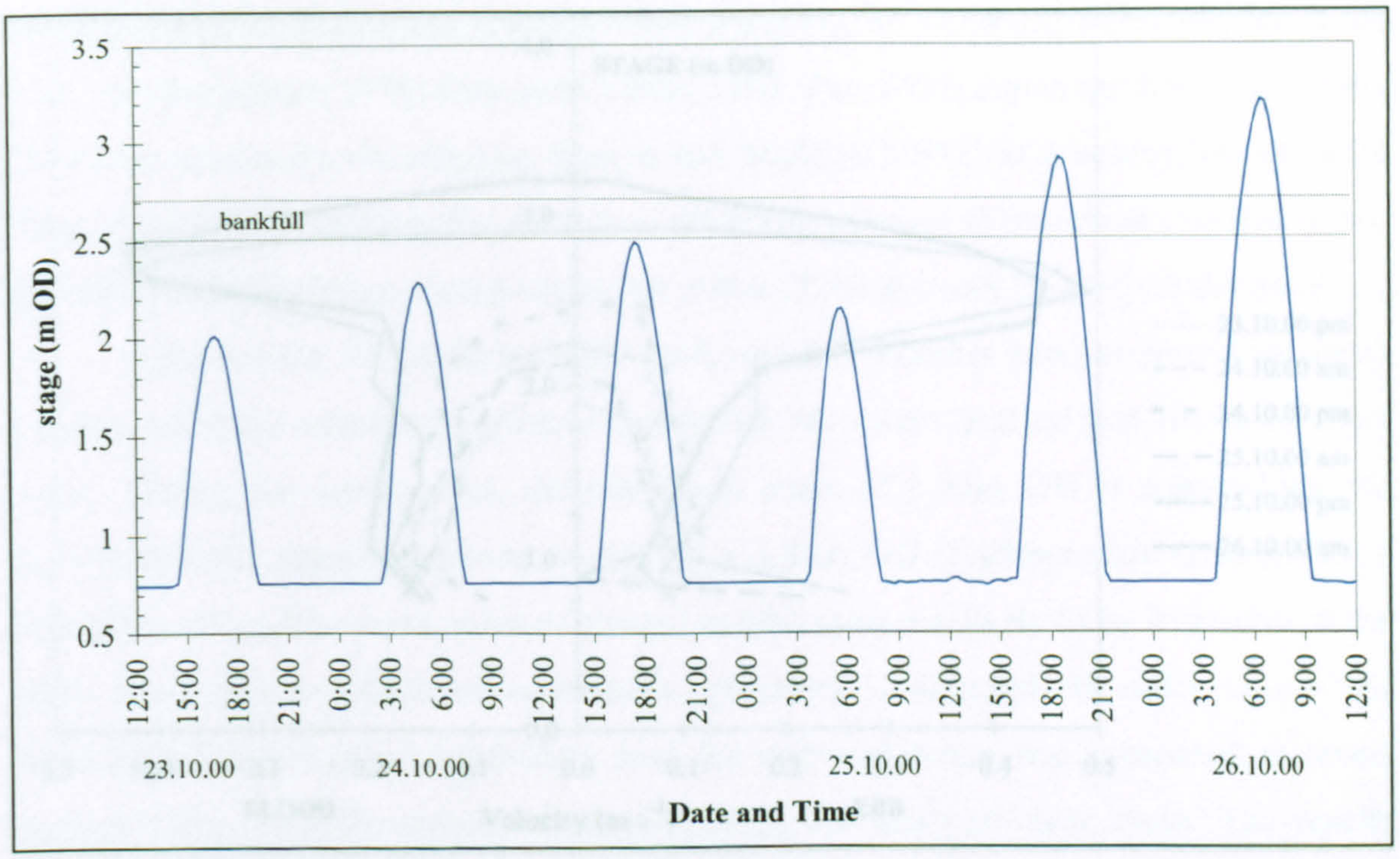

Figure 7.16 Stage-time curves for a sequence of tides at the Brancaster network. Over-marsh tides on 25-26th October 2000 clearly exceed bankfull elevation.

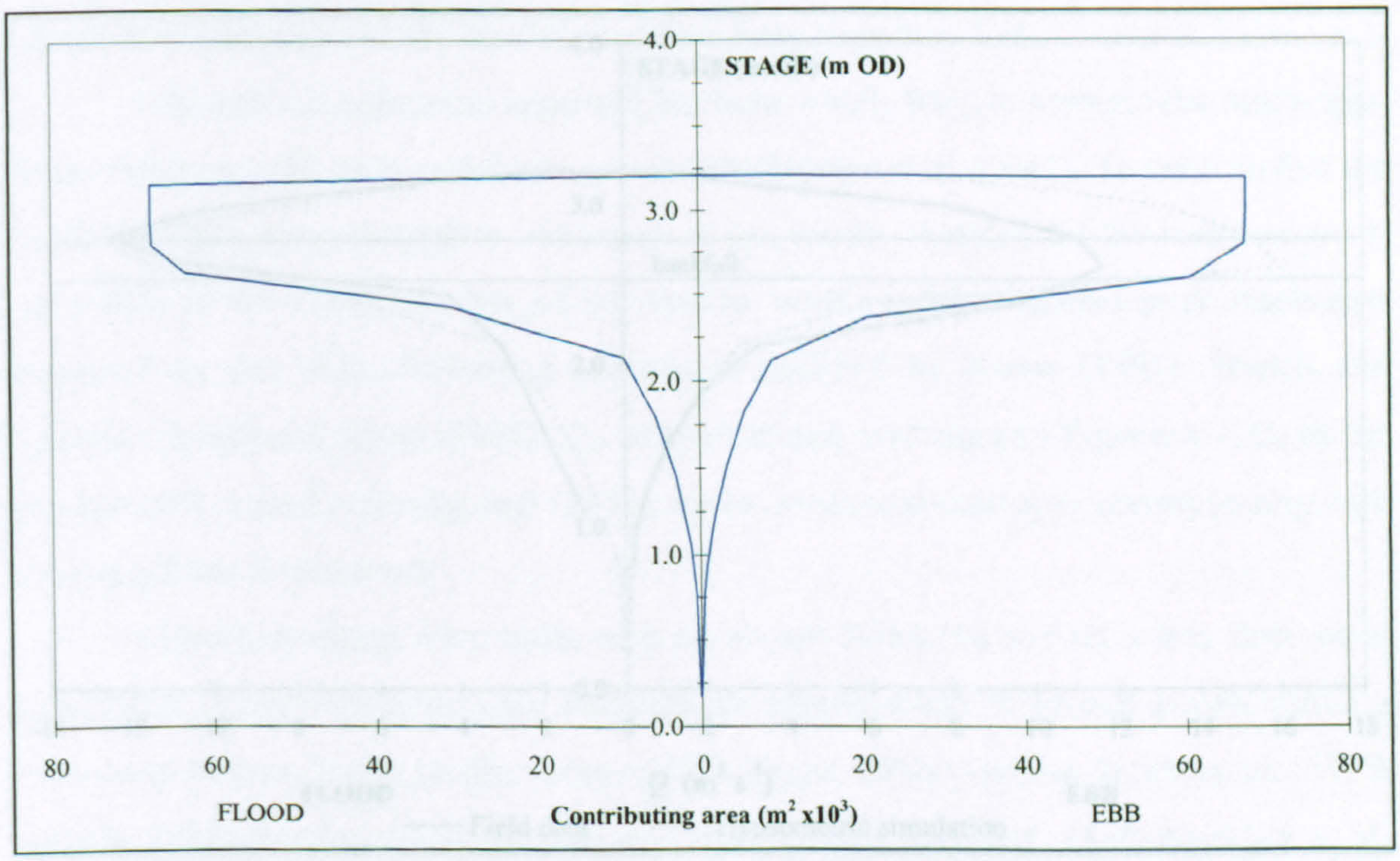

Figure 7.17 Area-stage plot showing an abrupt transition in the area contributing flow to the instrumental set-up station towards the mouth of the Brancaster network.

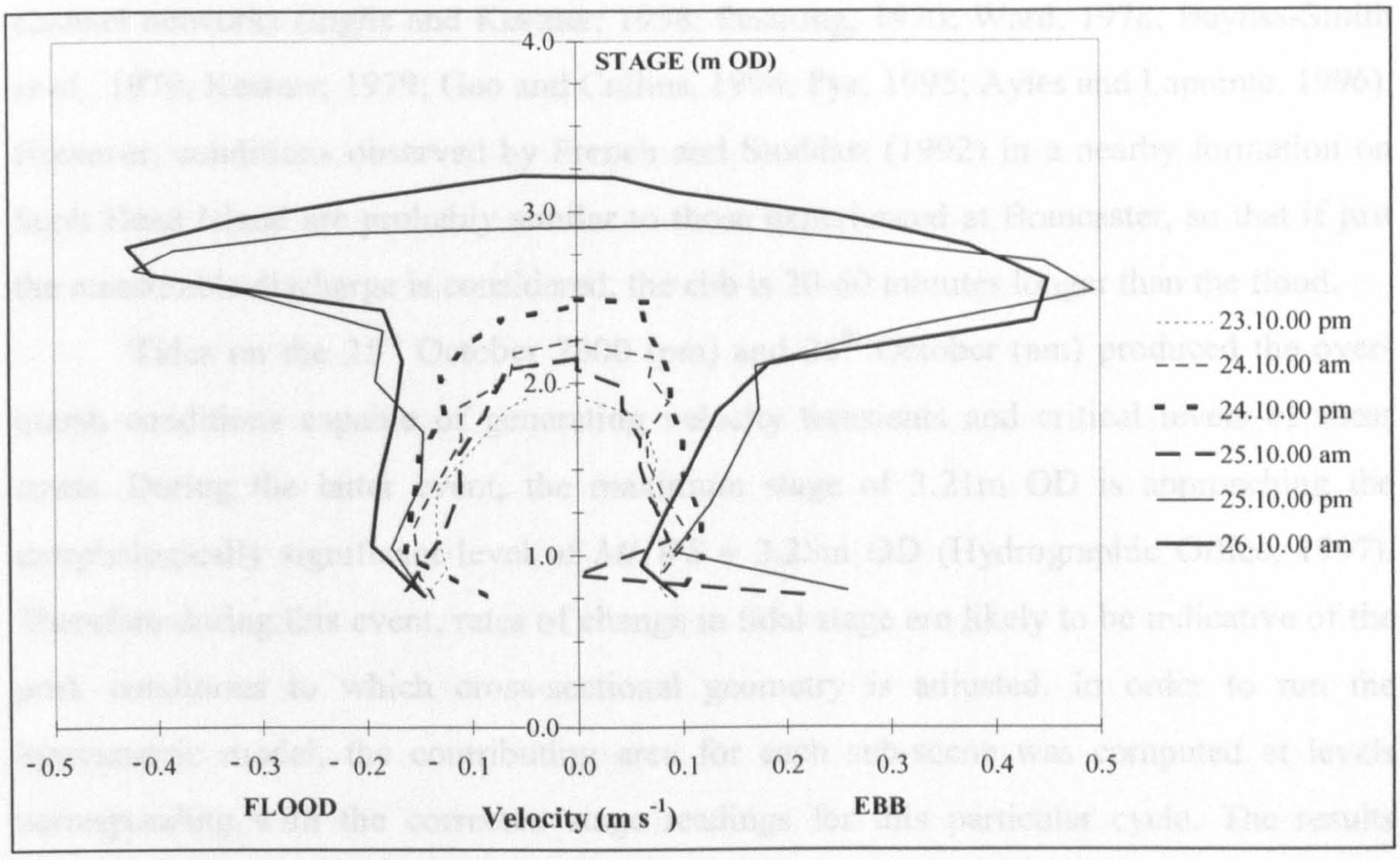

Figure 7.18 Velocity-stage curves for the sequence of tides at the instrumental set-up station towards the mouth of the Brancaster network.

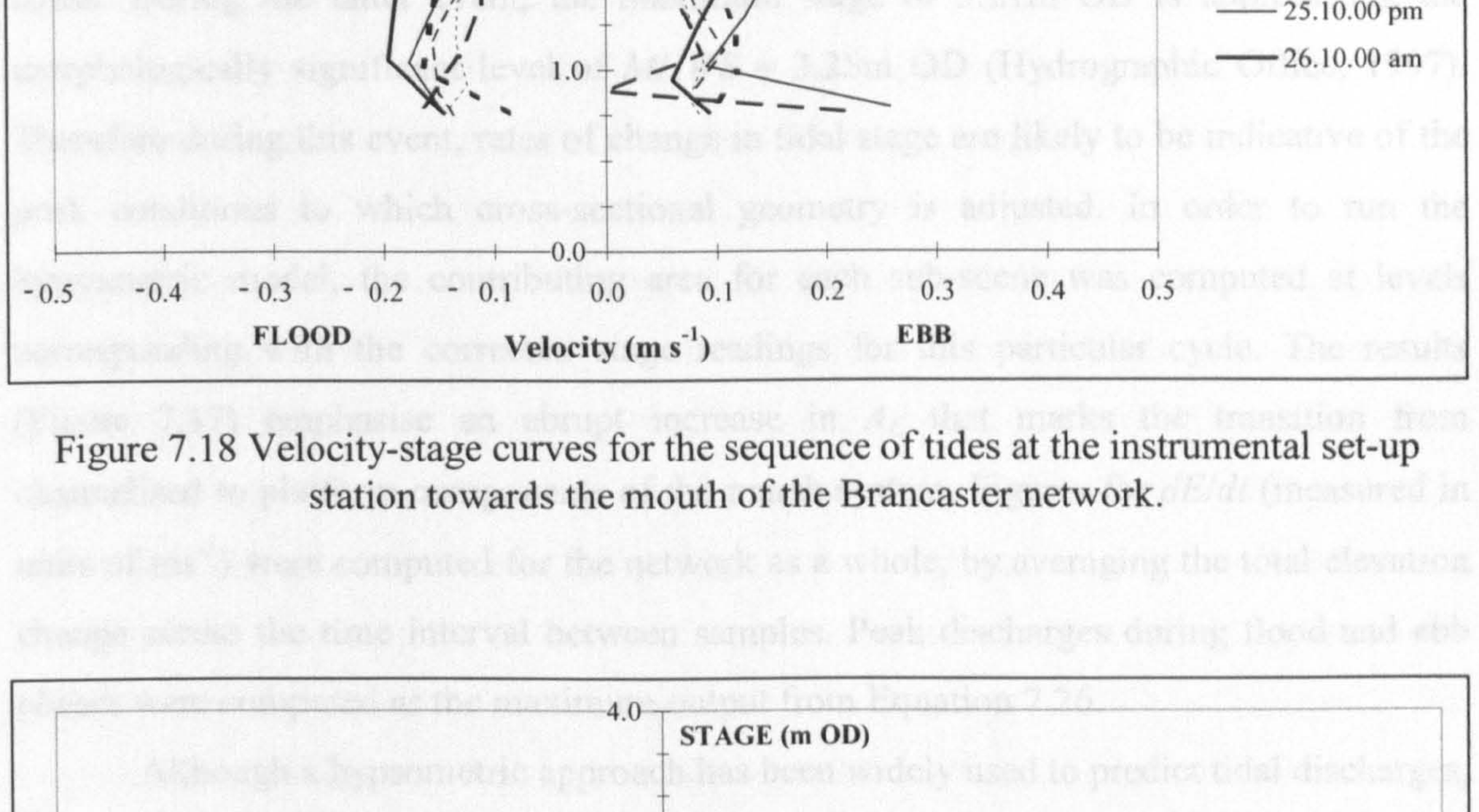

Figure 7.19 Stage-discharge plots computed using the hypsometric model and through field validation, for the instrument set-up station towards the mouth of the Brancaster network.

the present results exhibit the duration asymmetry that has been widely ascribed to tidal channel networks (Inglis and Kestner, 1958; Pestrong, 1970; Ward, 1978; Bayliss-Smith *et al.,* 1979; Kestner, 1979; Gao and Collins, 1994; Pye, 1995; Ayles and Lapointe, 1996). However, conditions observed by French and Stoddart (1992) in a nearby formation on Scolt Head Island are probably similar to those experienced at Brancaster, so that if just the measurable discharge is considered, the ebb is 20-60 minutes longer than the flood.

Tides on the 25th October 2000 (pm) and 26th October (am) produced the over-marsh conditions capable of generating velocity transients and critical levels of shear stress. During the latter event, the maximum stage of 3.21m OD is approaching the morphologically significant level of *MHWS* = 3.25m OD (Hydrographic Office, 1997). Therefore during this event, rates of change in tidal stage are likely to be indicative of the peak conditions to which cross-sectional geometry is adjusted. In order to run the hypsometric model, the contributing area for each sub-scene was computed at levels corresponding with the corrected stage readings for this particular cycle. The results (Figure 7.17) emphasise an abrupt increase in A_E that marks the transition from channelised to platform components of the marsh system. Figures for dE/dt (measured in units of ms^{-1}) were computed for the network as a whole, by averaging the total elevation change across the time interval between samples. Peak discharges during flood and ebb phases were computed as the maximum output from Equation 7.26.

Although a hypsometric approach has been widely used to predict tidal discharges, its predictive capability is called into question by Healey *et al.* (1981). To confirm that the model provides a representative indication of Q_P, results obtained for the instrument set-up station in the lower reaches of the system were validated against peak discharges measured in the field. Following procedures outlined by Hume (1991), French and Stoddart (1992) and Lessa (1996), Q_P was calculated according to Equation 7.23, as the product of: (1) peak velocity; and (2) the wetted cross-sectional area corresponding with the stage when v_P occurred.

Velocity readings were made with a Valeport BFM 104 self-recording flow meter (see Figure 7.15). While velocity readings are ideally taken at several points within a cross-section (see, for example, Boon, 1975; Ward, 1978; Bayliss-Smith *et al.,* 1979; Knight, 1981; Roman, 1984; Reed *et al.,* 1985; Ashley and Zeff, 1988; Stoddart *et al.,* 1987; De Jonge, 1992), such a rigorous measurement procedure is arguably more appropriate for detailed studies, where local variations in v are of importance. Considering the margins of uncertainty surrounding the prediction of Q_P using a hypsometric model, a

single flow meter should yield a sufficiently accurate cross-sectionally averaged statistic (Boon, 1975). The flow meter was positioned at 0.40 m above the channel bed, with readings sampled over 60 seconds at intervals timed to coincide with the stage record. Plotted as a function of stage, the resulting velocity data (Figure 7.18) exhibit the unsteadiness that is a characteristic feature of saltmarsh channel networks (Bayliss-Smith *et al.*, 1979; Green *et al.*, 1986; Reed, 1995; Stoddart *et al.*, 1989; French and Stoddart, 1992; Pringle, 1995). A basic distinction is evident between under-marsh or bankfull tides, and the two over-marsh flow events. Velocities are lower under the former, attaining a maximum of $v_P \sim 0.16$ ms^{-1} during the flood phase of the cycle. However, pronounced transients occur during the over-marsh tides, reaching a maximum of $v_P \sim 0.50$ ms^{-1} as the marsh platform emerges following inundation.

To complete the validation exercise, the cross-sectional profile at the instrument set-up station was surveyed with a Topcon GTS 300 and Psion logger running Survpro Software (NSS, 1998). The profile was tied into OD with a first order transformation of control points that could also be identified on the lidar coverage. The wetted cross-sectional area was then obtained at stages corresponding with velocity readings for the over-marsh event on 26th October 2000. After fitting a high order polynomial through the survey points, the empirical model was used to compute the area below a given water surface elevation according to the trapezium rule (Bostock and Chandler, 1994). For stages above bankfull, the area of channelised flow was defined by vertically extending the channel margins (see also Coates *et al.*, 1995). Values of A_E were combined with the velocity series to generate Q_E.

The stage-discharge curves (Figure 7.19) exhibit an encouraging correspondence between observations and model results. For the flood tide, the hypsometric maxima of $Q_P = 12.15$ m^{3}s^{-1} is within 3% of observed values, and occurs at a comparable tidal stage, as bankfull is exceeded. For the ebb tide, the more substantial departure of ~37% between the predicted $Q_P = 16.02$ m^{3}s^{-1} and observed $Q_P = 11.66$ m^{3}s^{-1} may be attributable to a number of factors. Firstly, French and Stoddart (1992) note that a proportion of the total discharge enters and leaves the system directly across the front of the marsh. The hypsometric model assumes that all flow is routed through the creek system. As such, it may over-estimate the volume exchanged, and thereby Q_P. Frictional retardation could also play a role. The hypsometric model assumes that each unit of marsh area, at or below a given stage, contributes to the component A_E. However, the drag presented by saltmarsh vegetation (see Leonard and Luther, 1995; Leonard *et al.*, 1995) will delay surface

drainage in some areas, so that the actual contribution is somewhat less than the potential figure. Overall, the hypsometric model provides a satisfactory representation of peak discharge. Its use in calculating Q_P for other cross-sections throughout the network is sufficiently justified, although a margin of uncertainty should be allowed for.

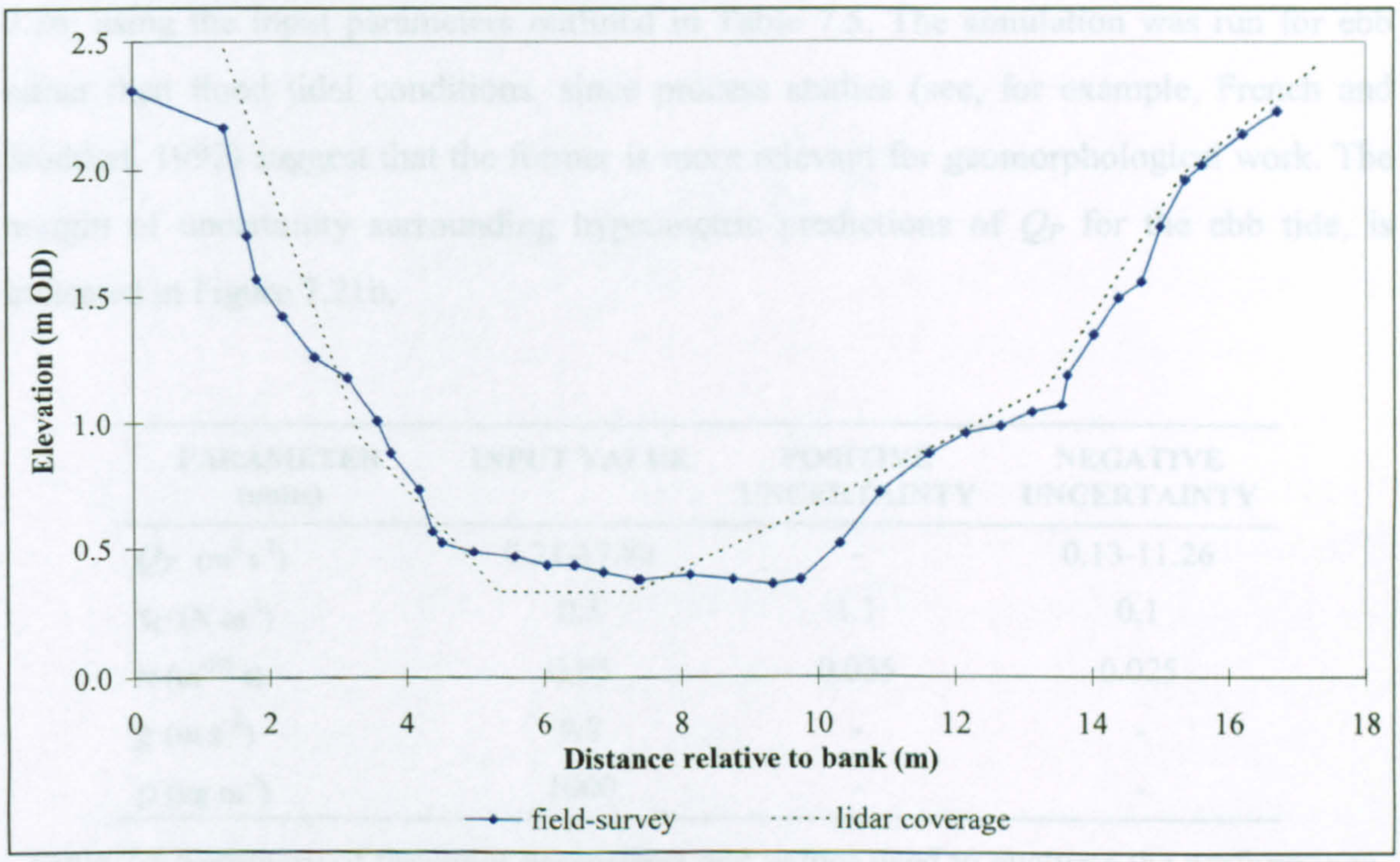

Figure 7.20 Comparison of cross-sectional profiles for the instrument set-up station acquired by field surveying and from the lidar coverage.

The final stage of model parameterisation involves obtaining the wetted cross-sectional area and hydraulic radius corresponding with Q_P, for comparison with values predicted by Equation 7.26. Following the procedure that was outlined in the context of hydraulic geometry (Section 7.2.5), the surface profiling tool of Imagine software was used to define the cross-sectional characteristics at each sample station. In order to verify the accuracy of this technique, the lidar cross-section for the instrument set-up station is plotted against the corresponding field survey data in Figure 7.20. Close agreement between the profiles supports the use of lidar data in calculating A_{SP} and R_P. Since Q_P and the stage at which it occurs is now known for stations throughout the network, the cross-sectional area below this elevation was computed using the trapezium rule. The wetted perimeter was computed as the total distance between successive points around the channel margin. The results were input into the left hand side of Equation 7.26, thereby generating the 'expected' cross-sectional geometry.

7.3.4 Model performance

The performance of the stability shear stress model, as a basis for explaining the cross-sectional adjustment of tidal channels to an imposed peak discharge, is summarised in Figure 7.21. The bivariate plot (Figure 7.21a) shows *predicted* values against *observed* readings. The predicted results were obtained according to the right hand side of Equation 7.26, using the input parameters outlined in Table 7.5. The simulation was run for ebb rather than flood tidal conditions, since process studies (see, for example, French and Stoddart, 1992) suggest that the former is more relevant for geomorphological work. The margin of uncertainty surrounding hypsometric predictions of Q_P for the ebb tide, is indicated in Figure 7.21b.

PARAMETER (units)	INPUT VALUE	POSITIVE UNCERTAINTY	NEGATIVE UNCERTAINTY
Q_P ($m^3 s^{-1}$)	0.21-17.88	-	0.13-11.26
τ_C ($N m^{-2}$)	0.5	1.1	0.1
n ($m^{-1/3} s$)	0.03	0.035	0.025
g ($m s^{-2}$)	9.8	-	-
ρ ($kg m^{-3}$)	1000	-	-

Table 7.5 Summary of the input parameters and values used to evaluate the performance of stability shear stress (τ_S) as a principle governing the cross-sectional geometry of Brancaster network.

From the scatter of points about the theoretical line (Figure 7.21a), it appears that 84% of the predicted readings fall at or below the level predicted by the stability shear stress criteria. With comparatively few responses above the upper margin of uncertainty, even when the error margin in ebb values is taken into account (Figure 7.21b), the general implication is that the critical shear stress (τ_C), obtained from consideration of the sedimentary characteristics of the channel floor, provides a reasonable lower bound on τ_S and an upper bound on the cross-sectional geometry of tidal creeks.

Interestingly, the data points exhibit a systematic departure from the theoretical line. The stability shear stress model tends to under-predict readings towards the lower end of the x-axis, and to over-predict responses at the upper end of the scale. At sample stations falling above the line, channel capacity is larger, τ_S lower, and the creek margin more easily eroded than would be expected from considerations of Q_P and τ_C alone. Cross-sectional profiles displaying these characteristics are concentrated within the upper

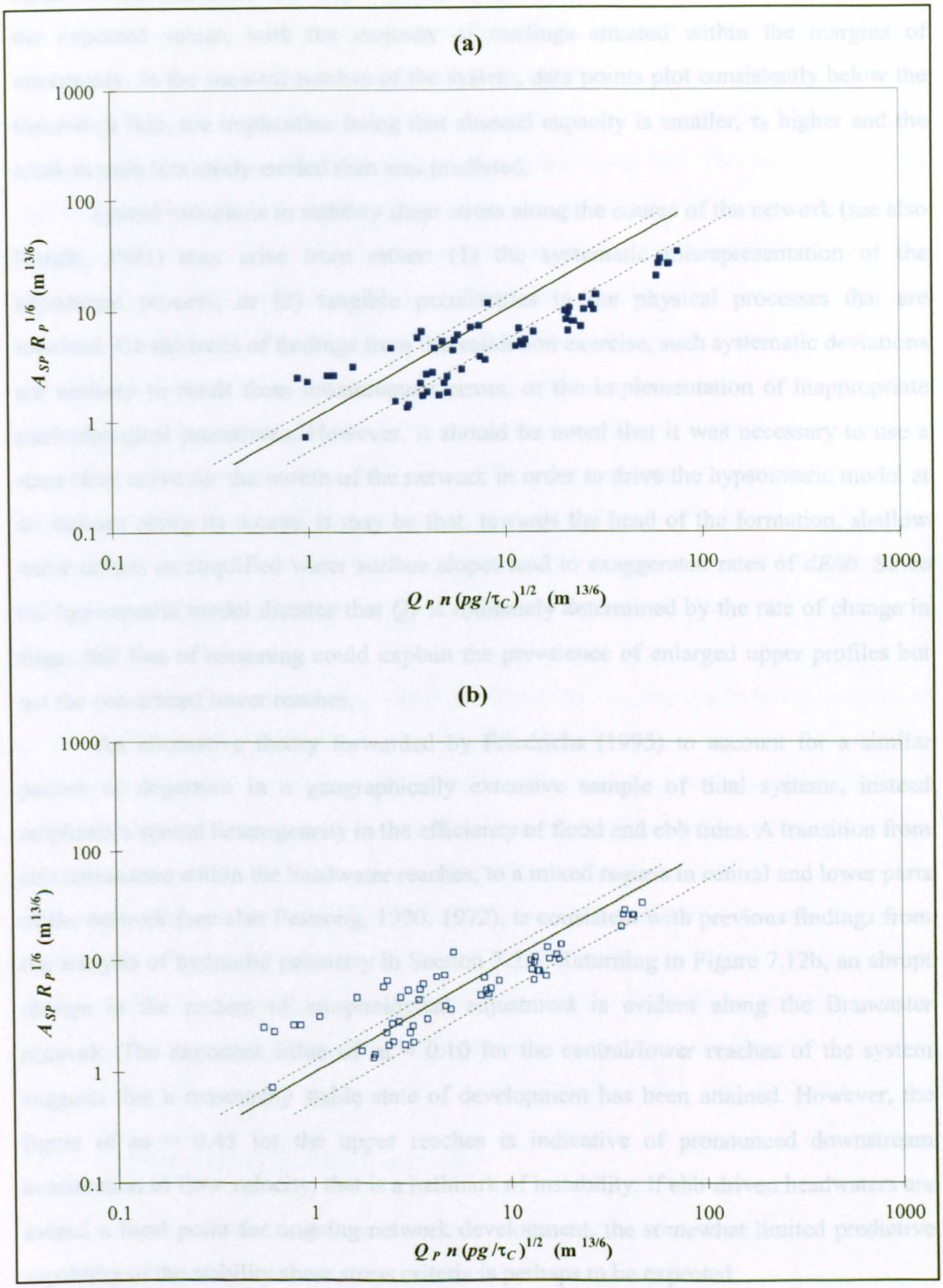

Figure 7.21 (a) Observations of the cross-sectional parameter $A_{SP}R_P^{1/6}$ as a function of Q_P and τ_C for 60 sample stations throughout the Brancaster network; and (b) observations of the cross-sectional parameter $A_{SP}R_P^{1/6}$ as a function of Q_P, and τ_C, taking into account a potential error margin of up to 37% in Q_P. The theoretical line (___) is given by Equation 7.26, with the error margins (_ _ _) reflecting cumulative uncertainty for the input series.

reaches of the Brancaster network. Predictions for stations in the central sector are close to the expected values, with the majority of readings situated within the margins of uncertainty. In the seaward reaches of the system, data points plot consistently below the theoretical line, the implication being that channel capacity is smaller, τ_S higher and the creek margin less easily eroded than was predicted.

Spatial variations in stability shear stress along the course of the network (see also Knight, 1981) may arise from either: (1) the systematic misrepresentation of the adjustment process; or (2) tangible peculiarities in the physical processes that are involved. On the basis of findings from the validation exercise, such systematic deviations are unlikely to result from measurement errors, or the implementation of inappropriate methodological procedures. However, it should be noted that it was necessary to use a stage-time curve for the mouth of the network in order to drive the hypsometric model at all stations along its course. It may be that, towards the head of the formation, shallow water effects or amplified water surface slopes lead to exaggerated rates of dE/dt. Since the hypsometric model dictates that Q_P is ultimately determined by the rate of change in stage, this line of reasoning could explain the prevalence of enlarged upper profiles but not the constricted lower reaches.

An alternative theory forwarded by Friedrichs (1995) to account for a similar pattern of departure in a geographically extensive sample of tidal systems, instead emphasises spatial heterogeneity in the efficiency of flood and ebb tides. A transition from ebb dominance within the headwater reaches, to a mixed regime in central and lower parts of the network (see also Pestrong, 1970, 1972), is consistent with previous findings from the analysis of hydraulic geometry in Section 7.2.5. Returning to Figure 7.12b, an abrupt change in the pattern of morphological adjustment is evident along the Brancaster network. The exponent value of **m** = 0.10 for the central/lower reaches of the system suggests that a reasonably stable state of development has been attained. However, the figure of **m** = 0.45 for the upper reaches is indicative of pronounced downstream acceleration in flow velocity, that is a hallmark of instability. If ebb-driven headwaters are indeed a focal point for ongoing network development, the somewhat limited predictive capability of the stability shear stress criteria is perhaps to be expected.

The failure of reaches in the central and lower parts of the system to achieve the capacity predicted by the model, may be due to the limiting effect of extraneous controls. As Bathurst (1988) notes, phenomena not taken into account are an important determinant of model applicability. In the present context, the physically-based mechanism of stability

shear stress may prove to be limited in several respects. First, the use of critical shear stress based on the sedimentary composition of the channel bed, fails to consider differences in bank material. In this network, the toe facet comprises a higher *%silt-clay* (Figure 6.11b), and may thus exert greater resistance to deformation. The additional strength afforded by vegetative binding action (Masterman and Thorne, 1994) is also ignored, together with the compressive strength attributable to both overlying bank material (Van Eerdt, 1985; Fenies and Faugeres, 1998) and the veneer of bed substrates (Stephens *et al.*, 1992; Friedrichs, 1995). Furthermore, the adjustment process is portrayed as a balance between forces arising at the channel margin during peak flow conditions and the resistive properties of the sedimentary material to *direct* entrainment. However, previous studies suggest that bank deformation may also occur through bio-erosion (Letzsch and Frey, 1980; Frey and Basssan, 1985) and processes of mass failure such as slumping, toppling and sliding (see, for example, Marshall, 1962; Bridges and Leeder, 1976; Allen, 1985a, 1989, 1997). Lastly, certain idiosyncrasies of the Brancaster system may actively resist deformation, such as its position on a resistant layer of sand and shingle (Pye, 1992).

This deterministic model, which is driven by the physically-based concept of stability shear stress, therefore provides a useful upper limit on cross-sectional geometry in the stable central and lower sectors of the Brancaster network, while its value is somewhat limited in the actively-developing headwaters. The predictive capability of the model appears to be curtailed by an incomplete understanding of interactions arising between motive forces during the drainage phase of the tidal cycle, and resistive forces determined by the strength of boundary materials. A more comprehensive parameterisation of the factors controlling critical shear stress along the creek margins may enable more satisfactory results to be obtained *throughout* the network.

7.4 SUMMARY OF KEY FINDINGS

Key findings from the preceding evaluation of the models of optimal angular geometry and equilibrium cross-sectional adjustment, are summarised as follows:

- For the model of optimal angular geometry, it was necessary to exclude ~50% of junctions within the Brancaster network from analysis, because of the strict selection criteria that must be satisfied. A review of the decision rules and methodological

procedures employed in the measurement of branching angles is required, to promote wider applicability of the model.

- Non-ebb aligned junctions are fairly common within the Brancaster network. Since these do not conform to the general requirements of the optimality model, they could not be accommodated within the evaluation. Discordant alignments are most common where source reaches adjoin master channels, suggesting that optimal behaviour is concentrated within the principal channels formed during the initial phase of creek development, rather than subsidiary reaches which were added later through network elaboration.

- As in fluvial systems, the major branching angle in tidal formations is on average closely aligned with the axial prolongation of the receiving stream. Minor branching angles are typically 10-20° wider than those of rivers studied by Roy (1985). This may reflect the dominance of asymmetrical confluences in tidal networks, together with the sequential manner in which the principal creeks and secondary tributaries are established. Junction angles are generally obtuse in tidal networks, but acute in their fluvial counterparts.

- The optimal model of angular geometry has a reasonable capacity to predict θ_1 and ψ, explaining 11-18% of the variance in recorded angles. The model is less successful in the case of θ_2, predicting <1% of the observed variation.

- Downstream hydraulic geometry exponents **m** and **z** are readily computed from high resolution lidar altimetry. While exponents are traditionally calculated using Q as the independent variable, geometric surrogates including P_{TM} and A provide a reasonable substitute, and are far easier to measure. However, topological proxies such as link frequency should not be used.

- The selected network at Brancaster Marsh exhibits discontinuous downstream variations in velocity. While active morphological change in the headwaters appears to be responsible for a rapid increase in velocity, the value of **m** ~ 0.1 recorded in central/lower sectors is more consistent with morphological stability.

- Angular geometry of the Brancaster network may simultaneously minimise several cost criteria. Minimum power loss, minimum resisting force and minimum total flow

resistance are the most likely candidates. Minimisation of channel volume is unlikely to be an important factor. The results agree with those obtained for fluvial networks by Roy (1985).

- The minimum power loss principle is consistent with a stable network that performs both drainage *and* dissipative functions. The branching structure at Brancaster Marsh may be regarded as both a morphological response to drainage of the ebbing tide from the marsh, and as a morphological device that effectively dissipates incident tidal energy.

- The Manning-Stricker equation provides a simple basis for modelling the equilibrium cross-sectional geometry of tidal channel networks, in terms of the balance defined by the critical shear stress between motive forces, represented by peak ebb tidal discharge, and effects resisting the entrainment of bed material.

- Novel techniques involved in the integration of remotely sensed imagery and field-based measurements are introduced. The availability of high resolution airborne lidar altimetry enables a hypsometric approach to be successfully employed in the calculation of peak discharge readings for stations throughout the upper, central and lower reaches of the network.

- The physically-based mechanism of stability shear stress provides a reasonable upper bound on the cross-sectional capacity of tidal channels. There is a systematic departure between predicted and observed results along the course of the Brancaster network. The model under-predicts channel capacity in actively developing headwater reaches, which exhibit a rapid acceleration in downstream velocity. Over-prediction of channel capacity in the central and lower reaches appears to be due to extraneous factors, which enhance critical shear stress levels at the creek margin.

- To improve the predictive capability of the stability shear stress model, a more accurate representation is required of the balance between motive and resistive forces, and also the processes involved in channel deformation. Nevertheless, stability shear stress provides a useful starting point for a more deterministic approach towards modelling the association between morphologically active forces arising during ebb tidal drainage and cross-sectional geometry.

8. DISCUSSION

8.1 EVALUATION OF SALTMARSH CHANNEL NETWORK MORPHOLOGY AND FUNCTION

The initial section of this two-part discussion revisits the first three thesis objectives, as outlined by the logistical framework diagram (Figure 2.1). These are:

- To characterise the morphology of saltmarsh channel networks
- To demonstrate how physical environmental controls relate to natural variability in saltmarsh channel network morphology
- To investigate relations between saltmarsh channel network morphology and function.

The evaluation of previous research on channel network geomorphology (Chapter 1), revealed a marked absence of comprehensive studies detailing the morphological characteristics of saltmarsh channel networks that have developed on the marine sedimentary shores of Britain. Although prevalent in the literature, process studies have tended to adopt an 'intensive' methodological approach, focusing on the characteristics of a particular cross-section or channel reach at a selected study locality, usually without considering the characteristics of the network as a whole, or placing the site-specific results within a broader regional or national context. In order to address these shortcomings, an 'extensive' mode of research (Sayer, 1992) was implemented, with emphasis placed on network-, rather than reach-scale characteristics, of a geographically diverse sample of saltmarshes from the coastlines of England and Wales. Considering the somewhat limited population of saltmarshes exhibiting a form of channel development (Pye and French, 1993), the subset of 30 networks represents a reasonable *large-N* sample. However, the decision to concentrate on commonplace branching systems, rather than the infrequent, localised class of anastomosing networks (typical, for example, of parts of the Blackwater Estuary in Essex), means that the latter remain largely undocumented.

Examination of the literature also suggested a fundamental lack of coherence between the methodological constructs in place for planimetric, longitudinal and cross-sectional characterisation. In the case of network planimetry, descriptive analysis has already been undertaken, and a number of morphometric descriptors translated from a fluvial to a tidal context. In contrast with the relative abundance of information on

planimetric adjustment, techniques involved in measuring cross-sectional and longitudinal features are less widely documented. Following the comparative evaluation of the merits and limitations of potential methods of characterisation from a wide range of fluvial and estuarine sources (Chapter 2), the data acquisition strategies employed in Chapters 3-5 provide a useful conceptual framework and methodological template for expressing patterns of behaviour exhibited by all three planes of morphological adjustment.

While field-based observation and survey are widely documented as primary data sources, the present study highlights the additional value of remotely sensed imagery in constructing an empirical morphological database. Without the overview provided by high resolution aerial photography, the acquisition of detailed planimetric data for such a large number of sites could not feasibly have been undertaken in the available time frame. With the advent of high resolution lidar altimetry, the amount of time and effort expended in obtaining cross-sectional and longitudinal measurements could be equally reduced. Lidar data has also proved its worth in the derivation of peak discharge readings via the implementation of a hypsometric model. The absence of detailed terrain data for the majority of saltmarsh localities around Britain precludes the accurate measurement of tidal prism. As shown in Chapter 6, the best alternative for P_{TM} that could otherwise be obtained given the data available, suffers from a lack of physical realism. To facilitate further modelling exercises that require prism or discharge terms, there is clear support for the more widespread acquisition of lidar coverage at saltmarsh localities around the British Isles.

Several other methodological issues, arising from the characterisation phase of the extensive analysis, deserve mentioning at this stage. First, the value of nominal descriptions is apparent where higher order measures are unavailable or inappropriate, and as a means of distinguishing subtle modes of adjustment that might be overlooked by statistical generalisation. Despite the increasing tendency to rely on quantitative methods, there are clear grounds for the continued implementation of descriptive techniques in geomorphological research. Second, the translation of area-based descriptors such as D and F to a tidal context is fraught with difficulties. In fluvial systems, the drainage basin comprises a fundamental measurement unit, and its boundary is readily defined by topography. Given the comparatively subdued terrain that is characteristic of saltmarsh environments, the delineation of an equivalent boundary poses both conceptual and pragmatic challenges. Although the persistence of drainage lines suggests that discrete flow pathways persist across marsh surfaces, measuring the area contributing flow to a

particular creek is problematic. While technological advances, such as the remote sensing of water surface gradients (using, for example, lidar altimetry), or dye tracing (see Leonard, 1997) may yield future insights, manual delineation of a boundary based on some type of equidistant decision rule is presently the only option. Third, the appropriateness of network-wide expressions for longitudinal and cross-sectional behaviour is called into question by the natural heterogeneity observed in the sample formations. Despite claims elsewhere in the literature that natural channels conform to a particular manner of adjustment, such as an exponential downstream change in width and depth (Wright *et al.,* 1973; Pethick, 1992), this is not always the case in the creeks analysed here. Since the exponential model cannot be reliably employed at all localities, an average measure focusing on the lower sector of each network provides a reasonable alternative. The susceptibility of conventional indices such as drainage density to scale dependence, also warrants the introduction of a new, scale-free expression *%C*. Together, these indices provide an improved basis for the comparative analysis of network-wide responses.

The theoretical distinguishing power of various morphometric descriptors has received some attention in the literature, with the most comprehensive study of data redundancy made by Gardiner (1978). Despite the assertion by Ichoku and Chorowicz (1994) that measures such as *D* and *F* are conceptually irreducible, these indices are essentially interchangeable for saltmarsh channel networks of the scale and complexity observed in the present study. Practical findings enable a subset of 'optimal' descriptors to be defined as *D*, *%C*, *L*, $L_{EXT/INT}$, *S*, G_N, *I*, w/d_L, A_{SL}, with *F*, L_{EXT} and L_{INT} simply mirroring their results. These measures provide a sound theoretical and practical basis for further exercises involving the morphometric characterisation of tidal creeks.

Considerable variation in the magnitude of responses exhibited by the extensive sample of networks for the above measures, points towards a multiplicity of external controls on morphological adjustment. Since previous observations concerning the nature of this interaction have been largely of a speculative nature (see, for example, Steers, 1977; Adam, 1990), the second objective of this thesis involves the formal testing of associations between morphometric and environmental variables, by rigorous statistical methods. The potential envelope of physical influences that emerged during the initial evaluation (Chapter 1) is usefully simplified into a number of classes through the construction of a conceptual model (Figure 2.8). Within the categories of: tidal forcing; erodibility; gradient effects; and miscellaneous considerations, certain measures are

difficult to parameterise. Limited data availability precludes the use of surge factor, flood:ebb duration asymmetry and soil moisture content. Since both the history of development and impact of human intervention are difficult to express in quantitative terms, causal associations are identified by subjective recognition, rather than statistical association. In consequence, apparent relations between the occurrence of: (1) relic steps above the creek margin and modifications to the tidal prism due to reclamation or training of the main tidal waterway; and (2) re-curved headwater reaches and 'coastal squeeze' arising from the construction of an embankment at the rear of the marsh, have yet to be formally established.

Signs of intervention are widespread throughout the sites studied (see also Nordstrom and Roman, 1996), the implication being that comparatively few saltmarshes around the coast of England and Wales have developed under entirely natural conditions. In many instances, creek formations accommodate changes in the local boundary conditions through land reclamation, dredging, or training of the adjoining waterway, without obvious signs of degradation. Nevertheless, factors responsible for the undesirable over-widening and internal degradation of networks, such as those in the River Orwell, require further investigation. The fate of these marshes clearly depends on mitigating such detrimental effects. Unless identified and counteracted, they could potentially limit the success of future saltmarsh restoration schemes.

A combination of bivariate and multivariate techniques are effectively employed in assessing the extent to which environmental controls account for natural variability in the morphometric descriptors. The positive association between tidal prism and cross-sectional geometry dominates bivariate relations. Not only does this finding indicate that the association observed in other tidal inlets (Hume, 1991) and estuarine channels (Wright *et al.*, 1973) can be extended to saltmarsh creeks, it further suggests that morphological adjustment may be driven by the conveyance function performed during over-marsh tides. This feedback mechanism has hitherto been implied by process studies (French and Stoddart, 1992), and observed in natural channel systems (see Jacobson, 1988; Knighton *et al.*, 1992; and Allen, 1997). Despite a considerable margin of uncertainty surrounding the calculation of P_P, such a strong association clearly warrants further investigation. Considerable scatter between the remaining associations of statistical significance reflects the complex nature of channel network development, in addition to the randomness inherent in all natural systems. A degree of scatter is also likely to arise because formations in the Duddon Estuary, the River Leven, the River Ribble, at Burry Inlet and at

Holbeach, The Wash, appear to be only partly adjusted to contemporary environmental conditions. The assumption made at the outset, that the sample formations are in a stable state of adjustment with external influences, is challenged in these cases by the presence of diagnostic indicators, such as relic steps and infilled headwater reaches. The value of traditional field-based observation as a component of geomorphological investigations is once again evident, since effects such as these could otherwise pass unnoticed.

Multivariate analysis suggests that the respective sets of statistically significant environmental controls account for a high proportion of variability in D, L and G_N. However, a poor performance for the various sinuosity measures may reflect the inappropriate translation of these indices from a fluvial to a tidal context. Although the extensive methodological approach is valuable as a means identifying relations of connection between morphological characteristics and physical controls, it is limited in terms of the level of explanation that can be achieved. Useful initial insights, such as those previously described, underpin the empirical models that are a foundation of further work. However, the transition from 'black-box' empiricism (Kirkby *et al.*, 1987) towards a more theoretically-informed and physically-based approach clearly necessitates a shift in emphasis towards intensive methodological procedures. In this manner, process-form interactions are explored in greater detail, through a single illustrative case study.

The choice of Brancaster Marsh as a case study in part reflects its seemingly stable adjustment to contemporary environmental controls, its near-natural state (in the absence of obvious human intervention through reclamation or dredging of the adjoining waterway), and also the availability of high quality terrain data. Airborne lidar coverage of this site supports the implementation of methodological techniques that would not otherwise be possible. While details are provided of the techniques employed in the measurement of upstream tidal prism according to the hypsometric model developed by Boon (1975) and Pethick (1980), lidar cover is also shown to provide cross-sectional data for the upper, central and lower reaches of the system. The spatial resolution of 2m precludes its similar application in the narrow headwaters, a limitation that could be overcome by reducing the altitude at which data is flown, or by increasing the sampling frequency.

Having gone some way towards establishing the morphological characteristics of tidal creeks and their relations with broad-scale physical environmental influences, the third objective of this thesis seeks to further investigate relations between channel network morphology and function. While the drainage function of saltmarsh creeks is

alluded to in the literature through the marked resemblance between fluvial and tidal networks, another function involving tidal energy dissipation during the flood phase of the tidal cycle (Pethick, 1992) is also cited as an important factor. Competition between these theories has resulted in a degree of confusion (see, for example, Toft *et al.*, 1994; Coates *et al.*, 1995) as to the principal function controlling network morphology. In order to resolve these differences in emphasis, two models are developed in Chapter 7. The results yield new insights into the manifestation of physical function within the branching characteristics and cross-sectional geometry of tidal creeks.

The theoretical model of optimal angular geometry retains a network-wide scale of analysis that few others have adopted in a tidal context, and is often absent at the more detailed level that is synonymous with an intensive methodological approach. It is noteworthy that this scale of analysis is particularly relevant to restoration schemes, which over and above the behaviour of individual reaches, are concerned with functions performed by the system as a whole. Interestingly, only a subset of junctions at the Brancaster network satisfy the basic criterion of ebb alignment, which is a prerequisite for inclusion in the optimality model. In the majority of those rejected, a source channel adjoins a much larger creek. The discordant adjustment between these links points towards the sequential nature of network initiation and elaboration at Brancaster Marsh. During the early stages of channel initiation, ebb alignment appears to result from the efficiency achieved through flow convergence across a gradually sloping, yet topographically homogenous surface. However, it may be envisaged that other factors, such as surface micro-topography, take precedence in later stages of network elaboration and extension, so that new tributaries adopt a variety of orientations. Since the principal creeks tend to retain their original alignment, the network has a dendritic appearance, despite the irregular nature of subsidiary creeks. It is reasonable to hypothesise that a comparable mode of adjustment operates in other tidal systems, although this of course requires further investigation.

Correspondence between the angular properties of the Brancaster network and fluvial systems documented by Roy (1985), points towards a degree of similarity in the functions performed. While the sedimentation function of tidal creeks is addressed elsewhere in the literature (Steers, 1959; Pestrong, 1970, 1972; Kestner, 1979; Letzsch and Frey, 1979; Hartnall, 1984; Stoddart *et al.*, 1989; French and Spencer, 1993; French *et al.*, 1995; Esselink *et al.*, 1998; Reed *et al.*, 1999), drainage and dissipative functions have, as noted previously, remained a subject of some debate. The difference in emphasis

between: (1) results obtained from process studies, in which channel morphology is typically dominated by formative processes during the ebb phase of the tidal cycle; and (2) the representation of creeks by Pethick (1992) as a morphological device to dissipate tidal energy, is largely reconciled by the finding that their branching geometry satisfies a cost criterion of minimum power loss. While this principle is synonymous with adjustment to perform a drainage function, such as that observed in fluvial networks, the state of relative stability that appears to have been attained in the central and lower reaches of the Brancaster formation suggests that a dissipative function is also being performed. As such, tidal creeks that are in a stable state of adjustment can be regarded as both a morphological outcome of ebb tidal drainage, and as a morphological device, that effectively dissipates tidal energy. The apparent difference in emphasis is therefore largely a result of a conflation of the physical function performed by tidal creeks and the processes by which they are formed.

While the tendency towards a condition of minimum power loss appears to influence the angular geometry of the Brancaster network, other principles involving minimising the resisting force and the total flow resistance cannot be ruled out. On the basis of the present results, it seems likely that the network may simultaneously satisfy several cost criteria. However, the morphological signature of these functions defies a more indepth interpretation until the limit of the literature is extended.

The potential utility of Friedrichs' (1995) model of equilibrium cross-sectional geometry, applied here to the Brancaster network, is apparent from the use of empirical relations between tidal prism and cross-sectional area for inlet design (Hume, 1991) and their implementation by Coates *et al.* (1995) as a basis for restoration guidelines in the U.S.. Although the model originally focused on a limited number of reach-scale adjustments in an extensive sample of systems, it is extended in the present study to consider adjustment at stations throughout the sample network. Results indicate that stability shear stress provides a useful conceptualisation of the adjustment process, which yields reasonable predictions of cross-sectional capacity given a knowledge of peak discharges and the sedimentary composition of the channel boundary. Its performance in the upper reaches of the system was limited, as morphological adjustment is currently proceeding through network elaboration and extension. In the lower reaches, flow losses across the front edge of the marsh, together with the higher strength and critical shear stresses at the creek margins, appear to be responsible for the mismatch between observed and predicted geometries. Although the model requires improved parameterisation of

downstream variations in the stage-time curve and the balance between motive and resistive forces, the stability shear stress criterion could be used to generate a first approximation for the cross-sectional capacity required to serve a given area of marsh. As a potential basis for restoration schemes, the model usefully accommodates variability in factors such as boundary composition, which as shown in Chapter 6 impart a degree of freedom in explaining channel bed gradient. It also enables variations in tidal range to be accounted for through their influence over prism. However, any improvement in the predictive capability of the stability shear stress model is not to be expected until improved predictions become available for peak discharge at stations throughout the network. Effectively, this demands the application of a full hydrodynamic model, in order to more accurately represent the unsteady flows that are characteristic of tidal creeks.

Returning to the general aim of this thesis, the preceding discussion demonstrates a number of key areas in which the scientific understanding of saltmarsh channel network morphology and function has been extended. While the inventory of morphological characteristics, which was generated using an innovative research design and novel techniques of data acquisition, provides the framework for establishing important relations of connection with key environmental controls, it also represents a database of unprecedented extent that will inform future research in this field. Furthermore, the models of optimal angular geometry and equilibrium cross-sectional adjustment have been shown to provide potentially useful theoretical bases for investigating the morphological manifestation of physical functions within a given tidal network. Both of these approaches may prove to be of practical value, as one of several bases for channel network design, within saltmarsh restoration and flood defence realignment projects.

8.2 IMPLICATIONS FOR SALTMARSH RESTORATION

In addition to academic interest in the morphology and function of saltmarsh channel networks, knowledge of their behaviour is also important for habitat restoration (Williams and Harvey, 1983; Haltiner and Williams, 1987; Landin, 1993; Williams and Florsheim, 1994; Coates *et al.*, 1995; Johnson, 1996; Reed *et al.*, 1999), and for the successful implementation of flood defence realignment schemes (Leggett and Dixon, 1994; Burd, 1995; Dixon and Weight, 1996; French, 1996; French, 1997; Dixon *et al.*, 1998).

Present in > 90% of saltmarsh localities around the coast of Britain, creeks provide the transportation network for tidal flows conveying sediment to the marsh platform, and as demonstrated in Chapter 7, perform important drainage and dissipative

functions. In accordance with these key physical functions, the introduction of a creek system as an element of marsh restoration projects is seen to be of fundamental importance by a number of authors (see Coates *et al.,* 1995; French, 1996; Haltiner *et al.,* 1997; Reed *et al.,* 1999). However, it is further recognised that the establishment of a fully functional channel network is by no means an inevitability (Haltiner and Williams, 1987; Haltiner *et al.,* 1997). The correct balance between erosive and resistive forces has first to be attained, and if left to natural processes, creek formation may even then take a considerable amount of time. It is widely accepted that an element of design can hasten network development (Williams and Florsheim, 1994), and thereby marsh creation (Beeftink, 1977). However, the appropriate engineering foundations for this are by no means well established. Previous recommendations range from the reactivation of former creek systems that were infilled during reclamation (Burd, 1995; French, 1997), to empirical guidelines for planimetric and cross-sectional construction (see, for example, Coates *et al.* 1995) based on a neighbouring 'guidance marsh' (Zeff, 1999).

The insights into channel network morphology and function obtained from the present study, are of potential value in improving theoretical basis for the interpretation and design of creeks as part of restoration schemes in the U.K.. In recognition, the implications of the results obtained, for the engineering of functional channel systems within restored marshes, is stated as a fourth and final objective of this thesis (see Section 1.6). It is straight forward to envisage how findings from the extensive phase of the study may be implemented in 'post-project appraisal' (MAFF, 1993; French, 1997), as a means of establishing the degree to which engineered formations conform to patterns of adjustment exhibited by natural systems. Furthermore, the theoretical principles that were shown to be of value in modelling cross-sectional and angular adjustment, may serve as practical guidelines for network construction, by promoting the rapid development of a stable marsh formation, and helping to avoid pitfalls of creek design that could compromise the success of a project. The following discussion addresses each of these applications in greater detail, with reference to realignment projects currently being undertaken at Tollesbury and Abbotts Hall in the Blackwater Estuary, Essex.

8.2.1 Design guidelines

It is widely recognised that the creation of a stable saltmarsh can be accelerated through 'restoration design' (Williams and Florsheim, 1994). While previous studies by Williams and Harvey (1983), Haltiner and Williams (1987), Coates *et al.* (1995), Burd (1995),

Haltiner *et al.* (1997), French (1999) and Zeff (1999) emphasise the value of empirical relations and the use of a 'guidance' marsh, according to French and Reed (2001, p.208) a more robust approach would be '*to define more precisely the important physical functions performed by the corresponding natural system and to generalise from these a set of guidelines for the optimal engineering of desired characteristics*'. Modelling system-wide responses in terms of the theoretical bases outlined in Chapter 7, may go some way towards achieving this goal.

Considering the key physical functions ascribed to saltmarsh creeks, it is vital that guidelines result in a network that satisfies the basic requirements of:

- Drainage – surface drainage is necessary, otherwise a stable marsh system is unlikely to result due to waterlogging and die-back within the marsh interior
- Dissipation - unless tidal energy is effectively dissipated between the mouth of the system and upstream reaches, the network is unlikely to attain a stable state of adjustment, and may experience internal degradation and over-widening
- Sedimentation - without an adequate supply of sediment to the marsh platform the system will be unable to keep pace with sea level rise, resulting in enhanced degradation as the relative inundation frequency increases.

Bearing these requirements in mind, the challenge is to develop a series of recommendations, which can be employed as a guide for designing an operational creek system, as part of a restoration project. The following phase of the discussion introduces a conceptual model for channel design, which is based on the findings of Chapters 3-7. After summarising the components and assumptions of the model, it is applied in a theoretical simulation involving the design of angular and cross-sectional channel network characteristics.

The conceptual model in Figure 8.1 presents a sequence of guidelines for the arrangement and capacity of tidal networks, as part of a saltmarsh restoration scheme. The optimal model of angular geometry is employed, as a theoretical basis for creek alignment, while the physical mechanism of stability shear stress is used to define the cross-sectional area required to serve the upstream tidal prism. While the applicability of these models has already been established through an illustrative case study, it is important to justify their implementation in a more generic sense to localities throughout England and Wales.

The general applicability of optimality criteria, as a basis for angular geometry, is evident from the widespread occurrence of networks exhibiting dendritic behaviour of a

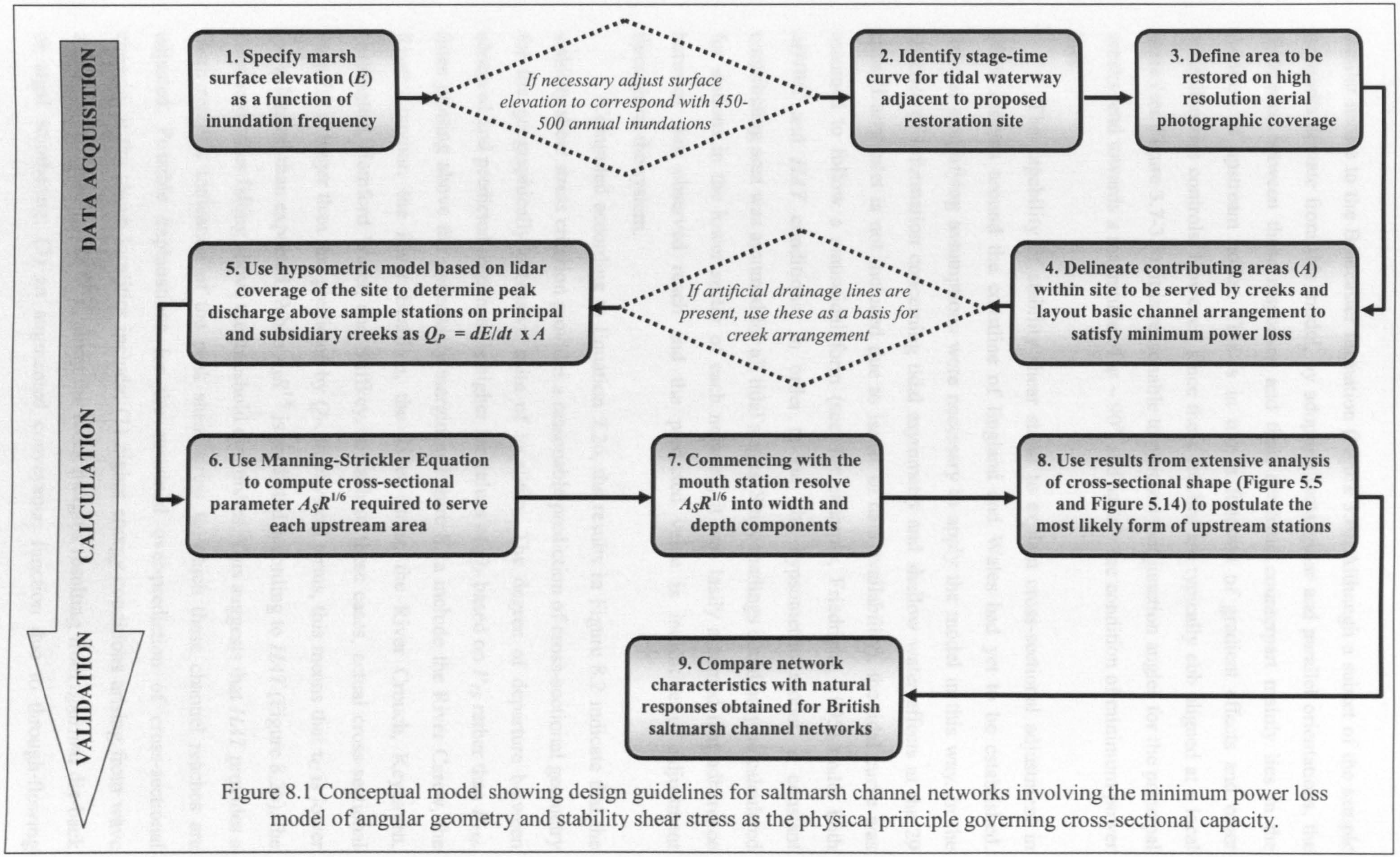

Figure 8.1 Conceptual model showing design guidelines for saltmarsh channel networks involving the minimum power loss model of angular geometry and stability shear stress as the physical principle governing cross-sectional capacity.

similar nature to the Brancaster formation (Figure 3.6). Although a subset of the sample networks deviate from this model, by adopting rectangular and parallel orientations, the difference between these responses and their dendritic counterpart mainly lies in the position of upstream nodes. This is in turn a function of gradient effects and other miscellaneous controls. However, since these reaches are typically ebb aligned at a local scale (see Figure 3.7-3.8), it is reasonable to propose that junction angles for the principal creeks tend towards a magnitude of $\psi \sim 90^{o}$, and satisfy the condition of minimum power loss.

The capability of stability shear stress to explain cross-sectional adjustment in other systems around the coastline of England and Wales had yet to be established. Several simplifying assumptions were necessary to apply the model in this way. In the absence of information concerning tidal asymmetry and shallow water effects at the 29 sites (Burry Inlet is not included due to issues of data availability), the tidal curve was assumed to follow a sinusoidal form (see, for example, Friedrichs, 1995) under both *MHWS* and *HAT* conditions. In order to run the hypsometric model, a constant contributing area was assumed for all tidal stages. Since readings could only be calculated for stations in the lower sector of each network, it was lastly assumed that adherence between this observed reach and the predicted value is indicative of adjustment throughout the system.

Computed according to Equation 7.26, the results in Figure 8.2 indicate that the stability shear stress criterion provides a reasonable prediction of cross-sectional geometry for the geographically extensive suite of localities. The degree of departure between observed and predicted responses is higher for values of Q_P based on P_{TS} rather than P_{TM}. Sites plotting above the uncertainty margin in Figure 8.2a include the River Carew, the River Loughor, the River Beaulieu, the River Stour, the River Crouch, Keyhaven, Lymington, Hamford Water, and Stiffkey. In each of these cases, actual cross-sectional capacity is larger than that predicted by Q_P. In physical terms, this means that τ_C is lower (or τ_P higher) than expected. When $A_S R^{1/6}$ is predicted according to *HAT* (Figure 8.2b), the number of sites falling above the threshold diminishes. This suggests that *HAT* provides a more realistic indication of the peak shear stress to which these channel reaches are adjusted. Possible explanations for the sustained over-prediction of cross-sectional capacity at the above localities include: (1) higher energy conditions arising from wave attack; (2) reduced levels of τ_c along the creek margins resulting from *Spartina* die-back or algal smothering; (3) an augmented conveyance function due to through-flowing

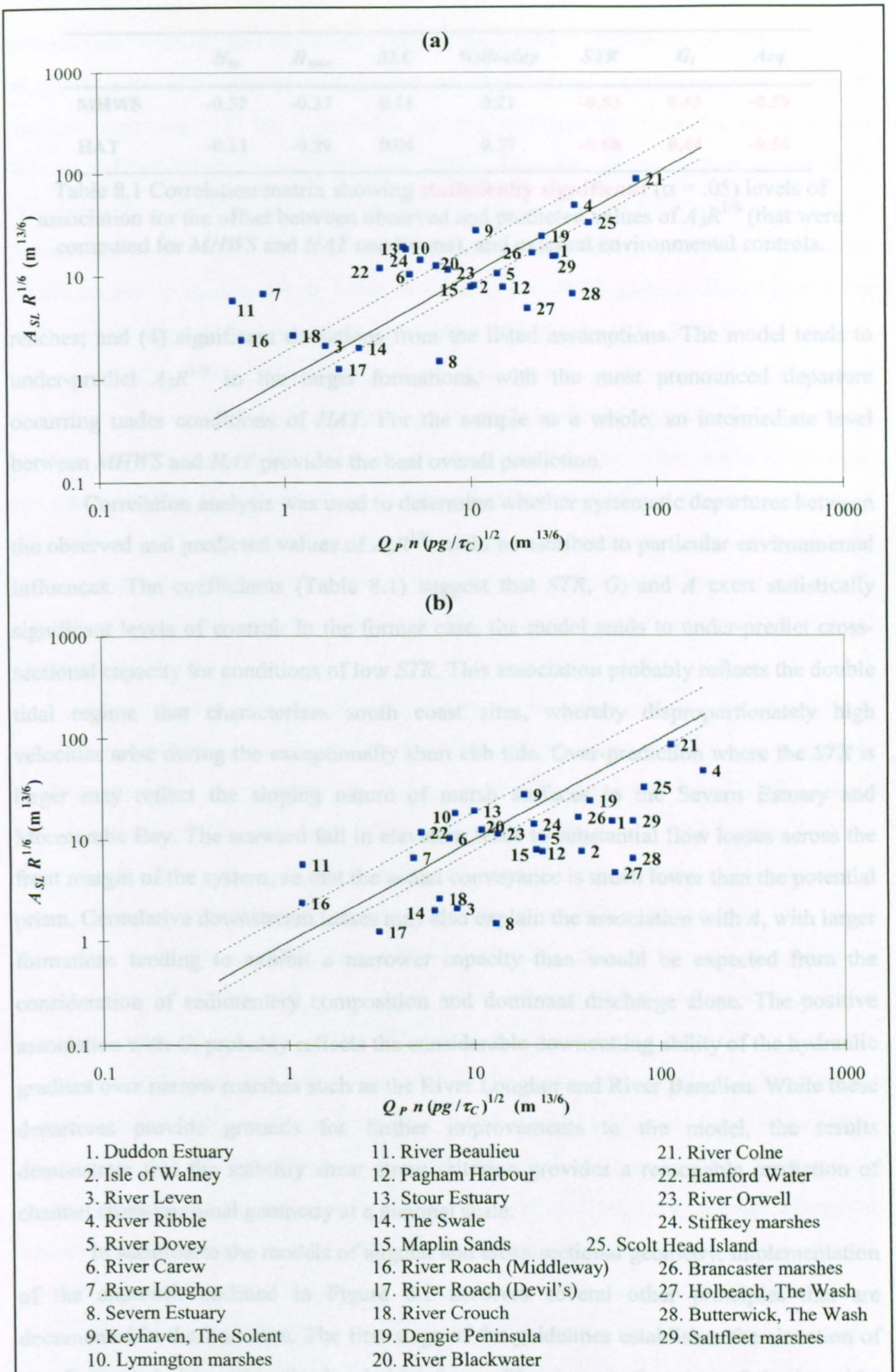

1. Duddon Estuary
2. Isle of Walney
3. River Leven
4. River Ribble
5. River Dovey
6. River Carew
7 .River Loughor
8. Severn Estuary
9. Keyhaven, The Solent
10. Lymington marshes
11. River Beaulieu
12. Pagham Harbour
13. Stour Estuary
14. The Swale
15. Maplin Sands
16. River Roach (Middleway)
17. River Roach (Devil's)
18. River Crouch
19. Dengie Peninsula
20. River Blackwater
21. River Colne
22. Hamford Water
23. River Orwell
24. Stiffkey marshes
25. Scolt Head Island
26. Brancaster marshes
27. Holbeach, The Wash
28. Butterwick, The Wash
29. Saltfleet marshes

Figure 8.2 Performance of the stability shear stress model for the extensive sample of channel networks, with Q_P driven by: (a) *MHWS* and (b) *HAT*.

	H_{sp}	H_{max}	*SLC*	*%silt-clay*	*STR*	G_I	*Aeq*
MHWS	-0.32	-0.37	0.11	0.21	**-0.53**	**0.43**	**-0.50**
HAT	-0.13	-0.29	0.04	0.37	**-0.68**	**0.44**	**-0.54**

Table 8.1 Correlation matrix showing **statistically significant** ($\alpha = .05$) levels of association for the offset between observed and predicted values of $A_S R^{1/6}$ (that were computed for *MHWS* and *HAT* conditions), and external environmental controls.

reaches; and (4) significant deviations from the listed assumptions. The model tends to under-predict $A_S R^{1/6}$ in the larger formations, with the most pronounced departure occurring under conditions of *HAT*. For the sample as a whole, an intermediate level between *MHWS* and *HAT* provides the best overall prediction.

Correlation analysis was used to determine whether systematic departures between the observed and predicted values of $A_S R^{1/6}$ could be ascribed to particular environmental influences. The coefficients (Table 8.1) suggest that *STR*, G_I and *A* exert statistically significant levels of control. In the former case, the model tends to under-predict cross-sectional capacity for conditions of low *STR*. This association probably reflects the double tidal regime that characterises south coast sites, whereby disproportionately high velocities arise during the exceptionally short ebb tide. Over-prediction where the *STR* is larger may reflect the sloping nature of marsh surfaces in the Severn Estuary and Morecambe Bay. The seaward fall in elevation leads to substantial flow losses across the front margin of the system, so that the actual conveyance is much lower than the potential prism. Cumulative downstream losses may also explain the association with *A*, with larger formations tending to exhibit a narrower capacity than would be expected from the consideration of sedimentary composition and dominant discharge alone. The positive association with G_I probably reflects the considerable downcutting ability of the hydraulic gradient over narrow marshes such as the River Loughor and River Beaulieu. While these departures provide grounds for further improvements to the model, the results demonstrate that the stability shear stress criterion provides a reasonable prediction of channel cross-sectional geometry at a national scale.

In addition to the models of angular and cross-sectional geometry, implementation of the approach outlined in Figure 8.2 involves several other principles that are documented in the literature. The first stage of the guidelines establishes the elevation of the designated site within the local tidal frame. The correct elevation of the intertidal surface is deemed pivotal to the success of marsh restoration projects by a number of

authors (see Williams and Florsheim, 1994; French, 1997; Haltiner *et al.*, 1997; Reed *et al.*, 1999), since it determines the frequency and depth of tidal inundation. If the surface is too low, vegetation will fail to establish and the development of a stable marsh system will be delayed (Haltiner and Williams, 1987). However, if the surface is too high, experience from the U.S. cautions that there will be insufficient depth of flow and power to perform erosive work. This in turn will hinder channel elaboration and extension (Williams and Florsheim, 1994). While Haltiner *et al.* (1997) quote an elevation of 0.5m below mean highest high water as an appropriate level for the U.S., Burd (1995) provides a more general statistic of 450-500 annual inundation events as the optimum frequency for mid-marsh species. With respect to tidal datum, this inundation frequency falls between a level of *MHWN* and *MHWS*. Following Amos (1995), the marsh surface elevation corresponding with this condition can be identified by constructing a frequency-stage plot (Figure 8.3a). If the designated surface falls short of this requirement, U.S. schemes rely on the placement of fill to a suitable elevation (see, for example, Coates *et al.*, 1995), rather than natural sedimentation which may delay the colonisation process (Williams and Florsheim, 1994).

In anticipation of data requirements for the hypsometric model (which at present is the best available source of data for Q_P), the second stage of the design procedure involves specifying the stage-time curve associated with 'dominant' flows in the adjacent tidal waterway. In line with the original application of the model (see Section 7.3), the curve should generally correspond with over-marsh tidal conditions. Based on the preceding considerations of inundation frequency, it should more precisely relate to a stage that is intermediate between *MHWS* and *HAT*. For the present simulation, a maximum stage of 3.25m OD is employed, which together with the assumption of a near horizontal intertidal surface at 2.25m OD, results in a hydraulic duty of 1m.

Specifying the layout of channels within the proposed restoration scheme remains a considerable challenge, due to wide and varied number of factors that influence their arrangement in 'natural' formations. Although the minimum power loss models developed by Howard (1990) and Rodriguez-Iturbe *et al.* (1992) may provide a basis for future designs, at present recourse is made to a strategy employed in reclamation schemes bordering the Wadden Sea (see, for example, Steers, 1959; Beeftink, 1977a; Esselink *et al.*, 1998). This approach places emphasis on achieving the necessary functions, rather than replicating the planimetric form of natural creeks. Comprising regularly spaced ditches separated by brushwood groynes (see Figure 1.4), sedimentation fields on the

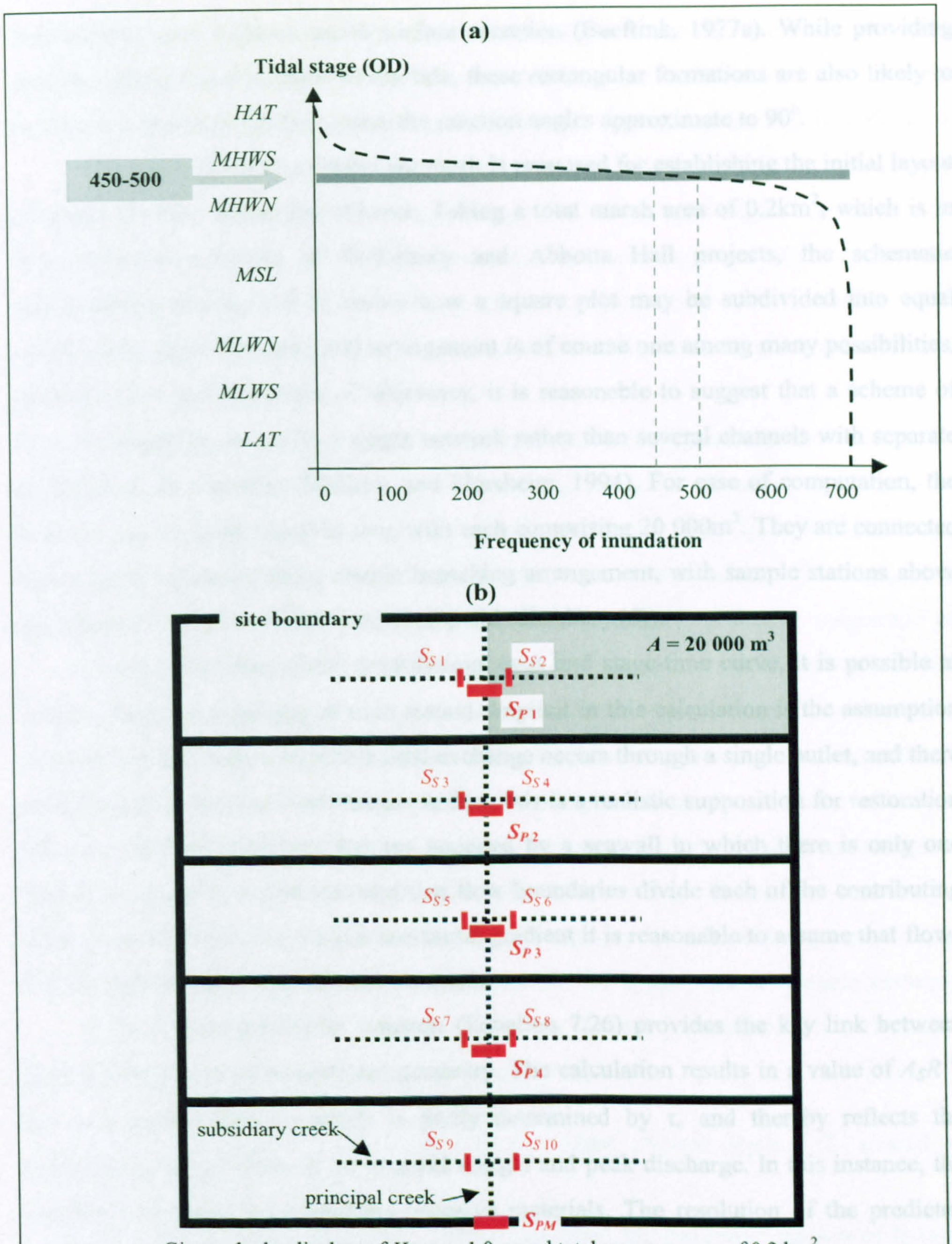

Given a hydraulic duty of $Hmax$ = 1.0 m and total area coverage of 0.2 km^2, when divided into 10 equal contributing areas of 20 000 m^3 ⇒

- Station $P1$ receives 2 x 20 000 x 1 = 40 000 m^3
- Station $P2$ receives 4 x 20 000 x 1 = 80 000 m^3
- Station $P3$ receives 6 x 20 000 x 1 = 120 000 m^3
- Station $P4$ receives 8 x 20 000 x 1 = 160 000 m^3
- Station PM receives 10 x 20 000 x 1 = 200 000 m^3
- Stations $S1$-$S10$ receive 1 x 20 000 x 1 = 20 000 m^3

Figure 8.3 Schematic representation of: (a) the frequency-stage plot enabling marsh surface elevation to be established for an inundation frequency of 450-500 annual events; and (b) the arrangement of contributing areas, principal (S_P) and subsidiary (S_S) creeks, and sample stations in a hypothetical restoration project of similar size to Tollesbury and Abbotts Hall schemes.

Netherlands coast enhance marsh surface accretion (Beeftink, 1977a). While providing drainage during the ebb phase of the tide, these rectangular formations are also likely to perform a dissipative function, since the junction angles approximate to 90°.

On these grounds, a similar approach is proposed for establishing the initial layout of creeks within a restoration scheme. Taking a total marsh area of 0.2km^2, which is in line with the coverage of Tollesbury and Abbotts Hall projects, the schematic representation in Figure 8.3b shows how a square plot may be subdivided into equal contributing areas. The proposed arrangement is of course one among many possibilities, although from considerations of efficiency, it is reasonable to suggest that a scheme of this size should be served by a single network rather than several channels with separate outlets (see, for example, Williams and Florsheim, 1994). For ease of computation, the areas A_1-A_{10} are made equal in size, with each comprising 20 000m^3. They are connected by channels organised into a simple branching arrangement, with sample stations above each junction categorised as principal (S_P) and subsidiary (S_S).

With knowledge of the contributing areas and stage-time curve, it is possible to compute the peak discharge at each station. Implicit in this calculation is the assumption of a semi-closed system, in which tidal exchange occurs through a single outlet, and there are no losses across the front margin. In fact, this is a realistic supposition for restoration schemes such as Tollesbury that are bounded by a seawall in which there is only one breach. Although it is also assumed that flow boundaries divide each of the contributing areas, in the absence of a marked horizontal gradient it is reasonable to assume that flows will initially move towards the nearest creek.

The Manning-Strickler function (Equation 7.26) provides the key link between peak discharge and cross-sectional geometry. The calculation results in a value of $A_S R^{1/6}$ for each sample station, which is partly determined by τ_c and thereby reflects the sedimentary composition of the channel margin and peak discharge. In this instance, the boundary is assumed to comprise cohesive materials. The resolution of the predicted values into width and depth components commences with the seaward station. At the outset, this procedure appears somewhat complicated, because the results involve expressions for both cross-sectional area and hydraulic radius. However, the term $R^{1/6}$ tends towards unity and, for the present solution, is assumed to take this value. During the characterisation of longitudinal adjustment, a number of the networks were seen to be perched high in the intertidal profile, with a principal channel that terminates far from the adjoining tidal waterway. However, examples from the River Loughor, the River

Beaulieu, Scolt Head Island and Brancaster indicate that at the seaward limit of a fully extended marsh system (see also Evans and Collins, 1987), channel floor elevation corresponds with the local base level. As such, depth at the outlet point may be defined as the offset between the marsh surface elevation (E) and base level (E_O). Assuming a rectangular cross-section, width is simply the quotient of area and depth. For the present example, the base level at the outlet is taken as 0m OD, resulting in a depth of 2.25m, and an associated width of w ~25m. Scenarios for prism readings of $10 < P_T < 300\text{m}^3$ x10^3 are depicted in Figure 8.4a, together with various combinations of channel width and depth.

The evaluation of cross-sectional shape (Section 5.3) suggests that the width:depth ratio of tidal creeks falls into distinct morphological categories according to the relative constraint on w and d. Recording a value of $w/d \sim 11$, station S_{PM} (Figure 8.4b) falls into the highest category in Figure 5.14. On grounds of the consistency observed in Figure 5.5, it is expected that stations in the lower reaches will exhibit a similar magnitude of response, while in the central sector $w/d > 5$ and in the upper sector $w/d > 3$. When compared with the theoretical responses (Figure 8.3b), it appears that w/d values of a similar magnitude to 'natural' channel networks result from limited permutations of width and depth. Together with the observation that the longitudinal profile of tidal creeks tends to follow an upwardly concave or linear pattern of descent from the headwaters through to the lower reaches of the network (Figure 4.6), it is this key finding that enables the specification of width and depth components throughout the rest of the system. Taking station S_{P4} as an example, several statements can be made with reasonable certainty concerning the cross-sectional characteristics of the channel required to convey the prism of 160 000m^3 (contributed by 8 upstream areas of 20 000m^3):

1) Given the assumption of a horizontal marsh surface, channel depth at S_{P4} should be less than at the downstream station
2) w/d should fall within the range of values obtained for the lower reaches of natural creeks, which may be similar to, or slightly less than, the value recorded at the downstream station.

Returning to Figure 8.4, these criteria are satisfied by $d \sim 2.0$m and $w \sim 24$m. By following the same guidelines for each station along the principal channel and the adjoining subsidiary reaches, a downstream cross-sectional geometry may be defined for the system as a whole.

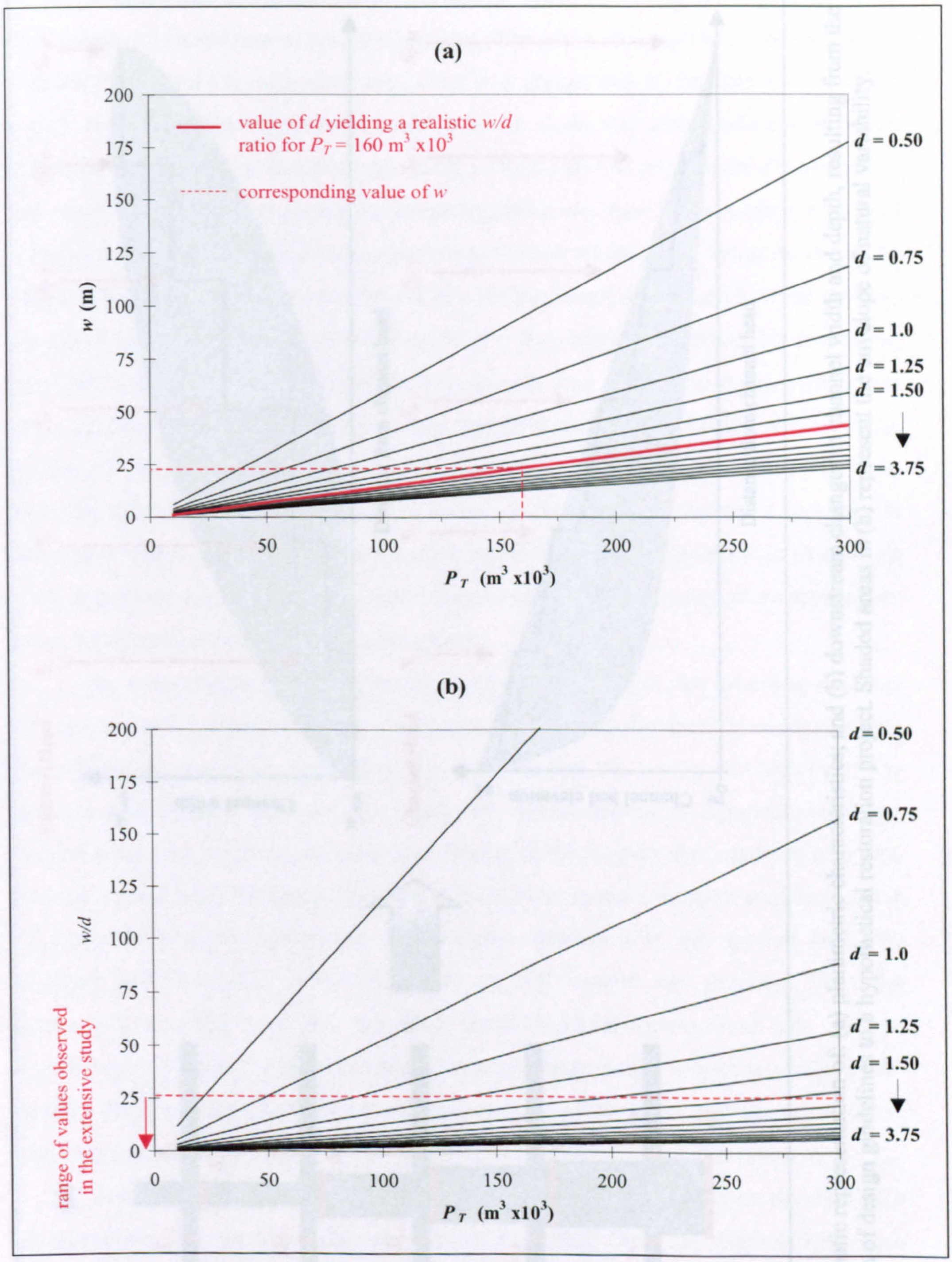

Figure 8.4 Graphical representation of: (a) creek width (*w*); and (b) width:depth ratio (*w/d*), expressed as a function of tidal prism for various scenarios of channel depth (*d*).

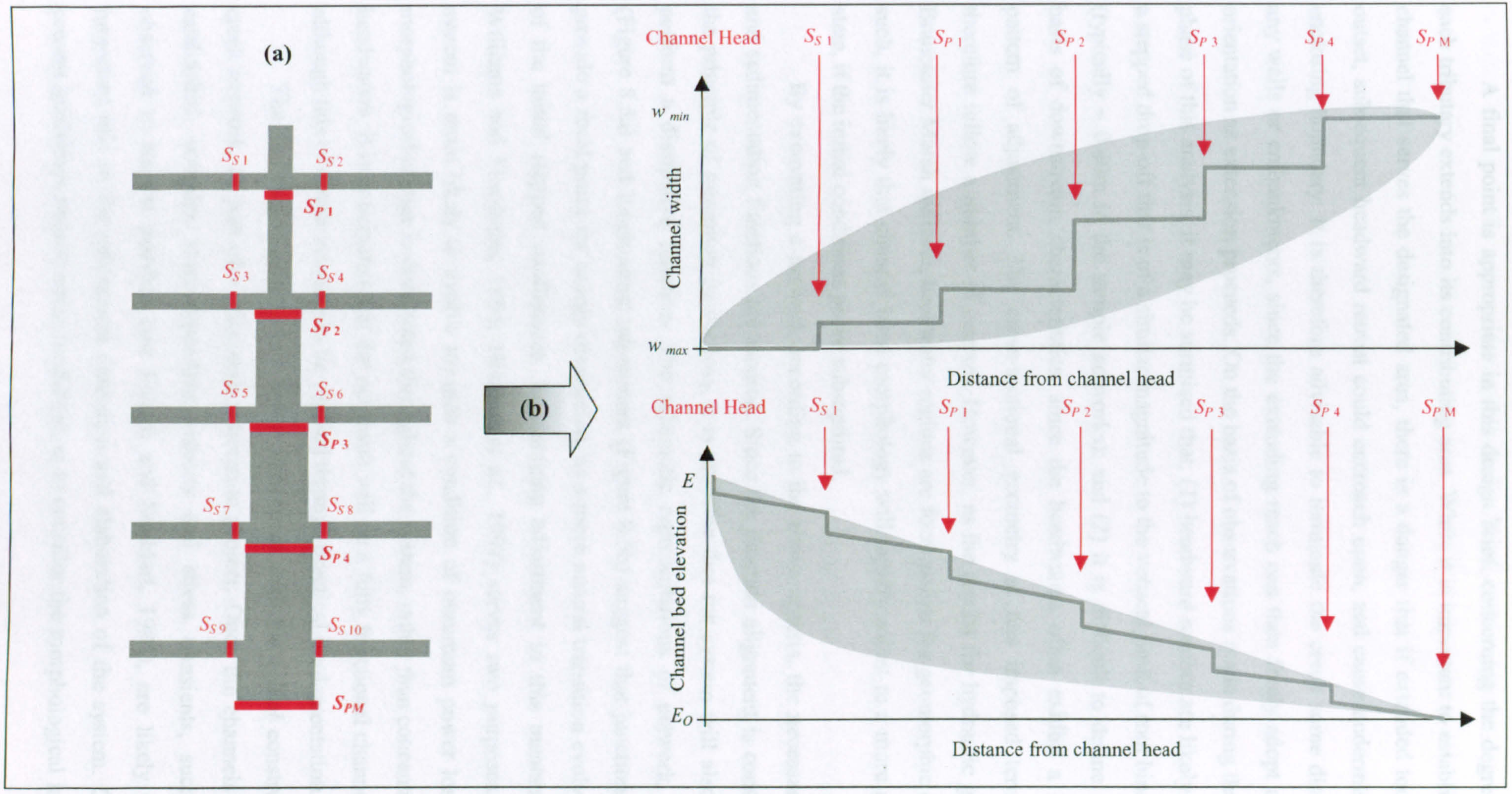

Figure 8.5 Schematic representation of: (a) planimetric characteristics; and (b) downstream changes in channel width and depth, resulting from the application of design guidelines to a hypothetical restoration project. Shaded areas in (b) represent the envelope of natural variability.

A final point is appropriate in this design brief, concerning the degree to which each tributary extends into its contributing area. While it is important to establish a proto-channel that serves the designated area, there is a danger that if extended too far at the outset, subsequent headward retreat could encroach upon, and cause undermining of, an enclosing boundary. It is therefore advisable to terminate the creek some distance from any walls or embankments, since the extending reach can then freely adopt a re-curved orientation as extension proceeds. On the basis of observations made during the extensive phase of this analysis, it may be surmised that: (1) headward reaches are likely to develop a stepped drop-off that is of a similar magnitude to the vertical limit of root binding action (typically ~ 0.40m in the sample networks); and (2) it is difficult to define *w/d* on the basis of downstream characteristics, since the headwaters often exhibit a contrasting pattern of adjustment. The cross-sectional geometry at this imposed terminus may therefore follow a number of courses. However, as the results for hydraulic geometry at Brancaster Marsh indicate, headwater regions are focal points for geomorphic change. As such, it is likely that channel head morphology will rapidly adjust to a more appropriate state, if the initial conditions prove sub-optimal.

By excavating a network according to the above criteria, the necessary drainage and sedimentation functions are assured. Since the junction alignment is consistent with the principle of minimum power loss, it is probable that the system will also evolve to perform a dissipative function. The schematic representations of network planimetry (Figure 8.5a) and longitudinal adjustment (Figure 8.5b) suggest that junctions may also provide a focal point for energy dissipation, as a more natural transition evolves in place of the initial stepped confluences. Encouraging adjustment in this manner (see also Williams and Florsheim, 1994; Haltiner *et al.*, 1997) serves two purposes. First, the system is more likely to evolve towards a condition of minimum power loss. Second, morphological change is distributed throughout the system, rather than concentrated in the headwaters. It is anticipated that the net result will be a fully functional channel network, although this of course remains to be verified through practical implementation.

The model previously described is concerned with the *initial* construction of a creek network, as part of a saltmarsh restoration project. Once the channels have been established, complex stage-dependent velocity and stress transients, such as those observed in natural marshes (see French and Stoddart, 1992), are likely to play an important role in the subsequent extension and elaboration of the system. Clearly, the present guidelines require some modification to consider the morphological implications

of such a change in the geomorphologically active forces. This represents just one of the many aspects of a future research agenda, through which findings from this study may be carried forward.

8.2.2 Post-project appraisal

Following completion, the appraisal of a project is critical to: (1) gauge its performance (Zeff, 1999); (2) improve the design and implementation of future schemes (French, 1997); and (3) avoid pitfalls which may compromise its long-term success (Haltiner *et al.*, 1997). In the context of channel network design as a component of saltmarsh restoration and flood defence realignment in Britain, post-project appraisal more specifically involves drawing a comparison between the morphological characteristics of creeks in restored marshes and natural formations. To illustrate the viability of this approach, the planimetric, cross-sectional and longitudinal characteristics of creeks systems in several recently restored marshes in the Blackwater Estuary are here compared with the envelope of responses obtained for the extensive sample of networks from England and Wales.

The example restoration schemes are located in the Blackwater Estuary, Essex. The first case study involves the inundation of reclaimed marshes at Tollesbury (Hazelden, 1996; Johnson, 1996; MAFF, 1996). Through opening a breach in the seawall, tidal activity was restored in 1995, to a 22 hectare (ha) site. As shown in Plate 8.1a, existing field drainage lines were utilised, by digging a small creek to connect them with the adjoining tidal waterway. The second example is nearby at Abbotts Hall (Dixon *et al.*, 1998), where in 1996 a closely controlled tidal exchange was returned through a pair of sluices to a 20ha tract of arable land. In this instance, the creek system comprises a series of excavated channels (Plate 8.1b), which are connected in a branching arrangement to the outlet points.

Using the optimal morphometric descriptors from Chapter 3-5, it is possible to determine the extent to which these artificial channel networks replicate the form of natural systems, and to propose likely evolutionary trajectories for their subsequent development. This is undertaken in Figure 8.6, using a 3D plot in which each plane of morphological adjustment is represented. $\%C$, w/d_L and G_N are taken to represent planimetric, cross-sectional and longitudinal form in Figure 8.6a. The results indicate that while the equivalent measures for Tollesbury and Abbotts Hall lie within the range of values recorded elsewhere for G_N and w/d_L, $\%C$ is presently below that observed in the 'natural' systems. Such a finding is not unexpected, since the drainage lines (see Plate 8.1)

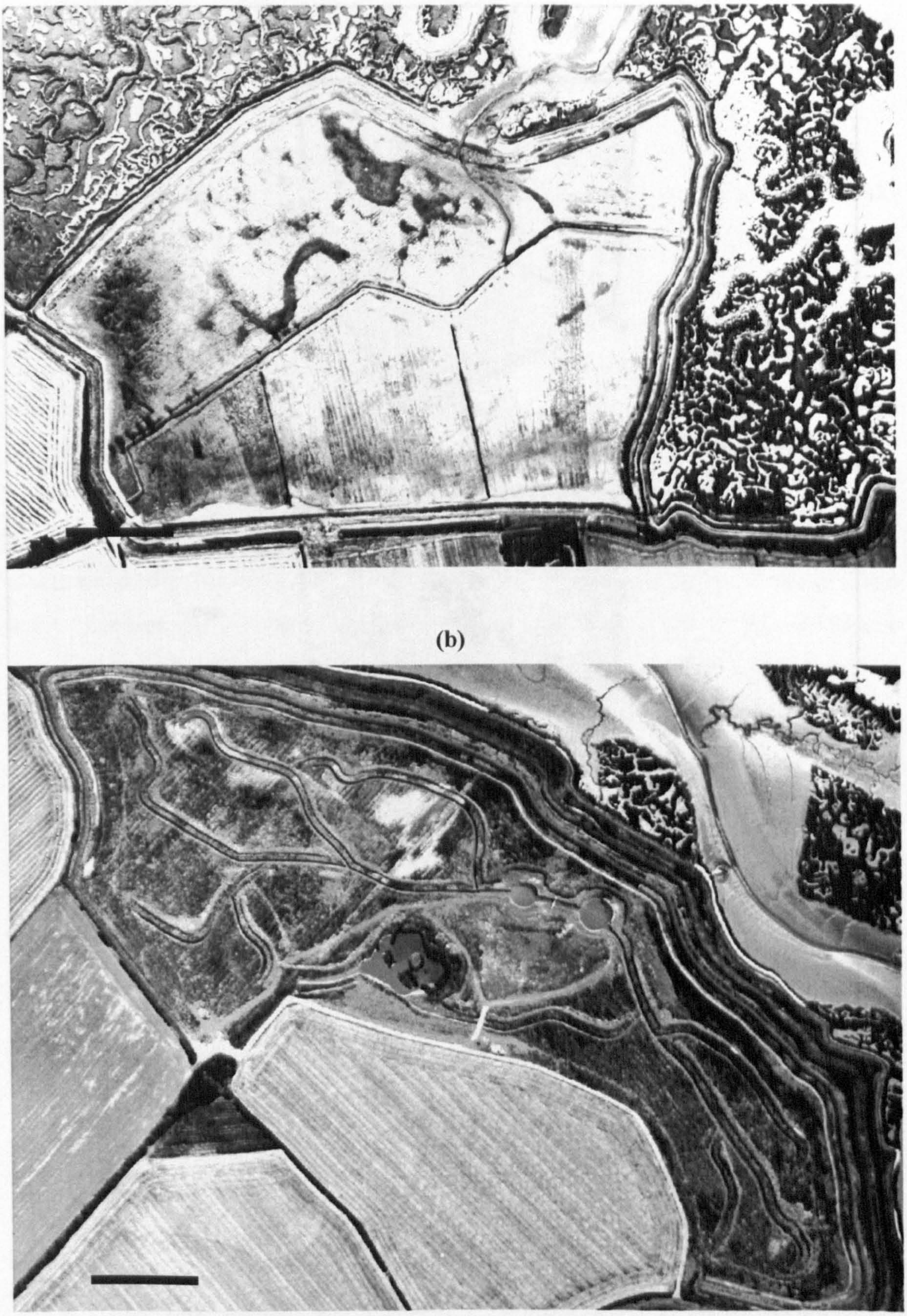

Plate 8.1 High resolution aerial photography showing saltmarsh restoration projects at: (a) Tollesbury; and (b) Abbotts Hall, in the Blackwater Estuary, Essex.
Scale bar represents 100 m.

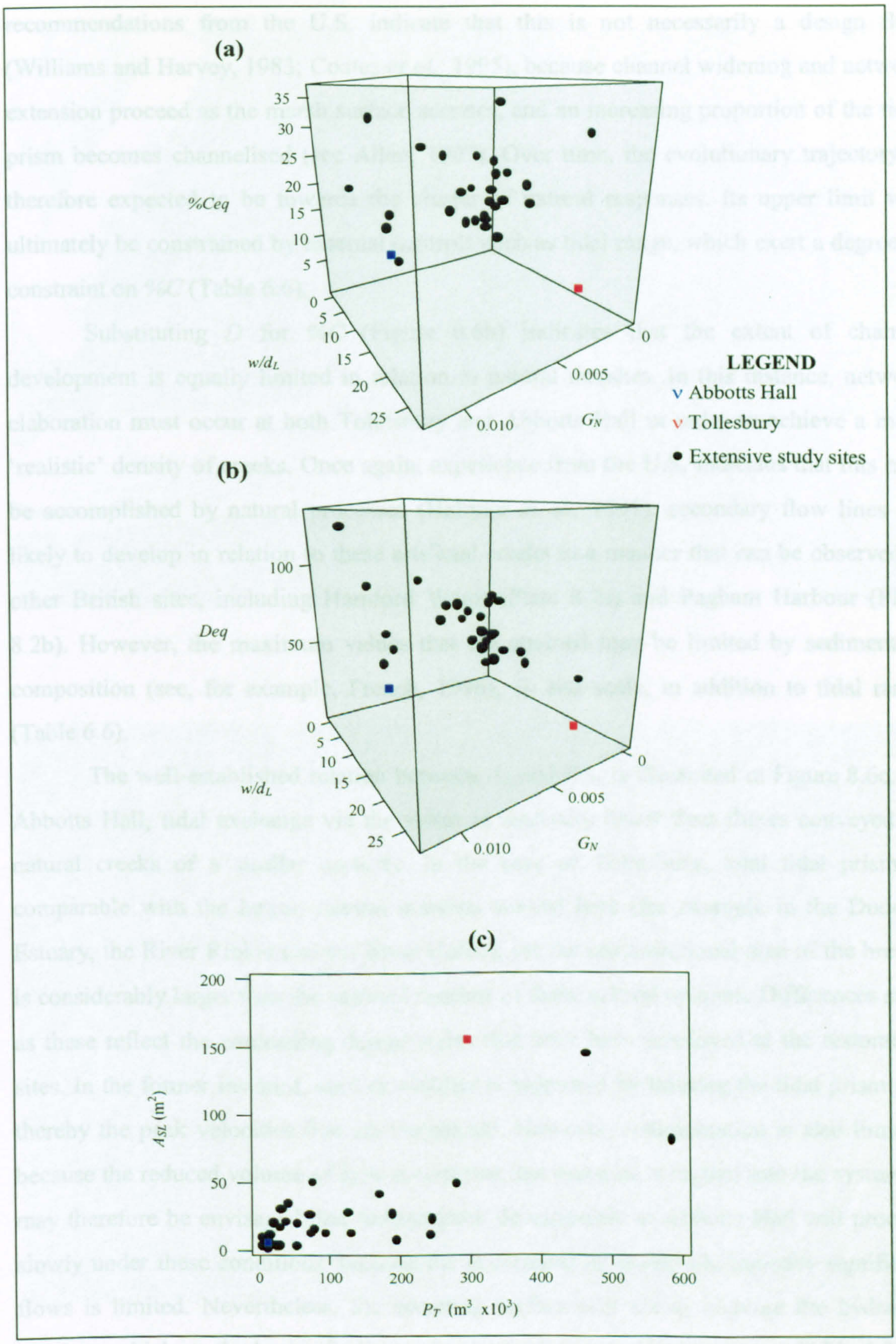

Figure 8.6 Comparison between the morphological characteristics of channel networks observed in saltmarsh restoration schemes at Abbots Hall and Tollesbury in the Blackwater Estuary and results obtained for 29 networks from throughout England and Wales.

are sparse compared with most natural creek systems (see Plate 3.1). However, recommendations from the U.S. indicate that this is not necessarily a design flaw (Williams and Harvey, 1983; Coates *et al.,* 1995), because channel widening and network extension proceed as the marsh surface accretes, and an increasing proportion of the tidal prism becomes channelised (see Allen, 1997). Over time, the evolutionary trajectory is therefore expected to be towards the cluster of natural responses. Its upper limit will ultimately be constrained by external controls such as tidal range, which exert a degree of constraint on *%C* (Table 6.6).

Substituting *D* for *%C* (Figure 8.6b) indicates that the extent of channel development is equally limited in relation to natural marshes. In this instance, network elaboration must occur at both Tollesbury and Abbotts Hall in order to achieve a more 'realistic' density of creeks. Once again, experience from the U.S. indicates that this may be accomplished by natural processes (Haltiner *et al.,* 1997): secondary flow lines are likely to develop in relation to these artificial creeks in a manner that can be observed at other British sites, including Hamford Water (Plate 8.2a) and Pagham Harbour (Plate 8.2b). However, the maximum values that are attained may be limited by sedimentary composition (see, for example, French, 1996), G_I and scale, in addition to tidal range (Table 6.6).

The well-established relation between A_S and P_{TM} is illustrated in Figure 8.6c. At Abbotts Hall, tidal exchange via the sluice is markedly lower than fluxes conveyed by natural creeks of a similar capacity. In the case of Tollesbury, total tidal prism is comparable with the largest natural marshes studied here (for example in the Duddon Estuary, the River Ribble and the River Colne), yet the cross-sectional area of the breach is considerably larger than the seaward reaches of these natural systems. Differences such as these reflect the contrasting design styles that have been employed at the restoration sites. In the former instance, surface stability is promoted by limiting the tidal prism and thereby the peak velocities that are exchanged. However, sedimentation is also limited, because the reduced volume of flow means that less material is carried into the system. It may therefore be envisaged that further creek development at Abbotts Hall will proceed slowly under these conditions, because the occurrence of geomorphologically significant flows is limited. Nevertheless, the accreting surface will act to increase the hydraulic gradient, which on the basis of adjustment observed in natural systems (see Table 4.2), is likely to initiate some headward extension. At Tollesbury, opportunities for geomorphological work are of considerably greater frequency. However, the low mean

(a)

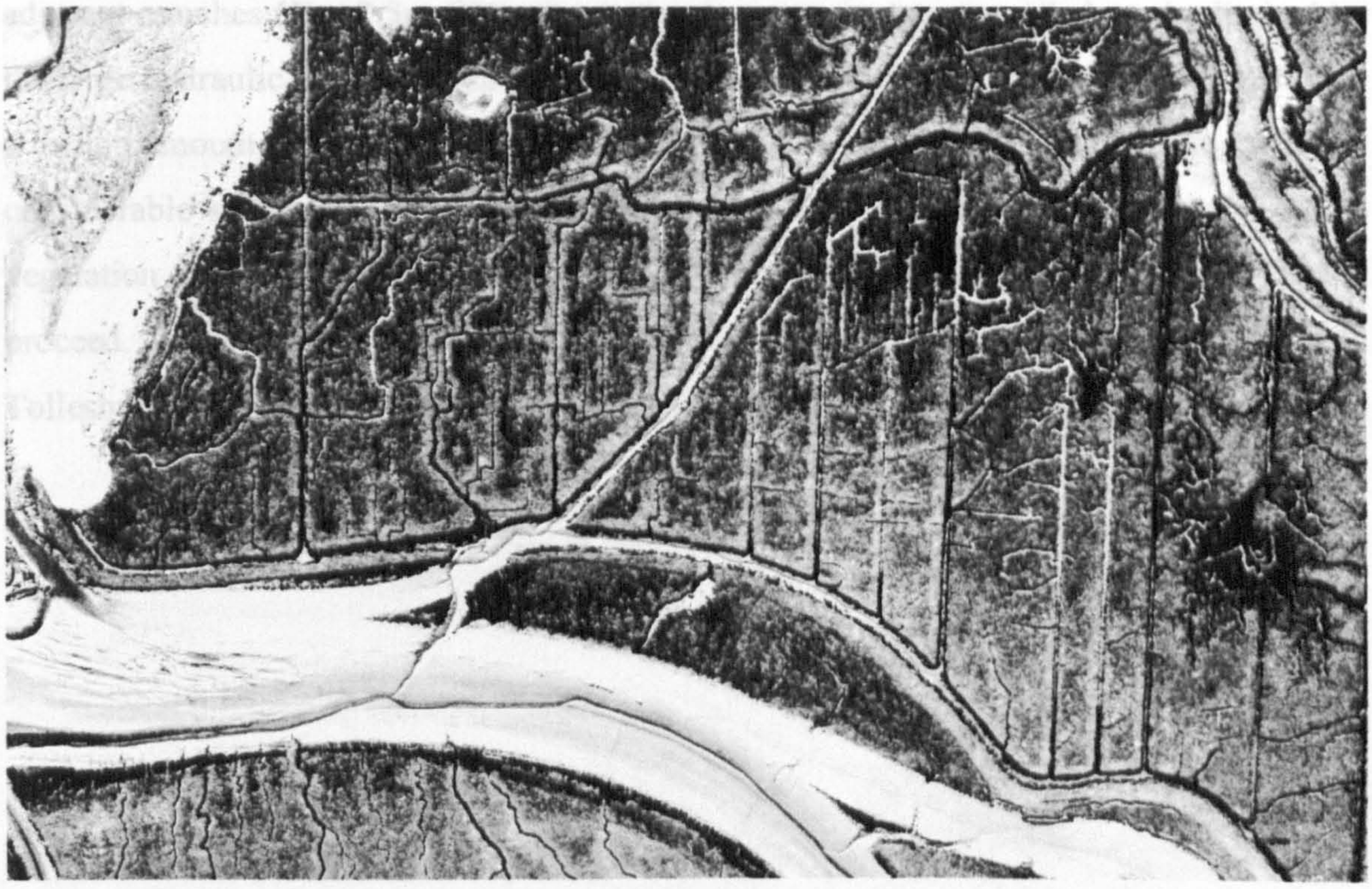

(b)

Plate 8.2 Development of secondary flow lines in relation to artificial 'creeks' comprising drainage lines on former reclaimed land, which has subsequently been restored to saltmarsh at: (a) Hamford Water, Essex; and (b) Pagham Harbour, Sussex.

elevation of the realignment site (E ~ 1.5m OD) is substantially below the level of adjacent marshes (E ~ 2.5m OD). Creek development is therefore likely to be limited by the large hydraulic duty and associated scouring experienced in areas of the site. Although a certain amount of flow convergence is to be expected around topographic irregularities, considerable surface accretion must occur before the system approaches a level where vegetation becomes established. At this point, channel initiation (see Figure 1.7) may proceed. While the formation of a fully functional creek system appears likely at both Tollesbury and Abbotts Hall, their development will clearly take some time.

9. CONCLUSIONS

9.1 SUMMARY OF KEY FINDINGS

1. Branching channel networks within a geographically extensive sample of coastal and estuarine saltmarshes in England and Wales exhibit broad diversity in planimetric, cross-sectional and longitudinal planes of morphological adjustment. Together with nominal descriptors of planimetric arrangement, a set of conceptually irreducible morphometric descriptors comprising: D; $\%C$; $L_{EXT/INT}$; S; G_N; I; w/d_L; and A_{SL}, provide a sound conceptual and practical basis for characterisation at a network-scale.

2. The morphological characteristics of saltmarsh creeks reflect a wide envelope of external environmental controls, relating to: the magnitude and dynamics of tidal forcing; substrate erodibility; and extraneous factors including the history of development and the extent of human intervention. The statistical significance of relations between cross-sectional form and tidal prism, suggest that channel capacity is adjusted to perform a conveyance function. This result agrees with the previous findings of process studies, and mirrors associations exhibited by larger-scale tidal inlets and estuarine systems.

3. Mathematical models involving the optimal branching geometry and equilibrium cross-sectional characteristics of tidal creeks, provide useful theoretical bases for investigating the manifestation of physical function in channel network morphology. An illustrative case study of a Norfolk saltmarsh shows that dendritic branching throughout the principal reaches strongly resembles fluvial networks documented by Roy (1985). In both cases, the networks satisfy a minimum power loss criterion, suggesting that drainage and dissipative functions are concurrently performed. The physical mechanism of stability shear stress yields a reasonable prediction of cross-sectional capacity throughout the case study network. Difference between observed responses and those predicted by a hypsometric model are believed to reflect instability in the upper creeks, and heightened resistance to erosion in the lower reaches of this network. Stability shear stress also yields reasonable predictions when applied to the lower reaches of networks throughout England and Wales.

4. The present study offers insights into creek morphology and function, which are relevant to the field of coastal engineering. The extensive characterisation provides a sound empirical basis for post-project appraisal, while the model of optimal angular geometry and concept of stability shear stress may contribute to the development of more formal guidelines for the design of tidal channel networks.

5. This study has been limited by the lack of high quality terrain data for most of the study sites. The case study has demonstrated the value of airborne altimetry (lidar) data as a means of extracting marsh surface and channel information. Expansion of the existing coverage should greatly assist future work concerned with the interpretation of natural saltmarsh function, and the implementation and appraisal of restoration schemes.

9.2 RECOMMENDATIONS FOR FURTHER RESEARCH

While the present study has clearly improved the scientific understanding of channel network morphology and function, a number of research challenges have emerged, which provide a focus for developing the methodological bases that have been employed, and also extending and applying the key theoretical findings.

The discussion in Chapter 8 provides strong support for the more widespread use of remotely sensed data as a primary source of information concerning channel network morphology. Although national archives of high resolution aerial photography of saltmarsh environments are fairly extensive, the spatial extent of airborne laser altimetry (which is a prerequisite for successful hypsometric modelling, and which affords considerable savings in terms of the time and effort required to extract cross-sectional and longitudinal profile information), is currently limited. Investment in terrain data of this nature would support further insights into important form-process interactions. Taking the elusive flow pathways across the marsh platform as an example, the techniques employed in Chapter 3 rely on subjective decisions, and at best point towards the 'most likely' contributing area. However, through the generation of high quality terrain models it may be envisaged how: (1) knowledge of the micro-topography could facilitate automated feature extraction of contributing areas; (2) an improved appreciation may be gained of the processes of network evolution, as the position of emerging creeks could be identified in the context of local controls. In a more applied context, the widespread availability of lidar data would also provide a secure empirical basis for post-project appraisal, with the

spatially distributed information enabling the detailed monitoring of morphological change, without recourse to labour-intensive and logistically challenging ground survey.

In theoretical terms, a number of fundamental questions concerning the morphology and function of tidal creeks remain only partly answered. First, the present study focuses on saltmarshes from the sedimentary shores of England and Wales. However, given the diversity of environmental conditions within which saltmarshes may develop in a global context (see Figure 1.3), it is important to consider how the present results compare with creeks that have evolved under fundamentally different controls. In this way, it can be established how physical conditions such as a diurnal tidal regime, or a more organic substrate composition, influence channel network morphology.

Second, the focus of the present study on the subset of branching networks, means that the morphological characteristics and functions of other arrangements, such as the anastomosing creeks of the Blackwater Estuary and 'complex' formations dominating the rocky shores of Scotland (Figure 2.3), remain to be addressed. While some of the methodological procedures are readily translated to these contrasting formations, it may be that certain morphometric descriptors are of limited value. This may necessitate the introduction of new indices, which encapsulate distinct aspects of planimetric, cross-sectional and longitudinal adjustment.

Third, the 10% of cases in which Pye and French (1993) record an absence of creeks deserve further consideration. Given the pivotal functions ascribed to tidal networks, it is reasonable to surmise that a lack of channel development is an undesirable scenario. The envelope of environmental conditions should be considered under which channel development is precluded, since the success of saltmarsh restoration schemes could be limited at coastal localities exhibiting these characteristics. Should this assumption prove unfounded, it is equally important to establish how saltmarshes can effectively function without a creek system.

Although the evaluation in Chapter 7 served to establish models of optimal angular and cross-sectional geometry as useful theoretical bases for investigating the morphological manifestation of physical function, there are a number of ways in which the performance and general applicability of these models could be extended. Adherence to the optimality principle by networks exhibiting a range of planimetric arrangements is of interest, since this has only been tested for a single dendritic formation. Furthermore, it would be useful to unpack the morphological consequences of other cost criteria, and the extent to which these are evident in saltmarsh creeks. As Howard (1990) points out,

branching geometry may be adjusted to other cost criteria, candidates for which include minimum shear stress and minimum stream power per unit width. However, it has yet to be established if either of these principles are important in the adjustment process. Further application of the stability shear stress criteria should focus on improving its performance in the headward and lower reaches of formations. This may be achieved through the acquisition of stage-time data at multiple stations along the course of a given network, an improved parameterisation of critical levels of shear stress, and the implementation of a more complete hydrodynamic model for predicting Q_P.

From a practical viewpoint, the appropriateness of optimality models of angular geometry and the concept of stability shear stress, as elements of design guidelines for saltmarsh restoration and flood defence realignment schemes, needs to be tested more fully. Engineered channel networks should also be subjected to more rigorous post-project appraisal, in order to determine the extent to which natural morphological characteristics and functions have been replicated.

REFERENCES

Abrahams, A.D. (1984) Channel networks: a geomorphological perspective, *Water Resources Research* **20**, 161-188.

Abrahams, A.D. and Flint, J.J. (1983) Geological controls on the topological properties of some trellis channel networks, *Geological Society of America Bulletin* **94**, 80-91.

Ackers, P. (1972) River regime: research and application, *Journal of the Institute of Water Engineers* **26**, 257-281

Adam, P. (1978) Geographical variation in British saltmarsh vegetation, *Journal of Ecology* **66**, 339-366.

Adam, P. (1981) The vegetation of British saltmarshes, *New Phytologist* **88**, 143-196.

Adam, P. (1990) *Saltmarsh Ecology*, Cambridge University Press: Cambridge.

Adams, B.J., French, J.R. and Clifford, N.J. (1998) Aerial photography as a source of saltmarsh channel network measurements: An analysis of errors, *Proceedings of the 24th Annual Conference of the Remote Sensing Society*, 695-702.

Adams, C.E., Wells, J.T. and Park, Y. (1990) Internal hydraulics of a sediment-stratified channel flow, *Marine Geology* **95**, 131-145.

Agnese, C., Asaro, F.D., Grossi, G. and Rosso, R. (1996) Scaling properties of topologically random channel networks, *Journal of Hydrology* **187**, 183-193.

Agriculture Select Committee (1998) *Sixth Report: Flood and Coastal Defence, Volume I*, HMSO: London.

Allen, G.P., Salomon, J.P., Bassoullet, P., Du Penhoat, Y and de Gradnpre, C. (1980) Effects of tides on mixing and suspended sediment transport in macrotidal estuaries, *Sedimentary Geology* **26**, 69-90.

Allen, J.R.L. (1985a) Intertidal drainage and mass-movement processes in the Severn Estuary: rills and creeks (pills), *Journal of the Geological Society of London* **142**, 849-861.

Allen, J.R.L (1985b) *Principles of Physical Sedimentology*, George Allen and Unwin: London.

Allen, J.R.L. (1989) Evolution of saltmarsh cliffs in muddy and sandy systems: a qualitative comparison of British west-coast estuaries, *Earth Surface Processes and Landforms* **14**, 85-92.

Allen, J.R.L. (1992) Tidally influenced marshes in the Severn Estuary, southwest Britain, In Allen, J.R.L. and Pye, K. (eds.) *Saltmarshes. Morphodynamics, Conservation and Engineering Significance*, Cambridge University Press: Cambridge, 123-147.

Allen, J.R.L (1997) Simulation models of saltmarsh morphodynamics: some implications for high-intertidal sediment couplets related to sea-level change, *Sedimentary Geology*, **113**, 211-223.

Allen, J.R.L. (2000) Morphodynamics of Holocene salt marshes: a review sketch from the Atlantic and Southern North Sea coasts of Europe, *Quaternary Science Reviews* **19**, 1155-1231.

Allen, J.R.L. and Duffy, J. (1998a) Medium-term sedimentation on high intertidal mudflats and salt marshes in the Severn Estuary, S.W. Britain: the role of wind and tide, *Marine Geology* **150**, 1-27.

Allen, J.R.L. and Duffy, J. (1998b) Temporal and spatial patterns of deposition in the Severn Estuary, southwestern Britain: intertidal studies at spring-neap and seasonal scales, 1991-1993, *Marine Geology* **146**, 147-171.

Allen, J.R.L. and Pye, K. (1992) Coastal saltmarshes: their nature and importance, In Allen, J.R.L. and Pye, K. (eds.) *Saltmarshes. Morphodynamics, Conservation and Engineering Significance*, Cambridge University Press: Cambridge, 1-18.

Amos, C.L. (1995) Siliclastic tidal flats, In Perillo, G.M.E. (ed.) *Geomorphology and Sedimentology of Estuaries*, Elsevier: Amsterdam, 273-306.

Anders, F.J. and Byrnes, M.R. (1991) Accuracy of shoreline change rates as determined from maps and aerial photographs, *Shore and Beach* **59**, 17-26.

Anderson, J.M and Mikhail, E.M. (1985) *Introduction to Surveying*, McGraw-Hill: New York.

Andresen, H., Bakker, J.P., Brongers, M. Heydemann, B. and Irmler, U. (1990) Long-term changes of salt marsh communities by cattle grazing, *Vegetatio* **89**, 137-148.

Ashley, G.M. and Zeff, M.L. (1988) Tidal channel classification for a low-mesotidal salt marsh, *Marine Geology* **82**, 17-32.

Astaras, T. (1985) Drainage network analysis of LANDSAT imagery of the Olympus-Pieria mountain area, Northern Greece, *International Journal of Remote Sensing* **6**, 673-686.

Astaras, T., Lambrinos, N. and Soulakellis, N. (1990) A drainage system analysis evaluation of, and comparison between, Landsat-3 RBV, Landsat-5 TM and SPOT PA imageries covering the central Macedonia district, Greece, *International Journal of Remote Sensing* **11**, 1549-1559.

Ayles, C.P. and Lapointe, M.F. (1996) Downvalley gradients in flow patterns, sediment transport and channel morphology in a small macro-tidal estuary: Dipper Harbour Creek, New Brunswick, Canada, *Earth Surface Processes and Landforms* **21**, 829-842.

Bannister, B. and Arbor, A. (1980) Joint and drainage orientation of S.W. Pennsylvania, *Zeitschrift fur Geomorphology N.F.* **24**, 273-286.

Bathurst, J.C. (1988) Flow processes and data provision for channel flow models, In Anderson, M.G. (ed.) *Modelling Geomorphological Systems*, John Wiley: Chichester, 127-152.

Bauer, B. (1980) Drainage density - an integrated measure of the dynamics and the quality of watersheds, *Zeitschrift fur Geomorphologie* **24**, 261-272.

Bayliss-Smith, T.P., Healey, R., Lailey, R., Spencer, T. and Stoddart, D.R. (1979) Tidal flows in salt marsh creeks, *Estuarine Coastal and Shelf Science* **9**, 235-255.

Beeftink, W.G. (1965) Vegetation and habitat of the saltmarshes and beach plains of the south-western part of the Netherlands, *Wentia* **15**, 83-108.

Beeftink, W.G. (1977a) Salt-marshes, In Barnes, R.S.K. (ed.) *The Coastline*, John Wiley: Chichester, 93-122.

Beeftink, W.G. (1977b) The coastal salt marshes of western and northern Europe: a ecological and phytosociological approach, In Chapman, V.J. (ed.) *Wet Coastal Ecosystems*, Elsevier: Amsterdam, 109-156.

Begin, Z.B. (1988) Application of a diffusion-erosion model to alluvial channels which degrade due to base level lowering, *Earth Surface Processes and Landforms* **11**, 487-500.

Begin, Z.B., Mayer, D.F. and Schumm, S.A. (1981) Development of longitudinal profiles of alluvial channels in response to base-level lowering, *Earth Surface processes and Landforms* **6**, 49-68.

Best, J.L. (1988) Sediment transport and bed morphology at river channel confluences, *Sedimentology* **35**, 481-498.

Boon, J.D. (1975) Tidal discharge asymmetry in a salt marsh drainage system, *Limnology and Oceanography* **20**, 71-80.

Boon, J.D. and Byrne, R.J. (1981) On basin hypsometry and the morphodynamic response of coastal inlet systems, *Marine Geology* **40**, 27-48.

Bostock, L and Chandler, S. (1994) *Core Maths for A-Level (2nd Edition)*, Stanley Thornes: Cheltenham

Brampton, A.H. (1992) Engineering significance of British saltmarshes, In Allen, J.R.L. and Pye, K. (eds.) *Saltmarshes. Morphodynamics, Conservation and Engineering Significance*, Cambridge University Press: Cambridge, 115-122.

Bridges, P.H. and Leeder, M.R. (1976) Sedimentary model for intertidal mudflat channels, with examples from the Solway Firth, Scotland, *Sedimentology* **23**, 533-552.

Brooke, J.S. (1992) Coastal defence: the retreat option, *Journal of IWEM* **6**, 151-157.

Brunsden, D. (1980) Applicable models of long term landform evolution, *Zeitschrift fur Geomorphology N.F.* **36**, 16-26.

Bruun, P. (1967) Tidal inlet housekeeping, *Journal of Hydraulics Divisions ASCE* **93**, 167-184.

Burd, F. (1989) *The Salt Marsh Survey of Great Britain*, NCC: Peterborough.

Burd, F. (1995) *Managed Retreat: A Practical Guide*, English Nature: Peterborough.

Butera, M.K. (1983) Remote sensing of wetlands, *IEEE Transactions of Geoscience and Remote Sensing* **GE21**, 383-392.

Cahoon, D.R., Lynch, J.C. and Powell, A.N. (1996) Marsh vertical accretion in a southern California estuary, USA, *Estuarine Coastal and Shelf Science* **43**, 19-32.

Carling, P.A. (1981) Sediment transport by tidal current and waves: observations from a sandy intertidal zone (Burry Inlet, South Wales), *Special Publication of the International Association of Sedimentologists* **5**, 65-80.

Carey, A.E. and Oliver, F.W. (1918) *Tidal Lands. A Study of Shore Problems*, Blackie: London.

Chorley, R.J. and Morgan, M.J. (1962) Comparison of morphometric features, Unaka Mountains, Tennessee and North Carolina and Dartmoor, England, *Geological Society of America Bulletin* **73**, 17-34.

Chadwick, A. and Morfett, J. (1993) *Hydraulics in Civil and Environmental Engineering (2nd ed.)*, E and FN Spon: London.

Chang, H.H. (1979) Minimum stream power and river channel patterns, *Journal of Hydrology* **41**, 303-327.

Chantler, A.G. (1974) The applicability of regime theory to tidal watercourses, *Journal of Hydraulic Research* **12**, 181-191.

Chapman, V.J. (1974) *Saltmarshes and Salt Deserts of the World (2nd ed.)*, Leonard Hill: London.

Chapman, V.J. (1977) Introduction, In Chapman, V.J. (ed.) *Ecosystems of the World I. Wet Coastal Ecosystems*, Elsevier: Amsterdam, 1-30.

Charbreck, R.H. (1988) *Coastal Marshes*, University of Minnesota Press: Minneapolis.

Chorley, R.J. (1957) Climate and morphometry, *Journal of Geology* **65**, 628-638.

Chorley, R.J. and Dale, P.F. (1972) Cartographic problems in stream channel delineation, *Cartography* **7**, 150-162.

Chorley, R.J. and Kennedy, B.A. (1971) *Physical Geography: A Systems Approach*, Prentice Hall: London.

Chorowicz, J., Ichoku, C., Riazanoff, S., Kim, Y. and Cervelle, B. (1992) A combined algorithm for automated drainage network extraction, *Water Resources Research* **28**, 1293-1302.

Christiansen, T., Wiberg, P.L. and Milligan, T.G. (2000) Flow and sediment transport on a tidal salt marsh surface, *Estuarine Coastal and Shelf Science* **50**, 315-331.

Clarke, R.T., Gray, A.J., Warman, E.A. and Moy, I.L. (1993) Niche modelling of salt marsh plant species, *Institute of Terrestrial Ecology Project T08059P1*.

Coates, R.M., Williams, P.B. and Cuffe, C.K. (1995) *Design Guidelines for Tidal Channels in Coastal Wetlands*, Phillip Williams Ltd.: San Francisco.

Collier, P., Fontana, D. and Pearson, A. (1995) GIS mapping of Langstone Harbour for an integrated ecological and archaeological study, *Cartographic Journal* **32**, 137-142.

Collins, L.M and Collins, J.N and Leopold, L.B. (1987) Geomorphic processes of an estuarine marsh: preliminary results and hypotheses, In Gardiner, V. (ed.) *International Geomorphology I*, John Wiley: Chichester, 1049-1072.

Courtney F.M. and Trudgill, S.T. (1976) *The Soil. An Introduction to Soil Study in Britain*, Edward Arnold: London.

Cracknell, A.P. (1999) Remote sensing techniques in estuaries and coastal zones - an update, *International Journal of Remote Sensing* **19**, 485-496.

Daiber, F.C. (1977) Saltmarsh animals: distributions related to tidal flooding, salinity and vegetation, In Chapman, V.J. (ed.) *Wet Coastal Ecosystems*, Elsevier: Amsterdam, 79-106.

Dalby, D.H. (1970) The saltmarshes of Milford Haven, Pembrokeshire, *Field. Studies* **3**, 297-330.

Davies, J.L. (1964) A morphogenic approach to world shorelines, *Zeitschrift fur Geomorphology* **8**, 127-142.

Davies, T.R.H. (1987) Channel boundary shape-evolution and equilibrium, In Richards, K. (ed.) *River Channels, Environment and Process*, Blackwell: Oxford, 228-248.

Davis, J.C. (1985) *Statistics and Data Analysis in Geology*, Wiley: New York.

Day, D.G. (1980) Lithologic controls of drainage density: a study of six small rural catchments in New England, N.S.W., *Catena* **7**, 339-351.

De Jonge, V.N. (1992) Tidal flow and residual flow in the Ems Estuary, *Estuarine, Coastal and Shelf Science* **34**, 1-22.

Dexter, A.R. (1995) The strength and stability of muds and sediments, In Sir William Halcrow and Partner Ltd (ed.) *Saltmarsh Management for Flood Defence*, NRA: Bristol, 64-74.

Dietrich, W.E. and Dunne, T. (1993) The channel head, In Beven, K. and Kirkby, M.J. (eds.) *Channel Network Hydrology*, John Wiley: Chichester, 175-220.

Dijkema, K.S. (1987) Geography of salt marshes in Europe, *Zeitschrift fur Geomorphology N.F.* **31**, 489-499.

Dingman, S.L. (1984) *Fluvial Hydrology*, W.H. Freeman and Co.: New York.

Dixon, A.M. and Weight, R.S. (1996) Managing coastal re-alignment – case study at Orplands sea wall, Blackwater Estuary, Essex, In Sir William Halcrow and Partner Ltd (ed.) *Saltmarsh Management for Flood Defence*, NRA: Bristol, 169-191.

Dixon, A.M., Leggett, D.J. and Weight, R.C. (1998) Habitat creation opportunities for landward re-alignment: Essex case studies, *Journal of CIWEM* **12**, 107-112.

Donoghue, D.N.M, Reed Thomas, D.C. and Zong, Y. (1994) Mapping and monitoring the intertidal zone of the east coast of England using remote sensing techniques and a coastal monitoring GIS, *Proceedings of the 2nd Thematic Conference on Remote Sensing Marine and Coastal Environments*, 665-676.

Donoghue, D.N.M and Shennan, I. (1995) Intertidal mapping of the Wash Estuary, *EARSeL Advances in Remote Sensing* **4**, 135-142.

Doody, J.P. (1992) The conservation of British saltmarshes, In Allen, J.R.L. and Pye, K. (eds.) *Saltmarshes. Morphodynamics, Conservation and Engineering Significance*, Cambridge University Press: Cambridge, 80-114.

Doornkamp, J.C. and King, C.A.M (1971) *Numerical Analysis in Geography*, Edward Arnold: London.

Druery, B.M., Britton, G.W. and Greentree, G.S. (1984) Discussion on shape and dimensions of stationary dunes in rivers, by J. Fredsoe, *Journal of the Hydraulics Division A.S.C.E.* **110**, 855-857.

Dury, G.H. (1971) Channel characteristics in a meandering tidal channel: Crooked River, Florida, *Geografiska Annaler* **53**, 188-197.

Dyer, K.R. (1997) *Estuaries. A Physical Introduction*, John Wiley: Chichester.

Dyer, K.R., Christie, M.C. and Wright, E.W. (2000) The classification of intertidal mudflats, *Continental Shelf Research* **20**, 1039-1060.

Environment Agency (1998) The implication of future shoreline management on protected habitats in England and Wales, *R & D Technical Report W150*, Environment Agency: Bristol.

Erdas (1997) *Erdas Imagine Field Guide*, Erdas: Cambridge.

Esselink, P., Kees, S.D., Reents, S. and Hageman, G. (1998) Vertical accretion and profile changes in abandoned man-made tidal marshes in the Dollard Estuary, The Netherlands, *Journal of Coastal Research* **14**, 570-582.

Evans, G. and Collins, M. (1987) Sedimentary supply and deposition in The Wash, In Doody, E. and Barrett, J. (eds.) *The Wash and its Environment*, NCC: Peterborough, 48-63.

Falconer, R.A. and Chen, Y. (1991) An improved representation of flooding and drying and wind stress effects in a two-dimensional tidal numerical model, *Proceedings of the Institute of Civil Engineers* **91**, 659-678.

Fenies, H. and Faugeres, J.C. (1998) Facies and geometry of tidal channel-fill deposits (Arcachon Lagoon, S.W. France), *Marine Geology* **150**, 131-148.

Ferguson, R.I. (1975) Meander irregularity and wavelength estimation, *Journal of Hydrology* **26**, 315-333.

Ferguson, R.I. (1978) Comment on the drainage density-basin area relationship, *Area* **10**, 350-352.

Ferguson, R.I. (1979) Stream network volume: an index of channel morphometry: discussion and reply, *Geological Society of America Bulletin* **90**, 606-608.

Ferguson, R.I. (1986) Hydraulics and hydraulic geometry, *Progress in Physical Geography* **10**, 1-31.

Fitzgerald, D.M. and Nummedal, E. (1983) Response characteristics of an ebb-dominated inlet channel, *Journal of Sedimentary Petrology* **53**, 833-845.

Flint, J.J. (1976) Link slope distribution in channel networks, *Water Resources Research* **12**, 645-654.

French, C.E., French, J.R., Clifford, N.J. and Watson, C. J. (2000) Sedimentation - erosion dynamics of abandoned reclamations: the role of waves and tides, *Continental Shelf Research* **20**, 1711-1733.

French, J.R. (1989) *Hydrodynamics and sedimentation in a macro-tidal salt marsh, Norfolk, England*, Unpublished PhD dissertation, University of Cambridge.

French, J.R. (1993) Numerical simulation of vertical marsh growth and adjustment to accelerated sea-level rise, North Norfolk, U.K., *Earth Surface Processes and Landforms* **18**, 1-19.

French, J.R. (1996) Function and optimal design of saltmarsh channel networks, In Sir William Halcrow and Partner Ltd (ed.) *Saltmarsh Management for Flood Defence*, NRA: Bristol, 85-95.

French, J.R. and Clifford, N.J. (1992) Estimation of turbulence parameters within intertidal saltmarsh channels, In Falconer, R.A., Shiono, K. and Matthew, R.G.S. (eds.) *Hydraulic and Environmental Modelling: Estuarine and River Waters, Proceedings of the 2nd International Conference*, Ashgate: Aldershott, 41-52.

French, J.R. and Clifford, N.J. (2000) Hydrodynamic modelling as a basis for explaining estuarine environmental dynamics: some computation and methodological issues, *Hydrological Processes* **14**, 2089-2108.

French, J.R. and Reed, D.J. (2001) Physical contexts for saltmarsh conservation, In Warren, A. and French, J.R. (eds.) *Habitat Conservation: Managing the Physical Environment*, John Wiley: Chichester, 179-227.

French, J.R. and Spencer, T. (1993) Dynamics of sedimentation in a tide-dominated backbarrier salt marsh, Norfolk, UK, *Marine Geology* **110**, 315-331.

French, J.R., Spencer, T., Murray, A.L. and Arnold, N.S. (1995) Geostatistical analysis of sediment deposition in two small tidal wetlands, Norfolk, U.K. *Journal of Coastal Research* **11**, 308-321.

French, J.R., Spencer, T. and Reed, D.J. (1995) Editorial – Geomorphic response to sea-level rise: Existing evidence and future impacts, *Earth Surface Processes and Landforms* **20**, 1-6.

French, J.R. and Stoddart, D.R. (1992) Hydrodynamics of saltmarsh creek systems: Implications for marsh morphological development and material exchange, *Earth Surface Processes and Landforms* **17**, 235-252.

French, P. W. (1997) *Coastal and Estuarine Management*, Routledge: London.

French, P.W. (1999) Managed retreat: a natural analogue from the Medway estuary, UK, *Ocean and Coastal management* **42**, 49-62.

Frey, R.W. and Bassan, P.B. (1985) Coastal salt marshes, In Davis, R.A. (ed.) *Coastal Sedimentary Environments*, Springer-Verlag: New York, 225-302.

Friedrichs, C.T. (1995) Stability shear stress and equilibrium cross-sectional geometry of sheltered tidal channels, *Journal of Coastal Research* **11**, 1062-1074.

Friedrichs, C.T. and Aubrey, D.G. (1994) Tidal propagation in strongly convergent channels, *Journal of Geophysical Research* **99**, 3321-3336.

Friedrichs, C.T. and Madsen, A.S. (1992) Nonlinear diffusion of the tidal signal in frictionally dominated embayments, *Journal of Geophysical Research* **97**, 5637-5650.

Gabet, E.J. (1998) Lateral migration and bank erosion in a saltmarsh tidal channel in San Francisco Bay, California, *Estuaries* **21**, 745-753.

Gao, S and Collins, M. (1994) Tidal inlet equilibrium, in relation to cross-sectional area and sediment transport patterns, *Estuarine Coastal and Shelf Science* **38**, 157-172.

Gardner, L.R. and Bohn, M. (1980) Geomorphic and hydraulic evolution of tidal creeks on a subsiding beach ridge plain, North Inlet, S.C., *Marine Geology* **34**, 91-97.

Gardiner, V. (1978) Redundancy and spatial organisation of drainage basin form indices: an empirical investigation of data from north-west Devon, *Transactions of the Institute of British Geographers New Series* **3**, 416-431.

Gardiner, V. (1979) Estimation of drainage density from topological variables, *Water Resources Research* **15**, 909-917.

Gardiner, V., Gregory, K.J. and Walling, D.E. (1977) Further notes on the drainage density-basin area relationship, *Area* **9**, 117-121.

Gardiner, V. and Park, C.C. (1978) Drainage basin morphometry: review and assessment, *Progress in Physical Geography* **2**, 1-35.

Geodata Institute (1994) *Pagham Harbour: Review of Physical and Biological Processes*, Geodata Institute: Southampton.

Gleason, M.L., Elmer, D.A., Pien, N.C. and Fisher, J.S. (1979) Effects of stem density upon sediment retention by salt marsh cord grass, Spartina alterniflora, *Estuaries* **2**, 271-273.

Glock, W.S. (1931) The development of drainage systems: a synoptic view, *Geographical Review* **21**, 475-482.

Gomes Pereira, L.M. and Wicherson, R.J. (1999) Suitability of laser data for deriving geographic information – a case study in the context of management of fluvial zones, *ISPRS Journal of Photogrammetry and Remote Sensing* **54**, 130-137.

Goodchild, M.F. and Klinkenberg, B. (1993) Statistics of channel networks on fractional Brownian surfaces, In Lamb, N.S. and De Cola, L. (eds.) *Fractals in Geography*, Prentice Hall: New Jersey, 122-157.

Goodman, P.J. (1960) Investigations into 'die back' in *Spartina Townsendii* agg. II: The morphological structure and composition of the Lymington sward, *Journal of Ecology* **48**, 711-724.

Goodman, P.J. and Williams, W.T. (1961) Investigations into 'die-back' in *Spartina Townsendii* agg. III: Physiological correlates of 'die-back', *Journal of Ecology* **49**, 391-396.

Gornitz, V. (1995) Sea-level rise: a review of recent past and near-future trends, *Earth Surface Processes and Landforms* **20**, 7-20.

Goudie, A. (1990) *Geomorphological Techniques* (2nd ed.), Unwin Hyman: London.

Gray, D.M. (1961) Interrelations of watershed characteristics, *Journal of Geophysical Research* **66**, 1215-1223.

Gray, A.J. (1972) The Ecology of Morecambe Bay. The saltmarshes of Morecambe Bay, *Journal of Applied Ecology* **9**, 207-220.

Green, E.P., Mumby, P.J., Edwards, A.J., Clark, C.D. and Ellis, A.C. (1998) The assessment of mangrove areas using high resolution multispectral airborne imagery, *Journal of Coastal Research* **14**, 433-443.

Green, H.M., Stoddart, D.R., Reed, D.J. and Bayliss-Smith, T.P. (1986) Saltmarsh tidal creek dynamics, Scolt Head Island, Norfolk, England, In Sigbjarnarson, G. (ed.), *Iceland Coastal and River Symposium Proceedings*, 93-101.

Greensmith, J.T. and Tucker, E.V. (1965) Salt marsh erosion in Essex, *Nature* **206**, 606-607.

Greensmith, J.T. and Tucker, E.V. (1966) Morphology and evolution of inshore shell ridges and mud-mounds on modern intertidal flats, near Bradwell, Essex, *Proceedings of the Geological Association* **77**, 329-346.

Gregory, K.J. (1977) Stream network volume: an index of channel morphometry, *Geological Society of America Bulletin* **88**, 1075-1080.

Gregory, K.J. and Walling, D.E. (1973) *Drainage Basin Form and Process*, Edward Arnold: London.

Groen, P. (1967) On the residual transport of suspended matter by an alternating tidal current, *Netherlands Journal of Sea Research* **3**, 564-574.

Hack, J.T. (1957) Studies of longitudinal stream profiles in Virginia and Maryland, *U.S. Geological Survey Professional Paper* **294B**.

Haggett, P. and Chorley, R.J. (1969) *Network Analysis in Geography*, Edward Arnold: London.

Haltiner, J. and Williams, P.B. (1987) Hydraulic design in saltmarsh restoration, In Kustler, J.A. and Brooks, G. (eds.) *Proceedings of the National Wetlands Symposium*, Chicago: National Wetlands Research Centre, 293-299.

Haltiner, J., Zedler, J.B., Boyer, K.E, Williams, G.D. and Calloway, J.C. (1997) Influence of physical processes on the design, functioning and evolution of restored tidal wetlands in California, U.S.A., *Wetlands Ecology and Management* **4**, 73-91.

Hamilton, L.C. (1990) *Modern Data Analysis: A First Course in Applied Statistics*, Brooks and Cole: Belmont.

Hardisky, M.A., Gross, M.F. and Clemas, V. (1986) Remote sensing of coastal wetlands, *Bioscience* **36**, 453-460.

Harleman, D.R.F. (1966) Tidal dynamics in estuaries: Part 2 real estuaries, In Ippen, A.T. (ed.) *Estuary and Coastline Hydrodynamics*, McGraw Hill: London, 522-545.

Hartnall, T.J. (1984) Salt-marsh vegetation and micro-relief development on the new marsh at Gibraltar Point, Lincolnshire, In Clarke, M.W. (ed.) *Coastal Research: U.K. Perspectives*, Geobooks: Norwich, 37-58.

Hauser, D.P (1984) Some problems in the use of stepwise regression techniques in geographical research, *Canadian Geographer* **18**, 148-158.

Hayes, M.O. (1979) Barrier island morphology as a function of tidal and wave regime, In Leatherman, S.P. (ed.) *Barrier Islands*, Academic Press: New York, 1-27

Haynes, J. and Dobson, M. (1969) Physiography, foraminifera and sedimentation in the Dovey Estuary (Wales), *Geological Journal* **6**, 217-257.

Hazelden, J. (1996) Soils and managed retreat at Tollesbury, Essex, In Sir William Halcrow and Partner Ltd (ed.) *Saltmarsh Management for Flood Defence*, NRA: Bristol, 75-84.

Healey, R.G., Pye, K., Stoddart, D.R. and Bayliss-Smith, T.P. (1981) Velocity variations in salt marsh creeks, Norfolk, England, *Estuarine, Coastal and Shelf Science* **13**, 535-545.

Henderson, F.M. (1966) *Open Channel Flow*, McMillan: New York.

Hey, R.D. (1988) Mathematical models of channel morphology, In Anderson, M.G. (ed.) *Modelling Geomorphological Systems*, John Wiley: Chichester, 99-125.

Hey, R.D and Thorne C.R. (1986) Stable channels with mobile gravel beds, *Journal of the Hydraulic Engineers ASCE* **112**, 671-689.

Hill, J.M., Graham, L.A., Henry, R.J. and Cotter, D.M. (2000) Highlight article: Wide-area topographic mapping and applications using airborne light detection and ranging (lidar) technology, *Photogrammetric Engineering and Remote Sensing*, **66**, 232-244.

Horton, R.E. (1932) Drainage basin characteristics, *Transactions of the American Geophysical Union,* 350-361.

Horton, R.E. (1945) Erosional development of stream and their drainage basins: Hydrophysical approach to quantitative morphology, *Geological Society of America Bulletin* **56**, 275-370.

Howard, A.D. (1967) Drainage analysis in geologic interpretation: a summation, *American Association of Petroleum Geologists Bulletin* **51**, 2246-2259.

Howard, A.D. (1971) Optimal angles of stream junction: geometric, stability to capture, and minimum power criteria, *Water Resources Research* **7**, 863-873.

Howard, A.D. (1990) Theoretical model of optimal drainage networks, *Water Resources Research* **26**, 2107-2117.

Howard, A.D and Hemberger, A.T. (1991) Multivariate characterisation of meandering, *Geomorphology* **4**, 161-186.

Huang, H.Q. and Warner, R.F. (1995) The multivariate controls of hydraulic geometry: a causal investigation in terms of boundary shear distribution, *Earth Surface Processes and Landforms* **20**, 115-130.

Huggett, R.J. (1988) Dissipative systems: implications for geomorphology, *Earth Surface Processes and Landforms* **13**, 45-49.

Hughes, R.G. (1999) Saltmarsh erosion and management of saltmarsh restoration: the effects of infaunal invertebrates, *Aquatic Conservation: Marine and Freshwater Ecosystems* **9**, 83-95.

Hume, T.M. (1991) Empirical stability relationships for estuarine waterways and equations for stable channel design, *Journal of Coastal Research* **7**, 1097-1111.

Hydrographic Office (1997) *Admiralty Tide Tables. Volume 1*, U.K. Hydrographic Office: Taunton.

Ichoku, C. and Chorowicz, J. (1994) A numerical approach to the analysis and classification of channel network patterns, *Water Resources Research* **30**, 161-174.

Ichoku, C., Karnieli, A., Meisels, A. and Chorowicz, J. (1996) Detection of drainage channel networks on digital satellite images, *International Journal of Remote Sensing* **17**, 1659-1678.

Inglis, C.C. and Kestner, F.J.T. (1958) The long-terms effects of training walls, reclamation, and dredging on estuaries, *Proceedings of the Institute of Civil Engineers* **9**, 193-216.

Inglis, C.C. and Kestner, F.J.T. (1959) Changes in The Wash as affected by training walls and reclamation works, *Proceedings of the Institute of Civil Engineers* **11**, 435-466.

Irish, J.L. and Lillycrop, W.J. (1999) Scanning laser mapping of the coastal zone: the SHOALS system, *ISPRS Journal of Photogrammetry and Remote Sensing* **54**, 123-129.

Jacobson, H.A. (1988) Historical development of the saltmarsh at Wells, Maine, *Earth Surface Processes and Landforms* **13**, 475-486.

James, W.R. and Krumbein, W.C. (1969) Frequency distributions of stream link lengths, *Journal of Geol.* **77**, 544-565.

Jarrett, J.T. (1976) Tidal prism-inlet area relationships, *US Army Coastal Engineering Research Centre GITI, Report 3*: Vicksburg Mississippi.

Jarvis, R.S. (1972) New measure of the topologic structure of dendritic drainage networks, *Water Resources Research* **8**, 1265-1271.

Jarvis, R.S. (1976) Stream orientation structures in drainage networks, *Journal of Geology* **84**, 563-582.

Jarvis, R.S. and Sham, C.H. (1981) Drainage network structure and the diameter-magnitude relation, *Water Resources Research* **17**, 1019-1027.

Jarvis, R.S. and Werritty, A. (1975) Some comments on testing random topology stream network models, *Water Resources Research* **11**, 309-318.

Johnson, D.E. (1996) Integrating science, technology and environmental management to achieve recreation of tidal wetlands: a regional approach, In Taussik, J. and Mitchell, J. (eds.) *Partnership in Coastal Zone Management*, Samara: Cardigan, 603-609.

Johnson, J.W. (1973) Characteristics and behaviour of Pacific coast tidal inlets, *Journal of the Waterways, Harbours and Coastal Engineering Division ASCE.*, 325-339.

Kesel, R.H. and Smith, J.S. (1978) Tidal creek and pan formation in intertidal saltmarshes, *Scottish Geographical Magazine*, 159-168.

Kestner, F.J.T. (1962) The old coastline of The Wash, *Geographical Journal* **128**, 457-471.

Kestner, F.J.T. (1979) Loose boundary hydraulics and land reclamation, In Knights, B. and Phillips A.J., (eds) *Estuarine and Coastal Land Reclamation and Water Storage*, Teakfield: Farnborough, 23-47.

Kirchner, J.W. (1993) Statistical inevitability of Horton's Laws and the apparent randomness of stream channel networks, *Geology* **21**, 591-594.

Kirkby, M.J., Naden, P.S., Burt, T.P. and Butcher, D.P. (1987) *Computer Simulation in Physical Geography*, John Wiley: Chichester.

Kirkby, M.J. (1996) A role for theoretical models in geomorphology?, In Rhoads, B.L. and Thorne, C.E. (eds.) *The Scientific Nature of Geomorphology: Proceedings of the 27th Binghampton Symposium in Geomorphology*, John Wiley: Chichester, 257-272.

Klein, G.D. (1985) Intertidal flats and intertidal sand bodies, In Davis, R.A. (ed.) *Coastal Sedimentary Environments*, Springer-Verlag: New York, 187-224.

Klein, M. (1981) Drainage area and variation of channel geometry downstream, *Earth Surface Processes and Landforms* **6**, 589-593.

Knight, D.W. (1981) Some field measurements concerned with the behaviour of resistance coefficients in a tidal channel, *Estuarine Coastal and Shelf Science* **12**, 303-322.

Knighton, A.D. (1975) Channel gradient in relation to discharge and bed material characteristics, *Catena* **2**, 263-274.

Knighton, A.D. (1987) River channel adjustments – the downstream dimension, In Richards, K. (ed.) *River Channels. Environment and Process*, Blackwell: Oxford, 95-128.

Knighton, A.D. (1998) *Fluvial Forms and Processes. A New Perspective*, Arnold: London.

Knighton, A.D. (1999) Downstream variation in stream power, *Geomorphology* **29**, 293-306.

Knighton, A.D., Woodroffe, C.D. and Mills, K. (1992) The evolution of tidal creek networks, Mary River, Northern Australia, *Earth Surface Processes and Landforms* **17**, 167-190.

Krishnamurthy, M. (1977) Tidal prism of equilibrium inlets, *Journal of the Waterway, Port Coastal and Ocean Division ASCE* **103**, 423-432.

Krumbein, W.C. and Shreeve, R.L. (1970) Some statistical properties of dendritic channel networks, *Technical Report 13 Office of Naval Research, Northwestern University, Illinois*.

Lambert, J.M. (1964) The Spartina Story, *Nature* **204**, 1136-1138.

Land, L.S. and Hoyt, J.H. (1966) Sedimentation in a meandering estuary, *Sedimentology* **6**, 191-207.

Landin, M.C. (1993) Wetland creation and restoration on the U.S. Pacific coast, In Magoon., A.T., Wilson, W.S., Converse, H. and Tobin, L.T. (eds.) *Coastal Zone '93*, American Society of Civil Engineers: New York, 2138-2146.

Lane, S.N. (1995) The dynamics of dynamic river channels, *Geography* **80**, 147-162.

Langbein, W.B. (1947) Topographic characteristics of drainage basins, *U.S. Geological Survey Water Supply Paper* **968-C**, 125-157.

Langbein, W.B. (1963) Hydraulic geometry of a shallow estuary, *Bulletin of the International Association of Scientific Hydrologists* **8**, 84-94.

Langbein, W.B. (1964) Profiles of river of uniform discharge, *U.S. Geol. Survey Prof. Paper* **501-B**, 119-122.

Lawrence, D.S.L. (1996) Physically based modelling and the analysis of landscape development, In Rhoads, B.L. and Thorne, C.E. (eds.) *The Scientific Nature of Geomorphology: Proceedings of the 27th Binghampton Symposium in Geomorphology*, John Wiley: Chichester, 274-288.

Leggett, D.J and Dixon, M. (1994) Management of the Essex saltmarshes for flood defence, In Falconer, R.A and Goodwin, P. (eds.) *Wetland Management*, Telford: London, 232-245.

Leonard, L.A., Hine, A.C. and Luther, M.E. (1995) Surficial sediment transport and deposition processes in a Juncus Roemerianus marsh, west-central Florida, *Journal of Coastal Research* **11**, 322-336.

Leonard, L.A. and Luther, M.E. (1995) Flow hydrodynamics in tidal marsh canopies, *Limnology and Oceanography* **40**, 1474-1484.

Leonard, L.A. (1997) Controls of sedimentary transport and deposition in an incised mainland marsh basin, southeastern North Carolina, *Wetlands* **17**, 263-274.

Leopold, L.B. (1971) Trees and streams: the efficiency of branching patterns, *Journal of Theoretical Biology* **31**, 339-354.

Leopold, L.B. and Bull, W.B. (1979) Base level, aggradation, and grade, *Proceedings of the American Philosophical Society* **123**, 168-202.

Leopold, L.B., Collins, J.N. and Collins, L.M. (1993) Hydrology of some tidal channels in estuarine marshland near San Francisco, *Catena* **20**, 469-493.

Leopold, L.B. and Maddock, T. (1953) The hydraulic geometry of stream channels and some physiographic implications, *U.S. Geol. Survey Professional Paper* **252**, 1-56.

Leopold L.B., Wolman, M.G. and Miller, J.P. (1964) *Fluvial Processes in Geomorphology*, W.H. Freeman and Co.: San Francisco.

Lessa, G. (1996) Tidal dynamics and sediment transport in a shallow macrotidal estuary, *Coastal and Estuarine Studies* **50**, 338-360.

Letzsch, W.S. and Frey, R.W. (1980a) Deposition and erosion in a holocene saltmarsh, Sapelo Island, Georgia, *Journal of Sedimentary Petrology* **50**, 529-542.

Letzsch, W.S. and Frey, R.W. (1980b) Erosion of salt marsh tidal creek banks, Sapelo Island, Georgia, *Senckenbergiana Maritima* **12**, 201-212.

Lincoln, J.M. and Fitzgerald, D.M. (1988) Tidal distortions and flood dominance at five small tidal inlets in southern Maine, *Marine Geology* **82**, 133-148.

Long, A.J. and Shennan, I. (1994) Sea-level changes in Washington and Oregon and the 'earthquake deformation cycle', *Journal of Coastal Research* **10**, 825-838.

Lubowe, J.K. (1964) Stream junction angles in the dendritic drainage pattern, *American Journal of Science* **262**, 325-339.

MAFF (1993) *Strategy for Flood and Coastal Defence in England and Wales*, MAFF: London.

MAFF (1996) *Managed Set-back Research. A Technical Briefing Note*, MAFF Flood and Coastal Defence Division: London.

Marshall, J.R. (1962) The Morphology of the Upper Solway Salt Marshes, *Scottish Geographical Magazine* **78**, 81-99.

Masterman, R. and Thorne, C.R. (1994) Flow resistance in gravel-bed channels with vegetated banks, In Kirkby, M.J. (ed.) *Process Models and Theoretical Geomorphology*, John Wiley: Chichester, 201-218.

Mather, P.M. (1987) *Computer Processing of Remotely Sensed Images. An Introduction*, John Wiley: Chichester.

Mehta, A.J., Birne, R.J. and DeAlteris, J.T. (1976) Measurement of bed friction in tidal inlets, *Coastal Engineering* **1**, 1701-1720.

Mehta, A.J. (1978) Bed friction characteristics of three tidal entrances, *Coastal Engineering* **2**, 69-83.

Melton, M.A. (1958a) Correlation structure of morphometric properties of drainage systems and their controlling agents, *Journal of Geology* **66**, 442-460.

Melton, M.A. (1958b) Geometric properties of mature drainage systems and their representation in an E4 phase space, *Journal of Geology* **66**, 35-56.

Miehle, W. (1958) Link length minimisation in networks, *Operational Research* **6**, 232-243.

Miller, T.K. (1991) A model of stream channel adjustment: assessment of Rubey's hypothesis, *Journal of Geology* **99**, 699-710.

Mitsch, W.J. and Gosselink, J.G. (1986) *Wetlands*, Van Nostrand Reinhold: New York.

Mock, S.J. (1971) A classification of channel links in stream networks, *Water Resources Research* **7**, 1558-1566.

Moeller, I., Spencer, T. and French, J.R. (1996) Wind wave attenuation over saltmarsh surfaces: preliminary results from Norfolk, England, *Journal of Coastal Research* **12**, 1009-1016.

Moglen, G.E. and Bras, R.L. (1995) The effect of spatial heterogeneities on geomorphic expression in a model of basin evolution, *Water Resources Research* **31**, 2613-2623.

Molnar, P and Ramirez, J.A. (1998a) An analysis of energy expenditure in Goodwin Creek, *Water Resources Research* **34**, 1819-1829.

Molnar, P and Ramirez, J.A. (1998b) Energy dissipation theories and optimal channel characteristics of river networks, *Water Resources Research* **34**, 1809-1818.

Montgomery, K. (1989) Concepts of equilibrium and evolution in geomorphology: the model of branch systems, *Progress in Physical Geography* **13**, 47-67.

Moore, L.J. (2000) Shoreline mapping techniques, *Journal of Coastal Research*, **16** 111-124.

Morisawa, M.E. (1962) Quantitative geomorphology of some watersheds in the Appalachian Plateau, *Geological Society of America Bulletin* **73**, 1025-1046.

Morisawa, M.E. (1964) Development of drainage systems on an upraised lake floor, *American Journal of Science* **262**, 340-354.

Morris, P.H. and Williams, D.J. (1997) Exponential longitudinal profiles of streams, *Earth Surface Processes and Landforms* **22**, 143-163.

Mosley, M.P. (1976) An experimental study of channel confluences, *Journal of Geology* **84**, 535-562.

Mosley, M.P. (1981) Semi-determinate hydraulic geometry of river channels, South Island, New Zealand, *Earth Surface Processes and Landforms* **6**, 127-137.

Mosley, M.P. (1987) The classification and characterisation of rivers, In Richards, K. (ed.) *River Channels*, Blackwell: Oxford, 295-320.

Mulrennan, M.E. and Woodroffe, C.D. (1998) Saltwater intrusion into the coastal plains of the Lower Mary River, Northern Territory, Australia, *Journal of Environmental Management* **54**, 169-188.

Murray, C.D. (1926) The physiological principle of minimum work applied to the angle of branching of arteries, *Journal of General Physiology* **9**, 835-841.

Myrick, R.M, and Leopold, L.B. (1963) Hydraulic geometry of a small tidal estuary, *U.S. Geological Survey Professional Papers* **422B**, 1-18.

Nixon, S.W. (1980) Between coastal marshes and coastal waters – a review of twenty years of speculation and research in the role of salt marshes in estuarine productivity and water chemistry, In Hamilton, R. and McDonald, K.B. (eds.) *Estuarine and Wetland Processes*, Plenum: New York, 437-525.

Norcliffe, G.B. (1977) *Inferential Statistics for Geographers. An Introduction*, Hutchinson: London.

NRA (1994) *East Anglian Salt Marshes*, NRA: Peterborough.

NRA (1995) *North Norfolk Shoreline Management Plan*, NRA: Peterborough.

NSS (1992) *National Survey Software User Guide*, NSS: Telford.

O'Brien, M.P. (1931) Estuary tidal prisms related to entrance area, *Civil Engineering ASCE* **1**, 738-739.

O'Brien, M.P. (1969) Equilibrium flow areas of inlets on sandy coasts, *Journal of the Waterways and Harbours Division ASCE* **95**, 43-52.

Patrick, W.H. and DeLaune, R.D. (1990) Subsidence, accretion and sea level rise in south San Francisco Bay marshes, *Limnology and Oceanography* **35**, 1389-1395.

Peakall, J., Ashworth, P. and Best, J. (1996) Physical modelling in fluvial geomorphology: principles, applications and unresolved issues, In Rhoads, B.L. and Thorne, C.E. (eds.) *The Scientific Nature of Geomorphology: Proceedings of the 27th Binghampton Symposium in Geomorphology*, John Wiley: Chichester, 221-253.

Pestrong, R. (1965) The development of drainage patterns on tidal marshes, *Stanford University Publications in Geology* **10**, 1-81.

Pestrong, R. (1970) Tidal flat sedimentation at Cooley Landing, S.W. San Francisco Bay, *Office of Naval Research, Technical Report 4430(00)*, Stanford University.

Pestrong, R. (1972) Tidal flat sedimentation at Cooley Landing, S.W. San Francisco Bay, *Sedimentary Geology* **8**, 251-288.

Pethick, J.S. (1975) A note on the drainage density-basin area relationship, *Area* **7**, 217-222.

Pethick, J.S. (1978) Comment. Drainage density-basin area relationship, *Area* **10**, 349-355.

Pethick, J.S. (1980) Velocity surges and asymmetry in tidal channels, *Estuarine and Coastal Marine Science* **11**, 331-345.

Pethick, J.S. (1984) *An Introduction to Coastal Geomorphology*, Edward Arnold: London.

Pethick, J.S. (1992) Saltmarsh geomorphology, In Allen, J.R.L. and Pye, K. (eds.) *Saltmarshes. Morphodynamics, Conservation and Engineering Significance*, Cambridge University Press: Cambridge, 41-62.

Pethick, J. (1993) Shoreline adjustments and coastal management: Physical and biological processes under accelerated sea-level rise, *Geographical Journal* **159**, 162-168.

Pethick, J. (1994) Estuaries and wetlands: function and form, In Falconer, R.A. and Goodwin, P. (ed.), *Wetland Management*, Thomas Telford: London, 75-87.

Pethick, J.S. (1996) The geomorphology of mudflats, In Nordstrom, K.F. and Roman, C.T. (eds.) *Estuarine Shores: Evolution, Environments and Human Alterations*, John Wiley: Chichester, 185-211.

Pethick, J.S.. Leggett, D. and Husain, L. (1990) Boundary layers under salt marsh vegetation developed in tidal currents, In Thornes, J.B. (ed.) *Vegetation and Erosion. Processes and Environment*, John Wiley: Chichester, 113-124.

Pickup, G. (1976) Adjustment of stream-channel shape to hydrologic regime, *Journal of Hydrology* **30**, 365-373.

Pickup, G. and Rieger, W.A. (1979) A conceptual model of the relationship between channel characteristics and discharge, *Earth Surface Processes* **4**, 37-42.

Pieri, D.C. (1984) Junction angles in drainage networks, *Journal of Geophysical Research* **89**, 6878-6884.

Pirazzoli, P.A. (1996) *Sea-level Changes. The Last 20 000 Years*, John Wiley: Chichester.

Pizzuto, J.E., (1984) Bank erodibility of shallow sandbed streams, *Earth Surface Processes and Landforms* **9**, 113-124.

Postma, H. (1961) Transport and accumulation of suspended matter in the Dutch Wadden Sea, *Netherlands Journal of Sea Research*. **1**, 148-190.

Pringle, A.W., (1995) Erosion of a cyclic saltmarsh in Morecambe Bay, north-west England, *Earth Surface Processes and Landforms* **20**, 387-405.

Pugh, D.T. (1987) *Tides, Surges and Mean Sea-Level. A Handbook for Engineers and Scientists*, John Wiley: Chichester.

Pye, K. (1992) Saltmarshes on the barrier coastline of north Norfolk, eastern England, In Allen, J.R.L. and Pye, K. (eds.) *Saltmarshes. Morphodynamics, Conservation*

and Engineering Significance, Cambridge University Press: Cambridge, 148-178.

Pye, K. (1995) Controls on long-term saltmarsh accretion and erosion in The Wash, eastern England, *Journal of Coastal Research* **11**, 337-356.

Pye, K. and Crooks, S. (1995) Geochemical controls on the moisture content and shear strength of saltmarsh sediments, In Sir William Halcrow and Partner Ltd (ed.) *Saltmarsh Management for Flood Defence*, NRA: Bristol, 55-63.

Pye, K. and French, P.W. (1993) *Erosion and Accretion Processes of British Saltmarshes*, Cambridge Environmental Research Consultants: Cambridge.

Queen, W.H. (1977) Human uses of salt marshes, In Chapman, V.J. (ed.) *Wet Coastal Ecosystems*, Elsevier: Amsterdam, 363-368.

Ragotzkie, R.A. (1959) Drainage patterns in saltmarshes, *Proceedings of the Saltmarsh Conference of the Marine Institute, University of Georgia*, 22-28.

Ragotzkie, R.A. and Bryson, R.A. (1955) Hydrography of the Duplin River, Sapelo Island, Georgia, *Bulletin of Marine Science for the Gulf and Caribbean* **5**, 297-314.

Randerson, P.F. (1979) A simulation model of salt-marsh development and plant ecology, In Knights, B. and Phillips, A.J. (eds.) *Estuarine and Coastal Land Reclamation and Water Storage*, Saxon House: Farnborough, 48-67.

Ranwell, D.S. (1972) *Ecology of Salt Marshes and Sand Dunes*, Chapman and Hall: London.

Redfield, A.C. (1965) Ontogeny of a salt marsh estuary, *Science* **147**, 50-55.

Redfield, A.C. (1972) The development of a New England salt marsh, *Ecological Monographs* **42**, 201-237.

Reed, D.J. (1987) Temporal sampling and discharge asymmetry in salt marsh creeks, *Estuarine Coastal and Shelf Science* **25**, 459-466.

Reed, D.J. (1990) The impact of sea level rise on coastal salt marshes, *Progress in Physical Geography* **14**, 24-40.

Reed, D.J. (1995) The response of coastal marshes to sea-level rise: survival or submergence?, *Earth Surface Processes and Landforms* **20**, 39-48.

Reed, D.J., Spencer, T., Murray, A.L., French, J.R. and Leonard, L. (1999) Marsh surface sediment deposition and the role of tidal creeks: implications for created and managed coastal marshes *Journal of Coastal Conservation* **5**, 81-90.

Reed, D.J., Stoddart, D.R. and Bayliss-Smith, T.P. (1985) Tidal flows and sediment budgets for a salt-marsh system, Essex, England, *Vegetatio* **62**, 375-380.

Reid Thomas, D.C., Donoghue, D.N.M. and Shennan, I. (1995) Intertidal mapping of the Wash Estuary, *EARSeL Advances in Remote Sensing* **4**, 135-142.

Reimold, R.J. (1977) Mangals and salt marshes of eastern United Sates, In Chapman, V.J. (ed.) *Wet Coastal Ecosystems*, Elsevier: Amsterdam, 157-164.

Rhoads, B.L. and Thorne, C.E. (1996) Observation in geomorphology, In Rhoads, B.L. and Thorne, C.E. (eds.) *The Scientific Nature of Geomorphology: Proceedings of*

the 27th Binghampton Symposium in Geomorphology, John Wiley: Chichester, 21-56.

Richards, F.J. (1934) The salt marshes of the Dovey estuary, *Annals Botanica* **48**, 225-259.

Richards, K. (1978) Yet more notes on the drainage density-basin area relationship, *Area* **10**, 344-348.

Richards, K. (1980) A note on changes in channel geometry at tributary junctions, *Water Resources Research* **16**, 241-244.

Richards, K. (1986) Fluvial geomorphology, *Progress in Physical Geography* **10**, 401-420.

Richards, K. (1988) Fluvial geomorphology, *Progress in Physical Geography* **12**, 435-456.

Richards, K. (1996) Samples and cases: generalisation and explanation in geomorphology, In Rhoads, B.L. and Thorne, C.E. (eds.) *The Scientific Nature of Geomorphology: Proceedings of the 27th Binghampton Symposium in Geomorphology*, John Wiley: Chichester, 170-190.

Rigon, R. and Rinaldo, A. (1993) Optimal channel networks: a framework for the study of river basin morphology, *Water Resources Research* **29**, 1635-1646.

Rinaldo, A., Fagherazzi, S., Lanzoni, S., Marani, M and Dietrich, W.E. (1999) Tidal networks. Watershed delineation and comparative network morphology, *Water Resources Research*, **32**, 3905-3917.

Rinaldo, A., Rodriguez-Iturbe, I. And Rigon, R. (1998) Channel networks, *Annual Review of Earth and Planetary Sciences* **26**, 289-327.

Rodriguez-Iturbe, I., Rinaldo, A., Rigon, R., Bras, R.L., Marani, A. and Ijjasz-Vasquez, E. (1992) Energy dissipation, runoff production, and the three-dimensional structure of river basins, *Water Resources Research* **28**, 1095-1103.

Roman, C.T. (1984) Estimating water volume discharge through saltmarsh tidal channels: An aspect of material exchange, *Estuaries* **7**, 259-264.

Rosgen, D.L. (1994) A classification of natural rivers, *Catena* **22**, 169-199.

Roy, A.G. (1983) Optimal angular geometry models of river branching, *Geographical Analysis* **15**, 87-96.

Roy, A.G. (1985) Optimal models of river branching angles, In Woldenberg, M.J. (ed.) *Models in Geomorphology*, Allen and Unwin: Boston, 270-285.

Roy, A.G. and Roy, R. (1988) Short communication. Changes in channel size at river confluences with coarse bed material, *Earth Surface Processes and Landforms* **13**, 77-84.

Roy, A.G. and Woldenberg, M. (1982) A generalisation of the optimal models of arterial branching, *Bulletin of Mathematical Biology* **44**, 349-360.

Roy, A.G. and Woldenberg, M. (1986) A model for changes in channel form at a river confluence, *Journal of Geology* **94**, 402-411.

Rubey, W.W. (1952) Geology and mineral resources of the Hardin and Brussels quadrangles, Illinois, *U.S. Geological Survey Professional Paper* **218**, 1-175.

Sanderson, E.W., Ustin, S.L. and Foin, T.C. (2000) The influence of tidal channels on the distribution of salt marsh plant species in Petaluma Marsh, CA, USA, *Plant Ecology* **146**, 29-41.

Sayer, A. (1992) *Method in Social Science. A Realistic Approach*, Routledge: London.

Schumm, S.A. (1956) Evolution of drainage systems and slopes in badlands at Perth Amboy, New Jersey, *Geological Society of America Bulletin* **67**, 597-646.

Schumm, S.A. (1997) Drainage density. Problems of prediction and application, In Stoddart, D.R. (ed.) *Process and Form in Geomorphology*, Routledge: London, 15-45.

Schuepfer, F.E., Lennon, G.P., Weisman, R.N. and Gabriel, R. (1988) Hydrodynamic model of Great Sound, New Jersey, *Marine Geology* **82**, 1-15.

Settlemyre, J.L. and Gardner, L.R. (1977) Suspended sediment flux through a salt marsh drainage basin, *Estuarine and Coastal Marine Science* **5**, 653-663.

Shaw, G and Wheeler, D. (1997) *Statistical Techniques in Geographical Analysis*, David Fulton: London.

Shepherd, R.G. (1985) Regression analysis of river profiles, *Journal of Geology* **93**, 377-384.

Shi., Z., Hamilton, L.J. and Wolanski, E. (2000) Near-bed currents and suspended sediment transport in saltmarsh canopies, *Journal of Coastal Research* **16**, 909-914.

Shi, Z., and Lamb, H.F. (1991) Post-glacial sedimentary evolution of a microtidal estuary, Dyfi Estuary, west Wales, U.K., *Sedimentary Geology* **73**, 227-246.

Shi, Z., Lamb, H.F. and Collin, R.L. (1995) Geomorphic change of saltmarsh tidal creek networks in the Dyfi Estuary, Wales, *Marine Geology* **128**, 73-83.

Shreve, R.L. (1966) Statistical law of stream numbers, *Journal of Geology* **74**, 17-37.

Shreve, R.L. (1967) Infinite topologically random channel networks, *Journal of Geology* **75**, 178-186.

Shreve, R.L. (1969) Stream lengths and basin areas in topologically random channel networks, *Journal of Geology* **77**, 397-414.

Shreve, R.L. (1975) The probabilistic-topologic approach to drainage-basin geomorphology, *Geology* **3**, 527-529.

Sivanesan, A. and Manners, J.G. (1972) Bacteria of muds colonised by *Spartina Townsendii* and their possible role in Spartina die-back, *Plant and Soil* **36**, 349-361.

Smart, J.S. (1969) Topological properties of channel networks, *Geological Society of America Bulletin* **80**, 1757-1774.

Smart, J.S. (1972) Channel networks, In Chow, V.T. (ed.) *Advances in Hydroscience*, Academic Press: New York, 305-346.

Smart, J.S. (1973) The random model in fluvial geomorphology, In Morisawa, M. (ed.) *Proceedings of the 4th Geomorphology Symposium*, Binghampton, 27-49.

Smart, J.S. (1978) The analysis of drainage network composition, *Earth Surface Processes* **3**, 129-170.

Smith, G.M., Spencer, T., Murray, A.L. and French, J.R. (1998) Assessing seasonal vegetation change in coastal wetlands with airborne remote sensing: an outline methodology, *Mangroves and Salt Marshes* **2**, 15-28.

Snow, R.S. and Slingerland, R.L. (1987) Mathematical modelling of graded river profiles, *Journal of Geology* **95**, 15-33.

Sonka, M., Hlavac, V. and Boyle, R. (1993) *Image Processing, Analysis and Machine Vision*, Chapman and Hall: London.

Spencer, T., Moeller, I. And French, J.R. (1996) Wind wave attenuation over saltmarsh surfaces, In Sir William Halcrow and Partner Ltd (ed.) *Saltmarsh Management for Flood Defence*, NRA: Bristol, 46-54.

Steel., T.J and Pye, K. (1997) The development of saltmarsh tidal creek networks: evidence from the U.K., *Proceedings of the Canadian Coastal Conference*, 267-280.

Steers, J.A. and Thomas, H. (1929) Vegetation and sedimentation as illustrated in the region of the Norfolk saltmarshes, *Proceedings of the Geological Association* **11**, 341-351.

Steers, J.A. (1959) Saltmarshes, *Endeavour* **18**, 75-82.

Steers, J.A. (1977) Physiography, In Chapman, V.J. (ed.) *Wet Coastal Ecosystems*, Elsevier: Amsterdam, 31-60.

Stephens, J.A., Uncles, R.J., Barton, M.L. and Fitzpartick, F. (1992) Bulk properties of intertidal sediments in a muddy, macrotidal estuary, *Marine Geology* **103**, 445-460.

Stoddart, D.R., French, J.R., Bayliss-Smith, T.P. and Raper, J. (1987) Physical processes on Wash saltmarshes, In Doody, P. (ed.) *The Wash and its Environment, Nature Conservancy Council Focus on Nature Conservation Series 7*, 64-76.

Stoddart, D.R., Reed, D.J. and French, J.R. (1989) Understanding salt-marsh accretion, Scolt Head Island, Norfolk, England, *Estuaries* **12**, 228-236.

Strahler, A.N. (1958) Dimensional analysis applied to fluvially eroded landforms, *Geological Society of America Bulletin* **69**, 279-300.

Strahler, A.N. (1962) Hypsometric (area-altitude) analysis of erosional topography, *Geological Society of America Bulletin* **63**, 1117-1142.

Strahler, A.N. (1964) Quantitative geomorphology of drainage basins and channel networks, In Chow, V.T. (ed.) *Handbook of Applied Hydrology*, McGraw-Hill: New York, 39-76.

Tarbuton, D.G., Bras, R.l. and Rodriguez-Iturbe, I. (1988) The fractal nature of river networks, *Water Resources Research* **24**, 1317-1322.

Taylor, J.R. (1982) *An Introduction to Error Analysis. The Study of Uncertainties in Physical Measurements*, Oxford University Press: Mill Valley.

Thieler, E.R. and Danforth, W.W. (1994) Historical shoreline mapping (I): improving techniques and reducing positioning errors, *Journal of Coastal Research* **10**, 549-563.

Thom, B.G. (1967) Mangrove ecology and deltaic geomorphology: Tabasco, Mexico, *Journal of Ecology* **55**, 301-343.

Thorne, C.R. and Tovey, N.K. (1981) Stability of composite river banks, *Earth Surface Processes and Landforms* **6**, 469-484.

Titus, J.G. (1991) Greenhouse effect and coastal wetland policy: How Americans could abandon an area the size of Massachusetts at minimum coast, *Environmental Management* **15**, 39-58.

Toft, A.R., Pethick, J.S., Burd, F., Gray, A.J., Doody, J.P. and Penning-Rowsell, E. (1994) A guide to the understanding and management of saltmarshes, *R&D Note 324*, NRA: Bristol.

Tsihrintzis, V.A., Vasarhelyi, G.M. and Lipa, J. (1996) Ballona wetland: A multi-objective salt marsh restoration plan, *Proceedings of the Institution of Civil Engineers - Water, Maritime and Energy* **118**, 131-144.

Tubbs, C.R. (1999) *The Ecology, Conservation and History of The Solent*, Packard Publishing: Chichester.

Tyler, A.C. and Zieman, J.C. (1999) Patterns of development in the creekbank region of a barrier island Spartina alterniflora marsh, *Marine Ecology* **180**, 161-177.

Van Dongeren, A.R. and De Vriend, H.J. (1994) A model of morphological behaviour of tidal basins, *Coastal Engineering* **22**, 287-310.

Van Eerdt, M.M. (1985) Salt marsh cliff stability in the Oosterschelde, *Earth Surfaces Processes and Landforms* **10**, 95-106.

Van Straaten, L.M.J.U. and Kuenen, P.H.H. (1957) Accumulation of fine grained sediments in the Dutch Wadden Sea, *Geologie En Mijnbouw* **19**, 329-354.

Wang, Y.P (1983) Spatial reasoning in remotely sensed data, *IEEE Transactions on Geoscience and Remote Sensing* **GE21**, 94-101.

Wang, Y.P., Zhang, R.S. and Gao, S. (1999) Geomorphic and hydrodynamic responses in salt marsh-tidal creek systems, Jiangsu, China, *Chinese Science Bulletin* **44**, 544-549.

Ward, L.G. (1978) Hydrodynamics and sediment transport in a salt marsh tidal channel, *Proceedings 16th Coastal Engineering Conference:* Hamburg, 1953-1970.

Ward, L.G. (1981) Suspended-material transport in marsh tidal channels, Kiawah Island, South Carolina, *Marine Geology* **40**, 139-154.

Wells, J.T., Adams, C.E., Park, Y., and Frankenberg, E.W. (1990) Morphology, sedimentology and tidal channel processes on a high-tide-range mudflat, west coast of South Korea, *Marine Geology* **95**, 111-130.

Werner, C. and Smart, J.S. (1973) Some new methods of topologic classification of channel networks, *Geographical Analysis* **5**, 271-295.

Werritty, A. (1972) The topology of stream networks, In Chorley, R.J. (ed.) *Spatial Analysis in Geomorphology*, Methuen: London, 167-196.

Wesolowsky, G.O. (1973) Location in continuous space, *Geographical Analysis* **5**, 95-112.

Wharton, G. (1995) The channel-geometry method: guidelines and applications, *Earth Surface Processes and Landforms* **20**, 649-660.

Williams, P.B. and Florsheim, J.L. (1994) Designing the Sonoma Baylands project, *California Coast and Ocean* **10**, 19-27.

Williams, P.B. and Harvey, H.T. (1983) California coastal saltmarsh restoration design, In Magoon, O.T. and Converse, H. (eds.) *Coastal Zone '83*, American Society of Civil Engineers: New York, 1444-1456.

Wolaver, T.G., Dame, R.F., Spurrier, J.D. and Miller, A.B. (1988) Sediment exchange between a euhaline salt marsh in South Carolina and the adjacent tidal creek, *Journal of Coastal Research* **4**, 17-26.

Woldenberg, M. (1972) Relations between Horton's Laws and hydraulic geometry as applied to tidal networks, *Harvard Papers in Theoretical Geography* **45**, 1-39.

Woldenberg, M. and Horsfield, K. (1983) Finding the optimal lengths for three branches at a junction, *Journal of Theoretical Biology* **104**, 301-318.

Woldenberg, M. and Horsfield, K. (1986) Relation of branching angles to optimality for four cost principles, *Journal of Theoretical Biology* **122**, 187-204.

Wolf, P.R. (1983) *Elements of Photogrammetry*, McGraw Hill: Singapore.

Wolpert, L. (1993) *The Unnatural Nature of Science*, Faber and Faber: London.

Woodworth, P.L. (1990) A search for accelerations in records of European mean sea level, *International Journal of Climatology* **10**, 129-143.

Woolnough, S.J., Allen, J.R.L. and Wood, W.L. (1995) An exploratory numerical model of sediment deposition over tidal saltmarshes, *Estuarine Coastal and Shelf Science* **41**, 515-543.

Wright, L.D., Coleman, J.M. and Thom, B.G. (1973) Processes of channel development in a high-tide-range environment: Cambridge Gulf-Ord River delta, western Australia, *Journal of Geology* **81**, 15-41.

Yalin, M.S. (1972) *Mechanics of Sediment Transport*, Pergamon Press: Oxford.

Yang, C.T. (1971) Potential energy and stream morphology, *Water Resources Research* **7**, 311-322.

Yang, C.T. and Song, C.C.S. (1979) Theory of minimum rate of energy dissipation, *Journal of the Hydraulics Division ASCE* **105**, 769-784.

Yang, C.T, Song, C.C.S. and Woldenberg, M.J. (1981) Hydraulic geometry and minimum rate of energy dissipation, *Water Resources Research* **17**, 1014-1018.

Yapp, R.H., Johns, D. and Jones, O.T. (1917) The saltmarshes of the Dovey estuary, *Journal of Ecology* **5**, 65-103.

Yatsu, E. (1955) On the longitudinal profile of the graded river, *Transactions of the American Geophysical Union* **36**, 655-663.

Zamir, M. (1976) Optimality principles in arterial branching, *Journal of Theoretical Biology* **62**, 227-251.

Zamir, M. (1986) Cost analysis of arterial branching in the cardiovascular systems of man and animals, *Journal of Theoretical Biology* **120**, 111-123.

Zamir, M. and Bigelow, D.C. (1984) Cost of departure from optimality in arterial branching, *Journal of Theoretical Biology* **109**, 401-409.

Zedler, J.B., Callaway, J.C., Desmond, J.S., Vivian-Smith, G., Williams, G.D., Sullivan, G., Brewster, A.E. and Bradshaw, B.K. (1999) California salt-marsh vegetation: an improved model of spatial pattern, *Ecosystems* **2**, 19-35.

Zeff, M.L. (1988) Sedimentation in a saltmarsh tidal channel system, southern New Jersey, *Marine Geology* **82**, 33-48.

Zeff, M.L. (1999) Saltmarsh tidal channel morphometry: applications for wetland creation and restoration, *Restoration Ecology* **7**, 205-211.

Zernitz, E.R. (1932) Drainage patterns and their significance, *Journal of Geology* **40**, 498-521.

APPENDIX 1: DETAILS OF AERIAL PHOTOGRAPHIC COVERAGE

Details of the nominal resolution, date of acquisition, and source of photographic coverage for each of the selected study localities, are summarised below.

	STUDY LOCALITY	PHOTOGRAPHIC RESOLUTION	DATE	SOURCE
1	Duddon Estuary	1:10 000	1992	Cambridge University
2	Isle of Walney	1:10 000	1992	Cambridge University
3	River Leven	1:4 900	1974	Cambridge University
4	River Ribble	1:3 000	1996	NERC*
5	River Dovey	1:13 000	1994	ITE**
6	River Carew	1:10 000	1998	Cambridge University
7	River Loughor	1:6600	1997	NERC
8	Burry Inlet	1:6600	1997	NERC
9	Severn Estuary	1:10 000	1988	Cambridge University
10	Keyhaven, The Solent	1:5 000	1997	EA*** (Southern Region)
11	Lymington River	1:5 000	1997	EA (Southern Region)
12	Beaulieu River	1:5 000	1997	EA (Southern Region)
13	Pagham Harbour	1:3 000	1997	EA (Southern Region)
14	Stour Estuary	1:5 000	1992	EA (Southern Region)
15	The Swale	1:5 000	1997	EA (Southern Region)
16	Maplin Sands	1:5 000	1997	EA (Anglian Region)
17	River Roach	1:5 000	1997	EA (Anglian Region)
18	River Crouch	1:5 000	1997	EA (Anglian Region)
19	Dengie Peninsula	1:5 000	1997	EA (Anglian Region)
20	River Blackwater	1:5 000	1997	EA (Anglian Region)
21	River Colne	1:5 000	1997	EA (Anglian Region)
22	Hamford Water	1:5 000	1997	EA (Anglian Region)
23	River Orwell	1:10 000	1997	EA (Anglian Region)
24	Stiffkey	1:5 000	1997	EA (Anglian Region)
25	Scolt Head Island	1:5 000	1997	EA (Anglian Region)
26	Brancaster Harbour	1:5 000	1997	EA (Anglian Region)
27	Holbeach, The Wash	1:5 000	1997	EA (Anglian Region)
28	Butterwick, The Wash	1:5 000	1997	EA (Anglian Region)
29	Saltfleet	1:5 000	1997	EA (Anglian Region)

Table 1. Spatial and temporal resolution of aerial photographic coverage for the selected study localities (courtesy of *Natural Environmental Research Council; **Institute of Terrestrial Ecology; and ***Environment Agency).

APPENDIX 2: DESCRIPTION OF EXTENSIVE STUDY LOCALITIES

This appendix provides the location of (as a six figure Ordnance Survey grid reference), and gives a brief site description for each study locality included in the extensive phase of this investigation. Detailed characteristics of each environmental setting are given in Chapter 6.

1. Duddon Estuary: Millom Marsh (SD 195 825)

Situated on the western shore of the Duddon Estuary, Millom Marsh extends seaward from an earth embankment, which fronts a railway line and agricultural land. Saltmarsh communities dominate upper reaches of the intertidal profile, while non-vegetated sandflats transcend the lower foreshore towards the Duddon channel. At the time of this study, the marsh is managed by Lansdale Estates, and is subject to livestock grazing.

2. Isle of Walney: Wylock Marsh (SD 202 642)

The area of Wylock Marsh included in the present study appears to be a comparatively new system (Pye and French, 1993), that has recently formed in the protected back-barrier setting afforded by the Isle of Walney. Bounded at its landward limit by higher terrain and a road, halophytic colonisation is evident throughout the upper reaches of the intertidal profile. Vegetation is absent from the central and lower sectors, which are nevertheless dissected by tidal creeks. These networks feed into Piel Channel, the migration of which is regulated upstream by a training wall. Broughton Estates and the Walney Island Wildfowlers Association manage the marsh. Nearby, older and higher marsh remnants occur landward of the younger tracts.

3. River Leven: Holker Marsh (SD 335 771)

Benefiting from the protected embayment setting of Morecambe Bay, Holker Marsh is situated on the east shore of the River Leven, in front of a raised concrete embankment along which a railway runs (see Gray, 1972). Saltmarsh occupies the upper reaches of the wide intertidal profile, and is fronted by sandflats that extend towards the main Ulverston Channel. Falling under the jurisdiction of Sand Gate Farm, the site is subject to intensive livestock grazing.

4. River Ribble: Warton Bank marshes (SD 383 267)

Warton Bank marsh is located on the north bank of the River Ribble. While the upper reaches of the estuary have been extensively reclaimed (Doody, 1992), the central sector within which the study site is situated, remains more-or-less in its natural state. As such, the selected formation extends landward until encountering an adjoining network, rather than an artificial obstruction. Saltmarsh comprises the upper and central reaches of the intertidal profile, with mudflats extending seaward to the main tidal waterway, which is constrained by a training wall throughout most of its length. Lytham and District Wildfowlers Association are presently responsible for the site.

5. River Dovey: Craig-y-penrhyn marshes (SN 647 948)

The saltmarsh at Craig-y-Penrhyn comprises a fairly narrow fringe on the southern bank of the River Dovey. Situated in the central sector of the estuary funnel (Shi and Lamb, 1991), the site is squeezed between an embankment along which a railway runs, and the local base level imposed by Pil Lodge. Managed by Lodge Farm, the marsh is intensively grazed by livestock.

6. River Carew: Williamston marshes (SN 030 054)

The Williamston marshes border the River Carew at a position just upstream of its junction with the River Cresswell (Dalby, 1970). Managed by the Pembroke Coast National Parks Authority, the saltmarsh has retained a fairly natural setting, backed by a gradual transition to higher terrain that is subject to agricultural use. Halophytic colonisation extends across the upper and central reaches of the foreshore, with the lower mudflats dissected by shallow creeks that adjoin the main tidal waterway.

7. River Loughor: Machynys marshes (SS 500 987)

The sandy spit, which has developed in a southerly direction from the North Docks at Llanelli, provides a protected setting for saltmarsh development. The landward limit of saltmarsh is marked by a seamless transition to sand dune communities, while halophytic vegetation extends across the entire width of the intertidal zone to the adjoining waterway of Afon Lliedi. The marshes are currently managed by the Countryside Commission for Wales.

8. Burry Inlet: Landimore Marsh (SS 462 944)

The extensive Landimore saltmarsh has developed in the sheltered setting of the south shore of Burry Inlet, in the lee of Whiteford Sands. The marsh area of interest is dissected by a mass of creeks, which are unconstrained at the landward limit, and feed into Great Pill. This large channel in turn connects with Burry Pill, which eventually leads to the main waterway of the River Loughor. Owned and managed by the National Trust, the site is also subject to intensive livestock grazing.

9. Severn Estuary: Sand Bay marshes (ST 327 656)

The saltmarsh at Sand Bay is situated at the transition between the Bristol Channel and Severn Estuary, which marks a switch in emphasis from wave- to tide-dominated conditions (Allen and Duffy, 1998a, 1998b). Vegetative cover extends from the landward limit imposed by an earth embankment, across the upper reaches of the intertidal zone. Central and lower sectors of the southern estuary bank comprise mudflats, on which proto creek development is evident towards the main waterway. The site currently falls under the jurisdiction of Sand Point Farm.

10. Keyhaven, The Solent: Keyhaven Lake marshes (SZ 308 909)

Hurst Castle Spit affords sufficient protection from wave activity within the Solent to support saltmarsh development throughout Keyhaven Lake. Comprising an extensive mosaic of interconnecting creeks, the marsh system of interest is bounded at the headwaters by a large muddy pool. Halophytic colonisation is evident throughout the central and lower reaches, extending to the banks of the adjoining tidal channel. Hampshire County Council and the Hampshire Wildlife Trust are responsible for the site.

11. Lymington River: Pylewell Lake marshes (SZ 344 946)

The marsh at Pylewell Lake is situated to the east of the main river channel, and sheltered in the lee of Lymington Spit. While the upper reaches of the site are adjusted relative to adjacent tidal networks, the lower boundary adjoins a through-flowing channel that effectively isolates the marsh from the mainland. Hampshire County Council and the Hampshire Wildlife Trust kindly granted access to the site.

12. Beaulieu River: Warren Farm Spit marshes (SZ 424 974)

Protection from wave-dominated conditions afforded by the shingle spit at Warren Farm, has enabled a narrow fringe of saltmarsh to develop at the mouth of the River Beaulieu (Tubbs, 1999). The rear of the marsh terminates at the base of the spit, while halophytic colonisation extends to a local base level defined by the adjoining waterway. Although owned by Beaulieu Estates, the site is overseen by English Nature.

13. Pagham Harbour: Ferry Channel marshes (SZ 863 969)

With the Isle of Wight affording protection from the south-west, the embayment setting of Pagham Harbour provides an ideal location for saltmarsh development. The site of interest has developed since a scheme to reclaim the entire area was abandoned in 1910, and tidal activity restored (Geodata Institute, 1994). The rear of the marsh is bounded by a former railway embankment, and extends seaward towards a local base level defined by Ferry Channel. The Environment Agency own most of the site, which is managed by West Sussex County Council, who uphold its designation as a Local Nature Reserve, Site of Special Scientific Interest and Special Protected Area.

14. Stour Estuary: Shell Ness marshes (TR 346 623)

Saltmarsh on the southern bank at the mouth of the River Stour has developed in the lee of the sand spit at Shell Ness. The marsh retains a natural setting, with a gradual transition to higher terrain at its landward boundary. The seaward limit of halophytic colonisation comprises a cliffed margin in close proximity to the main river channel. The site is managed by Kent Wildlife Trust.

15. The Swale: Shell Ness marshes (TR 044 675)

The Shell Ness marshes are bounded by an earth embankment, which protects low-lying agricultural land and fresh water marsh. Vegetative cover terminates some way from the main tidal waterway, although incised creeks transcend the remaining distance to base level. The site is overseen by English Nature.

16. Mapin Sands: Shelford Head marsh (TQ 994 894)

Situated on the eastern shore of Foulness Island, the marsh at Shelford Head is protected by Maplin Sands from the wave-dominated regime that is typical of open-coast localities. Vegetative cover extends over a small region of the foreshore, the landward limit of which is constrained by a seawall. The site is owned by overseen by the Defence Evaluation and Research Agency (DERA).

17. River Roach: Potton Point marshes (TQ 967 922)

Bordering the River Roach some distance upstream from its confluence with the River Crouch, the marshes at Potton Point are situated at a junction between waterways known as The Middleway and Devil's Reach. The narrow fringe of marsh is bounded at the rear by an embankment, and extends across upper and central reaches of the intertidal zone. The final descent to base level comprises a sloping mudflat, into which tidal creeks emanating from the marsh are incised. The site falls under the jurisdiction of DERA.

18. River Crouch: Foulness Point marshes (TR 046 953)

Known as Foulness Point, the northerly apex of Foulness Island also comprises the southern bank of the River Crouch. The saltmarsh is situated in the lee of a shell spit, which through its progressive shore parallel migration (Greensmith and Tucker, 1966), has isolated the area of interest from a regular semi-diurnal tidal regime. Flows into and out of the system now pass through a single breach at the southern end of the site, a condition that severely limits both the inundation frequency and pattern of drainage. Together with constraint of the landward boundary by a seawall, such limited access means that the marsh may soon become a closed system. The site is owned and overseen by DERA.

19. Dengie Peninsula: Grange Farm marshes (TM 037 023)

Situated between Howe and Grange outfall, the landward limit of the marsh is bounded by a channel connecting these two field drains. While the seaward limit of vegetative cover occurs in the upper reaches of the intertidal profile, the central and lower reaches comprise the Dengie Flats. These sand and mud banks afford protection from the wave-dominated regime that would usually prevent the formation of saltmarsh in an open-coast setting such as this. At the time of this investigation, the site is owned by Grange Farm.

20. Blackwater Estuary: Tollesbury Wick marshes (TL 982 098)

The small pocket of marsh fringing the Blackwater Estuary at Tollesbury Wick is constrained at its landward limit by an embankment. Halophytic vegetation transcends only the upper reaches of the northern foreshore, beyond which bare mudflats extend towards the main river channel. The marshes are currently managed by Essex Wildlife Trust.

21. River Colne: Lee Wick Farm marshes (TM 097 137)

The accumulation of a bar feature at the mouth of the River Colne has enabled saltmarsh to develop in the sheltered region of foreshore adjacent to Lee Wick Farm. Although an embankment protects the shoreline itself, the marsh effectively forms an island. Consequently, the system appears relatively unconstrained, bounded at the rear by an adjoining creek network and extending towards the local base level that is imposed by Ray Creek. The site is overseen by Essex Wildlife Trust.

22. Hamford Water: Oakley Creek marshes (TM 219 269)

The area of interest is situated in a northern branch of the Hamford Water embayment, adjacent to Bramble Island. The marsh is isolated from the shore, bounded to the rear by a large muddy pool and extending seaward to Oakley Creek. The base level imposed by this waterway may have experienced some past modification through dredging, since it leads to Great Oakley Dock. However, the dock no longer appears to be in use by the present owners, Exchem Organics Ltd.

23. River Orwell: Long Reach marshes (TM 227 375)

The marshes bordering Long Creek are situated on the southern bank of the River Orwell. The landward limit of saltmarsh development is constrained by higher terrain, which marks the transition to residential areas and agricultural land. The seaward boundary falls within the central reaches of the intertidal zone. Beyond the limit of vegetative cover, a considerable tract of muddy foreshore extends to the base level defined by the main river channel. There is evidence of past intervention within the saltmarsh system, in the guise of decaying sluices. Access to the site was granted courtesy of Hill House Farm.

24. Stiffkey: Lady Creek marshes (TF 975 445)

Despite the open-coast setting, marshes have formed in the upper reaches of the wide intertidal profile at Stiffkey, where fronting sand flats progressively mitigate excess wave energy. The area of interest is situated between higher terrain at the rear of the system and raised sand dunes marking the limit of vegetative cover. Beyond this point, a shallow channel connects with Patch Pit Creek, which in turn extends towards the distant base level imposed by mean low water. The site is managed by the National Trust.

25. Scolt Head Island: Hut marsh (TF 813 461)

The back-barrier setting of Scolt Head Island, which comprises a complex array of sand and shingle structures (Chapman, 1974), provides ideal conditions for saltmarsh development. Bounded to the rear by this natural topographic barrier, vegetative cover transcends upper and central reaches of the intertidal zone, with a rapid descent across the lower sector towards the local base level defined by Norton Creek. The site falls under the jurisdiction of English Nature.

26. Brancaster: Brancaster Marsh (TF 793 448)

The area of interest at Brancaster Marsh backs onto the golf course, which is situated in the lee of a sand dune complex. At the landward boundary, a natural transition is made to higher terrain, while the seaward limit of vegetative cover extends to a base level defined by Mow Creek. Although this channel provides access to Brancaster Harbour there is no evidence of intervention in the guise of dredging. The site is overseen by the National Trust, on behalf of Scolt District Commonholders.

27. Holbeach, The Wash: Cox's Creek marshes (TF 474 298)

Situated on the south-western shore of the Wash embayment, the marshes at Holbeach extend seaward, from the topographic boundary imposed by an embankment, towards Cox's creek. This channel in turn feeds into the Nene Outfall. The marshes of interest date back to 1865 (Inglis and Kestner, 1958; Chapman, 1974; Pye, 1995), having escaped more recent reclamation projects. The site is currently owned and overseen by the Ministry of Defence.

28. Butterwick, The Wash: Butterwick Low marshes (TF 417 439)

The marshes at Butterwick have attained their present status over the relative short period following a reclamation scheme that was completed in 1980 (Pye, 1995). While an embankment imposes the landward limit of vegetative cover, the seaward boundary falls within the central reaches of the intertidal zone. Extensive sand and mud flats extend beyond this point towards the adjacent tidal waterway known as Boston Deeps. The land is currently owned and overseen by Glebe Farm.

29. Saltfleet: Sand Haile marshes (TF 460 947)

Saltmarsh development is confined to the upper and central reaches of this open-coast setting, under the protection afforded by the fronting Sand Haile Flats. The landward limit of saltmarsh development is imposed by an embankment, while halophytic colonisation terminates with a ridge of sand dunes (see Steers, 1977). Interestingly, channel development is absent from upper reaches of the marsh, which instead forms a continuous platform. The central and lower sectors are, however, dissected by creeks in a more typical manner.